

Geotechnical, Geological and Earthquake Engineering

Gian Paolo Cimellaro

Urban Resilience for Emergency Response and Recovery

Fundamental Concepts and Applications

 Springer

Geotechnical, Geological and Earthquake Engineering

Volume 41

Series Editor

Atila Ansal, School of Engineering, Özyeğin University, Istanbul, Turkey

Editorial Advisory Board

Julian Bommer, Imperial College London, U.K.

Jonathan D. Bray, University of California, Berkeley, U.S.A.

Kyriazis Pitilakis, Aristotle University of Thessaloniki, Greece

Susumu Yasuda, Tokyo Denki University, Japan

More information about this series at <http://www.springer.com/series/6011>

Gian Paolo Cimellaro

Urban Resilience for Emergency Response and Recovery

Fundamental Concepts and Applications

 Springer

Gian Paolo Cimellaro
DISEG
Politecnico di Torino
Turin, Italy

ISSN 1573-6059 ISSN 1872-4671 (electronic)
Geotechnical, Geological and Earthquake Engineering
ISBN 978-3-319-30655-1 ISBN 978-3-319-30656-8 (eBook)
DOI 10.1007/978-3-319-30656-8

Library of Congress Control Number: 2016934208

© Springer International Publishing Switzerland 2016

This work is subject to copyright. All rights are reserved by the Publisher, whether the whole or part of the material is concerned, specifically the rights of translation, reprinting, reuse of illustrations, recitation, broadcasting, reproduction on microfilms or in any other physical way, and transmission or information storage and retrieval, electronic adaptation, computer software, or by similar or dissimilar methodology now known or hereafter developed.

The use of general descriptive names, registered names, trademarks, service marks, etc. in this publication does not imply, even in the absence of a specific statement, that such names are exempt from the relevant protective laws and regulations and therefore free for general use.

The publisher, the authors and the editors are safe to assume that the advice and information in this book are believed to be true and accurate at the date of publication. Neither the publisher nor the authors or the editors give a warranty, express or implied, with respect to the material contained herein or for any errors or omissions that may have been made.

Printed on acid-free paper

This Springer imprint is published by Springer Nature
The registered company is Springer International Publishing AG Switzerland

Dedicated to my family for supporting me through these years. Their presence and encouragement made this idea a reality.

Preface

Resilience is the ability of a system to bounce back after a crisis. It matters because it gives the system the capacity to resist, so more and more we should look for design-resilient structures, provided that crises cannot be avoided.

The book serves as introduction to the concept of Resilience-Based Design (RBD) as an extension of Performance-Based Design and presents some advanced applications for specialists. It provides different state-of-art methodologies to evaluate resilience and clarifies the difference between, vulnerability, resilience, sustainability, and risk. This book is targeted to graduate students, engineers, and researchers who are interested in the topic of resilience. In addition, the book can be used as supplementary text in graduate level courses in disaster resilience.

The resilience concept includes multiple factors describing temporal-spatial functionality of systems which encompass various types of uncertainties, both in definitions and quantifications. After introducing such definitions and focusing on losses, recovery processes, downtime, and their respective uncertainties, the book establishes the methods for evaluating them both analytically and heuristically. Starting from the definition of resilience originally introduced by the Multidisciplinary Center for Earthquake Engineering Research (MCEER), an extension of the methodology is provided to address Community Resilience introducing seven characteristic dimensions. The seven dimensions are summarized by the acronym PEOPLES: Population and demographics, Environmental/ecosystem, Organized governmental services, Physical infrastructures, Lifestyle and community competence, Economic development, Sociocultural capital. For each dimension, the components and the subcomponents are defined and the related indicators are provided. This book emphasizes the physical infrastructure dimension. It provides several examples of applications for transportation, hydraulic, gas and electric network. The problem of interdependencies and the domino effect is also taken into account during the analysis. Finally, one chapter focuses on the different methodologies to improve disaster preparedness and the engineering mitigation strategies. The last chapter describes the different computer platforms available in the market to evaluate community resilience.

The book contains three main parts:

- I. *Definition and Quantification of Theoretical Framework to Evaluate Resilience*
- II. *Applications of Resilience Concepts to Different Networks*
- III. *Resilience Mitigation Actions and Tools*

Part I defines resilience and describes the state of knowledge about the concept. It consists of seven chapters that together provide a systematic and comprehensive theoretical framework of resilience and presents methodologies to evaluate resilience by looking at the different spatial and temporal dimensions of the problem. Chapter 1 is an introduction to illustrate the importance and necessity of resilience in different dimensions of a community against natural and manmade hazards by highlighting some examples of recent community disasters. This chapter presents a broad definition of resilience as used in different fields. Chapter 2 introduces the concepts of resilience-based design (RBD) as an extension of performance-based design (PBD) starting from the early definition of resilience formulated in 2003 by researchers of the Multidisciplinary Center for Earthquake Engineering Research (MCEER). Different state-of-the-art methodologies to evaluate resilience are provided, clarifying the differences between resilience, vulnerability, sustainability, and risk. The concept of resilience-based design is formulated and presented. Chapter 3 focuses on the description of the different approaches to define and group resilience indicators. Chapter 4 focuses on the definition of a loss function which has been one of the first indicators used to define resilience. Different models to evaluate damage losses are provided, approaching the problem in probabilistic terms using fragility functions analyzing the different types of uncertainties which appear in the resilience assessment. Chapter 5 defines recovery models and downtime. Long-term and short-term recovery models are presented.

Finally, starting from the definition of resilience provided by MCEER, an extension of the methodology is provided in Chap. 6 which introduces seven dimensions of community resilience. The seven dimensions are summarized with the acronym PEOPLES: Population and demographics, Environmental/ecosystem, Organized governmental services, Physical infrastructures, Lifestyle and community competence, Economic development, Sociocultural capital. For each dimension, components and subcomponents are defined and the related indicators are provided. The chapter also presents a comprehensive mathematical formulation of the PEOPLES framework and provides performance metrics for the different dimensions of resilience. Chapter 7 describes a comprehensive methodology for the evaluation of infrastructure interdependencies, introducing a framework for the analysis of the degree of interdependency among lifelines. The method has been applied to the Fukushima Daiichi nuclear power plant disaster which is investigated as a case study.

Part II of the book provides different applications of resilience concepts and quantification metrics to evaluate community resilience which takes into account both organizational and technical aspects in different networks. Chapter 8 focuses on the application of resilience for the physical infrastructure dimension. Several

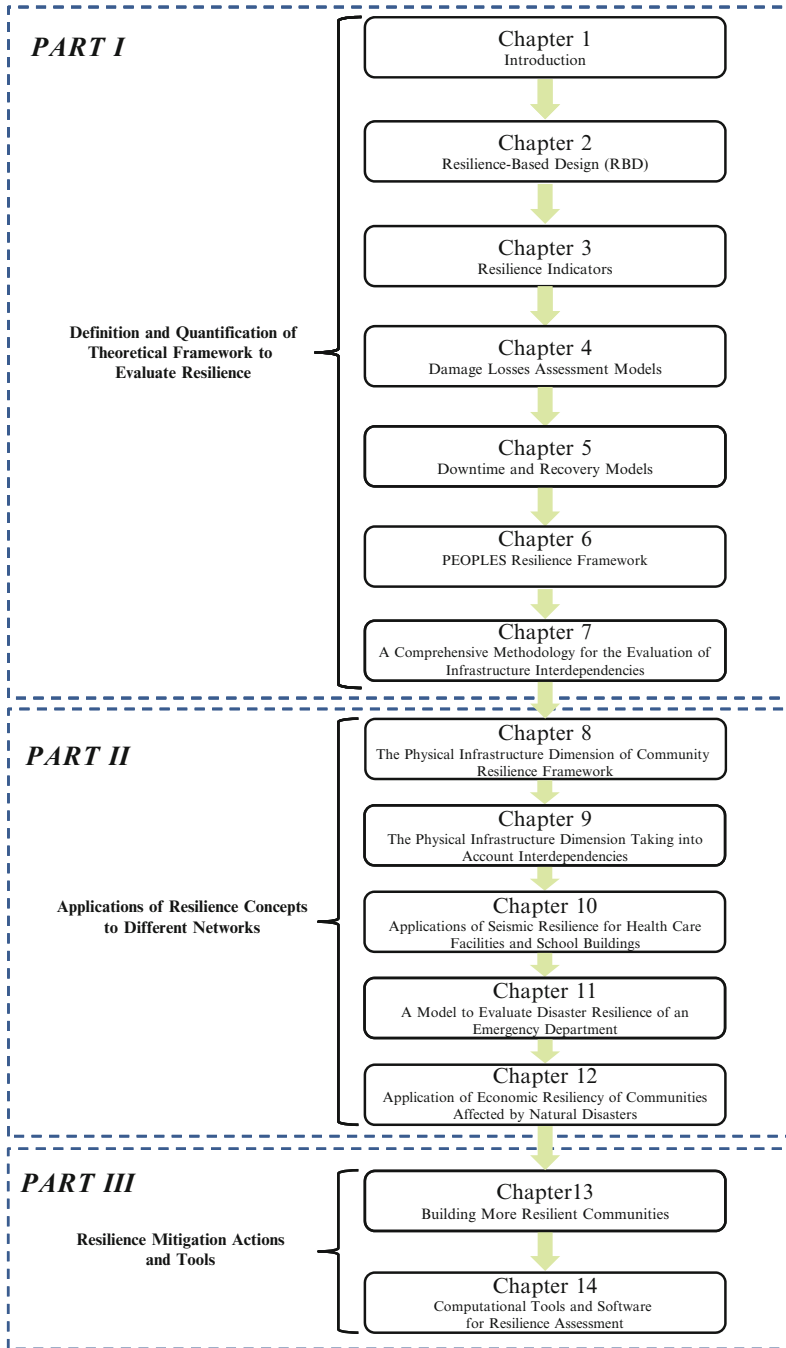


Fig. 1 Flowchart of the book

examples of applications are provided for the transportation, hydraulic, gas, electric, and telecommunication network.

The problem of interdependencies and the domino effect between infrastructures is taken into account in Chap. 9. Chapter 10 describes applications of seismic resilience for healthcare facilities and school buildings and evaluates repair cost and time by performing a loss analysis. Chapter 11 provides a model to evaluate disaster resilience of a health-care emergency department and proposes a metamodel to quantify the resiliency of the emergency department network. An application of economic resiliency for communities affected by natural disaster is described in Chap. 12, while an economic resilience index is defined.

Part III of the book describes methodologies to improve resilience and list the available tools in the market. Chapter 13 focuses on the different methodologies to improve disaster preparedness and the engineering mitigation strategies across a community. The last chapter (Chap. 14) focuses on the description of the different computer platforms available in the market to evaluate various aspects of community resilience. Finally, the Appendix provides complementary information, related, for example, to the probabilistic concepts used in the preceding chapters.

Turin, Italy
January, 2016

Gian Paolo Cimellaro

Acknowledgements

I am grateful to a number of people who helped me to prepare this book. Ali Zamani, my current PhD student, assisted in numerous ways and played an important role in completing the book. He edited the book and developed several figures which have been inserted in the text.

Several students, present and former, assisted in preparing the case study examples: Aldo Tinebra, Salvatore Pluchino, Maria Stella Tribulato, Marzia Malavisi, Paolo Fantini, Alba Chiara Trozzo, Sarah Moretti, Davide Martinelli, Vincenzo Arcidiacono, Giuseppe Scura, Alessio Vallero, Pietro Crupi, and Marzia Bianco.

Fabrizio Ozzello, Pietro Crupi, Omar Kamouh, Glen Dervishaj, Danial Mohebbat Doost, Maamak Poori, Erfan Sheikhi, Gerardo Leo, and Sebastiano Marasco did the word processing of some material and changes to the text in LaTeX.

I am also grateful to Bridget Bassi, visiting graduate student from MIT that helped in revising the English language of the book.

Prof. Andrei M. Reinhorn and Michel Bruneau read the first draft of the book, discusses with me monthly, and provided incisive criticism and substantive suggestions for improvements. Many other professors and students – too numerous to list here by name – offered valuable comments as well.

This book has been influenced by my own research experience in collaboration with my students, but I also wish to express my deep gratitude to Prof. Mahin for the influence he had on my professional growth in the last years.

This book was prepared over a period range of three years and part of this time was spent as sabbatical year at the University of California, Berkeley, a privilege for which I am grateful to the Politecnico di Torino.

Since this is a new book and it is new in this genre, if you have suggestions for improvements or clarifications or if you identify errors, please write to me (cimellaro@gmail.com). I thank you in advance for taking the time and interest to do so.

Turin, Italy

Gian Paolo Cimellaro

Contents

Part I Definition and Quantification of Theoretical Framework to Evaluate Resilience

1	Introduction	3
1.1	Motivations	3
1.1.1	Disasters Caused by Natural Hazard	4
1.1.2	Disasters Caused by Human Action (Manmade Disasters).....	7
1.2	Milestones for Preparedness Throughout History	14
1.3	What Is Disaster Resilience?	16
1.4	State of Art of Existing Resilience Frameworks	20
1.4.1	City Level Resilience Framework	22
1.4.2	State Level Resilience Framework	23
1.4.3	National Level Resilience Framework	24
1.5	From Performance-Based Design to Resilience-Based Design... ..	25
1.5.1	PEER Performance Assessment Methodology	25
1.5.2	History of the Development of the PEER Integral.....	26
1.6	Towards Resilience-Based Design (RBD)	27
1.7	Summary and Remarks	28
	References	28
2	Resilience-Based Design (RBD)	31
2.1	Resilience-Based Design in Structures	31
2.2	MCEER Pioneer Definition of Unidimensional Resilience	32
2.2.1	Spatial Distribution	34
2.2.2	Temporal Distribution	34
2.3	The Four Rs for Resilience	35
2.3.1	Rapidity	36
2.3.2	Robustness	37
2.3.3	Redundancy	38
2.3.4	Resourcefulness	38
2.4	Inherent vs. Adaptive Resilience	40

- 2.5 Resilience vs. Vulnerability 40
- 2.6 Resilience vs. Sustainability 41
- 2.7 Resilience vs. Durability 42
- 2.8 Resilience vs. Risk 43
- 2.9 The Risk Management of Complex Infrastructural Systems 44
 - 2.9.1 Aleatory Uncertainties 45
 - 2.9.2 Epistemic Uncertainties 45
- 2.10 Uncertainties in RBD 46
- 2.11 Communicating Risk in RBD 46
- 2.12 Summary and Remarks 47
- References 47
- 3 Resilience Indicators 49**
 - 3.1 Why Resilience Indicators? 49
 - 3.2 Type of Assessments 50
 - 3.3 Methodological Approaches 50
 - 3.4 List of Existing Indicators 51
 - 3.5 Classification of Indicators 56
 - 3.6 State of Art on Classification Methods 56
 - 3.7 Proposed Classification Method 57
 - 3.7.1 Hazard Type 58
 - 3.7.2 Temporal Scale 58
 - 3.7.3 Spatial Scale 59
 - 3.7.4 Building Type 60
 - 3.7.5 Level of Development 60
 - 3.7.6 Domains 60
 - 3.7.7 Measurement Method 61
 - 3.8 Aggregation of Indicators 63
 - 3.9 Selection of Key-Indicators for Specific Case Study 64
 - 3.10 Potential Challenges of Community Resilience Assessment Using Indicators 64
 - 3.11 Relationship Between Vulnerability Indicators and Resilience Indicators 65
 - 3.12 The Progress of Grounding Indicators Set 65
 - 3.13 Examples of Measurement Methods 66
 - 3.14 Remark and Conclusions 67
 - References 67
- 4 Damage Losses Assessment Models 71**
 - 4.1 State of Art on Loss Assessment Models 71
 - 4.2 Regional Seismic Losses Assessment Models (RSLA) for Ordinary Buildings 72
 - 4.3 Seismic Loss Assessment for Infrastructure Systems 73
 - 4.4 Loss Function as Resilience Indicator 74
 - 4.5 State of the Art on Fragility Curves 77

4.6	Analytical Formulation	78
4.7	Definition of Performance Limit States	82
	4.7.1 Multidimensional Performance Limit State Function ...	82
	4.7.2 Uncertainties of Limit States	85
4.8	Generation of Fragility Curves	89
4.9	Concluding Remarks	90
	References	90
5	Downtime and Recovery Models	93
5.1	Introduction	93
5.2	Analytical Recovery Models	94
	5.2.1 Long Term Recovery Models	94
	5.2.2 Short Term Recovery Models	97
5.3	Empirical Recovery Models	100
	5.3.1 Step Recovery Function	100
5.4	Definition of Downtime	100
	5.4.1 State-of-Art in Downtime	101
5.5	Concluding Remarks	107
	References	107
6	PEOPLES Resilience Framework	109
6.1	Literature Review on Resilience Framework	109
6.2	Formulation of a Theoretical Framework for the Analysis of Community Resilience	111
6.3	Population and Demographics	116
6.4	Environmental/Ecosystem	118
6.5	Organized Governmental Services	120
6.6	Physical Infrastructures	122
6.7	Lifestyle and Community Competence	124
6.8	Economic Development	125
6.9	Socio-cultural Capital	127
6.10	Mathematical Formulation of the PEOPLES Framework	129
6.11	Resilience Index and Performance Metrics	129
6.12	Resilience Performance Levels	132
6.13	Summary and Remarks	133
	References	134
7	A Comprehensive Methodology for the Evaluation of Infrastructure Interdependencies	139
7.1	Introduction	139
7.2	Interdependency	140
7.3	Type and Effect of Interdependency	142
	7.3.1 Dependence Patterns	144
	7.3.2 Types of Failure	146
7.4	Framework for the Evaluation of the Degree of Interdependency Among Lifelines	149

7.5	Modeling Temporal Networks	153
7.5.1	Existing Interdependence Models	153
7.5.2	Input-Output Inoperability Method.....	156
7.5.3	Modified IIM for Temporal Networks	160
7.5.4	Probability Risk Assessment	173
7.6	A Case Study: Fukushima Daiichi Nuclear Power Plant Disaster.....	181
7.6.1	Cooling Requirements of a NPS.....	184
7.6.2	Connection of Fukushima Daiichi NPS with Offside Power Supply	184
7.6.3	Time-Line of the Fukushima Daiichi NPS Disaster	185
7.6.4	Modelling the Nuclear Power Plant	189
7.6.5	Topology.....	190
7.6.6	Analysis of the System.....	195
7.6.7	Interdependencies that Occurred During the Disaster of Fukushima	214
7.7	Remarks and Conclusions	220
	References.....	221

Part II Applications of Resilience Concepts to Different Networks

8	The Physical Infrastructure Dimension of Community Resilience Framework	227
8.1	Lifelines	227
8.2	Example 1: Transportation Network	228
8.2.1	Literature Review	228
8.2.2	Proposed Methodology	230
8.2.3	Transportation System Models	230
8.2.4	Structural Damage Assessment.....	233
8.2.5	Functionality of Transportation Networks During a Disaster	234
8.2.6	Functionality of the Transportation Categories During a Disaster	234
8.2.7	Functionality and Resilience of Transportation System	236
8.2.8	The Case Study of Treasure Island in San Francisco Bay, California	237
8.3	Example 2: Water Distribution Network.....	238
8.3.1	Introduction.....	238
8.3.2	Definition of a New Performance Index for the Water Distribution Network	241
8.3.3	A Case Study of the WDN of Calascibetta, Italy	245
8.3.4	Characteristics of the Water Distribution Network	246

8.3.5	Model Description, Assumptions and Calibration	247
8.3.6	Seismic Damage Model for Water Pipes	248
8.3.7	Risk of Pipe Failure	251
8.3.8	Selection of Scenarios Event	251
8.3.9	Recovery Time and Restoration Process	254
8.3.10	Numerical Results and Lesson Learned	255
8.3.11	Restoration Plans	257
8.4	Example 3: Gas Network	261
8.4.1	Introduction	261
8.4.2	Performance Assessment Procedure of Natural Gas Distribution Network	263
8.4.3	Restoration Model	265
8.4.4	Description of the Italian Natural Gas Supply System	267
8.4.5	Simulation of Failure Modes of Pipelines	270
8.4.6	Description of the Natural Gas Distribution System in the Town of Sulmona, Italy	271
8.4.7	Geological Settings	274
8.4.8	Seismic Intensity	274
8.4.9	Seismic Damage Assessment of Distributing Elements and Scenario Selection	277
8.4.10	Scenario Earthquake and Numerical Results	280
8.5	Example 4: Electric Power Network	287
8.5.1	Seismic Performance of Power System	288
8.5.2	Risk Assessment of Power Systems	289
8.5.3	Risk Curves	289
8.5.4	Comparison Between Classical and Global Indicators of Power Distribution Networks	290
8.5.5	Resilience Framework and System Restoration	291
8.6	Example 5: Communication Network	292
8.6.1	Literature Review	295
8.6.2	Standard Earthquake Damage Assessment in Italy	297
8.6.3	Proposed Earthquake Damage Assessment Using Mobile Phone Technology	300
8.6.4	Survey on Building Earthquake Damage Assessment	303
8.6.5	Application of the Digitalized Earthquake Damage Assessment	308
8.7	Remarks and Conclusions	311
	References	312
9	The Physical Infrastructure Dimension Taking into Account Interdependencies	317
9.1	Interdependencies Between Networks	317
9.1.1	Literature Review	317

- 9.1.2 Restoration Curves of Physical Infrastructures After the 2011 Tohoku Earthquake 319
- 9.1.3 Evaluation of Interdependency Index 321
- 9.1.4 Evaluation of the Weight Coefficients of the Infrastructures 324
- 9.1.5 Evaluation of the Regional Resilience Index 325
- 9.1.6 Discussion on the Evaluation of the Interdependency Indices 328
- 9.1.7 Decomposition of the Restoration Curves in Intervals Ranging Between Two Consecutive Shocks 333
- 9.1.8 Calculation of the Weight Coefficients on the First Period 336
- 9.1.9 Numerical Results of the Regional Resilience Index 339
- 9.1.10 Remarks and Conclusions 343
- References..... 343
- 10 Applications of Seismic Resilience for Health Care Facilities and School Buildings 345**
 - 10.1 Introduction 345
 - 10.2 Buildings Description..... 346
 - 10.3 Ground Motion Selection..... 347
 - 10.4 Analysis-Models and Methods 349
 - 10.5 Comparison of Structural Response..... 349
 - 10.6 Loss Analysis 351
 - 10.6.1 Repair Cost and Repair Time 352
 - 10.7 Resiliency 357
 - 10.8 Remarks and Conclusions 358
 - References..... 359
- 11 A Model to Evaluate Disaster Resilience of an Emergency Department..... 361**
 - 11.1 Introduction 361
 - 11.2 Literature Review 363
 - 11.3 Methodology 364
 - 11.4 Discrete Event Simulation Model for the ED 365
 - 11.4.1 Description of the Case Study 365
 - 11.4.2 Description of the Model and Assumptions..... 367
 - 11.4.3 Calibration of the Model in Normal and Emergency Operating Condition..... 370
 - 11.4.4 Emergency Plan 372
 - 11.4.5 Numerical Results 373
 - 11.5 Metamodel for the ED of the Mauriziano Hospital 376
 - 11.5.1 Architecture of the Metamodel 376

11.5.2	Calibration of the Model in Normal Operating Condition	377
11.5.3	Calibration of the Model with the Emergence Plan	379
11.6	Generalization of the Metamodel	382
11.6.1	Validation of the Metamodel.....	383
11.7	Summary and Remarks	383
	References.....	385
12	Application of Economic Resiliency of Communities Affected by Natural Disasters	389
12.1	Introduction	389
12.2	Description of Methodology	390
12.2.1	Economic Loss Framework.....	390
12.2.2	Direct Time-Dependent Losses	391
12.2.3	Indirect Losses	397
12.2.4	Economic Resilience Index (R_{EC})	398
12.3	The San Francisco Bay Area Case Study	398
12.3.1	Sensitivty Analysis.....	400
12.4	Summary and Conclusions	402
	References.....	405
 Part III Resilience Mitigation Actions and Tools		
13	Building More Resilient Communities	409
13.1	Introduction	409
13.1.1	Disaster Risk Management	409
13.1.2	State-of-Art on Existing Plans for Developing Resilient Communities	410
13.2	Resilience as a Preventive Action	411
13.2.1	Improving Disaster Preparedness.....	411
13.2.2	Mitigating Natural Hazard	415
13.3	Resilience as Restorative Care	419
13.3.1	Post-disaster Recovery	419
13.3.2	The Role of Legislators	420
13.4	Land Use Intervention Planning.....	421
13.5	Public Policy	423
13.6	Role of Policy Makers	423
13.7	Policy Actors	424
13.7.1	Policy Insiders and Outsiders	424
13.7.2	Civil Society Policy	425
13.7.3	Policy Champions Processes of Reform	425
13.7.4	Sub-national Government.....	425
13.7.5	Scientific and Technical Bodies	426

13.7.6	International Actors	426
13.8	International Schemes for Disaster Risk Management	426
13.8.1	Yokohama Strategy for a Safer World (1994)	427
13.8.2	Hyogo Framework for Action (HFA) (2005)	428
13.8.3	Sendai Framework (2015)	430
13.8.4	Decision Making	431
13.9	Case Study of Hurricane Sandy	432
13.9.1	Initiatives Proposed in New York City	433
13.9.2	Initiatives for Utilities	434
13.9.3	Initiative for Liquid Fuel	445
13.9.4	Initiative for Transportation	450
13.10	Summary and Remarks	459
	References	460
14	Computational Tools and Software for Resilience Assessment	463
14.1	Introduction	463
14.2	RISe and SELeNa Software	464
14.2.1	Step-by-Step Procedure Using RISe and SELeNa	464
14.2.2	Seismic Risk and Loss Assessment Using RISe	467
14.3	REDARS	468
14.3.1	Seismic Risk Analysis Using REDARS	468
14.3.2	Earthquake Modeling and Hazards Module	471
14.3.3	Component Module	471
14.3.4	System Module	472
14.3.5	Economic Module	473
14.3.6	Advantages of REDARS 2	474
14.4	HAZUS	474
14.4.1	Risk Assessment Using HAZUS	475
14.4.2	Risk Assessment Process Using HAZUS-MH	476
14.5	GIRAFFE	484
14.5.1	Overview of the GIRAFFE Simulation	485
14.5.2	Hydraulic Network Analysis	488
14.5.3	Pipe Damage Modeling	489
14.5.4	Earthquake Demand Simulation	490
14.5.5	GIRAFFE Inputs and Outputs	491
14.6	OpenQuake of GEM	492
14.7	EQVIS	492
14.8	ResilUS	494
14.9	Virtual City Simulators	494
14.9.1	Comparison Between Virtual City Software Packages	495
14.10	Summary and Remarks	504
	References	506

Appendix A Probabilistic Formulation 509

- A.1 Important Definitions 509
- A.2 The Venn Diagram 509
- A.3 Mathematics of Probability 510
- A.4 Conditional Probability 511
- A.5 The Theorem of Total Probability 511
- A.6 Probability Distribution of a Random Variable 512
- A.7 Useful Probability Distributions 513
- A.8 Multiple Random Variables 514
- A.9 The Conditional and Marginal Distributions 515

Glossary 517

Index 519

Acronyms

ABV	Assembly-based vulnerability
ACU	Ambulatory care unit
AHP	Analytical hierarchy process
ANPP	Aboveground net primary productivity
BLS	Bureau of Labor Statistics
BWR	Boiling water reactor
CCA	Common-cause analysis
CCF	Cross-correlation function
CCSF	City and County of San Francisco
CDF	Cumulative distribution function
CI	Critical infrastructures
CRM	Consequence-based risk management
CRS	Community ratings
CSM	Capacity spectrum method
CST	Condensate storage tank
DBE	Design basis earthquake
DDA	Demand-driven analysis
DEA	Data envelopment analysis
DES	Discrete event simulation
DG	Distributed generation
DRM	Disaster risk
DRR	Disaster risk reduction
DV	Decision variable
EADT	Expected annual downtime
ED	Emergency department
EDAM	Earthquake damage assessment manager
EDP	Engineering demand parameter
EFV	Excess flow automatic gas shutoff valves
EMS	Emergency medical services
ENP	Emergency nurse practitioner
EOC	Emergency operation center

EP	Emergency plan
EPS	External power supply
ESV	Emergency shutoff valves
ETA	Event tree analysis
EV	Electric vehicle
FEMA	Federal Emergency Management Agency
FL	Fuzzy logic method
FTA	Fault tree analysis
GEM	Global Earthquake Model
GIRAFFE	Graphical Iterative Response Analysis for Flow Following Earthquake
GIS	Geographic information system
GRP	Gross regional product
HFA	Hyogo Framework for Action
HOV	High-occupancy vehicle
HPCI	High-pressure core injection system
HRA	Human reliability analysis
IC	Ideal community
ICG	International Center of Geohazards
IFRC	International Federation of Red Cross and Red Crescent Societies
IIM	Input-output inoperability matrix
IM	Intensity measure
IM	Interdependency matrix
INGV	Italian National Institute of Geophysics and Volcanology
ISIL	Islamic State of Iraq and the Levant
JST	Japan Standard Time
LP	Low pressure
MAE	Mid-America Earthquake Center
MCE	Maximum capable earthquake
MCEER	Multidisciplinary Earthquake Engineering to Extreme Events Center
MCS	Macro seismic intensities
MCS	Mercalli-Cancani-Sieberg
MMI	Modified Mercalli Intensity
MP	Medium pressure
MR	Multiregional
MTLS	Multidimensional threshold limit state
NCSA	National Center for Supercomputing
NDRF	National Disaster Recovery Framework
NDVI	Normalized Difference Vegetation Index
NEN	Neighborhood Empowerment Network
NIBS	National Institute of Building Sciences
NIR	Near infrared
NIST	National Institute of Standards and Technology
NOAA	National Oceanic and Atmospheric Administration
NPS	Nuclear power station

NYCDOT	New York City Department of Transportation
NYPD	New York City Police Department
OCIPEP	Office of Critical Infrastructure Protection and Emergency Preparedness
OECD-GSF	Organization for Economic Cooperation and Development-Global Science Forum
OEM	Office of Emergency Management
OLTPS	Office of Long-Term Planning and Sustainability
OSM	Open street map
OSSPAC	Oregon Seismic Safety Policy Advisory Commission
PACT	Performance Assessment Calculation Tool
PBD	Performance-based design
PBEE	Performance-based earthquake engineering
PBSE	Performance-based seismic engineering
PCCIP	President's Commission on Critical Infrastructure Protection
PCV	Primary containment vessel
PDA	Pressure-driven analysis
PDF	Probability density function
PDQ	Provider-directed queuing
PEER	Pacific Earthquake Engineering Research Center
PGA	Peak ground acceleration
PGD	Peak ground displacement
PGV	Peak ground velocity
PL	Performance Levels
PLS	Level of response for a certain functionality limit
PPD	Presidential Policy Directive
PRA	Probabilistic risk assessment
PRV	Pressure-reducing valves
PSA	Maximum pseudo spectral acceleration
PSHA	Probabilistic seismic hazard analysis
PSSRA	Probabilistic seismic structural response analysis
PV	Photovoltaic systems
QRA	Quantitative risk analysis
RAT	Risk Assessment Tool
RBD	Resilience-based design
RCIC	Reactor Core Isolation Cooling
RCRS	RoboCup Rescue Simulator
RE	Reynolds number
RHR	Residual heat removal
RPL	Resilience performance levels
RSLA	Regional seismic losses assessment
S _a	Pseudo acceleration
SBS	Select Bus Service
SCADA	Supervisory control and data acquisition
SFDRR	Sendai Framework for Disaster Risk Reduction

SGM	Structural growth model
SIRR	Special Initiative for Rebuilding and Resiliency
SP	Series parallel
SP	Suppression pool
SPUR	San Francisco Planning and Research
SRA	Seismic risk analysis
SSI	System serviceability index
T	Period (s)
TC	Typical community
TFPB	Triple friction pendulum bearing
TLC	The control time
TOSE	Technical, organizational, social, and economical
UHS	Uniform hazard spectrum
UNISDR	United Nations International Strategy for Disaster Risk Reduction
USCS	US Customary System
USGS	United States Geological Survey
VVC	Very vulnerable
WCDR	World Conference on Disaster Reduction
WCDRR	World Conference on Disaster Risk Reduction
WCED	World Commission on Environment and Development
WDN	Water Distribution Network
WT	Waiting time
WTC	World Trade Center

Part I
Definition and Quantification of
Theoretical Framework to Evaluate
Resilience

Chapter 1

Introduction

Abstract This chapter is an introduction to indicate the prominent function and necessity of resilience in different dimensions of a community against natural and manmade hazards by highlighting some examples of recent natural and manmade disasters. It is presented a broad definition of resilience concepts in different sciences by means of an extensive literature review. Different frameworks available in literature are described and compared. Finally, the concept of Resilience-Based design is presented as an extension of Performance-Based Design.

1.1 Motivations

Although substantial progress has been made in technology towards improved performance of the built environment, natural disasters, acts of terrorism, technological failures, wars, market collapses etc. have been responsible for loss of life, disruption of commerce and financial networks, damaged property loss of business continuity and essential services during the last two decades. Many facilities and infrastructures are vulnerable to natural hazards as well as manmade hazards, and the risk of damage due to hazardous events all over the world continues to increase as proven by recent events.

Some recent examples are provided to highlight the fragility of European communities and the world, specifically in the context of critical infrastructure failure and hazards (Caverzan and Solomos 2014). They have been grouped according to the hazard distinguishing between *natural* and *manmade hazard*, including in this category accidental human actions and terrorist attacks.

This classification is arguable, because there is a common opinion that all disasters can be seen as being human-made, because they are the result of human failure to introduce appropriate *disaster management measures*. Furthermore a specific disaster can initiate other disasters (e.g. earthquake causing tsunami causing coastal flooding etc.).

1.1.1 Disasters Caused by Natural Hazard

A natural disaster is a sudden event not caused by human being that generates widespread damage with loss of life. Natural disasters might be caused by

- earthquakes,
- flooding,
- volcanic eruption,
- landslide,
- hurricanes,
- wildfire, bushfire,
- tornadoes,
- avalanches,
- tropical cyclone,
- etc.

Although Europe is assumed relatively safe from severe natural hazards, significant risks do exist and can be extreme, especially due to the high density of population in the region. The European Environmental Agency (EEA 2011) recorded the highest number of fatalities from natural events to be caused by heat waves, while floods and storms caused the greatest economic loss, during the period of 1998–2009. These two are not the only categories of natural hazards which are prevalent. In April 2010, the eruption of the Eyjafjallajökull volcano in Iceland compromised European air traffic for weeks. This result exemplifies how an unexpected phenomenon can influence critical infrastructures, even if they are not directly hit (Figs. 1.1 and 1.2).

Obviously, Europe has been subject to and is prone to hazards just like any other country, such as the United States. For the U.S. in particular, two natural disastrous events significantly influenced the development of resilience concepts: Hurricane

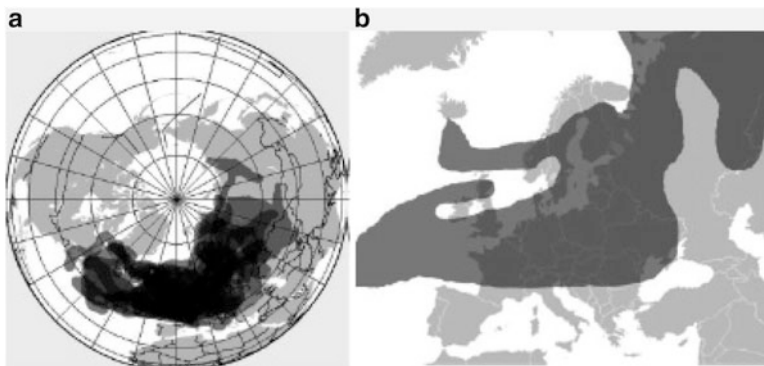


Fig. 1.1 Composite map of the volcanic ash cloud spanning in 14–25 April 2010 for the Eyjafjallajökull eruption (source <http://en.wikipedia.org>)

Fig. 1.2 Aerial image from Eyjafjallajökull volcano eruption. Ash cloud on April 17th, 2010 (source: <http://en.wikipedia.org>)

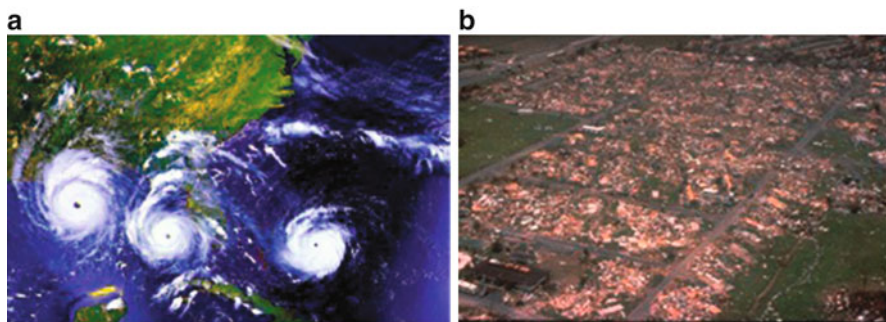


Fig. 1.3 Hurricane Andrew, (a) three views of Andrew on 23, 24 and 25 August 1992 as the hurricane moves from East to West (source <http://earthsky.org> Image credit: NASA), (b) An aerial view of Dade County, Florida, showing damage was hit by Hurricane Andrew (source: <http://en.wikipedia.org> image credited: FEMA)

Andrew in 1992 and Hurricane Katrina in 2005 (McAllister 2013). When Hurricane Andrew struck Dade County on August 24th, the storm devastated the area. It caused an estimated 25 billion dollars in damage and destroyed approximately 49,000 homes (Fig. 1.3).

Hurricane Katrina struck the Gulf Coast region in August of 2005 and rapidly escalated to a Category 5 with maximum sustained winds of 78 m/s. Storm surge and associated wave action caused breaches in the flood protection system in New Orleans, resulting in substantial structural damage to residences in the immediate vicinity of breaches and approximately three-quarters of the city became flooded (Fig. 1.4). Bridges were damaged by the uplift and lateral loads imparted by storm surge and associated wave action. An additional problem was the damage sustained by industrial facilities such as seaports, petrochemical facilities due to storm surge and flooding (NIST 2006). The extensive, multi-state destruction caused by Hurricane Katrina in 2005 serves as a reminder that natural disasters remain a significant threat to our livelihood. The unprecedented state of emergency brought

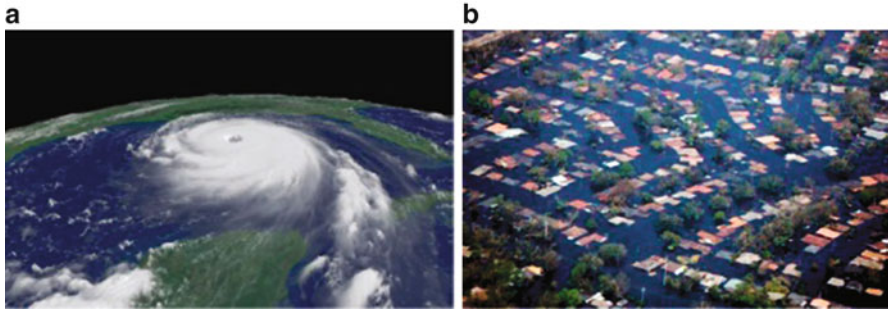


Fig. 1.4 Hurricane Katrina: (a) satellite image of the hurricane (source: image credited by NOAA); (b) flooding caused by Hurricane Katrina in the New Orleans area, August 31st, 2005 (source: <http://de.wikipedia.org>)



Fig. 1.5 Indian Ocean (Jan. 2, 2005) – A village near the coast of Sumatra lays in ruin after the Tsunami that struck South East Asia – (source: <http://en.wikipedia.org>)

renewed focus on the need to address protection from the threat of natural disasters, in addition to manmade hazards. As a result, the scientific community has been compelled to investigate the concept of resilience.

In the world, many other types of disasters happened in the last decade. The Indian Ocean earthquake which occurred on December 26th, 2004 with an epicentre off the west coast of Sumatra, in Indonesia was the third-largest earthquake ever recorded on a seismograph with a magnitude M_w between 9.1 and 9.3. The earthquake and the following tsunami (Fig. 1.5) killed 230,000 people in 14 countries, and inundating coastal communities with waves up to 30 m.



Fig. 1.6 An aerial view of the Sendai region with black smoke coming from the Nippon Oil refinery – (source: <http://en.wikipedia.org>)

The Great East Japan earthquake happened off the Pacific coast of Tohoku and was a magnitude 9.0 (Mw) undersea megathrust earthquake off the coast of Japan that occurred at 14:46 JST (05:46 UTC) on Friday 11 March 2011 (Fig. 1.6). The two Earth's tectonic plates collide in what is called a subduction zone, so East of Japan (the Pacific plate) slides beneath the overriding Eurasian plate. The total damages from the earthquake and tsunami are estimated at \$300 billion dollars (about 25 trillion yen), according to the Japanese government, while the number of confirmed deaths is 15,891 as of April 10, 2015. The tsunami caused a cooling system failure at the Fukushima Daiichi Nuclear Power Plant, which resulted in a level-7 nuclear meltdown and release of radioactive materials. The electrical power and backup generators were overwhelmed by the tsunami and the plant lost its cooling capabilities.

1.1.2 Disasters Caused by Human Action (Manmade Disasters)

Manmade disasters are those caused directly or indirectly by human action or inaction. They belong to this category:

- terrorism,
- civil disorders,
- criminality,
- wars,
- industrial and engineering accidents,

- waste disposal,
- fire,
- nuclear explosions/radiation,
- transport accidents,
- power outage,
- etc.

Below are reported some examples of disasters belonging to this category occurring in the last decade.

A key example is the Italian electrical blackout of September 2003 (Bacher et al. 2003). The origin of the blackout was two power lines in Switzerland which had flashed over in an alpine storm, causing the Italian grid to increase its demand and overload other lines that brought power to France, this subsequently caused blackouts across the entire Italian grid as well as failures in Switzerland. Another example is the 2003 Northeast blackout in US, a widespread power outage that occurred throughout parts of the Northeastern and Midwestern United States and the Canadian province of Ontario on Thursday, August 14, 2003 (Fig. 1.7). Power was restored within 7 h, but many others did not get their power back until two days later or even a week after in more remote areas. A software bug in the alarm system at a control room of the First Energy Corporation in Ohio was the blackout's primary cause. A lack of alarm left operators unaware of the need to re-distribute power after overloaded transmission lines hit unpruned foliage, which triggered a race condition in the control software.

This is not the only example of a failure involving the electrical grid. In fact, in 2006 another power outage occurred when a power line across the River Ems in Germany was switched off to allow a cruise ship to pass safely (Fig. 1.8). This outage unintentionally triggered blackouts that spread to France, Italy, Spain and

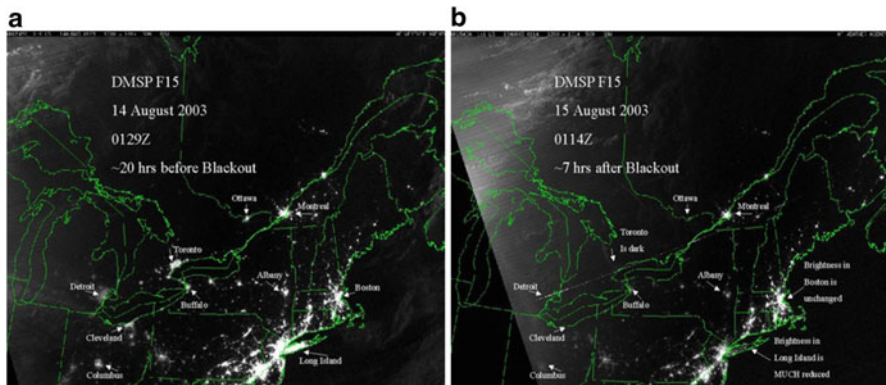


Fig. 1.7 Satellite images of the Northeastern United States blackout of August, 2003 which plunged millions of people into darkness (a) night Lights satellite image before the blackout, (b) night Lights satellite image after the blackout (source: NOAA credited by Air Force Weather Agency)



Fig. 1.8 Norwegian Pearl ship in the Papenburg, Germany, shipyard in November 2006. The ship indirectly caused a two-hour power outage on the evening of November 4, 2006 (source <http://news.nationalgeographic.com>)



Fig. 1.9 Aftermath of the fierce fire that claimed 39 lives in the Mont Blanc tunnel (source <http://www.tunneltalk.com>)

Portugal. Power system elements were also tripped in Austria, Hungary, Croatia, Bosnia, Ukraine, Romania and Morocco (UCTE 2007).

Tunnels are another example of important components of the transportation network. Many of the main cross-border routes in Europe are characterized by critical road and rail tunnels. Tunnels are vulnerable mainly to explosion and fire. Examples of disasters related to this component are the Mont Blanc and Tauern Tunnel fires (UN 2001), Figs. 1.9 and 1.10 and the Channel Tunnel fires of 1996 (Fig. 1.11), 2006 and 2008 (CTSA 1997; RAIB 2007; BEA-TT and RAIB 2010).



Fig. 1.10 The Tauern Tunnel fire. The main site in the rear burned at over 1000°C. A thick coat of foam covers the ground and parts of the roof hanging down against the fiery background (source <http://www.landroverclub.net>)



Fig. 1.11 Damage caused by the 1996 freight shuttle train fire in the Channel Tunnel (source <http://www.tunneltalk.com>)

When the protection of critical infrastructure is considered, *terrorism* remains a major concern. Europol (2012) recorded 316 attacks in the EU in 2009, 249 in 2010 and 174 in 2011 and an increase in the use of improvised explosive devices (IEDs) by terrorists of various affiliations. The components required for the construction of IEDs are easy to obtain, their production requires expertise that is available through open source information, and the chemical precursors can be obtained legally in EU Member States. In October 2011, improvised devices similar to incendiary devices (IIDs) were used in a coordinated attack targeting railway infrastructures in Germany.



Fig. 1.12 Terroristic attacks in rail transport system in Europe. (a) Madrid, 2004 (source <http://www.telegraph.co.uk>), (b) London, 2005 (source <http://www.dailymail.co.uk>)

Railway infrastructures and their occupants have been the target of terrorist attacks in major cities such as London and Madrid. Three days before the Spanish election, during the peak of Madrid morning rush hour on Thursday March 11th, 2004, ten explosions occurred on board of four commuter trains (Fig. 1.12a). All the target trains were traveling between Alcalá de Henares and the Atocha station in Madrid in the same direction.

There were three bombs which exploded in the Atocha station, two bombs in different carriages in the El Pozo del Tío Raimundo Station, one other explosion occurred in the Santa Eugenia Station and the last one exploded in different coaches of the train—approximately 800 m from Atocha Station. The explosions killed 191 people and wounded 1.800. One year after Madrid's attacks, on July 7th, 2005, a series of coordinated suicide attacks in central London were conducted by four terrorists (Fig. 1.12b). The attacks targeted civilians using the public transport system during the morning rush hour. Two attacks were conducted on Circle line sub-surface trains, while the third one targeted a Piccadilly line deep-level underground train traveling southbound from King's Cross-St. Pancras and Russell Square, and also damaged the surrounding tunnel. A final bomb was detonated on the top deck of a double-decker bus, 1 h after the first attack. Naturally these incidents caused serious disruptions in the rail transport system of both cities, and it took several days to regain full capacity.

Recently in France on November 13, 2015, a series of coordinated terrorist attacks occurred in Paris and Saint-Denis (Fig. 1.13). Three suicide bombers struck near the Stade de France in Saint-Denis, followed by suicide bombings and mass shootings at cafés, restaurant and a music venue. 130 people were killed (89 only at the Bataclan theatre), while 368 people were injured. Seven of the attackers died. This has been the deadliest attack in the European Union since the Madrid train bombing in 2004. The Islamic State of Iraq and the Levant (ISIL) claimed the attacks, saying it was in retaliation for the French airstrikes on ISIL targets in Syria and Iraq.



Fig. 1.13 Paris Shootings – The day after (Maya-Anais Yataghene [CC BY 2.0 <http://creativecommons.org/licenses/by/2.0>]) (via Wikimedia)



Fig. 1.14 Police officers, emergency vehicles, and journalists at the scene 2h after the shooting (“Charlie-Hebdo-2015-11” by Thierry Caro / Jérémie Hartmann – Own work. Licensed under CC BY-SA 4.0 via Commons – <https://commons.wikimedia.org/wiki/File:Charlie-Hebdo-2015-11.JPG/media/File:Charlie-Hebdo-2015-11.JPG>)

These attacks were anticipated by the Charlie Hebdo shooting on January 7, 2015 when two brothers, Saïd and Chérif Kouachi, forced their way into the offices of the French satirical weekly newspaper Charlie Hebdo in Paris. Armed with assault rifles, submachine guns and grenades, they killed 12 people and injured 11 others in the building (Fig. 1.14). Charlie Hebdo had attracted attention for its controversial depictions of Mohammed. Hatred for Charlie Hebdo’s cartoons, which made jokes about Islamic leaders as well as Mohammed, is considered to be the principal motive for the massacre.

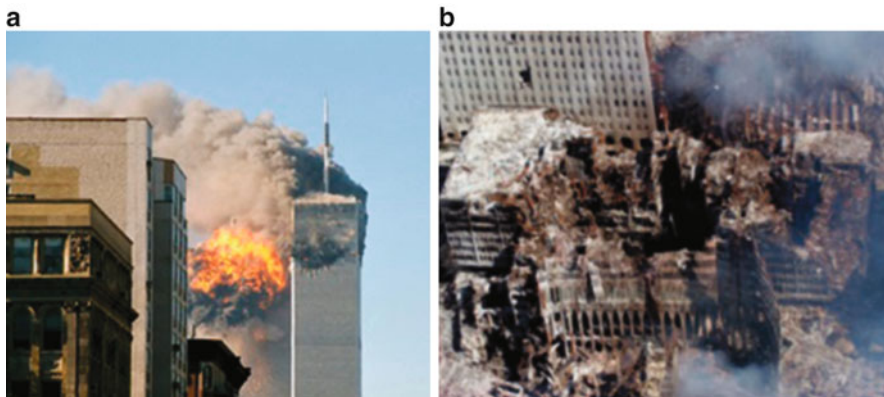


Fig. 1.15 The World Trade Center attack: (a) 9th September 2001, Flight 175 crashes into 2 WTC (source: <http://en.wikipedia.org>); (b) the remains of 6 World Trade Center, 7 World Trade Center, and 1 World Trade Center on September 17, 2001 (source <http://en.wikipedia.org>)

Outside of Europe, the most known terrorist attack happened in USA on September 11, 2001, when three large passenger aircrafts flew into the World Trade Center buildings and the Pentagon (Fig. 1.15). The fires following the impact caused the collapse of both the WTC 1 and WTC 2 buildings in less than 1.5 h. Once the buildings collapsed, the fire spread to the WTC 7 building where the emergency Operations Centre was located (Kendra and Wachtendorf 2003). The collapse of WTC buildings led to major damage of the surrounding buildings and the loss of power, communication and water in lower Manhattan as well as the interruption of financial markets. The loss of life by occupants and responders, and the damages to the surrounding buildings and infrastructure systems raised concern about how the destruction of a building can affect the entire built community around it NIST (2008).

Another example in US is the Boston marathon terrorist attack which occurred on April 15th, 2013. The bombs exploded 12 s and 190 m apart near the marathon finish line, killing 3 people and injured 264 who were treated in 27 local hospitals. The terrorists were two Chechen brothers: Dzhokhar Tsarnaev and Tamerlan Tsarnaev, which motivated by extremist Islamist beliefs and the wars in Iraq and Afghanistan. Units from Boston EMS, the Boston Police Department, and the Boston Fire Department were dispatched to assist emergency responders already on-scene (rescue workers and medical personnel) to assist runners and bystanders (Fig. 1.16).

The aftermath of these tragic events and the natural realization by researchers of the importance of considering resilience in their analyses, caused the shift in attention from vulnerability and risk assessment to new design and evaluation approaches based on resilience assessment, which involve many different disciplines: economics, political science, engineering, environmental planning, social science, etc. The evolution towards resilience thinking is far from trivial. “Resilience as a concept is more dynamic, it is non-linear and cross-linked, complex because it



Fig. 1.16 The area of the first blast a few minutes after the explosion

considers many factors and embraces uncertainty” (Stumpff 2013). Current work in the field of resilience is the product of theoretical and practical constructs that have seen refining and reshaping of the disaster paradigm over the past three decades. This has led to multiple definitions and the need for new terminology and/or metrics that will be harmonized. For this reason, various definitions are presented and discussed in the next section in order to establish the basic familiarity needed to develop further research in the field of critical infrastructure resilience.

1.2 Milestones for Preparedness Throughout History

The concepts of resilience and emergency response are not new or unique to recent history; they have actually been commonly practiced for human and organizational life around the world dating back to ancient times. Humans have been subjected to the adverse effects of disasters since the dawn of their existence and attempted to minimize their hazard vulnerability and exposure. Regardless of the actions that were taken, they have all had a similar purpose – to manage emergencies. Below is a list of some of the first examples of emergency authorities in the world, progressing to the recent ones.

- During the ancient Persian Achaemenid Empire (559–300BC), strategic, public and emergency management were well organized and efficient. They had already developed an alert system against flooding, disaster management programs following earthquakes and other types of disasters (e.g. robust shelters against extreme weather conditions were available at that time).

- Amenemhet III was a pharaoh of the Twelfth Dynasty of Egypt (ruled from c.1860 BC to c.1814 BC). He created a substantial river control project using a system of over 200 water wheels that diverted Nile floodwaters and allowed significant land reclamation.
- In AD 79, when the volcano Vesuvius began erupting, two towns in its shadow, Herculaneum and Pompeii, faced an impending catastrophe. Herculaneum, which was at the foot of the volcano and therefore directly in the path of its lava flow, was buried almost immediately. Conversely, the majority of Pompeii's population survived because the citizens of Pompeii had several hours before the volcano covered their city in ash, and the city's leaders organized a mass evacuation.
- St. Florian lived in the time of the Roman emperors Diocletian and Maximian. He was the commander of the imperial army in the Roman province of Noricum. In addition to his military duties, he was also responsible for organizing firefighting brigades in AD 303. He organized and trained an elite group of soldiers whose sole duty was to fight fires.
- Several Medieval cities were often set on fire during wars and natural disasters. For this reason, in 1254 AD by royal decree, King Saint Louis II of France created the *guet bourgeois* ("burgess watch"), an organization of private citizens who patrolled the streets in order to prevent crimes and fires.
- The Inca Empire was the largest empire in pre-Columbian America, expanding throughout the Andes Mountains in South America (during the thirteenth to fifteenth centuries). They built their cities on the peaks of rugged, though easily defensible, mountains, in order to prevent hostile attacks. In doing so, they placed themselves in a zone of high natural hazard risk (from landslides), which they maintained through land terracing.
- Kaifeng is the region located on the south bank of the Yellow River in China prone to devastating floods throughout its history. After the 1642 Yellow River flood caused about 300,000 life losses, Kangxi Emperor made the city as a rural backwater city of much less importance. They moved the people and thus they decreased the vulnerability against future floods.
- London suffered a devastating fire in 1666 which caused damages in area of about two square miles of the city. Before that, the city had no fire protection network. Subsequent to this event, private firefighting units were established by the insurance companies to extinguish fires in their clients' property.
- After the fire of 1802 in New Hampshire, the U.S. Congress provided financial assistance to the city to rebuild it. This is one of the first examples of U.S. government investment in the emergency management and recovery functions.
- Nagoya city in Japan suffered severe damages after the 1891 Nobi earthquake of magnitude 8. Afterwards, an Earthquake Disaster Prevention Investigation Council was formed in 1892 by the Japan government to focus on the earthquake disasters and to develop damage mitigation plans.
- The Flood Control Act of 1934 in the United States is one of the significant steps toward emergency management in this country and reflects the belief that natural disasters could be controlled by humans. After this act, design and

construction of flood control systems were investigated more by the U.S. Army Corps of Engineers to eliminate the risk of floods.

- In response to the damaging consequences brought about by major disastrous events, individuals and societies have attempted to minimize their hazard vulnerability by developing mitigation plans. This effort resulted in a number of guidance documents and tools to use for assessing hazards and for developing approaches to reduce or eliminate those vulnerabilities. For example the United States Federal Emergency Management Agency (FEMA), which grew out of the Federal Civil Defense Act of 1950, has produced a series of frameworks to address the spectrum of prevention, protection, mitigation, response, and recovery. Canadas Office of Critical Infrastructure Preparedness and Emergency Preparedness (OCIEPP), and Great Britains disaster management agency are the other efforts which form the basis for modern disaster and emergency management. On October 23rd, 2001 the EU Council established the Community Mechanism for Emergency authority, which is a tool to enhance community cooperation in civil protection matters. A recast of this Council Decision was adopted on November 8th, 2007.

This list of early milestones of *Preparedness* and *Resilience* all over the world show that these are key concepts and have recently been spreading within the engineering community.

The following sections of this chapter provide general information on the state-of-practice in resilience-based design (RBD) and current frameworks available. Then is illustrated the transition from performance-based design (PBD) towards resilience-based design (RBD). The main aspects of the resilience-based design framework that might prove useful in the development of resilience-based guidelines are identified.

1.3 What Is Disaster Resilience?

Latest disasters all over the world have shown clearly that not all threats can be averted. The natural and manmade disasters over the past years with which the human society had to cope with had stressed the necessity to be prepared and to be able to recover in a short time from a sudden and unexpected change in the communities technical, organizational, social and economical condition. The concepts of “risk reduction”, “vulnerability”, “recovery”, and “resilience” have become keywords when dealing with hazardous events. Modern societies as States are trying to enhance their resilience against extreme events of any kind, after realizing that they cannot prevent every risk from being realized, but rather they must manage risks and adapt by minimizing the impact on human beings and other systems. When a disaster strikes, the community affected requires immediate help to survive, resources, and efforts to recover in a short time. In other words, the community needs to be “prepared” and less “vulnerable”, in order to achieve a high “resilience”.

Resilience, according to the dictionary, means “the ability to recover from (or to resist being affected by) some shock, insult or disturbance”. Resilience in general is defined as the ability of systems to rebound after severe disturbances, or disasters. The concept of resilience has several definitions, because of its broad utilization in ecology, social and political sciences, economy, and engineering fields with different meanings and implications.

In earlier work by the authors, resilience was defined including technical, organizational, social and economic aspects (Bruneau and Reinhorn 2004). Various attempts have been made to provide a comprehensive definition, but recent literature review collected by Manyena (2006) points out that the current definition is too vague to be useful in the field of disaster risk reduction. In his research, Manyena reviews the concept of resilience in terms of definitional issues, its relationship with the concept of vulnerability, its application in the field of disaster management and risk deduction. Manyena (2006) evaluating all the possible definitions provided from the 90 to nowadays, suggests that Resilience could be viewed as the “intrinsic capacity of a system, community or society predisposed to a shock or stress to adapt and survive by changing its non-essential attributes and rebuilding itself”. As regards its relationship with the concept of vulnerability, it can be accepted that the latter is closely associated to the level of resilience, but it is a complementary aspect of the community preparedness.

As Klein et al. (2003), the term derives from the Latin word “*resilio*” that means “to jump back”. The field in which the term was first used is in psychology and psychiatry in the 1940s, and it is mainly accredited to Norman Garmezy, Emmy Werner and Ruth Smith.

In physics and engineering, the term resilience describes the property of a material to absorb energy when it is elastically deformed and then, when unloaded, to recover energy. Later, the concept of resilience was established in the field of ecology by Holling (1973), who stated that the resilience of an ecological system is “a measure of the persistence of systems and of their ability to absorb change and disturbance and still maintain the same relationships between populations or state variables. Stability represents the ability of a system to return to an equilibrium state after a temporary disturbance; the more rapidly it returns to equilibrium and the less it fluctuates, the more stable it would be”.

The researchers in resilience have continued to study it deeper and in a wider way. An extended literature review has elaborated upon resilience for years (Table 1.1), each contribution has added new nuances. Primarily, resilience has been defined in the context of the speed of systems going towards equilibrium (Adger 2000), capability to cope and bounce back, ability to adapt to new situations (Comfort 1999), to be inherently strong and flexible and adaptive (Tierney and Bruneau 2007), and to withstand external impacts and recover with least outside interferences (Mileti 1999). After the original definition of resilience in ecological systems, the word’s meaning was expanded to *engineering*, *social*, and *economical* fields.

In the engineering field, resilience is defined as the capability of a system to maintain its functionality and to degrade gracefully in the face of internal and external changes (Allenby and Fink 2005). The main difference in defining

Table 1.1 Literature review about resilience definitions

Author	Definition
Holling (1973)	Ecological systems resilience is a measure of the persistence of systems and of their ability to absorb change and disturbance and still maintain the same relationships between populations or state variables
Wildavsky (1991)	Resilience is the capacity to cope with unanticipated dangers after they have become manifest, learning to bounce back
Horne and Orr (1998)	Resilience is the ability of a system to withstand stresses of environmental loading... [it is] a fundamental quality found in individuals, groups, organizations, and systems as a whole
Haimes (1998)	Resilience is the ability of system to return to its optimal condition in a short period of time. Considering resilience one of four strategies for hardening a system, together with security, redundancy and robustness
Mileti (1999)	Local resiliency with regard to disasters means that a locale is able to withstand an extreme natural event without suffering devastating losses, damage, diminished productivity, or quality of life and without a large amount of assistance from outside the community
Comfort (1999)	Resilience is the capacity to adapt existing resources and skills to new situations and operating conditions
Adger (2000)	Social resilience is the ability of groups or communities to cope with external stresses and disturbances as a result of social, political, and environmental change
Gunderson et al. (2002)	Engineering resilience is the speed of return to the steady state following a perturbation ecological resilience is measured by the magnitude of disturbance that can be absorbed before the system is restructured
Fiksel (2003)	Resilience is the essence of sustainability the ability to resist disorder
Bruneau et al. (2003)	Resilience is defined in terms of three stages: the ability of a system to reduce the probability of an adverse event, to absorb the shock if the adverse event occurs, and to quickly re-establish normal operating conditions. So resilience thus encompasses the four characteristics of robustness, redundancy, resourcefulness, and rapidity. Are considered four types of resilience: technical; organizational; economic; and social
Allenby and Fink (2005)	Resiliency is defined as the capability of a system to maintain its functions and structure in the face of internal and external change and to degrade gracefully when it must
Rose and Liao (2005)	Regional economic resilience is the inherent ability and adaptive response that enables firms and regions to avoid maximum potential losses
Hollnagel (2006)	Resilience is defined as the intrinsic ability of an organization (system) to maintain or regain a dynamically stable state, which allows it to continue operations after a major mishap and/or in the presence of a continuous stress
Manyena (2006)	Evaluating all the possible definitions provided from the 1990s to nowadays, resilience could be viewed as the intrinsic capacity of a system, community or society predisposed to a shock or stress to adapt and survive by changing its non essential attributes and rebuilding itself

(continued)

Table 1.1 (continued)

Author	Definition
Woods (2006)	Resilience is defined as the ability of systems to anticipate and adapt to the potential for surprise and failure
Holmgren (2007)	Resilience is the ability of the system to return to a stable condition after a disruption. Distinguishing robustness and resilience, using robustness to imply that the system will remain (nearly) unchanged even in the face of disruption
Tierney and Bruneau (2007)	Resilience is both the inherent strength and ability to be flexible and adaptable after environmental shocks and disruptive events
DHS-RSC (2008)	Resilience is the ability of systems, infrastructures, government, business, and citizenry to resist, absorb, recover from, or adapt to an adverse occurrence that may cause harm, destruction, or loss of national significance
Haines (2009)	Resilience is defined as the ability of the system to withstand a major disruption within acceptable degradation parameters and to recover within an acceptable time and composite costs and risk
Vugrin et al. (2010)	Given the occurrence of a particular disruptive event (or set of events), the resilience of a system to that event (or events) is the ability to efficiently reduce both the magnitude and duration of the deviation from targeted system performance levels

resilience arises between the engineering approach where resilience occurs by moving towards the previous stable state (Bruneau et al. 2003), and the ecological approach where resilience is achieved moving towards a different system state (Handmer and Dovers 1996).

Social resilience is the ability of groups or societies to cope with external stresses and disturbances as a result of social, political, and environmental change (Adger 2000). Economic resilience is the inherent ability and adaptive response that enables firms and regions to avoid maximum potential losses (Rose and Liao 2005). It has mainly been studied in the context of seismic response and recovery (Tierney 1997), community behavior (Chang and Shinozuka 2004) and disaster hazard analysis (Rose 2004).

The outcomes of the 2005 World Conference on Disaster Reduction (WCDR) confirmed the importance of the entrance of the term resilience into disaster discourse and gave birth to a new culture of disaster response. Among the experts in disasters, however, the definitions of resilience are various and sometimes contrasting. Resilience can be considered as a desired outcome or, in a broader way, as a process leading to a desired outcome. Reducing resilience to an outcome does not take into account the performance of the process itself, or the effort to reach a certain result.

The definition of the resilience for the NIST framework (National Institute of Standards and Technology) is contained in Presidential Policy Directive 21 (PPD 2013) and “withstand and recover rapidly from disruption” (PPD 2013). The first phrase “the ability to prepare for and adapt to changing conditions” according to the NIST disaster resilience framework (2015) refers to “preparing for conditions that are likely to occur within the lifetime of a facility or infrastructure system, such as a hazard event, and hazard intensities or physical conditions that may change over time. Changing conditions include the effects of aging infrastructure systems and climate change, such as sea level rise in coastal areas. Changing conditions also include changes in our use of infrastructure systems”. The second part “withstand and recovers rapidly from disruptions must be examined for the anticipated range of possible hazard event. In a resilient community, a hazard event at the design level should cause only local disruptions that the community can tolerate without long term detrimental effects. If an unanticipated or extreme event occurs, the resilience planning and preparation should reduce the extent of disruption and recovery time. Additionally, communities that have a well-developed resilience plan are prepared to recover in a way that improves sustainability and resilience”. As related to the built environment, resilience means “the ability of identified buildings and infrastructure systems to return to full occupancy and function, as soon as they are needed, to support a well-planned and expedited recovery”. Under this definition resilience includes “activities already conducted by some communities, such as disaster preparedness, hazard mitigation, code adoption and enforcement, and emergency response” (NIST 2015).

On the other hand, *disaster resilience* can be viewed as a deliberate process (leading to desired outcomes), which is comprised of a series of events, actions, or changes to augment the capacity of the affected community, places emphasis on the human role in disasters. Disaster resilience is considered a quality, characteristic, or result that is generated or developed by the processes that foster or promote it.

1.4 State of Art of Existing Resilience Frameworks

Several frameworks are currently available in literature and a compact comparison of them is given in Fig. 1.17 in term of features and applicability. The frameworks were evaluated on the basis of five broad categories, including: comprehensiveness, utility, impacts assessed, techniques used, and overall merit (with respect to the maturity, innovativeness, objectivity, and scientific merit). The criteria were assessed in the context of community resilience planning and assessment, particularly concerning the built environment. Below is given a brief description of existing framework which are grouped according to the spatial dimension in *City*, *State* and *National* level.

Group	Category	Sub-category	Existing Assessment Methodologies										Symbol	Description				
			SPUR	Oregon Res. Plan (ORP)	UNISDR Scorecard	CARRI CRS	CART	BRIC	Rockefeller CFR & CRI	NOAA CRI	FEMA Hazus	PEOPLES						
1	Comprehensiveness	Community size	●	●	+	+	+	+	+	+	+	+	+	+	+	Addresses a broad range		
		Hazards	●	●	+	+	+	+	+	+	+	+	+	+	+	●	Focused subset, but not inherently limited	
		Recovery time scales	+	+	?	?	?	?	?	?	?	?	?	?	?	-	Limitation	
		Systems Interdependencies	●	●	?	+	-	-	+	+	+	+	+	+	+	?	Additional information required	
2	Utility	User friendliness	●	●	+	+	+	+	+	+	+	+	+	+	+	+	High	
		Utility without hired or volunteer SMEs	-	-	+	●	?	?	?	?	?	?	?	?	?	?	Moderate	
		Value of outputs for resilience planning	+	+	●	?	?	?	?	?	?	?	?	?	?	?	-	Low
		Consistency with PPD-21	+	+	●	+	+	+	+	+	+	+	+	+	+	?	Additional information required	
3	Impacts assessed	Physical impacts and recovery times	+	+	●	●	●	●	●	●	●	●	●	●	●	●	Explicitly assessed	
		Economic impacts and recovery times	●	+	●	●	●	●	●	●	●	●	●	●	●	●	Partially or indirectly assessed	
		Social impacts and recovery times	●	●	●	●	●	●	●	●	●	●	●	●	●	●	-	Not assessed
																?	Additional information required	
4	Techniques used	Checklists	-	-	+	+	+	+	+	+	+	+	+	+	+	+	Yes	
		Interviews, Surveys	+	+	-	●	+	+	+	+	+	+	+	+	+	+	Optional	
		Ratings	+	+	+	+	+	+	+	+	+	+	+	+	+	+	●	No
		Existing national data sets	-	-	-	-	-	-	-	-	-	-	-	-	-	-	?	Additional information required
5	Critical Assessment	Physical inspections	+	+	●	●	●	●	●	●	●	●	●	●	●	●	Strength	
		Engineering analysis or expert opinion	+	+	●	●	●	●	●	●	●	●	●	●	●	●	Neither a strength nor a weakness	
		Statistical inference	●	●	●	●	●	●	●	●	●	●	●	●	●	●	Weakness	
		Simulations	●	●	●	●	●	●	●	●	●	●	●	●	●	●	?	Additional information required
5	Critical Assessment	Maturity	+	+	●	+	-	+	+	+	+	+	+	+	?	Strength		
		Unique/innovative	+	+	●	+	+	+	+	+	+	+	+	+	+	+	Neither a strength nor a weakness	
		Objective/repeatable	+	+	●	●	●	●	●	●	●	●	●	●	●	+	Weakness	
		Scientific merit	+	+	+	?	?	?	?	?	?	?	?	?	?	?	?	Additional information required

Fig. 1.17 Evaluation matrix of ten different resilience frameworks (Adapted from NIST 2015)

1.4.1 City Level Resilience Framework

NIST framework (National Institute of Standards and Technology, 2015)

Among the most recent ongoing projects which need to be mentioned is the NIST (National Institute of Standards and Technology) Community Resilience Program NIST (2015) which aims to evaluate the existing resilience frameworks on the basis of a comprehensive list of community parameters. The program aims to develop a new framework, which will assemble the potentialities of all available methods and assimilate new concepts surrounding resilience that have been explored in the latest research. In particular, NIST gives a summary of available guidance, metrics, and tools for the assessment of community resilience under a variety of natural and manmade hazards with considering the different levels of hazard intensity or magnitude for each. Furthermore, it presents three types of metrics that can be used by a community to measure improvements through the understanding and implementation of proactive planning: (i) *recovery times* for the restoration of function of building and infrastructure systems, (ii) *economic metrics* to represent business, tax base, income, local services and amenities as well as sustained growth, and finally (iii) *social metrics* representing survival, safety and security, sense of belonging, and growth and achievement to reflect the hierarchy of human needs (Maslow's Hierarchy of Needs, 1943).

Despite of comprehensiveness in concepts, the NIST does not provide a systematic and theoretical framework to evaluate resilience, but it provides a sort of guidelines of what a framework should look like. However several parts of these guidelines are not fully developed and there is no a specified description on how to apply these concepts in practice and to assess the performance of critical infrastructures and their interdependencies for example. Although this framework is not limited inherently, it is developed specifically for communities within the United States and it cannot be considered as an international guideline.

San Francisco Planning and Research Association (SPUR) Framework

Among the frameworks at the city level, it is necessary to mention the San Francisco Planning and Research Association (SPUR) Framework.

The SPUR framework aims to make San Francisco become a Disaster Resilient City through seismic mitigation policies. The policy recommendations and mitigation plans are focused on community demands before, during and after responding to hazard events. In general the stated goals of the SPUR report (2009) are summarized as:

- Define resilience concept in the context of disaster planning;
- Establish performance goals for the “expected” earthquake that supports the concepts of resilience;
- Development of real performance tools that help to reach the specified performance goals;
- Suggest next steps for San Francisco's new buildings, existing buildings and lifelines.

The SPUR methodology concentrates on defining performance goals for several clusters of buildings (i.e., groups of buildings that provide a community service, such as critical response facilities, emergency housing, or neighborhood services) and defining target recovery time for a specified earthquake scenario in the San Francisco Bay area. SPUR does not directly address both the economic and social dimensions of resilience for the city of San Francisco. Whilst the economic and social impacts and the consequences effects in the estimation of the recovery time are the key questions for community leaders, stakeholders, investors, or governments, this methodology does not provide a direct performance metrics to quantify them. On the other hand SPUR focuses on earthquakes as the primary hazard in San Francisco and it does not provide a comprehensive methodology that can also be used against other natural or manmade hazard events. In addition, SPUR restricts the size of the community to the city of San Francisco and therefore its framework can not be applied or extended to any other community.

UNISDR Disaster Resilience Scorecard for Cities The United Nations International Strategy for Disaster Risk Reduction (UNISDR) Disaster Resilience Scorecard for Cities “provides a set of assessments that will allow cities to understand how resilient they are to natural disasters.” The Scorecard is “intended to enable cities to establish a baseline measurement of their current level of disaster resilience, to identify priorities for investment and action, and to track their progress in improving their disaster resilience over time.” This framework catalogues different evaluation criteria in research, organization, infrastructure, response capability, environment and recovery. Each evaluation criterion is broken down according to the measured resilience dimension, the measurement scale and evaluated through a formal checklist. The tool does not offer a theoretical framework which clearly explains how to apply these methods in practice. Additional information is needed to evaluate the performance of critical infrastructures and their interdependencies. Furthermore there is not any specific approach and metric tool to assess the recovery times considering all community dimension such as economical and social parameters.

1.4.2 State Level Resilience Framework

Oregon Resilience Plan The Oregon Seismic Safety Policy Advisory Commission (OSSPAC) was managed by House Resolution 3 in 2011 in order “to lead and coordinate preparation of an Oregon Resilience Plan that reviews policy options, summarizes relevant reports and studies by state agencies, and makes recommendations on policy direction to protect lives and keep commerce flowing during and after a Cascadia earthquake and tsunami.” The Oregon Resilience Plan (2013) was built upon the SPUR methodology and the Resilient Washington State initiative in order to produce a statewide projection of the impacts of a single earthquake and tsunami scenario. Immediate impacts include lives losses, buildings destroyed or damaged, and households displaced.

A particular statewide vulnerability identified during the study was the Oregon's liquid fuel supply and the resulting cascade effects induced by a long-term disruption of the liquid fuel supply.

The OSSPAC has suggested eight task groups:

1. earthquake and tsunami scenario,
2. business and work force continuity,
3. coastal communities,
4. critical buildings,
5. transportation,
6. energy,
7. information and communications,
8. water and wastewater.

The framework determines the likely impacts of magnitude 9.0 Cascadia earthquake and tsunami and proposes a method to estimate the recovery time after such a hazard event. It also describes an acceptable time frame for each critical infrastructure classification to fulfill the expected resilience performance. When analyzing in detail, the Oregon resilience plan does not offer a unique and novel approach to make communities resilient, but it follows mostly SPUR methodology. In fact, Oregon resilience plan when compared with the SPUR framework provides a methodology to evaluate the economic dimension of resilience while the performance metrics to quantify the social aspects after hazard events are still missing. In addition there is not any specific tool or indicator to assess the resilience of a community against the manmade hazard events such as the terrorist attacks etc.

1.4.3 National Level Resilience Framework

FEMA Hazus Methodology The Federal Emergency Management Agency's (FEMA) Hazus methodology (Hazus 2014) "is a nationally applicable standardized methodology that contains models for estimating potential losses due to earthquakes, floods and hurricanes. Hazus uses Geographic Information Systems (GIS) technology to estimate physical, economic and social impacts of disasters. It graphically illustrates the limits of identified high-risk locations due to earthquakes, hurricanes and floods. Users can visualize the spatial relationships between populations and other fixed geographic assets or resources for the specific hazard being modeled – a crucial function in the pre-disaster planning process."

The Hazus methodology and data sets cover the entire United States, and the study region (i.e., community) can be defined as any combination of the US Census tracts. The framework considers immediate physical, economic and social impacts and leads to outputs on expected damage losses of different infrastructures. Estimated repair time is explicitly considered in economic loss estimates produced by the model, but the economic outputs are not tabulated or viewable as a function of time.

There are limitations in the framework that will not allow to apply the software to evaluate resilience indicators. First, all the performances are indicated or normalized to economic costs. Second, Hazus can be used to assess the losses that can be avoided through mitigation measures, but it does not estimate the mitigation costs and therefore does not estimate the return on investments. Third, all the losses are considered independent each other and therefore the cascading effects and all interdependencies following a hazard event are neglected in the framework. Finally, Hazus is a hazard specific framework that covers only three types of hazard, and although it has been tried to be extended to other nations as well, it is made to be applied in USA.

PEOPLES framework The PEOPLES framework has been developed at MCEER in 2009 and it was the result of a 1 year project sponsored by NIST (Cimellaro et al. 2016). According to the summary given in Fig. 6.1, the PEOPLES framework is not hazard specific and it is multidimensional, so it can be applied to different spatial (City, State and National level) and temporal dimensions, while taking into account interdependencies between different components. However some improvements should be envisioned in the techniques used to enhance its ability to evaluate the community resilience index. More detail about the PEOPLES framework are provided in Chap. 6.

1.5 From Performance-Based Design to Resilience-Based Design

1.5.1 PEER Performance Assessment Methodology

In the last decades, researchers at the Pacific Earthquake Engineering Research (PEER) Center have developed a seismic performance assessment methodology based on an equation framework, which incorporates various sources of uncertainty using the concepts of conditional probability and total probability theorem. Nowadays, seismic standards provide a set of prescriptive rules with the goal of human safety. Recent research suggests quantifying structural performance in more useful terms to simplify stakeholders' decisions. Therefore, PEER has suggested that *economic losses (dollars)*, *downtime*, and *number of fatalities (deaths)* are the indicators that should be used to evaluate building performances and they have developed a probabilistic framework that uses the results from seismic hazard analysis and response simulations to estimate damages and monetary losses incurred during earthquakes. The above-mentioned methodology is divided into four steps:

- The first step uses probabilistic seismic hazard analysis to generate a seismic hazard curve, which quantifies the frequency of exceeding a ground motion intensity measure (IM) for the site being considered.

- The second step involves using structural response analysis to compute engineering demand parameters (EDPs), and the collapse capacity of the structure being considered.
- The third step produces damage measures (DMs) using fragility functions, which are cumulative distribution functions relating EDPs to the probability of being or exceeding particular levels of damage.
- The fourth and final step determines decision variables (DVs), such as the economic losses, based on repair and replacement costs of damaged building components, which can be used by stakeholders to make more informed design decisions.

1.5.2 History of the Development of the PEER Integral

Initially, it was proposed that the following three sources of uncertainty should be considered for a probabilistic estimation of DVs:

- Uncertainty corresponding to the ground motion intensity,
- Uncertainty corresponding to the structural response,
- Uncertainty corresponding to the decision variable.

These kinds of uncertainties were taken into account in the PEER model by defining a random variable associated with that source of uncertainty. The uncertainty in estimating the seismic hazard at the site has been modeled by considering a ground motion intensity measure (IM, e.g. PGA, PGV, I, $S_a(T)$) as a random variable and estimating the mean annual frequency of exceedance of the seismic hazard at the site, $\nu(IM > im)$, by performing a Probabilistic Seismic Hazard Analysis (PSHA). The uncertainty in estimating the intensity of the structural response is incorporated by considering a vector of engineering demand parameters (EDP's) and estimating the conditional probability of the engineering demand parameter exceeding a certain intensity, edp , at different levels of ground motion intensity, $P(EDP > edp | IM = im)$. The uncertainty in estimating decision variables, DV's, is incorporated using the conditional probabilities of exceeding a certain level of dv at a level of edp , $P(DV > dv | EDP = edp)$. The original first version of the PEER framing equation was introduced to estimate the mean annual frequency of exceedance of a decision variable, $\nu(DV > dv)$, as follows (Cornell and Krawinkler 2000):

$$\nu_{DV}(DV > dv) = \iint P(DV > dv | DM = dm).dP \\ (DM > dm | EDP = edp).dv(IM > im) | \quad (1.1)$$

In a second version, it was proposed that a more realistic estimation of the decision variable can be achieved by estimating the decision variable as a function

of the level of damage experienced in the facility instead of estimating the decision variable as a function of the level of deformation.

A new random variable, which corresponds to the level of damage that can be experienced in a facility, was introduced into the PEER framework and in PEER's terminology has been called damage measure, DM. Consequently, the PEER framework Eq. (1.1), has been modified as follows (Krawinkler and Miranda 2004):

$$v_{DV}(DV > dv) = \iiint P(DV > dv | DM = dm) dP(DM > dm | EDP = edp) \cdot dP(EDP > edp | IM = im) \cdot dv(IM > im) \quad (1.2)$$

where P is the probability of exceedance of the decision variable, DV, conditioned to as DM, and $P(DM > dm | EDP > edp)$ is the probability of a damage state, DM, exceeding dm , when the engineering demand parameter, EDP, is equal to edp . For certain measures of seismic performance such as economic losses in individual building components, it is more appropriate to assume that damage measures are discrete. Therefore, it was proposed that economic losses in individual components are computed from the need to apply discrete repair and replacement actions that is triggered at discrete damage states (Miranda and Aslani 2003; Krawinkler and Miranda 2004).

1.6 Towards Resilience-Based Design (RBD)

Although the above described methodology is rapidly spreading, there are fundamental parts that the Performance based design (PBD) does not cover. This method can be applied to describe of a single building or structure, while does not provide an assessment of both the portfolio and community. Today, designer and engineers approach a structure as if it stands alone, without considering the interaction with the community. The performance of an individual structure is not governed by its own performance, but it interacts heavily with the performance of other entities within the same community.

Hospitals are clear examples of these interdependencies between the building and the community. Despite recent codes are considering more stringent criteria in design of this occupancy (e.g. occupancy category III, per ICC IBC, 2012), there are hospitals which are not able to remain functional without electricity and water even if the structure has no structural damage. Another example of the limitations of PBD is given by 2009 L'Aquila earthquake (Cimellaro et al. 2010), during which the small town of Castelnuovo was completely destroyed, except a single housing unit that was standing after the earthquake and suffered minor damage. According to the PBD the building was ok, because there were no damage to the structure, but from the resilience point of view the building was not functional, because the entire city

around the building was destroyed and abandoned. Resilience based design (RBD) is a new fundamental way of looking at the problem, because interdependencies exist between the analyzed system and other structural and infrastructural systems. In this methodology, the building is not considered alone, but as a group of buildings using the “Portfolio Approach” which will allow regional loss analysis. So it will be moved from the concept of “housing units” to the concept of “housing block”. More details on RBD are provided in Chap. 2.

1.7 Summary and Remarks

Some examples of recent natural and manmade disasters are provided to show the necessity to develop resilient communities. The definition of seismic resilience combines information from technical and organizational fields, from seismology and earthquake engineering to social science and economy. Different frameworks available in literature are described and compared. The Pacific Earthquake Engineering Research (PEER) has established a probabilistic framework to estimate damage and monetary losses incurred during earthquakes which is based on Performance-Based Design. In the evaluation of seismic performance, it's required to introduce Decision Variables, incorporating various sources of uncertainty such as those corresponding to the damage measures, the structural response and the ground motion intensity. However the PBD approach works well for single buildings, while when building blocks or entire communities are considered it is necessary to adopt Resilience-Based Design concepts.

References

- Adger WN (2000) Social and ecological resilience: are they related? *Prog Hum Geogr* 24(3): 347–364
- Allenby B, Fink J (2005) Toward inherently secure and resilient societies. *Science* 309(5737):1034–1036
- Bacher R, Näf U, Renggli M, Bühlmann W, Glavitsch H (2003) Report on the blackout in Italy on 28 september 2003. Report, Swiss Federal Office of Energy
- BEA-TT, RAIB (2010) Technical investigation report concerning the fire on eurotunnel freight shuttle 7412 on 11 september 2008. Technical report, Bureau d'enquêtes sur les Accidents de transport terrestre and Rail Accident Investigation Branch, Paris, France and Derby
- Bruneau M, Reinhorn A (2004) Seismic resilience of communities – conceptualization and operationalization. Performance-Based Seismic design-concepts and Implementations. In: Fajfar P, Krawinkler H (eds) Proceedings of international workshop on performance based seismic-design Bled – Slovenia, June 28–July 1, PEER report 2004/05, University of California, Berkeley, Sept. 2004, pp 161–172
- Bruneau M, Chang S, Eguchi R, Lee G, O'Rourke T, Reinhorn A, Shinozuka M, Tierney K, Wallace W, Winterfelt Dv (2003) A framework to quantitatively assess and enhance the seismic resilience of communities. *Earthq Spectra* 19(4):733–752. doi:[10.1193/1.1623497](https://doi.org/10.1193/1.1623497)

- Caverzan A, Solomos S (2014) Review on resilience in literature and standards for critical built-infrastructure. Report EUR, Scientific and Technical Research series, ISSN 1831-9424, EUR 27065 EN, Joint Research Centre, Institute for the Protection and Security of the Citizen
- Chang S, Shinozuka M (2004) Measuring improvements in the disaster resilience of communities. *Earthq Spectra* 20(3):739–755. doi:[10.1193/1.1775796](https://doi.org/10.1193/1.1775796)
- Cimellaro G, Christovasilis IP, Reinhorn AM, De Stefano A, Kirova T (2010) L'aquila earthquake of april 6, 2009 in italy: rebuilding a resilient city to withstand multiple hazards. Report MCEER Technical Report, MCEER-10-0010, MCEER, State University of New York at Buffalo (SUNY). doi:[1520-295X](https://doi.org/10.1520-295X)
- Cimellaro GP, Renschler C, Reinhorn AM, Arendt L (2016) PEOPLES: a framework for evaluating resilience. *J Struct Eng ASCE*. doi: [http://dx.doi.org/10.1061/\(ASCE\)ST.1943-541X.0001514](http://dx.doi.org/10.1061/(ASCE)ST.1943-541X.0001514)
- Comfort LK (1999) Shared risk: complex systems in seismic response. Pergamon, New York
- Cornell A, Krawinkler H (2000) Progress and challenges in seismic performance assessment. *Peer News* April 2000, 3(2)
- CTSA (1997) Inquiry into the fire on heavy goods vehicle shuttle 7539 on 18 november 1996. Technical report, Channel Tunnel Safety Authority, Department for Transport, London
- DHS-RSC (2008) DHS Risk Lexicon, (Risk Steering Committee). U.S. Department of Homeland Security, Washington, DC
- EEA (2011) Mapping the impacts of natural hazards and technological accidents in europe – an overview of the last decade. Report 13/2010, EEA (European Environment Agency). doi:[10.2800/62638](https://doi.org/10.2800/62638)
- Europol (2012) TE-SAT 2012 - EU terrorism situation and trend report. Europol, P.O. Box 908 50, 2509 LW, The Hague
- Fiksel J (2003) Designing resilient, sustainable systems. *Environ Sci Technol* 37(23):5330–5339
- Gunderson LH, Holling CS, Pritchard J (2002) Resilience of large-scale resource systems. *Resilience and the Behavior of Large-Scale Systems*, Washington, DC
- Haines YY (1998) Risk modeling, assessment, and management. Wiley, New York
- Haines YY (2009) On the definition of resilience in systems. *Risk Anal* 29(4):498–501
- Handmer J, Dovers S (1996) A typology of resilience: rethinking institutions for sustainable development. *Organ Env* 9:482–511
- Hazus (2014) Hazus®-MH MR5 technical manuals and user's manuals. Department of Homeland Security, Federal Emergency Management Agency, Mitigation Division, Washington, DC
- Holling CS (1973) Resilience and stability of ecological systems. *Annu Rev Ecol Syst* 4:1–23
- Hollnagel E (2006) Resilience – the challenge of the unstable. In: Hollnagel E, Wood D, Leveson N (eds) *Resilience engineering: concepts and precepts*. Aldershot, Ashgate/Hampshire, p 397
- Holmgren A (2007) A framework for vulnerability assessment of electric power systems. In: Murray AT, Grubestic TH (eds) *Reliability and vulnerability in critical infrastructure: a quantitative geographic perspective*. Springer, Berlin/Heidelberg
- Horne JF, Orr JE (1998) Assessing behaviors that create resilient organizations. *Employ Relat Today* 24(4):29–39
- Kendra J, Wachtendorf T (2003) Elements of resilience after the world trade center disaster: reconstituting New York city's emergency operations centre. *Disasters* 27(1):37–53
- Klein RJT, Nicholls RJ, Thomalla F (2003) Resilience to natural hazards: how useful is this concept? *Glob Environ Change Pt B: Environ Hazards* 5(1–2):35–45
- Krawinkler H, Miranda E (2004) Performance-based earthquake engineering, vol 1. Taylor and Francis/CRC Press, Boca Raton/Florida, book section 9, pp 9–1 to 9–59
- Manyena SB (2006) The concept of resilience revisited. *Disasters* 30:434. <http://www.ingentaconnect.com/content/bpl/disa/2006/00000030/00000004/art00004><http://dx.doi.org/10.1111/j.0361-3666.2006.00331.x>, [1] doi:[10.1111/j.0361-3666.2006.00331.x](https://doi.org/10.1111/j.0361-3666.2006.00331.x)
- McAllister T (2013) Developing guidelines and standards for disaster resilience of the built environment: a research needs assessment. Report, NIST Technical Note 1795, National Institute of Standards and Technology, U.S. Department of Commerce
- Mileti D (1999) *Disasters by design: a reassessment of natural hazards in the United States* (18 May 1999). Joseph Henry Press, Washington DC

- Miranda E, Aslani H (2003) Peer 2003/03 – probabilistic response assessment for building-specific loss estimation. Report, PEER – Pacific Earthquake Research Center
- NIST (2006) Performance of physical structures in hurricane katrina and hurricane rita: a reconnaissance report. NIST technical note 1476, National Institute of Standards and Technology, 100 Bureau Dr, Gaithersburg, MD 20899
- NIST (2008) World trade center disaster study recommendations. National Institute of Standards and Technology. Technical Report
- NIST (2015) Community resilience planning guide for buildings and infrastructure systems. Special Publication 1190 CODEN: NSPUE2, National Institute of Standards and Technology
- OSSPAC (2013) The Oregon resilience plan: reducing risk and improving recovery for the next Cascadia earthquake and tsunami. Oregon Seismic Safety Policy Advisory Commission, Report to the 77th Legislative Assembly, Salem
- PPD (2013) critical infrastructure security and resilience. Report, Presidential policy directive/ppd 21
- RAIB (2007) Fire on hgv shuttle in the channel tunnel 21 august 2006. Report, Rail Accident Investigation Branch, Department for Transport, Derby
- Rose A (2004) Economic principles, issues, and research priorities in hazard loss estimation. In: Advances in spatial science. Springer, Berlin/Heidelberg, pp 13–36
- Rose A, Liao SY (2005) Modeling regional economic resilience to disasters: a computable general equilibrium analysis of water service disruptions. *J Reg Sci* 45(1):75–112. <GotoISI>://WOS:000226572800004, times Cited: 22
- Stumpp EM (2013) New in town? on resilience and “resilient cities”. *Cities* 32:164–166
- Tierney K (1997) Business impacts of the northridge earthquake. *J Conting Crisis Manag* 5:87–97
- Tierney K, Bruneau M (2007) Conceptualizing and measuring resilience. *TR News* 250:14–17
- UCTE (2007) system disturbance on 4 november 2006. Technical report, Union for the Coordination of the Transmission of Electricity
- UN (2001) Recommendations of the group of experts on safety in road tunnels, final report. Technical report, Economic and Social Council, United Nation, Geneva
- Vugrin ED, Warren DE, Ehlen MA, Camphouse RC (2010) A Framework for assessing the resilience of infrastructure and economic systems. In: Gopalakrishnan K, Peeta S (eds) Sustainable and resilient critical infrastructure systems: simulation, modeling, and intelligent engineering. Springer, Berlin
- Wildavsky AB (1991) Searching for safety. Oxford Transaction Publisher, New Brunswick
- Woods DD (2006) Essential characteristics of resilience. In: Hollnagel E, Woods DD, Leveson NC (eds) Resilience engineering: concepts and precepts. Ashgate, Aldershot

Chapter 2

Resilience-Based Design (RBD)

Abstract This chapter introduces the concepts of Resilience-Based Design (RBD) as an extension of Performance-Based Design (PBD) starting from the MCEER definition of Resilience. The four attributes of resilience are introduced: Rapidity, Robustness, Redundancy and Resoucefulness. A state of art of the different methodologies to assess resilience is provided clarifying the differences among Resilience, Vulnerability, Sustainability and Risk. Some considerations on how to communicate risk on RBD are also provided.

2.1 Resilience-Based Design in Structures

A disaster resilient community is a society that can withstand an extreme event, natural or man made, with a tolerable level of losses, and is able to take mitigation actions consistent with achieving that level of protection (Mileti 1999). In the last decade, earthquake engineers have given more attention to deformations during their analysis and to life safety, while less attention has been given to socio-economic parameters. Nowadays, attention is shifting towards the necessity to develop a damage-free structure using risk assessment tools, which should develop more robust structures against uncertainties. Shorter recovery processes are possible at the building level if the structure has little or no damage; otherwise it might take months to recover. In order to reduce the losses, the emphasis has shifted to mitigations and preventive actions before the earthquake events. One of the options for achieving more resilient structures in face of an earthquake is to provide them with advanced technologies such as self-centering capabilities with minimum residual deformations, which will allow for a faster recovery process (Christopoulos and Filiatrault 2006). Mitigation actions can reduce the vulnerability of such facilities. However, in case of insufficient mitigation actions, or in case that the events exceed expectations, damage occurs and a recovery process is necessary in order to continue to have a functional community. Seismic resilience describes the loss and loss recovery required to maintain the function of the system with minimal disruption. While mitigation may emphasize use of technologies and implementation of policies to reduce losses, resilience also considers the recovery process including the behavior of individuals and organizations in the post disaster

phase. A wealth of information is available on specific actions, policies or scenarios that can be adopted to reduce the direct and indirect economic losses due to earthquakes, but there is little information on procedures on how to quantify these actions and policies. Seismic resilience can compare losses and different pre and post event measures verifying if these strategies and actions can reduce or eliminate disruptions in presence of earthquake events.

2.2 MCEER Pioneer Definition of Unidimensional Resilience

There is a broader debate in literature on how resilience is defined. An extensive description of the state-of-the art in the definition of resilience can be found in Cimellaro et al. (2009). After a careful analysis of the literature, the authors decided to follow the definition provided by Bruneau et al. (2003) which has been clarified and extended in Cimellaro et al. (2010a). Disaster resilience, as MCEER's resilience framework defines it, is the ability of social units (e.g., organizations, communities) to mitigate hazards, contain the effects of disasters, and carry out recovery activities in ways that will minimize social disruption, while also mitigating the effects of future disasters (Bruneau et al. 2003). Consequently, strength, flexibility, and the ability to cope with and overcome extreme challenges are the hallmarks of disaster-resilient communities. According to MCEER, Resilience (R) is defined as a function indicating the capability to sustain a level of functionality or performance of a given building, bridge, lifeline networks, or community, over a period defined as the control time T_{LC} . Analytically, Resilience is defined as

$$R(\mathbf{r}) = \int_{t_{0E}}^{t_{0E}+T_{LC}} Q_{TOT}(t)/T_{LC} dt \quad (2.1)$$

where $Q_{TOT}(t)$ is the global performance function of the region considered; T_{LC} is the control time of the period of interest that is usually decided by owners, or society (usually is the life cycle, life span of the system etc.); t_{0E} is the time instant when the event happens; \mathbf{r} is a vector defining the position within the selected region where the resilience index is evaluated Cimellaro et al. (2009, 2010a,b). The time T_{LC} includes the building recovery time, T_{RE} and the business interruption time that is usually smaller compared to the other one. The performance function is the combination of all functionalities related to different facilities, lifelines, etc. for the case when physical infrastructures, resources and services are considered, which will be described in the following paragraphs. In MCEER's terminology, the seismic performance of the system is measured through a unique decision variable (DV) defined as "Resilience" that combines other variables (economic losses, casualties, recovery time, etc.), which are usually employed to judge seismic performance. This

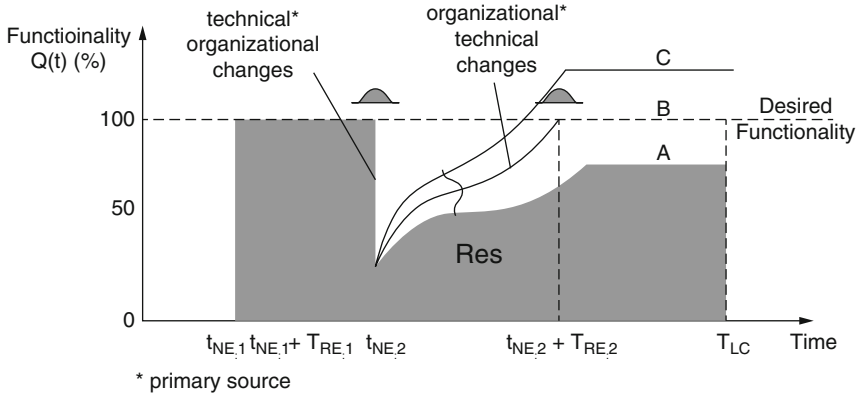


Fig. 2.1 Schematic representation of disaster resilience

Resilience is defined graphically as the normalized area underneath the performance function of a system defined as $Q(t)$. $Q(t)$ is a non-stationary stochastic process and each ensemble is a piecewise continuous function as the one shown in Fig. 2.1, where the functionality $Q(t)$ is measured as a dimensionless (percentage) function of time. For a single event, Resilience is given by the following equation (Cimellaro et al. 2005; Bruneau and Reinhorn 2007)

$$R = \int_{t_{OE}}^{t_{OE} + T_{LC}} Q(t) / T_{LC} dt \tag{2.2}$$

where

$$Q(t) = [1 - L(I, T_{RE})] [H(t - t_{OE}) - H(t - (t_{OE} + T_{RE}))] f_{REC}(t, t_{OE}, T_{RE}) \tag{2.3}$$

where $L(I, T_{RE})$ is the loss function; $f_{REC}(t, t_{OE}, T_{RE})$ is the recovery function; $H(t)$ is the Heaviside step function, T_{LC} is the control time of the system, T_{RE} is the recovery time from event E and; t_{NE} is the time of occurrence of event E . The recovery time and the recovery path are two key components for evaluating resilience, so they should be estimated accurately. Unfortunately in most common loss estimation models, such as HAZUS (2014), the recovery time is evaluated in simple terms and it assumed that within one year, everything returns back to normality. In reality, it should be taken into account that the system may not always return to the pre-disaster baseline performance (Fig. 2.1). Perhaps, it may exceed the initial performance (Fig. 2.1-curve C), particularly when the system can use the opportunity to fix pre-existing problems inside the system itself, or on the other hand the system may suffer permanent losses and equilibrate below the baseline

performance (Fig. 2.1-curve A). A clear example of the condition shown in Fig. 2.1-curve A is represented by Kobe earthquake that clearly demonstrates that certain kinds of long-term impacts losses do occur, at least in catastrophic disasters. In 1994, prior to the earthquake, the Port of Kobe was the world's sixth largest container port in terms of cargo throughput; in 1997, after repairs had been completed, it ranked seventeenth (Chang and Nojima 2001). In fact, performance and recovery of transportation systems often requires longer repair times than other lifeline systems and in the case of Kobe port, it appeared to play a major role in the development of long-term impacts. Transportation losses served to accentuate existing social and economic conditions of vulnerability, and they lead to permanent loss in business and therefore the port never came back to its pre-earthquake ranking. In general, the resilience index can be applied to different fields (e.g. engineering, economic, social science) and it can be used at various temporal and spatial scales. A Resilience Framework requires the combination of qualitative and quantitative data sources at various *temporal and spatial scales*, and as a consequence, information needs to be aggregated or disaggregated to match the scales of the resilience model and the scales of interest for the model output. Following sections present a description of each scale.

2.2.1 Spatial Distribution

Resilience can be considered as a dynamic quantity that changes over time and across space. It can be applied to engineering, economic, social, and institutional infrastructures, and can use various geographic scales. The first in quantifying the resilience performance index (R) is to define the *spatial scale* (e.g. building, structure, community, city, region, etc.) of the problem of interest. It is also important to mention that the entire recovery process is affected by the *spatial scale* of the disaster. Huge disasters will have longer recovery processes (Fig. 2.2). The *spatial scale* will also be used for defining the performance measures that will be considered in defining the global functionality of the system.

2.2.2 Temporal Distribution

The second step is to define the temporal scale (short term emergency response, long term reconstruction phase, midterm reconstruction phase, etc.) of the problem of interest (Fig. 2.2). The selection of the control period T_{LC} will affect the resilience performance index. Therefore when comparing different scenarios, the same control period should be considered. Figure 2.2 shows the spatial and temporal dimension of Resilience-Based design (RBD).

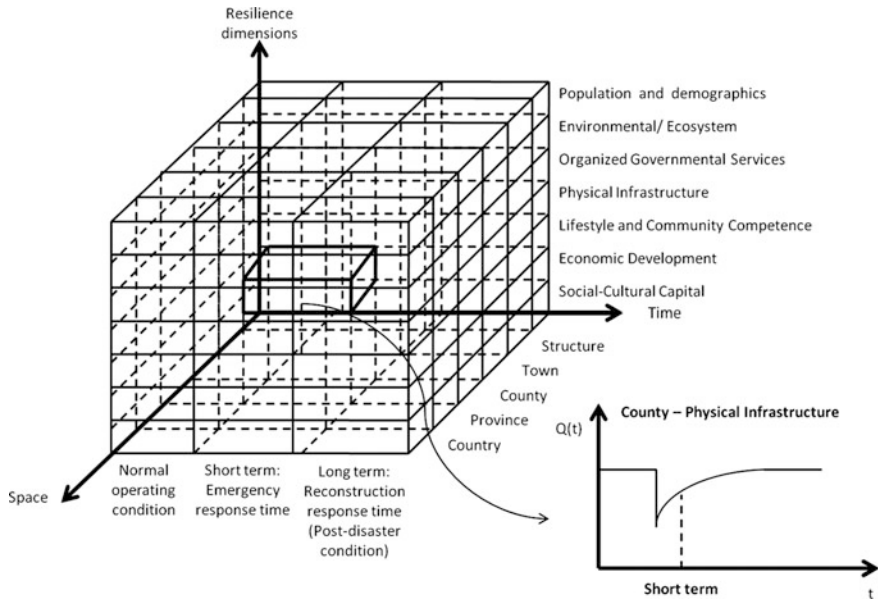


Fig. 2.2 Schematic representation of disaster resilience

2.3 The Four Rs for Resilience

While defining Resilience clearly presents a challenge, identifying the features of organizations and other social units that make them resilient is even more difficult. Resilience is an important concept for disaster management in complex systems. The objectives of enhanced Disaster Resilience are to minimize loss of life, injuries, disruption of important services, and economic losses; in short, to minimize any reduction in quality of life due to disaster. Inherent in the definition of disaster resilience are a number of characteristics that help to make it more tangible and measurable. Specifically, disaster resilience is characterized by:

- – *Reduced failure probabilities* – i.e., the reduced likelihood of damage and failures to critical infrastructure, systems and components;
- – *Reduced consequences from failures* – in terms of injuries, lives lost, damage and negative economic and social impacts; and
- – *Reduced time to recovery* – the time required to restore a specific system or set of systems to normal or pre-disaster level of functionality.

Based on these characteristics, resilience can be enhanced by reducing the likelihood of failure of critical infrastructure (thereby, reducing their impacts) and speeding up the time it takes to make a full recovery. In an effort to enhance these disaster resilience characteristics, researchers at the MCEER (Bruneau et al. 2003;

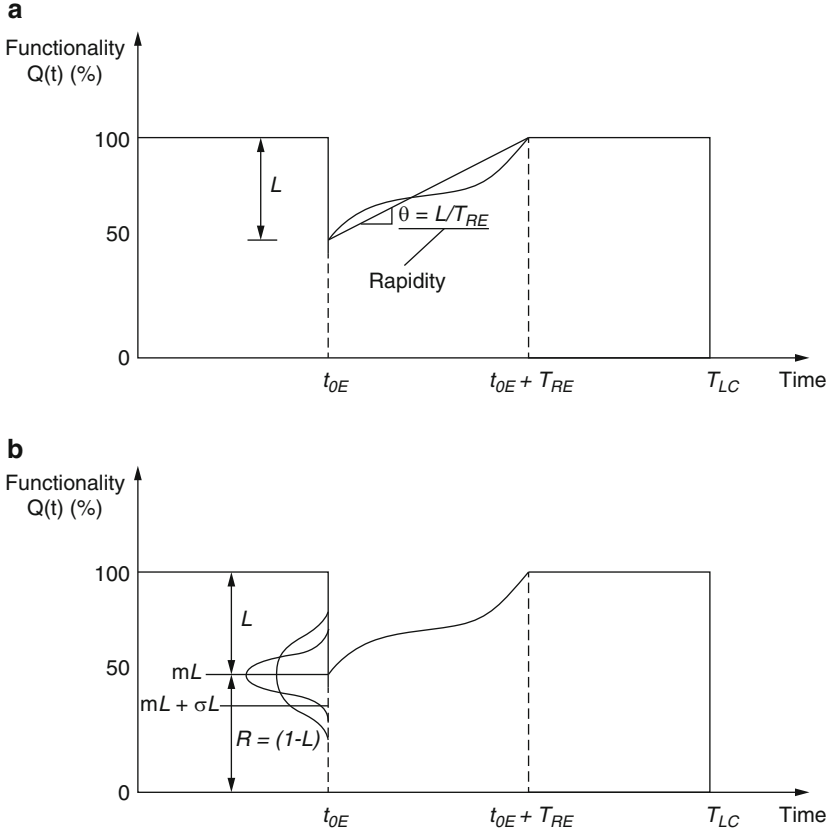


Fig. 2.3 Dimensions of resilience: rapidity (a) and robustness (b)

Bruneau and Reinhorn (2007) have identified four fundamental properties. These are *robustness*, *resourcefulness*, *redundancy*, and *rapidity*. These dimensions can better be understood by looking at the functionality curve shown in Fig. 2.3.

2.3.1 Rapidity

Rapidity is the “capacity to meet priorities and achieve goals in a timely manner in order to contain losses and avoid future disruption” (Bruneau et al. 2003). According to the NIST report (2015), rapidity is defined as “the speed with which disruption can be overcome and safety, services, and financial stability restored”. Mathematically, it represents the slope of the functionality curve (Fig. 2.3a) during the recovery-time and it can be expressed by the following equation

$$Rapidity = \frac{dQ(t)}{dt}; (t_{0E} \leq t \leq t_{0E} + T_{RE}) \quad (2.4)$$

An average estimation of rapidity can be defined by knowing the total losses and the total recovery time to regain 100 % of functionality, as follows

$$\text{Rapidity} = \frac{L}{T_{RE}} \quad (2.5)$$

where L is the loss, or drop of functionality, right after the extreme event.

2.3.2 Robustness

Robustness in the realm of to engineering systems is, “strength, or the ability of elements, systems or other units of analysis to withstand a given level of stress, or demand without suffering degradation or loss of function” (Bruneau et al. 2003). With respect to infrastructural qualities, NIST defines the robustness as “the inherent strength or resistance in a system to withstand external demands without degradation or loss of functionality”. It is therefore the residual functionality right after the extreme event (Fig. 2.3b) and can be represented by the following relation

$$\text{Robustness} = 1 - \tilde{L}(m_L, \sigma_L); \quad (2.6)$$

where \tilde{L} is a random variable expressed as function of the mean m_L and the standard deviation σ_L . A more explicit definition of robustness is obtained when the dispersion of the losses is expressed directly as follows

$$\text{Robustness} = 1 - \tilde{L}(m_L + a\sigma_L); \quad (2.7)$$

where a is a multiplier of the standard deviation corresponding to a specific level of losses. A possible way to decrease the uncertainty in the robustness of a system is to reduce the dispersion in the losses represented by σ_L . In this definition, robustness reliability is therefore the capacity of keeping the variability of losses within a narrow band, independently of the event itself (Fig. 2.3b). Two examples of systems with and without robustness, respectively, are the Emergency Operation Center (EOC) and the Office of Emergency Management (OEM) organization during the World Trade Center disaster in 2001 (Kendra and Wachtendorf 2003). The EOC facility, part of OEM, was not sufficiently robust to survive the September 11, attack (being located in the 23rd floor of the 7 World Trade Center). However, by the strength of its resourcefulness, OEM exhibited considerable robustness as an organization, demonstrating an ability to continue to function even after losing the WTC facility and a great part of its communications and information technology infrastructure. When the latter was restored, it contributed to the resilience of the OEM as a functional and effective organizational network.

2.3.3 *Redundancy*

According to the earthquake engineering field, *Redundancy* is “the quality of having alternative paths in the structure by which the lateral forces can be transferred, which allows the structure to remain stable following the failure of any single element” (FEMA 2000). In other words, it describes the availability of alternative resources in the recovery process of a system. In order to have a complete overview of the resilience problems, the definition of redundancy in the structural field is also referenced: “Structural redundancy refers to the multiple availabilities of load-carrying components or multiple load paths which can bear additional loads in the event of failure. If one or more components fail, the remaining structure is able to redistribute the loads and thus prevent a failure of the entire system. Redundancy depends on the geometry of the structure and the properties of the individual load-carrying elements.” (Frangopol and Curley 1987). Redundancy is “the extent to which elements, systems, or other units of analysis exist that are substitutable, i.e. capable of satisfying functional requirements in the event of disruption, degradation, or loss of functionality” (Bruneau et al. 2003). Simply, it describes the availability of alternative resources in the loss or recovery process. Redundancy, as NIST defines it, is “system properties that allow for alternate options, choices, and substitutions when the system is under stress”. Redundancy is a key attribute of resilience, since it represents the capability of using alternative resources, when the principal ones are either insufficient or missing. If the system is resilient there will always be at least one scenario allowing recovery, regardless of the extreme event. If this condition is not fulfilled by the system, then changes to the system can be made, such as duplication of components to provide alternative paths in case of failure. An example of a system without redundancy is well illustrated in the World Trade Center terrorist attack mentioned above, when the EOC facility was destroyed and there was no other office that could immediately, or instantaneously, replace the main facility. Redundancy should be developed in the system in advance, and it should exist in a latent form as a set of possibilities to be enacted through the creative efforts of responders, as indicated below.

2.3.4 *Resourcefulness*

Resourcefulness is “the capacity to identify problems, establish priorities, and mobilize resources when conditions exist that threaten to disrupt some element, system, or other unit of analysis; resourcefulness can be further conceptualized as consisting of the ability to apply material (i.e., monetary, physical, technological, and informational) and human resources to meet established priorities and achieve goals” (Bruneau et al. 2003). This is a property that is difficult to quantify, since it mainly depends on human skills and improvisation during the extreme event. Referring to infrastructural qualities, NIST defines resourcefulness as “the capacity

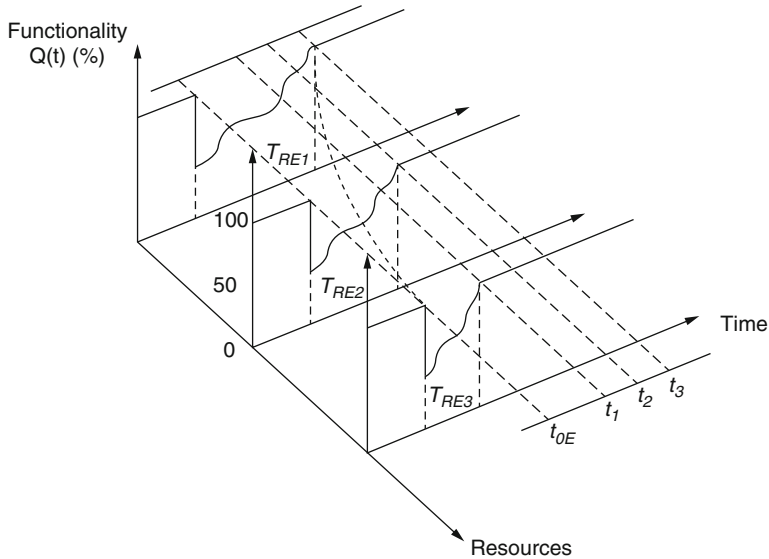


Fig. 2.4 The influence of resourcefulness on resilience (Bruneau and Reinhorn 2007)

to mobilize needed resources and services in emergencies”. Resourcefulness and Redundancy are strongly interrelated. For example, resources, and resourcefulness, can create redundancies that did not exist previously. In fact, one of the major concerns with the increasingly intensive use of technology in emergency management is the tendency to over-rely on these tools, so that if technology fails, or is destroyed, the response falters. To forestall this possibility, many planners advocate Redundancy. Changes in Resourcefulness and Redundancy will affect the shape and the slope of the recovery curve and the recovery time T_{RE} . As illustrated in Fig. 2.4, where a third axis is added to consider resourcefulness, adding resources can reduce time recovery beyond what is expected by the benchmark normal condition. In theory, if infinite resources were available, time recovery would asymptotically approach zero. Even in the presence of enormous financial and labor capabilities, a practical minimum time recovery exists. An example is the replacement of the Santa Monica freeway bridges following the 1994 Northridge earthquake. The replacement of this critical structure was accomplished 2.5 months faster than in the original planning, and a reported bonus cost of over 14 million of dollars was paid to the contractor for early completion. Likewise in less advanced societies where resources are scarce, time recovery could approach infinity. However, in resourceful societies the recovery time could be also significantly longer than necessary due to inadequate planning, organizational failures or ineffective policies. Resourcefulness and robustness are also linked. It can be argued that investing in limiting initial losses (improving the robustness) might, in some cases, be the preferred approach to enhance resilience as it automatically translates into a consequent reduction in time recovery; the retrofitting investment is an investment that pays benefit to both axes.

Resourcefulness also affects Rapidity and Robustness. It is through Redundancy and Resourcefulness (as means of resilience) that the Rapidity and Robustness (the ends of resilience) of an entire system can be improved.

2.4 Inherent vs. Adaptive Resilience

Inherent resilience means that the resilience analyzed is preexisting within a community or infrastructure (usually used as the baseline for measuring outcomes and change over time), while *adaptive* resilience is the ability to learn from an event and respond to changes (is a process involving social learning, but it can also have a measurable outcome). However, it is important to highlight that the disaster resilience can be considered as a dynamic process, so it may move from a pre-event inherent resilience to a post-event adaptive resilience, with both process and outcome measures (Norris et al. 2008; Rose 2007). This dynamic process feeds back into alterations in the inherent resilience of the community as suggested by the disaster resilience of place model (Cutter et al. 2008). However, at this stage the relationship between these two definitions of resilience is still at the theoretical level as the concept has not been empirically tested yet.

2.5 Resilience vs. Vulnerability

The difference between these two concepts is that resilience approach focuses on the quality of life of the people at risk and developing opportunities to generate a better outcome. In contrast, the vulnerability approach places stress on the production of nature (Smith and O’Keefe 1996) to resist the natural hazard. Engineers, guided by legislation, play a leading role in the quantification of vulnerability. Moreover, the concept of vulnerability has to be related with the definition of fragility. In order to better understand the relationship between these two concepts, it is useful to focus on the field of seismic engineering and provide two different methods of evaluating vulnerability and fragility. Given a certain control parameter (for example the shaking intensity), vulnerability (and in particular a vulnerability function) defines the loss, while fragility (more precisely a fragility function) gives the probability of some undesirable event (e.g. collapse). Thus the fragility function may assess the probability that a building will collapse as well as the probability that a factory may release hazardous materials into the atmosphere, given a certain seismic intensity. On the other hand, vulnerability functions would provide, as a function of the same control parameter, the damage factor for the building (e.g. valuated as repair cost divided by replacement cost) or the quantity of hazardous materials released. Resilience defines the capacity of a system to bounce back for a disruption. A distinction between the different terms is provided by Manyena in 2006 that also highlighted the necessity to develop a complementary “map of

Table 2.1 Difference between vulnerability and resilience (Manyena 2006)

N.	Vulnerability	Resilience
1	Resistance	Recovery
2	Force bound	Time bound
3	Safety	Bounce back
4	Mitigation	Adaptation
5	Institutional	Community – based
6	System	Network
7	Engineering	Culture
8	Risk assessment	Vulnerability
9	Outcome	Process
10	Standards	Institution

resilience and vulnerability” to create and increase the conscious role of the entire society in the restoration process. Furthermore, defining and mapping resilience has become an important tool in the decision-making process both for the engineering profession and the policy makers (Table. 2.1).

2.6 Resilience vs. Sustainability

The term sustainability appeared in the early 1970s as the rapid growth of the human race and the environmental degradation associated with increased consumption of resources raised concerns. Finding a way for consent between environment, advancement, and well-being of the world’s poor was discussed in the United Nation’s 1972 Stockholm Conference. “Sustainable development” was presented by Ward and Dubos (1972). The concept is not necessarily modern: (Gibson et al. 2010) imply that the concept of sustainability, as an old wisdom, has been around since the dawn of time in most communities. The definition of sustainability given by the Brundtland Commission, formally known as the World Commission on Environment and Development (WCED), was a turning point for government policy makers, scientists, politicians, sociologists, and economists. “The development that meet the needs of the present without compromising the ability of future generations to meet their own needs” (WCED 1987) is a definition for sustainability that challenged the traditional ways of doing business, changed the interpretation of the word development, and helped scientists and practitioners to understand not only the environmental impacts but also the social and economic effects of projects as the human race interacts with its surroundings.

Since, Among all definitions of resilience, according to Walker and Salt (2006) resilient systems are “sustaining ecosystems and people in a changing world” the resilience is intertwined with sustainability. Sometimes resilience is considered as one the indicators of sustainability. However the correlation between these two, is more complicated. Moreover, being resilient is essential to be really sustainable

and they cannot be taken into account separately. According to David Maddox, the future cities must have three inevitable characteristics. They must be **Sustainable**, **resilient** and **livable**.

It is possible to have sustainable cities which can reduce resource and energy consumption, optimize waste management and be economically efficient but not necessarily operative in case of shocks and major turbulence so that they are not resilient. Such cities are not truly sustainable. It is possible to have resilient cities that are not sustainable according to energy consumption, social equity, economical efficiency, and so on. They are not even resilient, but rather resistant, in the sense that they resist the hazardous situations. It is possible to have livable cities that are neither resilient nor sustainable. It is possible to have resilient and sustainable cities that are not livable, and so are not truly sustainable.

Although both sustainability and resilience are essential for future cities, the might work against each other in some cases.

Density is a good example. Usually dense and compact cities are considered sustainable cities, as they can reduce the energy consumption. For instance Public transportation requires a certain population density to be economically viable, but dense urban systems can make cities more vulnerable to extreme events. So, defining a limit of the for population density in a city might be the solution to have cities that are both sustainable and resilient. Resilience planning and management efforts needs to be linked with sustainability in order to move towards desired future sustainable systems.

For example, after the Superstorm Sandy hit New York City and the New Jersey coastline, there have been a lot of discussions about large technical infrastructure solutions for dealing with unexpected future storm surge and coastal flooding. One proposal was to build sea gates at the narrow section of the New York harbor entrance. However if the dam would have built, it would have caused serious economically unsustainable long-term maintenance costs with severe ecological side effects.

2.7 Resilience vs. Durability

Durability is the ability to endure for a system. A durable structure is a system which lasts longer, so less resources are required to bring back the system to the initial conditions.

In order to explain the correlation between durability and resilience let's consider two projects shown in Fig. 2.5.

Project 1 reaches the specific level of functionality in which the fundamental maintenance is required, before project 2, so it is less durable, so it will require more resources to go back to the initial conditions and it will be less resilient. On the other end project 2 is more durable, so it will require less maintenance and it will be faster to recover when an extreme event occurs. So this dimension has a positive effect on resilience.

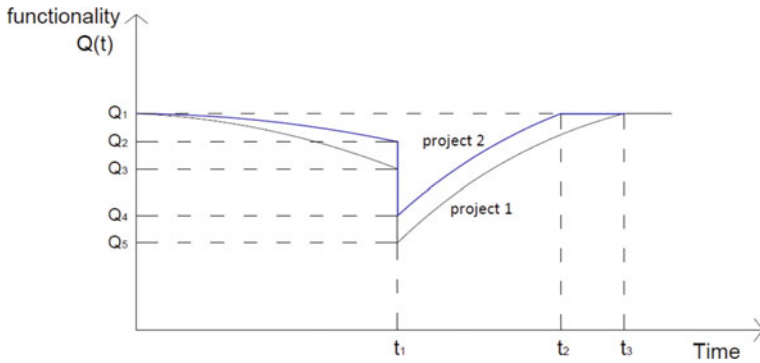


Fig. 2.5 Durability vs. resilience

2.8 Resilience vs. Risk

Risk analysis is an important tool for informed decision making and it is typically defined in terms of the probabilities of occurrence and the associated consequences of hazardous scenarios. Risk analysis is usually divided in:

1. *Risk assessment*, which means identifying, evaluating and measuring the probability and severity of risks
2. *Risk management* which means what to do about risk;

Risk analysis can be also divided in:

1. *Qualitative risk analysis* which uses words or colors to identify and evaluate risks or presents a written description of the risk
2. *Quantitative risk analysis (QRA)* which calculates numerical probabilities over the possible consequences;

QRA seeks assessing numerically probabilities for the potential consequences of risk, and is often called probabilistic risk analysis or probabilistic risk assessment (PRA). The analysis often seeks to describe the consequences in numerical units such as dollars, time, or lives lost.

Resilience analysis can be used to quantify the capacity to “bounce back” from extreme events of civil engineering assets. In certain sense is complementary to *Risk analysis*, which is used to quantify the safety of civil engineering assets, but they are also dependent each other as shown in Fig. 2.6. Both approaches are important for informed decision making.

1. **Risk analysis** is used to prioritize the **mitigation strategies** when running on limited budget.
2. **Resilience analysis** is used to prioritize the **restoration strategies** when running on limited budget.

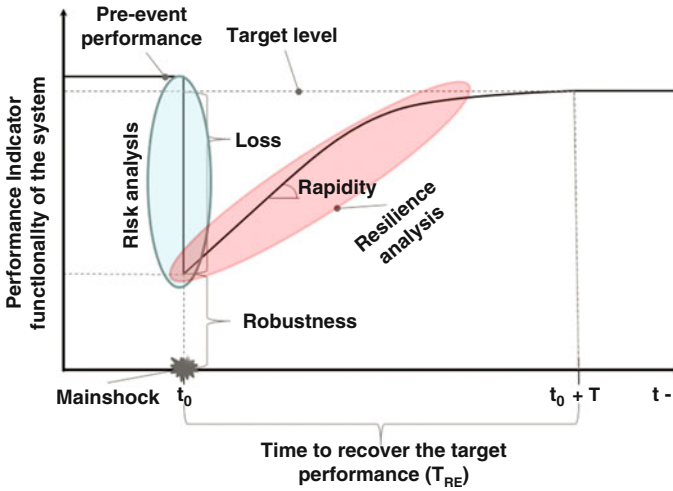


Fig. 2.6 Risk analysis vs. Resilience analysis

2.9 The Risk Management of Complex Infrastructural Systems

The first real problem to accomplish the administration of an articulated system is establishing the degree of risk exposure, and finding a method to numerically evaluate its percentage. Once this is done, the second step is to establish a procedure to lower the risks. The first method proposed in literature is a probabilistic methodology which has many inherent problems. A critical infrastructure is defined as a system including all elements necessary to provide sustainable services within the nation's power, transportation, waste management, water, telecommunication sectors, etc. Traditional risk assessment tools do not explicitly capture the influence of unpredictable factors on the system performance. Moreover, a significant of recent high consequence failures can be attributed directly to number cognitive uncertainties, at both the individual and organizational level (Watkins and Bazerman 2003). This means that neither civilians nor decision making administration know exactly how to behave in front of catastrophic events, also due to the fact that the models in their possession are not accurate enough to represent accurately the reality. The models' uncertainty includes both *unknown-knowable* (information exists, but it is not possible to properly utilize it; often rejected or not believed) and *unknown-unknowable* (information or knowledge does not exist). The first requirement is to evaluate how reliable the model is. This is possible through three different parameters:

1. **Face validity:** the degree to which a method appears to be appropriate for doing what it intends to do. It is based on justifications provided by the state-of-art and knowledge and experience;

2. **Content validity:** addresses the degree to which the method addresses the problem (issue) it is intended to address;
3. **Construct validity:** addresses the degree to which the results of the method can be accounted for by the explanatory constructs of a sound theory. Construct validity is demonstrated when measures that are theoretically predicted to be highly interrelated are shown in practice to be highly interrelated.

The *Probabilistic Approach* is defined as the “mathematical framework aimed at enhancing our understanding of the future”, and it is considered to be a good method to prevent disasters and organize prevention works. The probability theory does not provide a correct and sure answer to a problem, but rather it provides the “most probable” answer identified with a certain probability to be true. Due to real world complexity, when a model is made to perform tests, a series of uncertainties should be taken into account. In the late 1990s the risk analysis community actively adopted the aleatory and epistemic taxonomy to characterize uncertainty which are briefly described in Sects. 2.9.1 and 2.9.2.

2.9.1 Aleatory Uncertainties

Many phenomena or processes of concern to engineers contain randomness which means that the expected outcomes are unpredictable. Such phenomena are characterized by field or experimental data that contain significant variability, i.e., the observed measurements are different from one observation to another. Within a range of certain values may occur more frequently than others. The variability inherent in such data or information is statistical in nature, and the realization of a specific value involves probability.

2.9.2 Epistemic Uncertainties

Epistemic uncertainty is a representation of the analyst’s knowledge and ability to formulate a model that can predict the behavior of the system under consideration. As understanding is improved, perhaps as a function of research or observation, epistemic uncertainty can potentially be reduced (if not eliminated) via Bayesian updating according to the Bayes Rule. Examples of epistemic uncertainties are easy to find. They include: hurricane surge models, corroded pipeline burst models, earthquake attenuation relationships, “climate change” models etc. Epistemic uncertainties also include the strength for grades of structural steel and concrete, as well as soils under dynamic and pseudo-static loadings. In complex engineering systems it is often impossible and impractical to distinguish uncertainties in aleatory and epistemic categories, and this is why the *Amalgamatic (aka type III or mixed) uncertainty* was created. It is defined as having both aleatory and epistemic components.

2.10 Uncertainties in RBD

The RBD methodology can be used on a scenario basis (deterministic approach) or include uncertainties (probabilistic approach) when a particular level of confidence of achieving performance objective is of interest. In general, five types of random variables can be included in the probabilistic description of the resilience index. In this case, the joint probability density function is given by the following expressions

$$f_{R,T_{RE},Q,X,I}(r, t_{RE}, q, x, i) = f_{R,T_{RE},Q,X,I}(r|t_{RE}, q, x, i) \cdot f_{T_{RE},Q,X,I}(t_{RE}|q, x, i) \cdot f_{Q,X,I}(q|x, i) \cdot f_{X,I}(x|i) \cdot f_I(i) \quad (2.8)$$

The marginal probability density function (PDF) of the resilience index is given by

$$f_R(r) = \int_{t_{RE}} \int_q \int_x \int_i f_{R,T_{RE},Q,X,I}(r, t_{RE}, q, x, i) dt_{RE} \cdot dq \cdot dx \cdot di \quad (2.9)$$

Therefore the expected value of the resilience index, which is a random variable, is given by

$$m_r = E\{R\} = \int_{-\infty}^{\infty} r \cdot f_{R,T_{RE},Q,X,I}(r, t_{RE}, q, x, i) \cdot dr \quad (2.10)$$

where I = intensity measures; X = response measures; Q = performance measures; T_{RE} = recovery time measures; R = resilience index; m_r = mean resilience index.

2.11 Communicating Risk in RBD

Engineers need to know which measures of risk are most meaningful or relevant to decision makers, and then be able to communicate those risks, and the costs and benefits of mitigation, in concise, credible and meaningful terms. Keller and Blodgett (2006) have shown that when the problems are formulated in terms of frequencies rather than probabilities, the perceived threat of the risk is increased. The *probabilistic approach* described in Sect. 2.10 is more comprehensive and general, but the information provided to the public (e.g. decision makers, politicians, etc.) should be deterministic (scenario or event based), because it is simpler and easier to understand. In communicating risk effectively, the public has difficulty thinking in probabilistic terms (Patt and Schrag 2003). In fact, according to Kahneman and Tversky (2000), small probabilities (which are frequently associated with natural hazard events) are often underestimated. According to Samant's

personal communication 2011, “By eliminating probability, which is a confusing concept for a lot of people, the [risk] becomes way more impactful for the average person”. Many authors believe the scenario approach may also impact the emotions associated with an event.

2.12 Summary and Remarks

Disaster resilience combines information from technical and organizational fields, from seismology and earthquake engineering to social science and economics. The final goal is to integrate the information from these different fields into a unique function leading to results that are unbiased by uninformed intuition or preconceived notions of risk. Resilience is defined as the capability to sustain a level of functionality or performance over a period defined as the control time; in the plane of functionality versus time, it is represented by the area underneath the function. Furthermore, resilience can be considered as a dynamic quantity that changes over time and across space. The resilience of a system can be improved through four attributes:

- *Rapidity*, which is the capacity to contain losses and avoid future disruption. It represents the slope of the functionality curve during the recovery time;
- *Robustness*, which indicates the ability of a system to withstand a given level of stress maintaining its functionality;
- *Redundancy*, which refers to alternative resources in the recovery process when the principal ones are insufficient;
- *Resourcefulness*, which accounts for the human factor and, in particular, the capability to forecast dangerous events without over-relying on technological devices.

Comparison between Resilience and Vulnerability, Sustainability, Durability and Risk are provided to clarify confusion between these different concepts which are interdependent with the resilience dimension. Either a deterministic or a probabilistic approach can be used to study this characteristic of the system; however the first one is preferred over the second one for providing information to the public because it is easier to understand.

References

- Bruneau M, Reinhorn AM (2007) Exploring the concept of seismic resilience for acute care facilities. *Earthq Spectra* 23(1):41–62
- Bruneau M, Chang S, Eguchi R, Lee G, O’Rourke T, Reinhorn A, Shinozuka M, Tierney K, Wallace W, Winterfelt DV (2003) A framework to quantitatively assess and enhance the seismic resilience of communities. *Earthq Spectra* 19(4):733–752. doi:10.1193/1.1623497
- Chang S, Nojima N (2001) Measuring post-disaster transportation system performance: the 1995 kobe earthquake in comparative perspective. *Transp Res-A* 35(6):475–494

- Christopoulos C, Filiatrault A (2006) Principle of passive supplemental damping and seismic isolation. IUSS Press, Pavia
- Cimellaro GP, Reinhorn AM, Bruneau M (2005) Seismic resilience of a health care facility. In: Proceedings of the 2005 ANCER annual meeting, session III, paper N3, 10–13 Nov, Jeju
- Cimellaro G, Fumo C, Reinhorn AM, Bruneau M (2009) Quantification of seismic resilience of health care facilities. Report MCEER Technical Report-MCEER-09-0009, Multidisciplinary Center for Earthquake Engineering Research
- Cimellaro G, Reinhorn AM, Bruneau M (2010a) Framework for analytical quantification of disaster resilience. *Eng Struct* 32(11):3639–3649
- Cimellaro GP, Reinhorn AM, Bruneau M (2010b) Seismic resilience of a hospital system. *Struct Infrastruct Eng* 6(1–2):127–144
- Cutter S, Barnes L, Berry M, Burton C, Evans E, Tate E, Webb J (2008) A place-based model for understanding community resilience to natural disasters. *Glob Environ Change* 18(4):598–606
- FEMA (2000) Fema 356 prestandard and commentary for the seismic rehabilitation of buildings. Report, FEMA 356 Federal Emergency Management Agency
- Frangopol D, Curley J (1987) Effects of damage and redundancy on structural reliability. *ASCE J Struct Eng* 113(7):1533–1549
- Gibson R, Hassan S, Holtz S, Tansey J, Whitelaw G (2010) Sustainability assessment: criteria and processes, earthscan. Taylor & Francis Group, New York
- Hazus (2014) Hazus[®]-MH MR5 technical manuals and user's manuals. Department of Homeland Security, Federal Emergency Management Agency, Mitigation Division, Washington, DC
- Kahneman D, Tversky A (2000) Choices, values and frames. Cambridge University Press, New York
- Keller E, Blodgett R (2006) Natural hazards: earth's processes as hazards, disasters, and catastrophes. Pearson/Pretince Hall, Upper Saddle River
- Kendra J, Wachtendorf T (2003) Elements of resilience after the world trade center disaster: reconstituting new york city's emergency operations centre. *Disasters* 27(1):37–53
- Manyena SB (2006) The concept of resilience revisited. *Disasters* 30:434
- Mileti D (1999) Disasters by design: a reassessment of natural hazards in the United States (18 May 1999). Joseph Henry Press, Washington, DC
- NIST (2015) Community resilience planning guide for buildings and infrastructure systems. CODEN: NSPUE2, National Institute of Standards and Technology, Willie May, Acting Under Secretary of Commerce for Standards and Technology and Acting Director
- Norris FH, Stevens SP, Pfefferbaum B, Wyche KF, Pfefferbaum RL (2008) Community resilience as a metaphor, theory, set of capacities, and strategy for disaster readiness. *Am J Community Psychol* 41:127–150
- Patt AG, Schrag DP (2003) Using specific language to describe risk and probability. *Clim Change* 61(1–2):17–30
- Rose A (2007) Economic resilience to natural and man-made disasters: multidisciplinary origins and contextual dimensions. *Environ Hazards* 7(4):383–398
- Samant L (2011) Personal communication. 10 Mar 2011
- Smith N, O'Keefe P (1996) Geography, marx and the concept of nature. In: Agnew J, Livingstone DN, Rogers A (eds) *Human geography: an essential anthology*. Blackwell, Oxford/Cambridge, pp 282–315
- Walker B, Salt D (2006) Resilience thinking – sustaining ecosystems and people in a changing world. Island Press, Washington, DC
- Ward B, Dubos RJ (1972) Only one earth: the care and maintenance of a small planet, Mondadori
- Watkins MD, Bazerman MH (2003) Predictable surprises: the disasters you should have seen coming. *Harv Bus Rev* 81(3), 72
- WCED (1987) Our common future – Brundtland report United Nations World Commission on Environment and Development (WCED), Oxford

Chapter 3

Resilience Indicators

Abstract This chapter analyzes and classifies the different resilience indicators available in literature, since there is no a widely accepted type of indicator that should be used to measure resilience. A list of existing resilience indicators is provided together with different classification methods, which are based on the hazard type, the temporal scale, the measurement method etc.

3.1 Why Resilience Indicators?

The vagueness of the concept of resilience makes it difficult to define, but it becomes even more problematic when trying to measure it. The motivations and goals of resilience measurement are as different as the proponents advocating for them. Most researchers in the field emphasize that research on measuring community resilience is still in the early stages of development. There is no single or widely accepted method to the measurement issue as the landscape of resilience indicators is confusing and increasingly hard to navigate (Cutter et al. 2014). This is particularly the case for community resilience to disasters, since this concept raises not only questions related to the measurement of resilience, but also related to the definition and conceptualizations of communities. Since communities are interconnected systems whose indicators may apply to different scales and policy realms and also address different types of shocks. Resilience indicators can help to characterize the basic elements of the targeted system or unit of analysis and thus help to raise community awareness, because whenever there is a benchmarking, weak and strong points are identified and so it is easier to know where to address the funds to enhance the system. Being explicit about the objectives and motivations of measuring resilience is of critical importance for choosing the right approaches that integrate current conceptualizations and operationalizations of resilience.

3.2 Type of Assessments

Three main categories are defined for the different resilience assessment approaches:

- *indices*
- *scorecards*
- *tools and models*

Indices are those quantifiable that represent a selected characteristic of resilience and these individual indicators are combined to create an index. The relationship between the indicators and the phenomenon they are measuring may be more or less direct. Indices are a statistical approach that summarizes observations or measurements by aggregating multiple indicators into a single value.

Scorecards provide an evaluation of performance or progress toward a goal. A vastly used method of this kind are the checklist, a series of questions related to presence or absence of resilience-related items and actions. A score is then produced based on how often the items are present, used, and so forth. Scorecards can have numerical values (1–10), letter “grades” such as (A–F), or descriptors such as “excellent to poor”. Scorecards are normally based on qualitative assessments and then converted to scores, while indices mostly use quantitative data to derive the index value.

Tools and models. Models create simplified representations of processes using mathematical formulas to approximate and understand the relationships and the interactions in the real world. Models can characterize economic resilience or resilience of a specific place. Models can be used to characterize economic resilience (Rose and Liao 2005) in a computational way or to characterize the resilience of specific places (Renschler et al. 2010). *Tools* have been developed to provide a guidance for assessing resilience with sample procedures and survey instruments, or data for use in compilation of indices or scorecards.

3.3 Methodological Approaches

There are two main different types of approaches. The first one is an *idiographic measurements or bottom-up*, which are locally generated and customized to particular places (Pfefferbaum et al. 2014). Typically use qualitative methodology and stress the resilience using highly localized data that may not be widely available. Due to the local knowledge and information these kind of case studies are rich and detailed, but the ability to compare across places is difficult because of the variability of the data and the different contexts and meanings of resilience.

On the other hand there are the *nomothetic or top-down* type assessments, which strive toward comparisons across varying units of analysis. They tend to use larger spatial units such as states or nations. This allows comparing units of analysis using standardized data, which make these types of resilience indices more amenable for examining spatial variability, allocating resources, and/or monitoring progress—all done at state, national, or international scales.

3.4 List of Existing Indicators

Many frameworks are available in literature as shown in Chap. 1. Different frameworks propose similar indicators and most of them overlap each other. After an extensive comparison between different frameworks, below is reported a comprehensive list of resilience metrics which is mainly based on the work of Mileti (1999), Renschler et al. (2010), Cutter et al. (2014) and Burton (2015). The metrics are grouped according to five domains and are shown from Tables 3.1, 3.2, 3.3, 3.4, and 3.5.

Table 3.1 List of social resilience indicators

Social resilience indicators		
Category	Resilience metric	Data source
Educational attainment equality	Absolute difference between % population with college education and % population with less than high school education	Norris et al. (2008) and Morrow (2008)
Pre-retirement age	% population below 65 years of age	Morrow (2008)
Transportation	% households with at least one vehicle	Tierney (2009)
Communication capacity	% households with telephone service available	Colten et al. (2008)
English language competency	% population not speaking English as a second language	Morrow (2008)
Non-special needs	% population without sensory, physical, or mental disability	Center (2002)
Health insurance	% population with health insurance	Center (2002)
Mental health support	Psychological support facilities per 10,000 persons	Cutter et al. (2014)
Food provisioning capacity	Food security rate	Cutter et al. (2014)
Physician access	Physicians per 10,000 persons	Norris et al. (2008)
Social capacity	% population that is not institutionalized or infirmed; % population that is not a minority; % population with at least a high school diploma; % population living in high-intensity urban areas	Burton (2015)
Community health	Social assistance programs per 1,000 population	Burton (2015)
Well-being	Adult education and training programs per 1,000 population; child care programs per 1,000 population; community services (recreational facilities, parks, historic sites, libraries, museums) per 1,000 population; internet, television, radio, and telecommunications broadcasters per 1,000 population; health services per 1,000 population	Burton (2015)

(continued)

Table 3.1 (continued)

Social resilience indicators		
Category	Resilience metric	Data source
Equity	Ratio between the % of minority population to % non minority population	Burton (2015)
Population wellness	% black infant mortality rate	Norris et al. (2008)
Social vulnerability	SoVI index	Morrow (2008), Cutter et al. (2008), and Tierney (2009)
Racial/ethnic inequality	Value of difference in % of black & % of white	Norris et al. (2008) and Cutter et al. (2008)
Crime rate	Crime rate per 10,000	Colten et al. (2008)

Table 3.2 List of economic resilience indicators

Economic resilience indicators		
Category	Resilience metric	Data source
Home ownership	% owner-occupied housing units	Norris et al. (2008) and Cutter et al. (2008)
Employment rate	% labor force employed	Mileti 1999
Income distribution and equality	Gini coefficient	Norris et al. (2008)
Non-dependence on primary sector + tourism	% employees not in primary sectors (e.g. farming, fishing, forestry, extractive industry) and tourism	Berke and Campanella (2006)
Gender income equality	Female labor force participation	Bank (2015)
Business size	Ratio of large to small businesses	Norris et al. (2008)
Large retail-regional/national geographic distribution	Large retail stores per 10,000 persons	Cutter et al. (2014)
Federal employment	% labor force employed by federal government	Burton (2015)
Economic/livelihood	% female labor force participation rate (FLFP)	Burton (2015)
Stability	Per capita household income	Burton (2015)
	Median household income	Norris et al. (2008) and Cutter et al. (2008)
	Mean sales volume of businesses	Burton (2015)
Resource equity	Lending institutions per 1,000 population	Burton (2015)
	Ratio % white to % nonwhite homeowners	Norris et al. (2008)

Table 3.2 (continued)

Economic resilience indicators		
Category	Resilience metric	Data source
Economic	% commercial establishments outside of high hazard zones (flood, surge)	Burton (2015)
Infrastructure exposure	Density of commercial infrastructure	Burton (2015)
Poverty	Poverty percentage	Norris et al. (2008), Morrow (2008), and Enarson (2007)

Table 3.3 List of community capital indicators

Community capital indicators		
Category	Resilience metric	Data source
Place attachment	Net international migration	Morrow (2008)
	% population born in a state that still reside in that state	Vale and Campanella (2005)
Political engagement	% voting participating in presidential election	Morrow (2008)
Social capital-religious organizations	Population affiliated with a religious organization per 10,000 persons	Morrow (2008)
	Religious organizations per 1,000 population	Murphy (2007)
Social capital-civic organizations	Civic organizations per 10,000 persons	Morrow (2008)
		Murphy (2007)
Social capital-disaster volunteerism	Red cross volunteers per 10,000 persons	Cutter et al. (2014)
Citizen disaster preparedness and response skills	Red cross training workshop participants per 10,000 persons	Cutter et al. (2014)
Social capital	Social advocacy organizations per 10,000 population	Murphy (2007)
	Arts, entertainment, and recreation centers per 10,000 population	Burton (2015)
	Civic organizations per 10,000 population	Morrow (2008)
		Murphy (2007)
Creative class	% workforce employed in professional occupations	Burton (2015)
	Professional, scientific, and technical services per 1,000 population	Burton (2015)
	Research and development firms per 1,000 population	Burton (2015)
	Business and professional organizations per 1,000 population	Norris et al. (2008)
Cultural resources	National Historic Registry sites per square mile	Burton (2015)

Table 3.4 List of institutional resilience indicators

Institutional resilience indicators		
Category	Resilience metric	Data source
Mitigation plan capita	Ten year average per capita spending for mitigation projects	Cutter et al. (2008)
Jurisdictional coordination	Governments and special districts per 10,000 persons	Cutter et al. (2014)
Disaster aid experience	Presidential disaster declarations divided by number of loss-causing hazard events from 2000 to 2009	Cutter et al. (2014)
Local disaster training	% population in communities with Citizen Corps program	Cutter et al. (2014)
Performance regimes-state capital	Proximity of county seat to state capital	Cutter et al. (2014)
Performance regimes-nearest metro area	Proximity of county seat to nearest county seat within a Metropolitan Statistical Area	Cutter et al. (2014)
Population stability	Population change over previous five years	Cutter et al. (2014)
Nuclear plant accident planning	% population within 10 miles of nuclear power plant	Cutter et al. (2014)
Crop insurance coverage	Crop insurance policies per square mile	Cutter et al. (2014)
Hazard mitigation/ planning	% population covered by a recent hazard mitigation plan	Burby et al. (2000) and Godschalk (2007)
	% population participating in Community Rating System (CRS) for flood	Burby et al. (2000)
Mitigation and social connectivity	% households covered by National Flood insurance Program policies	Godschalk (2003, 2007)
	% population covered with Citizen Corps program	Godschalk (2003)
Municipal services	% workforce employed in emergency services (firefighting, law enforcement, protection)	Sylves (2007)
Development	% land cover change to urban areas from 1990 to 2000	Burton (2015)
Political fragmentation	Number of governments and special districts	Norris et al. (2008)
Housing types	% housing units which are not manufactured homes	Cutter et al. (2003)
	% housing that is not a mobile home	Cutter et al. (2003)
Evacuation potential	Major road egress points per 10,000 persons	Cutter et al. (2014)

(continued)

Table 3.4 (continued)

Institutional resilience indicators		
Category	Resilience metric	Data source
Housing stock construction quality	% housing units built prior to 1970 or after 1997	Mileti (1999)
Access and evacuation	Principal arterial in miles	NRC 2006
	Number of rail in miles	Burton (2015)
High speed internet infrastructure	% population with access to broadband internet service	Cutter et al. (2014)
Shelter capacity	% housing that is vacant rental units	Tierney (2009)
	Hotels and motels per square mile	Tierney (2009)
	Fire, police, emergency relief services, and temporary shelters per 1,000 population	Burton (2015)
	% fire, police, emergency relief services, and temporary shelters outside of hazard zones	Burton (2015)
	Schools (primary and secondary education) per square mile	Ronan and Johnston (2005)
Infrastructure exposure	Density of single-family detached homes	Burton (2015)
	% building infrastructure not in flood and storm surge inundation zones	Burton (2015)
	% building infrastructure not in high hazard erosion zones	Burton (2015)

Table 3.5 List of environmental resilience indicators

Environmental resilience indicators		
Category	Resilience metric	Data source
Local food suppliers	Farms marketing products through Community Supported Agriculture per 10,000 persons	Cutter et al. (2014)
Natural flood buffers	Wetlands loss	Gunderson (2009)
Efficient energy use	Megawatt hours per energy consumer	Cutter et al. (2014)
Pervious surfaces	Average percent perviousness	Cutter et al. (2014)
Efficient water use	Inverted water supply stress index	Cutter et al. (2014)
Risk and exposure	% land area that does not contain erodible soils	Cutter et al. (2008)
	% land area not in an inundation zone (100/500-year flood and storm surge combined)	Burton (2015)
	% land area not in high landslide incidence zones	Burton (2015)
	Number of river in miles	Burton (2015)

(continued)

Table 3.5 (continued)

Environmental resilience indicators		
Category	Resilience metric	Data source
Sustainability	% green space/undisturbed land	Cutter et al. (2008)
	% land area with no land-cover/land-use change, 1992–2001	Burton (2015)
	% land area under protected status	Burton (2015)
Protective resources	% land area that is arable cultivated land	Burton (2015)
	% land area that consists of windbreaks and environmental plantings	Burton (2015)
	% land area that is a wetland, swamp, marsh, mangrove, sand dune, or natural barrier	Burton (2015)
	% land area that is developed open space	Burton (2015)
Hazard event frequency	Frequency of loss-causing weather events (hail, wind, tornado, hurricane)	Burton (2015)

3.5 Classification of Indicators

An indicator, as can be inferred, simply “indicates” something or communicates information about a phenomenon of interest, which is called the *indicandum*. This phenomenon is sometimes difficult to analyze, difficult to measure or even it may not be measurable at all (Meyer 2011). Since resilience is difficult to define and analyze, there are several different ways to classify the indicators of resilience. During a classification process different methods, such as spatial scale, temporal scales, hazard type etc. can be considered. The majority of the indicators are time and spatial dependent and are difficult to be transferred from one scale to another. So it is important to distinguish between indicators which are specific to the case study considered and the ones that can be generalized and extended to different hazards, communities etc. (Weichselgartner and Kelman 2014). Another important characteristic of the indicators is their *relation to the phenomenon and resilience*, because it is a prerequisite for measuring resilience in quantitative terms. So it is possible to distinguish between indicators which can not be *ordered* or *ranked* (e.g. gender or hazard type), the ones that can only be ranked (e.g. education level) and the ones that can be ranked and ordered by quantifying the interval between classes (e.g. net income in Euro/year).

3.6 State of Art on Classification Methods

The first comprehensive work on classification about resilience metrics have been performed in the European project EMBRACE (Rodriguez-Llanes 2013) which proposed the following categories:

1. *Inherent or adaptive*
2. *Outcome or process*
3. *Domain*
4. *Relation with the phenomenon*
5. *Composite indicators*
6. *Scale of applications*
7. *Level of measurements*
8. *Resources & Capacities, Actions and Learnings*
9. *Generalization*
10. *Relation to resilience*
11. *General importance*
12. *Pre/Post-hazard event phase*
13. *Qualitative or quantitative*

However, the classification proposed in Embrace presents some limitations, because some of these categories overlap each other and they are not integrated in a useful manner, but they have the advantage of listing a series of characteristics of the indicators.

3.7 Proposed Classification Method

After reviewing the state of the art on classification methods, a new classification method is presented. Through this classification, it is possible to help decision makers in selecting the proper indicators for their problem at hand. This classification will allow them to assess resilience quantification properly and select the optimal resilience strategy. Based on these considerations, the resilience metrics listed from Tables 3.1, 3.2, 3.3, 3.4, and 3.5 have been classified according to 7 categories (or classification methods) below

1. *Hazard Type*
2. *Temporal scale*
3. *Spatial scale*
4. *Building type*
5. *Level of Development*
6. *Domain*
7. *Measurement method*

In the columns of Table 3.6 are shown the seven proposed classification methods, while in the rows are reported the different corresponding classes.

In the following paragraphs are described in detail the different classification methods.

Table 3.6 Classification method in PEOPLES framework

Classification method in PEOPLES framework						
Hazard type	Temporal scale	Spatial scale	Building type	Level of development	Domain	Measurement method
Natural (e.g. flood, earthquake, tsunami fire, tornado, hurricane etc.)	Pre-phase (Preparedness)	Building	Critical facility (e.g. hospital, cit-hall etc.)	Developed countries	Social/Cultural	Quantitative
Man-made (e.g. terrorism, wars, criminality, power outage, etc.)	Short-term (Emergency response)	Building block (Neighborhood)	Residential building	Under-developed countries	Economic	Qualitative
	Long term (Reconstruction phase)	City/State	No building type	Not in country scale	Ecological /Environmental	
		Region			Governmental/Welfare/Institutional	
		Country			Physical/infrastructural	

3.7.1 Hazard Type

In literature can be found resilience indicators that are just defined for a specific hazard corresponding to the specific case study presented. For example, Kafle (2012) developed a method (CRI) for measuring community resilience using process and outcome indicators in 43 coastal communities in Indonesia. He emphasized that community resilience can be measured, but in each measurement both location and hazard should be specified. It is also obvious that every community according to its geographic location, face with specific natural hazards, so it is essential to cope with them and not with all of the types. This is why considering this category is necessary for the indicators' classification.

3.7.2 Temporal Scale

Resilience, means “the ability to recover from (or to resist being affected by) some shock, insult or disturbance”. Recovery is a concept which is intertwined with time.

In this case, resilience can be considered as a dynamic quantity that changes over time. Three temporal levels can be defined:

- Pre-hazard event phase (Preparedness);
- Short-term post-hazard event (Emergency response phase);
- Long-term post-hazard event (Reconstruction phase);

The indicators within the *Pre-hazard event phase* evaluate how much the system, is ready to face unpredictable events. Indicators related to this phase mainly address the reduction of risks and vulnerabilities. For example, the existence of a mitigation plan is an indicator of this category. The indicators within the *emergency response phase* describe the ability and the speed of a system in responding the initial needs after an extreme event. Examples of these systems can be the fire, police, emergency relief services which are vital in the first moments of the turbulence situation. Finally the indicators within the category of the *reconstruction phase*, mainly address capacities to cope after a hazard event, measure the ability and the speed of a system to recover itself and reach its initial condition pre-event. As an example, home ownership, population income and poverty are indicators which affect the reconstruction phase level. It is also possible that some indicators can vary between all the temporal scales, such as population age etc.

3.7.3 Spatial Scale

This classification emphasizes the importance of quantifying place-specific indicators. In fact, the resilience indicators may refer to a small unit of analysis (e.g. single building unit), or can be related to a whole city or nation. This classification divide indicators according to five categories which are:

- Building unit;
- Building block;
- City/state;
- Region;
- Country;

At the *building unit scale* the resilience-based design considerations will be taken into account. For example, access/evacuation potential in buildings depends on the existence of emergency exit. The *neighborhood* is a part of a town or city, such as city center, immigrants quarter etc. The *region* is a part of a country that is different from other parts in some way, such as northern region, which can include some cities. The indicators in each category (neighborhood/city/region/country) are subsets of a larger group. The classification has been made just to facilitate resilience quantification in a proper scale. The first and the last groups will be also divided into smaller scales considering building type and the country level of development.

3.7.4 *Building Type*

This classification can be split in three groups:

- Critical facilities (e.g. hospitals, city-hall, etc.);
- Residential buildings;
- No building type;

Critical/essential facilities are those facilities that provide services to the community and should be operative after a hazard. They include hospitals, police stations, fire stations, schools etc. Examples of indicators which belong to the first group are for example the accessibility and the special needs for disabled, which is more necessary to take into account for essential facilities than residential buildings.

3.7.5 *Level of Development*

Two categories can be determined within this classification:

- Developed countries;
- Underdeveloped countries;

This classification is important because some indicators for lifelines (e.g. communication, transportation etc.) all depend on the country's infrastructures condition, which is different in *developed* and *under-developed* countries. So this classification affects the resilience assessment, because some indicators might not be applied in underdeveloped countries.

3.7.6 *Domains*

Indicators can also be classified according to their domains or perspectives. For example there are indicators referring to ecological and social-ecological resilience, psychological resilience, critical infrastructural resilience or organizational and institutional resilience (Birkmann et al. 2012). The categories which belong to this type of classification are:

- Social;
- Economic;
- Ecological/environmental;
- Governmental/welfare/institutional;
- Physical/infrastructural;

Below is given a brief description of each one of this category.

Social resilience: the ability of groups or communities to cope with external stresses and disturbances, such as Child and Elderly Services, Community Participation etc. *Economic resilience*: the ability of the economy to cope, recover, and reconstruct and therefore to minimize aggregate consumption losses. For example the economic development indicators that consist of financial services, industry- employment services and industry production. *Ecological/Environmental resilience*: is the capacity of an ecosystem to respond to a perturbation or disturbance by resisting damage and recovering quickly, such as biodiversity, water and air quality etc.

Governmental/welfare/institutional resilience: In contrast to the more or less spontaneous individual and neighborhood responses to extreme Events, governmental services are designed to allow an orderly response, for example legal and security services such as police, Emergency, and fire departments.

Physical/infrastructural resilience: this dimension focuses on a community's infrastructures, such as transportation, facilities, health care, etc.

3.7.7 Measurement Method

They belong to this classification two categories:

- qualitative indicators;
- quantitative indicators.

Whenever a description is made, qualitative or quantitative assessments are necessary because some aspects in life cannot be measured and shall be described without a scale. These indicators can be used to identify the important constituent characteristics that shape community resilience. However, the use of *qualitative indicator-based approaches* have the limitation that some indicators cannot be extent into further comparisons and it is not possible to generalize because sometimes these indicators propose their own frameworks and rely on specific perspectives. Aspects such as learning, reorganization, risk awareness or willingness are good examples of qualitative indicators. The use of these indicators is due to the fact that community resilience may be understood as a multi-faceted concept that goes beyond isolated capacities and views communities not only in spatial terms, but also recognize common interests, values and social structures (Twigg 2009). So, the disaster resilience community is defined as an ideal state, which in reality is never achievable.

An example of classification for qualitative indicators is to group them based on: *governance, risk assessment, knowledge and education, risk management and vulnerability reduction and disaster preparedness and response*. All these indicators include both outcome and process indicators and cover a broad range of topics. This classification has been provided by UNISDR and their “Making Cities Resilient” initiative (UNISDR 2012).

A different classification for qualitative indicators would be to organize the indicators on: organization and coordination, budget and incentives to invest in risk reduction, update data on *hazards and vulnerability*, *invest and maintain risk reducing infrastructure*, *assess the safety of critical infrastructure*, *enforce risk compliant building regulations*, *ensure education programs*, *protect ecosystems and natural buffers*, *install early warning systems* and last but not least, *ensure the needs of the affected population*. This kind of classification is done to address large communities, since most of the indicators focus on critical infrastructures, cover governmental aspects, education and training drills. The “Disaster Resilience Scorecard for Cities” (UNISDR 2012) is a good example of this type of approach. However a more common classification for qualitative indicators would be to gather the indicators in more general aspects such as: *external resources*, *assets*, *capacities and qualities*. Typical external resources are connections & information, services and natural resources. The assets can be split on human, social, political, environmental, economic and physical. The basic capacities to be considered resilient are *to be resourceful*, *to be flexible* and *to learn*. Finally, a resilient community has assets that are strong, well located, diverse, redundant and equitable. This classification was presented by the International Federation of Red Cross and Red Crescent Societies in 2012 about “Characteristics of a Safe and Resilient Community” (IFRC 2012).

It is important to highlight that is possible to make qualitative indicators “quantifiable”. There are several examples published like to use a “structured subjective” method (Forrester et al. 2015), coding schemes, to derive proxies or to use rating scale. However, it has to be noted that despite transferring qualitative indicators into quantitative metrics, the underlying information remains still subjective.

Qualitative indicator-based approaches take into account that resilience is a dynamic and multi-faceted concept that relates to multiple levels. Most approaches also define communities not only in spatial terms, but equally consider social and societal factors such as common interests and values of communities. These go beyond basic resources, capacities or assets of a disaster resilient community by identifying important qualities and processes.

On the other hand, *quantitative indicators* provide concrete metrics that are provided with data sources, justifications and sometimes the relationship to resilience. Aspects such as equity, diversity, efficacy, participation, coordination and communication are central pillars of such approaches indicators. The typical use of these indicators are single values that are added to a composite indicator, what makes them an attractive tool for informing the decision making process. However since not always is possible to quantify actions or aspects, quantitative indicators usually rely on proxy indicators, since often represent the only way to cover specific aspects of community resilience. One condition for quantitative indicators, in contrast to qualitative indicators, is that they have to be fully operationalized. For example, the indicator “percentage of citizens with access to a 4G connection mobile phones” is a fully operationalized quantitative/objective indicator, whereas “trust in politicians” is an example of qualitative/subjective indicator covering individual judgment or perceptions. One case of quantitative indicators

is to align them into domains such as social resilience (income and educational equality, presence of civic organizations, disaster volunteering, community health, well-being, equity...), economic resilience (livelihood stabilities, resource diversity...), community capital (as place attachment, political engagement, relationships between individuals...), institutional resilience (insurance coverage, disaster aid experiences, local disaster trainings, hazard mitigation and planning, urban development...), housing/infrastructural resilience (housing types, health care facilities, communication and transportation networks) and environmental resilience (risk and exposure, presence of protective resources, sustainability...) (Cutter et al. 2014). Another good example of quantitative indicator is the proposed by Cimellaro et al. (2015) to obtain a new resilience index for urban water distribution networks. This study proposes an index based on the product of three indicators: one describes the demand and is based on the number of users temporary without water; the second describes the capacity and is based on the tank water height; the third is based on the water quality. The first index is based on different indicators as number of households without water service, water volume, intensity, control time. The second one, related with capacity, takes into account the tank water level, the reserve capacity of the tank and the number of tanks. Finally, the index that estimates the quality of water uses qualitative indicators before and after the disruptive event. These indicators will help planners and engineers to evaluate the functionality of a water distribution system which consists in delivering a certain demand of water with an acceptable level of pressure and quality. The quantitative indicator-based approach provide concrete metrics which are able to cover different perspectives of community resilience.

3.8 Aggregation of Indicators

Typically the result of an analysis with different indicators, no matter the classification, is a **composite indicator** rather than numerous discrete indicators, since is easier to comprehend to the general public and to the policymakers as well (OECD 2008). Therefore decision makers request the aggregated results in most cases. The aggregation of indicators can support the illustration of a complex and multidimensional problem. In addition, the step of aggregation is combined often with a *weighting factor* for each indicator. Different weights might influence the aggregation results to a smaller or larger extent, generating a loss of underlying information. Moreover, when dealing with complex phenomena, a combination of individual components means often to compare datasets that have been generated from data sources of various statistical and scale levels. Therefore, the decision whether to aggregate should be carefully considered. The purpose of the study should be taken always into account, since is the main criterion. An aggregation may be useful if the outcome is intended to identify hot spots or to support the allocation of resources based on the comparison of different regions or communities. However, when the study main objective is to identify those aspects that lead to low resilience or has the main aim to develop strategies or select future activities to

increase resilience, the step of aggregation may be disregarded in favor of a more holistic view of how the disaggregated indicators fit into the bigger picture.

Whenever an aggregation is carried out it is absolutely necessary to make transparent which methodology has been applied and with which weight each individual indicator has contributed to the overall result. It is also highly recommended to keep hold of the information of the underlying individual components to be able to explain the reasons behind aggregating results.

3.9 Selection of Key-Indicators for Specific Case Study

The classification methods given in Sect. 3.7 may be used to select the *key-indicators* for a specific case study (e.g. building, community, etc.) from the list given in Sect. 3.4. Then in detail, the *key-indicators* are defined as indicators that:

- *are rated with a high importance by the case studies;*
- *are universally applicable;*
- *show a clear relation to resilience;*
- *were mentioned by more than one case study.*

Once the characteristics are established, a list with all the important indicators is ready to be composed. Some important indicators might not be considered in this list due to the applied criteria (especially the criteria “mentioned by more than one case study” reduces the list significantly), but this way of filtering allows communities to create a list of indicators that is concise and substantive.

3.10 Potential Challenges of Community Resilience Assessment Using Indicators

There exist potentials and advantages of *indicator-based approaches* for assessing community resilience and presents indicators that enable transferring theoretical and conceptual considerations into specific applications. The theoretical basis for grounding the indicators resides in the theory of change held by case study practitioners. These indicators can be classified or systematized in different groups for an easy understanding.

Community resilience is sometimes considered as a dynamic and steadily reshaping process that can be neither assessed through a static snapshot in time nor, alternatively, by considering “the resilient community” as an achievable end goal. Going beyond the assessment of only that which is simply measurable, it is aimed at capturing community resilience in its constituent facets including transformative aspects of resilience as well as different perspectives of communities.

Indicator-based approaches for assessing resilience are promising tools, because they allow – when evaluated at regular intervals – monitoring changes over time in both magnitude, direction and space (Cutter et al. 2010). They allow identifying

the major weaknesses or drawbacks of resilience. Resilience indicators help setting policy priorities, allocating resources – financial, personnel, technical, etc. – before and after a hazard event and evaluating the effectiveness of risk reduction efforts or emergency activities. The use of *qualitative indicators* for constant comparison and evaluation of changes in the spatial and temporal domain is more difficult than with *quantitative indicators*, because the data are subjective.

3.11 Relationship Between Vulnerability Indicators and Resilience Indicators

Resilience and *vulnerability* are related terms, even though the relationship between both concepts is not clearly defined.

Vulnerability focuses more on static stressors such as the exposure and sensitivity, and, respectively the hazard, exposure and disaster risk of the system, while resilience is a dynamic concept which adds transformative aspects such as learning, critical reflection or re-organisation.

Whereas research efforts on *vulnerability indicators* have increasingly provided useful indicators that are being applied in different fields of application (e.g. climate change vulnerability, hazard mitigation planning, social vulnerability etc.), the research efforts in *resilience indicators* is relatively slow due to the challenges that occur when implementing operational frameworks of resilience, and to the transformative nature of resilience.

3.12 The Progress of Grounding Indicators Set

Indicators can be grouped taking into account several aspects such as: the indicator title, the type of measurement used, the relationship of the indicator to resilience, the methods of data collection, the scale of application, the context- and hazard-specificity, the effort of indicator development and an evaluation of the overall importance of the indicator for determining resilience.

One of the main challenges of the indicator analysis is to synthesize the indicators identified by the different case studies, since they may differ considerably in terms of the applied scales, methods of data collection, types of natural hazards, and perspectives of community resilience. Some of the indicators for example may be related to the individual scale and be measured through interviews or questionnaires (e.g. “Belief in”), while others apply at the community scale and have to be measured with quantitative survey or existing statistics (e.g. “% of”). Therefore, first, it is useful to distinguish the indicators according to some criteria distinguishing indicators that can be measured with the help of qualitative research methods from indicators that can be better measured with quantitative methods; and also separating the indicators that can be applied across contexts from indicators that have to be used with local-context or hazard specificity.

3.13 Examples of Measurement Methods

In Table 3.7 is given a list of the different measurements methods to assess resilience categorized according to its *type*, the *spatial scale* and the *method*. Communities employing a bottom-up approach can develop or adapt simple measurement schemes to gauge their own baselines, capacities, assets or some combination of these. State and federal entities can equally develop comparative assessments of

Table 3.7 Methodologies to evaluate resilience

Measure name	Type	Spatial	Focus	Method
APIRE	Tool	Country	Whole community	Top down
BRIC	Index	USA counties	Whole community	Top down
CART	Tool	Community	Whole community	Botton up
CC RAM	Tool	Community	Whole community	Botton up
CDRI	Index	USA coastal counties	Whole community	Top down
Coastal Resilience index	Score-card	Community	Whole community	Botton up
CoBRA	Tool	Community	Whole community	Botton up
Community Resilience system	Tool	Community	Whole community	Botton up
Community Resilience index	Index	Community	Asset	Top down
CREAT	Tool	Infra-structures	Whole community	Top down
DFID Resilience	Tool	Country	Whole community	Botton up
FAO Livelihoods	Index	Community	Asset	Botton up
Financial system Resilience	Index	Infra-structures	Asset	Top down
FM Global Resilience	Index	Infra-structures	Whole community	Top down
NIST	Tool	Infra-structures	Whole community	Top down
Oxfam GB	Index	Community	Whole community	Botton up
PEOPLES	Tool	Community	Whole community	Top down
RCI	Index	USA metro areas	Asset	Top down
ResilUS	Tool	City	Asset	Top down
RMI	Index/Tool	Infra-structures	Whole community	Top down
Rockfeller 100 Resilience cities	Tool	Community	Whole community	Botton up
RRI	Index	Community	Whole community	Botton up
SPUR	Score-card	Community	Asset	Botton up
Surging Seas	Tool	USA coastal countries	Whole community	Top down
TNC Coastal Resilience	Tool	Coastal areas	Whole community	Top down
UNISDR Resilient cities	Tool	Cities	Whole community	Botton up
USAID Resilience	Tool	Countries	Whole community	Botton up

baseline or capacity indicators, but these must be approached differently and use consistent types of data to standardize the inputs. The progresses in enhancing resilience will generate changes in policy at local, state, and federal levels and within the public and private sectors. Such changes will require the development of a new set of tools and indicators that are co-produced and address the social dynamics and decision making within communities, as well as assessing baseline conditions and capacities in short, medium, and long terms.

3.14 Remark and Conclusions

Measurement tools and indicators cannot create a resilient community, but they can assess resilience and provide a community the directions for becoming safer, stronger, and more vibrant in the face of unanticipated events. This chapter emphasizes that it is important to decide and establish a norm to classify the indicators, but this classification can vary throughout the different case studies and/or projects. Several classifications are presented showing that there are many options available, so the more suitable classification should be determined based on the parameters that are going to be analyzed.

References

- Bank W (2015) Female labor force participation rate. <http://data.worldbank.org/indicator/SL.TLF.CACT.FE.ZS>
- Berke PR, Campanella TJ (2006) Planning for postdisaster resiliency. *Ann Am Acad Polit Soc Sci* 604(1):192–207
- Birkmann J, Chang Seng D, Abeling T, Huq N, Wolfertz J, Karanci N, İkizer G, Kuhlicke C, Pelling M, Forrester J, Fordham M, Deeming H, Kruse S, Julich S (2012) Systematization of different concepts, quality criteria, and indicators. emBRACE project
- Burby RJ, Deyle RE, Godschalk DR, Olshansky RB (2000) Creating hazard resilient communities through land-use planning. *Nat Hazards Rev* 1(2):99–106
- Burton CG (2015) Validation of metrics for community resilience to natural hazards and disasters using the recovery from hurricane katrina as a case study. *Ann Assoc Am Geogr* 105(1):67–86. doi:[10.1080/00045608.2014.960039](https://doi.org/10.1080/00045608.2014.960039)
- Center H (2002) Human links to coastal disasters. Report, Heinz Center for Science, Economics, and the Environment
- Cimellaro GP, Tinebra A, Renschler C, Fragiadakis M (2015) New resilience index for urban water distribution networks. *J Struct Eng, ASCE*. doi:[10.1061/\(ASCE\)ST.1943-541X.0001433](https://doi.org/10.1061/(ASCE)ST.1943-541X.0001433)
- Colten CE, Kates RW, Laska SB (2008) Three years after katrina: lessons for community resilience. *Environ: Sci Policy Sustain Dev* 50(5):36–47
- Cutter S, Boruff B, Shirley W (2003) Social vulnerability to environmental hazards. *Soc Sci Q* 84(2):242–261
- Cutter S, Barnes L, Berry M, Burton C, Evans E, Tate E, Webb J (2008) A place-based model for understanding community resilience to natural disasters. *Glob Environ Change* 18(4):598–606
- Cutter S, Burton C, Emrich C (2010) Disaster resilience indicators for benchmarking baseline conditions. *Homel Secur Emerg Manag* 7(1). doi:[10.2202/1547-7355.1732](https://doi.org/10.2202/1547-7355.1732)

- Cutter S, Ash K, Emrich C (2014) The geographies of community disaster resilience. *Glob Environ Change* 29:65–77
- Enarson E (2007) Identifying and addressing social vulnerabilities. ICMA, Washington, DC, pp 258–378
- Forrester J, Cook B, Bracken L, Cinderby S, Donaldson A (2015) Combining participatory mapping with q-methodology to map stakeholder perceptions of complex environmental problems. *Appl Geogr* 56:199–208
- Godschalk DR (2003) Urban hazard mitigation: creating resilient cities. *Nat Hazards Rev* 4(3):136–143
- Godschalk DR (2007) Mitigation. In: William JW, Kathleen Tierney L (eds) *Emergency management: principles and practice for local government*. ICMA press, Washington, DC, pp 89–112
- Gunderson LH (2009) Comparing ecological and human community resilience, CARRI research report 5. Community and Regional Resilience Institute, Oak Ridge
- IFRC (2012) Characteristics of a safe and resilient community. Community based disaster risk reduction study. Report, International Federation of Red Cross and Red Crescent Societies
- Kafle S (2012) Measuring disaster-resilient communities: a case study of coastal communities in indonesia. *J Bus Contin Emerg Plan* 5(4):316–326
- Meyer W (2011) Measurement: indicators – scales – indices – interpretations. In: Stockmann R (ed) *A practitioner handbook on evaluation*. Edward Elgar, Cheltenham, pp 189–219
- Mileti D (1999) *Disasters by design: a reassessment of natural hazards in the United States*. Joseph Henry Press, Washington DC, 18 May 1999
- Morrow B (2008) Community resilience: a social justice perspective (the community and regional resilience initiative research report 4). Community and Regional Resilience Initiative, Oak Ridge
- Murphy BL (2007) Locating social capital in resilient community-level emergency management. *Nat Hazards* 41(2):297–315
- Norris FH, Stevens SP, Pfefferbaum B, Wyche KF, Pfefferbaum RL (2008) Community resilience as a metaphor, theory, set of capacities, and strategy for disaster readiness. *Am J Community Psychol* 41:127–150
- OECD (2008) *Handbook on constructing composite indicators: methodology and user guide*. Report, <http://www.oecd.org/std/42495745.pdf>
- Pfefferbaum RL, Pfefferbaum B, Nitiéma P, Houston JB, Van Horn RL (2014) Assessing community resilience: an application of the expanded cart survey instrument with affiliated volunteer responders. *Am Behav Sci*. doi:10.1177/0002764214550295. <http://abs.sagepub.com/content/early/2014/09/24/0002764214550295.abstract>
- Renschler C, Frazier A, Arendt L, Cimellaro GP, Reinhorn AM, Bruneau M (2010) A framework for defining and measuring resilience at the community scale: the peoples resilience framework. Report NIST Technical Report GCR 10-930, NIST – U.S. Department of Commerce & National Institute of Standards and Technology
- Rodriguez-Llanes JM, Vos F, Yilmaz L, Guha-Sapir D (2013) Developing indicators and indicators systems of societal resilience to disasters: what prevent us from doing better? emBRACE project
- Ronan K, Johnston D (2005) *Promoting community resilience in disasters: the role for schools, youth, and families*. Springer, New York
- Rose A, Liao SY (2005) Modeling regional economic resilience to disasters: a computable general equilibrium analysis of water service disruptions. *J Reg Sci* 45(1):75–112. <GotoISI>://WOS:000226572800004, times Cited: 22
- Sylves R (2007) Budgeting for local emergency management and homeland security. In: waugh WL, Tierney K (eds) *Emergency management: principles and practice for local government*. International City Managers Association, Washington DC, pp 183–206
- Tierney K (2009) *Disaster response: research findings and their implications for resilience measures*. Report, CARRI Research Report 6, Community & Regional Resilience Institute

- Twigg J (2009) Characteristics of a disaster-resilient community: a guidance note (version 1) for the dfid disaster risk reduction interagency coordination group. Report, Community Research and Development Information Service
- UNISDR (2012) How to make cities more resilient: a handbook for local government leaders. United Nations, Geneva/New York
- Vale LJ, Campanella TJ (2005) The resilient city: how modern cities recover from disaster. Oxford University Press, Oxford
- Weichselgartner J, Kelman I (2014) Geographies of resilience: challenges and opportunities of a descriptive concept. *Prog Human Geogr*. doi:[10.1177/0309132513518834](https://doi.org/10.1177/0309132513518834)

Chapter 4

Damage Losses Assessment Models

Abstract The chapter focuses on the definition of a loss function which has been one of the first indicators used to determine resilience. Different models to evaluate the damage losses are provided, approaching the problem in probabilistic terms using fragility functions and analyzing the different type of uncertainties which appear in the resilience assessment.

4.1 State of Art on Loss Assessment Models

One of the biggest challenges faced when a seismic event occurs on a structure is to assess the magnitude of the effects caused by a catastrophic event in order to quantify the damages and provide a recovery strategy. Starting from the assumption that it is not possible to assess the aftermath of an earthquake until after it has happened, it may be possible instead to approach the problem in *probabilistic terms* and evaluate the losses through the use of numerical simulations. One of the inherent problems with current structural design practice is that seismic performance is not explicitly quantified. Instead, building codes rely on prescriptive criteria and overly simplified methods of analysis and design that result in an inconsistent level of performance. One way of quantifying earthquake performance that has been proposed by research Aslani and Miranda (2005), is the use of economic losses as a metric to gauge how well structural systems respond when subjected to seismic ground motions. While society and building owners main concern is the protection of life, there are other risks that have traditionally been ignored in earthquake-resistant design, such as the control of economic losses or the definition of an acceptable level of probability that a structure could maintain its functionality after an earthquake. Advancements in Performance-Based Earthquake Engineering (PBEE) methods have demonstrated the need for better quantitative measures of structural performance during seismic ground motions and have improved methodologies for estimating seismic performance. In order to provide a comprehensive discussion about this topic, it is convenient to follow the path taken by The Pacific Earthquake Engineering Research (PEER) Center, who has conducted a significant amount of research to address this need, by formulating a framework that quantifies performance in metrics that are more relevant to stakeholders, namely, deaths (loss

of life), dollars (economic losses) and downtime (temporary loss of use of the facility). The PEER methodology uses a probabilistic approach to estimate damage and the corresponding loss based on the seismic hazard and the structural response. The facility performance levels can be expressed qualitatively or quantitatively as shown in Sect. 4.7. *Qualitative performance levels* are the current state of practice and are related to the structural characteristics of the elements based on engineering ad-hoc judgments. On the other hand, *quantitative performance levels* permit to rigorously relate the performance levels of a facility to the structural characteristics of the facility. Economic losses in a facility due to earthquakes could represent a qualitative measure of seismic performance. It is useful to focus the attention on a classification of the economic losses due to a seismic event, assuming that the economic losses in a facility can be categorized as direct and indirect losses. Direct losses are those closely associated with repair or replacement costs of building components, whereas indirect losses are those resulting from the temporary loss of function (downtime) of the facility. In order to express a correct prediction of economic losses that may occur due to earthquake ground motions, it is first necessary to make an accurate prediction of the response of the structure when subjected to earthquake ground motions of different levels of intensity. One of the possible solutions to reach the objective is to use a Probabilistic Seismic Hazard Analysis (PSHA): a rational procedure through which it is possible to estimate the annual probability of exceedance of spectral ordinates at a given site by taking into account the location and seismicity of all possible seismic sources that can affect the site. The next step would be a Probabilistic Seismic Structural Response Analysis (PSSRA), which extends a PSHA to the estimation of the annual probability of exceedance of the Engineering Demand Parameter (EDP). The use of response history analyses applying accelerograms scaled at various levels of intensity to investigate the response of structures at various levels of ground motion intensity has been also referred to as “dynamic pushover analysis” (Luco and Cornell 1998) or “incremental dynamic analysis” (Vamvatsikos and Cornell 2001).

4.2 Regional Seismic Losses Assessment Models (RSLA) for Ordinary Buildings

Most of the research related to PBEE has focused on quantifying the possible risks to individual buildings. However, parties interested in a group of geographically distributed buildings, such as policy makers, insurers, practicing engineers working in city planning and real-estate developers, need to make risk-informed decisions on a regional or portfolio, rather than an individual building, basis (Liel and Deierlein 2012). For this reason, over the past decade, researchers have developed methods to extend PBEE to assess the risk of earthquake-induced losses for groups of buildings (hereafter referred to as “Regional Seismic Loss Assessment of buildings (RSLA)”). These methods predict the expected loss, as well as the variation therein, recognizing

that risk-informed decision-making depends upon quantifying the likelihood of experiencing rare, but catastrophic levels of loss (Haimes 1998).

There are many sources of uncertainty affecting the prediction of earthquake-induced regional losses, such as those associated with the characteristics of earthquakes, the properties of ground shaking at different sites, the building response and capacity, the fragility of building components, the costs of repairing damage, etc.

Probabilistic regional seismic loss assessment methods rely on Monte Carlo simulation because of the elevated number of uncertainties and the lack of closed-form solutions available to propagate them through the loss assessment process. This amounts to repeating the loss assessment for different sets of probabilistically characterized input random variables to develop a suite of “regional loss realizations” from which statistics for the mean and variance in regional loss can be obtained.

Regional loss studies aim at the estimation of economic losses for a large number of buildings, while on the other hand the Building-specific loss estimation studies aim at providing more accurate estimations of economic losses for specific buildings located at specific sites. Regional methods do not provide the necessary level of detail required by performance-based earthquake engineering (Aslani and Miranda 2005), but they can be used when Resilience analyses want to be taken at the regional level. Regional loss estimations attempt to quantify losses for a large number of buildings within a specific geographic area. One of the first investigations to explicitly consider the probabilistic nature of seismic-induced monetary losses was the study by Whitman et al. (1973), which introduced the concept of damage probability matrices into loss estimation methodology, where damage ratios were used to describe the amount of estimated damage, and seismic intensity was expressed as a function of Modified Mercalli Intensity (MMI), which was the selected ground motion intensity measure. In 1992, the Federal Emergency Management Agency (FEMA) and the National Institute of Building Sciences (NIBS) began funding the development of a geographic information system (GIS)-based on regional loss estimation methodology which eventually was implemented in the widely-used computer tool (Hanus 2014). HAZUS is a natural hazard loss estimation methodology implemented through PC-based Geographic Information System (GIS) software developed under agreements with the National Institute of Building Sciences (NIBS). HAZUS as well as the more recent regional loss estimation studies have been conducted developing empirical fragility functions for different classes of building constructions, different typologies of buildings and for several time- and frequency-dependent ground motion parameters. More details about the software can be found in Sect. 14.4.1.

4.3 Seismic Loss Assessment for Infrastructure Systems

In the past decades, research has been focusing on the response of a complex urban lifeline system under external perturbations. Some approaches adopt *analytical system reliability frameworks* to estimate the probabilities of complex system

events (Dotson and Gobien 1979; Kang et al. 2008; Li and He 2002; Song and Der Kiureghian 2003) while others rely on *simulation models* to estimate seismic performance of a lifeline system (Hwang and Shinozuka 1998; Shinozuka et al. 2007; Werner et al. 2000). These approaches generally incorporate the vulnerability of components represented by fragility curves in a system level analysis.

Analytical system reliability approaches evaluate statistical measures, such as the probability of system events (e.g., availability of a path from a node to another node) and their associated cut-sets. These approaches are flexible and applicable to generic networks, but they are not applicable to large networks, because the number of system events related to computation is an exponential function of the size of networks, and additional measures beyond statistical ones (e.g., imbalance between supply and demand in power grid and drivers' delay in transportation networks) are required to predict the functional loss of a system (Li and He 2002; Hwang and Shinozuka 1998). On the other hand, *simulation-based approaches* generally use system-specific flow analysis algorithms to compute properties of interests in a system that cannot be obtained from system reliability analysis. Although the simulation-based approaches can require a large number of simulations to achieve acceptable accuracy, and computer run time can be excessive, the obtained properties provide important information to social scientists for quantifying socioeconomic impacts, which is beneficial in comprehensive pre-disaster planning and consequence estimation.

4.4 Loss Function as Resilience Indicator

In statistics a loss function represents the a measure of the degree of inexactness (generally the difference between the estimated value and the true or desired value). Loss estimation has to be defined using damage descriptors that can be easily translated in monetary terms and a series of parameter units that can be measured or counted (e.g. the number of bridges available in a network, or the total length of viable roads). The loss estimation procedure is by itself a source of uncertainty and therefore the problem has to be taken into account in probabilistic terms. In fact, earthquake losses are by nature highly uncertain, and assume a different value for every scenario considered. Despite this, it is still possible to identify some common parameters affecting those losses.

The loss function $L_{I,T_{RE}}$ can be defined in general as a function of earthquake intensity I and recovery time T_{RE} . The total losses can be divided into two types: Structural losses (L_S), which occur “instantaneously” during the disaster, and Non-Structural losses (L_{NS}), which also have temporal dependencies.

$$L(I, T_{RE}) = L_S(I) + L_{NS}(I, T_{RE}) \quad (4.1)$$

For simplicity, and L_{NS} are described in such a way that it is possible to express the physical structural losses as ratios of building repair and replacement costs using the following relation

$$L_s(I) = \sum_{j=1}^n \left[\frac{C_{S,j}}{I_s} \cdot \prod_{i=1}^{T_i} \frac{(1 + \delta_i)}{(1 + r_i)} \right] \cdot P_j \left\{ \bigcup_{i=1}^n (R_i \geq r_{lim_i}) / I \right\} \quad (4.2)$$

where P_j is the probability of exceeding a performance limit state j if an extreme event of intensity I occurs, I is also known as the fragility function; $C_{S,j}$ are the building repair costs associated with a j damage state; I_s are the replacement building costs; r is the annual discount rate; t_i is the time range in years between the initial investments and the time of occurrence of the extreme event; δ_i is the annual depreciation rate. The description of the different methodologies to build fragility curves using performance limit states which might be also uncertain is given in Sect. 4.7.2. Equation (4.2) assumes that the initial value of the building is affected by the discount rate, but the value also decreases with time according to the depreciation rate δ_i , which may vary with time. The nonstructural losses L_{NS} consist of four contributions:

1. Direct economic losses $L_{NS,DE}$ (or Contents losses);
2. Direct Causalities losses $L_{NS,DC}$;
3. Indirect economic losses $L_{NS,IE}$ (or Business interruption losses);
4. Indirect Causalities losses $L_{NS,IC}$;

They are all function of the recovery period. Nonstructural direct economic losses $L_{NS,DE(I)}$ are obtained for every non-structural component k used in the affected system via a formulation similar to Eq. (4.1). The total non-structural direct economic losses are obtained using a weighted average expression as

$$L_{DE}(I) = \left(\sum_{k=1}^N w_k \cdot L_{NS,DE,k}(I) \right) / N_{NS} \quad (4.3)$$

where $L_{NS,DE,k}(I)$ is the non-structural direct economic losses associated with the component k , N_{NS} is the total number of non-structural components in the buildings and w_k is an importance weight factor associated with each non-structural component in the building, that have to be considered in the general model. Direct causalities losses $L_{NS,DC}$ are measured as a ratio of the number of damaged items N_{in} and the total number of items presented before the event N_{tot} . In the particular case of loss estimation for a building, it can be the ratio between the number N_{in} of injured people (including deaths) over the total number N_{tot} of people in the building.

$$L_{NS,DC}(I) = \frac{N_{in}}{N_{tot}} \quad (4.4)$$

The *indirect economic losses* $L_{NS,IE}(l, T_{RE})$ are time dependent. Because of the different forms these losses can take, they are the most difficult to quantify among the post-earthquake losses. For example, they mainly consist of business interruptions, relocation expenses, rental income losses, etc. Losses of revenue, both permanent and temporary, can be the consequence of damage suffered by structures and contents; this aspect is fundamental and must be taken into account during evaluations of lifelines. A good example may be the structural damage due to the collapse of a bridge span in a major highway. This event generates direct losses, as well as indirect losses subsequent to the loss of revenues as a consequence of impact on the traffic to businesses served. In other cases, there may be some indirect losses due to the disruption that can be more significant than the direct losses. Starting from these considerations, a model is evaluated in which losses due to business interruption should be modeled considering both the structural losses, and the time necessary to repair the structure T_{RE} (Scott and Stephanie 2006). Those quantities are related because the recovery time T_{RE} increases with the extent of structural damage $L_S(I)$. In addition, indirect casualties losses L_{IC} belong to the group in Eq. (4.4).

So, in summary the total non-structural losses L_{NS} can be expressed as a combination of the total direct losses $L_{NS,D}$ and the total indirect losses $L_{NS,I}$.

Direct losses $L_{NS,D}$ and indirect losses $L_{NS,I}$ are also expressed as combination of economic ($L_{NS,IE}$, $L_{NS,DE}$) and casualties ($L_{NS,IC}$, $L_{NS,DC}$) losses as follows

$$L_{NS} = (L_{NS,D} + \alpha_1 L_{NS,I}) \quad (4.5)$$

where

$$L_{NS,D} = L_{NS,DE}^{\alpha_{DE}} (1 + \alpha_{DC} L_{NS,DC}) \quad (4.6)$$

$$L_{NS,I} = L_{NS,IE}^{\alpha_{IE}} (1 + \alpha_{IC} L_{NS,IC}) \quad (4.7)$$

and where α_I is the weighting factor related to indirect losses, α_{DE} is a weighting factor related to construction losses in economic terms; α_{IE} is a weighting factor related to general business interruption; α_{DC} , α_{IC} are the weighting factors related to the nature of occupancy (i.e. schools, critical facilities, density of population). These weighting factors are all determined by socio-political criteria (i.e. cost benefit analyses, emergency functions, social factors, etc.). In the end, L_S and L_{NS} are summed together to obtain the total loss function. The loss function can be used as possible resilience indicator that is time dependent, because it includes the immediate losses caused by the disaster and the post disaster losses with change through the time. However to have a complete description of resilience it is necessary to define the restoration process which is described in the next Chap. 5. Before moving in the description of the recovery models it is necessary to define the different methodologies to determine the probability P_j of exceeding a performance limit state.

4.5 State of the Art on Fragility Curves

Awareness of the potential seismic hazard and the corresponding vulnerability of structures affecting urban areas that created serious economic and social impact have been increasing following recent earthquakes. The prediction of structural damage is critical for the evaluation of the economic losses in earthquake regions and it should be estimated with an acceptable degree of credibility, in order to mitigate potential losses dependent on the seismic performances of structures. Performance can be characterized through fragility functions that express the conditional probability that the building or a component is in, or exceeds, a particular damage state. Major efforts were made in the past in defining, evaluating and quantifying the fragility of structures, following different strategies and approaches. Various studies used Monte Carlo simulations to calculate fragility functions related to a specified structural model, such as Hwang and Huo (1994), Fukushima et al. (1996), Shinozuka et al. (2000a), Karim and Yamazaki (2001), and Kafali and Grigoriu (2005). Other studies developed empirical fragility functions using damage records resulting from past earthquakes, such as Basoz and Kiremidjian (1997) and Shinozuka et al. (2000b). Reinhorn et al. (2001) developed an analytical procedure to evaluate fragility of inelastic structures based on spectral response-capacity analysis and a probabilistic estimate of dynamic response. Karim and Yamazaki (2001) developed an analytical approach for constructing fragility curves of piers of bridges, using nonlinear dynamic response of an equivalent single degree of freedom model of the pier obtained by static pushover analysis. Gardoni et al. (2002) developed a methodology to construct probabilistic capacity models of structural components using a Bayesian approach where the originality of their method consisted in adding correction terms that explicitly describe the inherent systematic and random errors to existing deterministic models already available in literature. However, the developed model can be only applicable to structural systems that have geometry and material properties within the range of observations used to assess the model. Ramarmoorthy et al. (2006) developed fragility curves to assess the seismic vulnerability of a generic two stories reinforced concrete frame using a Bayesian methodology that takes into account aleatoric and epistemic uncertainties. Chaudhuri and Hutchinson (2006) presented an analytical evaluation of fragility curves for a range of rigid, sliding dominant equipment mounted on bench surfaces. In their study, the authors included the uncertainties of friction coefficient and supporting characteristics separately. Goulet et al. (2007) presents a state-of-the-art seismic performance assessment where fragility curves are used to evaluate probabilities of component damage. The emphasis of this study is on the estimation of the expected annual losses and the uncertainties involved in the evaluation of this decision variable, while less effort is made in presenting the procedure of evaluating the fragility curves. Porter et al. (2007) summarized six procedures to evaluate experimental fragility functions, which are considered in the development of a standard for (ATC-58), however not all the procedures available in literature are addressed. More recently, Williams et al. (2009) presented

a decision-making methodology to evaluate the benefit of seismically retrofitting existing structures, focusing on the effect of loss reduction, investment return period and retrofitting costs on the feasibility of seismic retrofitting and evaluating the probability of failure combining the conditional probability with the probability of occurrence of a seismic event. Although several works are referenced in this introduction, the survey is by no means comprehensive and it is presented here to highlight several distinct techniques. The limit of the approaches above is that they cannot be verified by laboratory testing, because such verifications require multiple physical models, brought to failure, which are prohibitively expensive and of long duration. Recently FEMA (2007) proposed a standard protocol developed for ATC-58 to evaluate performance of structural and nonstructural components that tries to solve the economical constraints of laboratory specimens by using multiple initial assumptions.

4.6 Analytical Formulation

Seismic fragility functions represent the probability that the maximum response $\mathbf{R}(\mathbf{x}, I, t) = \{R_1, \dots, R_n\}$ of a specific component, structure, or family of structures, exceeds a threshold $\mathbf{R}_{LS}(\mathbf{x}, I) = \{R_{LS1}, \dots, R_{LSn}\}$ associated with a desired limit state, conditional on the *earthquake intensity measure*, I . The response \mathbf{R} and the response thresholds \mathbf{R}_{LS} are functions of the same structural/nonstructural properties of the system \mathbf{x} , the ground motion intensity I and the time t . In the formulation, it is assumed that the response threshold $\mathbf{R}_{LS}(\mathbf{x})$ does not depend on the ground motion history, while the i th response $R_i(\mathbf{x}, I, t)$ of any component or structure is represented by its maximum value over the duration of the response history, $R_i(\mathbf{x}, I)$. The detailed description of dependence of the response, $\mathbf{R}(\mathbf{x}, I)$, on \mathbf{x} and I , and the dependence of the response threshold $\mathbf{R}_{LS}(\mathbf{x})$ on \mathbf{x} will be omitted in the following formulation for simplicity of presentation. Additionally, the chapter follows the standard convention of denoting random variables in capital letters and constants in lowercase letters. With these assumptions, the general definition of fragility F_{RLS} based on earthquake intensity I can be written as

$$F_{RLS}(i) = P(R_i \geq r_{LSi} | I = i) \quad (4.8)$$

where R_i = i th random variable of the response that can be either a deformation quantity, such as interstory drifts, or a force quantity, such as bending moment or shear force, or a combination thereof, or any other measure of damage for which adequate capacity models exist (Badillo-Almaraz and Cimellaro 2006); $r_{LS,i}$ = response threshold, or limit state, related to a certain functionality or damage; I = *earthquake intensity measure*, which can be represented by PGA = Peak Ground Acceleration; PGV = Peak Ground Velocity; PVS = Pseudo Velocity Spectrum; MMI = Modified Mercalli Intensity scale etc.; and i = a given earthquake intensity value. Even though the earthquake intensity measures above have mostly been used

in seismic fragility analysis, a definition of fragility based on *earthquake hazard* (e.g. return period T_r of a given earthquake event, annual probability of exceedance λ , etc.) can also be valuable because seismic hazard curves or maps are generally represented using the return period of the design earthquake. Therefore, in this chapter seismic fragility curves are developed as a function of the return period by utilizing the probability density function interpolation technique (Cimellaro et al. 2006; Yi et al. 2007). In order to find the expression of fragility curves as function of the earthquake hazard, two assumptions are necessary: (i) the structural responses are log-normally distributed under earthquake ground motions corresponding at the same probability of exceedance in Eq.(4.8); (ii) the *seismic hazard curves* of the structural responses are described by the following expression (Cornell 1996):

$$\lambda = H(r_{LS})_{1yr} = P(R \geq r_{LS})_{1yr} = 1/T_r = K_0 \cdot r_{LS}^{-K_1} \quad (4.9)$$

where λ = average annual frequency of exceedance of a given response threshold; $H(\cdot)$ = seismic hazard curve function; T_r = return period between two exceeded response thresholds, K_0 and K_1 = parameters representing the seismic hazard curve. The estimate of λ is a function of the geometry and material properties of the specific structure and therefore it needs to be estimated for each specific building.

In order to determine the fragility function based on *earthquake hazard* H , it is necessary to determine the probability density function (PDF) of an arbitrary maximum structural response, R_i , at a given annual probability of exceedance. Therefore, it is assumed that the maximum structural response R is log normally distributed and expressed as follows

$$f_R(r) = \begin{cases} \frac{1}{r\sigma_{\ln R}\sqrt{2\pi}} \cdot e^{-\frac{(\ln(r)-m_{\ln R})^2}{2\sigma_{\ln R}^2}} & r \geq 0 \\ 0 & elsewhere \end{cases} \quad (4.10)$$

where $m_{\ln R}$ and $\sigma_{\ln R}$ are the log-mean and the log-standard deviation values, respectively. According to Eq. (4.10), the two seismic hazard curves of the median (m_R) and deviated (σ_R) values of the response R are expressed as follows:

$$\lambda_{m_R} = H(r_{LS})_{1yr} = P(m_R \geq r_{LS})_{1yr} = K_{0,m} \cdot r_{LS}^{-K_{1,m}} \quad (4.11)$$

$$\lambda_{\sigma_R} = H(r_{LS})_{1yr} = P(\sigma_R \geq r_{LS})_{1yr} = K_{0,\sigma} \cdot r_{LS}^{-K_{1,\sigma}} \quad (4.12)$$

where $K_{0,m}$, $K_{1,m}$, $K_{0,\sigma}$ and $K_{1,\sigma}$ = constants of the median m_R and the deviated σ_R values, respectively, which are calculated using linear regressions. The log-mean $m_{\ln R}$ and the log-standard deviation $\sigma_{\ln R}$ values are related to the median m_R and the deviated σ_R values through the following expression:

$$m_R = e^{m_{\ln R}}, \sigma_R = e^{m_{\ln R} - \sigma_{\ln R}} \quad (4.13)$$

Therefore, the log-mean $m_{\ln R}$ and the log-standard deviation $\sigma_{\ln R}$ values at a given annual frequency of exceedance (or return period t_r) are given by the following expression:

$$m_{\ln R}(t_r) = -\frac{1}{K_{1,m}} \log\left(\frac{1}{t_r \cdot K_{0,m}}\right) \quad (4.14)$$

$$\sigma_{\ln R}(t_r) = m_{\ln R} + \frac{1}{K_{1,\sigma}} \log\left(\frac{1}{t_r \cdot K_{0,\sigma}}\right) \quad (4.15)$$

Back-substituting Eqs. (4.14) and (4.15) into Eq. (4.10), the PDF of the maximum structural responses corresponding to a given annual frequency λ or return period t_r is obtained as follows:

$$f_R(r, t_r) = \begin{cases} \frac{1}{r\sigma_{\ln R}(t_r)\sqrt{2\pi}} \cdot e^{-\frac{(\ln(r) - m_{\ln R}(t_r))^2}{2\sigma_{\ln R}(t_r)^2}} & r \geq 0 \\ 0 & elsewhere \end{cases} \quad (4.16)$$

Finally, the definition of fragility based on *earthquake hazard H* is given by the following integral:

$$F_{R_{LS}}(t_r) = P(R_i \geq r_{LSi} | T_r = t_r) = \int_{r_{LS}}^{\infty} f_R(r, t_r) dr \quad (4.17)$$

where the hazard is given by the return period, t_r of a given earthquake event. It is important to mention that there is not a one-to-one correspondence between earthquake intensity, I , and earthquake hazard, H as shown in Fig. 4.1.

In fact, different values of earthquake intensities I (PGA , PGV , PVS , S_a and etc.) can correspond to a unique earthquake hazard (e.g. T_r , the annual frequency of exceedance λ etc.).

The advantage of the second formulation in Eq. (4.17), with respect to Eq. (4.8), is that it takes into account directly the uncertainties of occurrence in estimating the earthquake intensity parameters I at the site. Therefore, in professional practice, buildings are designed according to a given return period T_r , that is related to a given earthquake event. It is possible to directly use the expression of fragility function given in Eq. (4.17) for evaluating directly the probability of functionality, or damage, of the system. The details about the method for generating fragility curves according to Eq. (4.17) are given in the following paragraphs. When the number of response parameters to be checked is n , the definition of fragility given in Eq. (4.17) can be written in the following form:

$$F_{R_{LS}}(t_r) = P\left(\bigcup_{i=1}^n (R_i \geq r_{LSi}) | T_r = t_r\right) = \int_{r_{LS}}^{\infty} f_R(r, t_r) dr \quad (4.18)$$

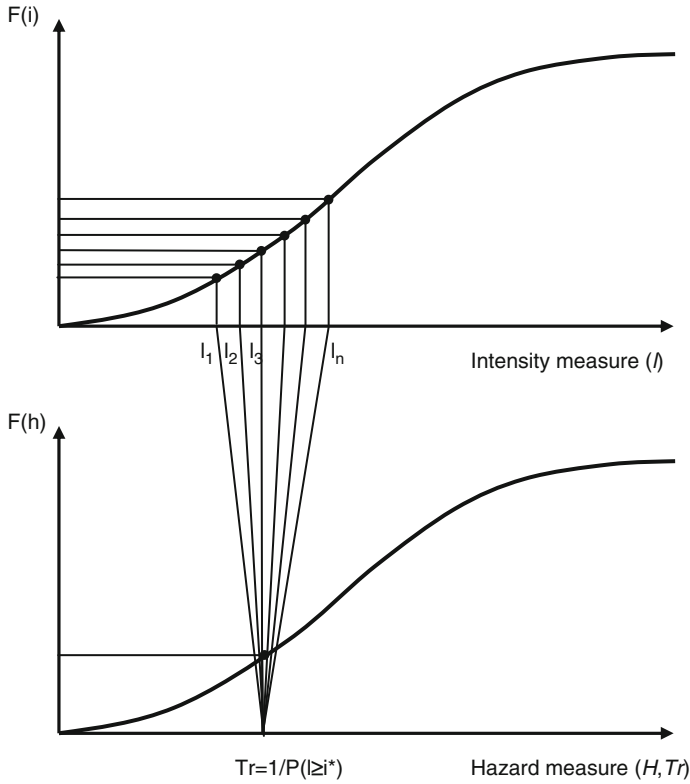


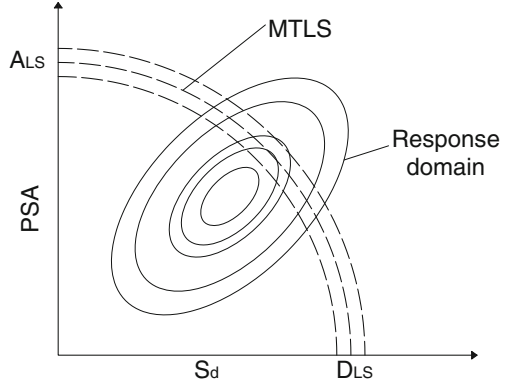
Fig. 4.1 Earthquake intensity versus earthquake hazard fragility curves

where the first right term of Eq. (4.18) is the conditional probability based on the earthquake hazard of the multi-component response exceeding a multidimensional limit state. When the problem is reduced to a bi-dimensional case considering for instance, displacements and accelerations at a specific story of a building, the fragility curve in Eq. (4.18) can be determined using the following expression:

$$\begin{aligned}
 F_{\mathbf{R}_{LS}} \left[\begin{array}{c} D_{LS} \\ A_{LS} \end{array} \right] (T_r = t_r) &= P((\Delta \geq D_{LS}) \cup (Z \geq A_{LS}) | T_r = t_r) = P((\Delta \geq D_{LS}) | T_r = t_r) + \\
 &+ P((Z \geq A_{LS}) | T_r = t_r) - P((\Delta \geq D_{LS}) (Z \geq A_{LS}) | T_r = t_r)
 \end{aligned}
 \tag{4.19}$$

where Δ = a random variable representing the displacement response, Z = a random variable representing the acceleration response, D_{LS} = displacement threshold, A_{LS} = acceleration threshold and $(\Delta \geq D_{LS})$ and $(Z \geq A_{LS})$ are assumed to be two independent events. The response of the structure can be visually represented for two variables by a “bell surface” (Bruneau and Reinhorn 2007) where the

Fig. 4.2 Response domains and the multidimensional threshold limit state



x-axis is the spectral displacement S_d , the y-axis is the pseudo-spectral acceleration, designated here as S_a , and the z-axis is the probability of occurrence (Fig. 4.2). This surface is the joint probability density function of the response expressed in terms of the two variables, the maximum spectral displacement S_d and the maximum spectral acceleration S_a that are assumed to be log-normally distributed.

4.7 Definition of Performance Limit States

4.7.1 Multidimensional Performance Limit State Function

The evaluation of fragility requires a definition of a threshold vector R_{LS} , representing the given limit state. The response vector R and the threshold vector R_{LS} being used in the estimation of fragility must have the same components (e.g. acceleration, drift etc.). Usually, the components of the threshold vector are assumed mutually independent. However for various systems in a structure or substructure, combinations of mutually dependent components, such as accelerations, displacements, drift, velocities, etc., can represent their limits of functionality, or damage. The generalized **Multidimensional Threshold Limit State** (MTLS) function provides a tool that allows consideration of these dependencies among different components of the threshold vector related to different quantities. The MTLS function $g(R, R_{LS})$ for the case in which n different types of response parameters are considered simultaneously can be defined in n -dimensional form by the mathematical “surface”

$$g(\mathbf{R}, \mathbf{R}_{LS}) = \sum_{i=1}^n \left(\frac{R_i}{R_{LS,i}} \right)^{N_i} - 1 \quad (4.20)$$

where R_i = i th component of the response vector (e.g. drifts, accelerations, forces, velocities, etc.); $R_{LS,i}$ == i th component of the threshold vector, representing the

one-dimensional (1D) limit states and N_i = interaction factors determining the shape of the n-dimensional surface. The limit state defining the boundary between desired and undesired performance corresponds to $g = 0$. When $g < 0$ the structure is safe, while when $g \geq 0$ the structure is not safe (undesired performance). The relation among different thresholds' parameters can be determined through calibration of the MTLs function that is obtained using probabilistic analysis, or engineering judgment based on field reconnaissance data collected after an earthquake or derived from laboratory tests. The model can also be continuously updated as soon as more data are available using the Bayesian approach proposed by Gardoni et al. (2002) and adding correction terms to the proposed limit state function. The MTLs function can be used "locally" to describe the limit state of a single nonstructural component (e.g., scientific equipment, piping and utility systems, etc.) or "globally" to describe the limit state of a part of a sub-structural system (e.g. building story level) or to describe the entire building structure including its nonstructural components. This model can be used to construct fragility curves considering different response parameters (e.g. forces, displacements, velocities, accelerations etc.) combined in a unique fragility formulation. In the proposed formulation, the limit states can be considered either linear or nonlinear dependent, or independent. All these options can be formulated as particular cases of the more general case, with a suitable choice of the parameters involved. In bi-dimensional form, the MTLs function in Eq. (4.18) can be seen in Fig. 4.2 and expressed by the following equation:

$$g(\mathbf{R}, \mathbf{R}_{LS}) = \left(\frac{A}{A_{LS}} \right)^{N_a} + \left(\frac{D}{D_{LS}} \right)^{N_b} - 1 \quad (4.21)$$

where A_{LS} and D_{LS} = acceleration and drift limit thresholds, respectively; A and D = peak acceleration and displacement response, respectively; N_a and N_b = coefficients determining the shape of the limit state surface. The thresholds A_{LS} , D_{LS} and the coefficients N_a and N_b are determined from either (1) field investigations after an earthquake or from (2) laboratory experiments. The first procedure implies collecting past earthquake field data (Shinozuka et al. 2000a,b). Damage data are related to drifts and they can be determined by field observations, while acceleration thresholds can be determined in the field only when the building is monitored with accelerometers. However, other types of damage data can be determined from laboratory experiments (e.g. number of tiles that fell out of a suspended ceiling) (Badillo-Almaraz and Cimellaro 2006; Retamales et al. 2006). The advantage of the latter procedure is that a range of earthquake intensities can be applied in a controlled fashion to the structure of interest, and inter-story drifts, accelerations, or other parameters, can be monitored and measured more accurately than in the field. However, both methods require multiple outcomes (e.g. structural collapses), which are prohibitively expensive in costs (in laboratory experimental tests) and human lives (in real earthquakes). Therefore, such limit thresholds would have to be derived by numerical analyses using basic engineering principles and rules of mechanics. When the MTLs function is calibrated, A_{LS} and D_{LS} can be assumed as either random variables, or deterministic quantities, either dependent or independent.

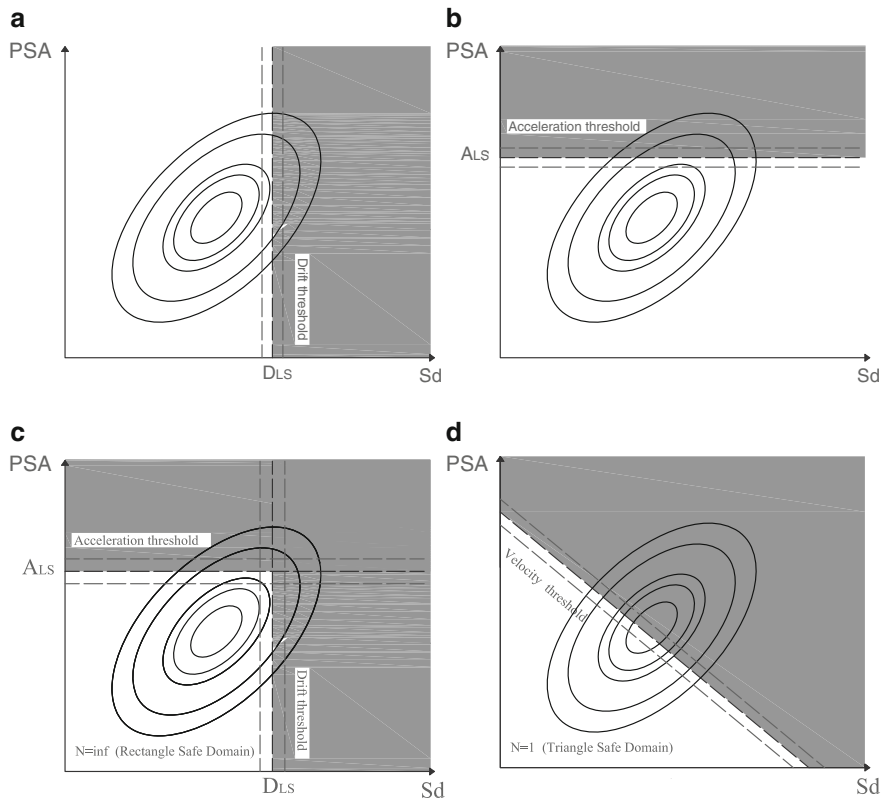


Fig. 4.3 Threshold limit states: (a) drift threshold limit state; (b) acceleration threshold limit case; (c) independent acceleration and inter-story drift limit states; (d) velocity limit state

All cases can be considered as particular realizations of the general Eq. (4.18). The two-dimensional (2D) MTLs function in Eq. (4.19) is considered for illustrative purposes. For example, the most common and simplest form of performance function considers only the drift as one-dimensional threshold and it can be obtained assuming $A_{LS} = \infty$; therefore Eq. (4.19) becomes

$$g(\mathbf{R}, \mathbf{R}_{LS}) = \left(\frac{D}{D_{LS}} \right)^{N_b} - 1 \quad (4.22)$$

where D = displacement response; D_{LS} = displacement threshold that can be either a deterministic or a random variable (Fig. 4.3). In order to be safe, $g \leq 0$ implies $D \leq D_{LS}$. Alternatively, if acceleration limit state is given, then this can be determined assuming $D_{LS} = \infty$, therefore Eq. (4.19) becomes

$$g(\mathbf{R}, \mathbf{R}_{LS}) = \left(\frac{A}{A_{LS}} \right)^{N_a} - 1 \quad (4.23)$$

As shown in Fig. 4.3b where A = acceleration response; A_{LS} = acceleration threshold that can be either a deterministic or a random variable. In order to be safe, $g \leq 0$ implies $A \leq A_{LS}$. The shape of the performance function is useful for nonstructural components such as acceleration sensitive equipment (i.e. computers, electric devices, lab equipment, etc.). Damage to this type of nonstructural components has gained significant attention following recent earthquakes, because in essential facilities like hospitals, failure of such equipment may hinder emergency response immediately after an earthquake. Most of these components are short and rigid and are dominated by a sliding-dominated response (Chaudhuri and Hutchinson 2006). The case in which both accelerations and inter-story drifts thresholds are considered as independent limit states can be determined from the generalized MTLs function in Eq. (4.19) by imposing $N = N_a/N_b = \infty$ (Fig. 4.3c)

$$g(\mathbf{R}, \mathbf{R}_{LS}) = \left(\frac{A}{A_{LS}}\right)^{\infty} + \left(\frac{D}{D_{LS}}\right) - 1 \quad (4.24)$$

In fact, if $A/A_{LS} \leq 1$ then ; therefore Eq. (4.24) reduces to

$$g(\mathbf{R}, \mathbf{R}_{LS}) = \frac{D}{D_{LS}} - 1 \quad (4.25)$$

that corresponds to the inter-story drift limit state given in Eq. (4.24). By imposing the safety condition ($g \leq 0$) in Eq. (4.24), then, therefore Eq. (4.24) becomes the acceleration limit state given in Eq. (4.23). On the other hand, assuming a linear relationship between acceleration and inter-story drift limit states for $N = N_a/N_b = 1$, a velocity limit state is obtained, as shown in Fig. 4.3d.

4.7.2 Uncertainties of Limit States

The PLS represent the level of response for a certain functionality limit, or for a specific damage condition. The limits of functionality or of damage depend on mechanical properties, such as strength and deformability, which are in themselves uncertain and therefore in literature are available Bayesian approaches that properly account for all the most relevant uncertainties (Gardoni et al. 2002). Unfortunately, current engineering practice in developing fragility curves is still based on deterministic PLS, usually obtained from scientific/engineering laws, observational data from laboratory experiments or field investigations, design standards, engineering experience, subjective judgment and etc. The main reason for this choice is justified by the fact that the uncertainty in the earthquake load is considerably larger than the uncertainty in the PLSs themselves. In this section, PLSs are considered as random variables, and are defined in terms of both inter-story drifts and accelerations, since the functionality and the failure modes in the case study (presented later) are

governed by both. Several cases are considered for the estimation of the fragility related to specific PLS, assuming that the limit thresholds are random variables. For simplicity of explanation, only two response parameters are considered: inter-story drift and floor acceleration. It is assumed that the peak responses have a lognormal distribution, which is used to model positive random variables, following Clough and Penzien (1993). Additionally, Cimellaro et al. (2009) have verified the assumption comparing different PDF (normal, Gumbel, and log-normal) for different structural configurations and results showed that the lognormal distribution is the best fit for the response distribution. For each case, different assumptions are made regarding the random variables considered. An analytical solution is formulated to calculate the probability of exceeding a certain performance limit state, given the probability distribution function of the response and of the limit states. The simplest case is where the inter-story drift threshold d is considered as a deterministic quantity, and is compared with the random variable $\delta\check{T}$ of the inter-story drift response that takes only positive values and is assumed to be log-normally distributed as follows

$$f_{\Delta}(\delta) = \begin{cases} \frac{1}{\delta\sigma_{\Delta}\sqrt{2\pi}} \cdot e^{-\frac{(\ln(\delta) - m_{\Delta})^2}{2\sigma_{\Delta}^2}} & \delta \geq 0 \\ 0 & elsewhere \end{cases} \quad (4.26)$$

In this case the fragility function describing the probability of exceeding the given performance limit state d is

$$F_d(t_r) = P(\Delta \geq d | T_r = t_r) = 1 - F_{\Delta}(d) = 1 - \int_0^d f_{\Delta}(\delta) d\delta \quad (4.27)$$

Instead, if the inter-story drift threshold is also a random variable that takes only positive values (but it is assumed independent from Δ), then the fragility function describing the probability of exceeding the given performance limit state D in Eq. (4.27) becomes

$$\begin{aligned} F_D(t_r) &= P(\Delta \geq D | T_r = t_r) = P\left(\underbrace{\frac{\Delta}{D}}_Y \geq 1\right) = P(Y \geq 1) = 1 - F_Y(1) \\ &= 1 - \int_0^{\infty} f_D(u) F_{\Delta}(1 \cdot u) du; \end{aligned} \quad (4.28)$$

where

$$\begin{aligned}
 F_Y(y) &= \int_0^\infty \int_0^{y \cdot u} f_\Delta(\delta) f_D(u) d\delta du = \int_0^\infty f_D(u) \int_0^{y \cdot u} f_\Delta(\delta) d\delta du \\
 &= \int_0^\infty f_D(u) F_\Delta(y \cdot u) du;
 \end{aligned} \tag{4.29}$$

where u and δ = auxiliary variables; y = specific real number of a real value random variable Y . If both the drift response Δ and the acceleration response Z are considered in the formulation, then these two variables are assumed dependent random variables because generally for every type of structure, experimental observations seem to confirm this assumption. For example for linear SDOF systems, the following relation holds

$$\frac{Z}{\omega^2} = \Delta \tag{4.30}$$

where $\omega = 2\pi/T$ is the circular frequency of a SDOF of period T . Based on this relationship, the problem is reduced from two-dimensional to one-dimensional:

$$\begin{aligned}
 F_{RLS}(t_r) &= P(\Delta \geq d \cup Z \geq a | T_r = t_r) = P(\Delta \geq d \cup \Delta \omega^2 \geq a | T_r = t_r) = \\
 &= P(\Delta \geq \min(d, a/\omega^2) | T_r = t_r) = 1 - F_\Delta(\min(d, a/\omega^2)) = \\
 &= 1 - \int_0^{\min(d, a/\omega^2)} f_\Delta(\delta) d\delta
 \end{aligned} \tag{4.31}$$

The probability of exceeding the limit state can be evaluated when the probability density functions of inter-story drift $f_\Delta(\delta)$ is known. Both parameters of the density functions can be calculated using the maximum likelihood method. While in the two cases shown above, the inter-story drift performance limit state d and the acceleration performance limit state a were considered deterministic quantities, they can also be assumed as random variables log-normally distributed as discussed previously. It is assumed that the acceleration response Z and the displacement response Δ are related in the elastic range, so that the relation $\Delta = Z/\omega^2$ holds, while the performance limit state of inter-story drift D and acceleration A are assumed independent random variables. This assumption is reasonable because, nonstructural components such as electronic devices (e.g. computers, etc.) for example, that are acceleration sensitive, cannot be related to the building PLSs that are typically displacement sensitive. In order to simplify the formulation, two new non-dimensional random variables $X = \Delta/D$ and $Y = Z/A$, are assumed.

In this case, the probability of exceeding the given performance limits state can be expressed as

$$\begin{aligned}
 F_{RLS}(t_r) &= P(\Delta \geq D \cup Z \geq A | T_r = t_r) = P\left(\underbrace{\frac{\Delta}{D}}_X \geq 1 \cup \underbrace{\frac{Z}{A}}_Y \geq 1 | T_r = t_r\right) = \\
 &= P\left(\underbrace{\frac{\Delta}{D}}_X \geq 1 \cup \frac{\Delta}{\frac{A}{\omega^2}} \geq 1 | T_r = t_r\right) = P\left(\underbrace{\frac{\Delta}{D}}_X \geq 1 \cup \left(\frac{\omega^2 D}{A}\right) \cdot \underbrace{\frac{\Delta}{D}}_X \geq 1 | T_r = t_r\right) = \\
 &= P\left(\underbrace{\frac{\Delta}{D}}_X \geq 1 \cup \underbrace{\frac{\Delta}{D}}_X \geq \frac{A}{\omega^2 D} | T_r = t_r\right) = P\left(X \geq \min\left(1, \frac{A}{\omega^2 D}\right) | T_r = t_r\right) = \\
 &= 1 - F_X\left(\min\left(1, \frac{A}{\omega^2 D}\right)\right) = 1 - \int_0^{\infty} f_D(u) F_{\Delta}\left(\min\left(1, \frac{A}{\omega^2 D}\right) u\right) du; \tag{4.32}
 \end{aligned}$$

Hence, for the evaluation of the exceedance probability in this case, only the probability density function of the inter-story drift response and the probability density function of the inter-story drift limit state are required. In case that inter-story drift performance limit state, D , and the acceleration performance limit state, A , are nonlinearly related through Eq. (4.21), then the probability of exceedance the *MTLS function* is obtained by substituting Eq. (4.21) in Eq. (4.32)

$$\begin{aligned}
 F_{rLS}(t_r) &= P(\Delta \geq d \cup Z \geq a | T_r = t_r) = P(\Delta \geq d \cup \Delta \omega^2 \geq a | T_r = t_r) = \\
 &= P(\Delta \geq \min(d, a/\omega^2) | T_r = t_r) = \\
 &= 1 - F_{\Delta}\left(\min(d, A_{LS}/\omega^2 (1 - (D/D_{LS})^N))\right) = \\
 &= 1 - \int_0^{\min(d, A_{LS}/\omega^2 (1 - (D/D_{LS})^N))} f_{\Delta}(\delta) d\delta \tag{4.33}
 \end{aligned}$$

The advantage of this formulation is that a limit state can be expressed as function of the other components, once the coefficients of the model have been calibrated; in this case, only a single parameter is needed to limit both displacements and accelerations. Once the probability of exceeding the PLS is computed analytically, the procedure can be repeated again for different intensity measures, generating the fragility curves using the procedure described in the next section.

4.8 Generation of Fragility Curves

In this section, the method for generating fragility curves uses the return period as the intensity measure to take into account the ground motion parameter I at the site, it is described in the following steps:

- *Step I:* for a given value of earthquake hazard H (e.g., return period T_r of an earthquake event), consider n synthetic or real earthquake records.
- *Step II:* analyze the structural system under each of the earthquake records generated in Step I that is consistent with the given hazard level. Compute the maximum pseudo spectral acceleration (PSA) and spectral displacement (S_d) response for every structural and nonstructural component at each story level. Note that nonstructural components are assumed rigid and rigidly connected to the structure for the particular case study considered.
- *Step III:* estimate the mean and the standard deviation from the δ response samples of Step II and evaluate the lognormal PDF of δ the response distribution.
- *Step IV:* evaluate the probability of exceeding, using the analytical expressions given in previous paragraphs, for the case when uncertainties in the limit states are taken in account. The limit states considered are partly dictated by structural safety (displacements) and partly dictated by functionality (accelerations) at each floor level and they are defined as “story PLS.”
- *Step V:* repeat Steps I to IV for different hazard levels and locate all the points corresponding to the different probability P of exceeding the limit state in the plane of probability of exceeding versus earthquake hazard. The number of hazard levels (represented by the return period of the earthquake event), available for design in the USGS database (Petersen et al. 2014), is usually four, which is equal to the number of points available to determine the fragility curves as function of the return period.
- *Step VI:* fit the points obtained in Step V using the lognormal cumulative distribution function. The fragility function is described by the following equation:

$$F_Y(y) = \Phi \left[\frac{1}{\beta} \ln(y/\theta_Y) \right] \quad y \geq 0 \quad (4.34)$$

where Φ = standardized cumulative normal distribution function; θ_y = median of y ; and β = standard deviation of the natural logarithm of y . A straightforward optimization algorithm based on chi-square χ^2 goodness-of-fit test allows the estimation of the optimal parameters of the lognormal distribution (θ_y and β).

- *Step VII:* repeat Steps I to VI for every story level and develop floor fragility curves. Then, the performance level of the most critical story is suggested to represent the global PLS for the structure.

The reason of the choice in *Step VII* is justified by the fact that in reality, most structures are a combination of series and parallel systems (Nowak and Collins 2000): structures may not fail when a single member fails, but they can fail

before all members fail. In a complex structural system like a hospital, structural and nonstructural components interact with each other, therefore identifying series and parallel systems may be difficult. However, the problem can be simplified assuming the hospital is a series system that demonstrates a weakest link system, because failure of the system corresponds to failure of the weakest element in the system. The proposed approach with respect to other methods available in literature (e.g., Zion method described by Kennedy and Ravindra (1984)) addresses *PLSs* as functions of combined multiple structural parameters and also allows consideration of dependencies among different limit thresholds and uncertainties in the limit states themselves. Therefore, the proposed approach can be considered as an alternative method for describing the vulnerable behavior of nonstructural components that are sensitive to multiple parameters, like partition walls that are drift sensitive during the earthquake in the initial vibration cycles but become acceleration sensitive as cantilever type structures, when they disconnect from the top boundary. Another example of nonstructural components that are sensitive to both accelerations and drifts are the piping systems. The disadvantage of the proposed method is that is based on nonlinear time history analysis coupled with Monte Carlo simulations that are used to characterize the demands in terms of their joint density function $f_D(d)$ where d =generic demand parameter. Therefore, the proposed approach may be prohibitive for complex structural systems where excessive computational demand is required.

4.9 Concluding Remarks

The chapter describes different types of loss assessment models to evaluate regional seismic losses of both ordinary buildings and infrastructures. Then attention shifts toward the definition of a loss function which has been one of the first indicators used to define disaster resilience. Different models to evaluate the damage losses are provided, approaching the problem in probabilistic terms using fragility functions and analyzing different types of uncertainties which appear in the resilience evaluation such as the uncertainties in the limit states.

References

- Aslani H, Miranda E (2005) Probability-based seismic response analysis. *Eng Struct* 27(8):1151–1163. doi:10.1016/j.engstruct.2005.02.015. <GotoISI>://WOS:000230132200003, iSI Document Delivery No.: 940GR Times Cited: 25 Cited Reference Count: 52 Aslani H, Miranda E, Elsevier Science
- (ATC-58) ATC (2007) Guidelines for seismic performance assessment of buildings 35 % draft, Redwood City
- Badillo-Almaraz H, Cimellaro GP (2006) Seismic fragility of suspended ceiling systems. Report, University at Buffalo, The State University of New York (SUNY), New York. <http://ntis.library.gatech.edu/handle/123456789/2034>

- Basoz N, Kiremidjian AS (1997) Risk assessment of bridges and highway systems from the northridge earthquake. California Department of Transportation
- Bruneau M, Reinhorn AM (2007) Exploring the concept of seismic resilience for acute care facilities. *Earthq Spectra* 23(1):41–62. <http://link.aip.org/link/?EQS/23/41/1>
- Chaudhuri SR, Hutchinson TC (2006) Fragility of bench-mounted equipment considering uncertain parameters. *J Struct Eng ASCE* 132(6):884–898
- Cimellaro G, Reinhorn A, Bruneau M, Rutenberg A (2006) Multidimensional fragility of structures: formulation and evaluation. Report MCEER, Technical report MCEER-06-0002, University at Buffalo, The State University of New York, New York, pp 123. doi:ISSN: 1520-295X
- Cimellaro GP, Roh H, De Stefano A (2009) Spectral and fragility evaluations of retrofitted structures through strength reduction and enhanced damping. *Earthq Eng Eng Vib* 8(1):115–125
- Clough RW, Penzien J (1993) Dynamics of structures, 2nd edn. Mc Graw Hill, New York
- Cornell A (1996) Calculating building seismic performance reliability: a basis for multi-level design norms. Elsevier Science Ltd
- Dotson WP, Gobien JO (1979) A new analysis technique for probability graphs. *IEEE Trans Circuits Syst* 26:855–865
- FEMA (2007) Fema 461: interim testing protocols for determining the seismic performance characteristics of structural and nonstructural components. Federal Emergency Management Agency and U.S. Army Corps of Engineers
- Fukushima S, Kai Y, Yashiro K (1996) Study on the fragility of system part 1: structure with brittle elements in its stories. In: Proceedings of the 11th world conference on earthquake engineering Pergamon, vol 1. Elsevier Science, Oxford, Paper No. 333
- Gardoni P, Der Kiureghian A, Mosalam KM (2002) Probabilistic capacity models and fragility estimates for reinforced concrete columns based on experimental observations. *J Eng Mech ASCE* 128(10):1024–1038
- Goulet CA, Haselton CB, Mitrani-Reiser J, Beck JL, Deierlein GG, Porter KA, Stewart JP (2007) Evaluation of the seismic performance of a code-conforming reinforced-concrete frame building from seismic hazard to collapse safety and economic losses. *Earthq Eng Struct Dyn* 36(13):1973–1997
- Haimes Y (1998) Risk modeling, assessment, and management. Wiley, New York
- Hazus (2014) Hazus[®]-MH MR5 technical manuals and user's manuals. Department of Homeland Security, Federal Emergency Management Agency, Mitigation Division, Washington, DC
- Hwang H, Huo JR (1994) Generation of hazard-consistent fragility curves for seismic loss estimation studies. Technical report NCEER-94-0015. National center for earthquake engineering research, State University of New York at Buffalo, Buffalo
- Hwang H, Shinozuka M (1998) Seismic performance assessment of water delivery systems. *J Infrastruct Syst* 4(3):118–125
- Kafali C, Grigoriu M (2005) Rehabilitation decision analysis. IOS Press
- Kang W-H, Song J, Gardoni P (2008) Matrix-based system reliability method and applications to bridge networks. *Reliab Eng Syst Saf* 93(11):1584–1593
- Karim KR, Yamazaki F (2001) Effects of earthquake ground motions on fragility curves of highway bridge piers based on numerical simulation. *Earthq Eng Struct Dyn* 30(12):1839–56
- Kennedy R, Ravindra M (1984) Seismic fragility analysis for nuclear power plant risk studies. *Nucl Eng Des* 79(1):47–68
- Li J, He J (2002) A recursive decomposition algorithm for network seismic reliability evaluation. *Earthq Eng Struct Dyn* 31(8):1525–1539
- Liel AB, Deierlein GG (2012) Using collapse risk assessments to inform seismic safety policy for older concrete buildings. *Earthq Spectra* 28(4):1495–1521. doi:doi:10.1193/1.4000090. <http://earthquakespectra.org/doi/abs/10.1193/1.4000090>
- Lucco N, Cornell CA (1998) Effects of random connection fractures on the demands and reliability for a 3-story pre-Norridge SMRF structure. In: Proceedings of the 6th U.S. national conference on earthquake engineering, Seattle, 31 May–4 June 1998
- Nowak A, Collins K (2000) Reliability of structures. Mc-Graw Hill, Boston

- Petersen MD, Moschetti MP, Powers PM, Mueller CS, Haller KM, Frankel AD, Zeng Y, Rezaeian S, Harmsen SC, Boyd OS, Field N, Chen R, Rukstales KS, Luco N, Wheeler RL, Williams RA, Olsen AH (2014) Documentation for the 2014 update of the United States national seismic hazard maps: U.S. geological survey open-file report 2014–1091, 243 p. <http://dx.doi.org/10.3133/ofr20141091>
- Porter K, Kennedy R, Bachman R (2007) Creating fragility functions for performance-based earthquake engineering. *Earthq Spectra* 23(2):471–489
- Ramarmoorthy SK, Gardoni P, Bracci JM (2006) Probabilistic demand models and fragility curves for reinforced concrete frames. *J Struct Eng ASCE* 132(10):1563–1572
- Reinhorn AM, Barron-Corverra R, Ayala AG (2001) Spectral evaluation of seismic fragility of structures. In: Corotis et al. (eds.) *Proceedings ICOSSAR 2001*. Swets & Zeitlinger/Balkema Publishers, Newport Beach, 17–21 June 2001
- Retamales R, Mosqueda G, Filiatrault A, Reinhorn AM (2006) Experimental study on the seismic behavior of nonstructural components subjected to full-scale floor motions. In: *Proceedings, 8th US national conference on earthquake engineering*, San Francisco. Earthquake Engineering Research Institute (EERI)
- Scott BM, Stephanie EC (2006) Modeling community recovery from earthquakes. *Earthq Spectra* 22(2):439–458. <http://link.aip.org/link/?EQS/22/439/1>
- Shinozuka M, Feng M, Kim H, Kim S (2000a) Non linear static procedure for fragility curve development. *ASCE J Eng Mech* 126(12):1287–1295
- Shinozuka M, Feng M, Lee J, Naganuma T (2000b) Statistical analysis of fragility curves. *ASCE J Eng Mech* 126(12):1224–1231
- Shinozuka M, Dong X, Chen TC, Jin X (2007) Seismic performance of electric transmission network under component failures. *J Earthq Eng Struct Dyn* 36(2):227–244
- Song J, Der Kiureghian A (2003) Bounds on system reliability by linear programming. *J Eng Mech ASCE* 129(6):627–636
- Vamvatsikos D, Cornell CA (2001) Incremental dynamic analysis. *Earthq Eng Struct Dyn* 31(3):491–514
- Werner SD, Taylor CE, Moore JEI, Walton JS (2000) A risk - based methodology for assessing the seismic performance of highway systems. Report MCEER-00-0014. MCEER multidisciplinary center for earthquake engineering research
- Whitman RV, Reed JW, Hong ST (1973) Earthquake damage probability matrices. In: *Proceedings of the 5th world conference on earthquake engineering*, Rome, pp 2531–2540
- Williams RJ, Gardoni P, Bracci JM (2009) Decision analysis for seismic retrofit of structures. *Struct Saf* 31(2009):188–196
- Yi JH, Kim SH, Koshiyama S (2007) Pdf interpolation technique for seismic fragility analysis of bridges. *Eng Struct* 29(7):1312–1322. doi:10.1016/j.engstruct.2006.08.019. <GotoISI>://WOS:000247755500005, ISI Document Delivery No.: 186CA Times Cited: 3 Cited Reference Count: 21 Yi, Jin-Hak K, Sang-Hoon K, Shigeru, Elsevier Science

Chapter 5

Downtime and Recovery Models

Abstract The chapter addresses different recovery models for communities and infrastructures. The recovery models have been categorized by distinguishing between analytical and empirical recovery models. Finally the definition of downtime is provided together with a state-of-the-art of the different models available for downtime assessment.

5.1 Introduction

Recovery is a complex process that is influenced by time dimensions, spatial dimensions (e.g., different neighborhoods may have different recovery paths) and by interdependencies between different economic sectors that are interested in the recovery process. For example, different critical facilities (e.g. hospitals) that belong to the same community, but are located in different neighborhoods, have different recovery paths and in some areas (mainly poor areas), these essential facilities may experience long term or permanent losses (Chang 2000). Therefore, since the recovery process among different systems shows disparities in rates and quality of recovery, even if belonging to the same community, modeling the recovery of single facility or of an entire community is a complex undertaking. Once these complex recovery models are available, it is possible to describe the relationships across different scales-socioeconomic agents, neighborhoods, institutions and communities, and to study the consequences of decision making. These models should aim at increasing the community's resilience and reducing its social vulnerability. Generally the recovery model depends on the type of indicator selected such as *the population, the number of household residences, and the occupancy rates, wide-ranging different neighborhoods and socio-economic groups, number of hospitals and its agility*. Generally, the indicator selected to measure the performance of a community and/or a system during transient analysis is function of time t and other parameters that depend on the type of community considered. Consequently, the functionality at a time t is given by an expression that also depends on other parameters involved in describing the recovery model ($x_1 \dots x_n$)

$$Q(t) = f(t, x_1, \dots, x_n) \tag{5.1}$$

Several models have been presented in Cimellaro and Reinhorn (2010a) to describe the recovery function, which can vary according to the system and society awareness level and can be either *analytical* or *empirical* depending on the source of data and the type of analysis.

5.2 Analytical Recovery Models

Analytical recovery functions are developed from community response data obtained through analysis of the system using numerical simulations. For instance, in the case of earthquake events, they can be obtained from nonlinear time history analysis, response spectral analysis, etc.. These kinds of functions use statistical data and accurate mathematical models to represent a determined physical phenomenon. The probability of going up to or even exceeding a damage state at a specified ground motion level is reflected in the fragility curve in statistical terms. These functions are obtained by computing the conditional probabilities of reaching or surpassing that damage state at various levels of ground motion. Since the recovery process is characterized by uncertainties, the parameters considered in the model are designated as random variables to quantify the uncertainties in the system. These uncertainties can be divided in aleatoric and epistemic uncertainties (Ang and Tang 2007). Several models can be suited to the observed data, and afterwards, model selection can be carried out using a goodness of fit measure, such as the r^2 value. The essential requirement of the analytical recovery models is simplicity, therefore the model should be selected so that it is easy to adapt to real or numerical observation data and the number of parameters involved should be as low as possible. Below five different recovery models are discussed, which are grouped according to the two control periods (*short term* vs. *long term*). *Long term recovery models* are used when the reconstruction phase needs to be modeled, whereas *short term recovery models* are applied in the case that the emergency phase after the extreme episode needs to be focused upon.

5.2.1 Long Term Recovery Models

Several *long term recovery models* are proposed in Cimellaro et al. (2010c). They can be arranged according to the number of parameters (one, two or three parameters). Complex recovery models with more parameters can be proposed, however simpler mathematical models have some benefits over more complex ones, because fewer experiments are needed and there are less chance of “overfitting”.

The simplest recovery model is the *uniform cumulative distribution (cdf)* recovery function (also known as the *linear model*). This model is usually adopted when there is no information regarding the preparedness, resources available, societal response, etc.

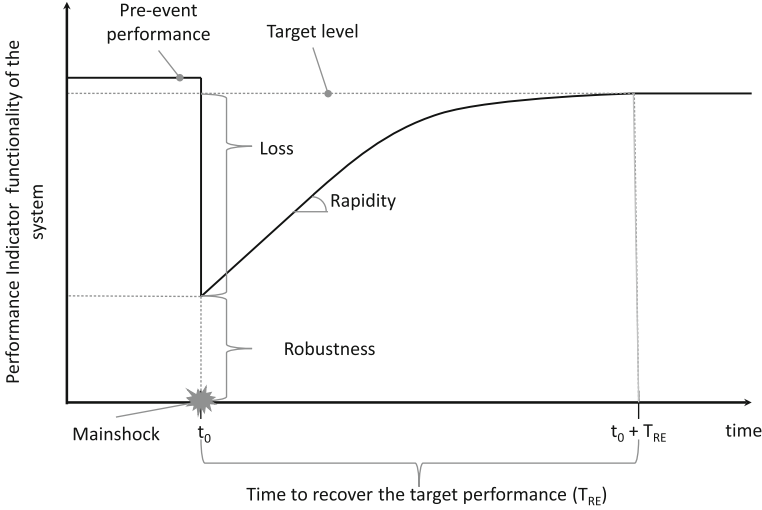


Fig. 5.1 Resilience (Adapted from Cimellaro et al. (2010b))

$$Q(t) = Q_0 + F(t/t_0, t_0 + T_{RE}) \cdot [Q_R - (Q_0 - L_0)] \tag{5.2}$$

where Q_0 is the initial functionality after the drop; L_0 is the initial total loss of functionality after the drop; Q_R is the residual functionality after the recovery process ends (Fig. 5.1); and $F(t/t_0 + T_{RE})$ is the uniform cumulative distribution function which is given by

$$F(t/t_0 + T_{RE}) = \frac{(t - t_0)}{T_{RE}} I(t/t_0 + T_{RE}) \tag{5.3}$$

where $I(t_0, t_0 + T_{RE})$ is the interval step function.

The model is characterized by only one parameter (Fig. 5.2), which defines the slope of the curve and represents rapidity (Cimellaro and Reinhorn 2010a). The model can also be generalized by dividing the recovery process into several time intervals, using a *multilinear model*, which is given by

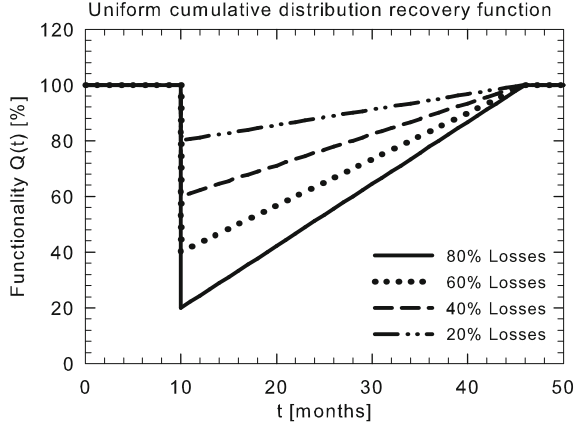
$$Q(t) = Q_1 + \sum_i H(t - t_i) \frac{(t - t_i)}{(t_{i+1} - t_i)} (Q_{i+1} - Q_i) \tag{5.4}$$

where Q_i is the residual functionality at the step i and Q_{i+1} is the residual functionality at the step $i + 1$; $H()$ is the Heaviside step function.

Alternatively, *lognormal cumulative distribution* (cdf) recovery function can be adopted. This has three parameters (L_0, θ, β), and it is given by

$$Q(t) = Q_0 + F(t/\theta, \beta) \cdot [Q_R - (Q_0 - L_0)] \tag{5.5}$$

Fig. 5.2 Resilience (Adapted from Cimellaro et al. (2010b))



where

$$F(t/\theta, \beta) = \frac{1}{\beta \sqrt{2\pi}} \int_{-\infty}^t \frac{e^{-\frac{(\log(x)-\theta)^2}{2\beta^2}}}{x} dx \quad (5.6)$$

This model combines both the exponential recovery pattern proposed by Kafali and Grigoriu (2005) and the trigonometric recovery model proposed by Chang and Shinozuka (2004). The parameter L_0 in Eq. (5.5) can be used to define the initial total loss of functionality after the drop (Fig. 5.3a)

The parameter θ can be used to define the time frame (Fig. 5.3b) when the societal response and recovery are driven by lack or limited organization and/or resources. As soon as the community organizes itself, with the help of other communities (for example), then the recovery system starts operating and the rapidity of recovery increases (Fig. 5.3a, b). For example, such a recovery occurred after Nisqually Earthquake (Filiatrault et al. 2001). The parameter β defines the rapidity of the recovery process (Fig. 5.3c).

Another recovery model presented in Cimellaro and Reinhorn (2010a) is the *harmonically over-damped* recovery function having three parameters (L_0, ω, ζ). It is defined as

$$Q(t) = Q_0 + \left\{ 1 - e^{-\alpha t} \left[\left(\frac{\alpha + \beta}{2\beta} \right) e^{\beta t} + \left(\frac{\beta - \alpha}{2\beta} \right) e^{-\beta t} \right] \right\} [Q_R - (Q_0 - L_0)] \quad (5.7)$$

where L_0 defines the initial total loss of functionality after the drop (Fig. 5.4); $\alpha = \omega \zeta$; $\beta = \omega \sqrt{(\zeta^2 - 1)}$; ω and ζ are related to the rapidity dimension ($\zeta \geq 1$; $\omega \geq 1$).

Furthermore, rapidity of recovery increases when either ω increases or ζ reduces as shown in Fig. 5.4b, c. For critically-damped systems ($\zeta = 1$), placing the same initial condition $Q(0) = 1 - L_0$ and $\dot{Q}(0) = 0$, the solution is given by

$$Q(t) = 1 - L_0 e^{-\omega t} (1 + \omega t) \quad (5.8)$$

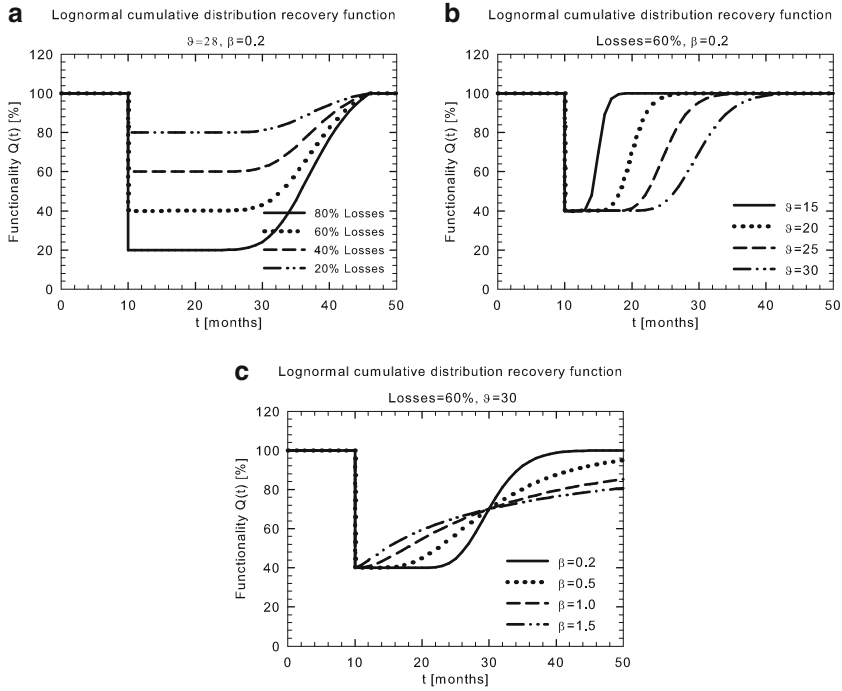


Fig. 5.3 Lognormal cumulative distribution recovery functions

This curve for values of ω close to 1 resemble an exponential recovery function and can be used for example when the societal response is driven by an initial inflow of resources, but then the rapidity of recovery decreases as the process nears its end.

5.2.2 Short Term Recovery Models

The main difference between this kind of model and long term models is that these models use *probability density functions (pdf)* instead of using the *uniform cumulative distribution (cdf)* recovery function. The simplest recovery model after the linear model proposed in (5.1) for the *uniform cumulative distribution* is the *Rayleigh* probability function recovery model, and it is defined as

$$Q(t) = 1 - L_0 \frac{f(t|b)}{\max(|f(t|b)|)} \tag{5.9}$$

where

$$f(t|b) = \frac{t}{b^2} e^{\left(\frac{-t^2}{2b^2}\right)} \tag{5.10}$$

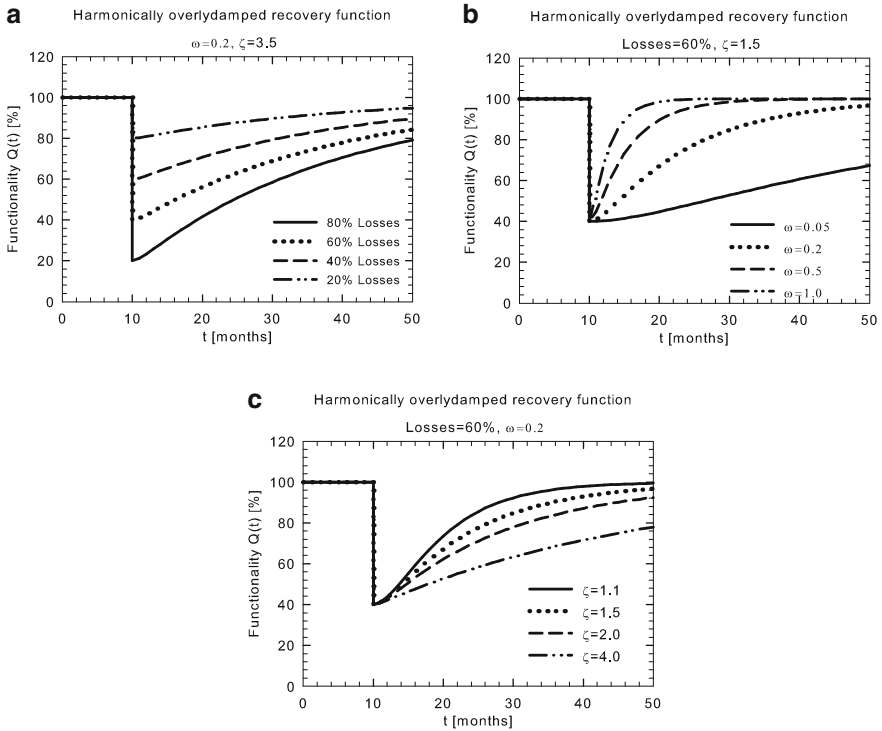


Fig. 5.4 Harmonically overly damped recovery function

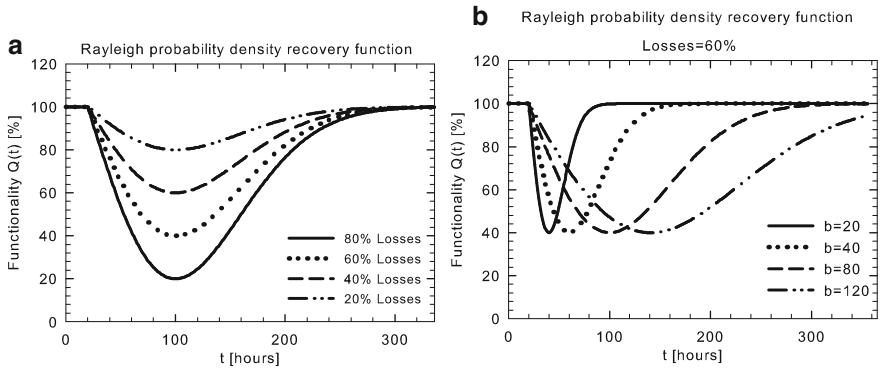


Fig. 5.5 Rayleigh probability density recovery function

The model is calibrated using two parameters: L_0 is related to the robustness dimension (Fig. 5.5a) while b is related to the rapidity and the delay in the recovery process (Fig. 5.5b).

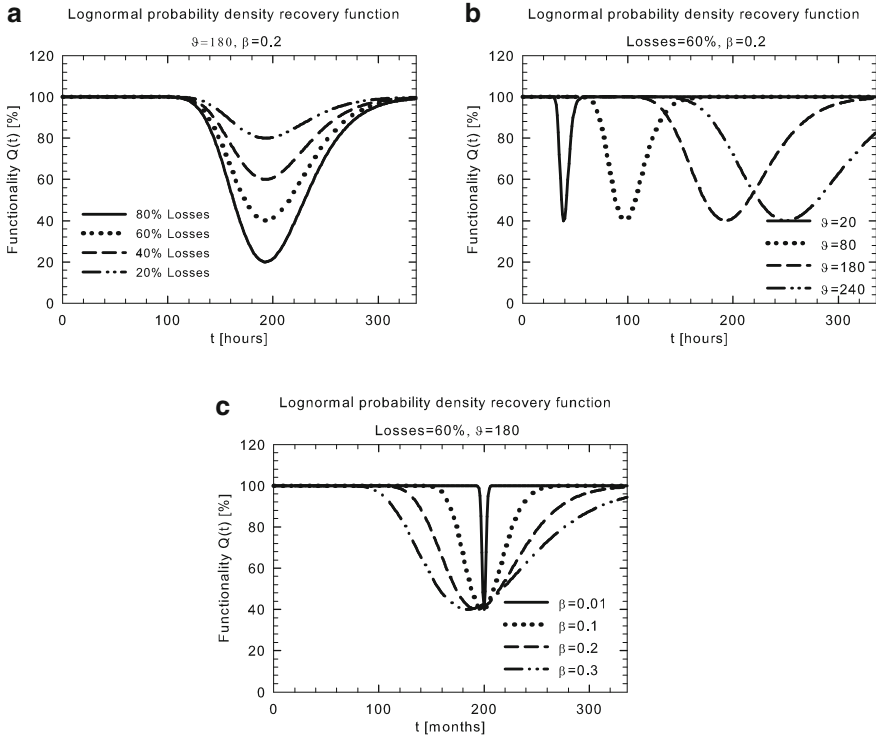


Fig. 5.6 Lognormal probability density recovery function

Another model is the *lognormal probability density recovery function*, which is given by

$$Q(t) = 1 - L_0 \frac{f(t|\theta, \beta)}{\max(|f(t|\theta, \beta)|)} \tag{5.11}$$

where

$$f(t|\theta, \beta) = \frac{1}{x\beta\sqrt{2\pi}} e^{-\frac{(\log(x)-\theta)^2}{2\beta^2}} \tag{5.12}$$

The sensitivity of the three parameters in the recovery process is shown in the Fig. 5.6.

In the *short term* emergency response, more complex analytical recovery are available, such as the *metamodel* for describing the organizational performance of a hospital facility (Cimellaro et al. 2010b). The model is based on a *double exponential function* and its parameters are calibrated based on simulated data obtained by a discrete event simulation model. The *metamodel* is capable of

estimating the hospital capacity and dynamic response in real-time, incorporating the influence of structural and non-structural damaged components on the entire organization model. It is important to mention that the constants in all the models presented can be continuously updated using Bayesian approach, as soon more data are available.

5.3 Empirical Recovery Models

These functions are based on test or field interpretation and engineering judgment. They can be built using the maximum likelihood method, based on data reported from past extreme events as Monte Carlo simulations of specified community models, or with the use of experimental reports obtained from laboratory tests. Since the complexity of the problem will change case by case and few of the insights collected from empirical studies have been formalized within a modeling framework, there is a dearth of these models. Furthermore, owing to the frequency of observed earthquakes, it is difficult to find enough actual damage data to generate empirical fragility curves. An example of empirical recovery model is the one by Shinozuka et al. (2000). Shinozuka developed both kinds of curves, empirical and analytical fragility curves, employing statistical analysis. Empirical fragility curves were developed making use of bridge damage data obtained from the 1995 Kobe earthquake, considering that the development of fragility curves required the use of quasi-static and design-code consistent analysis, damage data associated with past earthquakes, and numerical simulation based on dynamic analysis.

5.3.1 Step Recovery Function

In reality the majority of restoration curves do not have a smooth trend as the one shown in previous section, but they follow more the shape of a step function as shown in Fig. 5.7. This is due to the fact that in practice the restoration process is dictated for example from the resources available which are usually provided at discrete intervals. The restoration process of a building is managed by dividing the area in zones, so that it is possible to work independently.

5.4 Definition of Downtime

The recovery time (downtime) T_{RE} , according to MCEER, is the time necessary to restore the functionality of a community or a critical infrastructure system (water supply, electric power, hospital etc.) to a desired level below, same or better than the original, allowing proper operation of the system. In PEER's performance

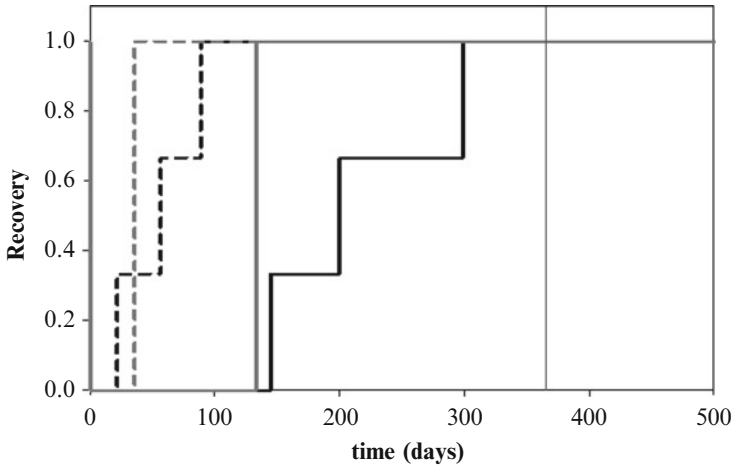


Fig. 5.7 Step recovery function

assessment methodology, downtime is one of three key decision variables (deaths, dollars, and downtime) used to predict potential losses and societal impacts when assessing buildings performance in earthquakes. In detail downtime is the time between the occurrence of a seismic event and the completion of the building repair effort and includes the time necessary to plan, finance, and complete repairs on facilities damaged in earthquakes or other disasters. Thus the performance assessment strategy outlined by PEER assumes downtime as the time required for re-occupancy.

The recovery time $T_{RE}(I, location)$ is a random variable with high uncertainties. It typically depends on the intensity of the hazard event and the type of area considered, the availability of resources such as capital, materials and labor following major seismic event. For these reasons this is the most difficult quantity to predict in the resilience function and nowadays its assessment is still in progress.

5.4.1 State-of-Art in Downtime

The first loss modeling approaches were proposed by Czarnecki (1973) who proposed an analytical method for estimating the repair cost using a structural model to evaluate the building response of its components which are then related to physical damage and repair cost. Later Kustu et al. (1982) added the use of empirical relationships between structural response and building-component damage, which is then related to repair cost, explicitly separating the analysis of damage from that of repair cost. Computer models for loss estimation began in 1980s and 90s due to the demand of the insurance and reinsurance industry. First loss models consisted in linking data through Geographic Information System (GIS) mapping programs.

The Federal Emergency Management Agency (FEMA) funded a series of studies on how to perform and use loss earthquake estimation techniques and developed the Hazus (1997) loss estimation software, which attempted to address regional impact of earthquakes. Hazus (1997) was the first edition of risk assessment software package built on GIS technology, used for mapping and displaying hazard data and the results of damage and economic loss estimates for building and infrastructure. HAZUS 97 was subsequently upgraded three times. The First time Mander and Basöz (1999) developed the fragility curves for the highway transportation module of HAZUS. They developed a complete description on the theoretical background of the damage functions and associated each damage state with the corresponding downtime, developing the first attempt to assess downtime losses. Later on, FEMA developed the multihazard version of HAZUS. This version was called HAZUS-MH and was released in 2004, while the last update became available in 2012. HAZUS methodology provides an estimate of the effects of an extreme event of given intensity. Estimating downtime is a subroutine within a larger methodology, used to generate the secondary economic losses and the specific functional losses for different structures and critical lifelines. The downtime in HAZUS is derived from the structural and nonstructural damage probabilities. At lower damage states, the repair time is equal to the estimated construction time, whereas the extensive damage state includes also the time for finance, design, and permits. HAZUS treats business and service interruption as a function of repair time, assuming that alternate ways of operating will be found. In HAZUS, the downtime is an interim step for assessing the long-term economic impact, so median values apply for large inventories. The downtime for essential facilities (e.g. schools and hospitals) is also derived from the estimates of the dollar losses. For the transportation systems and the utility lifeline systems, an algorithm for estimating the time needed for repair is used which is based on the number of breaks in the system.

Porter et al. (2001) developed a methodology called Assembly-Based Vulnerability (ABV) which estimated downtime through vulnerability curves. Later on, Ghorawat (2011) extended the approach for damage from Mander and Sircar (2009) to estimate death and downtime. The loss model was developed by multiplying the probabilities of being in each of the damage states using vulnerability curves by the corresponding downtime losses and summing those losses across all damage states to give composite downtime with respect to an engineering demand parameter, like drift. The calibrated loss model is incorporated into a direct four-step probabilistic loss modeling framework. The four-step approach is subdivided into four distinct tasks: hazard analysis, structural analysis, loss analysis of both direct and indirect losses and the total loss estimation due to damage, death and downtime. This approach relates seismic hazard to structural response and hence structural response to downtime losses from which scenario losses or the expected annual downtime losses (EADT) for all earthquake hazards are calculated.

Krawinkler and Miranda (2004) defined the downtime as something more than the time needed to complete repairs. In their work, they say: “*The basic difficulties in quantifying length of downtime are great uncertainties associated with the availability of labor, materials, and capital following a major seismic event, and difficulties*

relating quantifiable damage and the needs for repair with loss of function. Even if downtime could be quantified with confidence, the associated losses will be highly uncertain and strongly case and scenario specific. Estimation of downtime losses is and will remain perhaps the biggest challenge of seismic performance assessment and risk management.” Following this idea of quantifying downtime, Comerio (2006) introduced a new concept of downtime which is defined as the time necessary to plan, finance, and complete repair facilities damaged by earthquakes or other disasters and is composed by rational and irrational components (Comerio 2006). Rational components include construction costs and time, while irrational components take into account the time needed to mobilize for repairs and include financing, relocation of functions, workforce availability, regulatory changes, and economic uncertainty. Comerio (2006) determined: “*It is not possible to estimate the time a building will be closed after an earthquake solely on the estimate of damage to the structure. Instead, we need to examine the process involved in building repair in order to understand which elements affect the time needed for repairs.*” This statement was based on work field, where the repair times for closed buildings on Stanford University campus after the Loma Prieta earthquake ranged from 0.4 to 2.6 years, and the total downtime for these ranged between 0.9 and 9.3 years (Comerio 2006). This gap between repair time and total downtime suggests that the irrational components of downtime require serious consideration. Later on, the downtime data from the Northridge and Loma Prieta earthquakes focuses on time to occupancy measures by tag color, by building type and by single family versus multi-family (Comerio and Blecher 2010). These categories were used as they were defined as the most relevant for residential buildings and they have consistent and recognized definitions among interested parties (such as building authorities, construction professionals, owners and academics). To model downtime it is required a formula that combines three critical elements (Comerio and Blecher 2010). These three critical elements are: (1) an estimate of construction repair time for individual facilities damaged by a disaster; (2) an estimate of the mobilization time needed for various building stocks; and (3) a representation of the economic conditions in the region at the time of the event. Together, these inputs adequately represent the relationship between prevailing economic conditions and the rate of building stock recovery.

Mitrani-Reiser (2007) developed and implemented an analytical approach for PBEE (Performance-Based Earthquake Engineering) to evaluate the performance of a new reinforced-concrete moment-frame office building. This methodology estimates the direct economic losses due to repair costs as well as two types of indirect economic losses, which are produced by building downtime and by human facilities. In order to estimate downtime, the analytical approach was carried out through a hazard analysis, a structural analysis and a damage analysis. This last step involves the use of fragility functions that express the probability that a facility component is in or exceeds a particular damage state as a function of an EDP (Engineering Demand Parameter). The different damage states for each damageable group are indicative of the corresponding repair efforts needed to restore that component type to an undamaged state. The rational component of downtime is

estimated using a methodology modified from a repair-time model introduced by Beck et al. (1999), which considered several repair schemes for calculating building life-cycle costs. The time needed to repair the building damage caused by an earthquake, was estimated using the output of the damage analysis and the repair times determined by a professional cost estimator (Hecksher, 2006, Component downtime estimates, Report, Personal communication). The repair duration for each damageable building assembly group (set of damageable components of the same type that are sensitive to the same EDP) is dependent on the repair crew and particulars of the damage; therefore, these durations should be treated as uncertain. Probability distributions for these uncertain durations were developed using the means and 90th percentiles of the repair times, provided by the professional cost estimator (Hecksher, 2006, Component downtime estimates, Report, Personal communication) for the benchmark building assembly groups. One method that best exploits the results from the damage analysis and the available empirical data is a model for these mobilization delays conditioned on the results of the visual inspector results. The delay associated with the waiting for the engineer to perform a detailed inspection will vary from owner to owner since it will depend on the owner's relationship with the engineer and their financial standing; this delay is highly variable and difficult to approximate from the available empirical data. If a building is red tagged, it is unsafe to inhabit the building and will likely require demolition or extensive repairs. The mobilization delay for those buildings that are red tagged and not demolished/replaced is substantial (Comerio 2006). The theorem of total probability is used to estimate the expected total mobilization time conditioned on the building safety-tagging result of the virtual inspector.

In addition to HAZUS, FEMA released in 2012 the FEMA P-58 and a Performance Assessment Calculation Tool (PACT), which is an electronic tool for performing the probabilistic assessment of losses for individual buildings (FEMA-P58 2012). PACT (FEMA-P58 2012) uses a methodology for seismic performance assessment of individual buildings that properly accounts for uncertainty in the ability to accurately predict response. FEMA-P58 (2012) enables estimates of direct losses attributable to earthquake damage to an individual building and its contents, as well as the repair or reconstruction time. Performance is directly related to the damage a building may experience and the consequences of such damage such as loss of use, repair, and reconstruction costs. The methodology divides the performance assessment into a number of elements that can be resolved rigorously and consistently; i.e., earthquake intensity measures, engineering demand parameters, damage measures, and decision variables. The PACT (FEMA-P58 2012) methodology is divided in five steps. The first one consists in assembling building performance model through collection of data to define building assets at risk and their exposure to seismic hazards. The building components are categorized into fragility and performance groups. Then it is needed to define earthquake hazards by quantifying the intensity and the probability that effects of a given intensity will be experienced. From this analysis, it is possible to analyze building response, which usually includes peak values of story drift ratio, floor velocity, floor acceleration and residual drift ratio. Once the building response has been analyzed,

it is needed to develop collapse fragility functions and consequence functions in order to assess the performance. Collapse fragility functions define the probability of incurring structural collapse as a function of ground motion intensity, while consequence functions are relationships that indicate the potential distribution of losses and repair-time as a function of the damage state. Each damage state has an associated consequence function, from which the repair cost and repair time associated with the level of damage in the component is estimated.

Since there are many factors that can affect the building performance, such as the ground motion intensity, the quality of construction, the building response, or the vulnerability of contents, there is significant uncertainty in the predicted building performance. These uncertainties can be accounted for by means of Monte Carlo simulations. Within PACT, the uncertainties are accounted for by defining a value of dispersion to the building definition and a value of dispersion to the analytical model. The total repair time is evaluated as sum of the repair time of each single component, where the repair times are summed in a logical way taking into account both the *labor allocation* and the *repair scheme*. The *labor allocation* is setup following the instructions of FEMA while the *repair scheme* can be chosen in parallel or in series. A *repair scheme* in parallel means that the work is done simultaneously at each floor, while in series means that the work is done floor by floor following a sequence from the bottom to the top. For each realization, PACT software uses the maximum residual story drift together with the building repair fragility to determine if the building is repairable. If irreparable, the repair cost and repair time coincide with the building replacement costs and construction time.

One of the most recent effort on evaluating downtime derives from the Resilience-based Earthquake Design Initiative (REDi) rating system Almufti and Willford (2013) presented by ARUP. The REDi guidelines propose a detailed downtime assessment methodology by accounting for both direct repairs, based on PACT (FEMA-P58 2012), and impeding factors Comerio (2006) as well as also accounts for utility disruption.

REDi sets that there are several significant limitations in FEMA-P58 (2012) in relation to quantifying downtime, which must be addressed. These limitations are: the repair time estimates are based on potentially unrealistic labor allocation and repair sequence logic, repair time estimates are only associated with the time required to achieve full recovery and that it doesn't take into account for delays neither for utilities disruption. SEAONC defines three recovery states, as follows: *reoccupancy of the building*, *pre-earthquake functionality*, and *full recovery* (Bonowitz 2011). Reoccupancy occurs when the building is safe enough to be used for shelter, although functionality may not be restored. Functional recovery occurs when the building regains its primary function, i.e., it is operational. Full recovery occurs when the building is restored to its pre-earthquake condition; it comes after functional recovery, once additional repairs for aesthetic purposes have been completed. All these three recovery states can be estimated through REDi. The REDi guidelines provide a detailed downtime assessment methodology for individual buildings and identify the likely causes of downtime such that these can be mitigated to achieve a more resilient design. The methodology identifies the

extent of damage and criticality of building components that may hinder achieving a recovery state through the introduction of repair classes. Repair classes are assigned to the each damage state for each building component. Repair classes dictate whether the damage in the component hinders building reoccupancy, functional recovery, or full recovery. If the damage in any component hinders achieving a certain recovery state, the component needs to be repaired before such recovery state can be achieved. Once the components that need repairing to achieve a certain recovery state have been identified, the methodology includes delay estimates associated with impeding factors, defined as those factors which may impede the initiation of repairs. Impeding factors include post-earthquake inspection, engineering mobilization, contractor mobilization, financing, permitting, and long-lead-time components. Impeding factors are presented in the form of lognormal cumulative distribution functions, impeding curves. The REDi guidelines provide a logical approach for labor allocation and repair sequencing of structural and nonstructural components on a floor-per-floor basis. The repair sequence defines the order in which repairs take place. The repair sequence defined by REDi determines that structural repairs need to be conducted at any given floor before repairs to other building components at that level (or above) can commence. Nonstructural repairs are divided into the following categories: egress (stairs and elevators), façade (exterior partitions and cladding), and MEP and office fitouts (HVAC, partitions, and ceiling tiles). Once structural repairs at any given floor are complete, repair of nonstructural components can start, in parallel, following a rational approach. The overall repair time is estimated based on the repair times dictated by PACT, which are expressed in number of days for a single worker to complete the work and the labor allocation for each floor in the building. Downtime is lowered proportionally to the number of workers, which is a function of the square meters of the building. Furthermore, the total number of workers in the building is also limited by the number of workers allocated to a project. To account for subcontractor resource limitations, the number of workers repairing a certain type of component is limited. Utility disruption is also considered when estimating downtime for functional recovery. Disruption to water, natural gas, and electrical systems is considered. Total downtime is computed as the sum of impeding factors, repair times and utility disruption in a logical sequence.

Recently Terzic et al. (2014) presents the results of a study undertaken to illustrate the ability of simplified PBEE procedures to identify cost-effective strategies for reducing life-cycle earthquake induced costs during the preliminary stages of seismic design, including business downtime. In her study business downtime is considered as the time required to identify damage, design repairs or upgrades, obtain permits and financing, to mobilize supplies and manpower, and to restart operations. To obtain the repair time of each damage cost, it has been used the computer software PACT. Once the repair time is obtained, business downtime is calculated considering the order of building repair and accounting for mobilizing factors that can significantly delay the start of the building repairs (Comerio 2005a,b). These mobilization factors are related to the components that are essential for a building's functionality and the extent of damage of the components and their

effect of the business interruption. The problem with the mobilization factors are the uncertainties associated with the mobilization times of the different activities, since they depend greatly of innumerable factors as socio-political, economy of the affected area, and size and importance of the affected region. Terzic et al. (2014) employs lognormal functions to describe the mobilization times, but among other parameters, these are related to the severity of damage, total number of damage components and building loss ratio. They assumed that in order to calculate downtime to damage repair, some of the tasks can be done in sequence (series), while other can be done simultaneously (parallel): 1. First of all are repaired the structural elements in order to insure overall structural integrity. 2. Then the stairs, elevators, and electric power are repaired in parallel. 3. Finally, simultaneous repairs for piping and interior finishing; exterior enclosure; and mechanical units. The business downtime due to repair is equal to the maximum repair time for any floor level. At last, the total business downtime is estimated as the sum of the business downtime due to mobilization factors and due to repair. Finally, downtime is computed for different hazards and for different building retrofits. Terzic et al. (2014) considered three different situations (three different magnitudes for an earthquake) with five different retrofit equipments. The final results showed the importance of mitigating damage to the structure and other critical components, since delays due to building closure and subsequent mobilization issues can significantly increase business downtime.

5.5 Concluding Remarks

The chapter describes different types of recovery models to assess resilience for buildings, infrastructures and communities in general. Then attention shifts toward the definition of downtime which is the most uncertain variable in the resilience assessment, because it is affected by many parameters. A literature review of the different methods to assess downtime currently available are provided.

References

- Almufti I, Willford M (2013) REDiTM rating system, resilience-based earthquake design initiative for the next generation of buildings. Report, Arup
- Ang A, Tang W (2007) Probability concepts in engineering. Emphasis on applications to civil and environmental engineering. Wiley, New York
- Beck J, Kiremidjian A, Wilkie S, King S, Achkire Y, Olson R, Goltz J, Porter K, Irfanoglu A, Casari M (1999) Decision support tools for earthquake recovery of businesses. Interim report for CUREe-Kajima phase III project, vol 2. California Universities for Research in Earthquake Engineering, Richmond
- Bonowitz D (2011) Resilience criteria for seismic evaluation of existing buildings: a 2008 special projects initiative report to structural engineers association of northern california. Report, Structural Engineers Association of Northern California (SEAONC)

- Chang SE (2000) Transportation performance, disaster vulnerability, and long-term effects of earthquakes. In: Proceedings of the second Euro conference on global change and catastrophe risk management. International Institute for Applied System Analysis, Laxenburg
- Chang SE, Shinozuka M (2004) Measuring improvements in the disaster resilience of communities. *Earthq Spectra* 20(3):739–755
- Cimellaro GP, Reinhorn AM (2010a) Multidimensional performance limit state for hazard fragility functions. *J Eng Mech* 1(1):156. [http://link.aip.org/link/?EMX/1/156/1http://dx.doi.org/10.1061/\(ASCE\)EM.1943-7889.0000201](http://link.aip.org/link/?EMX/1/156/1http://dx.doi.org/10.1061/(ASCE)EM.1943-7889.0000201)
- Cimellaro GP, Reinhorn AM, Bruneau M (2010b) Seismic resilience of a hospital system. *Struct Infrastruct Eng* 6(1–2):127–144
- Cimellaro G, Reinhorn AM, Bruneau M (2010c) Framework for analytical quantification of disaster resilience. *Eng Struct* 32(11):3639–3649. doi:10.1016/j.engstruct.2010.08.008
- Comerio MC (2005a) Estimating downtime in loss modeling. *Earthq Spectra* 22(2):349–365
- Comerio MC (2005b) Downtime modeling for risk management – safety and reliability of engineering systems and structures. In: Augusti G, Schueller G, Ciampoli M (eds.) Proceedings of the ninth international conference on structural safety and reliability (ICOSSAR05). Millpress, Rotterdam/Rome
- Comerio MC (2006) Estimating downtime in loss modeling. *Earthq Spectra* 22(2):349–365
- Comerio MC, Blecher HE (2010) Estimating downtime from data on residential buildings after the northridge and loma prieta earthquakes. *Earthq Spectra* 26(4):951–965
- Czarnecki RM (1973) Earthquake damage to tall buildings. M.I.T. Department of Civil Engineering, Cambridge
- FEMA-P58 (2012) Seismic performance assessment of buildings. Report, FEMA P-58. Applied Technology Council, Federal Emergency Management Agency (FEMA), Washington, DC
- Filiatrault A, Uang CM, Folz B, Christopoulos C, Gatto K (2001) Reconnaissance report of the February 28, 2001 Nisqually (Seattle-Olympia) earthquake. Report, Department of Structural Engineering, University of California, San Diego
- Ghorawat S (2011) Rapid loss modeling of death and downtime caused by earthquake induced damage to structures. Thesis, Zachry Department of Civil Engineering, Texas A&M University, College Station
- Hazus (1997) Earthquake loss estimation methodology. Report, National Institute of Building for the Federal Emergency Management Agency
- Kafali C, Grigoriu M (2005) Rehabilitation decision analysis. In: Augusti G, Schueller GI, Ciampoli M. (eds.) Proceedings of the 9th international conference on structural safety and reliability, ICOSSAR05. IOS Press, Rome
- Krawinkler H, Miranda E (2004) Performance-based earthquake engineering. In: Bozorgnia Y, Bertero VV (eds) *Earthquake engineering: from engineering seismology to performance-based engineering*, chapter 9. CRC Press, Boca Raton
- Kustu O, Miller DD, Brokken ST (1982) Development of damage functions for high-rise building components. Report, URS/John A. Blume and Associates, Engineers, San Francisco
- Mander JB, Basoz N (1999) Seismic fragility curve theory for highway bridges. In: *Optimizing post-earthquake lifeline system reliability*. ASCE, New York, pp 31–40
- Mander JB, Sircar J (2009) Loss model for seismically damaged structures. In: Proceedings of the structures congress, ASCE, Austin, pp 1077–1086
- Mitrani-Reiser J (2007) An ounce of prevention: probabilistic loss estimation for performance-based earthquake engineering. Thesis, California Institute of Technology, Pasadena
- Porter KA, Kiremidjian AS, LeGrue JS (2001) Assembly-based vulnerability of buildings and its use in performance evaluation. *Earthq Spectra* 17(2):291–312
- Shinozuka M, Feng M, Lee J, Naganuma T (2000) Statistical analysis of fragility curves. *J Eng Mech ASCE* 126(12):1224–1231
- Terzic V, Mahin SA, Comerio MC (2014) Comparative life-cycle cost and performance analysis of structural systems. In: Proceedings of the 10th national conference in earthquake engineering. Earthquake Engineering Research Institute, Anchorage

Chapter 6

PEOPLES Resilience Framework

Abstract This chapter is proposing a framework for measuring community resilience at different spatial and temporal scales. Seven dimensions are identified for measuring the community resilience: *Population and Demographics, Environmental/Ecosystem, Organized Governmental Services, Physical Infrastructures, Lifestyle and Community Competence, Economic Development, and Social-Cultural Capital*. They are summarized with the acronym PEOPLES. Each dimension is characterized by a corresponding performance metric that is combined with the other dimensions using a multi-layered approach. Therefore, once a hybrid model of the community is defined, the proposed framework can be applied to measure its performance against any type of extreme event during emergency and in long term post-disaster phases. A resilience index can be determined to reflect all, or part, of the dimensions influencing the events.

6.1 Literature Review on Resilience Framework

After all the recent disasters, the international society has become aware that *Resilience* is the key to approach natural and manmade disasters. The goal of Resilience-Based Design (RBD) is to make individual structures and communities safe and resilient, through advanced technologies (e.g. base isolation, passive dampers, etc.) and resilience actions that allow each structure and/or community to recover its functionality in a short time.

As the research advances, it has been realized that resilience must be studied on a global level and not on an individual basis. Bruneau et al. (2003) identified four types of resilience that should be adequately measured: *technical; organizational; social; and economical*, (TOSE). Technical and economical resilience are mainly related to the physical systems, while organizational and social resilience are related to the society and the non physical systems. *Technical resilience* describes the capability of a system to perform its functionality. *Organizational resilience* describes the ability of the organization(s) to manage the system. For example, measures of organizational resilience could include how well emergency units function, how quickly spare parts are replaced, how quickly repair crews are able to reach the affected components of a system, etc. *Social resilience* concerns how well

society copes with the loss of services as a result of a blackout. For severe blackouts, social resilience can be the most critical dimension of resilience. Finally, *economic resilience* describes the capability to reduce both indirect and direct economic losses Rose and Liao (2005).

After the framework by Bruneau et al. (2003), other frameworks have been developed identifying different performance metrics for evaluating resilience. For example, Chang and Shinozuka (2004) refined the method proposed by Bruneau et al. (2003), and then applied it to the case study of the Memphis water system. Their method proposed a metric of system performance Q , which is evaluated by comparing the extreme events scenario with the pre-event conditions. Miles and Chang (2006) presented a comprehensive restoration model, which establishes the relationships between a community household business and lifeline networks.

The same year Cagnan et al. (2006) developed a discrete event simulation model for modeling the post-earthquake restoration process of an electric power network. The resilience concept as *input to decision support methodologies* has been applied to *hospitals* (Cimellaro et al. 2010b; Cimellaro and Piqué 2016), *lifeline structures* (Ouyang and Duenas-Osorio 2011; Cimellaro et al. 2014a,b) and *cities* (Chang et al. 2014) using different optimization methods based on *economic* (Chang and Shinozuka 2004), *downtime* (Cagnan et al. 2006) or *multi-criteria analysis* (Javanbarg et al. 2012).

More specifically, when considering infrastructures, several methods for the quantification of resilience have been proposed which can be grouped into *probabilistic methods* (Miller-Hooks et al. 2012; Queiroz et al. 2013), *graph theory methods* (Berche et al. 2009; Dorbritz 2011), *fuzzy methods* (Heaslip et al. 2010) and *analytical methods* (Cimellaro et al. 2010a; Tamvakis and Xenidis 2013). In particular, Tamvakis and Xenidis (2013) proposed a framework based on entropy theory concepts. Entropy describes the system disorder at a given point in time and is measurable in a single metric analogously to resilience, which describes the system potential to recover to a desired condition of the system. Although the idea seems promising, the research fails to provide details about the method and applications which show the feasibility of the methodology.

Of course, the literature review presented above cannot be exhaustive, but many of the works cited are based on the review of previous works to quantify resilience, therefore this review is still adequate to identify the different trends in quantifying resilience of infrastructures and communities in general. Furthermore, it is clear that a comprehensive model to quantify resilience of a metropolitan area, while considering all infrastructures and their interaction, is still missing in literature- due to the complexity of modeling it.

The present chapter identifies the gaps in the definitions and quantification of resilience at the community level and presents a novel framework for evaluating resilience in a community and for assessing the performance of critical infrastructures and their interdependencies while taking into account the influence of the human behavior and its emotions. The suggested framework combines different dimensions together and each category is a system with its performance indicator.

The framework is based on seven dimensions which are used to measure resilience at different scales. They are: *Population and Demographics, Environmental/Ecosystem, Organized Governmental Services, Physical Infrastructure, Lifestyle and Community Competence, Economic Development, and Social-Cultural Capital*. These are identified with the acronym PEOPLES.

The framework describes the methodology and introduces a few performance indicators for the different dimensions, components and sub-components, which are key parameters for the definition of the resilience index. These indicators can be as complex as needed, involving several parameters some of which still need to be defined and quantified, even though several applications of the framework are already available in literature. The framework can be used for resilience-based design (RBD) at different spatial (local, regional etc.) and temporal (emergency response, reconstruction phase, etc.) scales. It can be used by decision makers for resilience management minimizing all the possible consequences following an extreme event, both natural and manmade allowing the perturbed system to return to the initial conditions as quickly as possible.

6.2 Formulation of a Theoretical Framework for the Analysis of Community Resilience

Disaster resilience is often divided between technological units and social systems. On a small scale, when considering critical infrastructures, the focus is mainly on technological aspects. On a larger scale, when considering an entire community, the focus is broadened to include the interplay of multiple systems such as human, environmental, and others which together add up to ensure the healthy functioning of a society. At the community level, the human component is central, because in the case of a major disruptive event, resilience depends first and foremost on the actions of the people operating at the individual and neighborhood scale (Fig. 6.1). Community resilience also depends heavily on the actions of different levels of government and its agencies at the local and regional scales when a disruptive extreme event occurs (geographic scales II and III in Fig. 6.1). In order to emphasize the primary role of the human system in community resilience and sustainability, the authors suggest (Renschler et al. 2010; Cimellaro et al. 2016) using the acronym “PEOPLES” (Fig. 6.2). This nomenclature highlights both the physical and environmental assets as well as the socio-economic-political/organizational aspects of a particular community.

The *PEOPLES* Resilience Framework is built from and expands upon the initial research developed at the Multidisciplinary Center of Earthquake Engineering Research (MCEER), and it links the previously identified resilience characteristics (*technical, organizational, societal, and economic*) and resilience attributes (r^4 : *robustness, redundancy, resourcefulness, and rapidity*) (Bruneau et al. 2003; Bruneau and Reinhorn 2007; Cimellaro et al. 2010b). *PEOPLES* incorporates

Fig. 6.1 PEOPLES resilience framework, spatial scales

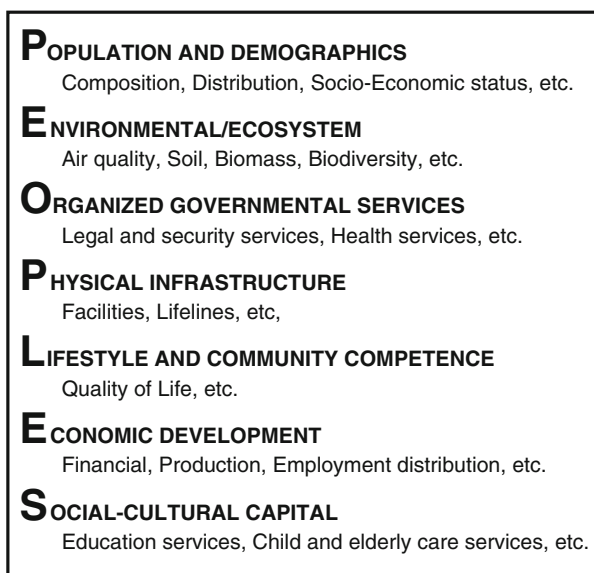
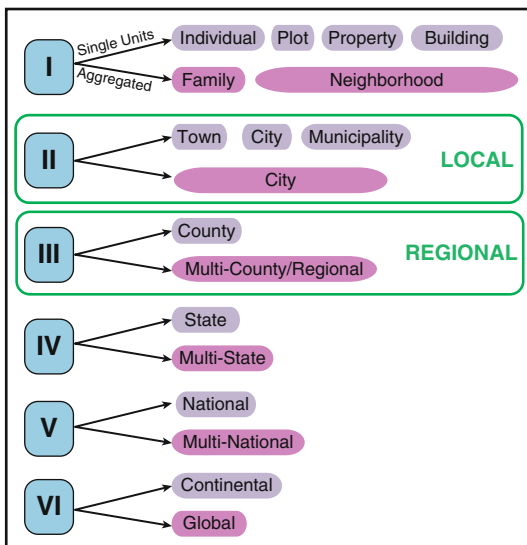


Fig. 6.2 PEOPLES resilience framework, dimensions

MCEER widely accepted definitions of service functionality, its components (assets, services, demographics) and the parameters influencing their integrity and resilience which are assembled using a layered approach (Fig. 6.3). While the components have different weights and values, the order of these dimensions in the acronym is not indicative to their importance. The *PEOPLES* Resilience Framework defines

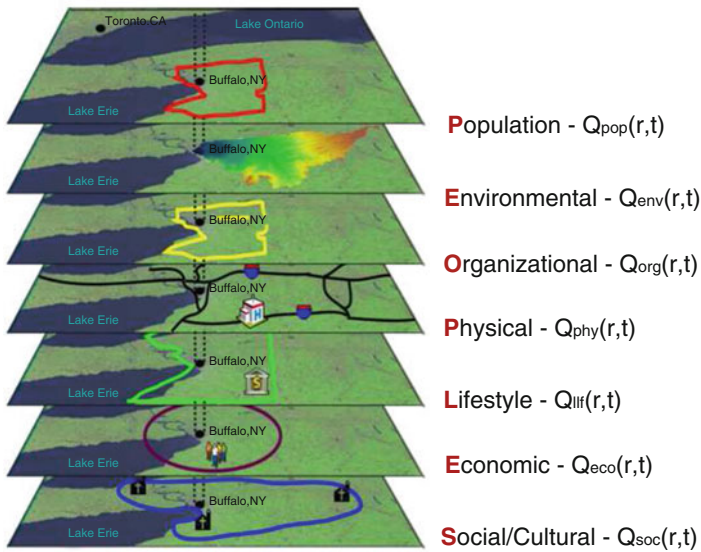


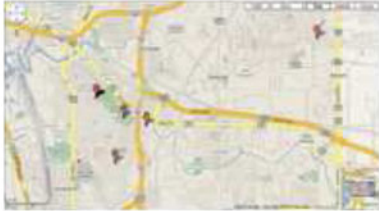


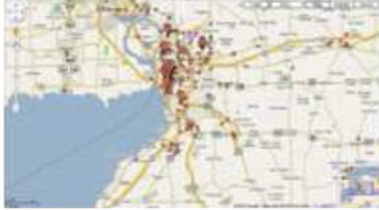

Fig. 6.3 PEOPLES framework layered model

components of functionality using a geospatial-temporal distribution within its geographical influence boundaries.

Interdependencies between and among these components are the key to determining the resilience of communities. *PEOPLES* enables the use of various **community resilience indicators** that integrate, over space and time, the system functionality and services of a community in a landscape setting. In this particular dimension, historical and continuously gathered information through remote sensing and Geographic Information Systems (GIS) play a major role in assessing the resilience of all integrated systems, and feed a predictive resilience model. Resilience can be considered as a dynamic quantity that changes over time and across space. As shown in Fig. 6.1 and Table 6.1, the landscape perspective in the *PEOPLES* Resilience Framework is based on basic community organizational units at a local (i.e., neighborhoods, villages, towns or cities) and regional scale (i.e., counties/parishes, regions, or states).

Table 6.2 shows the extended list of components and sub-components of the *PEOPLES* Framework. In the following sections a detailed description of each of the seven component-dimensions associated with the *PEOPLES* Resilience Framework and some potential indicators is complemented by attempts of quantification. The dimensions are neither orthogonal nor synonymous. While they are discussed as distinct dimensions and while we anticipate developing measures that are often independent, the nature of community resilience is such that interdependence between and among the dimensions is expected.

Table 6.1 PEOPLES resilience framework, scales I to V (Western New York)

<i>PEOPLES</i> community scale	Healthcare and veterinary facilities
<p>Scale I – neighborhood Neighborhoods directly surrounding Mercy Hospital (A) in West Seneca (note that this facility is the largest and most important facility at this scale)</p>	
<p>Scale II – local (town) Towns directly surrounding Mercy Hospital (D) near the map center ("ii" is subscale of "II" indicating that there are facilities in similar size close by)</p>	
<p>Scale III – local (city) City close to Mercy Hospital (F) (the facility is one of several in a densely populated location, e.g. Buffalo)</p>	
<p>Scale IV – regional (county) : Larger administrative boundary surrounding Mercy Hospital (F) (the facility is one of several in Erie County)</p>	
<p>Scale V – regional (multi-county) Mercy Hospital (mapped as a dot only) is among a lot of facilities in Western New York (Rochester, Pennsylvania and Southern Ontario are in this map it includes also Scales IV and V)</p>	

The potential indicators are intended to be illustrative rather than exhaustive. Importantly, the indicators that are identified are those that may be used to describe a community and its resilience at any time, and not simply the state of post-extreme event. Ultimately, the value of the *PEOPLES* Resilience Framework is that it (a) identifies the distinct dimensions and related key indicators but also (b) aggregates the dimensions in ways that reflect community realities. The *PEOPLES* Resilience

Table 6.2 A complete list of components and subcomponents of PEOPLES framework

1-Population and demographics			
(a) Distribution/density (i) Urban (ii) Suburban (iii) Rural (iv) Wildland	(b) Composition (i) Age (ii) Gender (iii) Immigrant status (iv) Race/ethnicity	(c) Socio-economic status (i) Educational attainment (ii) Income (iii) Poverty	(iv) Home ownership (v) Housing vacancies (vi) Occupation
2-Environmental/ecosystem			
(a) Water quality/quantity (c) Biomass (vegetation)	(b) Air quality (f) Other natural resources	(c) Soil quality	(d) Biodiversity
3-Organized governmental services			
(a) Executive/administrative (i) Emergency response (iii) Schools	(ii) Health and hygiene	(b) Judicial	(c) Legal/security
4-Physical infrastructure			
(a) Facilities (i) Residential (1) Housing units (ii) Commercial (1) Distribution facilities (2) Hotels-accommodations (iii) Cultural (i) Entertainment venues (ii) Museums (iii) Religious institutions	(2) Shelters (3) Manufacturing facilities (4) Office buildings (iv) Schools (v) Sports/recreation venues	(b) Lifelines (i) Communications (1) Internet (2) Phones (3) TV (4) Radio (5) Postal (ii) Healthcare (1) Acute care (2) Long-term acute care (3) Psychiatric (4) Primary care (5) Specialty (iii) Food supply (iv) Utilities (1) Electrical (2) Fuel/gas/energy (3) Waste (4) Water (v) Transportation (1) Aviation (2) Bridges (3) Highways (4) Railways (5) Transit (6) Vehicles (7) Waterways	
5-Lifestyle and community competence			
(a) Collective action and decision making (i) Conflict resolution	(ii) Self organization	(b) Collective efficacy and empowerment	(c) Quality of life
6-Economic development			
(a) Financial services (i) Asset base of financial institutions (ii) Checking account balances (personal and commercial) (iii) Consumer price index (iv) Insurance (v) Number and average amount of loans (vi) Number of bank and credit union members (vii) Number of bank and credit unions (viii) Saving account balances (personal and commercial) (ix) Stock market	(b) Industry-employment services (i) Agriculture (ii) Construction (iii) Education and health services (iv) Finance, insurance and real states (v) Furtune 1000 (vi) Furtune 500 (vii) Information, professional business, others (viii) Manufacturing (ix) Leisure and hospitality	(x) Number of corporate headquarters (xi) Other business services (xii) Professional and business services (1) Employment services (a) Flexibilities (b) Opportunities (c) Placement (2) Transport and utilities (3) Wholesales and retails	(c) Industry-production (i) Food supply (ii) Manufacturing
7-Social/cultural capital			
(a) Child and elderly services (c) Education services	(b) Commercial centers (f) Non-profit organization	(c) Community participation (g) Place attachment	(d) Cultural and heritage services

Framework requires the combination of qualitative and quantitative data sources at various temporal and spatial scales, and as a consequence, information needs to be aggregated or disaggregated to match the scales of the resilience model and the scales of interest for the model output.

6.3 Population and Demographics

The *Population and demographics* dimension describes and differentiates the communities using specific parameters (e.g. *the median income, the age distribution* etc.) which might be critical for understanding its economy, health etc. Table 6.3 shows fundamental elements of this dimension. The knowledge of, for instance, the median income and age distribution of a community, is critical to understanding its economic health and potential resilience. Communities tend to differ on key demographics; to the extent that two or more communities may be similar, Community A and Community B, we can predict Community A’s hypothetical response to a disaster based on Community A’s actual response to a disaster.

One measure of performance metric (Q_p) for the *Population and Demographic* dimension within a given community could be quantified by using the social vulnerability index (SoVI) proposed by Cutter (1996), which integrates exposure to hazards with the social conditions that make people vulnerable to them. Social vulnerability (a counterpart of social resilience) is defined as the *incapacity of societies, organizations and citizens to resist multiple undesirable events to which they are exposed*. These events are generated by the interaction in the society, the institutions and the systems of cultural values.

Social vulnerability is a pre-existing state of the community that affects the capacity of the society to get ready for and recover from undesirable disruptive

Table 6.3 Elements of population and demographics dimension

Dimension	Component	Sub-component
Population and demographics	Distribution/density	Urban
		Suburban
		Rural
		Wildland
	Composition	Age
		Gender
		Immigrant status
		Race/ethnicity
	Socio-economic status	Educational attainment
		Income
		Poverty
		Home ownership
		Housing vacancies
	Occupation	

event. However, *Vulnerability* and *Resilience* are two different concepts. In fact, *Vulnerability* focuses on the capacity of the community to resist the natural hazard, while *Resilience* looks for opportunities to enhance the outcome and focuses on the quality of life of the citizens at risk. The first to emphasize these differences is Manyena (2006) who has compared the concept of *resilience* vs. *vulnerability* summarizing all the different definitions provided from the 1990s up until the present.

This dimension of vulnerability can be measured using a social index that describes the socioeconomic status, the composition of the population (e.g. elderly and children), the population density, the rural agriculture, the race, the gender, the ethnicity, the infrastructure employment, and the county debt/revenue. The social index described is based on Cutter's Hazards-of-Place Model of Vulnerability framework that integrates exposure to hazards with the social conditions that make people vulnerable to them (Cutter and Mitchell 2000; Cutter 1996). High SoVI indicates high vulnerability, and conversely, low SoVI indicates low vulnerability. Analytically, the performance metric of the *Population and Demographic dimension* is given by:

$$Q_P(\mathbf{r}, t) = 1/(f_1, f_2, f_3, f_4, f_5, f_6, f_7, f_8, f_9, f_{10}, f_{11}) \quad (6.1)$$

where f_1, f_2, \dots, f_n are 11 independent factors which are: *socioeconomic status, elderly and children, development density, rural agriculture, race, gender, ethnicity, infrastructure employment, and county debt/revenue*. Additionally, key qualitative and quantitative indicators about population and demographics from the US Census database can be added into this index, such as the educational attainment, the

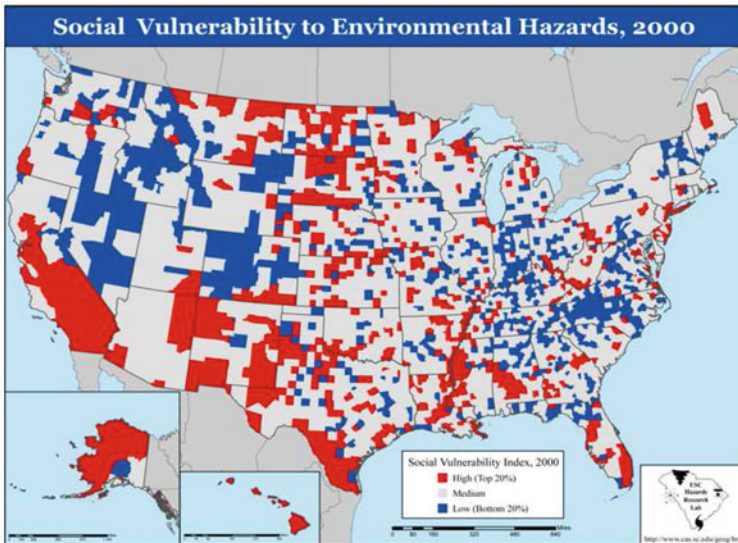


Fig. 6.4 Social vulnerability to environmental hazards, 2000 (HVRI 2013)

marital status, the annual income, the age, the gender, the race/ethnicity distribution, etc. The index is a comparative metric that helps users examine differences in social vulnerability among counties. SoVI graphically illustrates the geographic variation in social vulnerability (Fig. 6.4). It shows where there is uneven capacity for preparedness and response and where resources might be used most effectively to reduce the pre-existing vulnerability. SoVI is also useful as an indicator for determining the level of recovery from disasters.

6.4 Environmental/Ecosystem

While it is critical for and the sustainability of desirable ecosystem states in the face of unknown futures and variable environments (Elmqvist et al. 2003), resilience is not a quality that is easily assessed (Adger 2000). The resilience of a system depends on various factors such as time scale, the actual disturbance, the structure of the system, and control measures or policies that are available to be implemented (Ludwig et al. 2002). This dimension measures the capability of an ecosystem to deal with disturbance, as well as the amount of disturbance an ecosystem can absorb without considerably varying its processes, functionalities and structure (Gunderson et al. 2002).

In the *PEOPLES* Framework, the environmental and ecosystem dimension measures the capability of the ecological system to return to or approach its pre-event condition. In order to measure the environmental/ecosystem dimension of resilience, key indicators should be integrated together such as air, water and soil quality, biodiversity, and other natural resources (Table 6.4). One possible performance metric for this dimension is the *Normalized Difference Vegetation Index* (NDVI), which is evaluated from satellite-derived remote sensing images that analyze the density of green vegetation across an area. The *Normalized Difference Vegetation Index* (NDVI, Fig. 6.5) uses the visible and near-infrared bands of the electromagnetic spectrum, and is adopted to analyze remote sensing measurements and assess whether the target being observed contains live green vegetation or not (Rouse et al. 1973).

Table 6.4 Elements of environmental/ecosystem dimension

Dimension	Component
Environmental/ecosystem	Water quality/quantity
	Air quality
	Soil quality
	Biodiversity
	Biomass (vegetation)
	Other natural resources

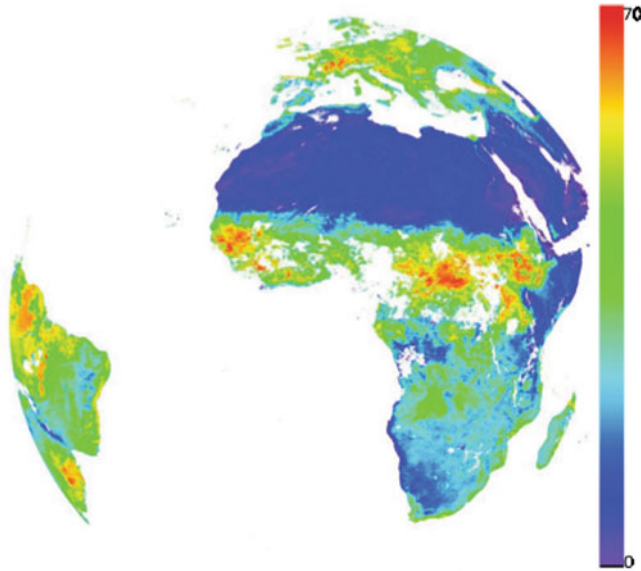


Fig. 6.5 Example of the NDVI encoded product for 31 August 2011

NDVI has found a wide application in vegetative studies and has been used to estimate crop yields, pasture performance, and rangeland carrying capacities, among other capacities. It is often directly related to other ground parameters, such as percent of ground cover, photosynthetic activity of the plant, surface water, leaf area index and the amount of biomass.

NDVI can be used in the framework as a proxy for ecosystem productivity and is calculated using the visible (red) infrared absorption bands (Red) and near infrared (NIR) absorption bands:

$$NDVI = (NIR - Red)/(NIR + Red) \quad (6.2)$$

Indeed, the NDVI index is highly correlated with the *Aboveground Net Primary Productivity* (ANPP) index (Pettoirelli et al. 2005; Olofsson et al. 2007), which is based on field measurements of the biomass accumulation and therefore can be considered as an indicator of the ecosystem resilience. Several applications can be found in literature where the NDVI values obtained from Landsat images have been used to observe the restoration of the vegetation after a fire (Diaz-Delgado et al. 2002) and using time series analysis (Simoniello et al. 2008). Building on previous research, the NDVI index can be used to quantify the Environmental/Ecosystem dimension by comparing the NDVI values before and after the event to determine the variations of ecosystem productivity through the space and the time caused by natural disasters such as fire, flood, hurricanes, tsunami, etc. In the case of other



Fig. 6.6 Green roofs in New York city

types of disasters, such as blizzards, terrorist attacks etc., the variation of this index could be negligible, because the vegetation density might not be altered, while other indicators would be more relevant. As with the other dimensions, ecological resilience is the integration of all key indicators that include air, water and soil quality, biodiversity, and other natural resources. In the city of New York, in the United States, is possible to find an example of an ecosystem based on disaster risk management. New York is seasonally untreated by storm water and its sewage usually floods the streets due to the aging sewerage system that is no longer sufficient. Most of water, after heavy rains, flows directly into the two rivers of the city instead of reaching one of the numerous water treatment plants. The City Council has decided to invest 5.3 billion U.S. dollars in green infrastructure on roofs (Fig. 6.6), streets and sidewalks. These green spaces will absorb more rainwater than before and will reduce the load on the city sewage system.

6.5 Organized Governmental Services

In contrast to the more or less spontaneous individual and neighborhood responses to extreme events, *organized governmental services* are designed to allow an orderly response (Table 6.5).

The *Organized governmental services* dimension includes legal and security services (e.g. Police, emergency Departments, fire Departments, the military etc.), as well as the public health, the hygiene Departments, the cultural heritage Departments etc. Each of the above mentioned organized government services play a key role in sustaining societies before and after an extreme event.

Table 6.5 Elements of organized governmental services dimension

Dimension	Component	Sub-component
Organized governmental services	Executive/administrative	Emergency response and rescue
		Health and hygiene
	Judicial	
	Legal/security	

The deficiency of this resilience dimension has been observed during the 2010 Haiti Earthquake, where the lack of government services and orderly control has been observed, along with a general perception that the government was not able to deal with the disaster. Instead, the value of this dimension was high during the 2010 Darfield earthquake in New Zealand which was characterized by a quick restoration on local, territorial and national government services. The organizational response during an emergency is most likely to be effective and resilient when it blends discipline and agility (Harrald 2006).

Agility, flexibility, adaptability, and improvisations are entities which enhance resilience of a society, through volunteers, spontaneous helping behavior, and emergency groups which infuse resources and creativity into disaster response activities (Stallings and Quarantelli 1985; Drabek and McEntire 2002). Discipline together with a proper reaction is guaranteed by emergency plans, training activities, exercises and mutual aid agreements, which encourage action toward common goals (Weick 2005, 1995). Flexibility, adaptability, and improvisation among responding entities make their own distinctive contributions to resilience. Organizational expansion, extension, and emergence are key bases of resilient disaster responses (Sutton and Tierney 2006).

The concept of collaborative emergency management seeks to engage all critical community sectors in preparing for and responding to disasters, including local elected and appointed officials; subject matter experts; community-based, faith based and other non-governmental organizations, the general public, including both community members that belong to groups such as community emergency response teams and volunteers; the private sector and business networks; and the mass media (Patton 2007).

Collaborative management, as opposed to top-down direction, is another characteristic of resilient systems. Hierarchies tend to stand in the way of upward information flow, the form of communication that is most essential during disasters. Less hierarchical forms of organization work best in all types of turbulent environments, including disasters. This is in part because they encourage a free flow of ideas, but also because flatter organizations and decentralized networks are more nimble in responding to those environments (Burns and Stalker 1961; Waugh and Streib 2006).

Key indicators for this dimension include the number of available response units and their capacity. Population and demographic numbers would be used to

normalize the number and capacity of these services. In addition to assessing the availability of government services in terms of personnel and equipment, this dimension also includes an evaluation of emergency preparedness planning. For example, surveys may reveal the extent to which organized government services have developed memoranda of understanding (MOUs) and other types of mutual aid agreements, and the extent to which various organized government services participate in emergency and evacuation drills and table-top exercises (Tierney 2009).

An example of how conscious a government should be is the behavior of councilor Nada Yamout, from Beirut, Lebanon. The city is situated east of the Mediterranean Sea, a hazard prone area, and in the city there are several heritages to be protected and preserved. Just after she had been elected, at the Third Global Platform for Disaster Risk Reduction she stated her concern about disaster risk reduction. Her government created a Campaign City in October 2010 to work on this task. They allocated a budget to risk reduction activities, evaluated the needs of the city and took stock of what was available. They focused in four main points: financial, technical, national government support and involvement of the private sector and civil society, and the actions that must be taken at all levels, at national, provincial and city government.

6.6 Physical Infrastructures

The *physical infrastructure dimension* includes both *facilities* (e.g. housing, commercial facilities, and cultural facilities) and *lifelines* (food supply, health care, utilities, transportation, communication networks, etc.) within a built environment (Cimellaro et al. 2014a). Table 6.6 shows fundamental elements of physical infrastructures dimension.

Table 6.6 Elements of physical infrastructure dimension

Dimension	Component	Sub-component
Physical infrastructure	Facilities	Residential
		Commercial
		Cultural
	Lifelines	Communications
		Health care
		Food supply
		Utilities
		Transportation

Lifelines are essential utilities which serve communities across all jurisdictions and locales. Lifelines are thus components of the nation's critical infrastructure, which also includes medical, financial, and other infrastructure systems that create the fabric of modern society. For clarity, lifeline infrastructures are simply called *lifelines* in this report and include: (a) energy utilities (e.g. power and natural gas networks (Cimellaro et al. 2014c)); (b) transportation systems (e.g. highways, railroads, airports, seaports etc.); (c) water, storm-water and sewerage pipelines; (d) communication systems; and (e) health care facilities (e.g. hospitals, emergency facilities, etc.) (Cimellaro et al. 2011), etc.

Physical infrastructures have an important impact on the restoration process following a disaster; therefore the organized government services work actively to restore their functionality after the disaster (e.g. they clean roadways of structural debris etc.). Following Hurricane Katrina in 2005, after the evacuation of New Orleans, attention has shifted towards the restoration of the physical infrastructures. The pictures of damages have been used to communicate the consequences of the hurricane and of the subsequent flood (e.g. collapse of critical facilities such as churches, schools, and hospitals) to the media all over the world. These critical facilities were not able to provide their services without water and electricity, while the damaged schools affected the community's self confidence to overcome the disaster and restore the initial functionality. The roads full of debris create an obstacle to the supply chain, therefore the economy in the region cannot restart, because even if shops and companies re-open they can be inaccessible and if they relocate for a short term, the older customers might have some difficulties in finding the new facility.

After a disaster, the restoration of physical infrastructures remains a technical problem, which is also related to the socio-political events and the economic situation. The resilience dimension should also take into account these interdependencies between the different infrastructures and sectors during the analysis (Cimellaro et al. 2014b). Different performance metrics for this dimension are available in literature (Cimellaro et al. 2014c,a,b) and they vary for every type of infrastructure (e.g. gas, water, transportation, etc.).

For example, a possible performance metric for *housing units* might be the proportion of housing stock not rated as substandard or hazardous, and vacancy rates for rental housing (Tierney 2009). Examples of performance metrics for the communication networks might be the (i) satisfactoriness of linkages between official and unofficial information sources, (ii) the number of ties between the mass media and the emergency management entities, (iii) the sufficiency of the measures for communicating the public's need and information after the disaster (Tierney 2009). There are several actions that can be carried out before the disaster occurs. To strengthen protective infrastructure it is useful to adopt city policies and to manage different strategies for all kind of hazards. It is important to assess the risk of each system and develop programs for each risk as it is broken down. But over all, it is critical to ensure that roads and sites have been designed to be accessible in case of any kind of emergency, including fire or earthquakes, ensure that all public buildings and infrastructures follow seismic codes adapted to the

area. Critical infrastructure can be protected by assessing the vulnerability of the existing to natural hazards, adopting measures to prevent damage and developing capital investment in the long-term to retrofit or replace the most critical lifelines.

6.7 Lifestyle and Community Competence

As suggested by Harrald (2010), “Resilience [] requires the building of collaborative relationships that will enable communities and businesses to better absorb, adapt, survive, and thrive when confronted with extreme events.” Norris et al. (2008) describe community resilience as “a metaphor, theory, set of capabilities and strategy for disaster readiness” (p. 127). One of the capabilities they discuss is community competence. Community competence is essential to community resilience in the same way that individual competence is essential to personal hardiness. *Lifestyle Community Competence* dimension deals with flexibility, creativity and problem-solving skills of a community, also through political partnerships (Norris et al. 2008).

Table 6.7 shows principal elements of *Lifestyle Community competence dimension*. This dimension captures both the raw *abilities* of a community (e.g., skills to find multifaceted solutions to complex problems through the engagement in political networks) and the *perceptions* of a community (e.g. perception to have the ability to make a positive change through a common effort that relies on peoples’ aptitude to resourcefully envision a new future and then move in that direction) (Brown and Kulig 1996/97). In fact, the societies that believe that they can restore, renew and rebuild themselves are expected to be more determined when facing a disaster or in general, any type of changes. Quality of life surveys can be used as indicators of this perception, because they reveal whether people inside the community are devoted to their community and willing to engage in the activities necessary to maintain the community alive, before and after the disaster strikes. Examples of performance metrics for the community competence in normal condition before the disaster might be the number of immigrants, the number of citizens involved in politics, etc. Specific performance metrics for this dimension directly related to the disaster might be the extensiveness of community warning procedures and plans, measured

Table 6.7 Elements of lifestyle and community competence dimension

Dimension	Component	Sub-component
Lifestyle and community competence	Collective action and decision making	Conflict resolution
		Self-organization
	Collective efficacy and empowerment	
	Quality of life	

using for example: the number of citizens involved, the number of organizational disaster training programs, etc. (Tierney 2009).

6.8 Economic Development

According to Radloff (2006), “A community needs to have access to resources to grow and react to changes. The difference between resilient and non-resilient resources is that the former focus on addressing local needs are often locally based sources of employment, skills, and finances” (p. 16). There are six points to this dimension of resilience:

1. Employment in the community is diversified beyond a single employer or employment sector;
2. Major employers in the community are locally owned;
3. The community has a strategy for increasing independent local ownership;
4. There is openness to alternative ways of earning a living and economic activity;
5. The community looks outside itself to seek and secure resources (skills, expertise, finance) to address areas of identified weakness;
6. The community is aware of its competitive position in the broader economy (The Centre for Community Enterprise (CCE), 2000: 15–16).

The *economic development dimension* is composed of both a *static* and *dynamic* assessment. The *static* assessment is the *economic activity* of the current economy of a community, while the dynamic assessment corresponds to the economic development which is the community’s ability to continuously sustaining the economic growth (Table 6.8). The *economic activity* takes into account the supply of labor for the production of economic goods and services (Project 2010), which includes:

All production and processing of primary products whether for market, for barter or for own consumption, the production of all other goods for the market and, in the case of households which produce such goods and services for the market, the corresponding production for own consumption.

The economic development addresses the future, the growth and the community’s efforts to increase its:

Productive capacities . . . , in terms of technologies (more efficient tools and machines), technical cultures (knowledge of nature, research and capacity to develop improved technologies), and the physical, technical and organizational capacities and skills of those engaged in production.

Resilient communities are characterized by the community’s capacity to replace goods, services, shift employment patterns when is needed. In other words, they are associated with the employment, the variety in production and services. The economic dimension consists of three sub-categories: (i) the production within the industry, (ii) the distribution of employments within the industry, and (iii) the financial services.

Table 6.8 Elements of economic development dimension

Dimension	Component	Sub-component
Economic development	Financial services	Asset base of financial institutions
		Checking account balances (personal and commercial)
		Consumer price index
		Insurance
		Number and average amount of loans
		Number of bank and credit union members
		Number of banks and credit unions
		Savings account balances (personal and commercial)
		Stock market
		Industry-employment services
	Construction	
	Education and health services	
	Finance, insurance and real estate	
	Fortune 1000	
	Fortune 500	
	Information, professional business, other	
	Leisure and hospitality	
	Manufacturing	
	Number of corporate headquarters	
	Other business services	
	Professional and business services	
	Industry-production	Food supply
Manufacturing		

The key indicators of the economic development dimension can be: (i) the percentage of the inhabitants that are working in the diverse industries, (ii) the variability of the distribution of employments in the different industries which are in the community, (iii) the literacy rate, (iv) the life expectancy and (v) the poverty rates. Other examples of indicators for this dimension that are related to the community performance following a disaster are the following: (i) the adequacy of plans for inspecting damaged buildings following disasters, (ii) the extent of evacuation plans and drills for high-occupancy structures and (iii) the adequacy of plans for post-disaster commercial restoration, etc. (Tierney 2009). Because of these indicators, this dimension is interdependent with the *Population and Demographics dimension*.

6.9 Socio-cultural Capital

Similar to the Norris et al. (2008) conceptualization of social support, the Community Resilience Model's first dimension is "Resilient People", which consists of the eight points:

1. Leadership is diversified and representative of age, gender, and community cultural composition;
2. Elected community leadership is visionary, shares power, and builds consensus;
3. Community members are involved in significant community decisions;
4. The community feels a sense of pride;
5. People feel optimistic about their community's future;
6. There is a spirit of mutual assistance and co-operation in the community;
7. People feel a sense of attachment to their community;
8. And the community is self-reliant and looks to itself and its own resources to address major issues;

There is a strong belief in and support for education at all levels (CCE 2000).

According to Norris and her colleagues (Norris et al. 2008), "individuals invest, access, and use resources embedded in social networks to gain returns" (p. 137). For our purposes, the *Social/cultural capital dimension* includes numerous sub-categories such as: (i) education services, (ii) child and elderly services, (iii) cultural and heritage services and (iv) community participation etc. (Table 6.9). Social/cultural capital is prerequisite to community competence (Norris et al. 2008) in that it incorporates the array of services that the community has chosen to provide for itself, understanding that community health requires more than good jobs and infrastructure. It also includes several intangible "goods", such as social support, sense of community, place attachment, and citizen participation (Norris et al. 2008).

In addition, the *social support* inspires several services connected with the social/cultural capital, such as "helping behaviors within family and friendship networks" and the "relationships between individuals and their larger neighborhoods and communities" (Norris et al. 2008). In fact, the inhabitants of a community tend

Table 6.9 Elements of social/cultural capital dimension

Dimension	Component
Social/cultural capital	Child and elderly services
	Commercial centers
	Community participation
	Cultural and heritage services
	Education services
	Non-profit organizations
	Place attachment

to manifest their sense of community and to bond with other members of the same group by providing social and cultural services. However, this emotional connection to the community is not necessarily related to the residents which inhabit those places (Manzo and Perkins 2006).

For example, several displaced residents of New Orleans after Hurricane Katrina expressed the desire to return home with a strong “place attachment”, regardless of the job they had and the people they knew. These residents are an important resource for the community, because if they will be provided with housing and employment after the disaster, and they will act in order to restore the community to the initial condition before the disaster. The citizen participation in community organizations (e.g. religious congregations, school and resident associations, neighborhood watches, self-help groups etc.) is a way of demonstrating one’s care for their community, one’s care for meeting and understanding one’s fellow citizens and it increases individuals’ circle of influence and perception of control (Norris et al. 2008).

Measuring social/cultural capital requires acquisition of tallies. The key indicators in normal condition for this dimension are: (i) the number of members belonging to the diverse civil and community organizations, (ii) the surveys of leaders and their perception (e.g., quality of life surveys). The key indicators in emergency conditions are: (i) the existence of community plans targeting transportation-disadvantaged residents, (ii) the adequacy of post-disaster sheltering plans, (iii) the adequacy of plans for incorporating volunteers into official response activities, (iv) the adequacy of donations management plans, (v) the community’s plans to manage various networks (Tierney 2009).

6.10 Mathematical Formulation of the PEOPLES Framework

The main part of the methodology consists of developing a community hybrid model, coupling the *Network models* which will be used to model the *physical infrastructures networks* such as the power and the water, with the *Agent based models* which will be used to model the *socio-technical networks* such as the Emergency Medical Technicians and the fire brigade (Fig. 6.7). Inside the ABM models, the emotions in the agents will be modeled using the extended version of Belief-Desire-Intention modeling framework proposed by Zoumpoulaki et al. (2010), which has been expanded and adapted to the proposed methodology (Fig. 6.8).

Both types of models will be integrated into a hybrid framework, and a matrix approach will be used to describe the interdependencies between the different layers. Each layer represents an infrastructure (Figs. 6.7 and 6.8) and is described by an adjacency matrix \mathbf{A} , while a \mathbf{D} matrix will describe the interdependencies between the nodes of the different layers (e.g. $\mathbf{D}_{\text{WaterPower}}$) which will be obtained using an *extended version of the Haimes' input-output inoperability matrix (IIM)* (Haimes et al. 2005). Let's clarify everything with an example shown in Fig. 6.7. The hospital, which is a node of the EMT layer, is interdependent with the power and the water network. Therefore, a \mathbf{D} matrix describing the interdependencies between the EMT layer and the water and power layer will be determined using Haimes model. The proposed approach will require substantial computational power if the spatial and temporal dimensions of the problem increase, therefore the use of parallel computing is recommended in these cases.

6.11 Resilience Index and Performance Metrics

Once the *hybrid model* in Fig. 6.7 is built, it is necessary to identify the performance metrics to estimate the resilience of each infrastructure. Several approaches exist in literature for hospitals (Cimellaro et al. 2011), lifeline structures (Ouyang and Duenas-Osorio 2011; Cimellaro et al. 2014b) and cities (Chang et al. 2014). Once the proper performance metric is selected, the degree of interdependency between an infrastructure x and y is described using a matrix $\mathbf{D}_{x \rightarrow y}$ which is able to identify the exact location of the interdependency in the network (e.g. node or link). However, sometimes it is also useful to identify a global index I , which measures the degree of interdependency between the different infrastructures, in order to have a global evaluation of the community performance and to assign an unbiased evaluation of the weight (or importance factor) to each infrastructure. This index can be determined using time series analysis (Cimellaro et al. 2014b) or from linear algebra manipulation of the $\mathbf{D}_{x \rightarrow y}$ matrix etc. Then the indices I can be grouped into an infrastructure Interdependency Matrix (\mathbf{IM}). The infrastructures considered in the

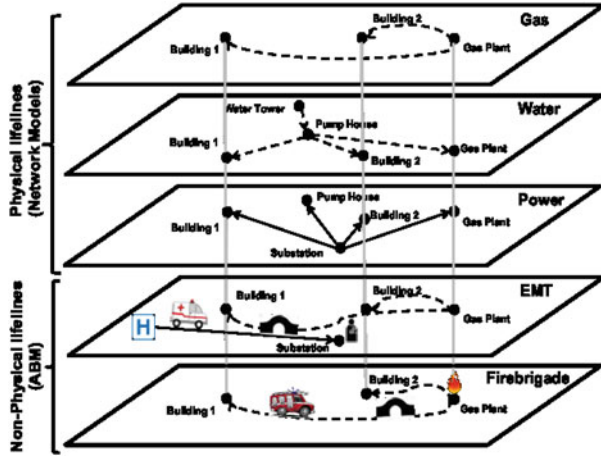


Fig. 6.7 Hybrid layered model for infrastructures within a community

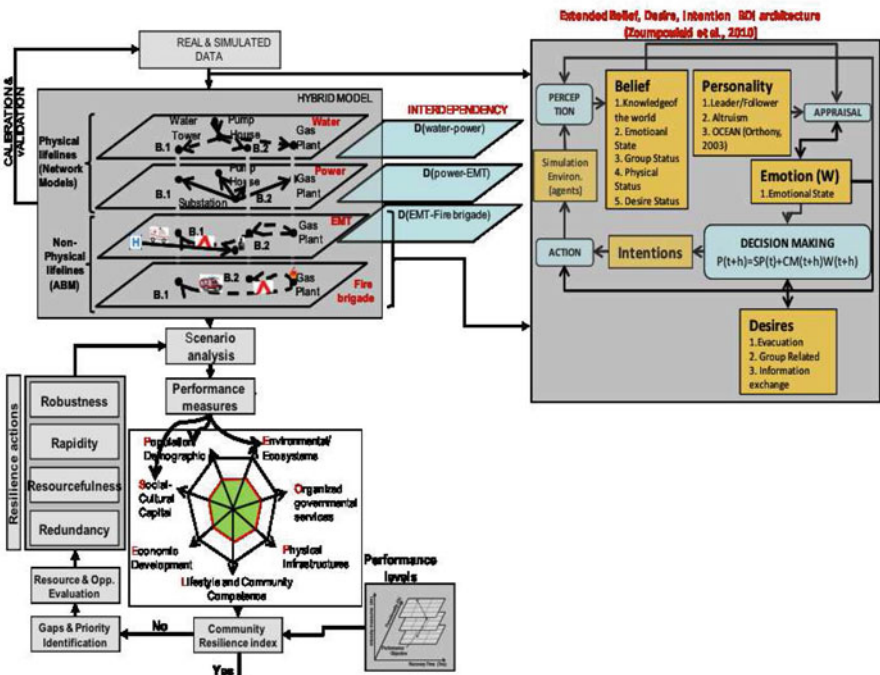


Fig. 6.8 Methodology for resilience-based design

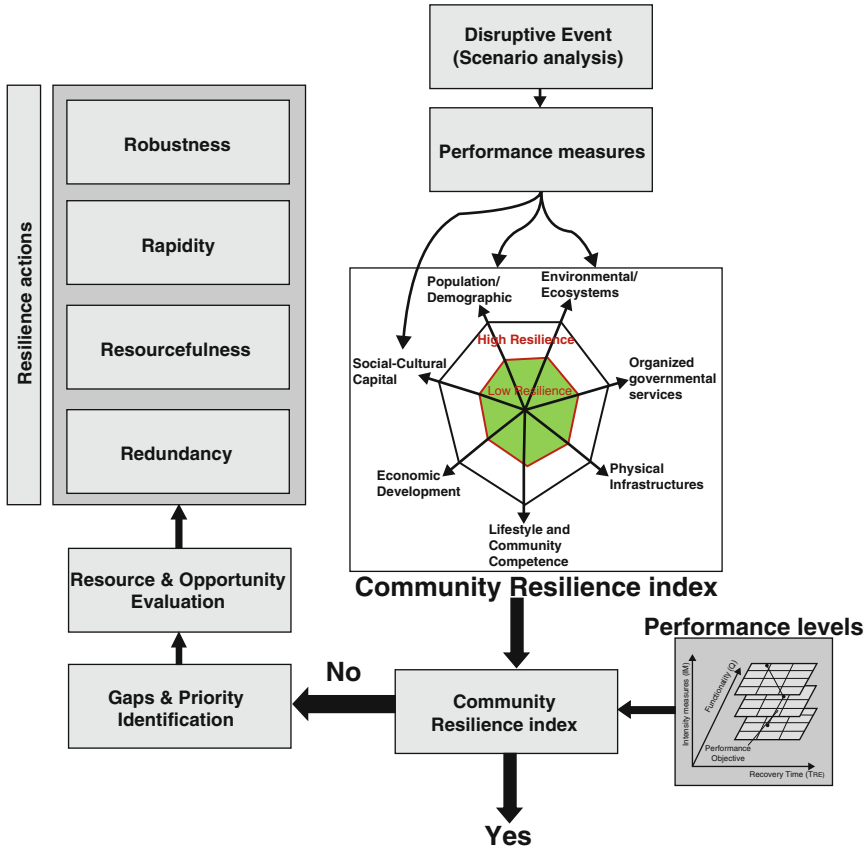


Fig. 6.9 Methodology for resilience-based design (RBD) based on control (feedback loop) approach

analysis of the community are listed in the rows and the columns, while in each cell the degree of interdependency (from 0 to 1), to which the infrastructures are coupled, is represented. The sum over the columns gives the *dependence factor* of the specific lifeline, while the sum over the rows gives the *importance factor* of a specific lifeline. Ideally, the target is to obtain a community in which all lifelines are independent, so **IM** will be an identity matrix. As mentioned above, the **IM** can also be used to have an unbiased estimation of the weight coefficients to assign to each infrastructure considered in the layered approach shown in Fig. 6.7. The approach allows taking into account the infrastructure interdependencies in the proposed resilience framework and it is described in detail in (Cimellaro et al. 2014b). Then, following the PEOPLES framework, the performance indicator of a community is a combination of the performance metrics related to each of the seven dimensions and is given by

$$Q_{TOT}(t) = Q_{TOT}(Q_P, Q_{Env}, Q_O, Q_{Ph}, Q_L, Q_{Eco}, Q_S, \dots) \quad (6.3)$$

where Q_{TOT} = total performance index; and Q_x = general performance indicator of one of the seven dimensions defined above. In each dimension, its indicator is a combination of functionalities of their respective subsystems. For example, the functionality of the physical infrastructure Q_{ph} is defined as follows:

$$Q_{Ph}(t) = Q_{Ph}(Q_{Hosp}, Q_{Ele}, Q_{Road}, Q_{Water}, \dots) \quad (6.4)$$

where Q_{hosp} = performance indicator of a hospital; Q_{Ele} = performance indicator of the electric network; Q_{Road} = performance indicator of the road network; Q_{Water} = performance indicator of the water distribution network; etc. The selection of the proper performance metric for the critical infrastructures plays a key role in the analysis. Even if a realistic and predictive model is developed, the results might be affected by the selection of the final performance function adopted to evaluate the community resilience index using the methodology shown in Fig. 6.9. Different innovative approaches to measure functionality are available in literature, including agent-based modeling, input-output models, mathematical models and game theory (Pederson et al. 2006)

Therefore, once the approach and the geographic scale is selected, the global performance indicator Q_{TOT} can be plotted over the region of interest using a contour plot at a given instant of time t , so the time-dependent functionality maps can be obtained. When the control time TLC is defined, the resilience contour map of the region of interest can also be plotted. The *Resilience contour maps* are obtained by integrating the functionality maps over time using Eq. (2.1), therefore the resilience maps will be time independent, but they will vary in space from point to point in the selected region. Finally, the community resilience index R_{com} is given by the double integral over time and space as follows:

$$R_{com} = \int_{A_c} R(r)/A_c dr = \int_{A_c} \int_{t_{OE}}^{t_{OE}+T_{LC}} Q_{TOT}(t)/(A_c T_{LC}) dt dr \quad (6.5)$$

where A_c is the area of the selected region. The contour plot of each dimension can be combined with the other plots using a layered approach. Then a radar graph is built (Fig. 6.9) and the internal area will determine the final score of the resilience index which will be used to recognize the priority resilience actions to be taken in the community.

6.12 Resilience Performance Levels

The objective of Performance Based Seismic Engineering (PBSE) is to design, construct and maintain facilities with better damage control, coupling the expected or desired performance levels with the levels of seismic hazard. Generally the levels focus on the performances a structure can hold during the shaking and are

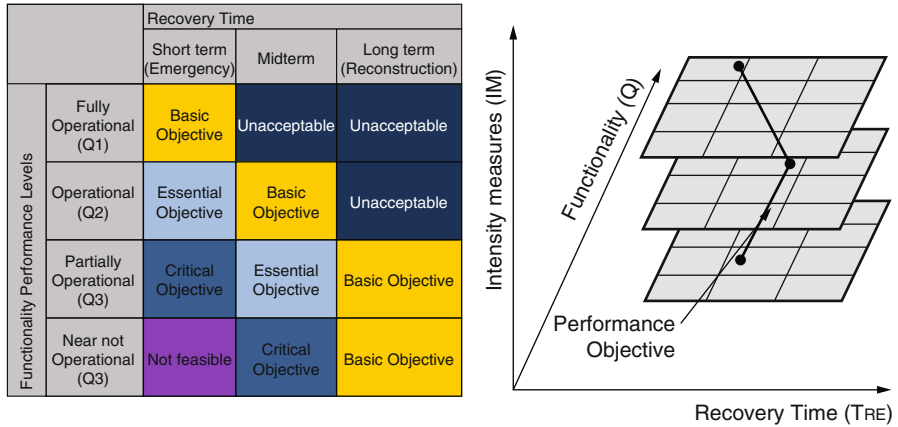


Fig. 6.10 Tridimensional resilience performance levels matrix for structures, communities, systems etc

related to engineering demand parameters such as deformations. More recently, SPUR (Bonowitz 2009), which is the San Francisco planning and Urban Research Association, introduced other definitions of performance levels for infrastructures based on recovery target states which take into account the safety as well as the recovery time. Five performance measures for buildings have been identified: (i) Safe and Operational; (ii) Safe and usable during repair; (iii) Safe and usable after repair; (iv) Safe but not repairable; (v) Unsafe.

The proposed Resilience Performance Levels (RPL) focus on building performance after the earthquake, recognizing the importance of the temporal dimension (Recovery time T_{RE}) in the assessment of the RPLs of structures and communities in general.

In this chapter, a 2-dimensional performance domain consisting of Performance Levels $PL(i, j)$ which are defined by the combination of *functionality* (index j) and *recovery time* (index i), is proposed. By accounting for the effect of the temporal dimension, a 3-dimensional performance matrix (Fig. 6.10) can be visualized as a set of predefined joined performance domains (“masks”) for different seismic intensity level, IM and different RPLs. The resilience performance levels can be defined using expert opinions as well as public interviews. This will allow the identification of the acceptable and desired performance levels by citizens for different type of infrastructures, for example.

6.13 Summary and Remarks

The evaluation of resilience takes into account, beside the technological aspects, also the human component, because the system response depends highly on people’s actions. MCEER researchers have developed the PEOPLES Resilience Framework

to model and describe seven different categories of community resilience indicators. The considered dimensions are:

- Population and Demographics data, which are related to the inability of the society to withstand adverse impacts and to rebuild, using the social vulnerability index;
- Environmental/Ecosystem Index, which represents the ability of the ecological system to return to or near its pre-event state. This ability could be estimated using normalized difference vegetation index, which is correlated to green vegetation density across a region;
- Organized Governmental Services, which indicate how all the community sectors are prepared to respond to disasters;
- Physical Infrastructures, which incorporate facilities and lifelines that have to be restored in the immediate aftermath of a disaster;
- Lifestyle and Community Competence, which describes how the community reacts to extreme events. This index is not only concerned with the raw abilities of the community, but also to the perceptions of its ability to effect positive exchanges;
- Economic Development, which is an index of the future growth of a community. It is linked to the proportion of the population that is employed within the various industries and to the adequacy of prevention standards existing inside them;
- Socio- Cultural Capital, which describes a community place attachment with its neighborhood or city that gives the motivation to bounce back after a disaster.

In summary, a schematic step-by-step procedure of the methodology is the following:

1. Define the extreme event scenarios (e.g. PSHA and ground motion selection);
2. Definition, calibration and validation of the hybrid model of the community;
3. Run the analysis and evaluate the response of the model;
4. Evaluate the performance metrics (e.g. losses, restoration time, performance index, resilience index) for different scenarios and compare with different performance levels;
5. Recognize remedial mitigation actions (e.g. advanced technologies such as base isolation, passive dampers, etc.) and/or resilience actions (e.g. resourcefulness, redundancy, etc.);

The proposed design approach has analogies with the feedback loop taken from control theory and it can be applied both to communities and single structures (e.g. hospital, city hall, etc.).

References

- Adger WN (2000) Social and ecological resilience: are they related? *Prog Hum Geogr* 24(3):347–364
- Berche B, von Ferber C, Holovatch T, Holovatch Y (2009) Resilience of public transport networks against attacks. *Eur Phys J B* 71(1):125–137

- Bonowitz D (2009) The dilemma of existing buildings: private property, public risks. Report, San Francisco Planning Urban Research Association (SPUR)
- Brown D, Kulig J (1996/97) The concept of resiliency: theoretical lessons from community research. *Health Can Soc* 4(1):29–52
- Bruneau M, Reinhorn AM (2007) Exploring the concept of seismic resilience for acute care facilities. *Earthq Spectra* 23(1):41–62. <http://link.aip.org/link/?EQS/23/41/1>
- Bruneau M, Chang S, Eguchi RT, Lee GC, O'Rourke TD, Reinhorn AM, Masanobu S, Kathleen T, Wallace WA, Winterfeldt Dv (2003) A framework to quantitatively assess and enhance the seismic resilience of communities. *Earthq Spectra* 19(4):733–752. <http://link.aip.org/link/?EQS/19/733/1>
- Burns T, Stalker G (1961) The management of innovation - burns,t, stalker,gm. *International Labour Review* <GotoISI>://WOS:A1961CFS6500013, iSI Document Delivery No.: CFS65 Times Cited: 0 Cited Reference Count: 1 [Anonymous] INT LABOR OFFICE WASHINGTON BRANCH
- Cagnan Z, Davidson RA, Guikema SD (2006) Post-earthquake restoration planning for Los Angeles electric power. *Earthq Spectra* 22(3):589–608. <http://link.aip.org/link/?EQS/22/589/1>
- CCE (2000) The community resilience manual: a resource for rural recovery & renewal. Centre for Community Enterprise (CCE), Port Alberni
- Chang S, Shinozuka M (2004) Measuring improvements in the disaster resilience of communities. *Earthq Spectra* 20(3):739–755. doi:10.1193/1.1775796
- Chang S, McDaniels T, Fox J, Dhariwal R, Longstaff H (2014) Toward disaster-resilient cities: characterizing resilience of infrastructure systems with expert judgments. *Risk Anal* 34(3): 416–434
- Cimellaro GP, Piqué M (2016) Resilience of a hospital Emergency Department under seismic event. *Adv Struct Eng* 1–12. doi:10.1177/1369433216630441
- Cimellaro GP, Reinhorn AM, Bruneau M (2010a) Framework for analytical quantification of disaster resilience. *Eng Struct* 32(11):3639–3649. doi:10.1016/j.engstruct.2010.08.008
- Cimellaro GP, Reinhorn AM, Bruneau M (2010b) Seismic resilience of a hospital system. *Struct Infrastruct Eng* 6(1–2):127–144
- Cimellaro GP, Reinhorn AM, Bruneau M (2011) Performance-based metamodel for health care facilities. *Earthq Eng Struct Dyn* 40(11):1197–1217. doi:10.1002/eqe.1084
- Cimellaro GP, Renschler C, Reinhorn AM, Arendt L (2016) PEOPLES: a framework for evaluating resilience. *J Struct Eng ASCE*. [http://dx.doi.org/10.1061/\(ASCE\)ST.1943-541X.0001514](http://dx.doi.org/10.1061/(ASCE)ST.1943-541X.0001514)
- Cimellaro GP, Scura G, Renschler C, Reinhorn AM, Kim H (2014a) Rapid building damage assessment system using mobile phone technology. *Earthq Eng Vib* 13(3):519–533. doi:10.1007/s11803-014-0259-4
- Cimellaro GP, Solari D, Bruneau M (2014b) Physical infrastructure interdependency and regional resilience index after the 2011 tohoku earthquake in Japan. *Earthq Eng Struct Dyn* 43(12):1763–1784. doi:10.1002/eqe.2422
- Cimellaro GP, Villa O, Bruneau M (2014c) Resilience-based design of natural gas distribution networks. *J Infrastruct Syst ASCE*. doi:10.1061/(ASCE)IS.1943-555X.0000204
- Cutter S (1996) Vulnerability to environmental hazards. *Prog Hum Geogr* 20(4):529–539
- Cutter SL, Mitchell JT (2000) Revealing the vulnerability of people and places: a case study of Georgetown county, South Carolina. *Ann Am Geogr* 90(4):713–737
- Diaz-Delgado R, Lloret F, Pons X, Terradas J (2002) Satellite evidence of decreasing resilience in Mediterranean plant communities after recurrent wildfires. *Ecology* 83(8):2293–2303. doi:10.2307/3072060. <GotoISI>://WOS:000177434200023, iSI Document Delivery No.: 583WP Times Cited: 92 Cited Reference Count: 85 Diaz-Delgado R, Lloret F, Pons X, Terradas J, ECOLOGICAL SOC AMER
- Dorbritz R (2011) Assessing the resilience of transportation systems in case of large-scale disastrous events. In: The 8th international conference on environmental engineering, Vilnius, 19–20 May 2011, pp 1070–1076
- Drabek T, McEntire D (2002) Emergent phenomena and multiorganizational coordination in disasters: lessons from the research literature. *Int J Mass Emerg Disaster* 20:197–224

- Elmqvist T, Folke C, Nystrom M, Peterson G, Bengtsson J, Walker B, Norberg J (2003) Response diversity, ecosystem change, and resilience. *Front Ecol Env* 1(9):488–494. doi:10.2307/3868116
- Gunderson LH, Holling CS, Pritchard J (2002) Resilience of large-scale resource systems. Resilience and the behavior of large-scale systems. Island Press, Washington, DC
- Haimes YY, Horowitz BM, Lambert JH, Santos JR, Lian C, Crowther KG (2005) Inoperability input-output model for interdependent infrastructure sectors. I: theory and methodology. *J Infrastruct Syst* 11(2):67–79
- Harrald J (2006) Agility and discipline: critical success factors for disaster response. *Ann Am Acad Political Soc Sci* 604:256–272
- Harrald JR (2010) New paradigms for private sector preparedness. 111th congress (Second Session) before the Subcommittee on State, Local, and Private Sector Preparedness and Integration Committee on Homeland Security and Governmental Affairs U.S. Senate
- Heaslip K, Louisell WC, Collura J, Serulle NU (2010) A sketch level method for assessing transportation network resiliency to natural disasters and man-made events. The 89th annual meeting of the transportation research board, Transportation Research Board Business Office, 500 Fifth Street, NW, Washington, DC, USA, 10–14 Jan 2010
- HVRI (2013) Social vulnerability index for the united states – 2006-10. Report, Hazards & Vulnerability Research Institute (HVRI), Department of Geography, University of South Carolina
- Javanbarg MB, Scawthorn C, Kiyono J, Shahbodaghkhan B (2012) Fuzzy ahp-based multicriteria decision making systems using particle swarm optimization. *Expert Syst Appl* 39(1):960–966
- Ludwig D, Walker BH, Holling CS (2002) Models and metaphors of sustainability, stability, and resilience, resilience and the behavior of large-scale systems, vol 60. Island Press, Washington, DC. <GotoISI>://WOS:000182751600002
- Manyna SB (2006) The concept of resilience revisited. *Disasters* 30:434. <http://www.ingentaconnect.com/content/bpl/disa/2006/00000030/00000004/art00004http://dx.doi.org/10.1111/j.0361-3666.2006.00331.x>, [1] doi:10.1111/j.0361-3666.2006.00331.x
- Manzo L, Perkins D (2006) Finding common ground: the importance of place attachment to community participation and planning. *J Plan Lit* 20:335–350
- Miles S, Chang S (2006) Modeling community recovery from earthquakes. *Earthq Spectra* 22(2):439–458. <http://link.aip.org/link/?EQS/22/439/1>
- Miller-Hooks E, Zhang X, Fatouche R (2012) Measuring and maximizing resilience of freight transportation networks. *Comput Oper Res* 39(7):1633–1643
- Norris FH, Stevens SP, Pfefferbaum B, Wyche KF, Pfefferbaum RL (2008) Community resilience as a metaphor, theory, set of capacities, and strategy for disaster readiness. *Am J Community Psychol* 41(1–2):127–150
- Olofsson P, Eklundh L, Lagergren F, Jonsson P, Lindroth A (2007) Estimating net primary production for scandinavian forests using data from terra/modis. *Space Res* 39:125–130
- Ouyang M, Duenas-Osorio L (2011) An approach to design interface topologies across interdependent urban infrastructure systems. *Reliab Eng Syst Saf* 96(11):1462–1473. doi:10.1016/j.res.2011.06.002. <GotoISI>://WOS:000295436700006
- Patton A (2007) Collaborative emergency management. Emergency management: principles and practice for local government, International City and County Management Association, Washington, DC
- Pederson P, Dudenhoeffer D, Hartley S, Permann M (2006) Critical infrastructure interdependency modeling: a survey of U.S. and international research (D. o. E. N. Laboratory, ed., Idaho National Laboratory)
- Pettorelli N, Vik J, Mysterud A, Gaillard J, Tucker C, Stenseth N (2005) Using the satellite-derived ndvi to assess ecological responses to environmental change. *TRENDS Ecol Evol* 20(9):503–510
- Project RP (2010) <http://web.uct.ac.za/depts/ricsa/projects/publicli/poverty>

- Queiroz C, Garg SK, Tari Z (2013) A probabilistic model for quantifying the resilience of networked systems. *IBM J Res Dev* 57(5). doi:10.1147/jrd.2013.2259433. <GotoISI>://WOS:000327262900004, times Cited: 0
- Radloff K (2006) Community resilience, community economic development, and saskatchewan economic developers. Report, Community-University Institute for Social Research
- Renschler C, Frazier A, Arendt L, Cimellaro GP, Reinhorn AM, Bruneau M (2010) Developing the “PEOPLES” resilience framework for defining and measuring disaster resilience at the community scale. In: Proceedings of the 9th US national and 10th Canadian conference on earthquake engineering (9USN/10CCEE), Toronto, 25–29 July 2010, paper 1827
- Rose A, Liao SY (2005) Modeling regional economic resilience to disasters: a computable general equilibrium analysis of water service disruptions. *J Reg Sci* 45(1):75–112
- Rouse JW, Haas RH, Schell JA, Deering DW (1973) Monitoring vegetation systems in the Great Plains with ERTS. In: Stanley EPM, Freden C, Becker MA (eds.) Third Earth Resources Technology Satellite-1 (ERTS) symposium, NASA SP-351 vol I, NASA, Washington, DC, pp 309–317
- Simoniello T, Lanfredi M, Liberti M, Coppola R, Macchiato M (2008) Estimation of vegetation cover resilience from satellite time series. *Hydrol Earth Syst Sci* 12:1053–1064
- Stallings RA, Quarantelli EL (1985) Emergent citizen groups and emergency management. *Public Adm Rev* 45:93–100. doi:10.2307/3135003. <GotoISI>://WOS:A1985AAR3600014
- Sutton J, Tierney K (2006) Disaster preparedness: concepts, guidance and research. Report, Natural Hazards Center, Institute of Behavioral Science, University of Colorado, Boulder, Report to Fritz Institute
- Tamvakis P, Xenidis Y (2013) Comparative evaluation of resilience quantification methods for infrastructure systems. Selected papers from the 26th Ipma (International Project Management Association). *World Congr* 74:339–348
- Tierney K (2009) Disaster response: research findings and their implications for resilience measures. Report, CARRI Research Report 6, Community and Regional Resilience Institute
- Waugh WL, Streib G (2006) Collaboration and leadership for effective emergency management. *Public Adm Rev* 66:131–140. doi:10.1111/j.1540-6210.2006.00673.x. <GotoISI>://WOS:000242352800014
- Weick KE (1995) Sensemaking in organizations (Foundations for Organizational Science). SAGE Publications, Thousand Oaks
- Weick KE (2005) Managing the unexpected: complexity as distributed sensemaking. Springer, Berlin, pp 51–65. *Understanding Complex Systems-Springer Complexity*
- Zoumpoulaki A, Avradinis N, Vosinakis S (2010) Multi-agent simulation framework for emergency evacuations incorporating personality and emotions. *Lecture notes in computer science*, vol 6040. Springer, Berlin/Heidelberg, pp 423–428. doi:10.1007/978-3-642-12842-4-54

Chapter 7

A Comprehensive Methodology for the Evaluation of Infrastructure Interdependencies

Abstract The chapter defines different types of infrastructure interdependencies, and provides a literature review of existing interdependent models. A reference nomenclature for infrastructures based on the analysis of the literatures in the field is proposed. Finally, a method for the analysis of the degree of interdependency among the infrastructures (lifelines) of a community is proposed. An index is evaluated using a matrix approach that takes into account the effect that any infrastructure can have on another through the use of temporal networks. Finally the method is applied to the Fukushima Daiichi nuclear power plant disaster.

7.1 Introduction

Nowadays, infrastructure networks have become the basis of life and economy of every community, large or small. These infrastructures have always had a certain degree of interdependency among them, therefore when the community is subjected to a shock (earthquake, terrorism, hurricanes, floods, etc.) it is more vulnerable when the degree of interdependency among infrastructures is higher.

In literature there are many definitions relating to the interdependencies that exist among the lifelines of a community. According to President's Commission on Critical Infrastructure Protection (PCCIP 1997), infrastructure "is a network of interdependent, mostly privately-owned, man made systems and processes that function collaboratively and synergistically to produce and distribute a continuous flow of essential goods and services". Infrastructure is also defined as the framework of interdependent networks and systems including identifiable industries, institutions (both people and procedures), and distribution capabilities that provide a reliable flow of products and services essential to the defense and economic security, the smooth functioning of governments at all levels, and society as a whole (PPD63 1998).

In the fundamental work of Rinaldi et al. (2001), dependency is defined as a connection between two infrastructures, through which the state of one infrastructure is correlated to the state of the other (unidirectional relationship). A distinction of dependencies is also made for different periods in which the perturbation may occur (normal operating conditions, which can vary from peak

to off-peak conditions, times of severe stress or disruption, or times when repair and restoration activities are under way), as well as between supported and supporting infrastructures. Interdependency is defined as a bidirectional relationship between two infrastructures through which the state of each infrastructure influences or is correlated with the state of the other. In other words, two infrastructures are interdependent when each one is dependent on the other, and interdependencies are connections among components in different infrastructures in a general system of systems. Consequently, the risk of failure or deviation from normal operating conditions in one infrastructure can be a function of risk in a second infrastructure if the two are interdependent (Banerjee and Prasad 2012; Kakderi et al. 2011).

Knowledge of the degree of interdependency is necessary for planning a resilient community. Increasing the resilience of systems is fundamental for ensuring sustainability of a community over time. This chapter establishes two core resilience objectives: Broad-based resilience which aims to improve capabilities of families, communities, private-sector organizations, and all levels of government to sustain essential services and functions, and Infrastructure resilience which increases the ability of critical infrastructure systems, networks, and functions to withstand and rapidly recover from damage and disruption and adapt to changing conditions.

In this chapter, a reference nomenclature based on the analysis of the literatures in the field is proposed. Sixteen types of infrastructures which compose each community are identified: seven core infrastructures (Electricity, Oil delivery, Transportation, Telecommunication, Natural Gas delivery, Water supply, Wastewater treatment) and nine non-core infrastructures (Financial system, Building services, Business, Emergency services, Food supply, Government, Health care, Education, Commodities). Finally, a method for the analysis of the degree of interdependency among the infrastructures (lifelines) of a community is proposed. An index is evaluated using a matrix approach that takes into account the effect that any infrastructure can have on another. This index depends on the type of failure that an infrastructure may cause to another (coupled and uncoupled) and on the number of systems affected.

7.2 Interdependency

Critical infrastructure systems are dependent and interdependent in multiple ways, where dependency refers to the unidirectional relationship and interdependence indicates the bidirectional interaction. They usually present upstream-downstream relationships and loop relationships, which turn their behavior into non-linear and non-stationary. Interdependencies are usually hidden during great part of infrastructure life, and may show up after a disrupting event. The forecast and analysis of cascading effects due to interdependence bonds are the principal problems addressed by various lifeline councils and committees all around the world. To clarify what interdependencies are and how they manifest, some examples are reported:

- *Example 1:* a loss of power can cause pump stations to fail since they need a constant supply of electricity to function.
- *Example 2:* flooding and damages to roads and bridges can affect repair crews' ability to get to areas where the infrastructure is damaged, further delaying normal water service.
- *Example 3:* pipelines may run along roads and bridges, which if damaged in a storm, can cause breaks and leaks.
- *Example 4:* rail and air infrastructure are vulnerable to power outages, both short term and extended. Rail switch facilities rely on a constant source of power to coordinate the movement of freight and rail trains, which often share the same tracks. Rail crossing guards are also dependent on electricity to close gates as trains approach road crossings. Airports rely on power to operate control towers and radar functions. A power outage that disrupts communication capabilities can threaten airport security and safety if the control tower and pilots cannot communicate with one another.

Many authors have tried to identify a common taxonomy in the field (Kakderi et al. 2011), however as of today a unique nomenclature related to lifelines' interdependency within a community, does not exist. In this chapter, the following definitions will be used (Fig. 7.1):

- *Community:* all the social and physical infrastructures (or lifelines) which contribute to the normal daily life of an organized group of people who live in a given area (e.g. a nation).
- *Infrastructure (lifeline):* the set of all the systems that contribute to the creation and operation of a physical or social network within a community (e.g. national electric distribution network).
- *System:* a set of sub-systems placed together with a specific order and a specific behavior (e.g. wind power plant).
- *Sub-system:* a combination of units which create a machinery or equipment or procedure that have defined and specific characteristics and properties (e.g. wind turbine).

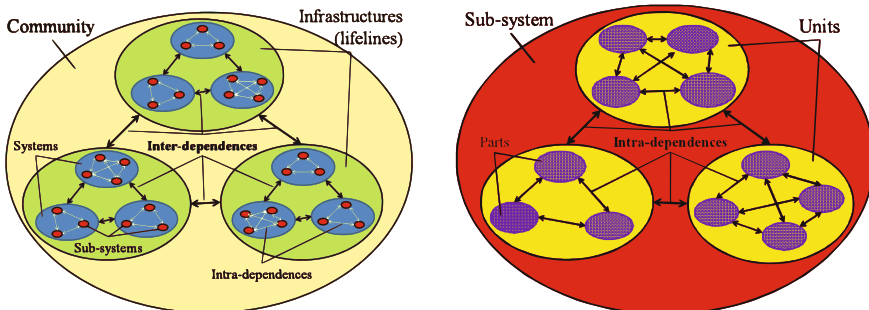


Fig. 7.1 Taxonomy used in the book

- *Unit*: the set of all components (or parts) assembled with a certain order. A unit is an object or a procedure that, by itself, does not have a unique goal (e.g. the gearbox of the wind turbine).
- *Part*: it is the fundamental element with which a unit can be built (e.g. the ball bearing of the gearbox of the wind turbine, Fig. 7.1).

The relationships between the various elements that make up a community do not have a unique definition. Two types of internal relationships have been identified (Fig. 7.1) in the proposed framework:

- First *interdependencies*: Bidirectional relationship between the different infrastructures (lifelines) that make up a community and between the different systems that compose an infrastructure (lifeline).
- Second *intradependencies*: Bidirectional relationship among the different sub-systems that compose a system, among the different units that make up a sub-system and between the different parts that compose a unit.

After the work of Kongar and Rossetto (2012), 16 infrastructures (lifelines) have been identified in a community, which are: Electricity (Power delivery), Oil delivery, Transportation, Telecommunication, Natural Gas delivery, Water supply, Wastewater treatment, Financial system, Building services, Business, Emergency services, Food supply, Government, Health care, Education, Commodities. For Kongar and Rossetto (2012) there is a core group of infrastructures that are widely recognized as being lifelines: power delivery, telecommunications, transportation, water supply, wastewater treatment, oil delivery and natural gas delivery. The common factor among these infrastructures is that although there is a human behavior involved to support their operations, they are largely physical systems.

7.3 Type and Effect of Interdependency

Thus far, a clear classification about the types of interdependencies among infrastructures has not been made. Many authors over the years have given their contribution in attempts to approach this problem. The most relevant ones are summarized in Table 7.1. Rinaldi et al. (2001) and Peerenboom et al. (2001) described four general categories of infrastructure interdependencies: *Physical*, *Cyber*, *Geographic* and *Logical* interdependency. Instead for Pederson et al. (2006) there are six general categories of infrastructure interdependencies: *Physical*, *Cyber*, *Geographic*, *Logical*, *Policy/Procedural* and *Societal interdependency*. More recently Zhang and Peeta (2011) identified the following interdependencies among the infrastructures: *Functional*, *Physical*, *Budgetary*, *Market* and *Economic interdependency*. In this section, seven different types of interdependencies (Kakderi et al. 2011) are identified (Fig. 7.2):

- *Physical interdependency*: a physical reliance on material flow from one infrastructure to another. This definition is close to the ones of physical

Table 7.1 Interdependence types according to different authors

Authors	Interdependence types
Rinaldi et al. (2001)	Physical, Cyber, Geographic, Logical
Zimmerman (2001)	Functional, Spatial
Dudenhoeffer et al. (2006)	Physical, Geospatial, Policy, Informational
Peerenboom et al. (2001)	Physical, Cyber, Geographic, Logical, Policy/Procedural and Societal interdependency
Lee et al. (2007)	Input, Mutual, Shared, Exclusive, Co-located
Zhang and Peeta (2011)	Functional, Physical, Budgetary, Market and Economic
Cimellaro et al. (2013)	Physical, Cyber, Geographical, Policy/Procedural, Societal, Budgetary, Market & Economy

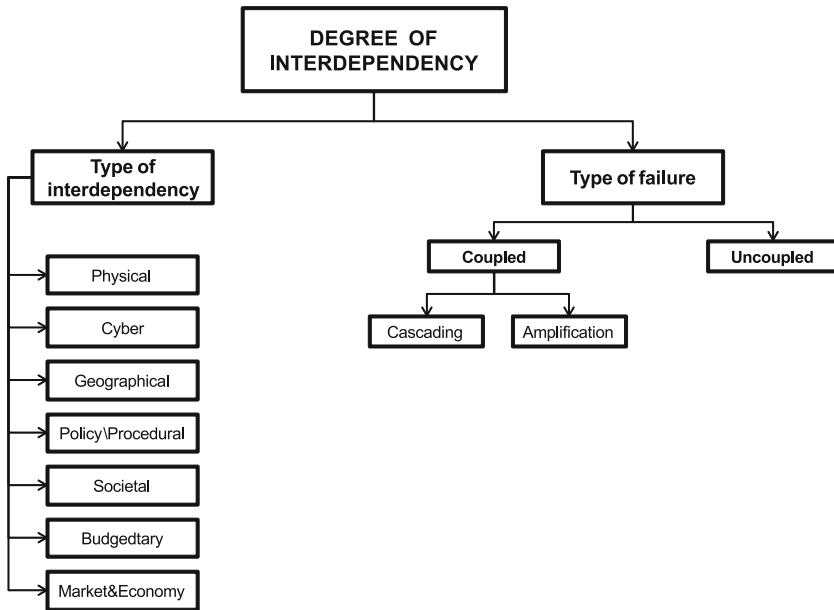


Fig. 7.2 Interdependency index: dependencies on type of interdependency and on type of failure

interdependence by Rinaldi et al. 2001 and Dudenhoeffer et al. (2006), of functional interdependence by Zimmerman (2001), Zhang and Peeta (2011) and of input interdependence by Wallace et al. (2001). An example is given by the reliance of electric power plants to the water network for cooling purposes. Also another physical dependency is the reliance on road and rail networks to move crews and equipment.

- *Cyber interdependency*: a reliance on information transfer between infrastructures. It means that if the reliance on transfer between infrastructures is not about physical quantities but about information, then there is a cyber interdependence. This definition is close to the ones of *cyber interdependence* by Rinaldi et al. (2001), of *informational* interdependence by Dudenhoeffer et al. (2006), of

functional interdependence by Zimmerman (2001), Zhang and Peeta (2011) and of input interdependence by Wallace et al. (2001). Cyber dependencies include the reliance on telecommunications for supervisory control and data acquisition (SCADA) systems and information technology for e-commerce and business systems. An example can be the disruptions on communication services which affects the situational awareness and control of electric power and water systems and caused their partial failures due to lack of observability.

- *Geographical interdependency*: a local environmental event affects components across multiple infrastructures due to physical proximity. This definition is close to the ones of *geographic* interdependence by Rinaldi et al. (2001), of *spatial* interdependence by Zimmerman (2001), of *geospatial* interdependence by Dudenhoefter et al. (2006), of *co-located* interdependence by Wallace et al. (2001) and of *physical* interdependence by Zhang and Peeta (2011). Geographical dependencies include, for example, common corridors that natural gas pipelines share with electric power lines and/or telecommunications lines.
- *Policy/Procedural interdependency*: An interdependency that exists due to policy or procedure that relates a state or event change in one infrastructure sector component to a subsequent effect on another component. Note that the impact of this event may still exist given the recovery of an asset.
- *Societal interdependency*: The interdependencies or influences that an infrastructure component event may have on societal factors such as public opinion, public confidence, fear, and cultural issues. Even if no physical linkage or relationship exists, consequences from events in one infrastructure may impact another infrastructure. Furthermore this influence may be time sensitive and may decay over time.
- *Budgetary interdependency*: Many infrastructure systems involve some level of public financing, especially under a centrally-controlled economy or during disaster recovery, leading to resource allocation budget interdependencies.
- *Market & Economy interdependency*: Shared market resources imply that all systems are interacting sectors in the same economic system. Another example of this interdependency is when these infrastructure systems serve the same end-users who determine the final demand for each commodity/service subject to budget constraints. Further interdependencies exist due to the shared regulatory environment where the government agencies control and impact the individual systems through policy, legislation or financial means such as taxation or investment. An example is how fuel prices can affect both supply and demand for transportation, which in turn can affect the supply and demand for fuel.

7.3.1 Dependence Patterns

To see how the above mentioned types of interdependence manifest on real infrastructure systems, it is important to determine which of the dependence patterns are present. Critical infrastructures rely on each other during business-as-usual condition and moreover they do during emergency situations; it is important to study

the topology of dependence patterns in both cases. During ordinary operations, electricity, telecommunications and transportation are the sectors most relied on by other utilities, while during emergencies the importance of dependencies changes according to the needs of responders (Pressly 2014).

7.3.1.1 Ordinary Period

It is unlikely that two infrastructure systems fail at the same time in ordinary period. If we consider that one system at a time fails, the cascading effects on the others will probably be mitigated by backup devices and redundancies. Anyway, even during ordinary periods, there are some systems which can significantly affect the operability of the other ones, which have a strong dependence on them.

- *Dependence on Electricity:* During business-as-usual operations, electricity is the utility that most others are dependent upon, and is required to operate all the other lifeline utilities to some degree. Because of this reliance, all other utilities have backup generation at most of their critical sites. However, backup mobile generator resources for other sites are generally sufficient to maintain a few sites only. After a certain period of time, a widespread regional power outage would impact on telecommunications, water supply, wastewater, fuel supply and traffic management services.
- *Dependence on Telecommunications:* Even if most utilities could continue services at near full capacity without telecommunication, a failure of this network can have a high impact on the other lifeline businesses. Some utilities would need to revert to manual operation and monitoring of facilities, and response to service requests would be impaired. There is a high reliance on the cellular network for voice communications. This network may become overloaded during or shortly after an event. However the copper, fiber and wireless infrastructure provides diversity and is highly resilient. Most utilities use a combination of the above technologies to monitor their own infrastructure and some have their own dedicated network of links and radio.
- *Dependence on Transportation:* Short-term road failures are unlikely to directly impede other utilities' ability to provide service in ordinary period, because the transportation network is usually redundant and rather resilient. However, as with telecommunications failure, response to service requests and asset failures would be affected. Road failures can become critical in the case of long-term road failures for services like fuel transportation and access of the personnel to other facilities. Only the long-term failure of ports and airports would impact other utility services, because imported supplies (such as water treatment chemicals) could be affected.

7.3.1.2 Emergency Situation

In normal operating conditions, some interdependencies are invisible, but under some disruptive scenarios, they can emerge. In a major disaster many lifelines can

be affected at the same time, and priority is given to responders operation rather than to guarantee a regular service for users. The following utilities become more critical:

- *Telecommunications and roads*: utility organizations need to coordinate their response and recovery efforts and access sites to do repairs or supply fuel to backup systems. Some agencies have their own backup communications networks.
- *Electricity and fuel*: if electricity is affected, diesel supply to critical sites (such as central city telecommunications hubs and water treatment plants) becomes critical. Even those sites with on-site diesel storage only hold a few days of supply. Refueling of generators deployed to other critical facilities will become a significant logistical issue.
- *Telecommunications/broadcasting*: for managing public information.

Cascading effects are usually amplified by simultaneous failures of different systems, generating an increase of the recovery time. An effective or non-identification of the system or component where to intervene first remarkably influences the evolution of the situation.

7.3.1.3 The San Andreas Fault Earthquake Scenario for the City of San Francisco

To evaluate the level of interdependency between critical infrastructures, the City of San Francisco (CCSF 2014) defined the critical “upstream” dependencies that each lifeline system has on other lifelines, as well as the “downstream” dependencies that a system’s disruption can have on other systems. Both dependencies are critical to understand and improving lifeline system resilience.

Figure 7.3 summarizes the level of interaction and dependence that lifeline operators interviewed for this study expect to have on other lifeline systems to maintain and restore service after a M7.9 earthquake scenario. Shading represents the overall level of interaction and dependency that could affect system performance and service restoration in San Francisco. In Fig. 7.4 is an illustration of the combined effects of damage levels and service disruption that may cause potential delays in restoration for different lifeline systems and the level of interdependence between them.

7.3.2 Types of Failure

In addition to the type of interdependency is useful to understand what type of failure a lifeline endures. As shown in Fig. 7.2, the type of failure is classified as follows:

	Regional Roads	City Streets	Electric Power	Natural Gas	Telecom	Water	Auxiliary Water	Wastewater	Transit	Port	Airport	Fuel
Regional Roads												
City Streets												
Electric Power												
Natural Gas												
Telecom												
Water												
Auxiliary Water												
Wastewater												
Transit												
Port												
Airport												
Fuel												

v Significant interaction and dependency on this lifeline system for service delivery and restoration efforts
 v Moderate interaction and dependency on this lifeline system for service delivery and restoration efforts
 v Limited interaction and dependency on this lifeline system for service delivery and restoration efforts

Fig. 7.3 City of San Francisco lifeline system interdependencies following a scenario M7.9 earthquake on the San Andreas Fault (Source: CCSF 2014)

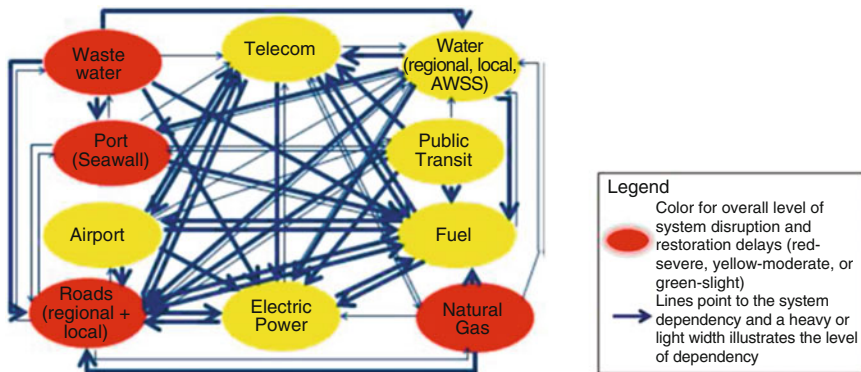


Fig. 7.4 Combined effects of damage service disruption that may cause delays in individual system restoration as well as the interdependencies among lifeline systems (Source: CCSF 2014)

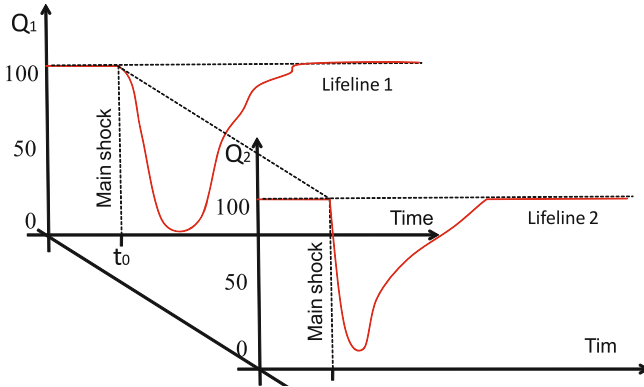


Fig. 7.5 A coupled failure: example of cascading failure

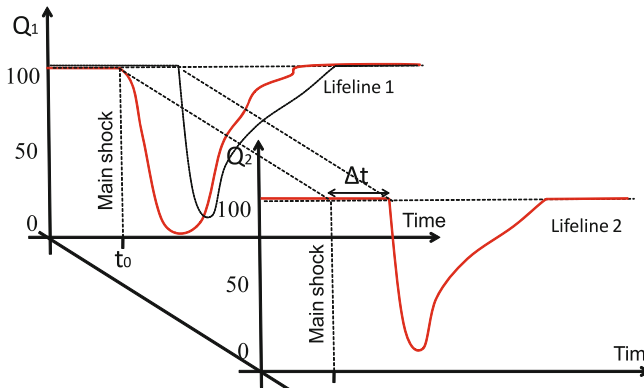


Fig. 7.6 A coupled failure: example of amplification failure. The failure in the second lifeline occurs with a time-delay Δt

- *Coupled failure*: A drop in the functionality of an infrastructure, due to a single perturbation (damaging event) in a community, causes the functionality of at least another lifeline to drop. If this drop of functionality takes place at the same time for both lifelines, this failure is called *Cascading failure* (Fig. 7.5), while if this drop of functionality takes place in these two lifelines (at least) with a certain time-delay, this failure is called *Amplification failure* (Fig. 7.6);
- *Uncoupled failure*: A drop of functionality of one infrastructure, due to a single perturbation (damaging event) in the community, that does not cause any failure in other infrastructures. There is no propagation of failure among infrastructures (Fig. 7.7).

The degree of interdependency is function of the *type of failure*, the *type of interdependency*, and the *importance factor* of each lifeline's system. This system depends on the degree of interconnection and the degree of importance that the system has with respect to other lifelines in the community.

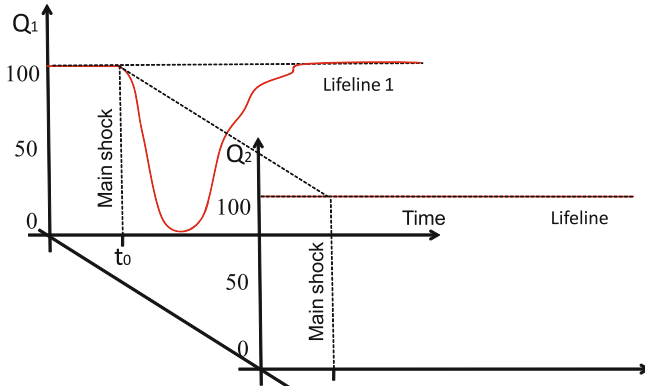


Fig. 7.7 Example of uncoupled failure

7.4 Framework for the Evaluation of the Degree of Interdependency Among Lifelines

For the evaluation of the degree of interdependency among lifelines, it is necessary to analyze the dependencies at the systems level, subdividing each lifeline into systems and assigning a value of dependency of each system of the considered lifelines among the 16 lifelines that are part of the community (Cimellaro et al. 2013). The degree of dependencies among lifelines in a community will be analyzed using the step-by-step procedure proposed below:

- Divide each lifeline in systems, according to the definition of system given in Fig. 7.1.
- Classify the systems according to the seven types of interdependencies defined in Fig. 7.2 (*Physical, Cyber, Geographic, Policy/Procedural, Societal, Budgetary, Market & Economy interdependency*).
- For each system and for each group, a degree of interdependency is assigned, which is function of two values assigned to each lifeline. The first value is assigned as a function of the *type of failure* (Cascading, Amplification, and Uncoupled); the second value is assigned as a function of the *importance factor* that each lifeline's system has.
- The values defined above are combined giving the degree of interdependency among the two lifelines under examination. The result is one degree of interdependency for each group (e.g. seven values for each pair of lifelines). So, finally there are seven matrices of the degree of interdependency, one for each type of interdependency.
- The seven matrices that are obtained are then assembled together using different weight coefficients for different types of interdependencies (Fig. 7.8) (Cimellaro and Solari 2014). Further studies will be able to address the determination of the weight coefficients for each type of interdependency.

the ↓	can affects ↓ in this points:															Leadership index	
	Electricity	Oil delivery	Transportation	Telecommunication	Natural Gas delivery	Water supply	Wastewater treatment	Financial system	Building services	Business	Emergency services	Food supply	Government	Health care	Education		Commodities
Electricity	1	1	0,6	1	1	0,6	0,6	0,6	0,6	1	0,6	1	1	0,6	0,3	0,6	12,1
Oil delivery	0,6	1	0,6	0,3	0,3	0,3	0,3	0,6	0,6	0,6	0,6	0,6	0,6			0,6	7,6
Transportation	0,3	0,6	1		0,6			0,6	0,6	1	1	1	0,6	0,6	0,3	1	9,2
Telecommunication	0,3	0,3	0,3	1	0,3	0,3	0,3	1		1	1	0,6	1	0,3		0,3	8
Natural Gas delivery	0,6		0,3		1			0,6	0,3	0,6	0,6	0,6	0,6	0,3	0,3	0,3	6,1
Water supply	0,6	0,3		0,3	0,3	1		0,3	1	0,6	0,6	1	0,6	0,6	0,6	0,6	8,4
Wastewater treatment		0,3			0,3	0,6	1			0,3	0,6	0,3	0,3	0,3	0,6		4,9
Financial system	0,3	0,3	0,6	0,3	0,3	0,3	0,3	1	0,6	1	0,3	0,6	1	0,3		1	8,2
Building services	0,3	0,3	0,6	0,3	0,3	0,3	0,3	0,6	1	0,6	0,6		0,3			0,6	6,1
Business	0,3	0,6	1	0,6	0,6	0,3	0,3	1	0,6	1		0,6	1			1	8,9
Emergency services	0,6	0,6	0,6	0,6	0,6	0,6			1	0,3	1	1	1	1	0,6		10,5
Food supply	0,3	0,3	0,6		0,3	1	0,3	1	0,3	1	0,6	1	1	0,6	0,6	0,3	9,2
Government	0,6	0,6	0,6	0,6	0,6	0,6	0,6	1	0,6	1	1	1	1	1	1	0,6	12,4
Health care			0,3						0,3	0,3	0,3	1	0,6	1	0,3	0,3	5,4
Education	0,3	0,3	0,3	0,3	0,3	0,3	0,3	1	0,3	0,6	1	0,3	1	0,6	1	0,3	8,2
Commodities	0,3	0,3	1	0,3	0,3	0,3	0,3	1	0,6	1	0,3	0,3	1	0,3		1	8,3
Index of subordination (dependence)	6,4	6,8	8,4	5,6	7,1	6,5	4,6	11,6	8,0	12,9	10,5	10,5	13,0	7,8	5,0	8,8	

Fig. 7.8 Community interdependency matrix. In yellow are highlighted the core lifelines interdependency matrix

The matrix thus obtained is the interdependency matrix (S) which is a 16 × 16 matrix in which each row and each column represents a lifeline. The values are arranged such that the interdependence value S at row i and column j ($S_{i,j}$) is the value of interdependency of the lifeline on the row i with respect to the lifeline on the column j.

The matrix arrangement will allow some considerations. By summing the values per row in the matrix $S_{i,j}$ a number can be obtained that indicates the level of leadership (Leadership index in Fig. 7.8) that the lifeline of that row has with respect to the other 15 lifelines of the community (Paton and Johnston 2006). Instead, by summing the data per column in the matrix $S_{i,j}$ a number can be obtained that indicates the level of subordination (Subordination index in Fig. 7.8) that the lifeline of that column has with respect to the other 15 lifelines.

The lifeline that has the highest value of **Leadership index** is the most important and requires more attention, because if its functionality drops, the functionality of the entire community drops. Therefore, to increase the resilience of the entire community, this lifeline must have the lowest vulnerability vs. any kind of hazard, while its degree of interdependency among other lifelines should be reduced.

The lifeline that has the highest value of *Subordination index* is the one that has the greatest dependency on other lifelines within the same community. If

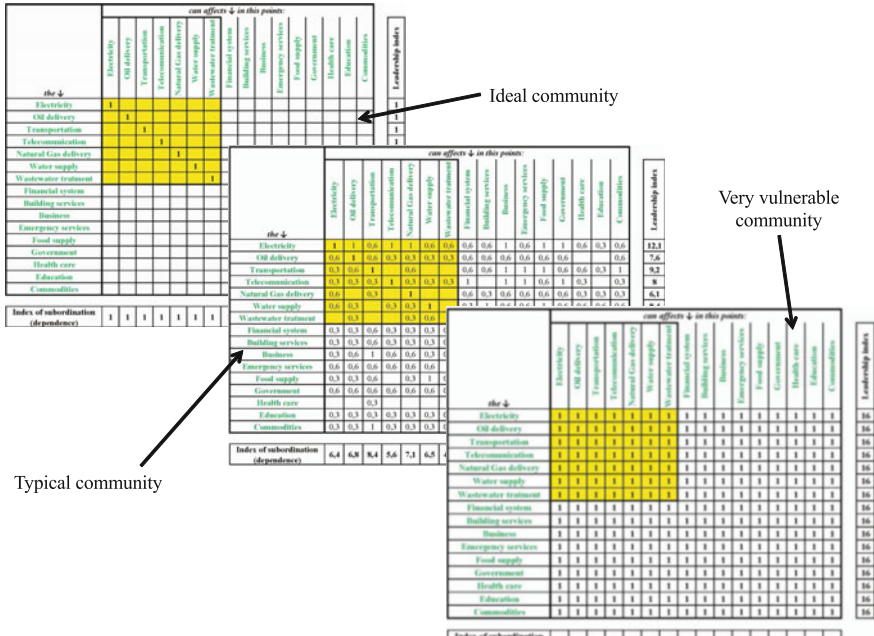


Fig. 7.9 Infrastructures interdependencies matrix. In *yellow* are highlighted the core lifelines interdependency matrix

the community suffers damage, this lifeline is the first that suffers the effects of damage propagation due to interdependencies even if it does not have direct damages. Therefore in order to increase the resilience of the entire community, the dependency of this lifeline with others should be as low as possible. In this situation the matrix of interdependency $S_{i,j}$ corresponds to an identity matrix. In general the interdependency matrix can assume three different shapes which are shown in Fig. 7.9:

- The matrix of interdependency (S) is a matrix of one's which correspond to *High vulnerable community (VVC)*.
- The matrix of interdependency (S') is a diagonal matrix where all the terms in the diagonal are ones. This situation corresponds to an *Ideal community (IC)* where all the lifelines in the given community are independent each other.
- The *Typical community (TC)* corresponds to all the situations between VVC and IC.

The proposed framework allows the decomposition of the *infrastructures* into *systems* and each *system* into *sub-systems*, reaching a higher level of detail for the evaluation of the interdependency using the same procedure described above. It is shown how a single value of the interdependency matrix among two specific lifelines can be exploded into a matrix of interdependencies of systems and sub-systems. This

type of analysis will be more detailed, because it will allow one to find the different levels of interdependencies, but it will be computationally expensive.

The level of detail of the calculation of the interdependency matrix can be selected based on the knowledge of the community and its lifelines, systems, sub-system, units and parts. The values of the interdependency matrix are not constant, but they can vary through time. These variations can occur due to different reasons:

- Improving of lifelines functionality (positive variation);
- Reduction of lifelines vulnerability (positive variation);
- Creation of a degree of redundancy among lifelines (positive variation);
- Creation of stocks and emergency systems (positive variation);
- Aging (negative variation);
- Negative human intervention on the lifeline (negative variation);
- etc.

It is important to point out that the degree of interdependency can change through time when human interventions are performed or because of aging effects, but they are not dependent on the magnitude or type of disaster faced. If the magnitude of an extreme event increases, only the “effects” of interdependency increase, but the degree of interdependency which is a property of the community remains the same (Fig. 7.10).

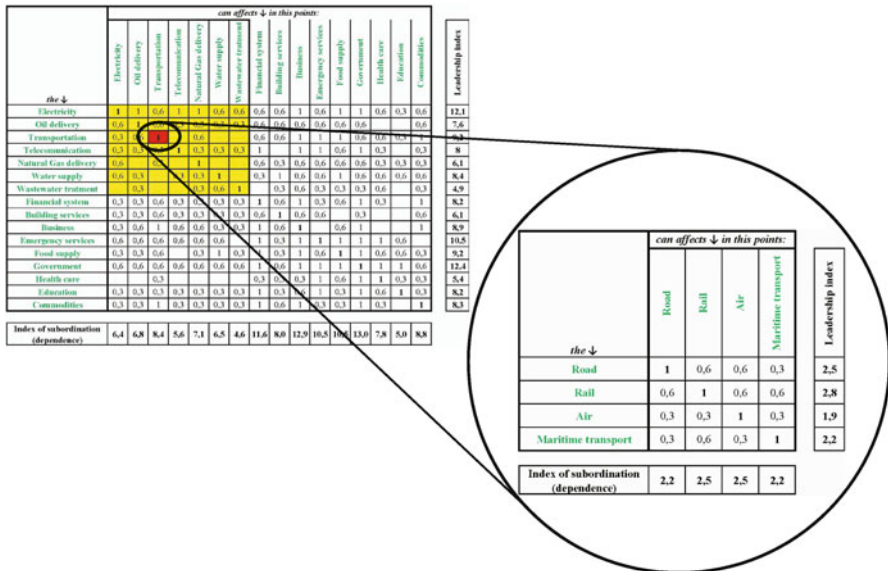


Fig. 7.10 Interdependency matrix of systems. In yellow are highlighted the core lifelines interdependency matrix

7.5 Modeling Temporal Networks

Lifelines, like many other networks, can change characteristics and topology over time. Being critical systems, they are designed to be reliable even during stress conditions. There is usually more than one possible configuration for performing the final scope; backup systems and lines are best practiced in this sense. To take into account the effect of time on networks, it is necessary to have a model capable of representing the current condition of the system at every time step.

The problem will be analyzed studying the connectivity of the system, rather than the physical phenomena involved. To begin this section, there is a brief introduction to the existing methods for evaluate connectivity features of networks. Among these, a focus will be devoted to the Input-output Inoperability Method, an important methodology for the evaluation of cascading effects in a system. From applications and limitations of the method, the need to implement some of its features brings to the definition of a new methodology able to model features, like the temporal variability of the topology. The suggested method is then compared to the Probability Risk Assessment method, used for the analysis of critical sites. The existing correlation between the two suggests the possibility of running analysis at different scales of detail, from the regional/extended one to the building/site one.

7.5.1 Existing Interdependence Models

This section groups and reviews the existing modeling and simulation approaches used for interdependence analysis. They are broadly categorized by the authors into six types: *system dynamics based models*, *network based approaches*, *empirical approaches*, *agent based approaches* and *economic theory based approaches*. After a presentation of each of this type, its strong and weak points are highlighted (Ouyang 2014).

7.5.1.1 System Dynamics Based Models

System dynamics based approaches model the dynamic and evolutionary behavior of the interdependent lifelines by capturing important causes and effects under disruptive scenarios. System dynamics based approaches take a top-down method to manage and analyze complex adaptive systems involving interdependencies. Feedback, stock and flow are the basic concepts in this type of approach. Feedback loops indicate connection and direction of effects between infrastructures system components. Stocks represent quantities or states of the system, the levels of which are controlled over time by flow rates between stocks. System dynamics based approaches model the interdependent infrastructures using two diagrams:

causal-loop diagram capturing the causal influence among different variables and *stock-and-flow diagram* describing the flow of information and products through the system.

This type of approach has some weaknesses. First, as the causal loop diagram is established based on the knowledge of a subject-matter expert, it is also a semi-quantitative method. Then, many parameters and functions in the models require calibration, which need a huge amount of data, which is not easily accessed. Lastly, due to the difficulty of obtaining relevant data, validation efforts usually consist of conceptual validation, so there is relatively limited validation of the model. These weaknesses call for integrating other modeling approaches in a uniform analysis framework for overall decision support (Bush et al. 2005).

7.5.1.2 Network-Based Models

Infrastructure systems can be described by networks, where *nodes* represent different system components and *links* mimic the physical and relational connections among them. Network-based approaches model single infrastructure by networks and describe the interdependencies by inter-links, providing descriptions of their topologies and flow patterns. Performance response of lifeline systems to hazards can be analyzed by firstly modeling the component failures from hazards at the component level, and then simulating the cascading failures at the system level (Patterson and Apostolakis 2007). Depending on whether or not they are modeling the particle flow, network-based studies are broadly grouped into topological models and physical-based models.

7.5.1.3 Empirical Approaches

The empirical approaches analyze lifeline interdependencies according to historical accident or disaster data and expert experience. The studies with this type of approaches can identify frequent and significant failure patterns and quantify interdependence strength metrics to inform decision making. Historical interdependence incidents can be used to uncover the interdependence structures or relationships between critical infrastructures under extreme events, such as the 2011 Tohoku earthquake in Japan. Establishing special databases from the incident reports and then analyzing the data can identify the frequent and significant failure patterns. Usually, interdependency incident records are collected from newspapers, media reports, Internet news outlets, official ex-post assessments, and utility owners and operators.

This type of approach has several weaknesses. First, due to the bias of reporting, some frequent interdependence failures that may have significant impact may be underreported. Second, scholars use different databases to collect failure data without a standardized data collection methodology for interdependent critical

infrastructure performance. Third, the reliance of the empirical approaches on previous failure records may not give good predictions for new disasters. These weaknesses call for other modeling and simulation approaches for additional decision support (McDaniels et al. 2007).

7.5.1.4 Agent Based Models

Agent based approaches are an effective way to model critical infrastructure systems and the related decision-making processes which characterize them during an emergency. These approaches adopt a *bottom-up method* and assume the complex behavior or phenomena emerge from many individual and relatively simple interactions of autonomous agents. Each agent interacts with others and its environment based on a set of rules, which mimic the way a real counterpart of the same type would react. Most critical infrastructure components can be viewed as agents.

Agent-based approaches model the behaviors of decision-makers and the main system participants in the interdependent lifelines. This enables them to capture all types of interdependencies among lifelines by discrete-event simulations, provide scenario-based analysis (“what-if”) and the effective assessment of different control strategies and allows an integration with other modeling techniques to provide more comprehensive analysis. However, this type of methods has some weaknesses. First of all, the quality of simulation is highly dependent on the assumptions made by the modeler regarding the agent behavior, and such assumptions may be difficult to justify, theoretically or statistically. Then, calibrating the parameters might be challenging due to lack of relevant data and the difficulties to model the participant behavior, because detailed information about each critical infrastructure system is considered sensible by utilities managers (Bonabeau 2002).

7.5.1.5 Economic Theory Based Models

Lifeline systems interdependencies can be analyzed through models of economic interdependencies. In the existing literatures, two types of economic theories are employed to model lifelines interdependencies: *input-output models* and *computable general equilibrium models* (Rose 2005). The *Inoperability Input-output Models* (IIM) can easily analyze how perturbations propagate among interconnected infrastructures and how to implement effective mitigation efforts. This model will be presented in detail in the next section. *Computable General Equilibrium based methods* extend the capacities of the Input-output methods, capture the nonlinear interactions among infrastructure systems, provide resilience or substitution analysis of single infrastructure and the whole economy, and enable the inclusion of different types of interdependencies in a single framework. The weaknesses of this type of methods are problem related to calibration and data acquisition (Partridge and Rickman 1998).

7.5.2 *Input-Output Inoperability Method*

Developed by Haimés and Jiang (2001), the IIM model is an adaptation of the *Leontief's input-output* (I-O) analysis of economic interdependencies (Leontief and Leontief 1986). However, instead of focusing on the economic impact of a perturbation, the IIM proposed in this section is intended to simulate the propagation of risk of inoperability in the infrastructure sector.

The inoperability is defined as the inability for a system to perform its intended function. It is quantified by a value between 0 and 1, determined from considerations of the likelihood and the level of failure. When the inoperability of an element is 0, it means that it is working at the top of its potentialities, instead when it is 1, it is completely inoperative. These risks of inoperability are propagated between different networks following the interdependency patterns. The Equation describing the IIM is the following:

$$q = [I - A]^{-1} \cdot c \quad (7.1)$$

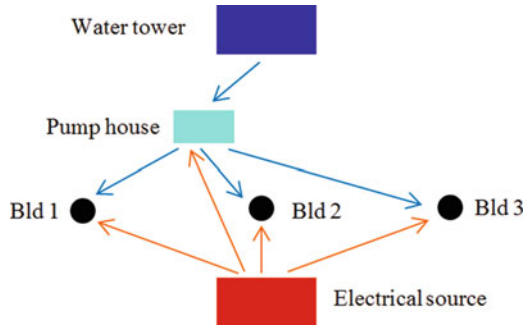
where q is the damage vector which contains the inoperability values for the n infrastructures considered; A is a matrix which depicts the extent of interdependence between infrastructures and is the transpose of the adjacency matrix which describes the topology of the system; I is an identity matrix and c is the scenario vector which include the effects of the perturbation (e.g. natural disasters, man-made attacks, intrinsic failures, etc.) on each infrastructure. The damage vector q is the output of the model and quantifies the level of inoperability of the infrastructures composing the system, following a perturbation which propagates according to the topology described by the interdependency matrix, A . Each element of this matrix quantifies the level of influence of the j th infrastructure on the i th infrastructure. They can be values between 1, indicating complete propagation of the scenario from j to i , and 0, no propagation from j to i . The A – matrix thus represents the probability of transferring inoperability across different infrastructures. The next paragraphs present an application of the IIM to a system of infrastructures and its main limitations in describing its performances.

7.5.2.1 *Application to Infrastructure Systems*

To give an example of which is the output of the IIM, the case of a six-node network developed by Valencia (2013) is reported. From now on it will be referred to as *Example 1* (Fig. 7.11). There are two networks: an electric and a water network, serving three buildings.

The hazard considered is infrastructure aging. To measure the impact of individual node decay across the network, it is computed the column summation of the damage vector q of each node i at each time t . This is the decay score:

Fig. 7.11 Graph representing Example 1 topology



$$dc_{s_i}(t) = \sum_{i=1}^j q_i(t) \tag{7.2}$$

7.5.2.2 Limitations of the IIM

The approach which is applied to a complex infrastructure network presents some limitations:

1. it does not take into account the redundancies of the system;
2. it does not consider the temporal evolution of the system, since it is a static model and neglect the temporal effects that can disrupt the system;
3. its inputs and outputs are not significant and end-user-oriented probabilistic quantities.

The following subsection focuses on the limitation relative to redundancies. A simple implementation is suggested to reduce this limitation.

7.5.2.3 Redundancies

If a new pump house is added in parallel to the first one, the network presents a redundancy, as shown in the system topology in Fig. 7.11.

Figure 7.12 shows the new topology of the so called *Example 2*. It is clear that the performance of the system is improved with respect to the previous case because both the pump houses can perform the same work and their simultaneous failure is more unlikely than the failure of just one.

It is expected that the impact of the water tower and of the electrical source remains the same, while the impact of each of the pump house decreases. If the results obtained in Fig. 7.13 are compared with the one-pump case (Fig. 7.14), it is observed that the expected trends are not there. The Electrical source and the water tower decay score dc_s increase, but the pump one doesn't change.

Fig. 7.12 System topology of Example 2

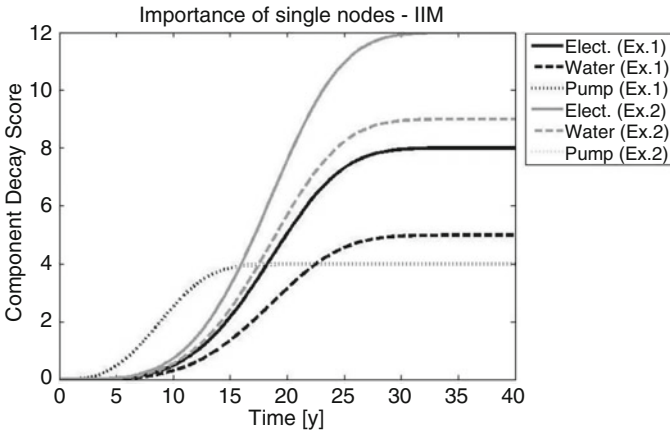
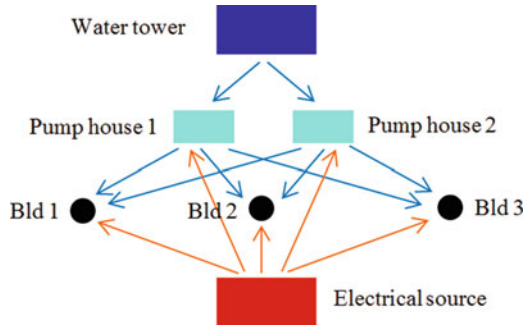


Fig. 7.13 Comparison of decay scores of Example 1 and Example 2, using the traditional IIM

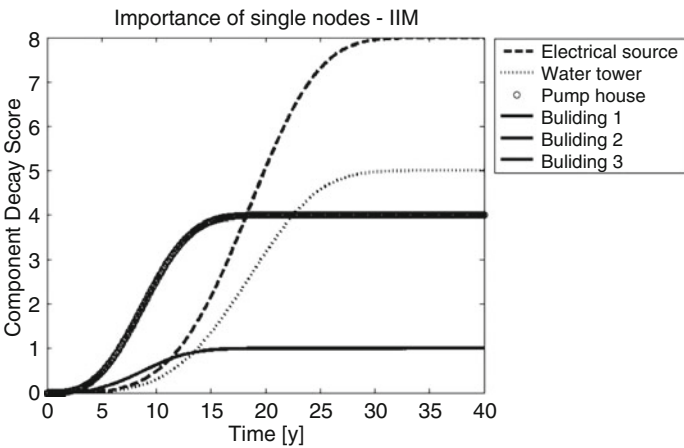


Fig. 7.14 Decay scores for Example 1

7.5.2.4 Implementation for Accounting Redundancies

In the case discussed in previous paragraph, the decay score dc_s of the electrical source and the water tower are increasing because the algorithm considers another node (the new pump) to be fed by them. To avoid the problem related to redundancies, the probabilities of failure of the nodes in parallel should be combined properly, by introducing the Series-Parallel Vector SP :

$$SP = \left\{ \begin{array}{c} 1/n_1 \\ 1/n_2 \\ \vdots \\ 1 \quad (forBLD) \end{array} \right\} \quad (7.3)$$

where n_i is the number of nodes redundant of node i . After having expanded it to the n -dimension, it is possible to add it to the damage vector equation:

$$SP^* = SP \times \{1 \ 1 \ \dots \ 1\}_{1 \times n} \quad (7.4)$$

$$q_i(t) = [I - A \cdot SP^*]^{-1} \cdot c_i \quad (7.5)$$

After this operation, the values of the electrical source and the water tower return to the proper values. when considering the pumps, if it is assumed that the failures of the two pumps are stochastically independent, the probability that both fail at a time is given by:

$$P(A \cap B) = P(A) \cdot P(B) \quad (7.6)$$

Results of this implementation reflect the initial expectations about redundancies effects and are shown in Fig. 7.15.

7.5.2.5 Sensitivity Analysis for Risk Reduction

Now that it is clear how an operation like the introduction of an additional pump can improve the performance of a system, it is necessary to develop an index assessing the performance of the entire system, and not just of single nodes. The proposed index is used to rate infrastructures systems at a specific time t , is dimensionless and varies in the range $0 \div \infty$. It is defined as follows:

$$sys_s(t) = \sum_k \frac{\sum dc_s_{k,i}(t)}{n_k^o} \quad (7.7)$$

where k is the type of node (i.e. electrical sources, water towers and pump houses). The final targets (i.e. buildings) are not considered when calculating the index sys_s .

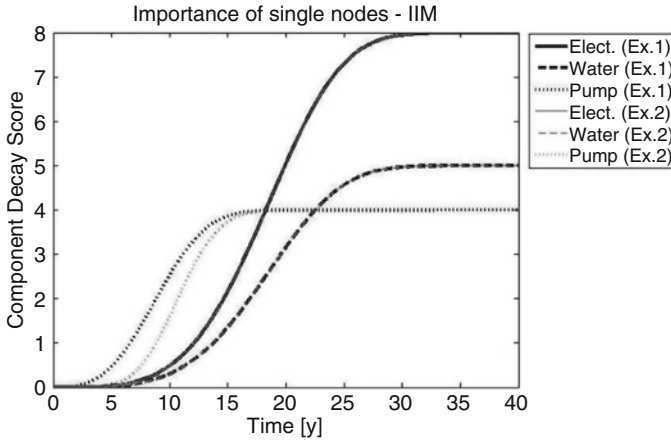


Fig. 7.15 Comparison of decay scores of Example 1 and Example 2, using the implemented IIM

A low value of the index sys_s indicates that the infrastructure has low risk of nodes failure, while a high values of the index indicates high risk. A threshold separating the low-risk region from the high-risk region needs to be calibrated on the basis of the importance of the system and minimum acceptable performance.

Through this new index, a sensitivity analysis can be performed, to establish which intervention is better to improve the performance of the system. A ten-building system is considered. Analyzed improvements are: (1) the spin off of the system in two smaller systems, (2) the introduction of redundant nodes and (3) a plan of maintenance interventions.

The positive effects of the spin off intervention in Fig. 7.16, is represented by the drastic lowering of the plateau of the index sys_s in Fig. 7.17. Looking at the redundancy intervention of Fig. 7.18 instead, it is noticeable that the plateau doesn't vary, but the sys_s in Fig. 7.19 decreases in the short term segment of the function.

Comparing these two pieces of evidence with the one obtained from planned maintenance interventions, it is clear that a spin off is the best solution for the long term. In the short term, the addition of redundancies is also effective. Maintenance interventions have a relevant positive effect in both the short and the long term and are probably the most feasible solution from the economic point of view. Results of the sensitivity analysis are shown in Fig. 7.20.

7.5.3 Modified IIM for Temporal Networks

Many extensions of the model have been proposed such as the Dynamic IIM (DIIM) and the Multi-Regional IIM (MR-IIM). However, the modified IIM model presented hereafter tries to overcome some of the limitations of the methodology proposed by Haines and Jiang (2001), while capturing the key aspects of infrastructure behavior

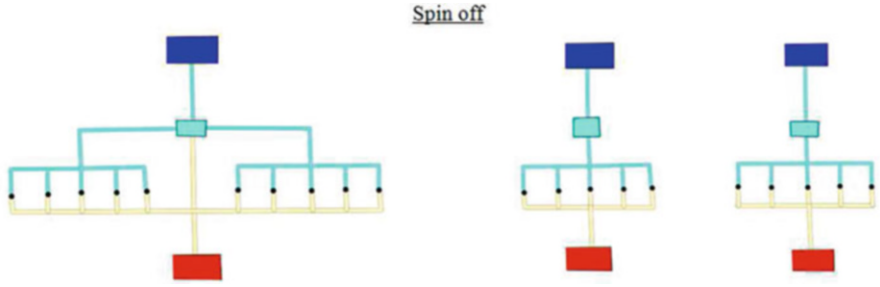


Fig. 7.16 Spin off intervention on Example 1

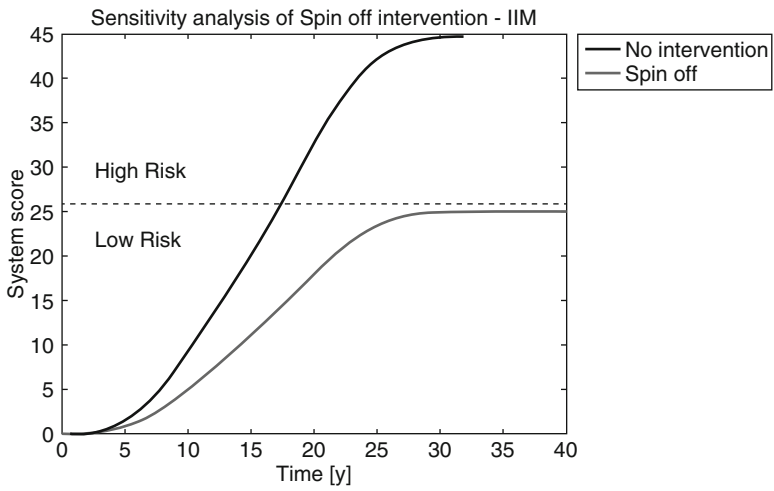


Fig. 7.17 System score before and after the spin off intervention on Example 1

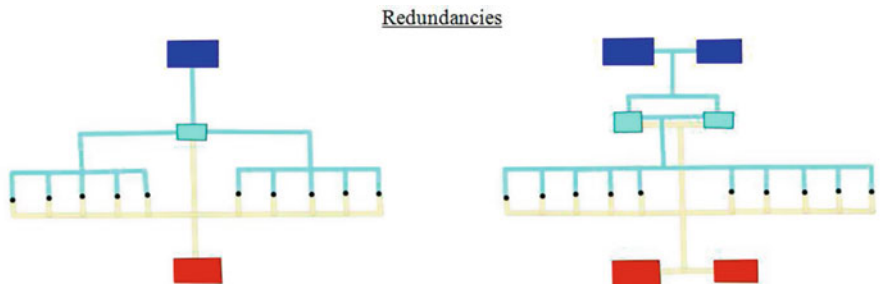


Fig. 7.18 Redundancies intervention on Example 1

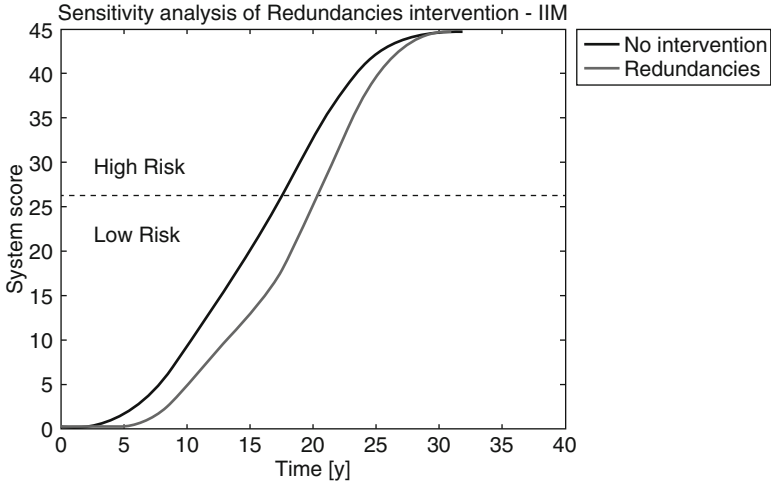


Fig. 7.19 System score before and after the redundancies intervention on Example 1

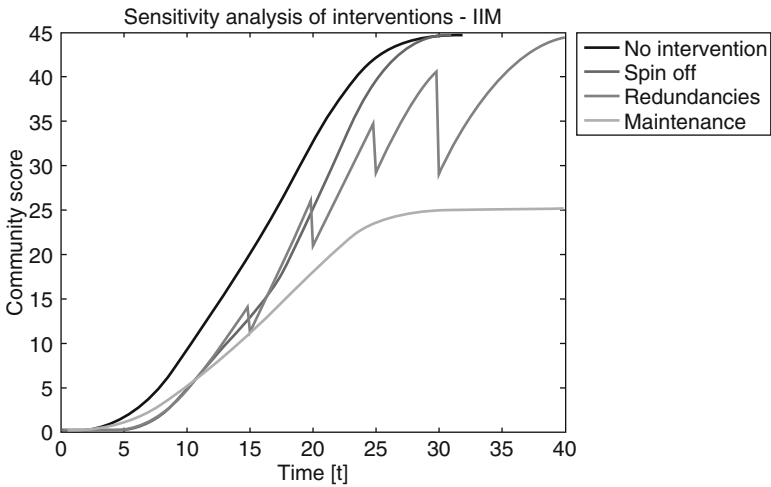


Fig. 7.20 Sensitivity analysis of interventions for risk mitigation on Example 1

during an emergency. A presentation of the theoretical framework of the model, followed by three different implementations of the IIM is proposed below.

7.5.3.1 Topology Formalization Using Graph Theory

Graph theory has been used to model infrastructure networks. The geographical, topological, and flow information of a network can be represented with a graph $G(V, E)$ which is formed by a set V of vertices, herein called nodes, and a

set E of edges. The definition of the nodes depends on the spatial scale of the problem considered which might be an entire infrastructure (e.g. electric network, water network, gas network) (Cimellaro and Solari 2014; Cimellaro et al. 2014), a sub-system (e.g. wind turbine) or even a unit (e.g. gearbox of the wind turbine). Specific features can be attributed to each node, such as hierarchy, resistance and autonomy, while edges do not have any features assigned in the proposed model, but they are oriented. The edges can link nodes intra-network (i.e. within a specific infrastructure) or inter-networks (i.e. across different infrastructures). The last one represents the interdependencies described in the A-matrix. Instead of attempting to specify the likelihood and the degree of interdependency in the A-matrix, this model describes that any inter-network link will be specified as Boolean, either 0 or 1. Thus, $a_{x,y}$ values will be 0 if the x th node belonging to the i th infrastructure is dependent on the y -th node belonging to the j th infrastructure.

With respect to existing formulations, the concept of *chains* is introduced in the model. A chain is a sequence of nodes from one vertex to another using the edges. The chains of interest are those that connect a source (i.e. a node without inflows) to a sink (i.e. a node without outflows). The task of every source is to feed all the sinks of the network, if the topology allows for it. If it doesn't, the source is called partial. An example of partial source is a photovoltaic plant on the roof of a building. This plant belongs to the general electric network of a city or a block, but it can just feed the building where it is settled and not the other ones. It is assumed that every node of a chain must have at most one inflow edge, but can have multiple outflow edges. This means that different supply lines exist in a critical infrastructure system. For example, besides the main supply line, there are usually backup lines present that can substitute the first in case of failure or malfunction. Each of these chains can guarantee the operability of the network, though they are mutually exclusive.

The hierarchy of their operation is defined by the design of the infrastructure. There are two possible kinds of hierarchy. The source hierarchy corresponds to the rank of priorities for the entry into operation of the sources. The path hierarchy instead corresponds to the rank of priorities for the activation of the different possible paths. It is assumed that source hierarchy is stronger than path hierarchy is. This means that if the first chain is not working, the network tries to maintain operation starting from the previous source and inquiring new paths (if possible). If no other path is available for that source, then it skips to the following one. This theoretical framework and notation will be adopted while discussing the implementation of the methodology to the IIM model.

7.5.3.2 Probabilistic Formulation of Inputs and Outputs

The proposed methodology modifies the IIM deterministic formulation in probabilistic terms, because while the damage score just gives a snapshot of the cascading propagation of inoperability, it does not say anything about the final state of the network. The probability of failure of a single node is obtained by combining the natural hazard with the infrastructure vulnerability and it refers to the status (fully

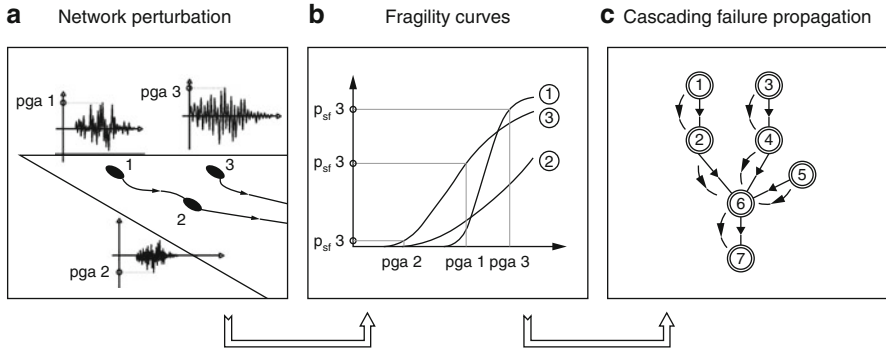


Fig. 7.21 Flowchart of the probabilistic approach. Starting from a network perturbation (a) probabilities of failure of nodes are computed on fragility curves (b) and then propagated according to the topology of the network (c)

operative or failed) of the node itself after the perturbation. Hereinafter it will be called self-failure probability (P_{sf}) and will substitute the scenario vector c .

The hazard component is represented by an event vector $E_{n \times 1}$, where n is the number of nodes in the system. At a given time \bar{t} every node will be disrupted by a natural event (e.g. earthquakes, tsunamis, fires, sabotages, etc.). The elements of the E -vector can be physical quantities such as the PGA , PGV , PGD , earthquake magnitudes, the height h_w of a tsunami wave, the megatons M_t of an explosion, etc. These quantities can vary from node to node, because infrastructures usually have a large spatial extension (Fig. 7.21a).

By performing different simulations, using different E -vector, it is possible to approach the problem in probabilistic terms. Each simulation has a weight which corresponds to the probability of occurrence of the event of a certain magnitude, which is taken directly from the hazard curves.

The vulnerability component of each node is represented by the fragility curves, which define the probability of failure of each node depending on the type of hazard considered (Fig. 7.21b). Therefore, for each node there are as many fragility curves as the type of hazard acting. Only complete failures fragility curves are used, while intermediate damage levels are not considered at this stage.

The probability of failure P_{sf} of a node under a specific event E , is obtained by inserting the value of the E -vector into the node fragility curve. The approach proposed by Valencia (2013) of summing up the elements of the q -vector to obtain a final score to evaluate the interdependency performances has obvious limitations, because they are not normalized to the dimension of the system (e.g. the longer the chain will be, the higher the score will be). Moreover, as already pointed out, the index proposed by Valencia (2013) does not take into account the benefits given by the redundancies present on the infrastructure. In the *modified IIM* proposed, the probability of failure P_f of every node is obtained by combining the P_{sf} with the cascading failure probability P_{cf} which is transmitted by the upstream nodes and is calculated using a step by step approach taking into account the ramifications of

the system (Fig. 7.21c). In other words, P_f is the probability of failure of each node, which is obtained as result of all the disrupting events and the cascading propagation effects.

7.5.3.3 Multilayer Approach for Spatial Interdependency

The more intuitive approach for analyzing a system of infrastructures is to solve each network separately and then consider their interaction. Infrastructure networks can be seen as layers which overlap each other and share some nodes which are presented in both networks and are virtually connected by inter-infrastructure edges. It is referred to as “virtually” connected, because there is not a real physical connection. Let’s consider the network of *Example 1*. The pump for operating needs both electricity and water, and so it belongs to both the electric and water networks. Using the layer visualization, a single node will be projected in the two layers and a virtual edge will link the two projections (Fig. 7.22).

The IIM model suffers from the incapability of dealing with different layers and adjacency matrices. In fact, it needs to store the topology in one general matrix, and hence considers the entire system as a single network. This is because the IIM can only use square matrices, while the inter-networks matrices are usually rectangular. To overcome this limitation, Valencia (2013) suggests the introduction of an *I-matrix*. These are $n \times m$ matrices, where n is the number of nodes of the j th infrastructure and m the number of nodes of the i th infrastructure, which is dependent on the j th. The idea is to increase the values of *c-vector* of infrastructure i , by adding the *q-vector* computed for the j th network. The following equation expresses this concept:

$$c_{j \rightarrow i} = I_{j \rightarrow i}^T \cdot q_j + c_i \tag{7.8}$$

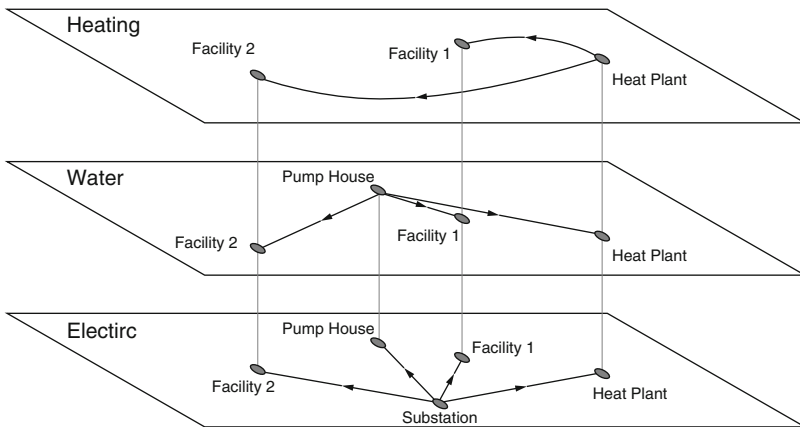


Fig. 7.22 Example of layer subdivision for interdependent networks

Inserting the output of the first network into the input of the second dependent one is the correct approach for the evaluation of the cascading effects. However, this formulation starts from the same deterministic values of before, so it cannot be considered satisfactory. The current method involves the combination of the P_{cf} of upstream and downstream networks:

$$P_{cf_i}^* = (I_{j \rightarrow i}^T \cdot P_{cf_j}) \cup P_{cf_i} \quad (7.9)$$

where the $P_{cf_i}^*$ can be considered cascading-failure probability which incorporates in the node all the information coming from upstream networks and upstream nodes of the current network that converge there.

This multilayer approach brings many benefits: (i) It discerns the analysis and results of layers and interdependencies and aids the understanding of where critic points are located and which are the tighter and more stressed inter-links. While the single infrastructure assessment is mature, the interdependency studies are still at a development stage and inquiring them is the real issue. (ii) Moreover, giving the possibility to each infrastructure manager of running the model of a given layer and then controlling the interaction between the different layers at a higher level is closer to the professional practice adopted during an emergency response phase. A model which considers all the elements of the system simultaneously won't be used in the real practice, because no one has the authority and competence to manage all the data. (iii) In the end, the diffusion of informatics tools, like Geographic Information Systems (GIS), in both the emergency response and the risk planning sector, suggests the adoption of a unified methodology. The GIS platform has great potentialities and it can be effectively used to organize input data and visualize outputs. Their relational databases are shaped with a layer structure which is in accordance with the one proposed above.

7.5.3.4 Tensor Notation for Accounting Temporal Effects

What has not been addressed yet is the temporal dimension. The first add-on, compared to the traditional static IIM, is the introduction of a timeline $\tau = \{t_0, t_1, t_2, \dots, T\}$, where the range $t_0 \div T$ must be extended enough to include all the events and their effects. The time step Δt of the elements of the τ - vector represent the time necessary for the propagation of the events across the entire system. This means that if at the time \bar{t} a landslide overwhelms an electricity pylon, before the time $\bar{t} + \Delta t$ the pylon must fail and the effect of this failure must propagate throughout the whole system. Therefore, the transmission of information in the system is immediate. The final situation, after having solved the system, at the time \bar{t} , will be the initial condition at the time $\bar{t} + \Delta t$. Given this timeline, it is clear that each event must be associated with a time of occurrence and that the model must run at every time step.

Now the model is not stationary, but is composed of temporal networks, denoted $G(t) = G(V, E(t))$. The P_f of nodes changes over time, in accordance with the sequence of events, and with the existence of edges. It appears that changes in the status of the nodes can result in changes in the topology of the system. For example, let's consider the node V_a , a water purification plant, the node V_b , a water collection pit, and the node V_c , an aqueduct. V_c is usually fed by V_a through the edge E_{ac} , but if V_a fails, the edge E_{ac} disappears and the edge E_{bc} is activated. The active chain has shifted from $a \rightarrow c$ to $b \rightarrow c$.

From this example, it can also be inferred that different chains of a network are not only spatial layers, but temporal layers. The multilayer approach is effective in modelling interdependencies among different networks, but here the networks are mutually exclusive, and not linked. The solution adopted is to pass from bi-dimensional matrices to a three-dimensional tensor notation. The topology of every network is now described by an adjacency tensor, whose elements are $a_{x,y_j}(t)$. Each temporal layer of the A -tensor represents a possible chain. The first in the hierarchy is the ordinary supply line, while the others are the backup lines. Figure 7.23 shows

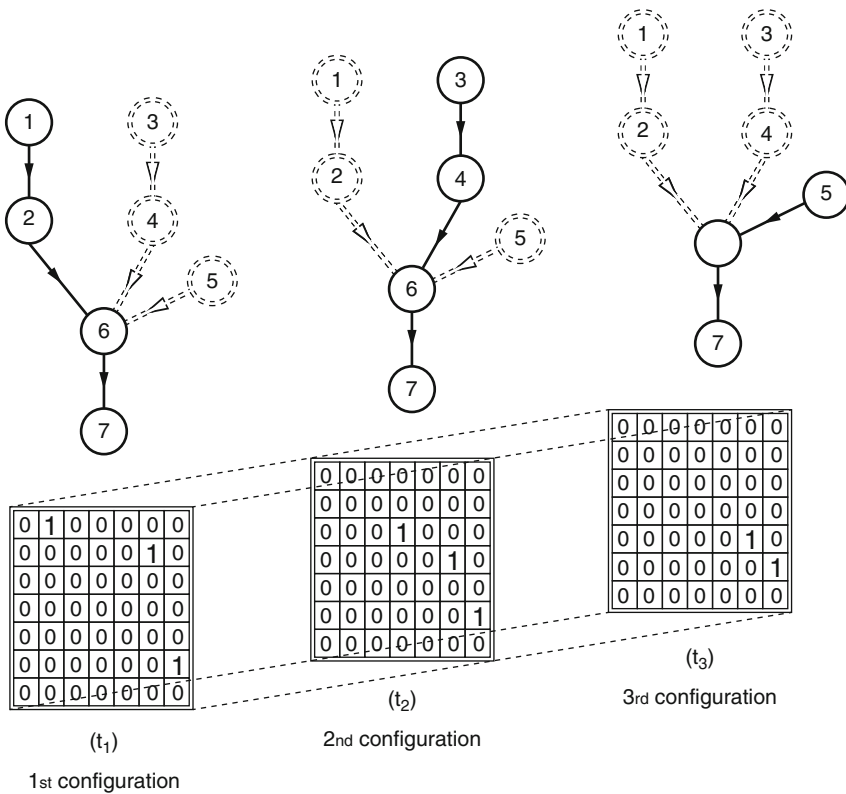


Fig. 7.23 Tensor notation for a network. An adjacency matrix is associated to each of the possible, and mutually exclusive, configurations of the network

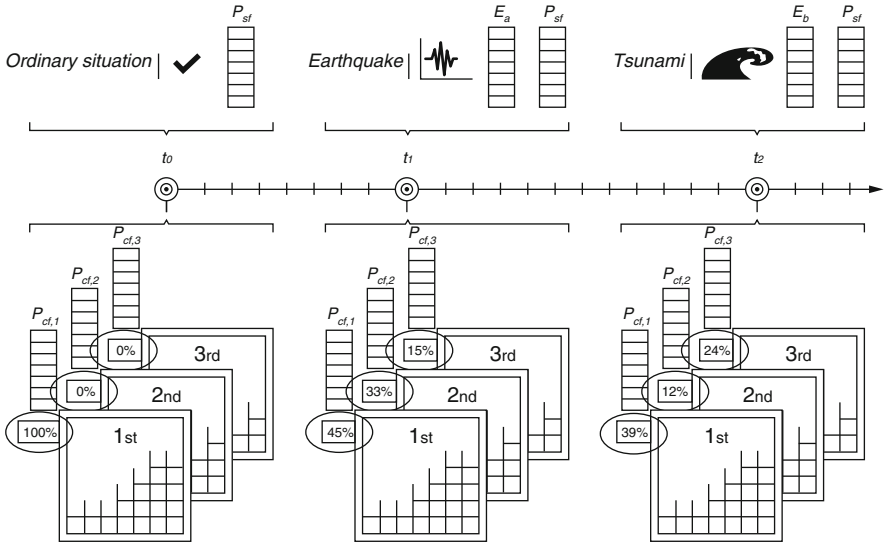


Fig. 7.24 Temporal variance of Operability Labels. Disruptive events tend to change their value and decrease the overall probability of operability ($\sum P_{occ}$)

the three different possible functional configurations which the seven-node network examined can assume. In the reminder of this section, this case will be referred to as Example 3.

To better understand which of the chains is active at the time \bar{t} , the probability of occurrence of a specific configuration P_{occ} is assigned to every layer (Fig. 7.24). This value expresses if the layer is “on” ($P_{occ} = 1$), or if it is “off” ($P_{occ} = 0$) at the considered time step. The condition for being “on” is that, in the current configuration, target nodes of the network do not fail and that configurations with higher degree of hierarchy are “off”. Transferring this concept in the probabilistic model means that values of P_{occ} become probabilities of being active. The sum of the probability of occurrence of a network is $0 \leq \sum P_{occ} \leq 1$ and the value $1 - \sum P_{occ}$ represents the percentage of lost capacity of the network (LoC).

Having understood how probable the activation of a chain is, it is useful to determine certain time effects not mentioned yet. Let’s consider, for example, that the primary power source of a hospital is not working due to a blackout. An emergency power generator is kicked-off to maintain the operability of the hospital, which is the target node. This UPS is fed by the fuel contained in a tank, so unless the time considered in the model is much smaller than the runtime of the tank, the unloading of the tank must be taken into account. The run out of autonomy of a node cannot be classified as an event, but its effects are well documented by various famous disasters. This work analyzes the effects of backup systems in lifelines, which can be considered as sources with a capacity which is limited in time. What emerges is that nodes can also have temporal features, like autonomy, that influence their status.

The tensor notation has many advantages with respect to the static bi-dimensional notation and they are listed below:

- (i) It is able to describe changes in the topology of the system that usually occurs after individual node failures;
- (ii) The separation of chains into different layers allows the computation of cascading failure responsibility of each node without considering the presence of parallel branches. The propagation of cascading effects is linear and the results of each layer should be weighted with respect to the value of their operability label;
- (iii) The P_{occ} furnishes direct information on the activity of each chain and allows the evaluation of time-related effects, like the autonomy;
- (iv) It is moreover possible to use the value $1 - \sum P_{occ}$ as an index for quantifying the loss of capacity of the network;
- (v) In the end, the possibility of varying the topology of the system gives the opportunity for adding new layers to existing networks. For example, if rescue teams modify their path or add a new provisional source, for recovering the operation of a network, a new layer will appear in the tensor.

7.5.3.5 Comparison with Traditional IIM

After having introduced the methodology and the potentialities of the modified IIM in comparison with the traditional method, a parallel between results furnished by the two methods can help to better understand the improvements given by the modifications. A first critic to the IIM and a relative simple implementation, for concerns regarding the accounting of redundancies, has been done in the last subsection. After having overcome the results of that partial implementation with this new methodology, let's see what improvements are achieved in the definition of meaningful and user-friendly outputs. Next results are relative to the network of Example 2.

7.5.3.6 Performance of the System

To evaluate the performance of the overall system, a *system score* is introduced, which is the sum of the terms of the q -vectors. Its weakness is that it doesn't really represent what the situation is at the target nodes and it also needs a threshold to evaluate the level of risk (Fig. 7.25). The calibration of this threshold is problematic.

The *modified IIM* instead deals with probabilities of failure, which don't need to be interpreted and furnish a precise and mathematical measure of the risk. For the evaluation of the performance of a system, it is possible to observe the P_f functions of target nodes. Figure 7.26 shows the P_f for what concerns the electric supply and the water supply of each building of Example 2. It is easy to see how they are completely not functional ($P_f = 1$) after 20 years, while from Fig. 7.25 this is not clear.

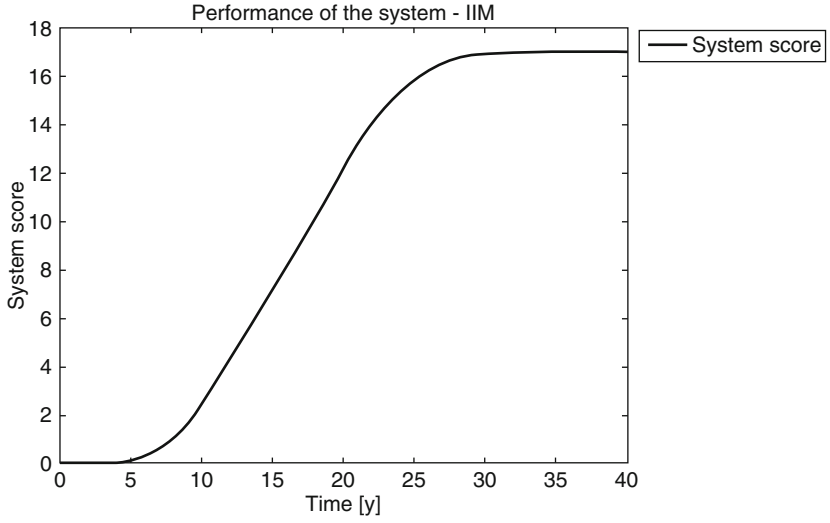


Fig. 7.25 Performance of the Example 2 network, according to the IIM

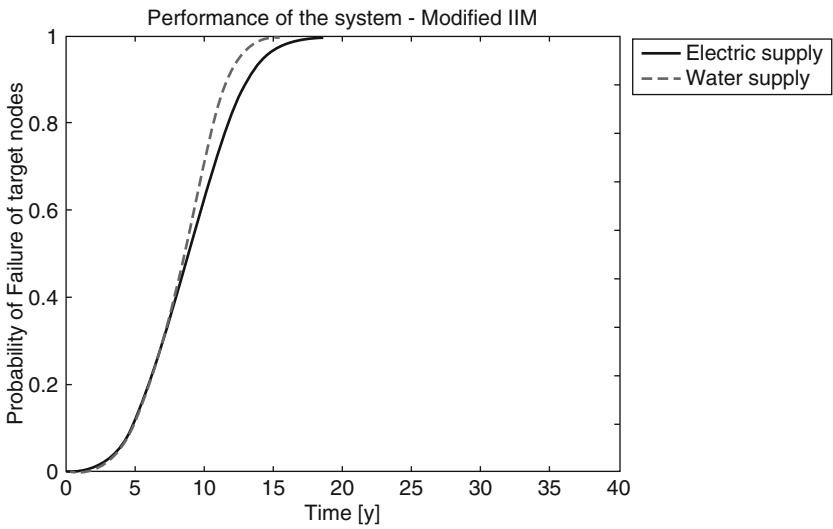


Fig. 7.26 Performance of the Example 2 network, according to the modified IIM

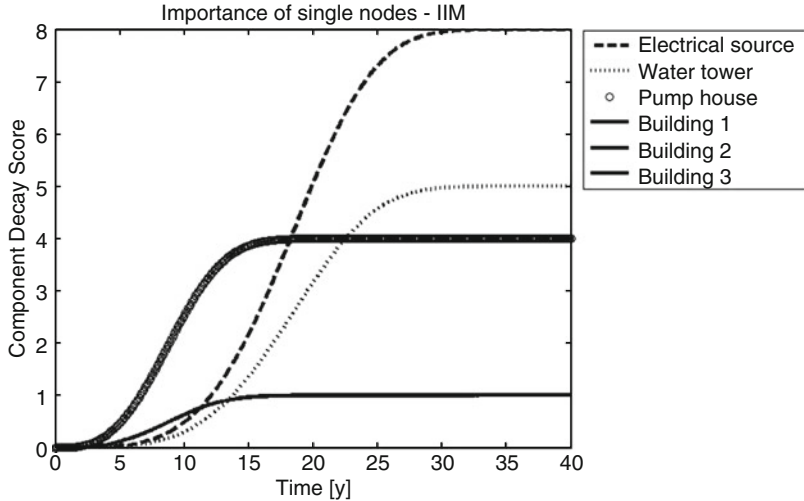


Fig. 7.27 Importance of nodes for the Example 2 network, according to the IIM

7.5.3.7 Importance of Single Nodes

The component decay score dc_s measures the importance of single nodes in the network. This index does not consider the mutual effects of the nodes in the network, but just multiplies the probability of self-failure P_{sf} for the number of nodes which are topologically located downstream (Fig. 7.27). Using the *modified IIM* instead, it is possible to determine the influence that each node has on the final failure of the target nodes. If it is computed the probability of failure of target nodes of a system in both the cases that the node of interest is considered subjected to events ($P_{sf} \geq 0$) and that it is not ($P_{sf} = 0$), it is possible to obtain curves shown in Fig. 7.28.

The difference between the two functions at every time step represents the effect that the node has on the entire system. The higher the difference, the more relevant is the damaging effect of the considered node propagating to target nodes. Plotting this difference, it is possible to obtain the curves of Figs. 7.29 and 7.30.

In Example 2, the numerical results show that the electric supply damages to buildings are much more relevant than damages to the electrical source. This is because the building fragility curves go to 0 faster than the ones of the electrical source, and once the buildings are down, no electric furniture can be available to users. For the water network it is possible to make the same consideration; the only difference is that here the buildings are less important than in the electric network, because the combination of probability of failure of electrical source, water tower and pumps is higher than the probability of failure of the electrical source itself.

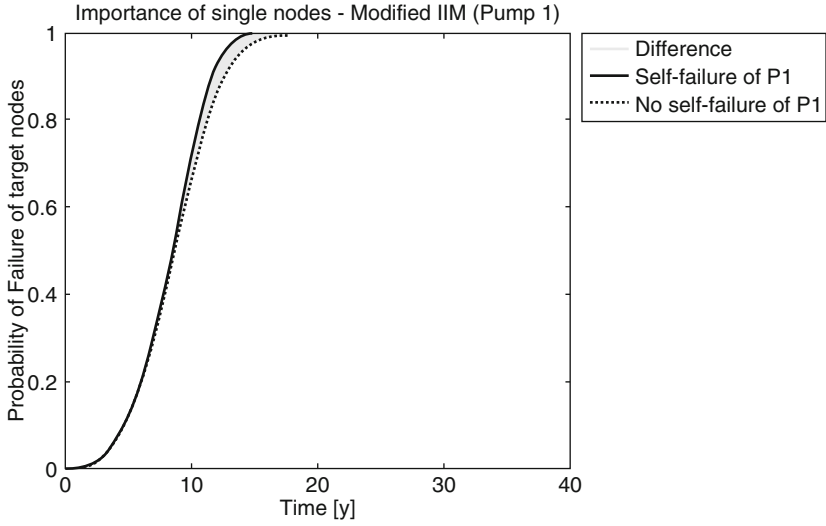


Fig. 7.28 Differences induced in the system by Pump 1 for Example 2 network

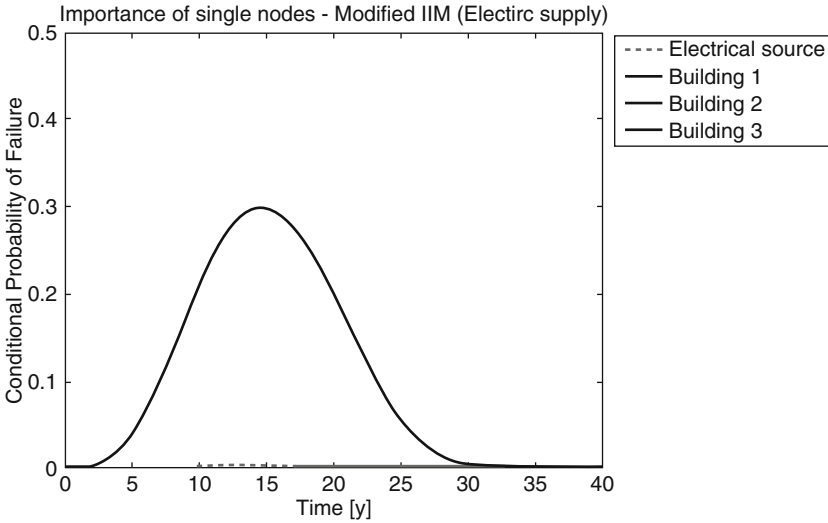


Fig. 7.29 Importance of nodes for the Example 2 network electric supply, according to the modified IIM

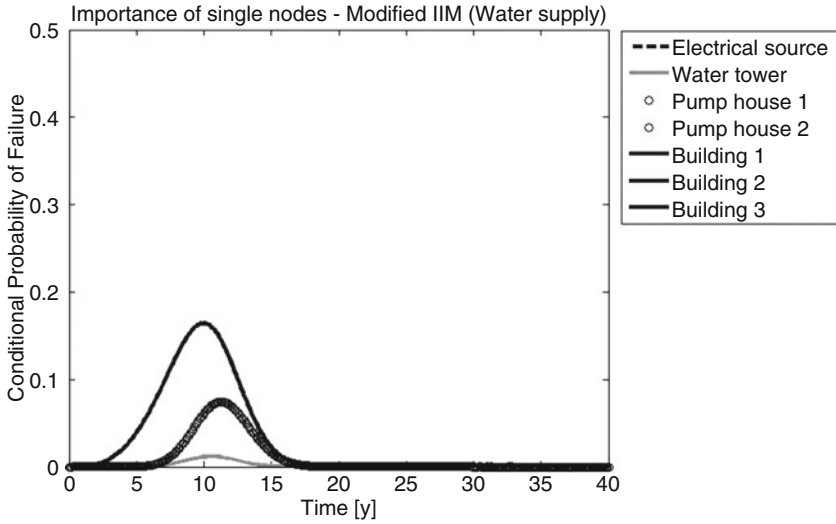


Fig. 7.30 Importance of nodes for the Example 2 network water supply, according to the modified IIM

7.5.4 Probability Risk Assessment

After introducing the *modified IIM* for lifeline networks, it is interesting to see how this method can be compared to the Probabilistic Risk Assessment (PRA) method, when considering critical sites. The aim is to see if the *modified IIM* can model both regional-scale and local-scale networks.

PRA is a systematic and comprehensive methodology to evaluate risks associated with every life-cycle aspect of a complex engineered technological entity (e.g., power plant, facility or spacecraft) from concept definition, through design, construction and operation, and up to removal from service. In a PRA, risk is characterized by two quantities: the magnitude, or severity, of the adverse consequences that can potentially result from the given activity or action, and the likelihood of occurrence of the given adverse consequences. If the measure of consequence severity is the number of people that can be potentially injured or killed, risk assessment becomes a powerful analytical tool to assess safety performance. Probabilistic Risk Assessment usually answers three basic questions:

1. What can go wrong with the studied technological entity, or what are the initiators or undesirable initiating events that lead to adverse consequences?
2. What and how severe are the potential detriments, or the adverse consequences that the technological entity may be eventually subjected to as a result of the occurrence of the initiator?
3. How likely are these undesirable consequences to occur, or what are their probabilities or frequencies?

The answer to the first question requires technical knowledge of the possible causes of a given activity or action leading to detrimental outcomes. PRA studies can be performed for internal initiating events, as well as for external initiating events. Internal initiating events are defined here to be hardware or system failures or operator errors in situations arising from the normal mode of operation of the facility. External initiating events are those encountered outside the domain of the normal operation of a facility. Initiating events associated with the occurrence of natural phenomena (e.g. earthquake, storm, etc.) are typical examples of external initiators.

The answers to the second and third questions are obtained by developing and quantifying accident scenarios, which are chains of events that link the initiator to the end-point detrimental consequences. Focusing on the third question, the answer is obtained by using Boolean Logic methods for model development and by probabilistic or statistical methods for the quantification portion of the model analysis. Boolean logic tools include inductive logic methods like event tree analysis (ETA) and deductive methods like fault tree analysis (FTA). It is easy to get confused between these two techniques. Indeed, these techniques are in fact complimentary and often used together, but focus on opposite sides of an undesirable event. Figure 7.31 shows how they fit together. A more comprehensive description of these methods is shown in next subsections.

In addition to the above model development and quantification, PRA studies require special analysis tools like human reliability analysis (HRA) and dependent-failure or common-cause analysis (CCF). HRA deals with methods for modeling human error while CCF deals with methods for evaluating the effect of inter-system

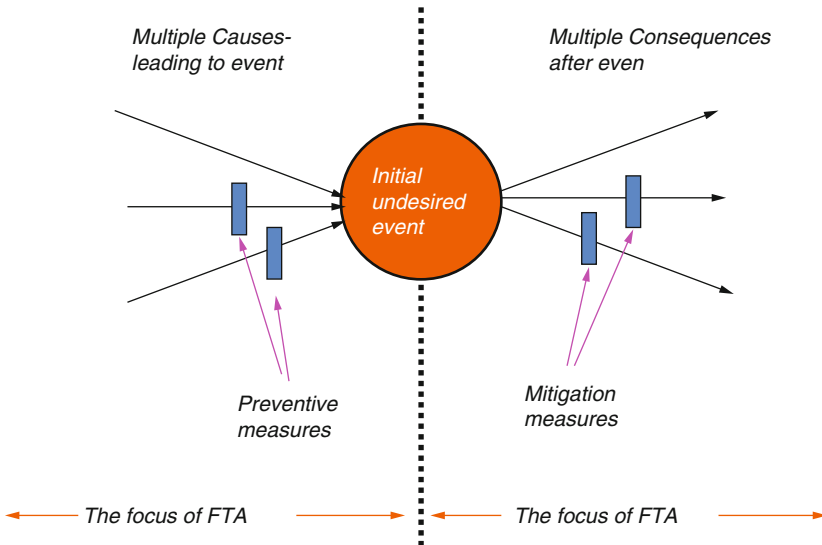


Fig. 7.31 Looking at undesired event using failure tracing methods (Source: ICAO 2014)

and inter-component dependencies which tend to cause significant increases in overall system or facility risk.

The final result of a PRA is given in the form of a risk curve and the associated uncertainties. The risk curve is generally represented by the plot of the frequency of exceeding a consequence value as a function of the consequence values (ICAO 2014).

7.5.4.1 Fault Tree Analysis

In many cases there are multiple causes for an accident or other loss-making event. Fault tree analysis is one analytical technique for tracing the events which could contribute. It can be used in accident investigation and in a detailed hazard assessment.

The fault tree is a logical diagram based on the principle of multi-causality, which traces all branches of events which could contribute to an accident or failure. A fault tree diagram is drawn from the top down. The starting point is the undesired event of interest, called the ‘top event’. The process consists of logically working out the immediate contributory fault conditions leading to that event. These may each in turn be caused by other faults, and so on. The trickiest part of the whole thing is actually getting the sequence of failure dependencies worked out in the first place (Stamatelatos 2000).

7.5.4.2 Event Tree Analysis

This is a complimentary technique to FTA, but defines the consequential events which flow from the primary “initiating” event. Event trees are used to investigate the consequences of loss-making events in order to find ways of mitigating, rather than preventing, losses. Below is the step-by-step procedure for carrying out event tree analysis:

- Identify the primary event of concern.
- Identify the controls that are assigned to deal with the primary event such as automatic safety systems, alarms on operator actions.
- Construct the event tree beginning with the initiating event and proceeding through failures of the safety functions.
- Establish the resulting accident sequences.
- Identify the critical failures that need to be addressed.

There are a number of ways to construct an event tree. They typically use Boolean logic gates (i.e. a gate that has only two options such as success/failure, yes/no, on/off). They tend to start on the left with the initiating event and progress to the right, branching progressively. Each branching point is called node. Simple event trees tend to be presented at a system level, glossing over the detail (Stamatelatos 2000).

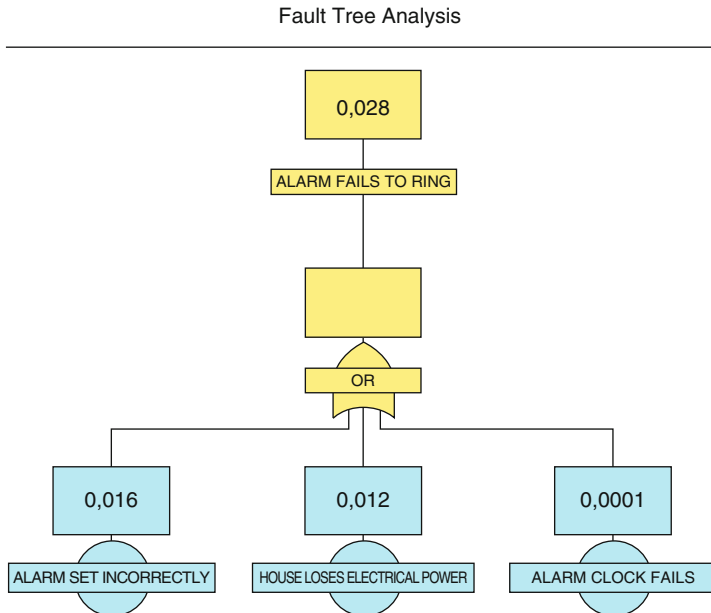


Fig. 7.32 Fault Tree Analysis of the probability of failure of the alarm clock in a working year period (Source: Wood et al. 2008)

7.5.4.3 Example of PRA

To clarify what is a PRA and how FTA and ETA work, a simple numerical example is presented. Hereinafter it will be called Example 4. The aim is to determine the frequency of being late at work because of oversleeping, over 1 year. After thinking about the problem, it is possible to construct a simple event tree model by defining an initiating event (i.e. it's a work day) and mitigating systems (i.e. an alarm clock and a backup person). Once defined the initiating event frequency, the model is solved by the determination of branch probabilities. For doing this, Fault Trees may be required, as shown in Fig. 7.32. As a convention for the ETA, upper branches are considered success (green probabilities) while lower branches are unsuccessful (red probabilities).

7.5.4.4 Limitations of PRA

Probabilistic Risk Assessment is a logical approach that suffers from analytical limitations. The three main problems pointed out by critic scholars are:

- it cannot account for the indirect, non-linear, and feedback relationships that characterize many accidents in complex systems;

- it does a poor job on modeling human actions and their impact on known and unknown failure modes;
- it is conceptually impossible to complete the construction of event-trees and fault-trees in mathematical sense.

The modified IIM suggested in the previous subsection overcomes the problems related to feedback relationships and rigorous mathematical formulation, because it allows loops of interdependence and uses analytical relations described by the IIM constitutive equation. For what concerns the second problem, agent based models can furnish more reliable human actions simulations. In conclusion, the modified IIM combined with temporal networks and agent based models, for the simulation of the human behavior, can determine the risk related to a system, without having the issue related to a PRA. The next subsection shows how results given by the two approaches can be compared.

7.5.4.5 Comparison with the Modified IIM

Even if inoperability and risk are similar measures for addressing the performance of a system, no correlation between the IIM and PRA have ever been done. As already shown, the modified IIM for temporal networks can model infrastructure networks at a regional scale; in the next paragraphs the application for analysis at the local level is presented. With the local level, it means for example the intern plant of a facility. Being the PRA based on logical tool, this analysis can also be done on non-conventional lifelines or infrastructure systems, and on logical scheme.

7.5.4.6 Fault Tree

One of the main implementations of the modified IIM is to be able to take into account the positive effect of redundancies in the system. Redundancies are computed, in both the PRA and the modified IIM, through the logic operator “OR”. Figure 7.33 shows how the tensor notation of the modified IIM can be used at this scope.

Figure 7.34 shows how the results of a numerical example coincide. The example of the clock failure presented in Fig. 7.32 is replicated with a simple 3-node network. Applied to each node is a probability of self-failure P_{sf} , equal to the frequency of failure of the oversleeping example. With the IIM algorithm, inoperability is propagated in the network and the result is given by the probability of failure P_f . The result obtained with the two methods coincides. In conclusion, the combination of events and cascading effects done by the modified IIM follows the same logic approach of FTA and give the same results.

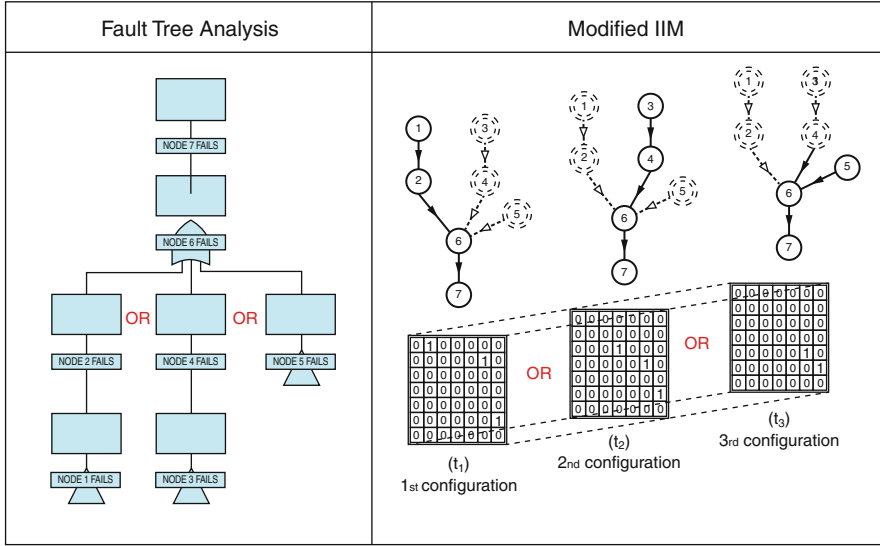


Fig. 7.33 Structure to obtain an “OR” operator with FTA and modified IIM

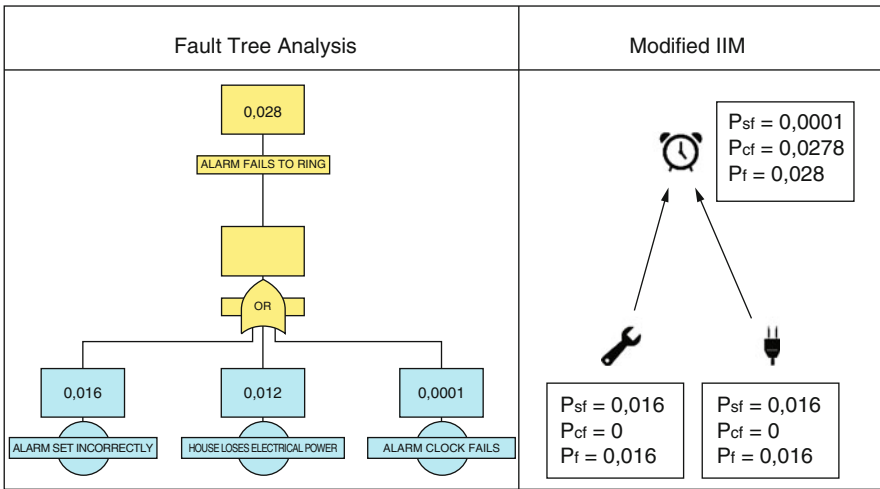


Fig. 7.34 Comparison between the FTA and the modified IIM for Example 4

7.5.4.7 Event Tree

Finding a correlation between the *modified IIM* and the ETA is more difficult than finding the correlation with FTA. The concept of sequences of events was not addressed by the traditional IIM, and was introduced in the proposed implementation with the tensor formalism. The sequences referred to in the modified IIM are

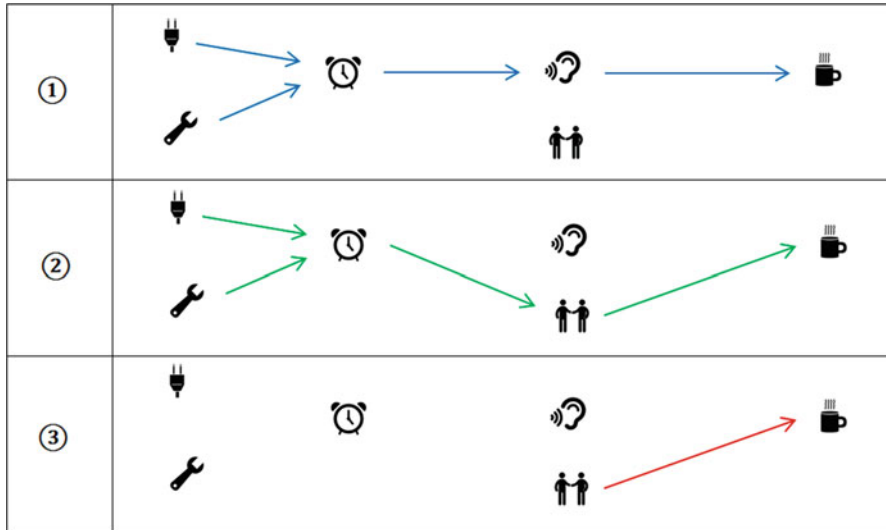


Fig. 7.35 Different configurations of a network simulating Example 4

the occurrences of different configurations of the network. If an Event Tree refers to sequences of event, which cannot be identified by the occurrence of a configuration, the modified IIM cannot obtain the same results, starting from the same data. In conclusion, there are some event sequences which can be simulated through the suggested model and not in the other.

Non-acceptable Event Sequences

When considering the example of oversleeping risk assessment, we can try to model it with the network of Fig. 7.35. The problem is that events (written in the columns) of Fig. 7.36, are not the success/failure of the three configurations of Fig. 7.36, but are the success/failure of single nodes. Modified IIM can only compute conditioned probability of occurrence of every configuration, but not the conditioned probability of single nodes.

Acceptable Event Sequences

If the Event Tree is structured in a way that every temporal sequence refers to the success/failure of a configuration of the system, the results obtained with the ETA and the *modified IIM* are the same. Figure 7.37 shows how, for Example 3, the P_{occ} and the loss of capacity LoC are the same for both methods. An event sequence is acceptable if is mutually exclusive with the others and if it represents the complete

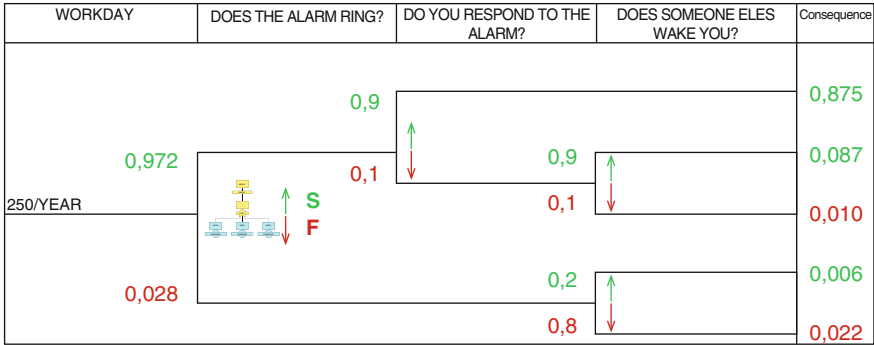


Fig. 7.36 Event Tree Analysis of Example 4, about the probability of being late at work because of oversleeping in a working year period (Source: Wood et al. 2008)

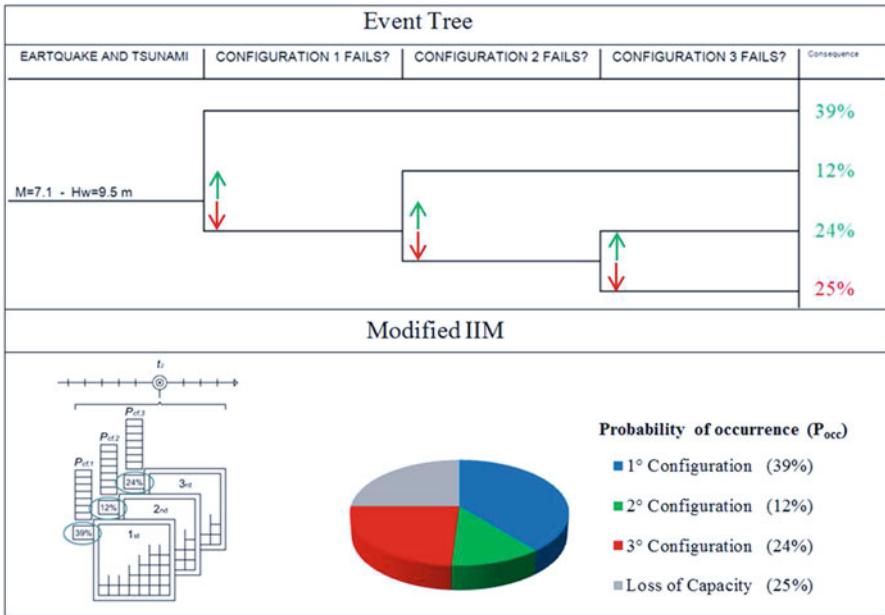


Fig. 7.37 Comparison between the ETA and the modified IIM for Example 3

flow, from the source to the sink, like configurations do for the modified IIM. In conclusion, the probabilities shown in the event tree of Example 4 are conditioned and they cannot be used as input in the *modified IIM*.

7.6 A Case Study: Fukushima Daiichi Nuclear Power Plant Disaster

This section focuses on the performance of lifelines serving critical sites such as a nuclear power plant. The choice of this case study to show the application of the methodology derives from the fact that nuclear power plants are dependent on extended regional scale infrastructures, but at the same time are strategic sites and have service plants at the local scale. In detail, the case study describes the 2011 Fukushima nuclear power plant disaster, which is one of the most complete examples of failure due to interdependence and temporal effects. The earthquake (Fig. 7.38) and tsunami (Fig. 7.39) that struck Japan's Fukushima Daiichi nuclear power station on March 11, 2011, knocked out backup power systems that were needed to cool the reactors at the plant, causing three of them to undergo fuel melting, hydrogen explosions, and radioactive releases (Fig. 7.40). Radioactive contamination from the Fukushima plant forced the evacuation of communities up to 25 miles away and affected up to 100,000 residents, although it did not cause any immediate deaths. This disaster marked a breaking point in the recent studies about safety engineering and showed that the complexity of the events and of the system were not accurately modeled by risk planners, and cascading effects resulted in major damage to the nuclear power plant. Fukushima Daiichi *Nuclear Power Station* (hereinafter referred to as NPS) is located in Okuma Town and Futaba Town, Fukushima Prefecture, facing the Pacific Ocean on the east side.

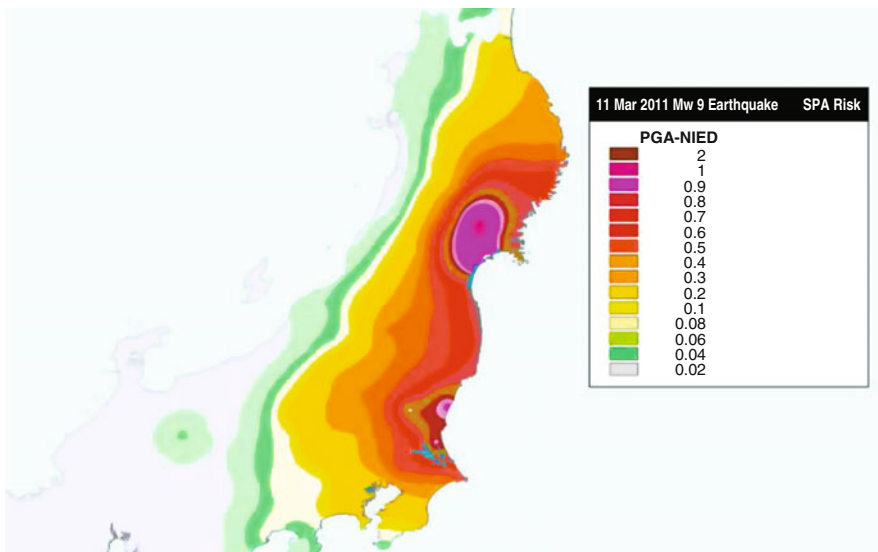


Fig. 7.38 Shake map of the Eastern Japan Coast after Tōhoku earthquake (Source: Coastal Engineering Committee, Japan Society of Civil Engineers)

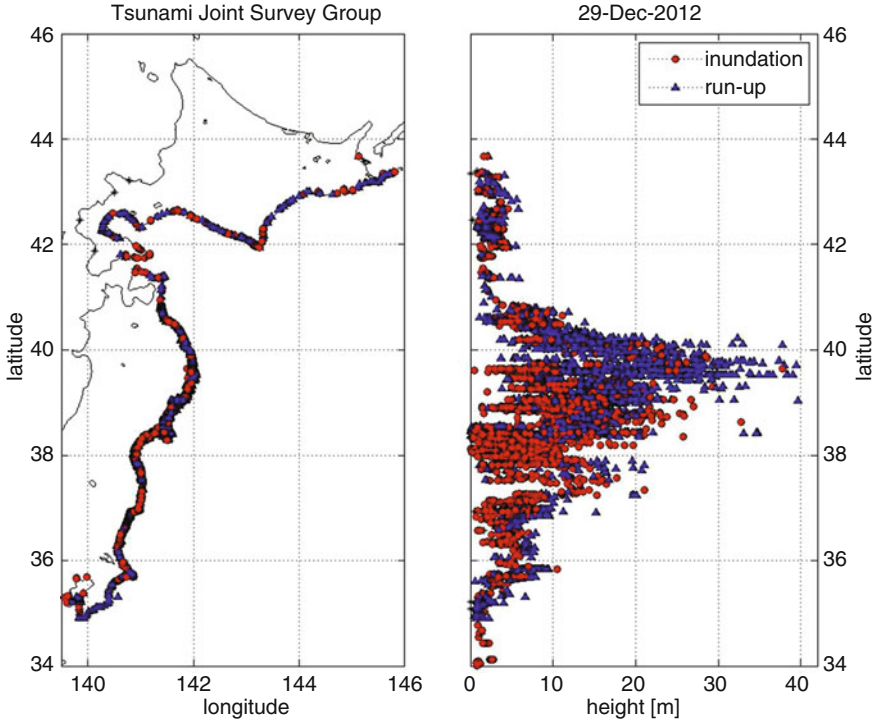


Fig. 7.39 Inundation map of the Eastern Japan Coast after Tōhoku tsunami (Source: Coastal Engineering Committee, Japan Society of Civil Engineers)

The site is a half oval shape with the long axis along the coastline and the site area is approx. 3.5 million square meters. This is the first nuclear power station constructed and operated by the Tokyo Electric Power Company, Incorporated (hereinafter referred to as TEPCO). Since the commissioning of *Unit 1* on March 1971, additional reactors have been constructed in sequence. Currently, there are six reactors (Fig. 7.41). The total power generating capacity of the facilities is 4,696 MW (Report of Japanese Government to the IAEA Ministerial Conference on Nuclear Safety – The Accident at TEPCO’s Fukushima Nuclear Power Stations).

The safety design procedures employed at Fukushima NPSs are the following:

- cooling system was connected to the *offsite power supply grids* via two or more power lines;
- Multiple *emergency power supply systems* such as diesel generators were installed independently in parallel with the offsite power supply system (redundant design).
- to cope with a short-period loss of all AC power sources, emergency DC power sources (batteries) were installed giving redundancy and independency to the safety system.



Fig. 7.40 Pictures of Fukushima nuclear power plant after the 2011 Tōhoku earthquake and tsunami

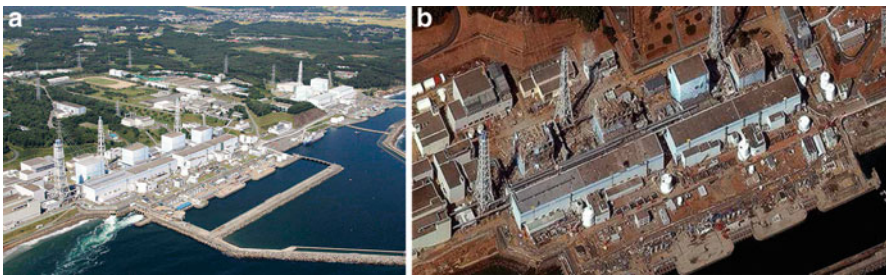


Fig. 7.41 Fukushima Daiichi Nuclear Power Plant before (a) and after (b) the disaster

On the day the earthquake occurred, *Unit 1* of the Fukushima Daiichi NPS was in operation at the constant rated electric power, *Units 2* and *3* were in operation at the constant rated thermal power. *Unit 4* was shut down for periodic inspection. Large-scale repair work was under way to replace the core shroud, and all fuel assemblies had been transferred to the spent fuel pool from the reactor core with the reactor well filled with water and the pool gate closed. *Unit 5* was also shut down for periodic inspection. All fuel assemblies were loaded in the reactor core and the pressure leak test for *Reactor Pressure Vessel* (hereinafter referred to as RPV) was underway. *Unit 6* was in periodic inspection too, and all fuel assemblies were loaded in the reactor core that was in cold shutdown condition.

7.6.1 Cooling Requirements of a NPS

To operate safely, a nuclear power plant needs to be cooled continuously, especially when the reactor is shut down, because it continues to generate heat even when the reaction chain is stopped because of the radioactive decay of unstable isotopes and fission products created by the process. The decay heat in the reactor core decreases for several days. Nuclear fuel rods that have reached cold shutdown temperatures typically require several years of water cooling in a spent fuel pool.

The reason that cooling is so essential for a nuclear reactor is that many of the internal components and fuel assembly cladding is made from Zircaloy (Zirconium alloys are solid solutions of zirconium or other metals, a common subgroup having the trade mark Zircaloy). At normal operating temperatures (of approximately 300 °C), Zircaloy is inert. However, when heated to above 500 °C in the presence of steam, Zircaloy undergoes an exothermic reaction and the Zircaloy oxidizes to produce hydrogen gas. The reaction between the zirconium cladding and the fuel can also lower the melting point of the fuel and thus speeds up core melt. The result of this problem is shown in Fig. 7.41b. When the reactor is shut down and it is not producing electricity, the pumps which circulate cooling water can be powered by other units off-site through the grid, or by diesel generators. In addition, the boiling water reactors have steam-turbine driven emergency core cooling systems that can be directly operated by steam which is still being produced after a reactor shutdown, and it can inject water directly into the reactor. The steam turbines reduce the dependency on the emergency generators, but they operate until the reactor is producing steam. Electric energy provided by batteries is otherwise necessary to operate the valves and the monitoring systems. The case study considered here is the failure of the cooling system, that led to the nuclear disaster.

7.6.2 Connection of Fukushima Daiichi NPS with Offside Power Supply

Okuma Lines No. 1 and No. 2 (275 kV) of the Shin-Fukushima Substation were connected to the switchyard for Units 1 and 2. Okuma Lines No. 3 and No. 4 (275 kV) were connected to the switchyard for Units 3 and 4, while Yonomori Lines No. 1 and No. 2 (66 kV, Fig. 7.42) were connected to the switching yard for Units 5 and 6.

In addition, the TEPCO Nuclear Line (66 kV) from Tomioka Substation of the Tohoku Electric Power was connected to Unit 1 as spare line. The three regular high voltage switchboards (6.6 kV) were used for Unit 1, for Unit 2, and for Units 3 and 4, respectively. The regular high voltage switchboards for Unit 1 and for Unit 2 were interconnected, and the regular high voltage switchboards for Unit 2 and for Units 3 and 4 were interconnected. When the earthquake occurred, the switching facilities for Okuma Line No. 3 in the switchyard for Units 3 and 4 were under construction, so that six lines were available for power of the NPS from offsite power supply.

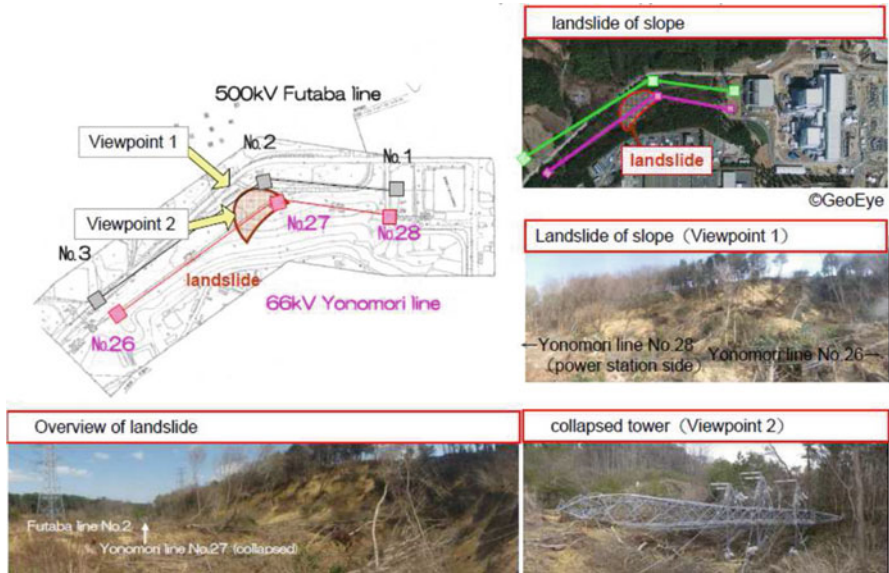


Fig. 7.42 Damage occurred at Yonomori Lines (66 kV)

7.6.3 Time-Line of the Fukushima Daiichi NPS Disaster

Below is the time line of the events after the main shock, given in Japan Standard Time (JST):

March 11, 2011 at 14:46: the earthquake occurred and brought all of the Fukushima Daiichi NPS Units 1, 2 and 3 in operation to an automatic shutdown of the reactors, and the station power supply was switched to the offsite power supply. However, the NPS was unable to receive electricity from offsite power transmission lines, mainly because some of the steel towers for power transmission outside the NPS site collapsed due to the earthquake (Fig. 7.42). For this reason, the emergency direct generators (DGs) of each Unit were automatically engaged to provide power to the cooling system of the reactors and the spent fuel pools. At 15:46 a 14 m tsunami (Fig. 7.43) overcomes the seawall designed to protect the plant, filling the Fukushima facility with seawater. All backup diesel generators were disabled, except one which was placed and sealed underground, while the fuel tanks were wiped away. All the emergency DGs except the one of Unit 6 stopped. Seawater systems that cooled the emergency DGs, and metal-clad switchgears were underwater, and the result was that all AC power supply were lost from Units 1 to 5 (Fig. 7.44).

At 16:36 on the same day, TEPCO figured out that it was not able to monitor the water level in the reactors of Units 1 and 2.

TEPCO opened the valve of the *Isolation Condensers* (hereinafter referred to as IC) (System A) of Unit 1, and in an effort to maintain the functions of the



Fig. 7.43 The tsunami overtops the 10 m high seawall designed to protect the Fukushima Daiichi NPS



Fig. 7.44 Flooding of the Fukushima Daiichi NPS due to the tsunami

IC, it continued to operate it mainly by injecting fresh water into its shell side. Immediately after the tsunami, TEPCO could not confirm the proper functioning of the *Reactor Core Isolation Cooling system* (hereinafter referred to as RCIC) of Unit 2. Only at 3:00 on March 12th it was confirmed that it was operating properly. Unit 3 was cooled using its RCIC system, and as a result, the *Primary Containment Vessel* (hereinafter referred to as PCV) pressure and water levels remained stable. In order to recover the power supply, TEPCO took emergency measures, such as making arrangements for power supply vehicles. It was later confirmed, around 23:00 on March 11th, that the radiation level in the turbine building of Unit 1 was increasing. In addition, at 0:49 on March 12th, TEPCO confirmed that there was a possibility that the PCV pressure of the Unit 1 had exceeded the maximum operating pressure.



Fig. 7.45 Massive explosion of Unit 1

At 5:46 on March 12th, the company began alternative fresh water injections in Unit 1 using fire engines. In addition, they began preparations for PCV venting because the PCV pressure was high, but the work ran into trouble because the radiation level in the reactor building was already high. It was around 14:30 on the same day that a decrease in the PCV pressure level was actually confirmed. Subsequently, at 15:36 on the same day, a hydrogen explosion occurred in the upper part of the Unit 1 reactor building (Fig. 7.45). A complete timeline of all the events occurring at Unit 1 is presented in Fig. 7.46. Meanwhile, the RCIC system of Unit 3 stopped at 11:36 on March 12th, but shortly after, the *High Pressure Core Injection system* (hereinafter referred to as HPCI) was automatically activated, in order to maintain a certain water level in the reactor. It was confirmed at 2:42 on March 13th that the HPCI system had stopped. After the HPCI system stopped, TEPCO performed wet venting to decrease the PCV pressure, and fire engines began alternative fresh water injection in the reactor around 9:25 on March 13. As the PCV pressure increased, PCV venting was performed several times, resulting in a decrease of the PCV pressure. At 11:01 on March 14th, a hydrogen explosion occurred in the upper part of the reactor building.

At 13:25 on March 14th, TEPCO determined that the RCIC system of Unit 2 had stopped because the reactor water level was decreasing, and began to reduce the RPV pressure and inject seawater into the reactor using fire-extinguishing system lines. TEPCO continued to cool the reactor core using the fire pumps loaned by a fire department. The wet venting line configuration had been completed by 11:00 on March 13th, but the PCV pressure exceeded the maximum operating pressure. At 6:00 on March 15th, an impulsive sound that could be attributed to a hydrogen explosion was confirmed near the *Suppression Chamber* (hereinafter referred to as S/C), and later, the S/C pressure decreased sharply. The total AC power supply for Unit 4 was also lost due to the earthquake and tsunami, and therefore, the functions

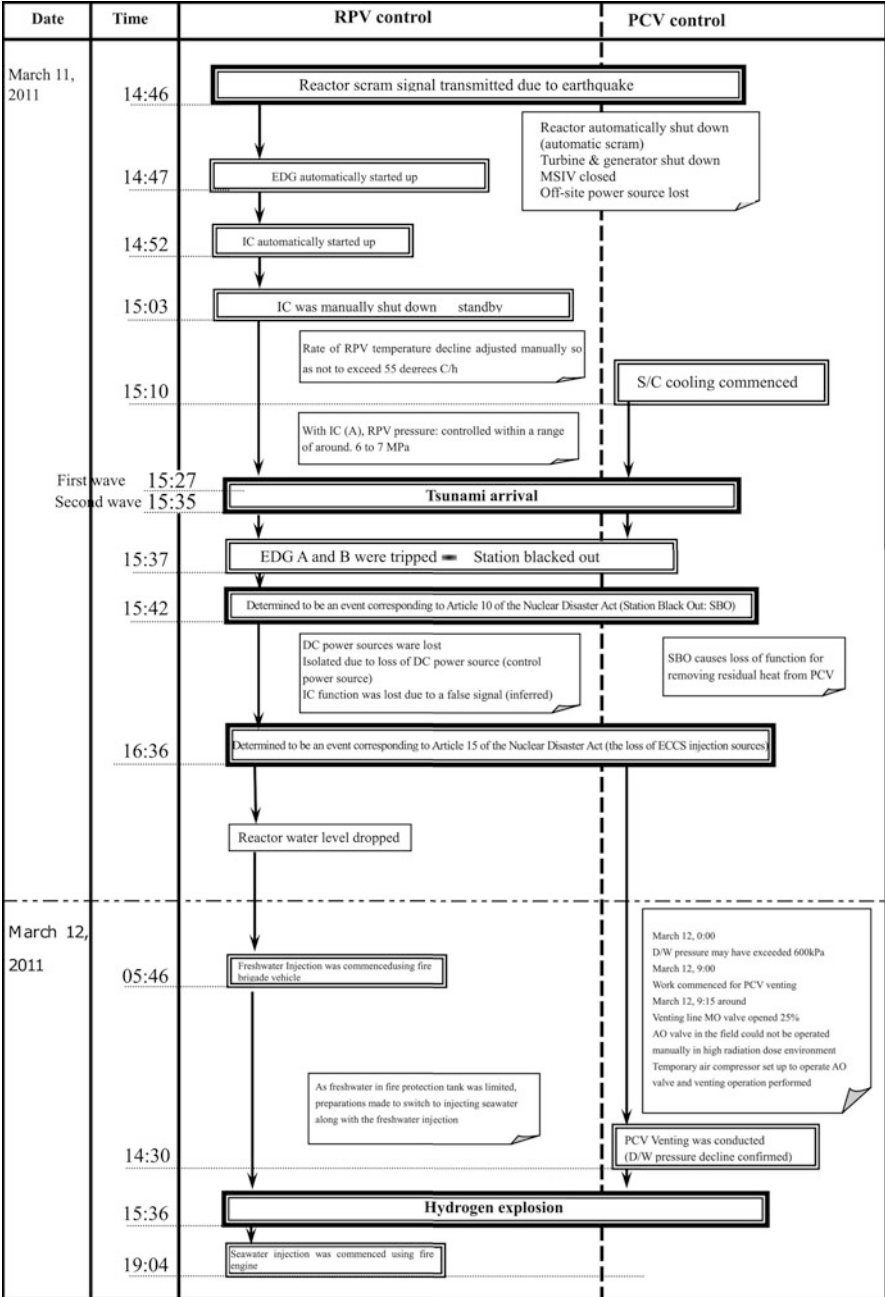


Fig. 7.46 Timeline of events occurring at Unit 1 of Fukushima Daiichi nuclear power plant (Source: TEPCO 2012)

of cooling and supplying water to the spent fuel pool were lost. Around 6:00 on March 15th, a hydrogen explosion occurred in the reactor building, damaging part of the building severely.

At 22:00 on March 15th the Minister of Economy, Trade and Industry of Japan ordered TEPCO to inject water into the spent fuel pool of Unit 4. On March 20th and 21st, fresh water was sprayed into the spent fuel pool of Unit 4. On March 22nd, a concrete pump truck started to spray seawater onto the pool, followed by the spraying of fresh water instead of seawater, which began on March 30th. On March 17th, a Japan Self-Defense Forces helicopter sprayed seawater into the spent fuel pool of Unit 3 from above. Later, seawater was sprayed into the pool using high-pressure water-cannon trucks of the National Police Agency's riot police and fire engines of the Self-Defense Forces. From March 19th to March 25th, Tokyo Fire Department, Osaka City Fire Bureau and Kawasaki City Fire Bureau, that were dispatched as Emergency Fire Response Teams, sprayed seawater for five times by using seawater supply system against fire and squirt fire engines. In addition, Yokohama City Fire Bureau, Nagoya City Fire Bureau, Kyoto City Fire Bureau and Kobe City Fire Bureau dispatched their fire engines to Fukushima Daiichi NPS. Niigata City Fire Bureau and Hamamatsu City Fire Bureau assisted with the set up of a large-scale decontamination system. Later, the concrete pump truck started to spray seawater into the spent fuel pool of Unit 3 on March 27th and into the spent fuel pool of Unit 1 on March 31st.

The total AC power supply for Unit 5 was also lost due to the earthquake and tsunami, resulting in a loss of the ultimate heat sink. As a result, the reactor pressure continued to increase, but TEPCO managed to maintain the water level and pressure by injecting water into the reactor by operating a Make-Up Condensing Water Pump after the power was supplied from Unit 6. Later, the company activated a temporary seawater pump, bringing the reactor to a cold shutdown condition at 14:30 on March 20th.

One of the emergency DGs of Unit 6 had been located uphill, and as a result, its functions were not lost, even when the NPS was hit by the tsunami, while the seawater pump was not functioning. TEPCO installed a temporary seawater pump while controlling the reactor water level and pressure by injecting water into the reactor and reducing the reactor pressure on a continuous basis. By doing this, the company recovered the cooling functions of the reactor, thus bringing the reactor to a cold shutdown condition at 19:27 on March 20th. After the accident, seawater was used for cooling the reactors and the spent fuel pools for a certain period of time, but the coolant had been switched from seawater to fresh water with consideration given to the influence of salinity.

7.6.4 Modelling the Nuclear Power Plant

Models of the lifeline networks serving a nuclear power plant have been put in place to try to replicate what happened at Fukushima. This work doesn't model the Unit 1 of Fukushima Daiichi NPP because data regarding this case study are not present,

or are at least unavailable to the author. The aim is to realize a model of a nuclear power plant equipped with a Boiling Water Reactor (BWR), similar in shape to the one present in Fukushima. The topology and data regarding disrupting events affecting the system are inspired by the Fukushima case study, but the parameters of the system components are generic and taken from the literature.

7.6.5 Topology

Nuclear power plants are served by a number of service plants, whose complexity is hard to grasp for people not in the industry. Focusing just on the connectivity of these networks, it is possible to follow logic schemes while setting the topology of a model. The plant scheme furnished by TEPCO (Fig. 7.47) was used as a reference for building nuclear power plant models. In the scheme are the electric network, the water network and the steam network. For the purposes of this analysis, the steam network has not been considered by itself but it has been combined with the water one. To prevent the spread of radioactive substances outside, cooling circuits are closed. These loops have been modeled with one-direction links from the source to the reactor core.

Apart from the water network, which is present at the local/building scale, there is also the electric network, which expands from the regional scale to the local one. This is a lifeline in a more appropriate sense than the cooling plant, but no distinction is made in this case study. The task is to run a performance analysis of all the

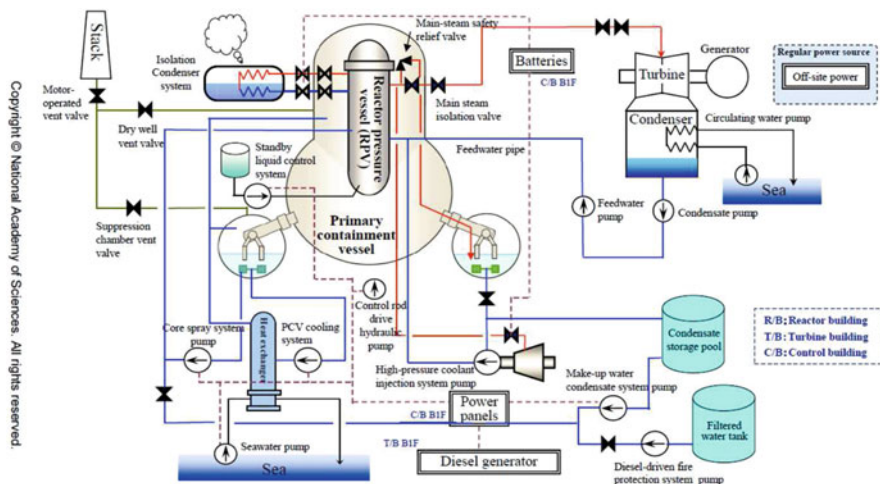


Fig. 7.47 Scheme of the Unit 1 Fukushima Daiichi reactor (Source: TEPCO 2012)

systems serving the reactor core, so all the components important for the success or failure of the reactor cooling have been modeled by nodes and connected following logical assumptions.

Two different models are presented. The first is a simplified version of the scheme of Fig. 7.47, while the second one is a more detailed one and integrates the physical infrastructures as well as emergency responders' networks.

7.6.5.1 Simplified Model

The simplified model shown in Fig. 7.48 is composed of an electric and a water network. The sources of the electric network are, in order of priority, the external electric network, diesel generators and DC batteries. All these possible configurations converge into a power panel which is feeding the pumps of the ordinary water network. The source of this water network is the sea, which is considered to have unlimited autonomy, as it does the external electric network. The first emergency cooling systems consists in the Isolation Condenser (IC), which cools the steam coming from the reactor in a pool and does not require electricity because the flow is gravity-driven. After this, the High Pressure Coolant Injection (HPCI) system can cool the core in emergency conditions. It draws water from the Condensate Storage Tank (CST) or from the Suppression Pool (SP) and injects it into the core, thus reducing the internal pressure. The pump used by this system is steam-driven so it feeds automatically once the plant is started. In conclusion we have three possible configurations for the electric network and four configurations for the water cooling one.

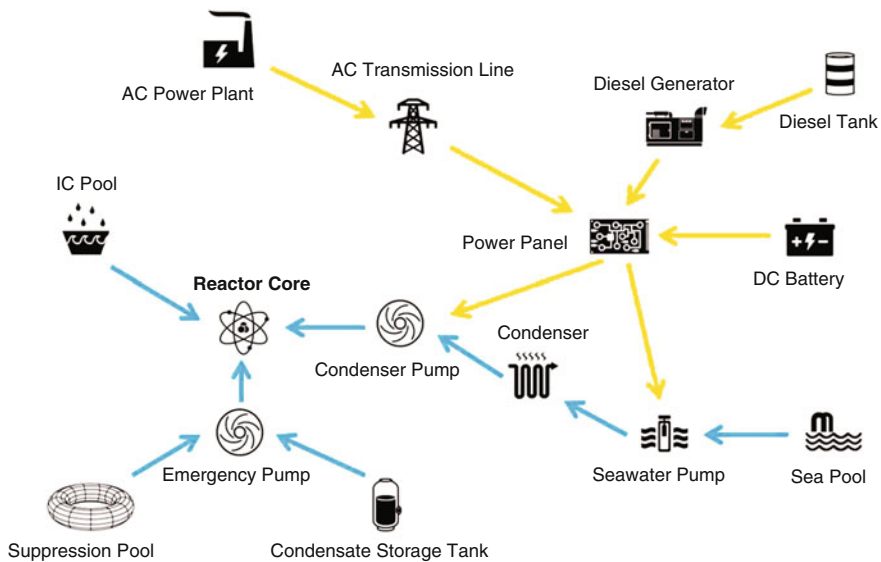


Fig. 7.48 Simplified model for lifelines serving a nuclear power plant

7.6.5.2 Detailed Model

More detail is necessary to accurately describe the Fukushima Unit 1 case study. Both the electric and the water networks have connections more complex than the one present in the simplified model. Starting from the electric sources, the self-sustainment guaranteed by the NPP power plant is introduced. Then every source and relative paths feed particular target nodes, not all of them. The ordinary cooling line, for example, is only fed by the NPP turbine and the off-site AC power, while the diesel generators feed the Residual Heat Removal (RHR) cooling system. The IC and HPCI systems, which were considered not dependent on electricity in the simplified model, are now indirectly dependent on it, because their activation is performed by valves which can be remotely controlled only with electricity supply. The DC battery is responsible for the functionality of these valves.

To better model possible human intervention to the system, three other networks have been added: the telecommunication network, the transportation network and the emergency service network. Some nodes and edges of these networks may not be active for certain periods of time. All the layers of these new models are interdependent, as shown in Fig. 7.49. The connections among nodes can be present at the *regional scale* (Fig. 7.50), at the *power plant scale* (Fig. 7.51) and at the *reactor scale* (Fig. 7.52).

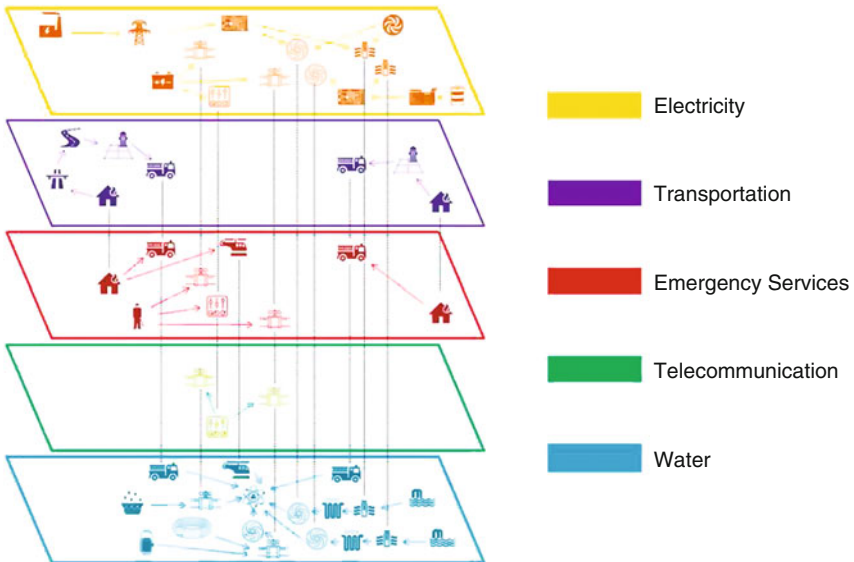


Fig. 7.49 Interdependent layers of the detailed model for lifelines serving a nuclear power plant

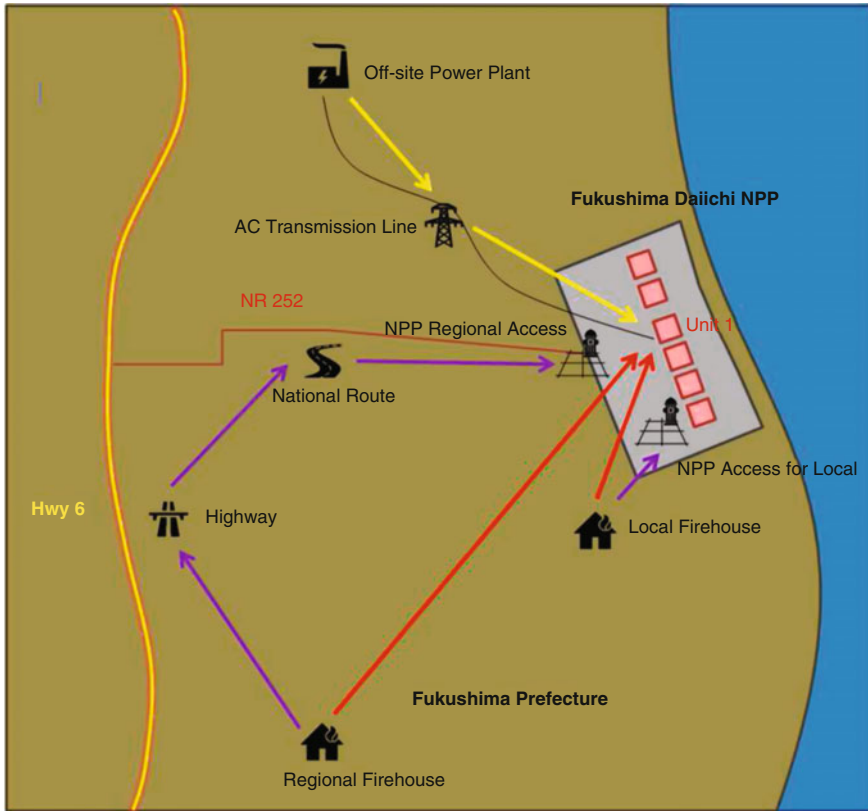


Fig. 7.50 Detailed model for lifelines serving a nuclear power plant at the regional scale

7.6.5.3 Hazards

The hazards considered for the analysis are the earthquake and the tsunami. The intensities of these hazards are considered deterministic and are taken from the real case study. In Table 7.2, the nodes have been classified according to their location and their altitude. Figures 7.53 and 7.54 show the plan and the section view of the power plant. It is then possible to estimate, through the data from the shake and the flow maps, what has been the intensity of the event for the considered node. To assemble the event matrix, the E-vectors should be positioned at the correct time step. The time steps are defined in accordance with the timeline present in Fig. 7.55.

7.6.5.4 Parameters

It is well known the difficulty in collecting reliable data about essential facilities and in the case of nuclear power plants it is even more difficult. So, the impossibility of

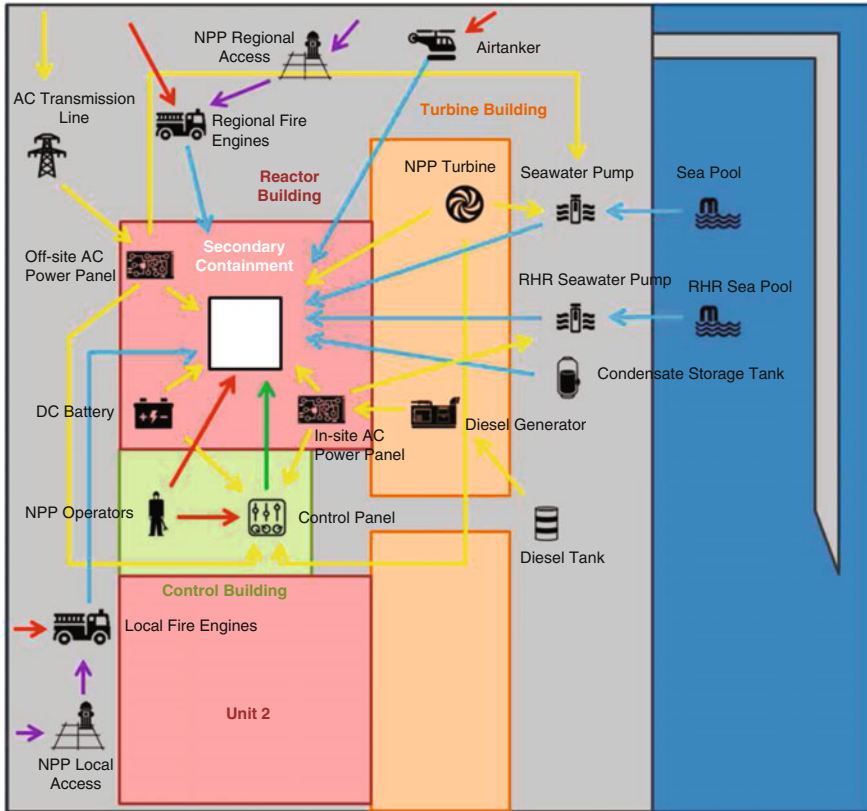


Fig. 7.51 Detailed model for lifelines serving a nuclear power plant at the power plant scale

finding data about Fukushima brought the author to the decision of discussing a generic nuclear power plant instead of that specific one.

After comparing different sources, credible parameters have been assigned to each component. Concerning earthquake and tsunami fragility functions, most of them have been taken from ATC13 (1985) “Earthquake damage evaluation data for California” (1985). These data are old and generic, but are still broadly employed in absence of more reliable and updated sources. ATC13 (1985) furnishes a series of damage probability matrices for structural and non-structural components, which are based on expert opinion. The objective of the analysis is to evaluate the performance of the systems, so it is necessary to make some assumption about the level of damage of the component which causes its inoperability. Other earthquake fragility curves have been taken from the Eidinger et al. (2001) and from the Hazus database (FEMA 2012).

Tsunami fragility curves have been considered linear functions between two values obtained from the ATC13 (1985) recommendations and considerations about the robustness of buildings. Autonomy curves instead, have been estimated to be

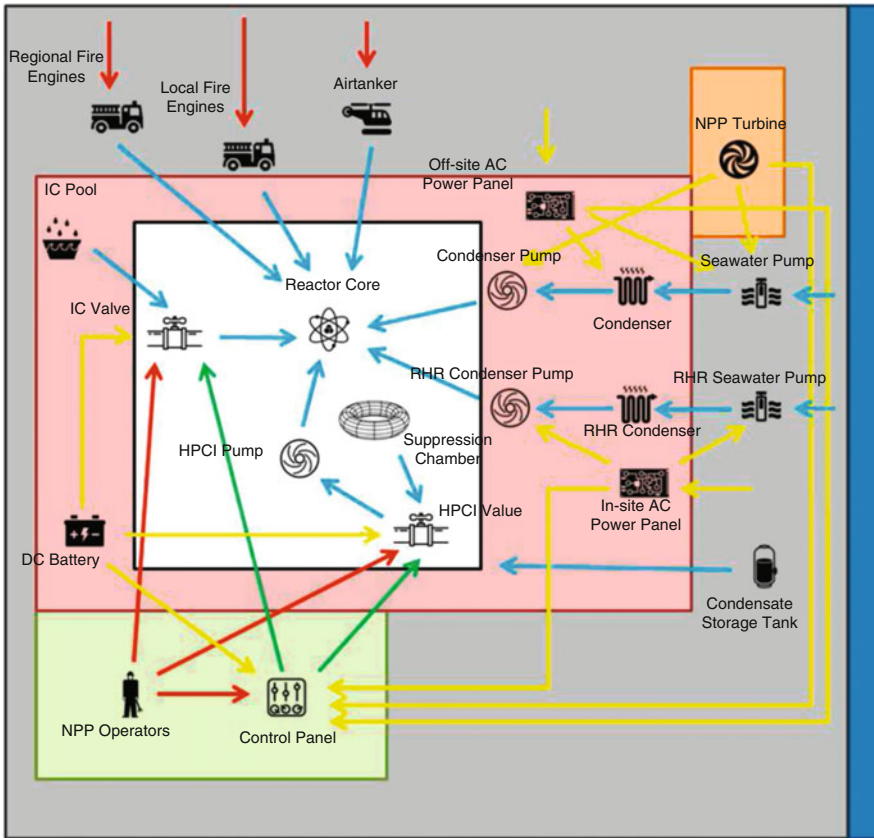


Fig. 7.52 Detailed model for lifelines serving a nuclear power plant at the reactor scale

a step function where the step is located in correspondence of the nominal value indicated by Moriya and Sato (2011).

Figures 7.55, 7.56 and 7.57 illustrate the fragility and temporal effects curves for the nodes of the water network. Similar functions were adopted for all the other networks.

7.6.6 Analysis of the System

Having defined all the necessary inputs, it is possible to run the model to compute the various probabilities of failure of the systems. This section shows the results relative to the electric network and the water network of both the simplified model and the detailed model of the NPP modelled. Analysis of other networks, composing the detailed model are not reported, because they are not directly comparable with

Table 7.2 Intensity of hazards for the nuclear power plant models

Node	Location	Altitude (m)	Earthquake PGA (g)	Tsunami depth of water (m)
NPP turbine	Turbine building	10	0.469	6
AC power plant	Hinterland	>50	0.415	–
AC line	Hinterland	>50	0.415	–
Off-site AC power panel	Turbine building	10	0.469	6
Diesel tank	NPP apron	10	0.469	3
Diesel generator	Reactor building	10	0.469	9
In-site AC power panel	Reactor building	10	0.469	9
DC battery	Reactor building	10	0.469	9
Highway	Hinterland	>50	0.415	–
Road	Hinterland	>50	0.415	–
Local firehouse	Hinterland	>50	0.469	–
NPP local access	NPP apron	10	0.469	3
Local fire engines	–	–	0.469	–
Regional firehouses	Hinterland	>50	0.415	–
NPP regional access	NPP apron	10	0.469	3
Regional fire engines	–	–	0.415	–
Airtanker	–	–	0.415	–
NPP operators	–	–	0.469	–
Control panel	Control building	10	0.469	6
Sea pool	Wharf	4	0.469	5
Seawater pump	Wharf	4	1	3
Condenser	Reactor building	10	0.469	9
Condenser pump	Reactor building	10	1	9
RHR sea pool	Wharf	4	0.469	5
RHR seawater pump	Wharf	4	0.469	3
RHR condenser	Reactor building	10	0.469	9
RHR condenser pump	Reactor building	10	0.469	9
IC pool	Reactor building	10	0.469	9
IC valve	Reactor building	10	0.469	9
Condensate storage tank	NPP apron	10	0.469	3
Suppression pool	Reactor building	10	0.469	9
HPCI valve	Reactor building	10	0.469	9
HPCI pump	Reactor building	10	0.469	9
PCV	PCV	20	0.469	16

the simplified model, but have been computed and influence the results of the water network presented. In the next subsections, a description of the results of the simulations and a comparison with the real events happened in Japan is given.

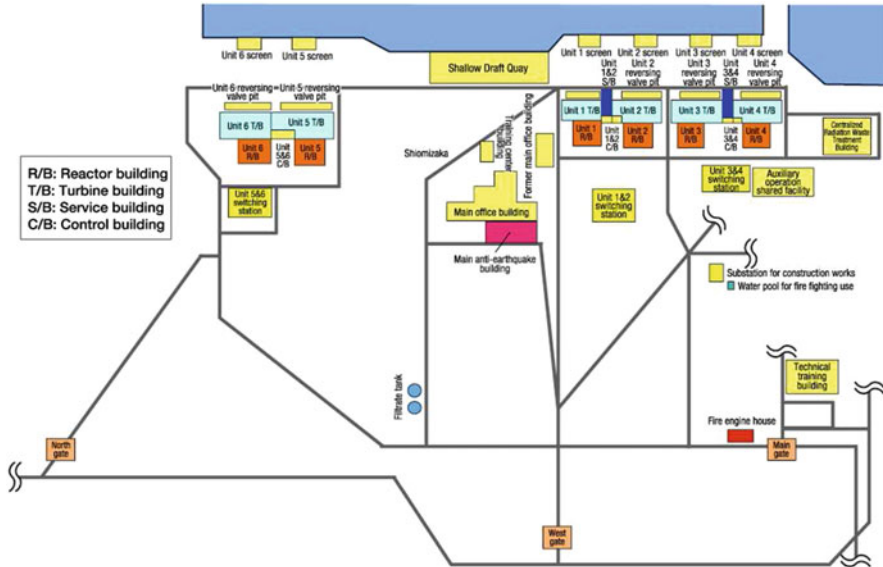


Fig. 7.53 Location of facilities at the Fukushima NPP (Source: TEPCO 2012)

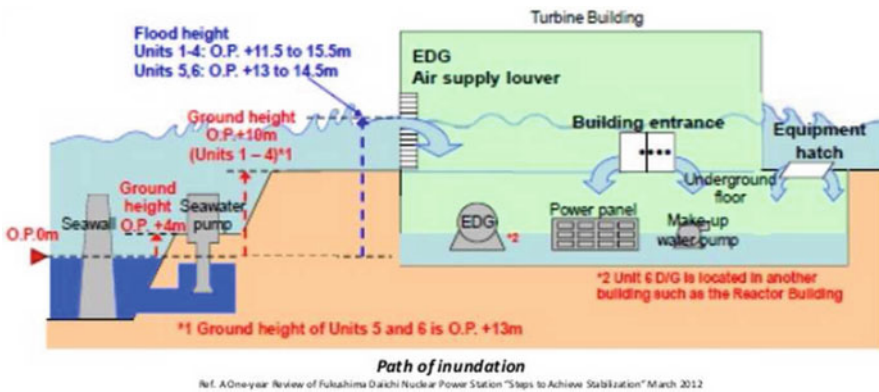


Fig. 7.54 Flooding path for the Fukushima NPP (Source: TEPCO 2012)

7.6.6.1 Simplified Model

In the simplified model, the earthquake is responsible for the shutdown of other power plants and for the collapse of the AC transmission line; this implies the loss of the off-site AC power, which represents the first configuration of the electric network. The electric network changes configuration and the power supply is guaranteed to the water network. Other components suffer few damages or no damages.

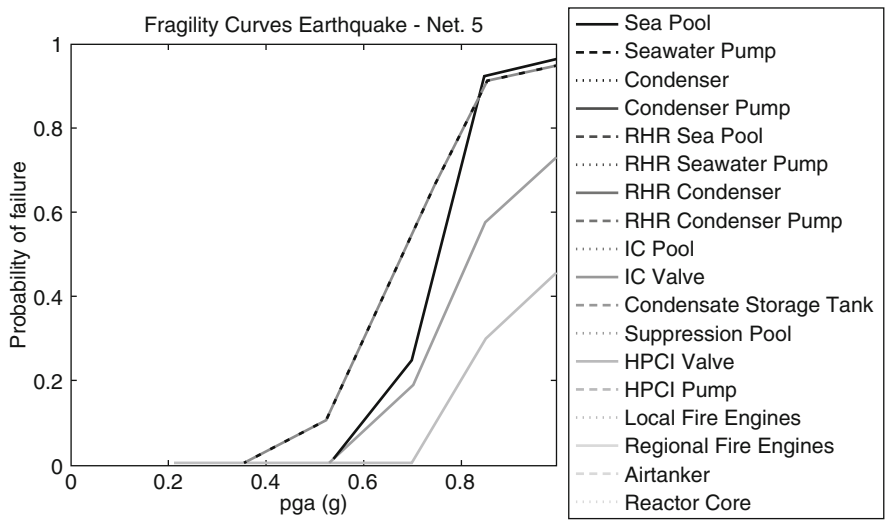


Fig. 7.55 Earthquake fragility curves for the nodes of the water cooling network

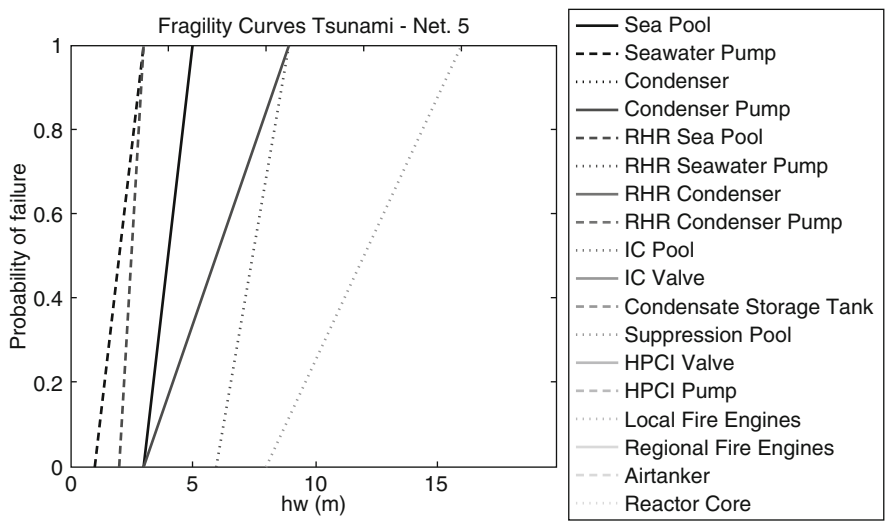


Fig. 7.56 Tsunami fragility curves for the node of the water cooling network

The arrival of the tsunami wave drastically changes the situation. Tanks placed in the NPP apron are swept away as well as the sea pumps. Diesel generators and the ordinary cooling line are out of order. Batteries are damaged too, but there is no need of them anymore since pumps they were feeding have failed. IC backup cooling system, which does not need electricity because it works by gravity, is initiated and the probability of failure of the reactor core cooling is still close to

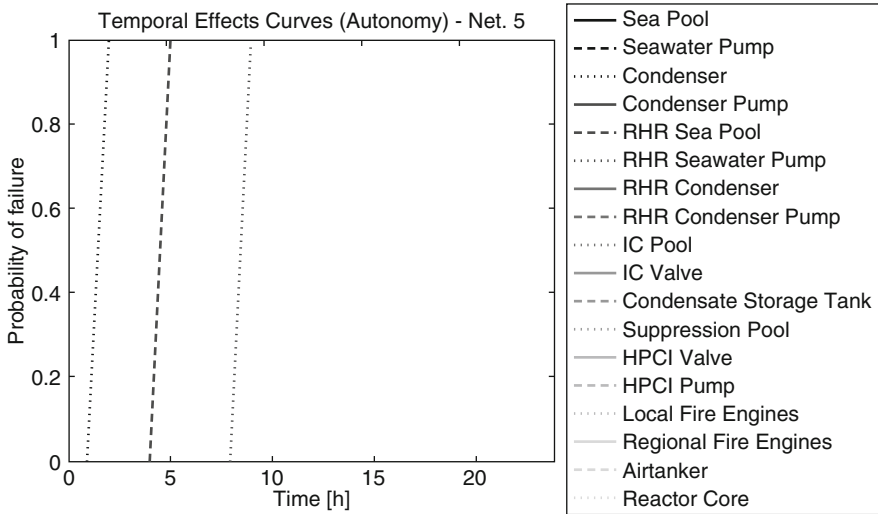


Fig. 7.57 Autonomy curves for the nodes of water cooling network

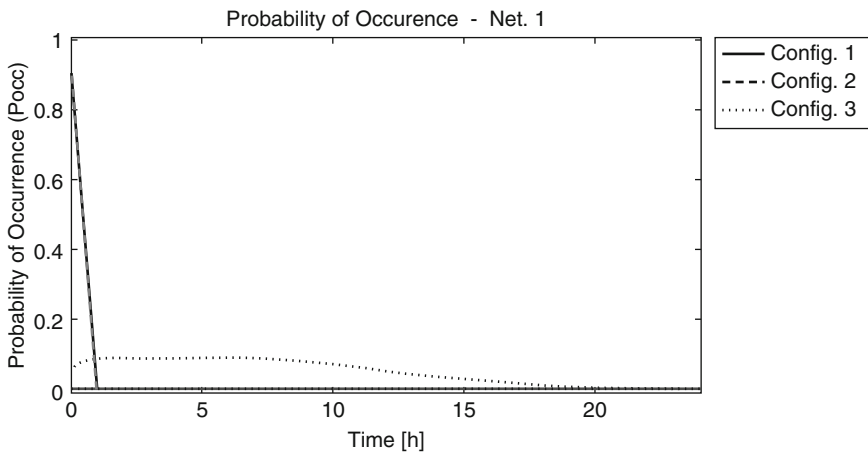


Fig. 7.58 Probability of occurrence of configurations of the electric network, for the simplified model

zero. Ten hours after the earthquake, the autonomy of the IC starts to decrease and it is substituted by the HPCI system, which does not need electricity because it is equipped with a steam driven pump. As the probability of failure of the IC increases because of autonomy run out, the probability of failure of the reactor core increases as well, because it now relies on the HPCI system, which was potentially damaged by earthquake and the tsunami. Figures 7.58, 7.59 and 7.60 summarize all this information (Figs. 7.61, 7.62, 7.63, 7.64, 7.65, 7.66, 7.67, and 7.68).

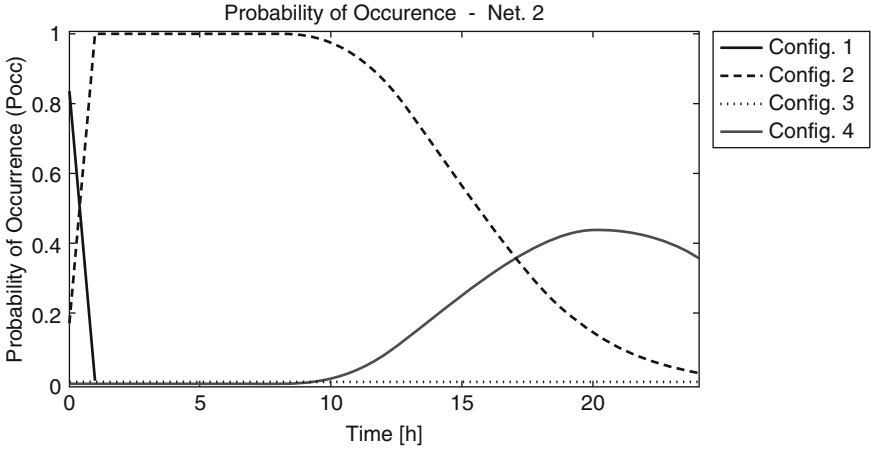


Fig. 7.59 Probability of occurrence of configurations of the water network, for the simplified model

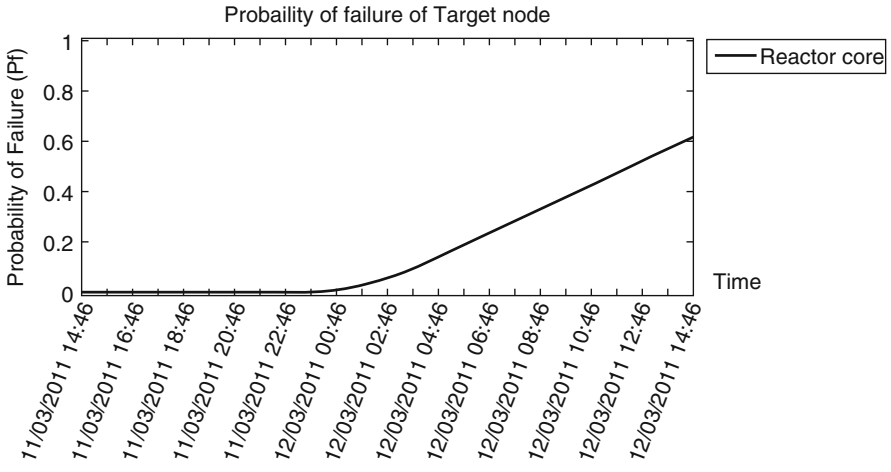


Fig. 7.60 Probability of failure of the reactor core cooling, for the simplified model

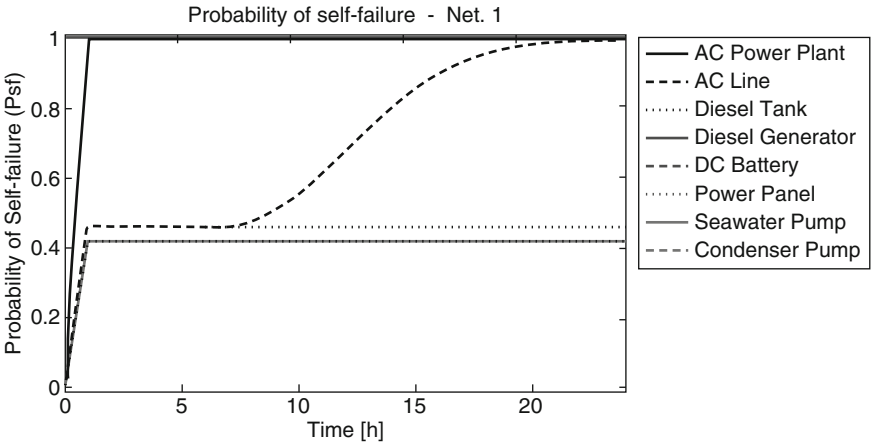


Fig. 7.61 Probability of self-failure of nodes of the electric network, for the simplified model

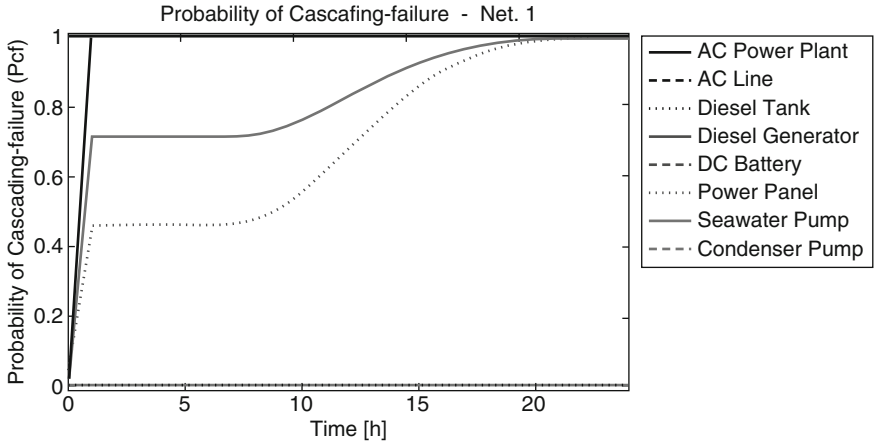


Fig. 7.62 Probability of cascading-failure of nodes of the electric network, for the simplified model

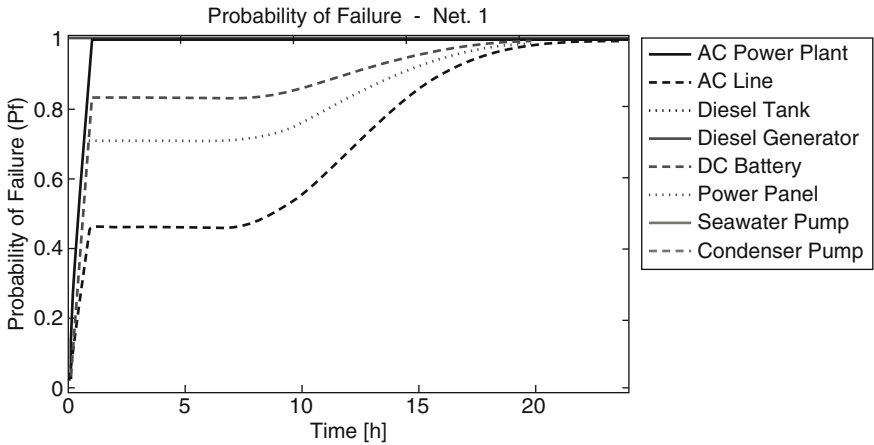


Fig. 7.63 Probability of failure of nodes of the electric network, for the simplified model

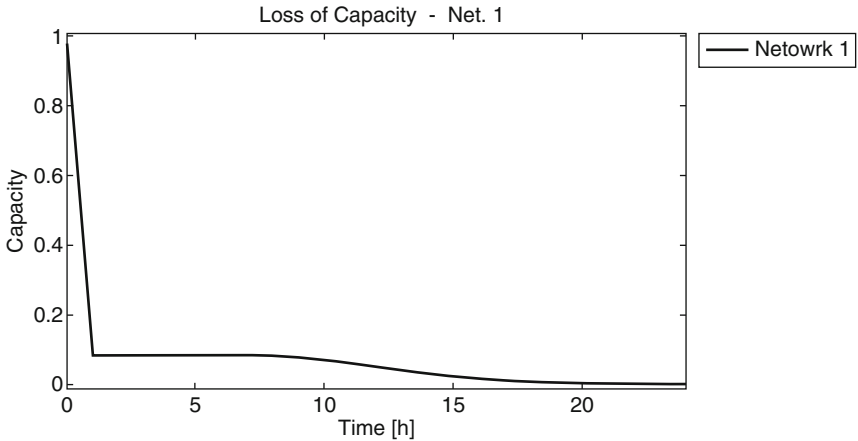


Fig. 7.64 Loss of capacity of the electric network, for the simplified model

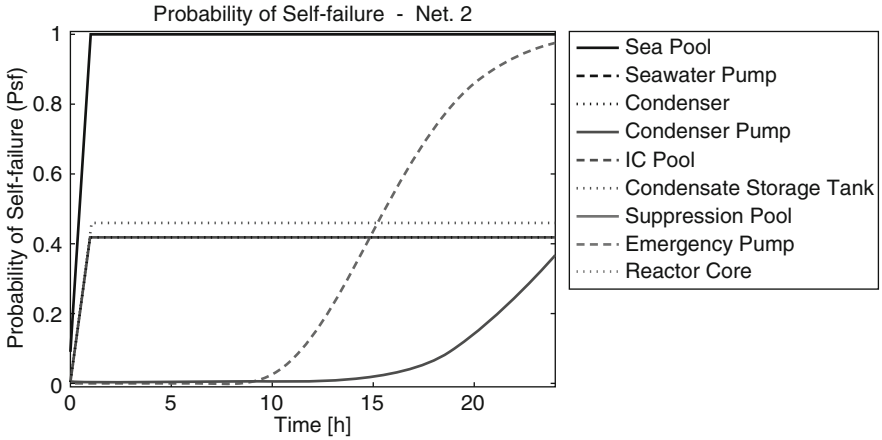


Fig. 7.65 Probability of self-failure of nodes of the water network, for the simplified model

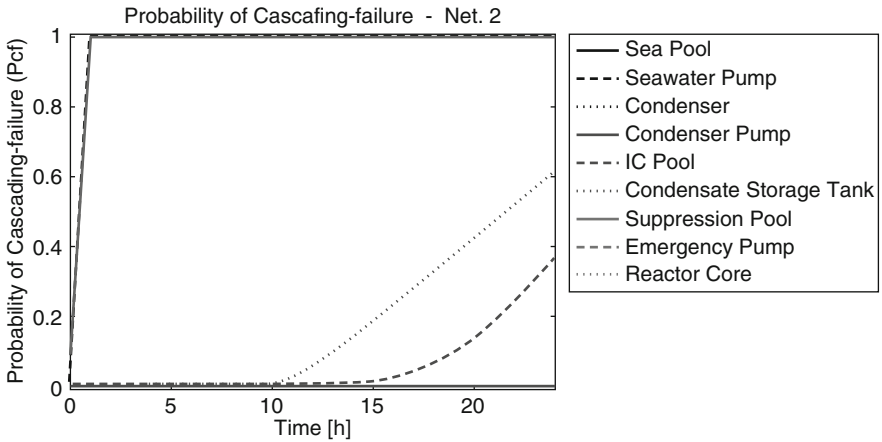


Fig. 7.66 Probability of cascading-failure of nodes of the water network, for the simplified model

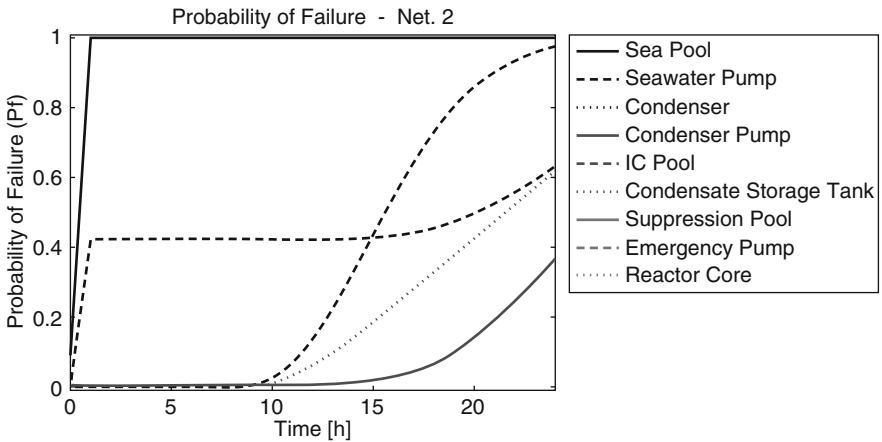


Fig. 7.67 Probability of failure of nodes of the water network, for the simplified model

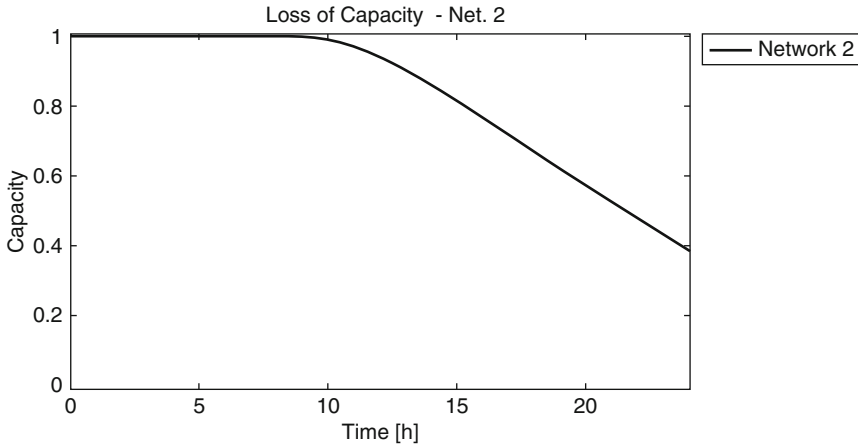


Fig. 7.68 Loss of capacity of the water network, for the simplified model

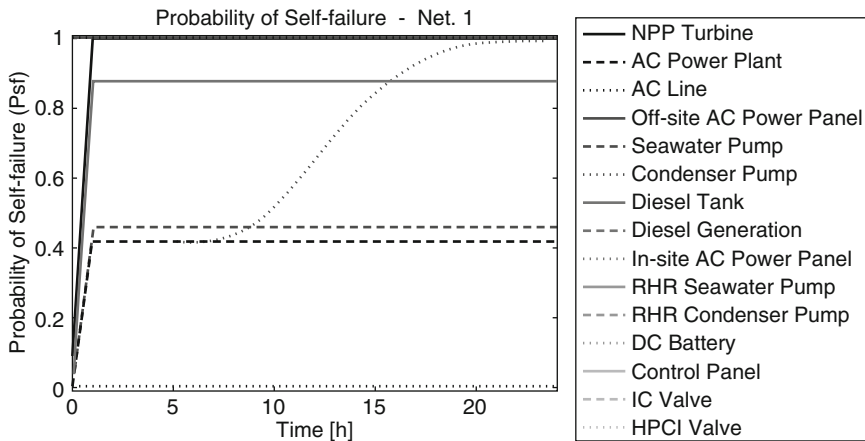


Fig. 7.69 Probability of self-failure of nodes of the electric network, for the detailed model

7.6.6.2 Detailed Regional to Local Scale Model

In the *detailed model*, as well as the previous one, the earthquake is responsible for the shutdown of the NPP turbine and the off-site AC power. AC transmission lines collapse. The loss of off-site AC power propagates the inoperability to the ordinary cooling configuration. Electricity is still provided by diesel generators which feed the RHR system and the control room. Damages caused by the earthquake to emergency cooling systems imply that all of the first three backup lines have a probability of occurrence $P_{occ} \neq 0$, but still the most likely to be active is the RHR (Figs. 7.69 and 7.70).

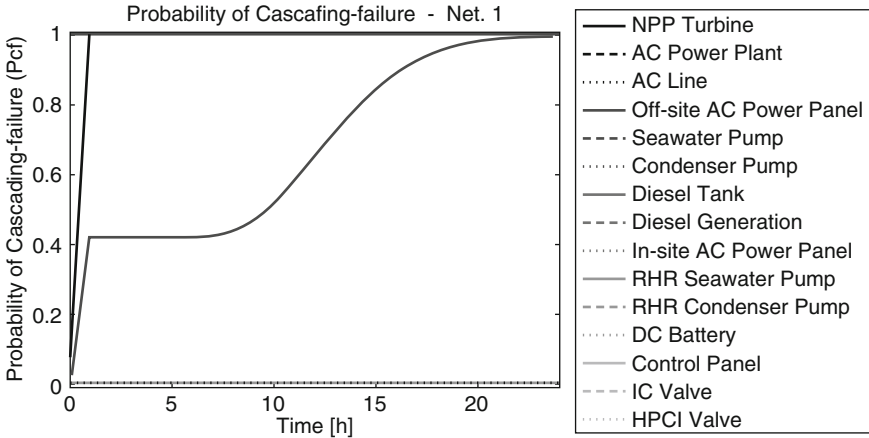


Fig. 7.70 Probability of cascading-failure of nodes of the electric network, for the detailed model

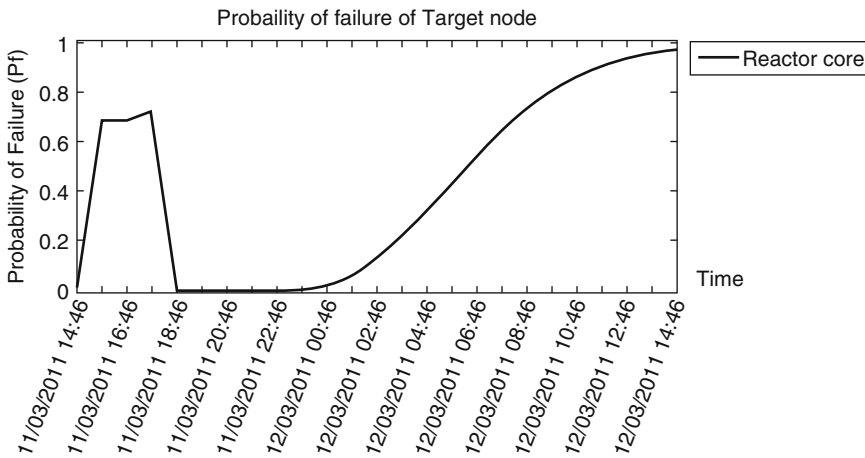


Fig. 7.71 Probability of failure of the reactor core cooling, for the detailed model

After the tsunami, diesel tanks, CSTs and seawater pumps are completely damaged. The NPP is unusable too, because access is obstructed by the debris deposited by the wave. Rescuers have difficulties in accessing and need time to restore a functional access. The water network tries to switch to the IC and HPCI configurations, but the DC power is needed to control their valves. There is a low probability that this is available because the batteries have high probability of failure, so the loss of capacity sharply increases. After three hours, the IC valves are manually opened and the cooling is provided by the IC, until its autonomy runs out and brings to a complete loss of capacity (Figs. 7.71, 7.72, 7.73, 7.74, 7.75, 7.76, 7.77, 7.78, and 7.79).

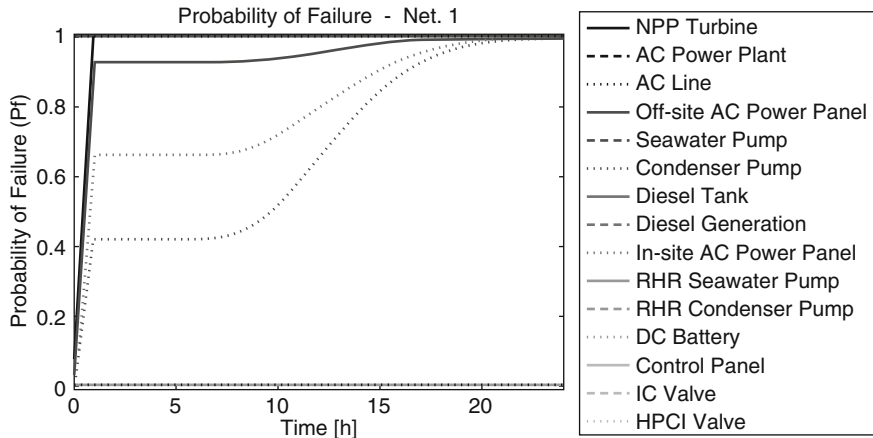


Fig. 7.72 Probability of failure of nodes of the electric network, for the detailed model

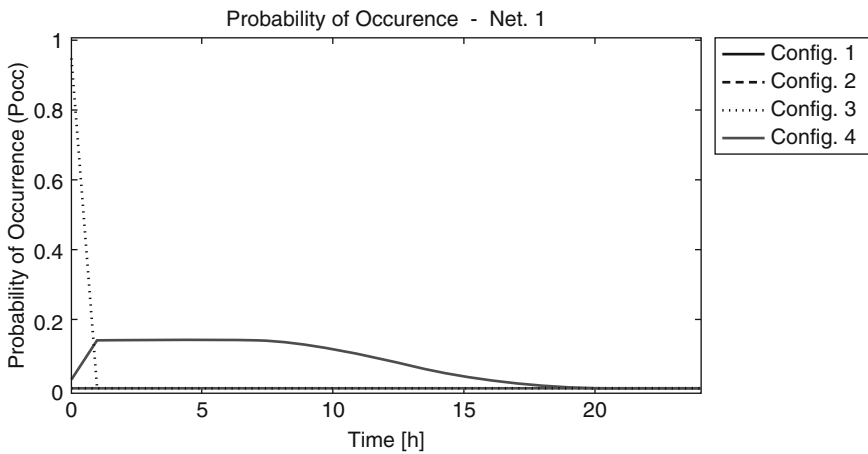


Fig. 7.73 Probability of occurrence of configurations of the electric network, for the detailed model

7.6.6.3 Comparison of Simplified and Regional Scale Model: The 2011 Fukushima NPP Disaster

Sensitivity analysis of results obtained by applying the *modified IIM* has been performed using both the *simplified* and the *regional scale model*. In fact, often in civil engineering, design and analysis starts with simple models and then becomes more refined with more complex ones. Here, it is shown how the level of detail is important as far as it conditions the sequence of events that take place. Given the fact

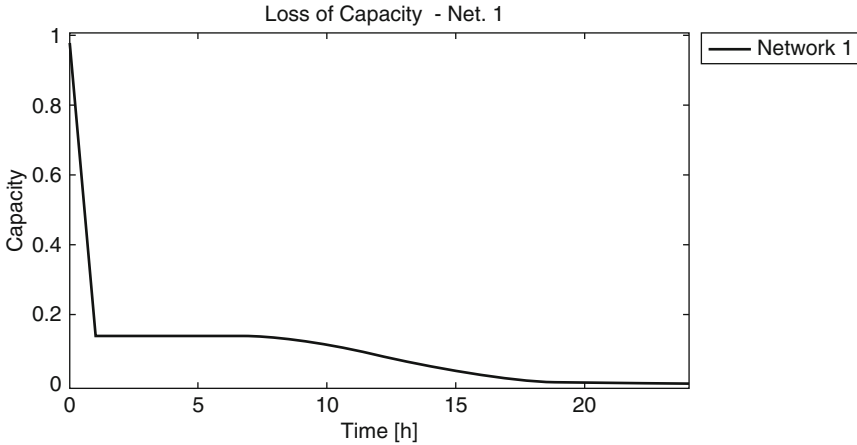


Fig. 7.74 Loss of capacity of the electric network, for the detailed model

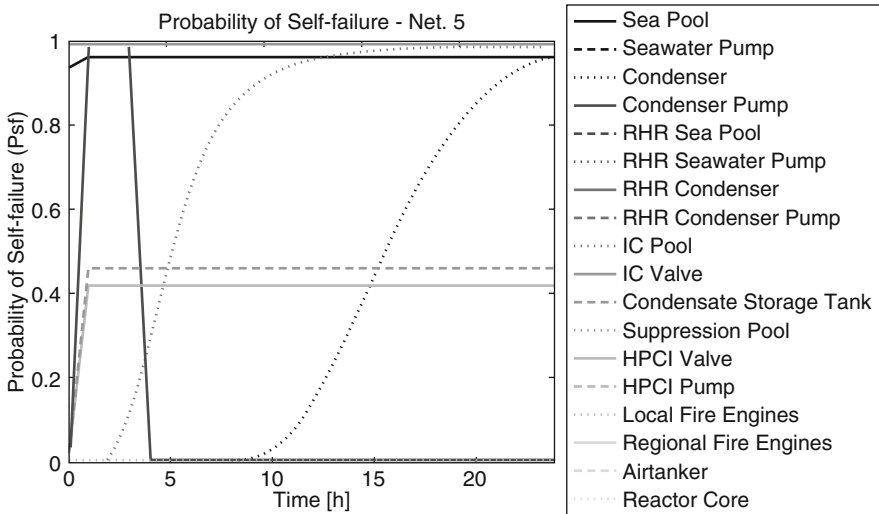


Fig. 7.75 Probability of self-failure of nodes of the water network, for the detailed model

that the model topology and parameters have been calibrated on a real case study, a comparison with the evidence of this one will indicate which is the best model and how relevant is to capture certain details.

In the next paragraphs, the events that took place on March 11th 2011 at the Unit 1 of the Fukushima Daiichi nuclear power station are represented in the form of event trees. The red line (Fig. 7.81) indicates the sequence of events which took place. The probability of occurrence of these configurations is of course $P_{occ} = 1$, because it is the real scenario. In Tables 7.2 and 7.3 are compared the P_{occ} obtained

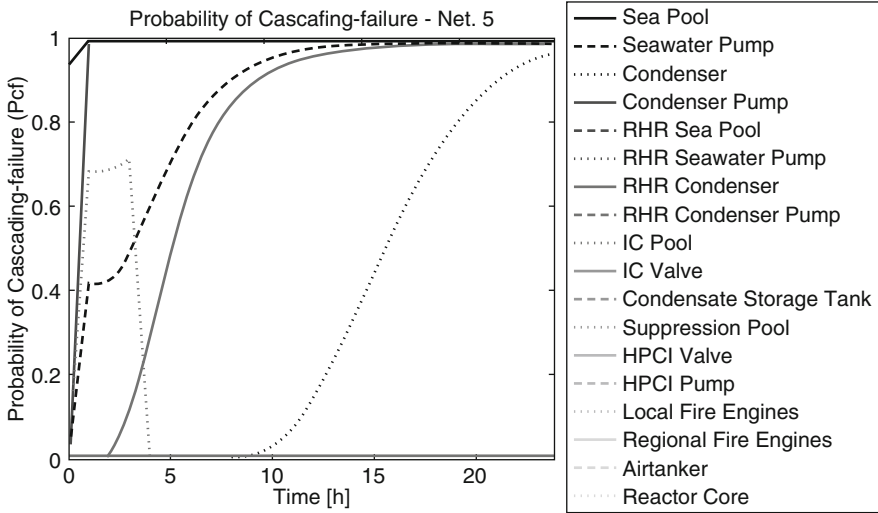


Fig. 7.76 Probability of cascading-failure of nodes of the water network, for the detailed model

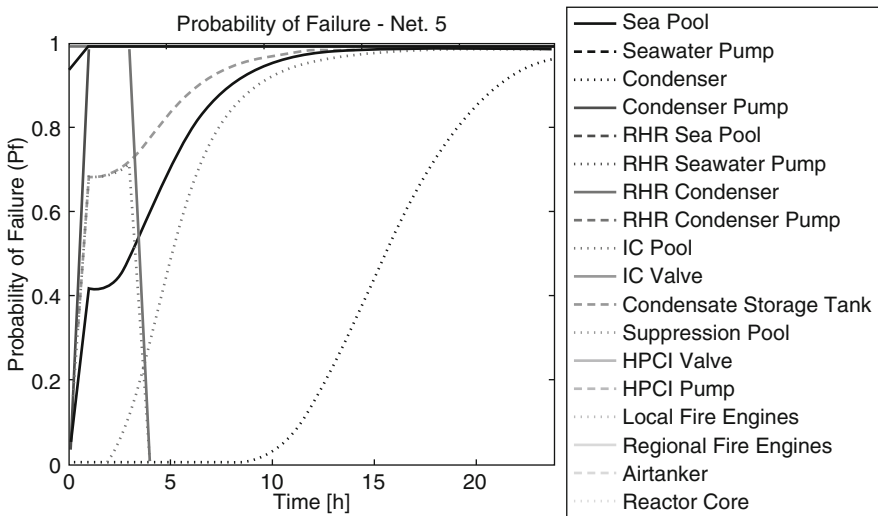


Fig. 7.77 Probability of failure of nodes of the water network, for the detailed model

from the simple model, the detailed model, and the real case study for both the electric and the water network. The problem is analyzed at three different time steps: (i) after the earthquake, (ii) after the tsunami, and (iii) before the arrival of rescuer at the NPP.

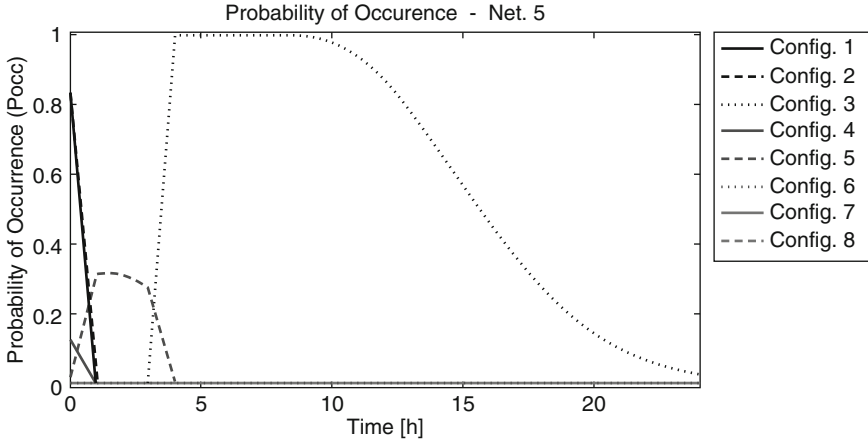


Fig. 7.78 Probability of occurrence of configurations of the water network, for the detailed model

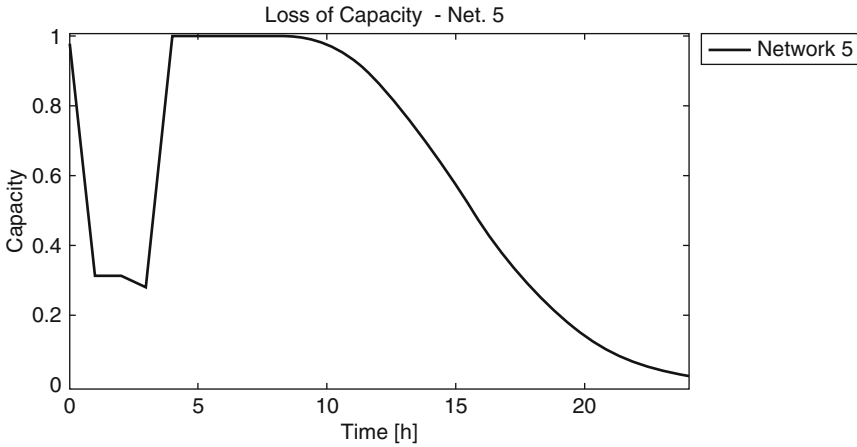


Fig. 7.79 Loss of capacity of the water network, for the detailed model

After the Earthquake

The situation at the reactor is shown in Fig. 7.80. The event trees show how the actual configuration for the power network was relying on diesel generators (Fig. 7.81), while for the water network both the RHR and the IC cooling systems were active (Fig. 7.82). The situation of the electric network is well represented by both models (Table 7.4), however for the water network, the *simplified model* assumes all the power sources supply power to the ordinary cooling line and so gives an inaccurate prediction (Table 7.5 and Fig. 7.83).

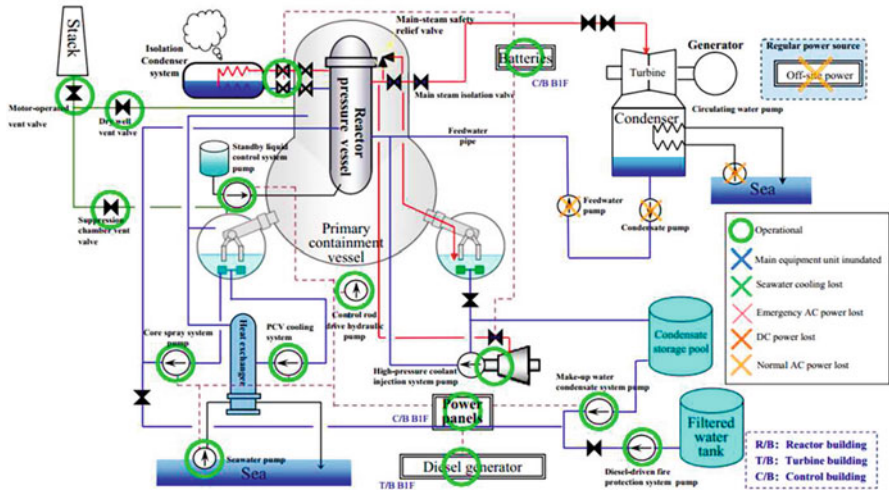


Fig. 7.80 Post-earthquake situation at Unit 1, Fukushima NPP (Source: TEPCO 2012)

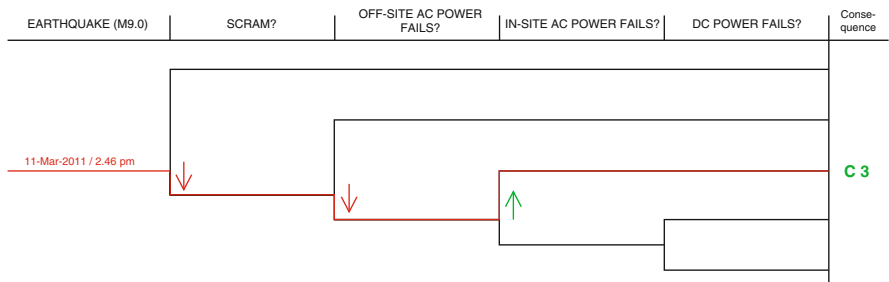


Fig. 7.81 Event tree of the post-earthquake situation for the electric network at Fukushima

Table 7.3 Comparison of results for the electric network after the earthquake

Configuration		Probability of occurrence (Pocc) after the earthquake		
		Fukushima NPP	Simplified model	Detailed model
Self-generation	*(-/1)	0 %	–	0 %
Off-site AC power	*(1/2)	0 %	0 %	0 %
In-site AC power	*(2/3)	100 %	92.4 %	95.1 %
DC power	*(3/4)	0 %	6.5 %	3.3 %
Loss of capacity		0 %	1.1 %	1.6 %

* Refers to (simplified model numeration/detailed model numeration)

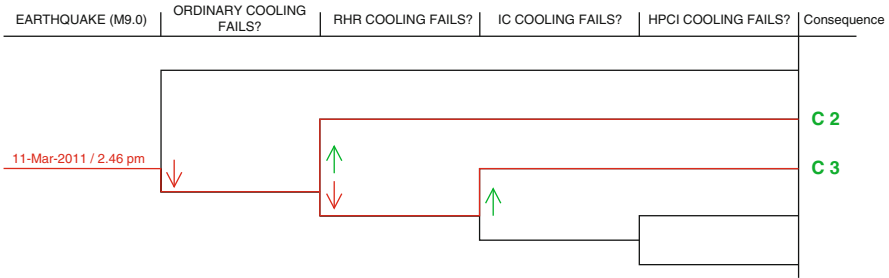


Fig. 7.82 Event tree of the post-earthquake situation for the water network at Fukushima

Table 7.4 Comparison of results for the water network after the earthquake

Configuration		Probability of occurrence (Pocc) after the earthquake		
		Fukushima NPP	Simplified model	Detailed model
Ordinary cooling	* (1/1)	0 %	83.9 %	0 %
RHR cooling	* (-/2)	100 %	16.1 %	85.6 %
IC cooling	* (2/3)			
HPCI cooling	* (3 + 4/4 + 5)	0 %	0 %	14.1 %
Loss of capacity		0 %	0 %	0.3 %

* Refers to (simplified model numeration/detailed model numeration)

Table 7.5 Comparison of results for the electric network after the tsunami

Configuration		Probability of occurrence (Pocc) after the tsunami		
		Fukushima NPP	Simplified model	Detailed model
Self-generation	*(-/1)	0 %	–	0 %
Off-site AC power	* (1/2)	0 %	0 %	0 %
In-site AC power	* (2/3)	0 %	0 %	0 %
DC power	* (3/4)	0 %	8.5 %	13.7 %
Loss of capacity		100 %	91.5 %	86.3 %

* Refers to (simplified model numeration/detailed model numeration)

After the Tsunami

At 15.35 the second tsunami wave hit the NPP. Both the electric and water networks lost their capacity because of the damage to their nodes and the cascading effects. However, while the electric network is simulated properly by both models, the water network is properly simulated only by the *detailed model*. The *simple model* lacks the presence of the IC valve, which in reality was closed and can not be remotely activated. In conclusion, the cooling system of the *simple model* relies on the IC, while in the detailed model the IC valve was considered closed and so the probability of a loss of capacity is $LoC = 86, 3 \%$ (Figs. 7.84, 7.85, and Table 7.6).

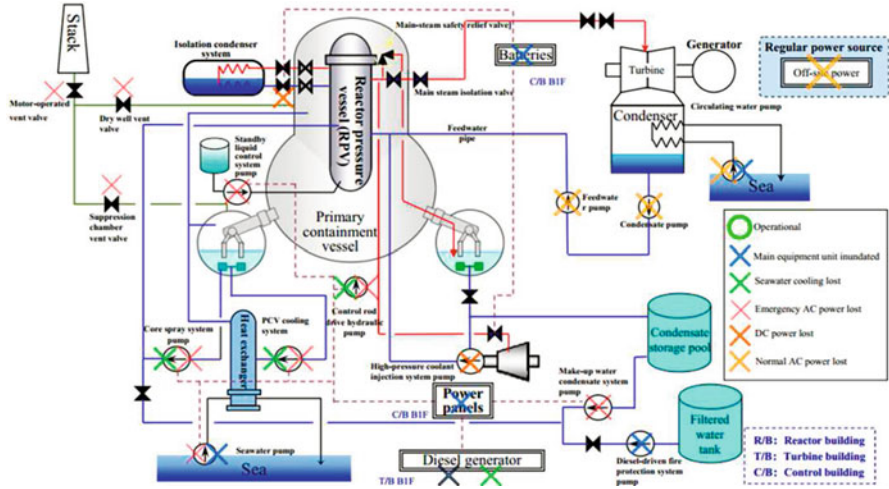


Fig. 7.83 Post-tsunami situation at Unit 1, Fukushima NPP (Source: TEPCO 2012)

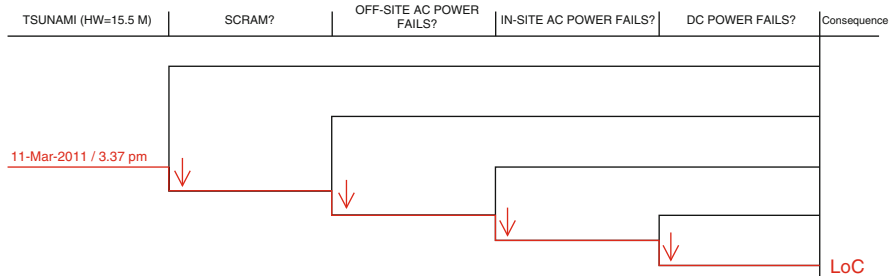


Fig. 7.84 Event tree of the post-tsunami situation for the electric network at Fukushima

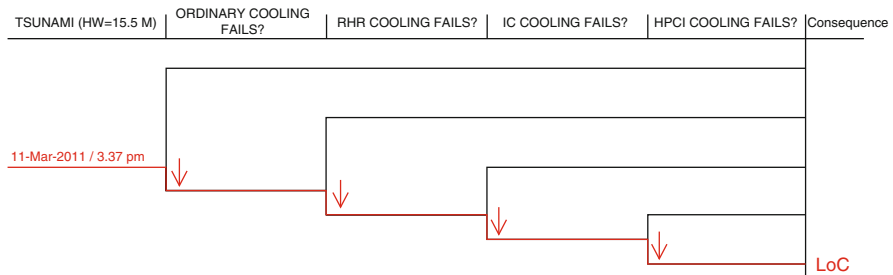


Fig. 7.85 Event tree of the post-tsunami situation for the water network at Fukushima

Table 7.6 Comparison of results for the water network after the tsunami

Configuration		Probability of occurrence (Pocc) after the tsunami		
		Fukushima NPP	Simplified model	Detailed model
Ordinary cooling	*(1/1)	0 %	0 %	0 %
RHR cooling	* (-/2)	0 %	-	0 %
IC cooling	* (2/3)	0 %	100 %	0.1 %
HPCI cooling	* (3 + 4/4 + 5)	0 %	0 %	31.4 %
Loss of capacity		100 %	0 %	68.5 %

* Refers to (simplified model numeration/detailed model numeration)

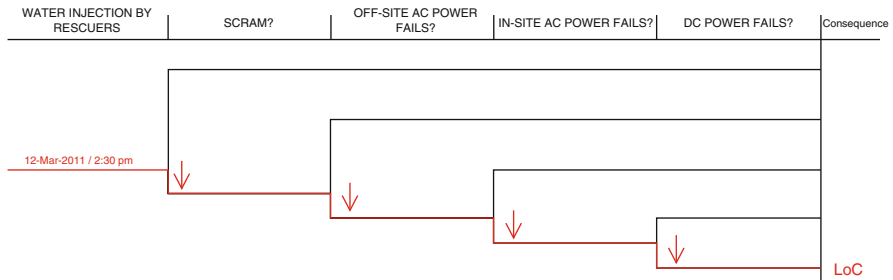


Fig. 7.86 Event tree of the electric network at Fukushima NPP before the water injection

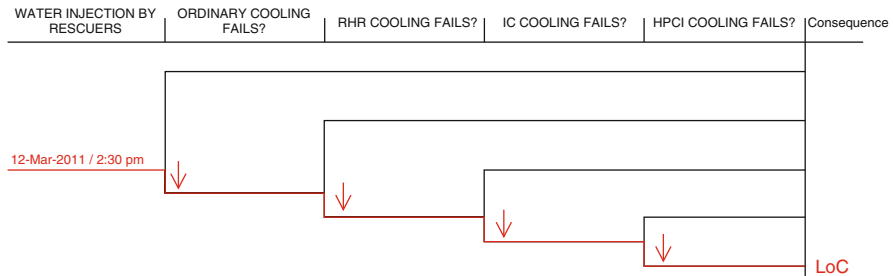


Fig. 7.87 Event tree of the before water injection situation for the water network at Fukushima

Before the Arrival of Rescuer at the NPP

Twenty-four hours after the earthquake, all the systems were down and the core was melting. Temporal effects has brought both the simplified and the detailed model towards the *capacity loss state* for both power and water networks. however, the *detailed model* is more accurate because it models the after-tsunami condition (Figs. 7.86, 7.87, Tables 7.7, and 7.8).

Table 7.7 Comparison of results for the electric network before water injection

Configuration		Probability of occurrence (Pocc) before water injection by rescuers		
		Fukushima NPP	Simplified model	Detailed model
Self-generation	*(-/1)	0 %	–	0 %
Off-site AC power	*(1/2)	0 %	0 %	0 %
In-site AC power	*(2/3)	0 %	0 %	0 %
DC power	*(3/4)	0 %	0.4 %	0.8 %
Loss of capacity		100 %	99.6 %	99.2 %

* Refers to (simplified model numeration/detailed model numeration)

Table 7.8 Comparison of results for the water network before water injection

Configuration		Probability of occurrence (Pocc) before water injection by rescuer		
		Fukushima NPP	Simplified model	Detailed model
Ordinary cooling	*(1/1)	0 %	0 %	0 %
RHR cooling	* (-/2)	0 %	–	0 %
IC cooling	*(2/3)	0 %	4.0 %	4.1 %
HPCI cooling	*(3 + 4/4 + 5)	0 %	39.2 %	0 %
Loss of capacity		100 %	56.8 %	95.9 %

* Refers to (simplified model numeration/detailed model numeration)

Considerations

From the analysis above, it appears that both models can effectively reproduce the behavior of the electric network, while there are some discrepancies in the results obtained for the water network. For the electric network there are not large differences because the only things that change from the two models are the number of power panels and the split of target nodes’ supply lines. Target nodes can not propagate upstream, so this implies null effect. Furthermore, the electric network is independent from all the other ones, so improving the model of the other networks will not affect the behavior of the electric network. Instead in the water network, different power sources provide energy to various configurations of the water network. The insertion of valves helps in controlling the risk of network inoperability under certain configurations that can be simulated only with the *detailed model*. For instance, specific scenarios, such as the malfunctioning of the HPCI for unknown reasons can only be simulated with the detailed model, while physical reactions, like the destabilization of reactor bars and the pressurization of the core can not be modeled at all. So it is possible to conclude that the *detailed model* describes better the timeline of the events that took place at the Fukushima NPP.

7.6.7 *Interdependencies that Occurred During the Disaster of Fukushima*

To analyze the interdependencies, it is necessary to define the problem at hand using the proposed nomenclature. Therefore, following the taxonomy proposed here, the *community* is Japan, the infrastructure (lifeline) is the electric network, while the *system* is the Fukushima Daiichi nuclear power plant.

The Fukushima Daiichi nuclear power plant (*system*) is interdependent with the Electricity and the Transportation network (*infrastructures*). During the reactor shut down, in order to guarantee the operability of the cooling system, an external power supply grid is necessary (in light of the dependency between electric network and nuclear power plant). If the external power grid is not available, then dependency between the transportation network and the power plant is evident because external batteries are provided to the site through the use of the road network. After the disaster, further interdependencies arise among the system (Fukushima Daiichi NPS) and *the Health care, Food supply, Business, Education and Emergency services*. In fact, the large amount of radiation released after the disaster required the immediate evacuation of people in a radius of 10 km from the Fukushima Daiichi NPS. The *system* can be divided in the following main *sub-systems* which are: *Reactors, Cooling system of Reactors, Emergency generator for the cooling system of Reactors, Control room of the power plant, Tsunami barriers, automatically shutdown system of Reactors*. The following physical intradependencies can be identified after the sequence of events described above:

- *Amplifying failure* of reactors if the cooling systems fail;
- *Amplifying failure* of reactors if the emergency generators fail;
- *Cascading failure* of the cooling systems if the emergency generators fail;
- *Amplifying failure* of reactors if the tsunami barriers fail;
- *Cascading failure* of cooling systems if the tsunami barriers fail;
- *Cascading failure* of emergency generators if the tsunami barriers fail;
- *Cascading failure* of reactors caused by the automatically shutdown system of reactors.

The *matrix of physical intradependency* among these sub-systems is shown in Table 7.9, where *R* = reactors, *CS* = cooling systems, *EG* = emergency generators for the cooling system, *CR*= control room, *TB* = tsunami barriers, *ASS*= automatically shutdown systems, *A* = Amplifying failure and *C* = Cascading failure.

Considering the same timeline, the following cyber intradependencies are identified:

- *Cascading failure* of automatically shutdown system of reactors if the control room fails;
- *Cascading failure* of emergency generators if the control room fails;
- *Cascading failure* of emergency generators if the automatically shutdown system fails.

Table 7.9 Physical intradependency index matrix among the sub-systems of the Fukushima Daiichi power plant system

	R	CS	EG	TB	ASS
R	1	-	-	-	-
CS	A	1	-	-	-
EG	A	C	1	-	-
TB	A	C	C	1	-
ASS	C	-	-	-	1

Table 7.10 Cyber intradependency index matrix among the sub-systems of the Fukushima Daiichi power plant system

	CR	ASS	EG
CR	1	C	C
ASS	-	1	C
EG	-	-	1

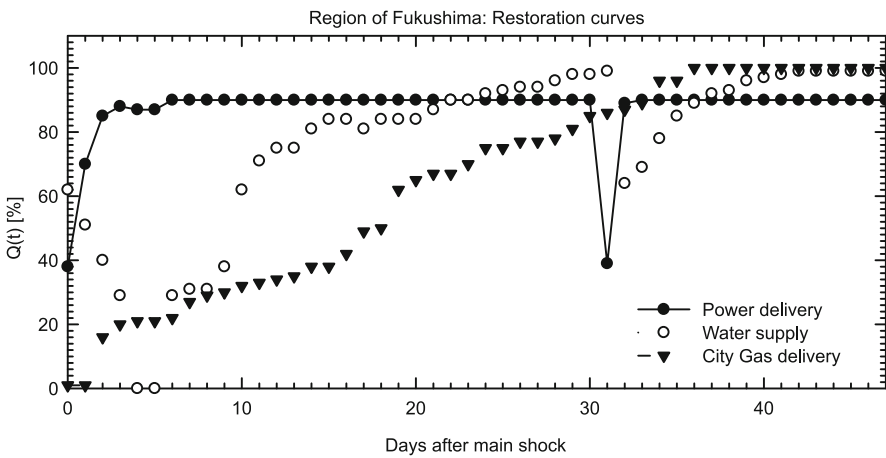


Fig. 7.88 Infrastructure restoration curves for the region of Fukushima

In addition, the *matrix of cyber intradependency* among these sub-systems is shown in Table 7.10.

Fukushima Daiichi NPS is a complex system; therefore a numerical quantification of every intradependency can not be possible. However, recently Cimellaro et al. (2013) have proposed a method based on the use of lifeline’s restoration curves. This method leads to a simplified evaluation of the interdependency index S , which comes from two restoration curves that contain information derived from the systems of which they are composed. In Fig. 7.88 an example of infrastructures restoration curves is shown for the region of Fukushima (Nojima 2011).

With this input, it is possible to evaluate only the interdependency index S among the infrastructures. The method proposed in this section is more detailed than the one proposed Cimellaro et al. (2013), because the evaluation of the interdependency index are based on the interdependencies that arise among different systems (or sub-systems). Every system contributes to the final value of interdependency and it is possible to identify which are the systems that cause more

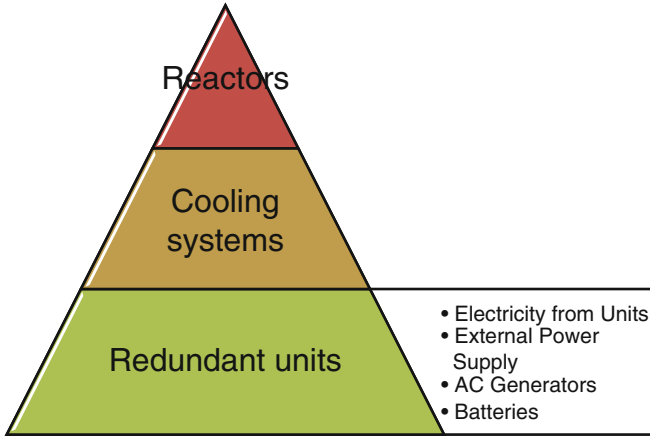


Fig. 7.89 Risk assessment of Fukushima Daiichi NPS

problems of interdependency into a lifeline, in order to adequate or improve only those systems, focusing only the available resources in order to maximize the ratio between invested money and reduction of interdependency. However the method proposed by Cimellaro et al. (2013) can give a numerical quantification (although simplified, because all the information about systems interdependencies are in a single restoration curve) of the interdependency index. However, it is possible to build some restoration curves related to the systems, to the sub-systems and to the units of each infrastructure. For example, in the case study of the Fukushima Daiichi NPS shown previously, a restoration curve of the system called “Fukushima Daiichi NPS” (which is a system of the infrastructure called “Electricity or Power delivery”) are shown in Fig. 7.94. These restoration curves are considering the power that the NPS plant produced at time t divided by the maximum power that the plant can produce:

$$q = Q(t) = \frac{MW_{produced}}{MW_{max}} \quad (7.10)$$

This kind of evaluation it is accurate only for a long term analysis, because at short term the security of the NPS is more important, instead of the production of electricity. The system called “Fukushima Daiichi NPS” can be divided into three main sub-systems: the *security sub-system*, the *electricity production sub-system* and the *controlling and management sub-system*. In this part, only the sub-system “security” is analyzed, because it is the one that had great influence on this nuclear disaster. The security sub-system can be divided into five main units: the electricity self-produced by the NPS (hereinafter called electricity from Units) used for supplying the cooling systems, the external power supply (hereinafter called EPS), the AC emergency diesel generators, the batteries and the cooling system. For the security of the NPS, the four units that give the power at the unit called “cooling system” work in parallel to guarantee a high degree of redundancy (and so

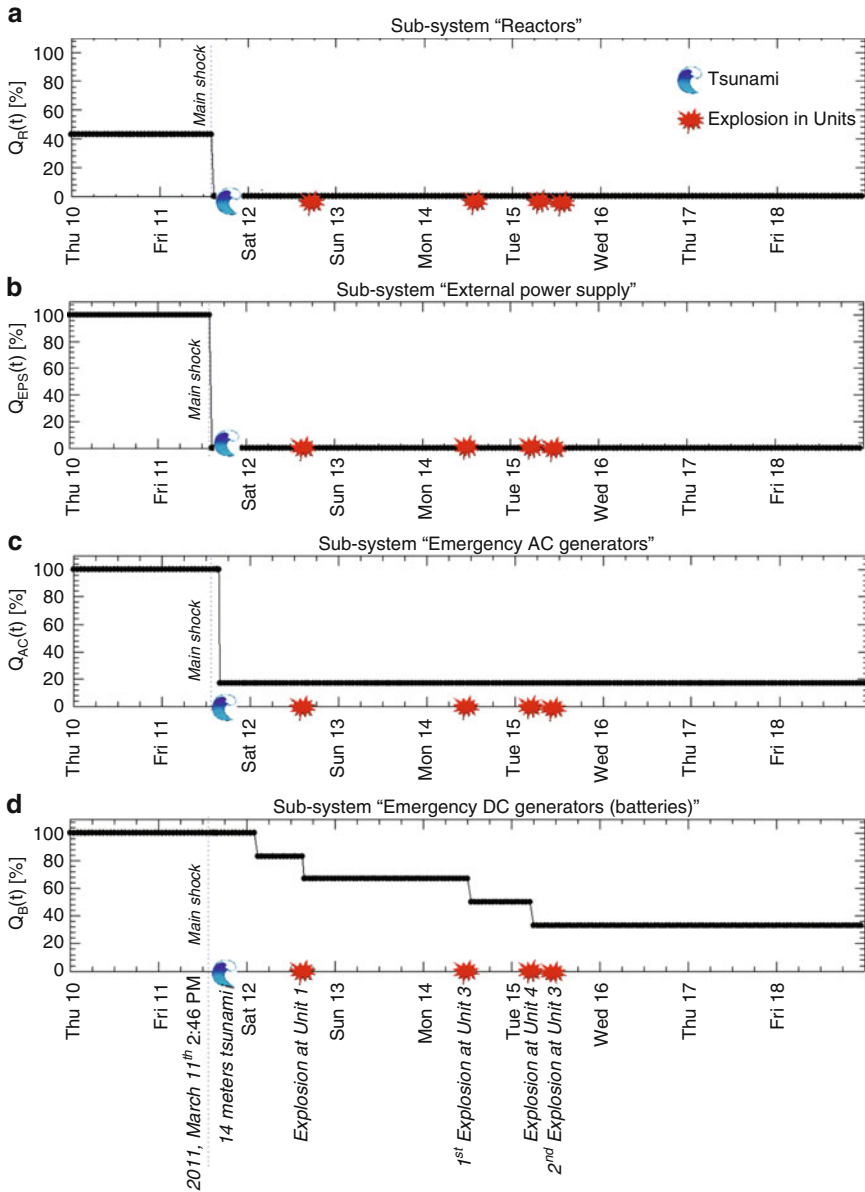


Fig. 7.90 "Redundant" Units restoration curves of the Fukushima Daiichi NPS

a low degree of intradependency among them). The risk assessment of a NPS can be the one shown in Fig. 7.89, where the maximum risk is the failure of the reactors, and the lowest risk is the failure of the redundant units that give electricity to the cooling system units.

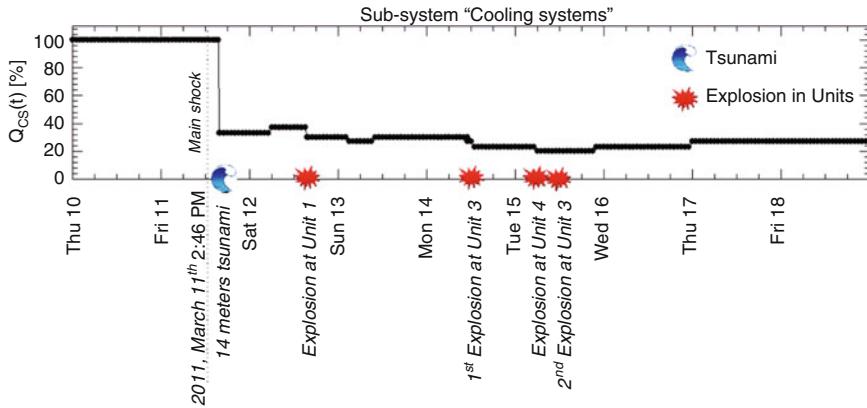


Fig. 7.91 Unit “Cooling system” restoration curves (the system is the Fukushima Daiichi NPS)

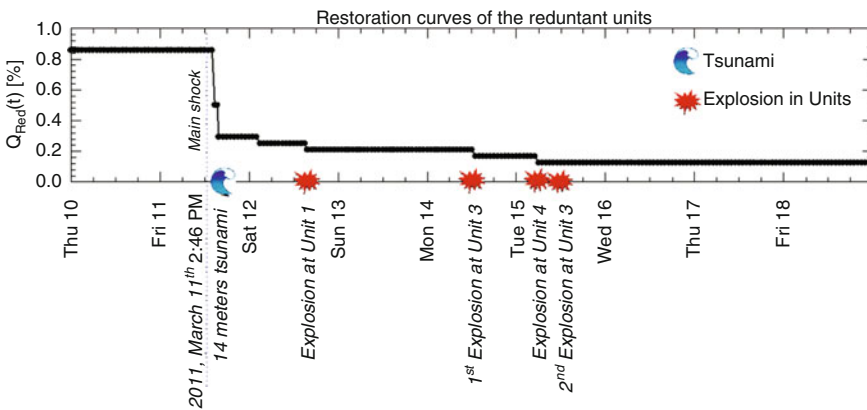


Fig. 7.92 Restoration curves of redundant units: combination of Q_R , Q_{EPS} , Q_{AC} and Q_B

It is possible to build the restoration curves of the five units, starting from the time-line of the Fukushima NPS disaster. The results are shown in Fig. 7.90 for the four redundant units (Q_R , Q_{EPS} , Q_{AC} and Q_B) and in Fig. 7.91 for the unit “cooling system”.

The time length of these curves is a week (the first week after the disaster), because of the significance that the first period had on the disaster and because the consequences of the disaster are still in evolution right now. The functionality is evaluated with the following equations:

$$Q_R(t)[\%] = \frac{MW_{produced}(t)}{MW_{max}} \cdot 100 \tag{7.11}$$

$$Q_{EPS}(t)[\%] = \begin{cases} 100 & \text{if } i_c > 0A \\ 0 & \text{if } i_c = 0A \end{cases} \tag{7.12}$$

$$Q_{AC}(t) [\%] = \frac{N_{AC,in \ function}}{N_{AC,tot}} \cdot 100 \tag{7.13}$$

$$Q_B(t)[\%] = \frac{N_{B,in \ function}}{N_{B,tot}} \cdot 100 \tag{7.14}$$

where i_c is the intensity of the current into every line that are linked with the NPS, N_{AC} is the number of AC generators, N_B is the number of the DC generators (batteries).

In order to evaluate the functionality curves of the redundant units which supply the power for the cooling system, Eq. 7.15 is used which gives, as first approximation, the same weight at every *redundant unit*:

$$Q_{Red}(t) = \frac{0.25 \cdot Q_R(t) + 0.25 \cdot Q_{EPS}(t) + 0.25 \cdot Q_{AC}(t) + 0.25 \cdot Q_B(t)}{100} \tag{7.15}$$

The result of this calculation is the functionality curve shown in Fig. 7.92.

The functionality curve of the security sub-system is then evaluated by combining the functionality curves of the redundant units (Q_{Red}) with the functionality curves of the cooling system unit (Q_{CS}) using Eq. 7.16:

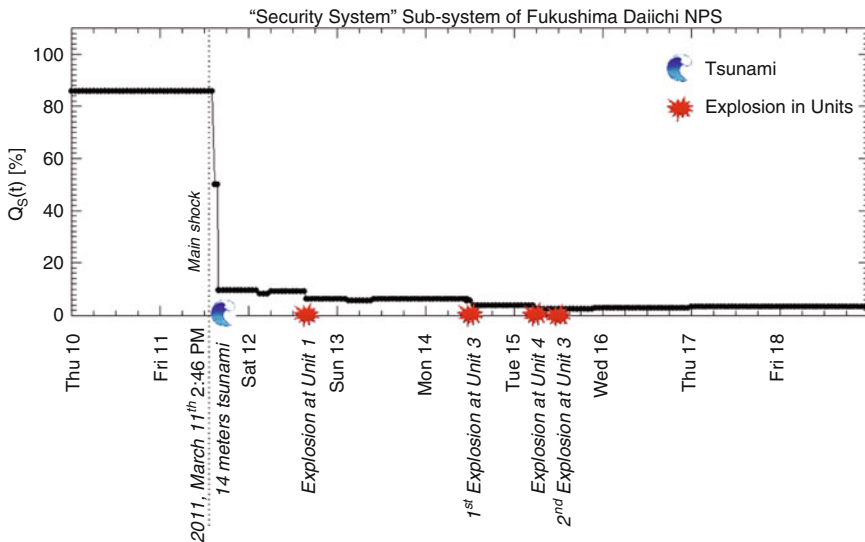


Fig. 7.93 Sub-system “Security system” restoration curves at short term (the system is the Fukushima Daiichi NPS)

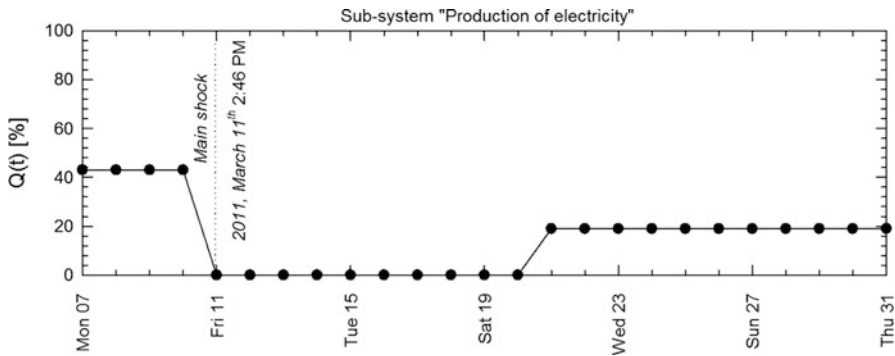


Fig. 7.94 Sub-system “Production of electricity” restoration curves at long term (the system is the Fukushima Daiichi NPS)

$$Q_S(t)[\%] = Q_{Red}(t) \cdot Q_{CS}(t)[\%] \quad (7.16)$$

The results are shown in Fig. 7.93.

This method is useful in the short term after a shock, when the security has the greatest importance with respect to the production of electricity, especially if the system affected is a NPS, while in a medium-long term the production of electricity is more important (Fig. 7.94).

The evaluation of the functionality curves with this method is more detailed than the same analysis at the level of infrastructures. This approach allows the use of the method proposed by Cimellaro et al. (2013). For example, it has been used to evaluate the interdependence that arises among the different sub-systems of the Fukushima Daiichi NPS, raising a high level of detail and significance. The method proposed in this section can be a useful framework to analyze the interdependency that arises among different lifelines and different systems into a community. It is also possible to choose the level of detail for the evaluation of the interdependency or the intradependency.

7.7 Remarks and Conclusions

In this chapter, a framework was proposed for evaluating the degree of interdependency between the infrastructures (lifelines) of a community. A reference nomenclature is defined, classifying sixteen infrastructures that compose each community: seven which are *core infrastructure* (Electricity, Oil delivery, Transportation, Telecommunication, Natural Gas delivery, Water supply, Wastewater treatment) and nine which are *non-core infrastructure* (Financial system, Building services, Business, Emergency services, Food supply, Government, Health care, Education, Commodities). Each lifeline is divided in systems, while interdependencies are subdivided in seven types (Physical, Cyber, Geographic, Policy/Procedural, Societal, Budgetary, Market and Economy interdependency).

For each system and for each type of interdependency, a degree of interdependency, which is function of two values assigned at every type of lifeline, is assigned. The first value is function of the type of failure (*Cascading, Amplification and Uncoupled*). The second value is function of the importance factor that each lifeline's system has. Lifeline interdependencies are evaluated by combining the values of interdependency of systems in which the different lifelines have been divided.

Finally, there are seven types of interdependencies for each lifeline's pair, which are organized in seven interdependencies matrices. The degree of interdependency (or interdependency index) can assume values between 0 and 1, where 0 represents the absence of interdependency, and 1 represents the maximum interdependency between the two infrastructures. It is possible to evaluate for each matrix the *Leadership index* (obtained by adding per row the data in the interdependency matrix $S_{i,j}$) that the lifeline of a given row has with respect to the other 15 lifelines identified in the community and the *Subordination index* (obtained adding per column the data in the interdependency matrix $S_{i,j}$) that the lifeline of a given column has with respect to the other 15 lifelines in the community. The lifeline that has the highest value of *Leadership index* is the most important lifeline in the community and requires more attention, because if its functionality fails, the performances of the community decrease dramatically.

It is important to know which lifeline with the maximum *Leadership index* is, and which lifeline with the maximum *Subordination index* is. All the available resources of the community should be focused on these two lifelines, not wasting resources while optimizing the global response of the community in terms of interdependency and sustainability. The lifeline that has the highest value of Subordination index is the one that has the greatest dependency on the other lifelines within the community. If the community suffers damage, this lifeline is the first that suffers the effects of propagation of damage due to the interdependencies, even if it does not suffer damages. Finally as case study, the 2011, March 11th, Fukushima Daiichi nuclear power plant disaster is analyzed. Sub-system intradependencies are highlighted and are placed into the proposed framework. The functionality curve of the "security sub-system" of the Fukushima Daiichi NPS system is evaluated starting from the functionality curves of the single units. With the functionality curves it is possible to use the methods based on cross-correlation to evaluate this intradependency. Further studies are necessary to give a numerical quantification of interdependencies at the system level (local level), in the same manner which is proposed at a global level, when infrastructures are considered as global entities.

References

- ATC13 (1985) Earthquake damage evaluation data for California. Technical report, Applied Technology Council – ATC
- Banerjee S, Prasad GG (2012) Seismic risk assessment of reinforced concrete bridges in flood-prone regions. Struct Infrastruct Eng Maint Manag Life-Cycle Des Perform. Available online. doi:10.1080/15732479.2011.649292

- Bonabeau E (2002) Agent-based modeling: methods and techniques for simulating human systems. *Proc Natl Acad Sci* 99(suppl 3):7280–7287
- Bush B, Dauelsberg L, LeClaire R, Powell D, DeLand S, Samsa M (2005) 3 critical infrastructure protection decision support system (cip/dss) project overview. In: *Proceedings of the 2005 system dynamics conference*, Boston
- CCSF (2014) City and county of San Francisco lifelines interdependency study. Technical report, Lifelines Council of the City and County of San Francisco
- Cimellaro GP, Solari D (2014) Considerations about the optimal period range to evaluate the weight coefficient of coupled resilience index. *Eng Struct* 69:12–24
- Cimellaro GP, Solari D, Bruneau M (2014) Physical infrastructure interdependency and regional resilience index after the 2011 Tohoku earthquake in Japan. *Earthq Eng Struct Dyn* 43(12):1763–1784
- Cimellaro GP, Solari D, Renschler C, Reinhorn AM, Bruneau M (2013) Community resilience index integrating network interdependencies. In: *Proceedings of the 2013 structures congress (SEI 2013)*, Pittsburgh, 2–4 May 2013, pp 1789–1799
- Dudenhoefter DD, Permann MR, Manic M (2006) Cims: a framework for infrastructure interdependency modeling and analysis. In: *Proceedings of the 38th conference on winter simulation, winter simulation conference*, Monterey, pp 478–485
- Eidinger JM, Avila EA, Ballantyne DB, Cheng L, Der Kiureghian A, Maison BF, O'Rourke TD, Power MS (2001) Seismic fragility formulations for water systems, part 1: guideline. Technical report, American Lifelines Alliance
- FEMA (2012) Seismic performance assessment of buildings: Fema p-58. Technical report, Applied Technology Council
- Haimes YY, Jiang P (2001) Leontief-based model of risk in complex interconnected infrastructures. *J Infrastruct Syst* 7(1):1–12
- ICAO (2014) Fault tree analysis (fta) and event tree analysis (eta). Technical report, NEBOSH National Diploma- Unit A: Managing Health and Safety
- Kakderi K, Argyroudis S, Ptilakis K (2011) State-of-the-art literature review of methodologies to assess the vulnerability of a “system of systems”. Technical report, Aristotle University of Thessaloniki
- Kongar I, Rossetto T (2012) A framework to assess the impact of seismic shocks on complex urban critical infrastructure networks. In: *15th world conference on earthquake engineering (15WCEE)*, Lisbon, pp 24–28
- Lee EE, Mitchell JE, Wallace W (2007) Restoration of services in interdependent infrastructure systems: a network flows approach. *IEEE Trans Syst Man Cybern Part C: Appl Rev* 37(6):1303–1317
- Leontief WW, Leontief W (1986) *Input-output economics*. Oxford University Press, New York. On demand
- McDaniels T, Chang S, Peterson K, Mikawoz J, Reed D (2007) Empirical framework for characterizing infrastructure failure interdependencies. *J Infrastruct Syst* 13(3):175–184
- Moriya K, Sato K (2011) Fukushima daiichi npp accident: plant design and preliminary observations. Technical report, Hitachi-GE Nuclear Energy Ltd
- Nojima N (2011) Restoration processes of utility lifelines in the Great East Japan earthquake disaster. In: *15th world conference on earthquake engineering (15WCEE)*, Lisbon
- Ouyang M (2014) Review on modeling and simulation of interdependent critical infrastructure systems. *Reliab Eng Syst Saf* 121:43–60
- Partridge MD, Rickman DS (1998) Regional computable general equilibrium modeling: a survey and critical appraisal. *Int Reg Sci Rev* 21(3):205–248
- Paton D, Johnston D (2006) *Disaster resilience an integrated approach*. Charles C Thomas publisher LTD, Springfield
- Patterson SA, Apostolakis GE (2007) Identification of critical locations across multiple infrastructures for terrorist actions. *Reliab Eng Syst Saf* 92(9):1183–1203

- PCCIP (1997) Critical foundations: protecting America's infrastructures: the report of the president's commission on critical infrastructure protection. Technical report, U.S. Government Printing Office, Washington, DC
- Pederson P, Dudenhoefter D, Hartley S, Permann M (2006) Critical infrastructure interdependency modeling: a survey of us and international research. Idaho National Laboratory, pp 1–20
- Peerenboom J, Fisher R, Whitfield R (2001) Recovering from disruptions of interdependent critical infrastructures. Technical report, CRIS/DRM/IIIT/NSF workshop on mitigating the vulnerability of critical infrastructures to catastrophic failures
- PPD63 (1998) The Clinton administration's policy on critical infrastructure protection: presidential decision directive 63. White paper, The White House, Office of the Press Secretary
- Pressly R (2014) Improving lifelines: protecting critical infrastructure for resilient counties. Technical report, National Association of Counties
- Rinaldi SA, Peerenboom JP, Kelly TK (2001) Identifying, understanding, and analyzing critical infrastructure interdependencies. *IEEE Control Syst Mag* 21(6):11–25. ISI Document Delivery No.: 495YT Times Cited: 144 Cited Reference Count: 26 Rinaldi, SA Peerenboom, JP Kelly, TK IEEE-INST ELECTRICAL ELECTRONICS ENGINEERS INC
- Rose AZ (2005) Tracing infrastructure interdependence through economic interdependence. Technical report, University of Southern California
- Stamatelatos M (2000) Probabilistic risk assessment: what is it and why is it worth performing it? Technical report, NASA Office of Safety and Mission Assurance
- TEPCO (2012) A one-year review of Fukushima Daiichi nuclear power station "Steps to Achieve Stabilization". Tokyo Electric Power Company Holdings, Inc.
- Valencia VV (2013) Network interdependency modeling for risk assessment on built infrastructure systems. Technical report, DTIC Document
- Wallace W, Mendonça D, Lee E, Mitchell J, Chow J (2001) Managing disruptions to critical interdependent infrastructures in the context of the 2001 world trade center attack. Technical report, Diss. Rensselaer Polytechnic Institute
- Wood S, Smith CL, Kvarfordt KJ, ST B (2008) Systems analysis programs for hands-on integrated reliability evaluations (saphire): summary manual. Technical report, U.S. Nuclear Regulatory Research, Washington, DC, 20555-0001
- Zhang P, Peeta S (2011) A generalized modeling framework to analyze interdependencies among infrastructure systems. *Transp Res Part B: Methodol* 45(3):553–579
- Zimmerman R (2001) Social implications of infrastructure network interactions. *J Urban Technol* 8(3):97–119

Part II
Applications of Resilience Concepts
to Different Networks

Chapter 8

The Physical Infrastructure Dimension of Community Resilience Framework

Abstract Part 2 of the book from Chap. 8 to Chap. 12 focuses on applications of the PEOPLES framework which was presented on Chap. 6. In particular this chapter focuses on the evaluation of Resilience metrics for physical infrastructures. Several examples of applications of the PEOPLES framework are provided for the transportation, water, gas and communication network.

8.1 Lifelines

In the last decade, the attention of Authorities has increased towards physical infrastructures networks, since a significant amount of damage was observed during recent disasters (e.g. Hurricane Katrina, Sandy storm, Nepal earthquake, etc.). This increased government attention has generated programs such as the *European Program on Critical Infrastructure Protection* and the institution of the *U.S. President's Commission on Critical Infrastructure Protection*. The physical infrastructures which are described in this chapter they all belong to the lifeline dimension of the PEOPLES framework (Fig. 8.1).

In particular, in the first case study, the PEOPLES framework is applied to evaluate the performance of the transportation system during extreme events. The damage states, the recovery time and the resilience index of the transportation network are evaluated. A methodology to model the interdependencies between infrastructure is proposed (Sect. 8.2). This method is able to evaluate the optimal recovery plan that maximizes the resilience index of the physical infrastructure (considering the building and transportation systems), minimizing the recovery time, with respect to physical, social, and economic constraints. Then the proposed methodology is applied to a case study in the San Francisco Bay area.

In the second case study, the PEOPLES framework is applied to evaluate the resilience performance of a water distribution network. A new resilience index to measure the performance of a water distribution network is proposed, which combines both the technical, the environmental and social dimension of the PEOPLES framework. The methodology considers both the initial losses and the restoration process of the system. Then the proposed methodology is applied to

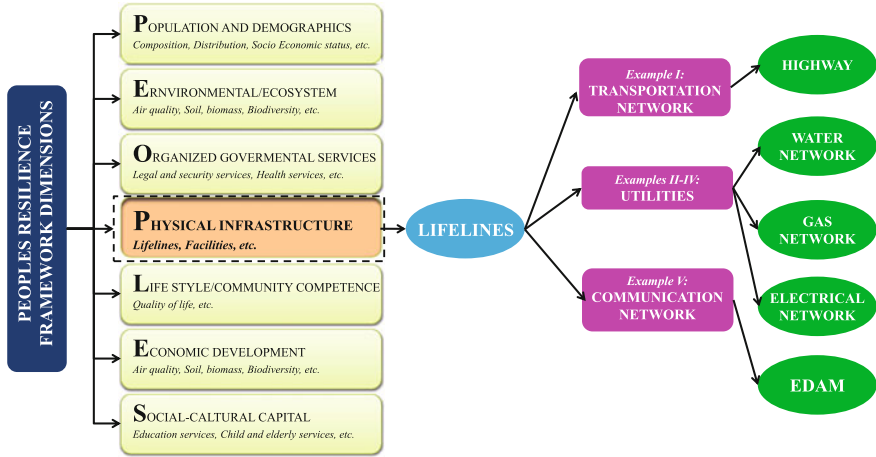


Fig. 8.1 Chapter 8 outline

the water distribution network of a small town in the south of Italy considering different disruptions scenarios.

In the third case study, the PEOPLES framework is applied to evaluate the physical dimension of a gas distribution network. A resilience index is proposed and applied to the gas distribution network of the municipalities of Introdacqua and Sulmona, two small towns in the center of Italy which were affected by 2009 earthquake.

In the fourth case study, the PEOPLES framework is applied to evaluate the resilience performance of the electric power network during extreme events. Different resilience-enabling schemes and risk evaluation methods of power systems are evaluated. In the fifth case study, a methodology to improve the field reconnaissance damage assessment of buildings following an extreme event is proposed. The methodology is based on a mobile application (EDAM) which is able to improve the performance of the communication network.

8.2 Example 1: Transportation Network

8.2.1 Literature Review

In the last decade numerous catastrophic events have shown that the transportation system is a key point for a community affected by a disaster, because it is vital for emergency services such as policeman, firefighters, health care facilities, etc. Hence, the concept of resilience has gained attention, because small damages can become catastrophes when the communities have no access to the emergency services.

Previous methodologies studied single components of the transportation system (i.e. road network, railway, waterways, airports, etc.) focusing on the concept of

risk assessment that analyzed only the disaster time neglecting the recovery phase. Hence, societies are turning their attention to increase the resilience of entire communities against various types of extreme events. Moreover, communities are getting aware that they cannot prevent every risk, but rather they must learn to adapt and manage risks in the fastest way that minimizes impact on human and other systems.

In literature are available several methods which are able to evaluate the effects of different hazards on different types of infrastructures. Among them one of the most popular is HAZUS method (Whitman et al. 1997) that was developed by the National Institute of Building Sciences (NIBS) and used by FEMA in 1997 to assess the earthquake losses within the US territory. The method works on inventory of the classification of various components such as population, buildings, transport systems, lifeline utilities, and hazardous materials. This method evaluates the status of a community – according to the direct and indirect losses due to social, economic, and physical aspects – with a multi-risk analysis. The losses are provided in probabilistic terms evaluating causalities, shelters, inundations, fires, debris, hazardous material release, damage states of physical infrastructure, and economic losses. The methodology considers all type of hazards, but not all the interdependencies among the structural components. For example, the damage of the transportation network generated by the building debris is not considered. Furthermore, the methodology is not considering the recovery phase; therefore it is a useful tool to design urban areas for example and prevent damages, but it is not able to manage communities during catastrophic events and design proper recovery plans.

After Kobe earthquake Miles and Chang (2006, 2011) have proposed a methodology that identifies the performance of the road network through three different indicators. These are defined as the ratio between the post- and pre-event conditions of the network identified by: (i) *length of available roads*, (ii) *minimum travel distance between the nodes of the network*, and (iii) *weighted minimum travel distances of different subareas*. Bocchini and Frangopol (2011) have proposed an index to define the road network functionality that is entirely based on a single parameter, which characterizes the entire network considering the status of the road network and its economic aspects. The evaluation of the functionality of the whole network is performed through two parameters: the distance and the total travel time spent on the network. However, both methodologies do not consider the travel path in both directions for a given road link and the accessibility of the network.

Section 8.2 focuses on the transportation network and answers to several questions:

- how is it possible to model the transportation system and its damage states?
- How can redundancies' network typology be modeled?
- How can be modeled interdependencies with the other elements of the community?
- Which are the performances of the transportation network during an extreme event?
- And how do we model functionality and resilience?

8.2.2 *Proposed Methodology*

The proposed methodology intends to analyze the transportation system of a community during catastrophic events, evaluating its resilience index and considering redundancies and interdependencies between categories and resilience dimensions, following the PEOPLES framework. In this section, the resilience index corresponds to the area underneath the global functionality function of the community evaluated over a control period (e.g. the recovery period until the reconstruction phase ends (T_{EW})).

Functionality of the transportation system depends on the interdependencies among different dimensions and categories. For example, the debris of a damaged building might prevent access to a road and consequently to some areas of the community, thus excluding all emergency interventions. Another example is the bridge collapse that not only interrupts the transportation network, but it can also interrupt the electric network, the gas and the water supply system that run on the bridge, so without water and electricity, critical facilities such as hospitals cannot effectively perform their primary functions. Additionally damage of subway stations, power grid etc. can also reduce or stop functionalities of subway systems, of electric railway systems etc. Hence, all these examples show that functionality of one component is not only a function of the damage state itself, but it also depends on the boundary conditions provided by the other components. Moreover, economic losses, during the recovery, may involve a slower recovery process, which corresponds to a reduction of the resilience index.

The transportation system is composed by three categories: transportation network systems (road network, bus network, railway, subway, etc.), ports, and airports (these for incoming traffic flow). The transportation networks depend on the structural functionality of the network, on the traffic sources (internal and boundary sources), and on the functionality of the facilities connected to the network typology. Two categories of the transportation network can be identified: (i) self-reliant (road network, bus network, etc.) and (ii) reliant (electric railway, subway, etc.). The internal sources are buildings and/or structures (airports, railway stations, ports, etc.) that contribute with an incoming flow, while, the boundary sources are points of the transportation network that stay on the boundary of the selected area and identify an incoming traffic flow. The buildings of the internal sources as well as the buildings of the transportation facilities are not an isolate system but they are interdependent with other services (water, electricity, heating, etc.).

8.2.3 *Transportation System Models*

The transportation system is divided into categories and sub-categories, to take into account different interdependences as shown in Fig. 8.2.

The airports, ports, and transportation facility structures are modeled as buildings, while the networks are modeled with graph theory using nodes and edges. The edges are the system's components (i.e. bridges, tunnels, major roads, districts, etc.),

Component	Category	Sub-category	
Transportation System	Ports (small, medium, large)	Waterfront Structures	
		Facilities	Cranes/Cargo Handling Equipment
			Ferry Terminals
			Dispatches
			Fuel Structures
			Maintenance
			Warehouses
			other
	Airports (small, medium, large)	Runways	
		Facilities	Control Towers
			Terminals
			Parking Structures
			Fuel Structures
			Maintenance and Hangars
			other
	Network Systems	Road Network	Bridges
			Tunnels
			Roads/Trucks/etc.
		Bus Network	Districts
		Railway System	Transportation Sources
		Facilities	other
Light Rail			Monitoring Center
Stations			
Subway System			Dispatches
Facilities		Fuel Structures	
	Maintenance		
	other		

Fig. 8.2 Transportation system typologies (categories and sub-categories)

while the nodes are the junctions between them. Nodes and edges near the transportation source can be used as traffic sources. The structure of the typology network T is defined by the adjacency matrix $A^T(t)$, where rows and columns are the nodes, while the values are the weight coefficients of the edges.

$$A_{h,j}^T(t) = L_j^T(t) = \text{equivalent edge length} = \begin{cases} l_i \cdot nl_i(t) & \text{standard edge} \\ \sum_{j=RIA_j} l_i \cdot nl_i(t) & \text{district edge} \end{cases} \tag{8.1}$$

where the indices h_j correspond to the position of the i th edge in the adjacency matrix (if $A_{h,j}^T(t)$ is greater than zero, the edge is open, otherwise it is closed); $L_j^T(t)$ is the equivalent edge length defined as the length of the lanes inside the influence area of the respective edge; l_i = average length of lanes of the i th component; $nl_i(t)$ = number of available lanes; and RIA_j = roads inside the influence area (IA_i).

The influence area IA_i for standard edges (e.g. bridges, tunnels, railway, major roads, etc.) is rectangular (Fig. 8.3a), while for district edges – which are a

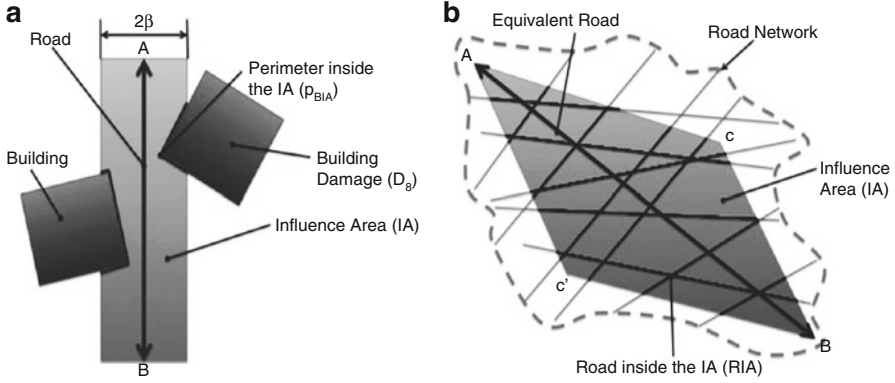


Fig. 8.3 Equivalent edge length for standard (a) and district (b) edges

discretization of redundant sub-networks such as the secondary roads inside the towns – it is rhomboidal (Fig. 8.3b). The district edges are modeled with an equivalent edge length in order to reduce the computational time.

Instead, the number of available lanes along the edge $nl_j(t)$, i.e. the edge functionality, is analytically defined as:

$$nl_i(t) = \begin{cases} f_j(t) & f_j(t) \geq L_j \\ 0 & f_j(t) < L_j \end{cases} \quad (8.2)$$

where $f_j(t)$ is the number of available lanes (decimal), and L_i is a lower bound limit that is function of the lane typology (e.g. road: $L_i = 70\%$, district: $L_i = 50\%$, and railway truck: $L_i = 100\%$). For example, the vehicles of firefighters (or ambulances, police cars, etc.), during the emergencies, can use a road lane with functionality less than one – this means that the entire road is not closed –, while a railway lane can be used by trains only if its functionality is 100%. The recovery curve for the number of available lanes $f_j(t)$ consists of two parts: the first is constant, while the second part has a log-normal shape. The function is analytically defined as follows:

$$f_j = \begin{cases} nl_j(T_j^-) & t < T_{Dis} \\ nl_j^{Dis} & T_{Dis} \leq t \leq T_j^{Ad} \\ nl_j^{Dis} + (1 - nl_j^{Dis}) \cdot r_j(t - T_j^{Ad}) & t > T_j^{Ad} \end{cases}$$

$$r_j(t) = \frac{\sum_{k=1}^4 W_k \cdot PDS_{j,k}^R \cdot \Phi\left(\frac{\ln(t) - \mu_k}{\sigma_k}\right)}{\sum_{k=1}^4 W_k \cdot PDS_{j,k}^R} \quad (8.3)$$

where: T_i^{Ad} = the administrative time, defined as the time elapsed from the disaster to the start of repair works of the edge according to the accessibility; T_{Dis} = the disaster

time defined as the time when the disaster occurred; $r_i(t)$ = restoration value; Φ = the lognormal function; σ and μ , are respectively the standard deviation and average value of the lognormal distribution (obtained by HAZUS database).

8.2.4 Structural Damage Assessment

The methodology works with any risk assessment, but this section will focus on earthquake damage assessment. HAZUS methodology has been chosen to evaluate the damage states of buildings, bridges, tunnels, etc. It identifies the damage states probabilities ($PDS_{j,k}^T$ where: k is the index of damage states 1: slight, 2: moderate, 3: extensive, and 4: complete) as a function of structural features of the peak ground acceleration (PGA_j).

$$PDS_{j,k}^T = f(PGA_j, \dots) \quad (8.4)$$

Instead, the damage states of other edges (e.g. railway, major roads, districts, etc.) essentially depend on the debris of the damaged buildings that drops on the lanes. In detail, the closure of an edge can be caused by damage of a single building, while for district edges, because they are more redundant, depend on the average damage of the buildings inside the influence area that is weighted with the buildings perimeter p_j and the length of the lanes l_j inside the influence area (IA_i). Hence, the damage states are defined as follows:

$$PDS_{j,k}^T = \begin{cases} \max(PDS_j, k^B \in PDS_j) & \text{standard edge} \\ \frac{\sum_{j=BLA_j} p_j^B \cdot PDS_{j,k}^B}{\sum_{j=RLA_j} l_j} \leq 1 & \text{district edge} \end{cases} \quad (8.5)$$

where: are the damage states probabilities of the buildings; BIA_i are the buildings inside the influence area; and p_j^B is the perimeter of the relative building inside the IA_i . Therefore, the number of available lanes of the edge after the disaster (nl_j^{Dis}) is analytically defined as follows:

$$nl_j^{Dis} = nl(T_{Dis}^-) \cdot \left(1 - \frac{\sum_{k=0}^4 W_k \cdot DPDS_{j,k}^T}{\sum_{k=0}^4 W_k} \right) \begin{cases} DPDS_{j,k}^T = 1 - PDS_{j,k+1}^T & k = 0 \\ DPDS_{j,k}^T = PDS_{j,k}^T - PDS_{j,k+1}^T & k = 1, 2, 3 \\ DPDS_{j,k}^T = PDS_{j,k}^T & k = 4 \end{cases} \quad (8.6)$$

where: k is the index of damage states (0: none; 1: slight; 2: moderate; 3: extensive; and 4: complete); w_k are weight coefficients defined in the case study as: $w_0 = 0$, $w_1 = 0.1$, $w_2 = 0.2$, $w_3 = 0.3$, and $w_4 = 0.4$ in order to give more importance to severe damage states involving more debris; $nl_i(T_{Dis}^-)$ is the number of available

lanes before the disaster time T_{Dis} (for district edge assumption is equal to 1); and $DPDS_{j,k}^T$ are the discrete probabilities of damage states.

8.2.5 *Functionality of Transportation Networks During a Disaster*

Performance of a road network can be measured using: (i) the *number of edges* immediately available after the disaster, (ii) the *accessibility* of the network (i.e. the possibility of reaching a zone from the transportation sources), (iii) the *traffic flow* during the disaster event (which is difficult to determine during the disaster due to lack of information), and (iv) the *travel time* (a good parameter to evaluate the functionality in normal operating conditions, but it is not meaningful during catastrophic events).

The proposed model for measuring network functionality adopted in this section was inspired by the human circulatory system, where the transportation sources can be compared to the heart, while the network is equivalent to the blood vessels. The capacity $C^T(t)$ of the network is defined as the equivalent length of the network that is available and accessible from the transportation sources with functionality greater than zero:

$$C^T(t) = \text{Capacity} = \sum_{j=N_{AR}} L_j^T(t) \quad (8.7)$$

where N_{AR} = number of available edges and L_i^T = equivalent edge length defined in Eq. 8.1. The accessibility (alternative routes, etc.) and the related recovery plan are evaluated studying the relation between the adjacency matrix $A^T(t)$ and the traffic sources. For example, during an emergency, the traffic directions are no longer respected, because traffic is rearranged to cover the weaknesses of the network. Hence, if the functionality $f_e^N(t)$ of the network typology is below a certain threshold, the adjacency matrix will be considered symmetric (both directions of traffic of the roads are allowed). The functionality is defined as the ratio between the capacities of post-disaster $C^T(t)$ and pre-disaster $C^T(T_{Dis}^-)$ as follows:

$$f_e^N(t) = \text{Network Functionality} = \frac{C^T(t)}{C^T(T_{Dis}^-)} \quad (8.8)$$

8.2.6 *Functionality of the Transportation Categories During a Disaster*

The subdivision of the transportation system in categories (P1, P2, P3: Ports, A1, A2, A3: Airports, R: Road Network, B: Bus Network, R: Railway, LR: Light Rail, S: Subway, and O: Other) and sub-categories (e.g. for the networks N:

Network, MC: Monitoring Center, S: Stations, D: Dispatch, F: Fuel Structures, M: Maintenance Structures, and O: Other) allows one to evaluate the redundancy rate of the building categories showing which are the critical infrastructures. The building category functionality $Q_h^{TC}(t)$, according to interdependencies and redundancies, has been defined as follows:

$$Q_h^{TC}(t) = \frac{\sum_{e=TC_h} W_{e,h}^{TC_e} \cdot f_e^E}{\sum_{e=TC_h} W_{e,h}^{TC_e}} \text{ with } f_e^E = \begin{cases} 0 & f_e \leq L_e^{CF} \\ f_e & f_e > L_e^{CF} \end{cases} \quad (8.9)$$

where: h is the transportation category index; TC_h are the transportation system elements that belong to the h th transportation category; $w_{e,h}^{TC_e}$ are the weight coefficients that identify the importance of a transportation system with respect to other systems that belong to the same transportation typology h th (e.g. a small airport has $w^{TC_e} = 3$, while a large airport has $w^{TC_e} = 10$); L_e^{CF} is a lower bound limit that is a function of the system transportation element e th (e.g. for small airports $L_e^{CF} = 60\%$, while for large airports $L_e^{CF} = 30\%$); and f_e is the functionality of the element transportation system defined as follows:

$$f_e = \begin{cases} f_e^N(t) \cdot [L_e^{CF} \cdot f_e^{CF}(t) + (1 - L_e^{CF})] \cdot [L_e^F \cdot f_e^F(t) + (1 - L_e^F)] & \text{Networks} \\ f_e^{MS}(t) \cdot [L_e^{CF} \cdot f_e^{CF}(t) + (1 - L_e^{CF})] \cdot [L_e^F \cdot f_e^F(t) + (1 - L_e^F)] & \text{Ports and Airports} \end{cases} \quad (8.10)$$

where L_e^F and L_e^{CF} are coefficients that identify the importance of facilities and critical facilities (e.g. the electricity supply system in the tram system controls 100% of the system functionality so $L_e^{CF} = 100\%$) respectively; f_e^{MS} , f_e^{CF} , and f_e^F are the functionalities of the main structures (e.g. waterfront structures, runways, etc.), of the critical facilities, and of the facilities respectively which are analytically defined in the equations below:

$$f_e^{CF}(t) = \frac{\sum_{f=CF_e} \left(W_{e,f}^{Fe} \cdot \frac{\sum_{j=CFB_f} W_{e,f,j}^{CFB} \cdot f_j^B}{\sum_{j=CFB_t} W_{e,f,j}^{FB}} \right)}{\sum_{f=CF_e} W_{e,f}^{CF}} \leq 1;$$

$$f_e^{MS}(t) = \frac{\sum_{f=MS_e} W_{e,f}^F \cdot f_j^B}{\sum_{f=MS_e} W_{e,f}^F} \leq 1; \quad (8.11)$$

$$f_e^F(t) = \frac{\sum_{f=Fe} \left(W_{e,f}^{Fe} \cdot \frac{\sum_{j=FB_f} W_{e,f,j}^{FB} \cdot f_j^B}{\sum_{j=FB_t} W_{e,f,j}^{FB}} \right)}{\sum_{f=Fe} W_{e,f}^F} \leq 1;$$

where: f_j^B = functionality of the j th building; CF_e , F_e , and MS_e are respectively the critical facilities, the facilities, and the main structures that belong to the e th system transportation element; FB_e , and CFB_f are the building facility and critical facility that belong to the f th facility's typology respectively ; w_{ef}^{CF} and w_{ef}^F are the weight coefficients of facility's typologies (e.g. for a road network, $L_e^F = 8\%$ and $L_e^{CF} = 0\%$ because it is a self-reliant system without critical facilities and it has $w_{e,MC}^F = 20$, $w_{e,S}^F = 0$, $w_{e,D}^F = 10$, $w_{e,F}^F = 60$, $w_{e,M}^F = 10$, and $w_{e,O}^F = 0$); and $w_{ef,j}^{CFB}$, $w_{ef,j}^{FB}$, and w_{ef}^{MS} are the weight coefficients of building typologies (that depend on the dimension and importance of the j th structures with respect to the f th group).

8.2.7 Functionality and Resilience of Transportation System

The resilience value of the transportation system R_T^{Ph} is the integral of its functionality $Q_T^{Ph}(t)$ over a control period T_{LC} and is given by:

$$R_T^{Ph}(T, T_{LC}) = \frac{\int_T^{T+T_{LC}} Q_T^{Ph}(t) \cdot dt}{T_{LC}} \text{ with } Q_T^{Ph}(t) = \frac{\sum_h W_h^{TC} \cdot Q_h^{BC}(t)}{\sum_h W_h^{TC}} \quad (8.12)$$

where: h is the transportation category index, and W_h^{TC} are the weight coefficients for each transportation category that depend on the community system, (e.g. for normal condition $w_P^T C = 8$, $w_A^T C = 12$, $w_R^T C = 40$, $w_B^T C = 3$, $w_{Rw}^T C = 8$, $w_{LR}^T C = 6$, and $w_S^T C = 4$; while, for an island $w_P^T C = 15$, $w_A^T C = 20$, $w_R^T C = 40$, $w_B^T C = 3$, $w_{Rw}^T C = 8$, $w_{LR}^T C = 6$, and $w_S^T C = 4$).

Therefore, the global resilience G_R^{Ph} and the global functionality Q_{Ph} of physical infrastructure dimension are defined as follows:

$$G_R^{Ph}(T, T_{LC}) = \frac{\int_T^{T+T_{LC}} Q_{Ph}(t) \cdot dt}{T_{LC}} \text{ with } Q_{Ph}(t) = \frac{\sum_c W_c^{Ph} \cdot Q_c(t)}{\sum_c W_c^{Ph}} \quad (8.13)$$

where: w_c^{Ph} is the weight coefficient associated with the c th component. Finally, the global resilience index GI_R^{Ph} and the resilience index of the transportation system I_T^{Ph} are the resilience value at the end of the recovery works T_{EW} (i.e. when the global functionality reaches 100%) starting from the disaster time T_{Dis} .

$$G_R^{Ph}(T, T_{LC}) = \frac{\int_T^{T+T_{LC}} Q_{Ph}(t) \cdot dt}{T_{LC}} \text{ with } Q_{Ph}(t) = \frac{\sum_c W_c^{Ph} \cdot Q_c(t)}{\sum_c W_c^{Ph}} \quad (8.14)$$

In conclusion, the proposed methodology uses as main parameters for evaluating the performances of the physical infrastructure dimension, the global resilience index GI_R^{Ph} and the recovery time T_{EW} .



Fig. 8.4 Buildings in Treasure Island, San Francisco Bay

8.2.8 *The Case Study of Treasure Island in San Francisco Bay, California*

The proposed methodology was tested – evaluating the interdependencies between road and building networks – in the case study of Treasure Island in San Francisco Bay in California. The road network (data from Open Street Map database, OSM) and 25 residential buildings (in white in Fig. 8.4) with realistic features (e.g. capacity curves, damping ratios, occupancy classes, repair costs etc.) have been modeled. In particular, the island is connected to San Francisco and Oakland through the Bay Bridge. The interdependencies between the road network and the building system were modeled considering the *accessibility* – i.e. if a building unit is not accessible from the road network it cannot be repaired, losing its functionality – and on the other side if a building unit collapses within the road influence area, this will lose its functionality.

Moreover, for the case study it is assumed: (i) an earthquake with a return period (Tr) of 2450 years; (ii) no-limit on the economic budget (EB); (iii) maximum of three simultaneous starts of construction building sites (CSS) during the recovery phase; and (iv) maximum of three construction sites per day (CS). The optimal solution of the recovery plan was selected performing a sensitivity analysis. Different recovery plans were compared in terms of resilience under certain boundary conditions (accessibility, economic budget, number of construction sites, etc.) varying the administrative times TA_{di} of each element of the model. The final outputs are: (i) the resilience index, (ii) the functionality values, and (iii) the optimal recovery plan of the analyzed system.

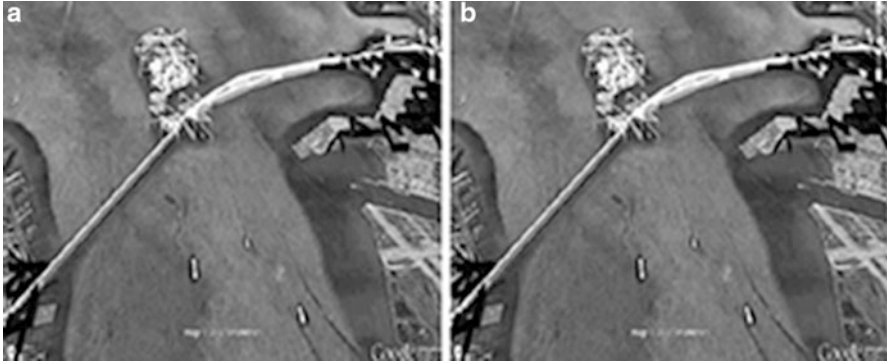


Fig. 8.5 (a) Discrete probability of damage states for buildings. (b) Functionality after the risk assessment

The discrete probability damage states for the buildings inside the island are shown in Fig. 8.5a with a 3D histogram plotted on Google Earth (in black no damage, in white collapse or unusable). The functionality of the buildings and the entire road network, immediately after the disaster, are shown in Fig. 8.5b. Initially, the entire Island is not accessible, because the bridges that connect it to the mainland collapsed. Hence, the building units and the district edges inside the Island are unusable, i.e. they have zero functionality.

The functionalities of the components of physical infrastructure dimension (transportation system and building system) and its global functionality Q_{Ph} , which was evaluated with equal weight coefficients w_c^{Ph} for the road network and the building system, are shown in Fig. 8.6a. When the first bridge that joins the island with the mainland is recovered (in 40 days according to the simulations) the global functionality has a leap, because the road network and the building units inside the island can be reused and repaired (Fig. 8.6b). In conclusion, the results of analysis are: a recovery time T_{EW} for the community of 3.19 years.; resilience indicators of 74.34% and 97.52% for building system and transportation system respectively; and a global resilience index equal to 85.93%.

8.3 Example 2: Water Distribution Network

8.3.1 Introduction

The increasing frequency of natural disasters and man-made catastrophes has caused major disruptions to critical infrastructures (CI) such as Water Distribution Networks (WDNs). Therefore, reducing the vulnerability of the systems through physical and organizational restoration plans is a prime concern for system engineers and utility managers responsible for the design, operation, and protection of

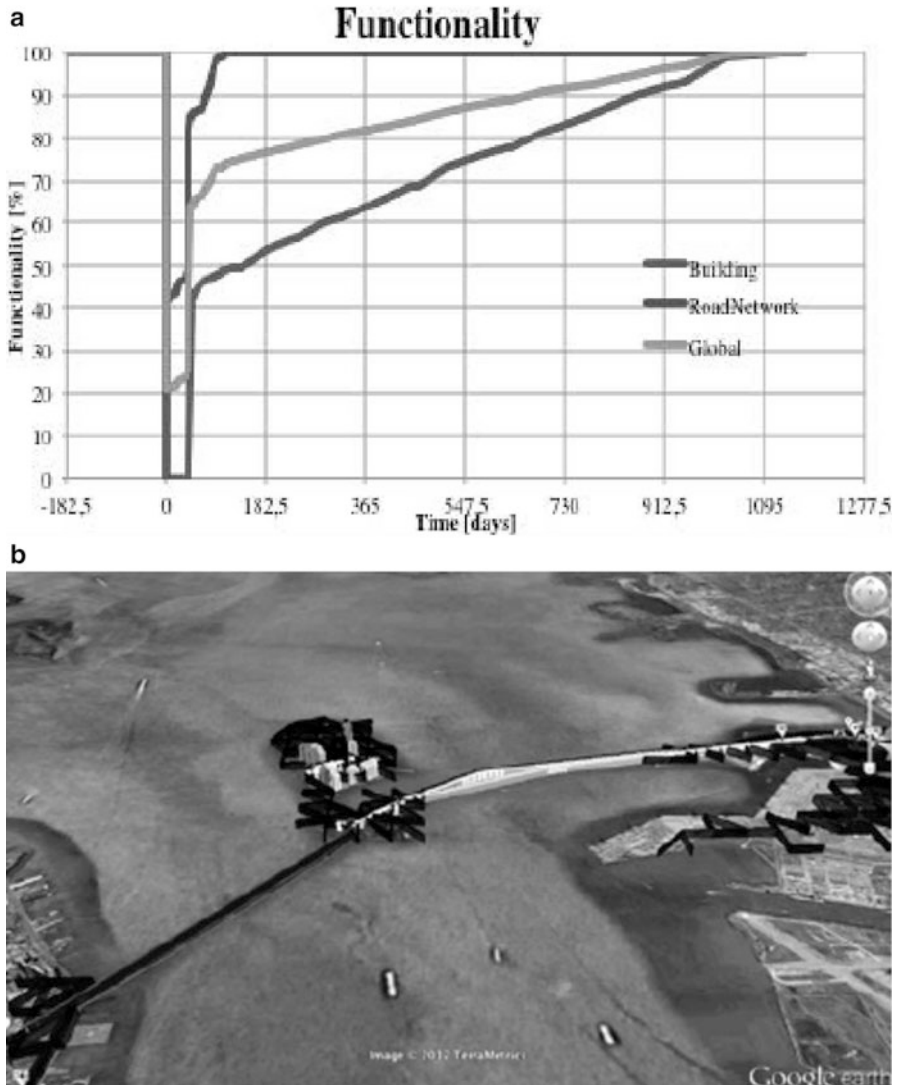


Fig. 8.6 (a) Functionality curves. (b) Functionality after the recovery of the first bridge in the Bay area

WDNs. Disruptions change the operability state of parts of the network (nodes and/or links), and the recovery involves a set of actions to restore functionality to the damaged parts of the network, allowing the performance of the system to return to nominal levels as quickly as possible. In the past, emphasis was given to the physical protection of water distribution networks, but now attention is shifting towards infrastructure resilience, defined as the ability of infrastructure systems to withstand, adapt to, and rapidly recover from the effects of a disruptive event.

“Resilience is the capability of over-coming stress or failure”. This definition is proposed by Todini (2000) in his study of the looped water distribution network design. The cost of the hydraulic network is related to two main factors: energy and pipe network cost. The cost of energy only appears if the water must be pumped, sometimes gravity driven water distribution systems can be applied and the cost of energy is neglected. On the other hand, if the pipes are too small, the pumping cost increases since the head losses are greater. It has been studied that the most efficient way to design the hydraulic network is the looped topology (Fig. 8.7), which guarantees the supply of enough capability in the system to go through local failures and the efficient distribution of water to users.

In contrast, in the tree shaped distribution network (Fig. 8.8), a pipe failure could have important consequences in terms of reliability, since some of the nodes would

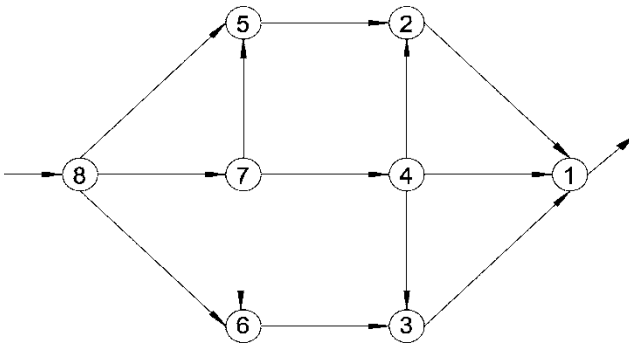


Fig. 8.7 Example of a looped network

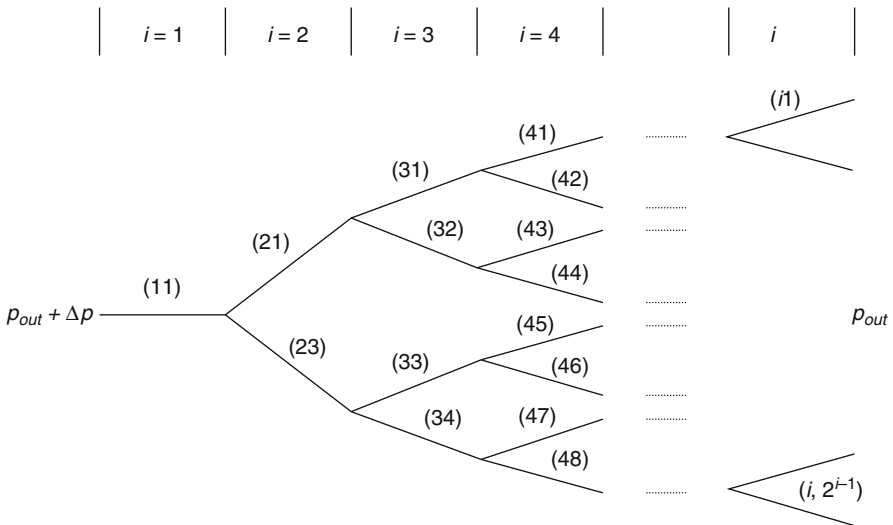


Fig. 8.8 Example of tree shaped network

not be served for a certain period or they would be poorly served. So it is better, whenever it is possible, to use the concept of topological redundancy by adding pipes and closing loops, so in the case of failure, the water will flow to the node through an alternative route. In the looped system, whenever the demand increases or a pipe fails, the water will flow at a higher pressure, so the original network is changed and now has higher internal losses. The water has to be delivered at a minimum pressure to the users. More power than is required would be provided to each node, in order to have enough surplus to be dissipated internally in case of failure.

One of the most important things for the WDNs is to define a Resilience Index (R) for a water distribution system in order to measure its performance. In the last decade, several metrics have been proposed in literature to measure the performance of WDNs. For example, Todini (2000) proposed an index which is a measure of the capability of the network to cope with failures and it is related indirectly to system reliability. Other authors have also extended this resilience index to overcome certain drawbacks (Prasad and Park 2004; Jayaram and Srinivasan 2008), such as the inapplicability of the index in networks with multiple sources. They have listed the theoretical advantages of their approaches, but none of them has compared the performance of these resilience indicators. Earthquake effects on water supply systems have been investigated extensively in literature and different methodologies for estimating the reliability and serviceability of water supply systems heavily damaged by earthquake are available in literature (Ballantyne et al. 1990; Taylor 1991; Shinozuka et al. 1992; Markov et al. 1994; Hwang et al. 1998). Recently, Davis (2014) in his work has defined five categories of water services. He has compared pre- and post-disaster services and has distinguished between operability and functionality.

In this section, a Resilience Index (R) for a water distribution system has been proposed to measure its performance. The proposed index R is defined as the product of three indicators: one describes the demand and is based on the number of users temporarily without water (R_1); the second describes the capacity and is based on the tank water height (R_2); the third (R_3) is based on the water quality. These indicators will help planners and engineers evaluate the functionality of a water distribution system which consists in delivering a certain demand of water with an acceptable level of pressure and quality. A small town located in a seismic region of Italy has been used as a case study. The WDN has been analyzed using the software EPANET 2.0 (Rossman 2000) and different restoration plans have been compared using the proposed resilience indicators.

8.3.2 Definition of a New Performance Index for the Water Distribution Network

The proposed index is composed of three parts which depend on the number of households that would suffer water outage, the tank water level and the

water quality. The first part of the index is proportional to the system serviceability index (SSI) proposed by Todini (2000), which is defined as the ratio of the sum of satisfied water demands after an earthquake to that before an earthquake. In detail, three performance functions $F_1(t)$, $F_2(t)$ and $F_3(t)$ have been presented. $F_1(t)$ relates to the number of households without water, therefore it is related to the social dimension of the resilience problem. Analytically it is defined as

$$F_1(t) = 1 - \frac{\sum_i n_{p,e}^i}{n_{Tot}} \text{ for } i = 1n \quad (8.15)$$

where $n_{p,e}^i$ are the equivalent number of users for each node that suffer insufficient pressure, n_{Tot} are the total number of users within the distribution system, n is the total number of nodes that suffer water outage. The Loss Function $L_1(I, T_R)$ is defined as

$$L_1(I, T_R) = 1 - \frac{\sum_i n_{d,e}^i(I, T_R)}{n_{Tot}} \text{ for } i = 1n \quad (8.16)$$

where $n_{d,e}^i$ are the number of Demand Nodes which are assumed to be directly proportional to the water volume lost W_{Lost} during the extreme event and the repair operations; I is an intensity parameter; T_R is the recovery period which is defined as the period necessary to restore the functionality of a system to a desired level that can operate or function the same, close to, or better than the original one (Cimellaro and Reinhorn 2010; Cimellaro et al. 2010). In detail, $n_{d,e}^i$ is given by the following equation

$$n_{d,e}^i = n_i \cdot \frac{W_{Lost}^i}{W_i} \quad (8.17)$$

where i indicates the general node in which the pressure is insufficient to ensure the demand water flow; n_i is the total number of entities connected to node i ; W_{Lost}^i is the water volume lost and W_i is the water volume that the entities would consume in normal operating conditions. To evaluate the volume of water lost and the volume of water in normal operating conditions the following equations have been used

$$W_i = \int_{t_j}^{t_{j+1}} Q_{Demand}(t) dt \quad (8.18)$$

$$W_{Lost}^i = \int_{t_j}^{t_{j+1}} [Q_{Demand}(t) - Q_i(t)] dt \quad (8.19)$$

where t_j and t_{j+1} are generic instants after the extreme event ($t > t_1$); Q_{Demand} is the demand water flow at instant t and Q_i is the real water flow at time t afterwards the damage of the pipe. For a given extreme event, the general form of $F_1(t)$ is

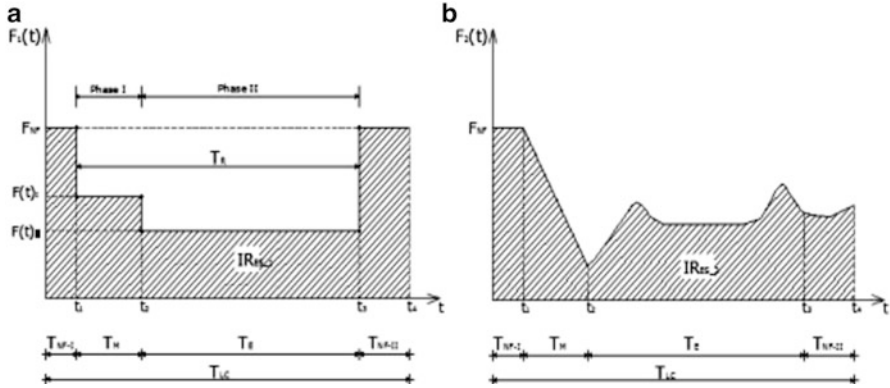


Fig. 8.9 (a) Functionality of water distribution system based on the number of users with suffered water outage and of (b) the tank water height $F_2(t) = h(t)/ h_{Reserve}$. IRES,1 and IRES,2 represent the area under the functionality curves

shown in Fig. 8.9a. The control time T_{LC} has been divided into four different period ranges. T_{NF-I} is the normal operating functionality period before the earthquake; T_M is the operating period range immediately after the earthquake and before the first emergency operations; T_E is the transition period during which the water system is partially in service; T_{NF-II} is the normal operating functionality after the repair operations. Moreover, t_1 is the time instant when the extreme event occurs, t_2 is the time instant when the damaged pipe is isolated, t_3 is the time instant when the repair operations are finished and t_4 is a generic instant when the system works in normal operating conditions. The difference between t_3 and t_1 corresponds to the Recovery Time T_R . Then the restoration process has been divided into two phases: Phase I is the time interval necessary for the first emergency operations and the isolation of the area where the damage happens, while Phase II is the time interval necessary for the repair operations. During Phase II, the users are temporarily without water, so, in this case, the water flow is equal to zero, while the ratio is equal to 1, since. Therefore, after the definition of the performance index $F_1(t)$ given in Eq. 8.15 the corresponding resilience index is defined as

$$R_1 = \int_0^{T_{LC}} \frac{F_1(t)}{T_{LC}} dt \tag{8.20}$$

where $F_1(t)$ is the performance function proportional to the number of equivalent households n_e w/o service; T_{LC} is the control time. The second performance function $F_2(t)$ relates to the tank water level, which is directly related to the reserve capacity of the tank and therefore to the technical dimension of the resilience problem. The analytical expression is defined as

$$F_2(t) = \begin{cases} \frac{h(t)}{h_{Reserve}} & h \leq h_{Reserve} \\ 1 & h > h_{Reserve} \end{cases} \tag{8.21}$$

where $h(t)$ is the water level in the tank at a given instant of time, while $h_{Reserve}$ corresponds to the reserve capacity in the tank. In detail, if the water level is above the height corresponding to the reserve capacity $h_{Reserve}$, $F_2(t)$ is equal to 1, but if the level decreases below $h_{Reserve}$, $F_2(t)$ has a value less than 1. In this case the Loss Function $L_2(I, T_R)$ is given by

$$L_2(I, T_R) = 1 - \frac{h(t, I, T_R)}{h_{Reserve}} \quad (8.22)$$

The loss function given in Eq. (8.22) provides information about how much water has been lost during the earthquake and allows us to establish what the optimal strategy is for recovering the Reserve Capacity. The definition of performance function in Eq. (8.21) can also be generalized and extended not only to tanks, but to pumps, by using the ‘‘Hydraulic head’’ or ‘‘Piezometric head’’ which is a specific measure of liquid pressure that can also be used for pumps. With respect to Eq. (8.16), for Eq. (8.22) it is not possible to define a fixed recovery time before the numerical simulations, because in this case T_R is directly related to the type of restoration plan adopted. Shown in Fig. 8.9b is a sketch of how $F_2(t)$ looks. The figure shows how $F_2(t)$ doesn’t return to 1 at the end of T_{LC} , but it can assume lower values, if a proper restoration strategy is not adopted. In this case, the Resilience Index is given by

$$R_2 = \int_0^{T_{LC}} \frac{F_2(t)}{T_{LC}} dt \quad (8.23)$$

where $F_2(t)$ is the water level in the tank; T_{LC} is the control time. Special attention is required in the definition of R_2 when multiple tanks are in the network. In this case, the index is given by

$$R_2 = \frac{\sum_i w_i R_2^i}{\sum_i w_i}; i=1,2 \quad (8.24)$$

where w_i are the weight coefficients of the n tanks in the network. These coefficients can be evaluated using two approaches. Assuming two tanks, in the first case, the weights w_1 and w_2 are proportional to the average flow loss on the two pipes in which the connecting pipe is divided after the earthquake. In the second case, the weights w_1 and w_2 are proportional to the reserve capacity.

Since WDNs have strict requirements for ensuring water quality, the global resilience index should also include a water quality index which is related to the environmental dimension of the resilience problem. Currently there is no globally accepted composite index of water quality. Most water quality indicators rely on normalizing, or standardizing data according to expected concentrations and some interpretation of ‘‘good’’ versus ‘‘bad’’ concentrations. Parameters are often then weighted according to their perceived importance of overall water quality and the

index is calculated as the weighted average of all the observations of interest. The authors do not want to enter in the discussion of which index is better to adopt, however once an index of water quality check Q is selected, it can be compared with its value before the earthquake event defining the following performance function

$$F_3(t) = \frac{Q(t)}{Q^*} \quad (8.25)$$

where Q^* and $Q(t)$ are the water quality indicators before and after the seismic event respectively. The final resilience index for water quality is defined as

$$R_3 = \int_0^{T_{LC}} \frac{F_3(t)}{T_{LC}} \quad (8.26)$$

Then the three indicators are combined together to have a comprehensive evaluation of the WDN, so the Global Resilience Index is defined as

$$R = R_1 R_2 R_3 \quad (8.27)$$

The R index summarizes the performance of the WDN considering the demand R_1 (users), the capacity R_2 (water level in the tank) and the water quality R_3 .

The metrics have been multiplied, because the global index R in Eq. (8.27) is more sensitive to the different scenario events when the three indicators are multiplied. In fact some scenarios in the case study below generate high values of R_1 , so it seems that damage did not cause any effect, but in reality the quantity of water loss has been relevant and this causes a reduction of the water reserve capacity in the tank and consequently of R_2 .

8.3.3 A Case Study of the WDN of Calascibetta, Italy

The methodology described above has been applied to the WDN of Calascibetta, an Italian town supplying 4600 inhabitants in the Enna Province, located on Erei Mountains (Fig. 8.10) in Sicily. The town did not suffer high intensity earthquakes except the “Noto valley earthquake” which occurred in 1693 and produced severe damages in the entire eastern side of the island. Its intensity was about XI of Mercalli–Cancani–Sieberg (MCS) scale, but in Calascibetta the intensity felt was about VII. Using the Neo-deterministic seismic hazard scenario proposed by Panza et al. (2012), the value of the peak ground velocity in the town of Calascibetta (14.4000 N 37.4000 E) is in the range between 15 and 30 cm/s (Panza et al. 2014). The Neo-determinist approach has been preferred with respect to the Probabilistic Seismic Hazard analysis, because the former provides non conservative results (Panza et al. 2014) at the specific site. The PGV used in the analysis is the average value of 22.5 cm/s, which can be assumed constant over the entire WDN, because of the limited extension of the network.

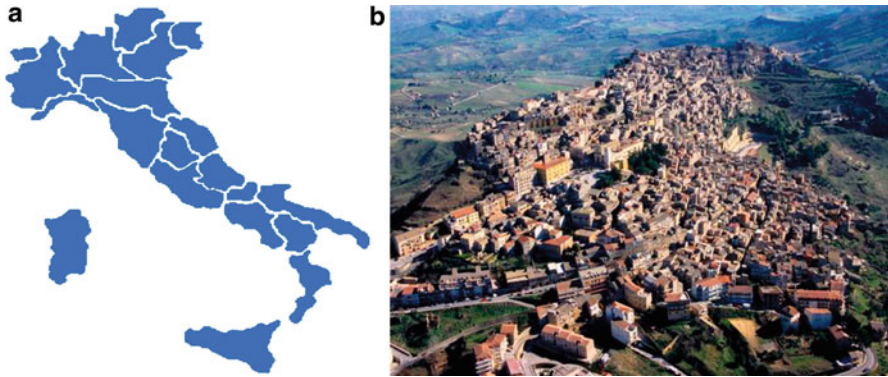


Fig. 8.10 Location and overview of Calascibetta Town in Sicily

8.3.4 *Characteristics of the Water Distribution Network*

The WDN consists of two tanks:

- the roof tank (Capacity = 50 m³) located in the highest part in the town;
- St. Peter's tank (Capacity = 500 m³), which is supplied by the pipes coming from the roof tank.

The water source capacity of the two tanks is the reservoir located at Ancipa Dam. The water is pumped to the roof tank from a station located at the bottom of the hill and from there, the water is distributed to district 1 and to the Saint Peter tank which supplies the entire city. This section deals only with the distribution network, while the adduction network is not considered in the analysis. The entire network is made by polyethylene pipes which are characterized by an easy process of installation, high elasticity that allows it to absorb modest land subsidence without damage on the structure, chemical inertness against the aggressiveness of land or percolated water or liquids conveyed. In Fig. 8.11 the plan view of the WDN of Calascibetta which is divided into eight districts is shown. All districts are connected through pipes which are normally closed under normal operating conditions, but they can be opened in case of emergency. Three diameters of respectively 63, 110 and 160 mm are installed in the network, while 32 mm diameter pipes have been used to connect the different services within the building.

The length of the 32, 63, 110 and 160 mm diameter pipes are respectively 3728.83 m, 8719.35 m, 4427.65 and 1115.35 m. Pressure reducing valves (PRV) have been installed in the network to maintain the pressure within certain limits, given in Table 8.1, while shut-off valves have been installed to close the pipes in case of emergency (Fig. 8.11).

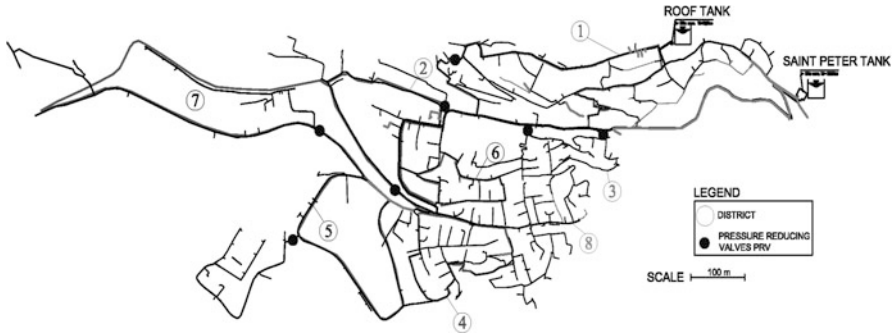


Fig. 8.11 Calascibetta water distribution network (WDN) organized by districts and pressure reducing valves (PRV)

Table 8.1 Characteristics of the pressure reducing valves

Id. code	Location	D (mm)	Meters head (m)
PRV1	Via Dranza	63	20.0
PRV2	Via Giudea	63	15.0
PRV3	Via Vita	63	20.0
PRV4	Via Roma	110	20.0
PRV5	Via Maddalena II	110	15.0
PRV6	Via Teatro	63	25.0
PRV7	Via Maddalena II	110	20.0

8.3.5 Model Description, Assumptions and Calibration

The WDN of Calascibetta has been modeled using EPANET 2.0 (Rossman 2000). The standard procedure used in the software to evaluate the nodes’ pressure and the flow in each pipe is the Demand Driven Analysis (DDA) . However, the limitation of this method is that the demand flow is fixed a priori in each node, so the DDA provides the same value of demand flow even if the pressure is below the threshold necessary to satisfy the demand in the WDN. For these reasons, the DDA works well under normal operating conditions when there are no failures in the pipes, but if one pipe fails, the pressure in some nodes could be below the threshold value necessary for satisfying the demand. In this case, the Pressure Driven Analysis (PDA) has been used. So all the simulations with pipe failures start with a DDA analysis and when the pressure in one node goes below the threshold necessary to satisfy the demand flow, it is transformed in an Emitter node (Rossman 2000).

The PDA analysis in presence of Emitters is characterized by less flow circulating in the network and consequently by reduced hydraulic head losses when compared with the first analysis (DDA). In the analyses, the pressure necessary for satisfying the demand flow at each node is set to 20 m of water column (2 bar), so that at least 5 m of water column are above the tallest house in Calascibetta which has an height of about 13 m. The Darcy-Weisbach formula has been used to evaluate the head losses which are given by

$$h = \lambda(\varepsilon, d, q) \frac{L \cdot v^2}{d \cdot 2g} \quad (8.28)$$

where λ is the friction factor (depending on the roughness ε , the diameter d and the flow rate q), L is the pipe length, v is the flow velocity, g is the acceleration of gravity. The friction factor λ is estimated with the use of different equations as a function of the Reynolds Number (RE). The roughness ε for the polyethylene pipes has been assumed constant and equal to 0.005 mm, because the pipes have been recently installed and in general, the polyethylene material maintains its hydraulics characteristics. The concentrated losses have been neglected. Pipes with the same features (e.g. diameter, roughness) have been combined into a single pipe with length equal to the sum of the lengths of each pipe. The pipes with diameter of 32 mm connecting to the services have been neglected. The roof tank has a cylindrical shape with a diameter of 3 m, while the St. Peter tank is composed of two tanks of rectangular shape that cover an area of 66 m² each. To simplify the modeling in EPANET the rectangular tank has been replaced with an equivalent tank with a diameter of 12.95 m that have a cylindrical shape of the same area ($D = \sqrt{\frac{4A}{\pi}} = \sqrt{\frac{4 \cdot 132}{\pi}} \simeq 12.95$ m). The variation of water flow demand over the 24 h has been determined using the data provided from the operator from July 2011 to June 2012.

In particular, the water flow demand is obtained as an average of a monthly time pattern for each district. For example, Fig. 8.12 shows the water flow demand related to District 1. Pipe breaks and leaks have been modeled in EPANET using the scheme shown in Fig. 8.13, however simulations have been focusing only on pipe breaks, which are assumed to happen in the middle point of the pipe. Then at the end-parts of the divided pipe, two reservoirs are added to simulate the water flow through the crack. The tanks have a hydraulic head equal to the elevation of the break point which is evaluated with a linear interpolation between the two nodes of the original pipe. Finally, a check valve is inserted on each new pipe so that the water can only flow from the broken pipe to the tanks and not vice-versa.

8.3.6 Seismic Damage Model for Water Pipes

Pipeline damage models for the seismic vulnerability assessment are usually formulated as the repair rate for unit length of pipes. These models can be derived from the data collected during previous seismic events or any other hazard which

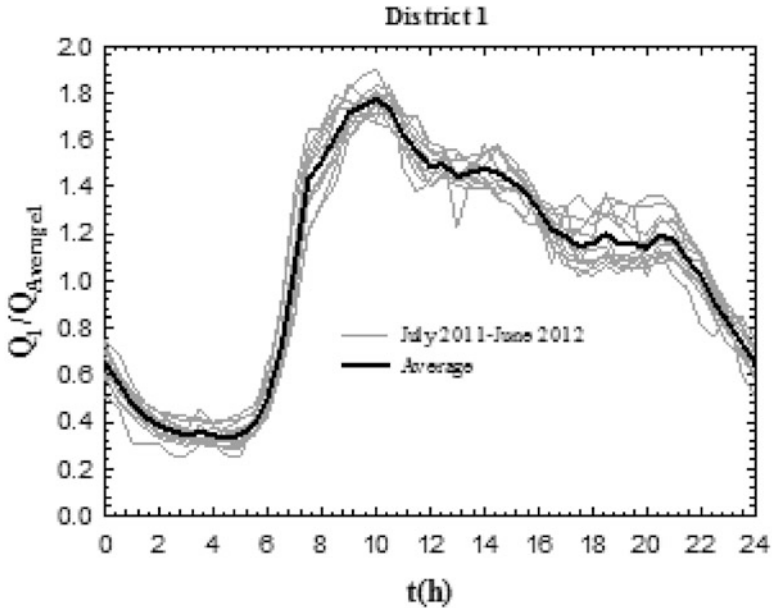


Fig. 8.12 Variation of demand of water flow of district 1 during 24 h

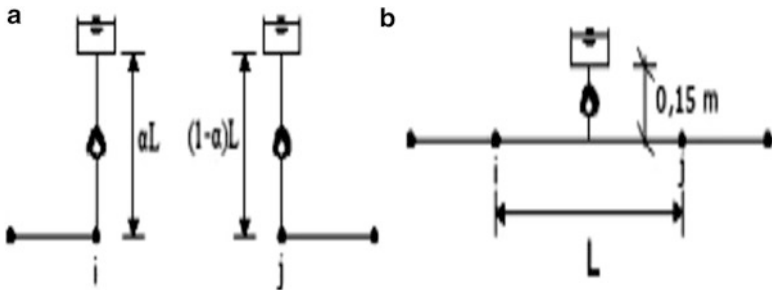


Fig. 8.13 Modeling of (a) pipe break simulation and (b) pipe leak simulation in EPANET 2.0 (GIRAFFE, 2008)

produced breakages in the pipes. In this example, the well known model in the American Lifeline Alliance (ALA 2001) has been used. In particular, the repair rate is defined as

$$RR = K(0.00187)PGV \tag{8.29}$$

where RR is the Repair Rate which is the number of pipe breaks per 1000 ft (305 m) of pipe, K is a coefficient determined by the pipe material, pipe joint type, pipe diameter, type of fitting and soil condition and the PGV is the peak ground velocity which is given in units of in/s. K is assumed 0.5, because in Calascibetta are

polyethylene pipes and the type of fitting adopted is rubber gasket, while the PGV is assumed equal to 22.5 cm/s (8.86 in/s). So applying Eq. (8.29), the value of RR is equal to 0.008. Furthermore, the WDN of Calascibetta consists of pipes of different importance, which have been distinguished in four groups: (1) main pipes, (2) pipes at the entrance of each district, (3) connecting pipes and (4) plain pipes within each district. In order to take into account the varying importance of each pipe, Eq. (8.29) has been modified introducing the importance factor (I_m), thus

$$RR = I_m K(0.00187) PGV \quad (8.30)$$

where I_m is assumed equal to 2, 1.5, 1 and 0.8, respectively. Finally, the probability of having a number n of breakages in a pipe of length L is given by the following expression

$$P(n) = \frac{(-RR \cdot L)^n}{n!} e^{-RR \cdot L} \quad (8.31)$$

where n is the number of pipe breaks, RR the repair ratio evaluated using Eq. (8.30) and L is the length of pipe (expressed in terms of 1000-ft segment USCS). Figure 8.14 shows the probability of having a certain number of breaks in the WDN of Calascibetta. The figure justifies the choice of selecting the scenarios with a single break, because the probability of having two breaks is negligible.

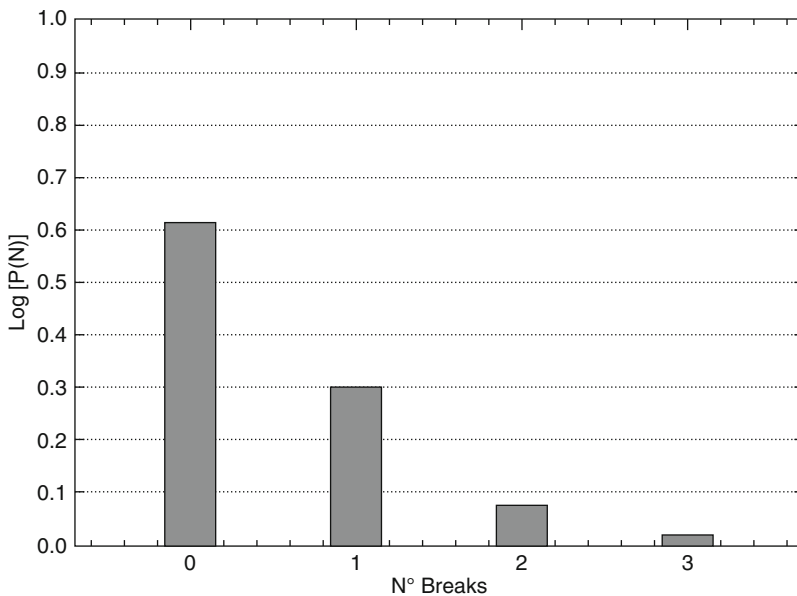


Fig. 8.14 Failure probability in the Calascibetta water distribution network

8.3.7 Risk of Pipe Failure

The risk of failure of a WDN can be obtained using its topology and the failure probability $P(n)$ of every pipe. The failure to deliver a sufficient amount of water from an inflow node i to an outflow node j , can be defined as the probability that the hydraulic head goes below a specified threshold value. Therefore, the probability of failure of a network can be obtained after the hydraulic analysis of a damaged network. Then Monte Carlo simulation is employed reducing the network topology by removing the pipes segments based on the failure probability of every pipe $P(n)$. Once the failed pipes are removed, an algorithm based on Graph Theory can be used to determine whether a path between an inflow and an outflow node exists. For every damaged network created, Monte Carlo simulations have been employed using 5000 runs in order to calculate the statistics of the hydraulic quantities of interest. The procedure is discussed in detail in Fragiadakis and Christodoulou (2014).

8.3.8 Selection of Scenarios Event

Classical risk analysis has different assumptions, objectives and methods which are not sufficient for resilient design, so the departure from the traditional design practices is necessary (Park et al. 2013). Resilience is a dynamic, emergent property that must be continually managed and is characterized by a lack of certainty. The uncertainty of potential future disruptions makes the use of scenarios important. In this part, four types of scenarios that cover a wide range of potential occurrences for the WDN of Calascibetta have been selected based on a “hybrid approach” which combines Monte Carlo based algorithm with engineering judgment. The Monte Carlo based algorithm allows assessment of preliminary failure probabilities in various locations within the network. The reason for combining the engineering judgment in the approach lies on the topology of the WDN of Calascibetta. The network is divided in eight districts connected with a main pipe and several connecting pipes.

The main and the connecting pipes are important because if they fail the entire district will be left without water, so additional scenarios were selected for explicitly assessing their significance. Less important pipe failures of smaller diameter pipes within the district have been also selected.

Four groups of scenarios (S_1 , S_2 , S_3 and S_4) have been selected to examine the effect of different types of pipe failures. S denotes a “Scenario” and the subscript number indicates the group that each scenario belongs (Fig. 8.15). In detail, the following groups of scenarios in Table 8.2 have been analyzed:

- Group S_1 includes scenarios with one break on the main pipeline and the supply pipe of the St. Peter Tank;
- Group S_2 includes all scenarios with breaks in the supply pipes of each district;
- Group S_3 includes all scenarios where the breaks occur in the districts;
- Group S_4 includes all scenarios where the breaks occur in the connecting pipes.



Fig. 8.15 Earthquake scenarios event divided by groups

Table 8.2 Scenarios considered in the analysis

Scenario	District location & group	Location	D (mm)	Average flow loss (l/s)
1	S1_Main Pipeline	Break of DN 160 PE pipe in Via Conte Ruggero	160	90.11
2	S2_District 1	Break of DN 160 PE pipe in Matrice Square	160	180
3	S2_District 2	Break of DN 63 PE pipe in Via Giudea	63	61.4
4	S2_District 3	Break of DN 63 PE pipe in Via Vita	63	48.63
5	S2_District 4	Break of DN 63 PE pipe in Via Nazionale SS 290	63	53.80
6	S2_District 5	Break of DN 110 PE pipe in Via Nazionale SS 290	110	77.35
7	S2_District 6	Break of DN 63 PE pipe in Via Teatro	63	53.82
8	S2_District 7	Break of DN 110 PE pipe in Via Maddalena II	110	48.36
9	S2_District 8	Break of DN 110 PE pipe in Via Nazionale SS 290	110	75
10	S3_District 1	Break of DN 63 PE pipe in Via Itria	63	33.48
11	S3_District 2	Break of DN 110 PE pipe in Via Giudea	110	66.61
12	S3_District 3	Break of DN 63 PE pipe in Via Minavento	63	21.51
13	S3_District 4	Break of DN 63 PE pipe in Via San Antonio	63	24.47
14	S3_District 5	Break of DN 110 PE pipe in Via Maddalena II	110	55.25
15	S3_District 6	Break of DN 63 PE pipe in Via Annunziata	63	29.55

(continued)

Table 8.2 (continued)

Scenario	District location & group	Location	D (mm)	Average flow loss (l/s)
16	S3_District 7	Break of DN 110 PE pipe in Via Maddalena II	110	38.78
17	S3_District 8	Break of DN 110 PE pipe in Via Nazionale SS 290	110	44.54
18	S4_D1-D2	Break of DN 63 PE pipe in Umberto Square	63	58.05
19	S4_D2-D6 (I)	Break of DN 110 PE pipe in Via Roma	110	71.75
20	S4_D2-D6 (II)	Break of DN 110 PE pipe in Via Roma	110	70.29
21	S4_D2-MP	Break of DN 110 PE pipe in Via Nazionale SS 290	110	87.59
22	S4_D3-D6 (I)	Break of DN 63 PE pipe in Via Fontana	63	33.01
23	S4_D3-D6 (II)	Break of DN 63 PE pipe in Via Aquila	63	33.29
24	S4_D3-D8 (I)	Break of DN 63 PE pipe in Via Scarlata	63	31.72
25	S4_D3-D8 (II)	Break of DN 63 PE pipe in Via Scarlata	63	28.49
26	S4_D4-D5	Break of DN 110 PE pipe in Via Chiusa	110	63
27	S4_D4-D8	Break of DN 63 PE pipe in Via Lucchese	63	27.94
28	S4_D6-MP	Break of DN 160 PE pipe in Umberto Square	160	78.04
29	S1_MainPipeline	Break of DN 110 PE pipe in Via P.D' Aragona	110	4.28

Within group S_3 , the scenarios inside each district have been selected, so that the impact of the pressure drop and of the number of users affected is maximized. Typically, eight damaged events for every district have been randomly created, with the exceptions of District 7 where six scenarios have been selected and District 1 where 12 scenarios have been selected (largest district). Figure 8.16 shows the scenarios considered for District 6, while in Fig. 8.17 are plotted the average pressures for each scenario and compared to the average pressure in normal operating conditions.

During the selection of the scenarios for every District, it is generally noticed that the peripheral areas inside each District have less influence on the global district pressure when one pipe fails. However, other factors can also affect the scenario selection, such as the topographic features of the district, the number of users and the valve distribution etc. For example in District 1, because for almost all the assumed scenarios the average pressure level is the same, the scenario with the highest number of users without water service has been selected.

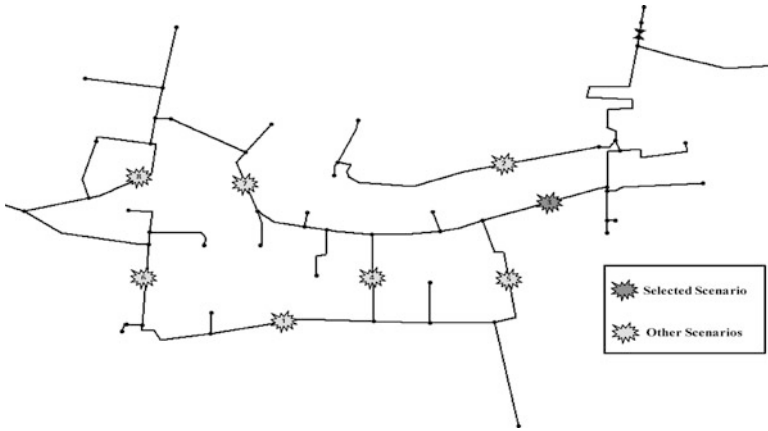


Fig. 8.16 Scenarios in district 6 for group S3

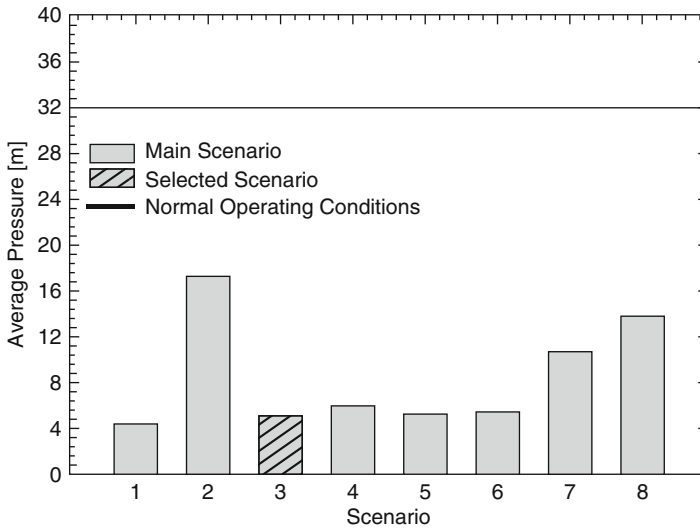


Fig. 8.17 Average pressure in district 6 for the eight failure scenarios in the district

8.3.9 Recovery Time and Restoration Process

In the case study, the control time T_{LC} is assumed equal to 48 h which is the time to repair the damaged pipe according to the emergency plan of the Water distribution provider in the region. According to the information provided by the operator (AcquaEnna S.C.p.A) of the WDN, after the earthquake, the first emergency operations (e.g. isolate the zone where the pipe is damaged) are completed within 1 h, while the repair operations, if the diameter is less than 600 mm, are completed

within a maximum of 12 h. An additional 24 h has been added, because that is the time necessary to inform in advance the residents of the repair operations. Finally, T_R has been assumed to equal 38 h (1 h has been added to include the uncertainties) and it is assumed constant for all the simulations.

8.3.10 Numerical Results and Lesson Learned

In Table 8.3 the resilience indicators are summarized, according to Eq. (8.20), Eq. (8.23) and Eq. (8.27) for the different scenarios selected. In the analyses, it is assumed that the water quality check (e.g. hardness, presence of contaminants, etc.) remains above the standards defined by the law and constant before and after the repair, therefore the index R_3 is not shown in the results. The index R_1 is a function of the number of households without water and it is lower in the districts where the pipe failure is selected, while it remains constant in other districts, because the effect of the pipe failure is confined in the district using valves. As expected, the lowest value of R_1 index is obtained with scenario 1, which corresponds to failure in the main pipeline. In this case, the seven districts supplied by the main pipeline, remain without water until the pipeline is repaired. This generates a drop of the function $F_1(t)$ and therefore of R_1 . The same observation applies to scenarios 21 and 28, which involve the main pipeline. The index R_2 is more sensitive than R_1 for the selected scenarios, because it is affected by the volume of water loss which is function of the pipe diameter and the location of the breakage. In fact, if the breakage affects a pipe which provides water to several households, during the repair operation when the pipe is isolated, the water tank level increase and so the value of R_2 .

For example, during Scenario 1, which corresponds to the main pipeline failure, the entire pipe is isolated and all districts are without water. Consequently, the water level in the tank increases because the seven districts are without water supply, and then the R_2 index increases. Scenario 9 (breakage at the input pipe of district 8) is the worst in terms of R_2 , because for the particular position of this pipe and for its diameter (110 mm), the flow rate loss is about 75 l/s and this leads to emptying of the St.Peter Tank. Because both indicators are equally important for describing certain scenarios, they have been combined together in a global index R which is the synthesis of the information obtained from R_1 and R_2 . Further considerations are necessary for the scenario 18 when the Index R_2 is evaluated. In this case, the failure is in the pipe connecting district 1 which is supplied by the Roof Tank and district 2 which is supplied by the St.Peter Tank, therefore, the index R_2 is determined using a weighted average which is given in Eq. (8.24) where w_1 and w_2 are weight coefficients of the Roof Tank and St.Peter Tank respectively.

Following the two approaches mentioned in previous section, the weights $w_1 = 0.3274$ and $w_2 = 0.6726$ are determined using the first approach, while $w_1 = 0.0693$ and $w_2 = 0.9307$ are determined using the second approach when they are proportional to the reserve capacity which is 31.62 m³ for the Roof tank and

Table 8.3 Resilience index summary for different scenario events

Scenario	R1	R2	R = R1R2	Scenario	R1	R2	R = R1R2	Scenario	R1	R2	R = R1R2
1	0.40	0.69	0.28	11	0.92	0.19	0.18	20	0.86	0.23	0.20
2	0.79	0.88	0.69	12	0.95	0.74	0.71	21	0.58	0.64	0.37
3	0.92	0.23	0.21	13	0.83	0.83	0.68	22	0.84	0.64	0.54
4	0.95	0.31	0.29	14	0.93	0.45	0.42	23	0.84	0.64	0.54
5	0.82	0.34	0.28	15	0.89	0.91	0.81	24	0.93	0.60	0.56
6	0.90	0.33	0.30	16	0.97	0.56	0.54	25	0.94	0.64	0.60
7	0.88	0.31	0.28	17	0.92	0.41	0.37	26	0.85	0.36	0.30
8	0.97	0.38	0.37	18	0.88	0.57	0.5	27	0.96	0.65	0.62
9	0.87	0.11	0.10	19	0.86	0.23	0.20	28	0.42	0.69	0.29
10	0.90	0.59	0.53					29	0.78	0.36	0.28

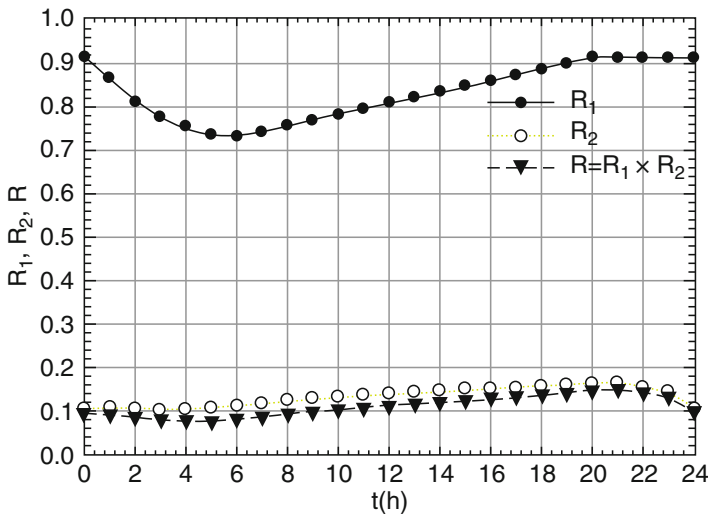


Fig. 8.18 Variation of resilience indices (a) R1, (b) R2 and (c) R depending on the instant when the failures happen during the day for scenario 9

424.82 m³ for San Peter tank, respectively. However, in all tables and figures the results related to scenario 18 refer to the second approach, which is more general.

The sensitivity of the Resilience indicators (R_1 , R_2 & R) to the time of the earthquake occurrence during the day is shown in Fig. 8.18 for the scenario 9. The Resilience Index R_2 , instead, does not have any significant variations with respect to the earthquake occurrence during the day. Instead, for index R_1 , if the earthquake occurs at 1 am and failure corresponds to scenario 9, then the St.Peter tank is emptied, because of the flow rate loss. However, because in the evening the demand flow is less than the input flow, the tank starts increasing its water level and in 24 h is able to cover the total demand flow. Instead, if the earthquake occurs at 6 am, the demand flow has its peak and the tank in less than 2 h decreases its water level until

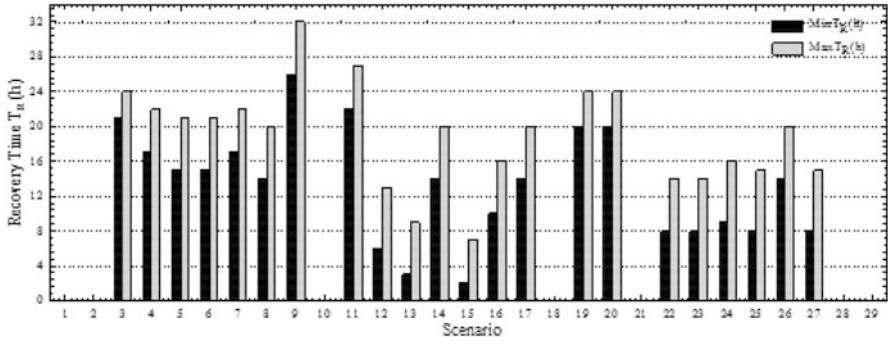


Fig. 8.19 Maximum variation of recovery time for all scenarios when the first restoration strategy (water tank closed) is applied

it empties to cover the demand and the flow rate loss. From that moment, the tank remains empty because the demand flow continues to be higher than the input flow. Only when the output flow is less than the input flow, does the water level begins to increase (Fig. 8.18).

8.3.11 Restoration Plans

Three different restoration plans have been proposed. The first restoration plan involves the closure of the tanks until the entire reserve capacity is recovered. The minimum and the maximum variation of recovery time T_R to restore the full capacity in the tanks for the different scenarios are plotted in Fig. 8.19. Please note that for the scenarios 1, 2, 10, 21, 28 and 29 the recovery time is not shown, because the reserve is automatically recovered during the time interval T_{LC} .

The maximum and minimum recovery time in Fig. 8.19 has been evaluated using the procedure described in Fig. 8.20 for scenario 12 where the tank water height vs. time (hours) right after the earthquake is plotted. The bold line represents the water level in normal operating conditions, while the gray line represents the water level when no recovery strategies have been applied. At the end of the control time T_{LC} , the final water height h_{Final} will be less than the reserve height $h_{Reserve}$ (4.47 m for the Roof Tank, 3.23 m for St. Peter Tank). This happens because under normal operating conditions, the final water height is higher than the water reserve height, because the reserve capacity of the tank is not used. However, when the pipe fails the water reserve capacity of the tank is used to satisfy the water demand, so the final water height will be lower than the water reserve height. The difference between these two values ($\Delta h = h_{Reserve} - h_{Final}$) has led to the construction of the gray dashed line in Fig. 8.20, which is the target to reach for recovering the reserve capacity. In particular, the grey line (No restore) is translated from Δh to have a curve that follows the water demand and that reaches the $h_{Reserve}$ at the end of the 48 h. The

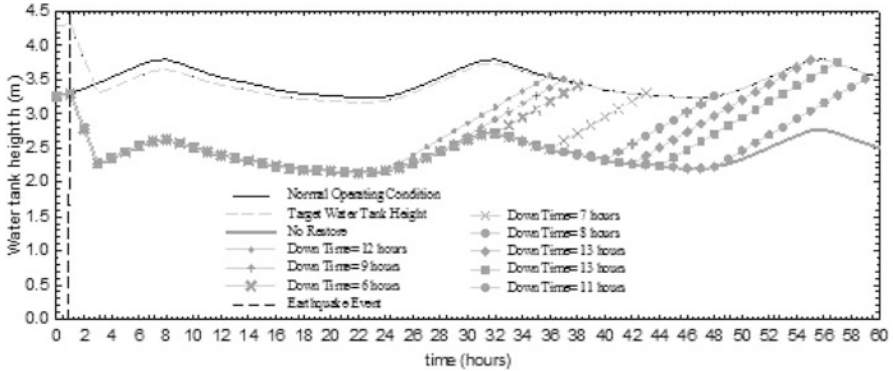


Fig. 8.20 Maximum variation of recovery time for all scenarios when the first restoration strategy (water tank closed) is applied

other curves correspond to different instants when the tank is closed. The straight lines derive from the assumption of constant water flow in the tank when it is closed, therefore they can estimate the time interval to recover the reserve capacity and when the entities suffer water outage. For example, in scenario 12, the maximum recovery time is 13 h and the minimum is 6 h. The minimum and the maximum recovery time will depend on Δh . With the restoration strategy above, no other costs of electricity due to the use of pumps must be added, but in that time interval, the users remain without water supply.

The second restoration plan involves the use of the maximum available flow from the pump station. Under normal operating conditions, the input flow to the distribution system is about 5.44 l/s. Neglecting the physiological water losses, the input flow in the roof tank is around 1.16 l/s, while the input flow in St.Peter tank is 4.28 l/s. In emergency conditions, the pump station can supply a maximum flow of 19 l/s. With this flow rate, the recovery times of the reserve capacity have been calculated for the selected scenarios, using the following equation

$$\frac{\Delta h \cdot A_T}{\Delta t \cdot (Q_e/1000)} = T_R(h) \tag{8.32}$$

where $\Delta h = h_{Reserve} - h_{Final}$ in m, A_T is the tank's area in m^2 , Q_e in l/s is the available flow to be added to recover the water reserve capacity, Δt is equal to 3600 s. In Fig. 8.21 the values of the recovery time T_R are shown for the second restoration plan. In the selected scenarios, the total reserve capacity which is recovered corresponds to the one of St.Peter Tank, that is equal to $Q_e = 13.56$ l/s, where $Q_e = (19 - 1.16 - 4.28) = 13.56$ l/s. Please note that for the scenarios 1, 2, 10, 18 and 28 the recovery time is not shown, because the reserve is automatically recovered. The higher recovery times are obtained for the scenarios with the lowest h_{Final} and consequently the lowest R_2 values. With this strategy, the recovery time T_R is reduced, but the cost of electricity, deriving from the use of pumps is increased.

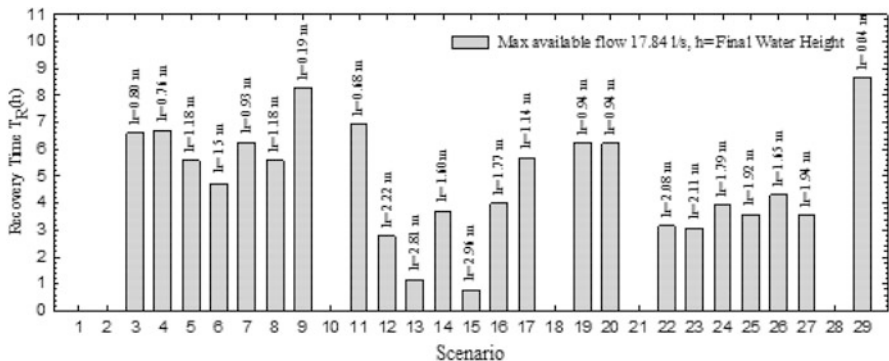


Fig. 8.21 Recovery time for the second restoration strategy with open water tank and the maximum available flow

The third restoration plan is a hybrid combination of the first two strategies. First, the water tank is closed for the first 7 h in the morning and then part of the available flow is used for recovering the water reserve capacity. The advantage of this restoration plan is based on the limited use of the available flow from the pump station and the reduced amount of downtime for the water tank, which will only be closed in the early morning, generating less discomfort for the residents. The available flow Q_e is obtained using the following equation:

$$Q_e = \frac{\Delta h \cdot A_T}{\Delta t \cdot T_R} \tag{8.33}$$

where the recovery time T_R is equal to 7 h (fixed), while $\Delta h = h_{Reserve} - h_{Final}$ will be higher than the value obtained in the second strategy, because the final water height increases after the closure of the tank. This strategy can be adopted for the scenarios in which the recovery time T_R is higher with respect to the other two strategies. In this case, the partial flow is limited to 7 h (at the time of the day when the demand is lower) as well as is limited the downtime of the tank. Please note that in this case the recovery time T_R is measured as sum of the period the tank is closed plus the period the pumps are operating. The use of the third restoration strategy produces an increase of the R_2 value, but also produces a decrease on R_1 value caused by the closure of the tank. The combined index R given in Eq. (8.24) does not change with respect to the condition when no retrofit strategies are applied.

For example, in scenario 12 the R_2 for the minimum recovery time (6 h) is 0.82; the corresponding R_1 is equal to 0.87 and then the combined index R is 0.71, which is the same when no restoration plans are taken into account. In this case, it is recommended to work with only one of the two indicators to appreciate the effect of the retrofit strategy proposed. These considerations also bring about the conclusion that the third restoration plan should be used only for scenarios where the recovery time T_R is short (e.g. scenarios 13, 15 and 29). The use of the second or

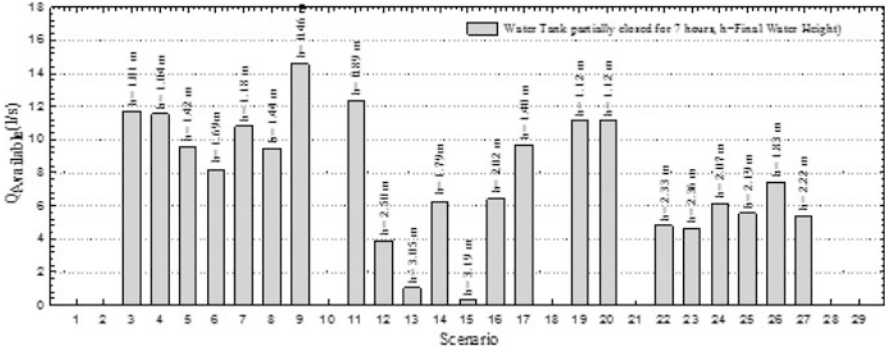


Fig. 8.22 Third restoration strategy with water tank partially Closed for 7 h and use of part of the available flow

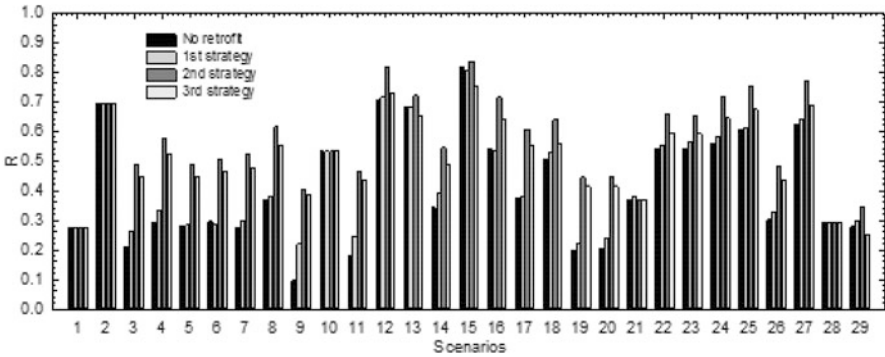


Fig. 8.23 Resilience index for the different retrofit strategies

third restoration plan produces an overall improvement of the indicators as shown in Figs. 8.21 and 8.22. In fact, with these strategies the index R_2 improves, while the index R_1 is maintained at the same level in the second strategy, and it undergoes a slight reduction in the third strategy. The improvement of the global index R with respect to the initial condition shows the validity of the selected retrofit strategies (Fig. 8.23).

Among the scenarios selected, scenario 18 is of interest, because in this case the two tanks (Roof and St.Peter) are working in parallel at the same time. This implies that the three restoration strategies should be applied on the two tanks simultaneously. For the first strategy, the recovery time T_r for the roof tank is between 3 and 9h, while for St. Peter tank is between 9 and 15h. For the second strategy, using the same weight coefficients described above, the flow in the roof tank and the flow in St.Peter tank are determined as weight average of the maximum available flow $Q_e = 13.56$ l/s. Using the second restoration plan the recovery times are 5h and 16min in the roof tank and 3h and 40min in St. Peter tank. For the

third restoration plan, the flow rate necessary to recover the reserve capacity is Q_e is 0.31 l/s ($h_{Final} = 3.52$ m) for the Roof tank, while for St.Peter tank Q_e is 5.8 l/s ($h_{Final} = 2.14$ m).

Scenario 29 also requires attention, because in this case the pipeline that supplies the St. Peter tank fails, so the tank is able to provide water to the distribution system for the first 32 h, but then it empties before the repair operations finish. In this case, the most suitable restoration strategies are the second and the third one. Once the pipeline has been fixed, the incoming maximum available flow permits the restoration of the reserve capacity in the water tank in about 9 h. For the third restoration plan, the available flow should be equal to 16.78 l/s. The restoration plan 1 cannot be used, because when the incoming pipe is under repair, no input flow can supply the tank which is closed, and the restoration of the reserve capacity doesn't occur.

So the lesson learned is that applying one strategy with respect to the other depends on several considerations such as the cost of electricity, the possibility to use the maximum available flow from the pumps, the extension of the tank downtime and its effects on consumers, etc.

8.4 Example 3: Gas Network

8.4.1 Introduction

The reliability assessment of infrastructure systems providing natural gas is an integral part of societal preparedness for unforeseen hazards (e.g. earthquakes, fire, etc.) and it has attracted great attention in recent years. In fact, a significant amount of damage has been observed especially in the gas distribution networks during recent earthquakes such as the 1995 Kobe, 1999 Kocaeli (Scawthorn and Johnson 2000), 1999 Chi-Chi (Chen et al. 2002), the 2011 Great East Japan Earthquake etc. These earthquakes occurred mainly close to urban areas and caused significant damage to buried pipelines because of their dimensions and because of the system vulnerabilities, due for example to aging and corrosion of rigid joints.

In the European Union, more than 20 % of the total energy consumption comes from natural gas (Montiel et al. 1996), which is currently one of the most important sources of energy. For instance, according to the national data in Italy from 1971 to 2006, the primary forms of energy include fossil fuels (i.e. coal, natural gas, and petroleum), which are responsible for most of the national electric energy supply, with most of the remainder being hydroelectric energy, and a smaller percentage being renewable sources (wind, solar, etc.). Then the gas distribution network has a significant impact on the Italian national economy; however, because of earthquakes and other extreme events such as landslides etc., it is often exposed to significant economic, social and physical disruptions.

One of the major hazards after earthquakes for gas pipelines is fire, because an escape of gas, either within a building or on a network, can result in a fire or explosion. The risk of fire or explosion due to gas leakages is significantly

higher inside a building than outside, however the hazard arising from gas leakages in a distribution system may be more severe than in the transmission pipelines, therefore the current section focuses on gas leakages in an urban gas distribution network. In fact, disruptions of the gas distribution network can induce significant consequences on the population and the economy of the community. The literature related to the seismic performance of the gas distribution networks has focused mainly on the seismic vulnerability of gas pipelines when subjected to permanent ground deformations and liquefaction (Jeon and O'Rourke 2005; Choo et al. 2007). More attention on the overall gas network performance has been provided by Shinozuka et al. (1999) which has focused on loss estimation methodologies for lifelines, considering loss of connectivity between substations, failure of substations and imbalance of the power system under a scenario earthquake in the Memphis area. Recently, Adachi and Ellingwood (2008) focused on infrastructure system interactions due to earthquakes using fault tree analysis and a shortest-path algorithm. When considering risk assessments methods for natural gas distribution networks, several approaches are available in literature, which can be grouped in *qualitative* and *quantitative* methods (Han and Weng 2011). *Qualitative methods* use indicators, which are based on pipeline length, flow rate, population density, external interferences, etc. Several approaches are available for qualitative methods such as Analytical Hierarchy Process (AHP), Event Tree Analysis (ETA), Data Envelopment Analysis (DEA), Fuzzy logic method (FL) (Markowski and Mannan 2009; Yuhua and Datao 2005). The limitation of these methods is that they can only identify the causes of the accidents, but are not able to identify the risk.

Quantitative methods are based on probability assessment, consequence analysis and risk evaluation of a gas distribution networks. This group includes the recent method proposed by Poljansek et al. (2012) which analyzed the seismic vulnerability of the gas and electric network from the topological point of view. However, the limit of these methods is that they fail to analyze the consequences of various accidents, which can cause different harms to people (Jo and Crowl 2008).

The studies summarized above consider the performance measures of the gas distribution network and other lifelines in general, while only a few studies on seismic risk analysis of gas distribution networks take into account all the aspects of the component of risk (hazard, vulnerability and loss), but none of them take into account the restoration process during the analysis. Therefore, further research is required to evaluate the economic and social consequences caused by the reduced functionality of a damaged gas distribution network and its consequences (Cimellaro 2013). In summary, this section introduces a performance assessment methodology for gas distribution networks including the restoration process right after an extreme event such an earthquake. This part is organized as follows:

First, this section outlines the motivations of the research and provides the formulations related to the seismic performance of the gas network. Second, the performance index is presented along with the required methodological steps for the natural gas distribution network. Then as a case study, a description of the Italian natural gas supply system is provided, both at the national and local level. This description includes the analysis of the restoration process. Third, the model's

assumptions in describing the network and the failure mode are described. Fourth, the method is applied to the gas distribution network of the municipalities of Introdacqua and Sulmona. These two small towns in the center of Italy were affected by 2009 earthquake, and have been used as case study to show the implementation issues of the proposed methodology. Different breakage scenarios due to an earthquake have been selected considering the disaggregated seismic hazard maps and the seismic damage assessment of the distributing elements. Then, the section analyzes the results of the numerical analysis and provides retrofit recommendations in practice. Finally, the major conclusions concerning the proposed performance assessment methodology of the gas distribution network are presented.

8.4.2 Performance Assessment Procedure of Natural Gas Distribution Network

As described in Chap. 2, the performance of a system can be measured through a unique decision variable defined as “Resilience” (R), which combines other dimensions (economic losses, casualties, recovery time, etc.) which are usually employed to judge the performance of a network. In other words, resilience is an index measuring the capacity to sustain a level of functionality or performance for a given infrastructure or community over a given period range and it can be defined graphically as the normalized shaded area underneath the functionality of a system $Q(t)$ given in Fig. 8.24.

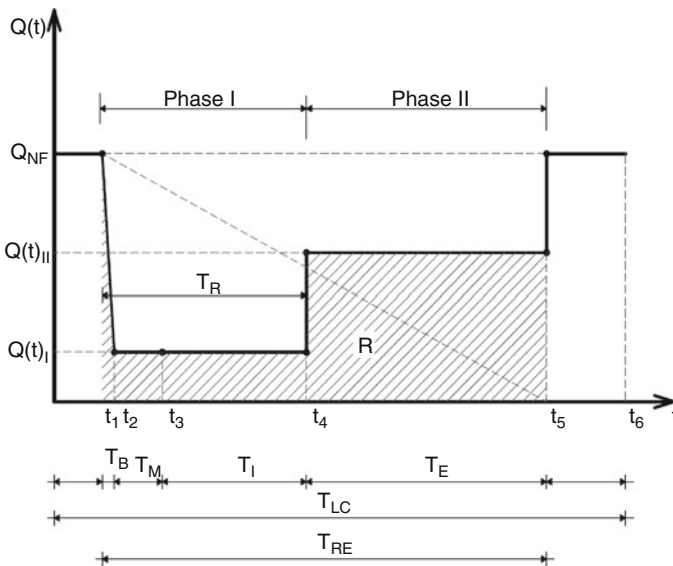


Fig. 8.24 Functionality of natural gas network after disruption

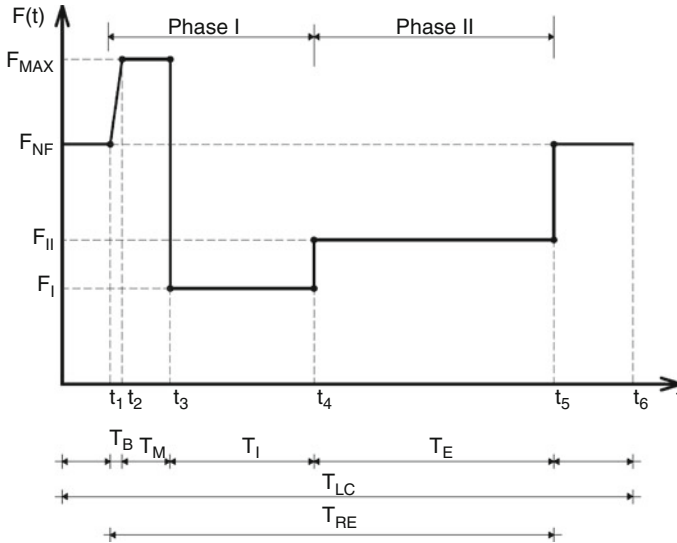


Fig. 8.25 Flow rate inside the pipelines after disruption

As shown in this figure, the Control period range T_{LC} has been divided in two phases, where Phase I corresponds to the period range necessary to repair the distribution network and go back to partial service after the extreme event. During this phase, there is no gas network in service, because the valves are closed, so pipes are empty. Phase II corresponds to the period range right after the first emergency intervention on the gas network, during which the network is partially in service, before reaching full restoration. Different period ranges can be distinguished inside the two phases: T_B = network balancing period range; T_M = operating period range which should be less than 1 h according to the ITALGAS regulations; T_I = repair period range to bring the network to partial service in Phase II; T_E = transition period during which the network is partially in service, which corresponds to Phase II; $T_{RE} = (T_B + T_M + T_I + T_E)$ = recovery period range. The gas flow in the network after disruption is shown in Fig. 8.25.

After the pipeline breaks, the flow in the network increases to the maximum system capability F_{MAX} (Phase I) during the balancing period T_B . Then, after repairing, the network goes back to partial service and the flow reduces to lower values with respect to the flow F_{NF} in normal operating conditions. The evaluation of Resilience using Eq. (8.5) necessitates the definition of the serviceability or functionality of the analyzed system.

Communities depend heavily on the availability of distributed civil infrastructure systems, such as the gas distribution networks. During the emergency, the serviceability of such systems can be measured by the ratio of the satisfied customer demand to the total customer demand within the area served. However, the serviceability can be directly correlated with the gas flow and the length of the

operating pipes. These are quantities that can be determined more easily during numerical analysis using commercial software available in the market. Therefore, based on these practical considerations, a new functionality index $Q(t)$ of the gas distribution network is proposed as a combination of the normalized gas flow rate and the total length of the network in service before and after the event. Therefore, $Q(t)$ of the gas network is given by the following expression

$$Q(t) = \left[w_1 \cdot \frac{F(t)}{F_{NF}} + w_2 \cdot \frac{L(t)}{L_{NF}} \right] \cdot 100; \quad (8.34)$$

where $\begin{cases} \text{if } t_3 \leq t \leq t_4 & w_1 = 1; w_2 = 0; \\ \text{if } t_4 \leq t \leq t_5 & \forall w_1 \in [0, 1]; w_2 = 1 - w_1; \end{cases}$

where F_{NF} = gas flow in normal operating conditions; L_{NF} = length in km of the gas network working in normal operating conditions; $F(t)$ = gas flow right after the extreme event and after the valve closure by the operator ($t \geq t_3$); L = length of gas network in partial service after the extreme event (e.g. earthquake etc.); w_1, w_2 = weight factors. The weights in Eq. (8.34) model the importance of the two combined indicators, which take into account both pipeline length and flow rate and can be determined using the *Reliability Engineering Theory* and the *Grey Correlation Theory*. Therefore, the evaluation of the weights is based on the real data of gas pipeline network such as operation information, environmental information and statistical analysis of historical accident data (Han and Weng 2011). However, when no information is provided, such as in the case study described below, both values can be assumed equal to 0.5. In fact, it has been proven that there is not much difference in the final results of the resilience index if more complex methods are provided for evaluating the weights, such as the one proposed by Cimellaro et al. (2014b).

8.4.3 Restoration Model

The restoration model and the recovery time T_{RE} , which corresponds to the time necessary to restore the gas distribution network to the initial conditions, are essential components for the resilience quantification of the gas network. In particular, T_{RE} is a parameter characterized by high uncertainties due to the difficulty of evaluation and distinguishing between the shutoff time and the repairing time. The restoration phase of the components of the gas distribution network has been evaluated using the technical reports made by ITALGAS (the distribution network operator in the region) which describes the repair and replacement activities following the earthquake. Unfortunately, the technical reports describing the repair activities right after the earthquake in the month of April 2009 are not available, because assistance and emergency support interventions were the main operations undertaken during the first month, with a limited activity of repair/restoration of the gas network.

However, on the reports from the following months, it could be observed that right after the main shock and during the first phase of the emergency, the gas network was shut down to avoid explosions, gas leaks and fires, and to allow emergency vehicles and Search and Rescue teams to act in the safest way possible. To ensure this priority, the entire network in the affected area was shut off via the closure of the three operating M/R stations in less than 2 h. In the days following the event, all the gas valves external to each residential building were closed as well. The recovery phase following the earthquake started gradually opening first the gas flow in the medium pressure network, after in the low-pressure network and finally in the external end-user valves of each residential building which were previously closed. The restoration process, which lasted a few days, was the only option for the emergency management authorities, because emergency shutoff valves were not inserted in the network. The presence of these valves would have avoided the shutdown of the entire network and limit the damaging effects as shown in the numerical example in this section.

In detail, the service reactivation was managed in the following four steps: (1) seal verification; (2) nitrogen check; (3) repair of damaged pipes and/or valves; (4) reopening. In the seal verification phase, the detection of broken pipes and/or the possible joint slip-off was made, acting in the first instance, from node to node, and further segmenting the network when necessary. The adopted strategy ensured the restoration of more than 90 % of the gas network in 3 months after the earthquake. Using the same restoration strategy described above, which is based on real information available from the most recent earthquake in the region, it has been assumed a recovery period T_{RE} of 4 months for the scenario events considered in the analysis in order to restore full functionality. It is important to clarify that during 2009 earthquake in the region, no damage to the gas facilities were detected; therefore the adopted restoration time which is a function of the failure mode, is valid only for pipeline failures due to permanent ground deformations which is the one that was observed during 2009 earthquake.

Other countries like Japan have developed advanced disaster countermeasures; therefore, the recovery time is shorter. In the case of 2011 Tohoku earthquake in Japan, the eight Japanese municipalities were able to go back to full functionality in less than a month. The reason for this fast recovery is justified from the analysis of Tokyo gas distribution network. About 4000 seismographs are installed in different locations throughout the supply area so that local gas supply for each district is shut off automatically in the event of a major earthquake. Segmentation of the gas network is carried out at two levels: one for medium-pressure (MP) lines and another for low-pressure (LP) lines (Fig. 8.26). Emergency shutoff of gas networks can be carried out for these units, called K-blocks for medium-pressure lines and L-blocks for low-pressure lines. In this way, it is possible to separate areas with more damage from areas with less damage, thus minimizing the impact on the less affected areas. This method can be used to quickly shut off the gas supply to the affected areas only. For the areas where the gas supply is shutdown, personnel are trained to restore the supply as early as possible.

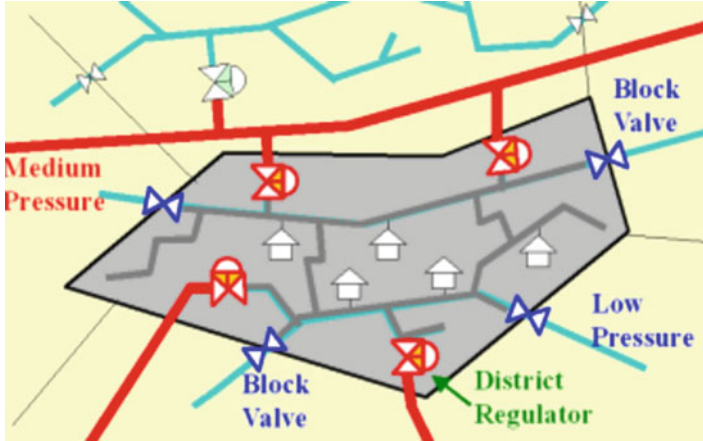


Fig. 8.26 Japanese district supply system

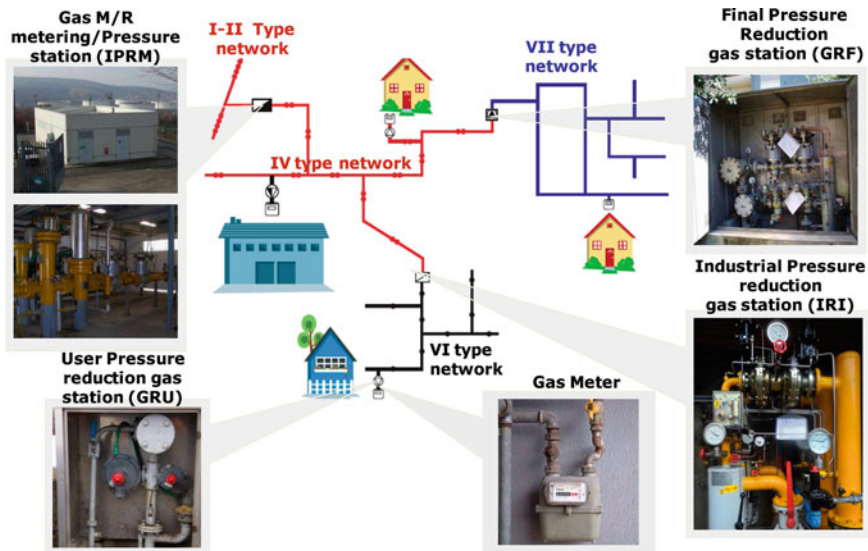


Fig. 8.27 Scheme of Italian gas network distribution system

8.4.4 Description of the Italian Natural Gas Supply System

The Italian gas supply system is divided into *transport*, *storage* and *distribution*. Principal components of the Italian gas supply system include (Fig. 8.27): (i) high-pressure transmission lines; (ii) metering pressure reduction stations (M/R); (iii) medium pressure distribution networks; (iv) reduction groups; (v) low pressure distribution network; (vi) demand nodes; (vii) gas meters.

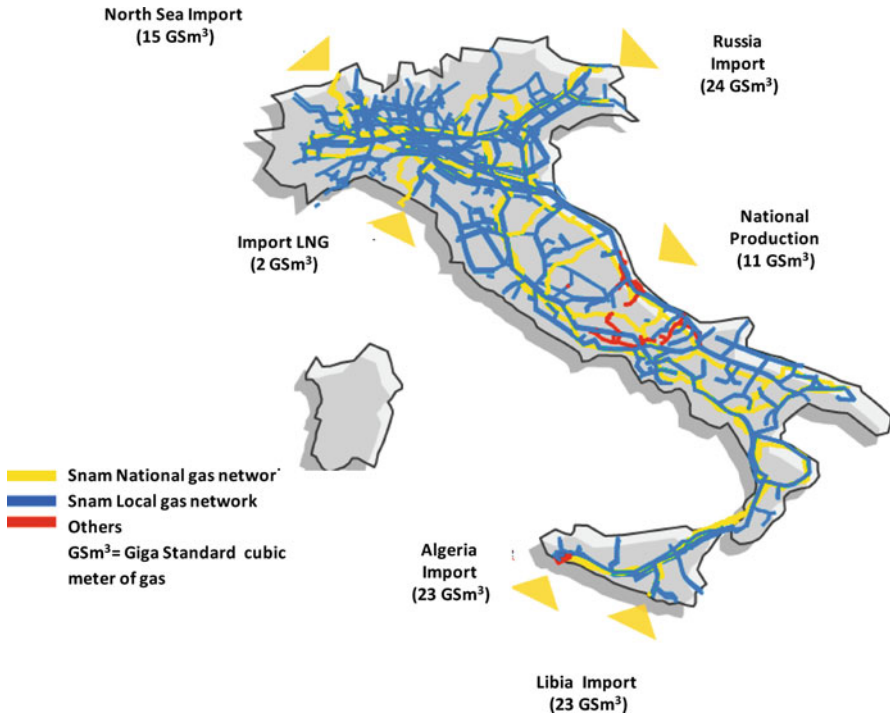


Fig. 8.28 National gas distribution network in Italy

The natural gas injected into the Italian National Network is mainly imported. It is injected into the National Network via seven entry points (Fig. 8.28) where the network joins up with the import pipelines (Tarvisio, Gorizia, Passo Gries, Mazara del Vallo, Gela) and the LNG regasification terminals (Panigaglia, Cavarzere).

Domestically produced gas is injected into the Network through 51 entry points from the production fields or their collection/treatment plants. Natural gas storage fields are also connected to the transmission network. The transportation of natural gas is a service connected with the pipelines coming from Russia, Northern Europe and North Africa, but the re-gasification plants and the production and storage points is located in Italy. From these points, the gas is delivered to local distribution utilities, large industries and power plants where the gas is redelivered to the end users. Pipes used in Italy for the gas distribution network are made by polyethylene (thermoplastic resin belonging to the family of polyolefin), steel and cast iron. However, cast iron pipes are used less nowadays, due to gas leakage and cracks resulting from aging.

The Italian gas distribution network is divided into 8 classes according to the gas pressure (Fig. 8.27). The RE.MI. “REgolazione di MISura” in (Italian) are metering pressure reduction stations which supply natural gas in the distribution network and allow the physical connection between the high pressure network and

the distribution network to the customer. Pressure reduction systems are designed to adjust the flow rate calibrating the gas supply pressure to a predetermined value, which depends on: (i) supply pressure of the utilities; (ii) type of downstream network.

Network Modeling of the Gas Distribution System

SynerGEE is commercial software (Advantica_Ltd. [Germanische-Lloyd](#)) for gas pipelines which analyzes close conduit networks using a set of non-linear mathematical equations that form the model of the piping system. This uses nonlinear fluid dynamic equations, which provide levels of pressure, flow etc. The first Kirchhoff law is used to analyze the mesh network and is given by

$$F_j = \sum_{i=1}^{\text{facilities adjacent to node } j} F_i + FN_j, j = 1 \dots NN \quad (8.35)$$

where F_i = is the facility flow, FN = the node flow and the summation is for all facilities incident to node j ; j = is the node number in the network, NN = is the total number of nodes in the network.

The iterative process inside the program solves simultaneous equations, and as the algorithms that govern these equations get closer to the solution, the program converges. In detail, the program solves for node pressure as a function of externally imposed system flows and the flow equation used. The fractional tolerance value used during a steady-state analysis to determine whether facility pressures and flows are considered solved is 0.0005. Each node equation expresses the pressure in terms of system demands, supplies, and physical parameters. The flow is evaluated using the general gas flow equation in a horizontal pipe which can be obtained after some manipulations that can be found in the papers of Hyman et al. (Hyman et al. (1975)) and Finch and Ko (Finch and Ko (1988))

$$F = C \frac{T_b}{P_b} D^{2.5} e \left(\frac{P_1^2 - P_2^2}{LGT_a Z_a f} \right)^{0.5} \quad (8.36)$$

where $C = 0.0011493$ (77.54 in US Customary System (USCS)); D = diameter of pipe in mm (*in* USCS); e = pipe efficiency; G = gas specific gravity; L = pipe length in km (mi USCS); P_b = base pressure at the standard gas state in kilopascal (PSIA USCS); P_1 = inlet pressure in kilopascal (PSIA USCS); P_2 = outlet pressure in kilopascal (PSIA USCS); T_a = average temperature in K (R USCS); T_b = base temperature in K (R USCS); Z_a = compressibility factor; f = Fanning friction factor. Usually pipes are not horizontal, so if the slope is smooth, a correction factor H_c for the static head of fluid can be incorporated in Eq. (8.36) and determined as follow:

$$F = C \frac{T_b}{P_b} D^{2.5} e^{\left(\frac{P_1^2 - P_2^2 - H_c}{LGT_a Z_a f} \right)^{0.5}} \quad (8.37)$$

where:

$$H_c = \frac{c_1 g (H_2 - H_1) P_a^2}{Z T_a} \quad (8.38)$$

where $c_1 = 0.06835$ (0.0375 USCS); Z = compressibility factor; g = local acceleration due to gravity; P_a = average pipeline pressure; H_1 = upstream hydraulic head; H_2 = downstream hydraulic head. Once all the nonlinear continuous equation matrices related to each node have been solved and node pressures reach the value of the convergence tolerance, the flow is calculated using Eq. (8.37).

8.4.5 Simulation of Failure Modes of Pipelines

The failure of the gas distribution network depends on the number of pipe breaks/km of pipe and the damage states of different facilities such as the gas metering/pressure stations, the user pressure reduction gas stations, the storage tanks and the other support facilities, which are described by their fragilities. However, after the analysis of the technical reports of ITALGAS, the seismic damage assessment of the facilities was not taken into account in the analysis, while the simulations are focusing on the seismic damage assessment of the distributing elements. Furthermore, from past observations, about 3% of natural gas pipeline failures in USA are due to the effect of ground movements by seismic events. The main seismic hazards that are responsible for pipeline failure can be described as:

1. Seismic wave propagation;
2. Abrupt permanent ground displacement (faulting);
3. Permanent ground deformation (PGD) related to soil features:
 - Longitudinal PGD;
 - Transverse PGD;
 - Landslide.
4. Buoyancy due to liquefaction.

Because of the geological settings in the Sulmona region, it was decided to consider only pipeline failure generated by PGD. Furthermore, the main failure modes of continuous pipelines (which are the one used in the Sulmona region) can be summarized as: (1) **tensile failure**; (2) *local buckling*; (3) *beam buckling*. Among them, the most common in steel pipes is the local buckling; therefore, the failure mode due to local buckling has been considered in the simulations. Local buckling in pipeline occurs due to local instability of the pipe wall. Once the wrinkling instability of the pressurized shell is initiated, all the subsequent wave propagation and geometric distortion caused by ground deformation tend to concentrate at these

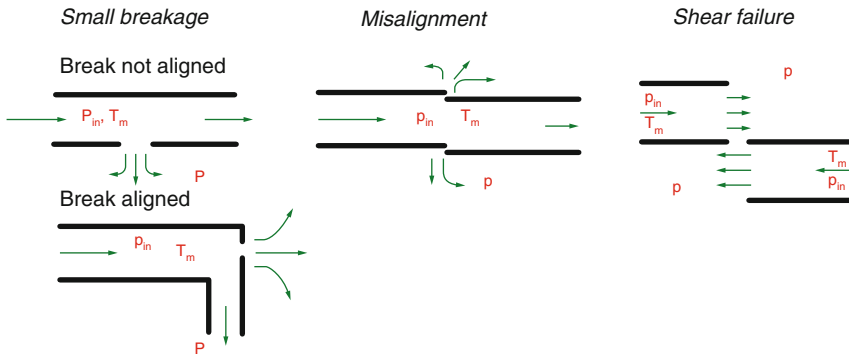


Fig. 8.29 Assumption of the pipeline failure mechanisms. P_{in} = upstream pressure, T_{in} = upstream temperature; P = downstream pressure

wrinkles. Thus, the local curvature in the pipe wall becomes large and leads to circumferential cracking of the pipe wall and leakage. Different disruptions due to local buckling of the gas distribution network in the town of Sulmona and Introdacqua are simulated assuming pipes shear failure in the medium and low-pressure network. Two failure locations have been considered: (i) Failure in the main pipes; (ii) Failure in the mesh network. The failure in the main pipes results in gas leakage from a single trunk of pipe, which is connected to the network. The shear failure in the mesh results in gas leakage from both sides of the pipes, therefore the total flow of gas released at the end of the transient discharge is equal to twice the flow released from each section. The pipe failure mechanism has been analyzed defining the typology and the value of gas flow released in the atmosphere. The Dutch TNO model (TNO 1997) has been used to describe the disruption behavior of pressurized pipelines. The gas is modeled using the equation of ideal gases and the flow is considered adiabatic and isentropic. Three types of failure mechanisms are considered in the model (Fig. 8.29):

- Small break;
- Misalignment;
- Shear Failure.

Small break failure appears when upstream pressure remains constant during the gas leakage, while *shear failure* appears when the pressure inside the pipes goes to zero.

8.4.6 Description of the Natural Gas Distribution System in the Town of Sulmona, Italy

The natural gas distribution system that involves the municipalities of Sulmona and Introdacqua is managed by ITALGAS, the largest gas distribution network operator

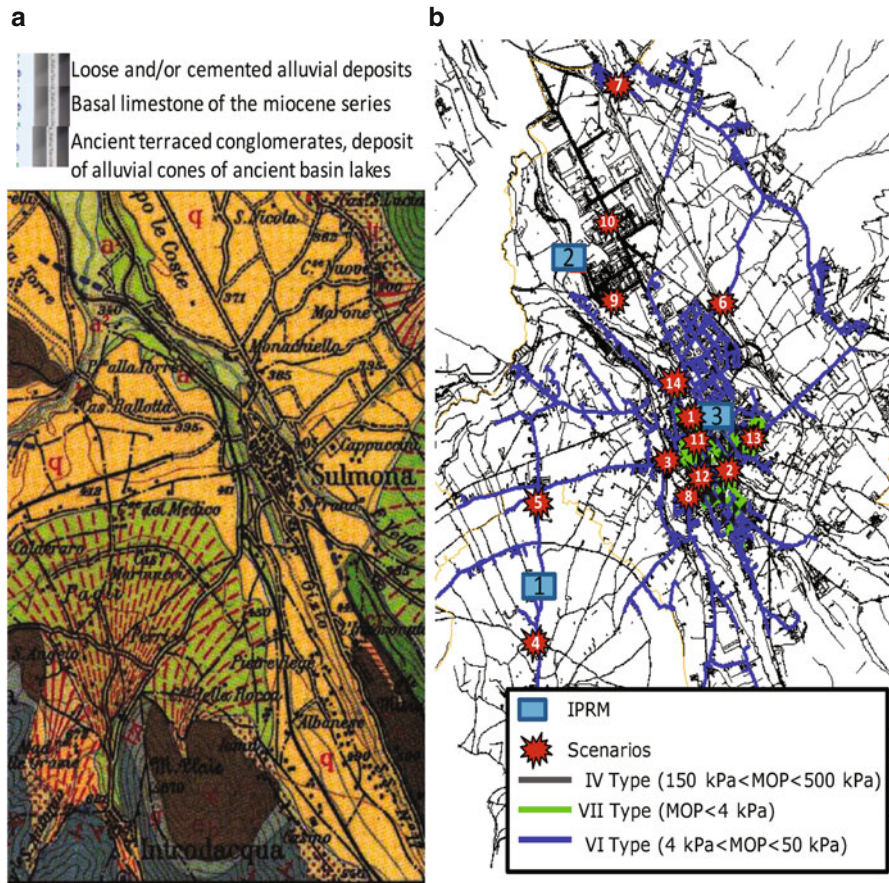


Fig. 8.30 Natural gas distribution network of the town of Sulmona and Introdacqua with the (a) geological map of the region and (b) the considered scenarios

Table 8.4 Metering/pressure reduction (M/R) stations

Identification code	Location	DN	Nominal flow for a Min. pressure of 600 kPa (103 m ³ /h)	Maximum flow (103 m ³ /h)
IPRM 1	Via La Torre, Introdacqua	DN 50	4.6	1.734
IPRM 2	Via del Lavoro, Sulmona	DN 80	11.5	0.290
IPRM 3	Via Lapasseri, Sulmona	DN 100	18.5	7.380

in Italy. Figure 8.30 shows the gas distribution network in the municipalities of Sulmona and Introdacqua.

The connection of Sulmona and Introdacqua distribution medium-pressure network (MP=64 MPa) to the national high-pressure transmission lines is operated via three Metering/Pressure Reduction (M/R) stations (RE.MI.) which are listed in Table 8.4 and shown in Fig. 8.30. Two of the three M/R stations in the region

Table 8.5 Final pressure reduction gas stations (GRF)

Identification code	Location	Diameter	Nominal flow (m ³ /h) for a pressure of		Simulated flow (m ³ /h)
			50 kPa	150 kPa	
GRF4	Sulmona – Via Mazzini/Trento	Dn50	800	1600	34
GRF5	Sulmona – Via Freda	Dn50	800	1600	184
GRF6	Sulmona – Via Celidonio	Dn50	800	1600	139
GRF7	Sulmona – Via d’Eramo	Dn50	800	1600	238
GRF8	Sulmona – Via Sauro	Dn50	800	1600	114
GRF9	Sulmona – Via Mazzini	Dn50	800	1600	113
GRF10	Sulmona – Via Maiella	Dn50	800	1600	163
GRF11	Sulmona – Via Circ.ne Orientale	Dn50	800	1600	205
GRF12	Sulmona – Via Pansa (ponte)	Dn80	1800	3600	407
GRF13	Sulmona – Pza Faraglia	Dn80	1800	3600	167
GRF14	Sulmona – Pza Iacovone	Dn65	1250	2500	246
GRF15	Sulmona – v.le Comunale	Dn65	1250	2500	384
GRF16	Sulmona – Pza Capograssi	Dn80	1800	3600	156
GRF17	Sulmona – via Comacchiana	Dn50	800	1600	164

Table 8.6 Pipeline length according to the material and pressure

Material	Total (km)	IV Type 150<MOP<500 (kPa)	VI Type 4<MOP<50 (kPa)	VII Network MOP<4 (kPa)
Steel	109.83	8.91	77.37	23.55
Polyethylene	27.11	0.39	23.04	3.67
Total	136.94	9.29	100.42	27.23

(IPRM1 and IPRM3) are connected to the national network of SNAM pipelines, which operates the high-pressure transmission lines in Italy. RE.MI. stations are hosting internal regulators and mechanical equipments (heat exchangers, boilers and bowls) under which the gas undergoes the following operations and processes: (i) gas preheating; (ii) gas-pressure reduction and regulation; (iii) gas odorizing; (iv) gas-pressure measurement (8.5). The 14 final pressure reduction gas stations (GRF) of the gas network considered in the case study are listed in Table 8.5. The distribution network of the two municipalities has a total length of approximately 136.9 km of which 109.8 km are steel coated pipes and 27.1 km are polyethylene pipes. Within the two groups, distinction can be made based on the pressure distribution, as shown in Table 8.6. Steel pipes have welded connections and are provided with a coating of bitumen-based material, but they are also currently protected cathodically with system of sacrificial sink at impressed current, equipped with automatic feeders.

8.4.7 *Geological Settings*

The Sulmona Basin is one of the larger and more external Quaternary continental intramontane basins of the Central Apennines thrust belt, and like other intramontane basins it is partially filled by continental Quaternary deposits. The chain is characterized by a complex Meso-Cenozoic paleogeographic setting and by a complicated Neogene-Quaternary structural setting (Fig. 8.30). In particular, the Sulmona valley is characterized by alluvial soils with loose natural deposits in the ancient basin lake, therefore the consolidation of cohesion-less fills and loose natural deposits during earthquakes can cause permanent ground deformations (PGD). Permanent deformations can generate differential ground movements, which can result in bending and tension or compression, depending on the relative orientation of the motion and the pipeline layout.

Minor liquefaction effects were observed in the region during 2009 L'Aquila earthquake where small volcanoes of liquefied sand appeared in the Aterno Valley. However, the liquefaction effects in the region were rather limited and they did not interest the municipality of Sulmona. This can be partially justified because according to the empirical relationships available in literature (Galli 2000), the maximum distance from the epicenter to have the liquefaction effect is 40 km. Instead the epicenter of 2009, L'Aquila earthquake had a distance of 67 km from the town of Sulmona. Additionally, the analysis of the historical earthquakes catalog in the region indicated that liquefaction effects are never observed through the centuries in the region.

From the empirical observations of the areas affected by liquefaction in Italy, it can be concluded that liquefaction appears:

- when the magnitude of the earthquake is bigger than 5.5;
- the layers are less than 15 m deep;
- the water depth is near the surface (less than 3 m).

The Sulmona region is characterized by stable geological conditions. The soil type is B, which corresponds to unsaturated firm soil (the water level is more than 3 m deep below the ground). So based on the observations above and references to literature, it can be concluded that the liquefaction effects and the possibility of pipe break caused by peak ground deformation (PGD) due to liquefaction (ALA 2001; Porter 1992; Eguchi 1983) can be neglected in the region.

8.4.8 *Seismic Intensity*

Sulmona is located on an 800 km long segmented normal fault system that accommodates the extensional deformations of the Apennines chain. Large earthquakes have occurred historically in this zone in 1349, 1461 and 1703 resulting in epicentral macro seismic intensities (MCS) between IX and X. According to 2003 Italian

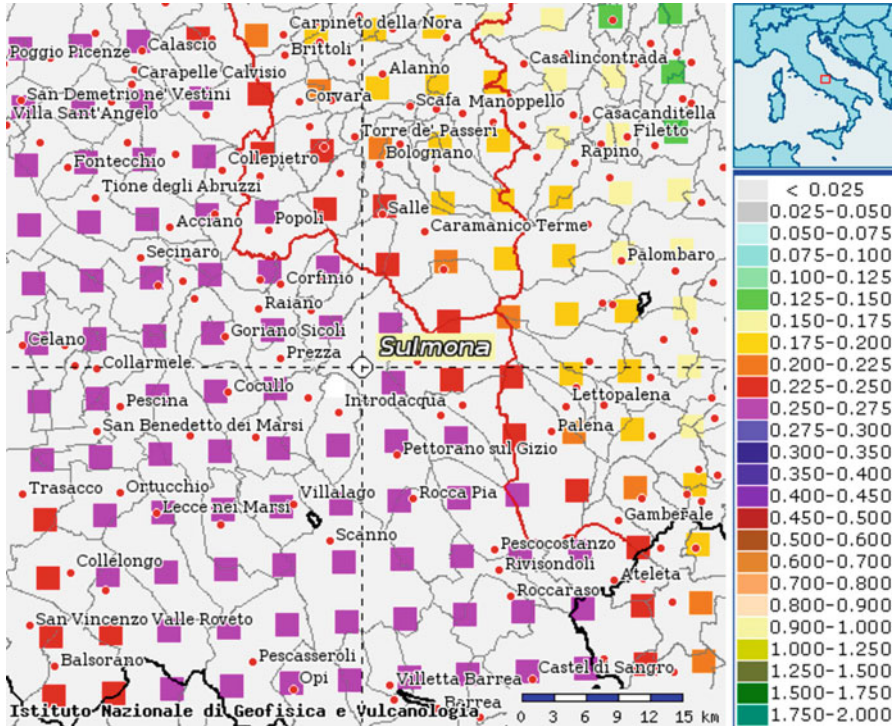


Fig. 8.31 Median peak ground accelerations for Sulmona region for 10 % PE in 50 years

seismic code (OPCM-3274, 2003), the town of Sulmona belongs to the second category zone (first category is the highest) with a PGA on stiff soil equal to 0.25g. The current Italian code (NTC-08, 2008) defines the PGA as a function of the geographic coordinates at the site; therefore, Sulmona has a PGA of 0.261g for soil type A (stiff), and for a probability of exceedance of 10 % in 50 years (Fig. 8.31).

Probabilistic seismic hazard analysis (PSHA) provides estimates of mean annual rate of occurrence or annual probability that ground motion exceeds a specific intensity over a range of intensities; therefore, this tool has become a common seismic risk assessment tool. However, results from PSHA are sometimes difficult for non-specialist decision makers to interpret, because the significant earthquake threats corresponding to the low probabilities of interest (e.g. 0.0004/year) represents an aggregation of earthquake events rather than one specific earthquake. Furthermore, the aggregated event cannot describe the spatial variability of damaging intensities across a region due to any particular severe earthquake, so it might not be appropriate for assessing risk of a distributed gas network system. On the other hand, a risk assessment based on scenario events avoids these difficulties, but the risk is conditioned on the occurrence of the scenario event. Appropriate scenario events can be determined from disaggregation, which identifies the dominant seismic events in

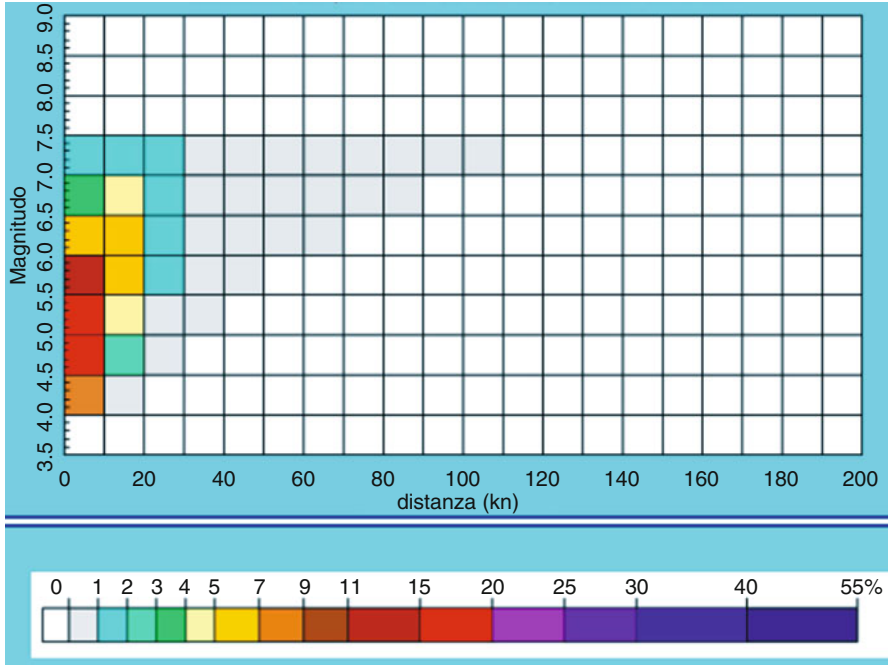


Fig. 8.32 Deaggregation hazard map for 22 % PE in 50 years (return period = 233 years)

the region contributing to an earthquake hazard of 22 % in 50 years. The appropriate scenario event used to illustrate the network vulnerability analysis in this section is determined from the disaggregation hazard maps provided by the Italian National Institute of Geophysics and Vulcanology (INGV) (Spallarossa and Barani 2007) (Fig. 8.32).

The maps corresponding to a return period of 230 years (22 % PE in 50 years) are selected based on the observations of the historical earthquake catalog in the region, which clearly shows the occurrence of an earthquake every 200–250 years. The identified dominant seismic event has a $M_w = 5.56$ with an epicentral distance of $R = 9.56$ km. The authors believe that inexperienced decision makers may more readily appreciate the threat to an urban area from such an event than the threat from 22 % in 50 year earthquake. Then, the seismic intensity at a site is determined using the Ambraseys et al. (2005) attenuation relationship which describes the median ground motion intensity as function of M_w and R , modified by local soil conditions, therefore the final peak ground velocity (PGV) at the site is 13.91 cm/s. PGV was determined because it is a common measure of earthquake intensity for assessing distributed civil infrastructure damage.

Median PGV contour maps for the deaggregated event in the Sulmona region are not provided from the Italian National Institute of Geophysics and Vulcanology (INGV). However the PGV contour map of April 6th, 2009 earthquake in the region

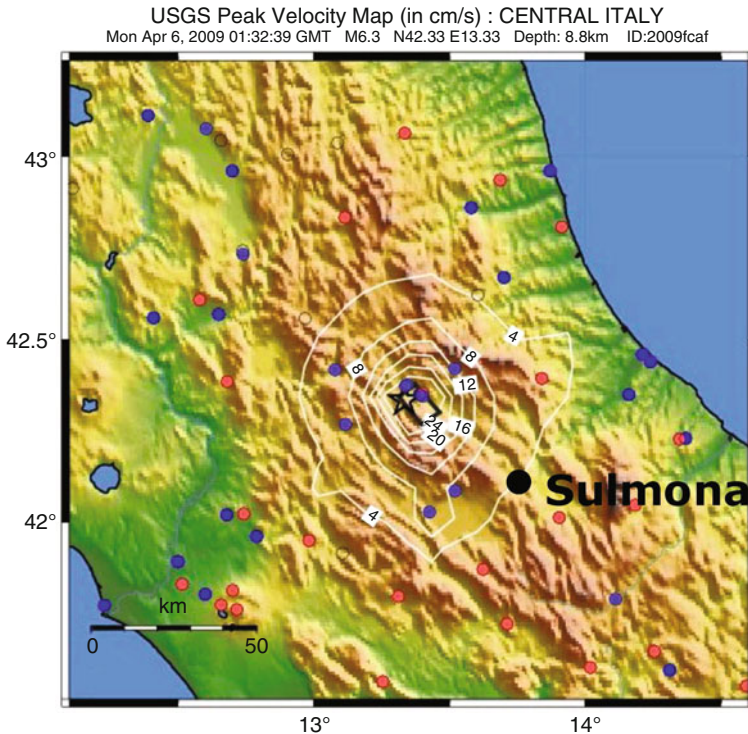


Fig. 8.33 Peak velocity map of April 6th, 2009 Central Italy earthquake

is available and shown in Fig. 8.33. It can be observed that the measured peak ground velocity at the site of Sulmona is approximately 4 cm/s, which is lower than the median value obtained at the site with Ambraseys et al. (2005) attenuation relationship. Because the 2009 earthquake is a single event, which can be below the median value, the PGV obtained by Ambraseys et al. (2005) has been used in the analysis.

8.4.9 Seismic Damage Assessment of Distributing Elements and Scenario Selection

In most of the available approaches for seismic vulnerability assessment, the pipeline damage is typically expressed in terms of the numbers of repairs occurring per unit length of pipeline. The available methods for seismic behavior of pipelines are generally based on observations about earthquake properties and pipeline response and damage. Several research projects have been developed across the world to assess the seismic loss in gas pipelines (Yamin et al. 2004). The Federal

Emergency Management Agency (FEMA) developed a general methodology to assess hazard vulnerability, called HAZUS (FEMA 2005). However, in the HAZUS model, it is assumed that pipeline damages caused by earthquakes are completely independent from the pipeline size, class, and mechanical specifications. Based on previous studies, damage to pipes caused by strong ground motion in the guidelines prepared by the American lifeline Alliance (ALA 2001) is given by

$$RR = K(0.00187)PGV \quad (8.39)$$

where RR = repair ratio, which is the number of pipe breaks/305 m (1000 ft USCS) of pipe length, K is a coefficient determined by the pipe material, pipe joint type, pipe diameter and soil condition and PGV = peak ground velocity which has the units of in/s USCS.

Pipes installed in Sulmona region are mainly non corrosive steel pipes with arc welded joints of diameters between 50 and 250 mm; therefore following the values provided in literature (ALA 2001) it is assumed $K = 0.3$, for steel pipes and $K = 0.5$ for polyethylene small pipes.

The repair ratio, using Equation and the peak ground velocity of the dominant seismic event, is respectively $RR = 0.003$ for steel pipes and $RR = 0.005$ for polyethylene pipes. Under the assumption that the seismic intensity leads to a uniform demand on a gas pipe connecting two facilities, the number of pipe breaks can be expressed by the Poisson probability law:

$$P[N = n] = e^{-RRL} \frac{(RRL)^n}{n!} \quad (8.40)$$

where N = a random variable denoting the number of occurrences of a broken pipe, $n = 0, 1, 2$, number of pipe breaks, RR = repair ratio at which the event occurs evaluated by Eq. (8.39), and L = length of pipe segment analyzed (expressed in terms of 1000-ft segment USCS), RRL = average number of occurrences occurring over length L of pipe that is being examined. The pipe segment is not able to deliver gas when there is at least one pipe break, therefore the failure probability of the pipe segment can be expressed by the exponential distribution:

$$P_f = 1 - P[N = 0] = 1 - e^{-RR \cdot L} \quad (8.41)$$

Even if the pipe failures are correlated, it is assumed that the events describing failure of each pipe segment are statistically independent, which is a necessary assumption to use the Poisson law. The probability of having a certain number of breaks in the steel and polyethylene pipes is shown in Fig. 8.34.

Due to computational resource limits, only 14 scenarios have been selected. In particular, the number of scenarios with one, two or three breaks has been selected to be proportional to the respective probability given in Fig. 8.34. However, the extension of the steel pipes is larger than the polyethylene pipes, which is only 20% of the entire network. Therefore, assuming a weight factor of 0.2 in the probability

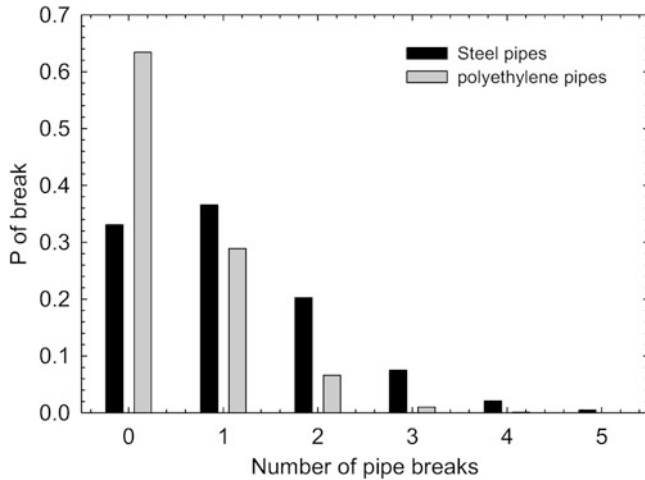


Fig. 8.34 Probability of pipe breaks in the Sulmona gas distribution network

of failure of polyethylene pipes and a weight factor of 0.8 in the steel pipes, then the probability of having one break in the polyethylene pipes is below 6 %.

Furthermore, additional evidence that polyethylene gas pipelines are sufficiently ductile and tough to sustain significant earthquake effects is also given by their good performance during Kocaeli (Izmir) earthquake (O'Rourke et al. 2000) and during l'Aquila earthquake. Finally based on the observations above, no breaks in the polyethylene pipes have been considered. Instead, according to Fig. 8.34, the most probable event for the steel pipes is the one corresponding to one pipe break, therefore we have 10 scenarios with one-break, three scenarios with two-breaks and one scenario with three-breaks, are selected.

Once the number of scenarios with one, two and three breaks has been selected, then their locations need to be determined within the gas distribution network. The locations have been selected based on engineering judgment and following what described in literature (ALA 2001). For example, continuous pipelines which are built with rigid welded joints, have shown generally good performance, therefore scenario events have been selected to address mainly leakage problems at the joint locations caused by poor quality welds or the presence of corrosion at the joint location. The scenarios have been selected by also considering the structural vulnerabilities of the gas distribution network that in several points is passing over bridges. Bridge collapse scenarios (1-2-3-7-8) have been selected since these links are considered vulnerable points of the road network and are coupled with the gas network sharing the same vulnerabilities. For all the other cases, it is assumed that what triggers the pipe failures are the permanent ground deformations and soil failures between two different soil layers during the ground shaking. For example, the scenarios 4, 5, and 6 (8.7) have been located at the intersection between the layers of alluvial deposits and ancient terraced conglomerates as shown in the geological map of the region in Fig. 8.30.

The 14 shear failures mechanisms of the gas distribution network have been selected in both the medium and in the low-pressure network. In particular, scenarios 1 and 3-4-5-6-7-8 correspond to shear failure in pipes of type VI ($4 \text{ kPa} < \text{MOP} < 50 \text{ kPa}$, where MOP = maximum operating pressure). Scenarios 9-10 correspond to shear failure in pipes of type IV ($150 \text{ kPa} < \text{MOP} < 500 \text{ kPa}$). Scenarios 11-12-13-14 correspond to shear failure in pipes of type VII ($\text{MOP} < 4 \text{ kPa}$).

In all the selected scenarios, only physical damages in the pipelines are considered, while damage to the facilities (e.g. gas reduction stations etc.) is not considered in this section, because no damage to the gas facilities are observed in the recent 2009 earthquake which affected the same region.

8.4.10 Scenario Earthquake and Numerical Results

Simulations have been performed considering the maximum flow per hour evaluated during the phase of maximum gas consumption which for the Sulmona is $9107 \text{ m}^3/\text{h}$, considering the daily gas flow behavior shown in Fig. 8.35 which is evaluated from the comparison between summer and winter annual gas consumption in the region provided by ITALGAS.

Listed in Table 8.5 are the values of gas flow, pressure and speed in the final Pressure Reduction stations (GRF) obtained from the numerical simulations in normal operating conditions. Then, for each damage scenario shown in Fig. 8.30 the flow, pressure and speed of the gas inside the distribution network are also evaluated. The gas flows F , resulting from the 14 damage scenarios in correspondence of the pipe breakage, are given in Table 8.7.

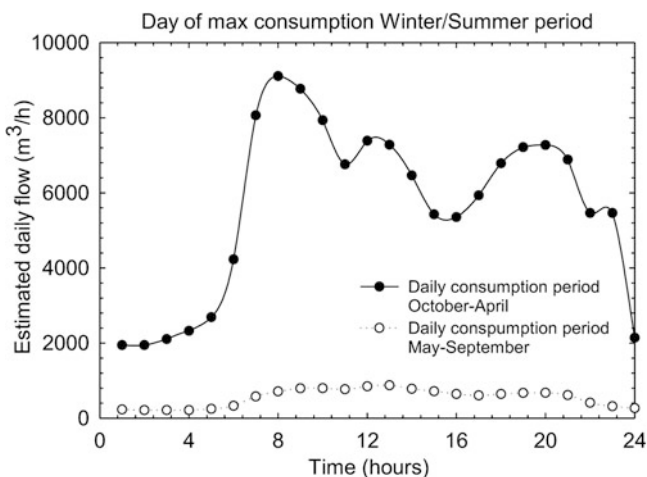


Fig. 8.35 Estimated daily gas flow during the day of max consumption in summer and winter period

Table 8.7 Brief description of the scenarios considered in the analysis

Scen.	Location	N. breaks	D nom.	Di (mm)	Max. OPE pressure (kPa)	P (kPa)	F ($10^3\text{m}^3/\text{h}$)
1	Collapse of the bridge in Via Iapasseri	1	DN 200	209.1	VI network $4 < \text{MOP} < 50$	49.3	10.512
2	Collapse of the bridge in Via Fiume	2	DN50	54.5	VI network $4 < \text{MOP} < 5$	35.5	0.648
			DN65	70.3	VII network $\text{MOP} < 4$	2.23	0.569
3	Collapse of the bridge in Via Arabona	1	DN150	160.3	VI network $4 < \text{MOP} < 50$	36.3	5.616
4	Collapse in Via Case del medico	1	DN200	209.1	VI network $4 < \text{MOP} < 50$	49.9	10.548
5	Collapse in Via Torrone	1	DN250	261.8	VI network $4 < \text{MOP} < 50$	48.0	16.344
6	Collapse in Via Lomaccio	1	DN200	209.1	VI network $4 < \text{MOP} < 50$	48.0	10.404
7	Collapse of the bridge in Via Bagnaturo	1	DN100	107.9	VI network $4 < \text{MOP} < 50$	44.1	2.700
8	Collapse of the bridge in Via Stazione	1	DN150	160.3	VI network $4 < \text{MOP} < 50$	33.8	5.544
9	Collapse in Via del Lavoro	1	DN100	107.9	IV network $150 < \text{MOP} < 500$	500	10.224
10	Collapse in Via dell'Industria	1	DN150	160.3	IV network $150 < \text{MOP} < 500$	500	22.572
11	Shear failure in DN50 steel pipe	1	DN50	54.5	VII network $\text{MOP} < 4$	2.0	0.382
			DN50	54.5	VII network $\text{MOP} < 4$	2.18	5.724
			DN150	160.3		2.18	0.662
12	Shear failure in DN50 and DN150 steel pipe	2	DN50	54.5	VII network $\text{MOP} < 4$	2.18	5.724
			DN50	54.5	VII network $\text{MOP} < 4$	2.18	0.662
			DN150	160.3		2.18	0.662
13	Shear failure in DN50, DN65 and DN100 pipe	3	DN50	54.5	VII network $\text{MOP} < 4$	2.25	2.610
			DN65	70.3		2.25	1.109
			DN100	107.9		2.25	0.666
14	Shear failure in DN65 and DN100 steel pipe	2	DN100	107.9	VII network $\text{MOP} < 4$	2.25	2.610
			DN100	107.9	VII network $\text{MOP} < 4$	2.25	2.610
			DN65	70.3		2.25	1.109

Table 8.8 Gas flow and length of gas network operating after the extreme event

Scenario	FI (103 m ³ /h)	FII (103 m ³ /h)	LI (km)	LII (km)
1	0.164	4.053	9.297	73.508
2	0.164	9.107	9.297	136.942
3	0.164	8.927	9.297	134.200
4	0.164	8.927	9.297	127.949
5	0.164	8.781	9.297	109.652
6	0.164	6.375	9.297	120.318
7	0.164	8.174	9.297	135.038
8	0.164	9.107	9.297	136.942
9	8.942	8.967	127.645	136.942
10	8.942	9.097	127.645	134.987
11	6.374	8.435	109.713	130.715
12	6.374	8.402	109.713	124.496
13	6.374	8.519	109.713	131.599
14	6.374	8.402	109.713	134.942

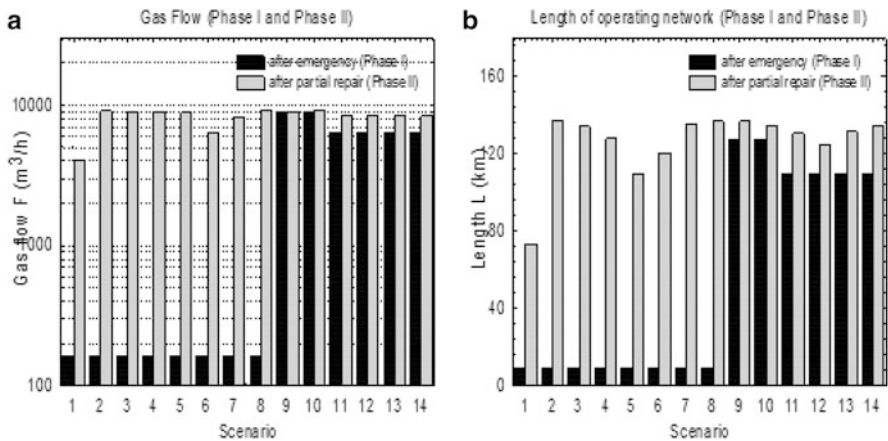


Fig. 8.36 (a) gas flow and (b) length of operating network after emergency and after partial repair

In Table 8.8, the gas flow and the length of operating network, respectively, are shown during the two phases for the different scenarios. In the medium pressure distribution network A (type VI), which corresponds to scenario 1–8, both the flow and the length of the operating network drops drastically in the hours right after the earthquake, while significant recovery is achieved after the partial repair (Phase II) of the network Fig. 8.36a, b. Then, three types of protective systems have been considered for retrofitting the gas distribution network:

- Seismic Automatic Gas shutoff Valves (ESV) (a–b);
- Excess Flow Automatic Gas Shutoff Valves (EFV) (-c);
- Manual shutoff Valves installed in correspondence of gas meter and/or underground gas connections.

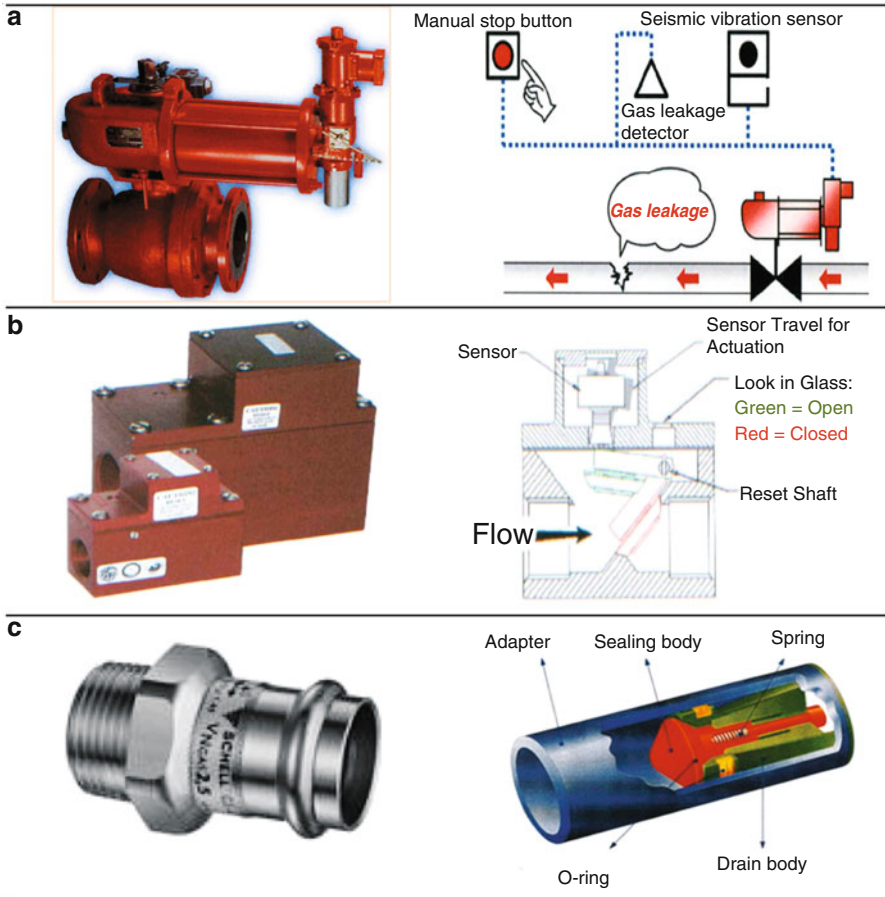


Fig. 8.37 (a) Emergency shutoff valves in the distribution network (by Tokico Technology Ltd); (b) AGV – Series Horizontally Mounted Earthquake gas shutoff valves; (c) Excess flow valves (EFV)

The first type has a seismic sensor (Fig. 8.37a, b) which is able to shut-off the network when there is an earthquake event and a predefined acceleration threshold is exceeded, or if there is a remote command, which is able to interrupt the gas flow in certain parts of the network to evaluate potential damage caused by earthquakes. When the valve closes, it can be opened after inspection only manually. The second type, *Excess Flow Automatic Gas Shutoff Valves* (EFV) are inserted in the M/R stations and they work when predefined flow rates are increased due to gas leakage (Fig. 8.37c). They can also be adopted near the end users and they shut off the flow rate if the downstream flow exceeds a certain threshold. They will automatically re-open again when the gas flow goes back to normal operating conditions. Since after an earthquake, these valves will most likely experience power outages, the

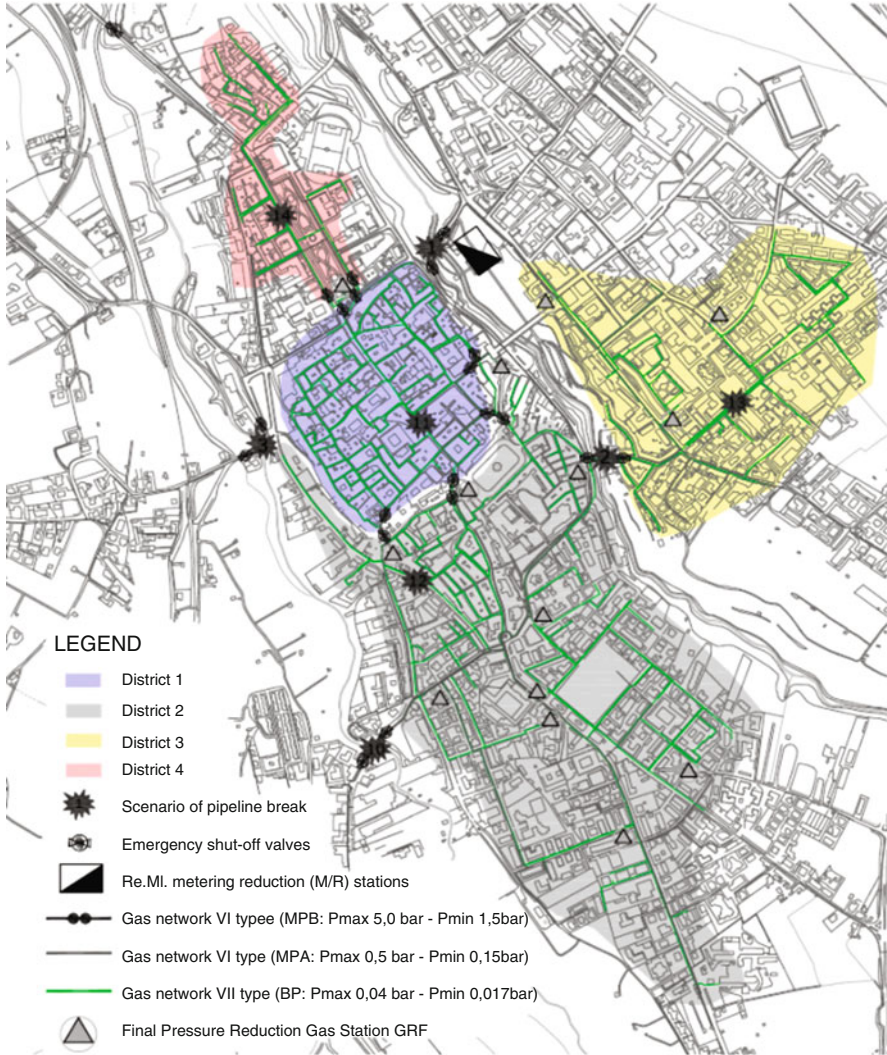


Fig. 8.38 Location of emergency shut-off valves in downtown Sulmona according to the districts

above-mentioned retrofit measures will have rechargeable batteries or accumulators to operate during the emergency.

The emergency shutoff valves (ESV) have been located near bridges, which can potentially collapse after earthquakes and in critical points inside the network. For example, the valves have been located to isolate the four districts that compose the gas distribution network of the town of Sulmona as shown in Fig. 8.38.

In addition, two flow dividers are also installed in both Metering/Pressure Reduction (M/R) stations, to divide the flow in different pipelines, and to control the

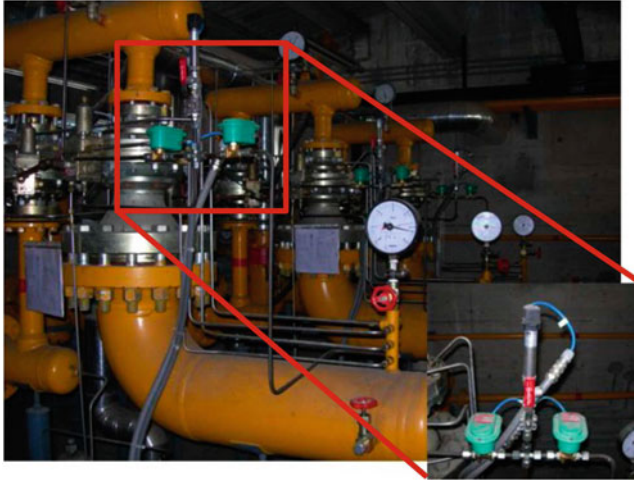


Fig. 8.39 Flow dividers installed in a M/R station

gas flow remotely, using an electric valve that decides the flow based on the actual flow and the pressure values (Fig. 8.39). In this way, both the acoustic emissions and the quantity of gas used can be reduced.

Finally, in all the pressure reduction gas stations valves that can control the gas flow remotely are also installed. In summary, the retrofit system that has been tested is composed of:

- Thirty two emergency shutoff valves (ESV);
- Two flow dividers;
- Sixteen valves at the pressure reduction gas stations.

The retrofit system described above has been tested for the 14 different scenarios; therefore, the results of the simulations are used to evaluate the resilience index before and after retrofit. The resilience values are listed in Table 8.9 and shown in Fig. 8.40.

Analyses show a relevant increment of the resilience index, an average of about 78 % especially when breaks happen under the medium pressure A distribution network (type VI – 4 kPap50 kPa). Instead, the increments are more modest, with about 13 % on average in the low-pressure network (type VII – p4 kPa). No significant increments of resilience has been observed before or after retrofit when pipe breaks happen in the medium pressure B distribution network (type IV – 150 kPap500 kPa) (Fig. 8.40). As shown in Table 8.9, the flow dividers (Fig. 8.39) do not improve the resilience index during the emergency as effectively as the emergency shutoff valves installed along the pipes, which improve the performance of the gas network for all the scenarios (Fig. 8.40). In particular, the resilience improvement is relevant in scenarios 1, 2 and 3, which correspond to bridge collapse as shown in Fig. 8.40. The functionality of the gas distribution network described

Table 8.9 Resilience index summary for different scenario events

Scenario	Resilience index (%)			
	Before retrofit	Flow dividers	Shutoff valves	After retrofit
1	11.35	11.45	52.53	52.63
2	11.80	11.83	99.77	99.81
3	11.35	11.45	97.50	97.60
4	34.44	34.87	94.32	94.75
5	34.44	34.87	89.42	89.65
6	17.35	17.53	80.83	81.02
7	14.46	14.61	93.89	94.03
8	11.35	11.45	99.32	99.42
9	94.30	94.73	96.61	97.04
10	94.30	94.73	96.61	97.04
11	83.33	83.38	95.76	95.81
12	80.78	81.21	91.60	92.03
13	80.98	81.38	93.92	94.34
14	81.27	81.62	94.59	94.95

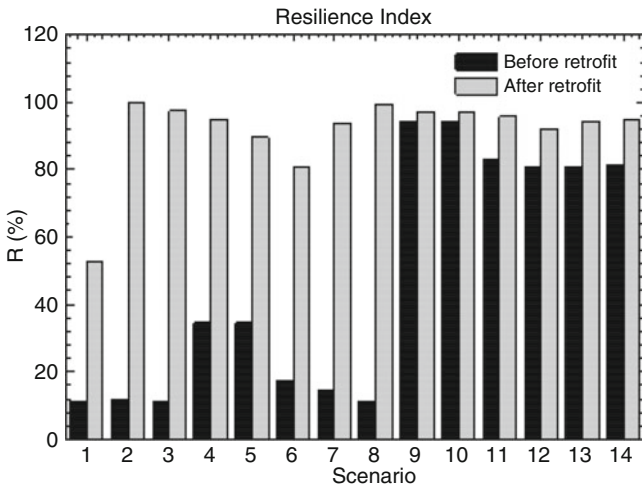


Fig. 8.40 Resilience index for the different scenario events before and after retrofit

by Eq. 8.34 related to scenario 2 is shown in Fig. 8.41, where the length of the operating network in the municipality of Sulmona, before and after retrofit assuming the bridge collapse in Via Fiume, is also shown.

From the simulated analyses, it appears that the worst scenarios correspond to shear failure on the medium-pressure network, which has a dramatic effect in the performance of the gas network, especially right after the earthquake event. The entire network performance can be improved by the insertion of Emergency Shutoff Valves, which allow dividing the gas network of Sulmona into four districts as

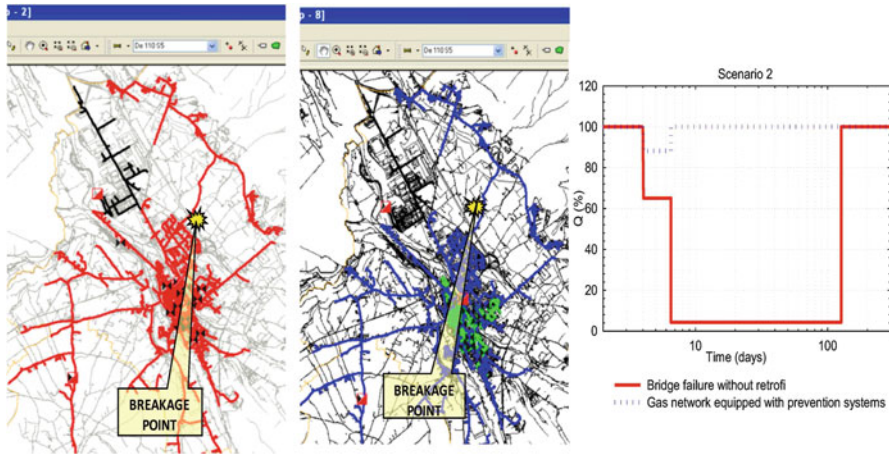


Fig. 8.41 Bridge collapse (scenario 2) of gas network w/ and w/o prevention systems

shown in Fig. 8.38. As a result of this division through the insertion of valves, it is possible to improve the resilience index of the gas distribution network by about 80 %, especially when failure happens in vulnerable elements of the network like bridges or shear failure of pipeline happen in the medium-pressure network.

The analyses performed require a number of assumptions on the spatial correlation of the seismic intensity. Epistemic uncertainties in response to distributing elements and in strong ground motion are not modeled; nor are any covariance in seismic intensity that may exist at adjacent points within the network considered. Furthermore, the inclusion in the analyses of the interdependency effects among other infrastructure systems could also have significantly affected the serviceability and resilience of the gas network. Future research, which is beyond the scope of this report, will focus on extending the model to determine the potential impact of these additional factors on the gas network serviceability and on the mitigation of seismic risk.

8.5 Example 4: Electric Power Network

Electric power is essential for almost every kind of urban and economic activity. Hence, the failure of the electric power network can cause important social as well as economic disruptions. These failures can have several origins such as natural disasters, terrorist attacks or technical accidents. Its damage can provoke huge losses and due to this fact it is imperative to be able to anticipate potential power system failures and try identifying efficient mitigation strategies.

Modeling the effects of electric power disruption is a complex problem which combines different sectors such as: civil, electrical, mechanical and economical and

social science disciplines. In fact it is necessary to assess how damage to individual pieces of electric power equipment affects power flow across the network, how the damage would be repaired, how electric power would be restored; and on the other hand it is necessary to calculate how the loss of electric power would affect households or business.

Fragility curves for electrical power equipments such as circuit breakers, transformers, buses in the transmission network and disconnected switches are used to study the seismic resilience of the power systems. Restoration models can also be developed by calibrating the restoration data of the case study earthquake. So, the restoration process can be simulated, taking into account the restoration process of the transmission equipments.

An added difficulty is that the electric power systems, as other urban infrastructures, are spatially distributed across a wide area. This fact increases the difficulty in simulating the network. In addition, it has to be taken into account that the hazard of study is not only spatially variant across a broad area, but it is also spatially correlated. This means that traditional probabilistic methods cannot be used for these spatially distributed networks.

It is important to carry out an in-depth study of the transmissions systems. Typically, a utility power system is integrated by generating stations, transmission systems and distribution networks. At the receiving stations there are many electric and mechanical components such as circuit breakers, transformers, lightening arresters, disconnected switches, current transformers, coupling voltage transformers, potential transformers, wave trap and circuit switches. All these components are integrated to transmission lines through buses at nodes. These transmission lines are the links between generating stations and distribution systems, and they lead to other power systems. If the voltage between two buses is different, then there must be at least one transformer between them. The node is an element that facilitates the movement of electric power and is protected by buses, circuit breakers and disconnected switches. Its configuration is complex and redundant to minimize the chance that the transmission lines become disconnected from the power network.

8.5.1 Seismic Performance of Power System

Several methods are available in literature to analyze the seismic performance of an electric power network. Below is shown one of the possible step-by-step procedure:

- Define all the earthquake scenarios and use the appropriate attenuation law to get the spatial distribution of the PGA;
- Simulate the state of damage of an equipment (e.g. transformer, etc.) with the fragility curves with and without rehabilitation for each scenario earthquake using Monte Carlo techniques;
- Simulate the state of damage of the transmission network for each scenario earthquake;

- The power flow is calculated using the IPFLOW code with the next network failure criteria:

1. Imbalance of power: supply/demand ratio outside the range;

$$1.05 \leq \frac{\text{Total supply}}{\text{Total demand}} \leq 1.1 \quad (8.42)$$

2. Abnormal voltage;

$$\left| \frac{V_{\text{int act}} - V_{\text{damaged}}}{V_{\text{int act}}} \right| > 0.1 \quad (8.43)$$

3. Frequency change;
4. Loss of connectivity.

- The seismic performance of the power network is evaluated in terms of percentage of power supply and households and business with power affected by the earthquake. The percentage is relative to the performance under the intact system condition;
- It is possible to develop a seismic risk curve. This curve plots the probability that the system performance will be reduced by more than a specific value due to the hazard, i.e. an earthquake;
- Examine the system performance with and without rehabilitation;
- Determine the effectiveness of rehabilitation;
- Develop risk curves for the loss of Gross Regional Product (GRP).
- Perform the power flow analysis 20 times under each scenario earthquake by using Monte Carlo techniques involving the fragility curves. Then take the average over all 20 simulations.

8.5.2 Risk Assessment of Power Systems

The “risk curves” graphically summarize the risk in terms of likelihood of performance degradation during a disaster. These curves are generated for performance parameters associated with different dimensions of resilience, including societal, economic, organizational and technical.

8.5.3 Risk Curves

The reduction in power supply, the reduction in GRP or the number of households without power following an earthquake are risk measures which are all related to technical, societal and economical dimension. These curves show the percentage of

reduction in the activities mentioned before. As for the details of evaluation in GRP, readers are referred to Shinozuka and Shi (2003/2004).

Percentage P_w of power supply

$$P_w = \frac{\sum_{m=1}^M \sum_{n=1}^N Pd(m, n)}{\sum_{m=1}^M P(m)} \times 100 \% \quad (8.44)$$

Percentage P_{wo} of reduction in power supply

$$P_{wo} = 100 \% - P_w \quad (8.45)$$

Percentage H_w of households with power

$$P_w = \frac{\sum_{m=1}^M \sum_{n=1}^N Rd(m, n) \times Hshld(m)}{\sum_{m=1}^M Hshld(m)} \times 100 \% \quad (8.46)$$

Percentage H_{wo} of households without power

$$H_{wo} = 100 \% - H_w \quad (8.47)$$

where m represents service area number; n is the simulation number ($1, 2, \dots, N$); $Pd(m, n)$ is the power output in service area m under n -th simulation; $P(m)$ is the power amount in service area m under normal conditions; $Rd(m, n)$ is the power amount ratio in service area m under the n -th simulation; and $Hshld(m)$ is the number of households in service area m .

8.5.4 Comparison Between Classical and Global Indicators of Power Distribution Networks

Reliability analysis of power networks is becoming more frequent nowadays, therefore the methods to assess it is also changing as well. In the past, *classical reliability indicators* in the field of electric networks were used such as:

1. failure rate λ (year⁻¹)
2. mean failure duration τ (h)
3. probability of failure-free operation R (-)
4. probability of failure Q (-)
5. mean time between failures t_S (h)

The *failure rate* is usually expressed as number of failures per time unit (year). The *mean failure duration* is given in hours (h) or days. The *probability of failure-free operation* and *probability of failure* are given as a proportional number (decimal fraction) or are given in per cents. The *mean time between failures* is stated in days or years and is a ratio of the total time of operation to the total number of failures during this time. The *mean time between failures* is proportional to the inverse value of the rate of failures. However, nowadays, the so-called *global reliability indicators* are starting to be applied increasingly, because they can be understood more easily from the energy customer's point of view and they are easy-to-determine from the analysis of individual power outages. Furthermore, classical reliability indicators are used mainly when the reliability indicators of the individual elements of the reliability diagram are known and this lead to the determination of the reliability of the electric network in a certain point. Instead if the reliability of the electric network in a given area wants to be determined, then global reliability indicators should be used. Examples of these global indicators are the following:

1. **SAIFI** = System Average Interruption Frequency Index (int./year. cust) = Total number of customer interruptions/Total number of customers served
2. **SAIDI** = System Average Interruption Duration Index (h/year. cust) = Customer interruption durations/Total number of customers served
3. **CAIFI** = Customer Average Interruption Frequency Index (int./year. cust) = Total number of customer interruptions/Total number of customers interrupted
4. **CAIDI** = Customer Average Interruption Duration Index (h/year. cust.) = Customer interruption durations/Total number of customer interruptions = SAIDI/SAIFI
5. **CTAIDI** = Customer Total Average Interruption Duration Index (h/year. cust) = Customer interruption durations/Total number of customers interrupted
6. **ENS** = Total Energy Not Supplied (kwh/year.) = Unserved Energy **UE**.
7. **AENS** = Average Energy Not Supplied = (kwh/year. Cust.) = Total energy not supplied/Total number of customers served
8. **LOLP** = Loss of Load Probability = The probability that the total production in system cannot meet the load demand

SAIFI indicator, in principle, coincides with the failure rate λ . The frequency of outages can also be expressed as a ratio of the number of customers affected by one outage per year to the total number of customers. SAIDI indicator is basically equal to the mean failure duration τ . The value of this index can also be defined as a ratio of the number of customers affected by a minute's outage per year to the total number of customers. CAIDI indicator is basically equal to the probability of failure.

8.5.5 Resilience Framework and System Restoration

The resilience of power network can be defined using two main concepts: robustness and rapidity which are part of the restoration process. This can be understood

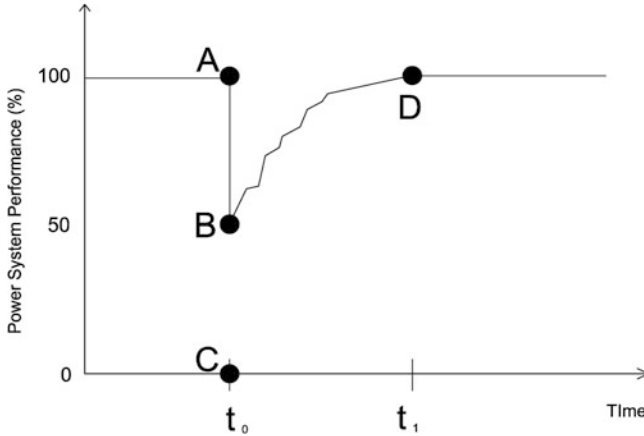


Fig. 8.42 Example of restoration curve

using the restoration curve shown in Fig. 8.42 where t_0 represents the time at which earthquake occurs and t_1 is the time at which power supply is restored 100%. B-C is the robustness, the performance percentage, and can be expressed as

$$\text{Robustness} = B - C \text{ (in percentage)} \quad (8.48)$$

and the rapidity can be quantify as the elapsed time for the total restoration ($t_1 - t_0$)

$$\text{Rapidity} = \frac{A - B}{t_1 - t_0} \text{ (average recovery rate in percentage/time)} \quad (8.49)$$

It has been demonstrated that the restoration time for the power network seems to be faster with respect to the gas, water and transportation network.

8.6 Example 5: Communication Network

Communication networks and information systems are becoming essential part of critical infrastructure in our daily lives. Communities today are thoroughly dependent on smart devices that with their development over the past decade are offering several new services raising the expectation that communication networks are readily available all the time.

The social needs of a community include the needs of citizens, businesses, industry, and government, all of which directly rely on communication networks and information systems.

For example, the banking system relies on the Internet for financial transactions, businesses need to have Internet and telephone service to communicate with their

Table 8.10 Communication and information infrastructure components

(a) Landline telephone systems	(b) Internet systems	(b) Internet systems
(i) Central offices	(i) Internet exchange points (IXP)	(i) Cell towers
(ii) Transmission and distribution	(ii) Internet Backbone	(ii) Free standing/ mounted cell phone towers

clients and suppliers have begun to use social networking sites for collaboration, marketing, recruiting etc. People now use laptops, smart phones, and tablets to read news on the Internet and watch movies and television shows, documents are transferred via Internet between businesses and e-mail is a primary means of communication. When these services are not available, a massive set of failures can affect performance to the point where the degradation can disrupt our daily lives, resulting in human losses and significant financial costs in the worst cases. In Table 8.10 are shown the critical components of the communication and information network. However, during a natural disasters these components might be damage. Therefore the communication network might not be available at the time when is most needed (e.g. for communication between citizens and emergency responders, between family members to check their status, between government and public agencies, etc) in order to coordinate the recovery plan between the first responders and the community leaders.

In addition, all other critical infrastructures within a community are becoming more dependent on communication networks and information systems to provide their services.

Specific to the communications and information system,

For example the emergency repair crews of power networks need to communicate efficiently for repairing their network after a disaster. Traffic signals and hubs of the transportation network also rely on communications systems. For example, the traffic signals use the communication network for the synchronization of green lights to ensure a smooth traffic flow, and the transportation hubs use the communication network to transmit schedules for inbound/outbound passenger traffic. Buildings and facilities need their communications and information systems to function properly. Similar interdependencies between the communication and the water distribution network also exist. In fact if the cellular network is down for an extended period of time following a disaster event, the recovery process of the water distribution network can take longer, since there will be limited coordination in the recovery efforts.

Understanding communication network behavior under perturbations can improve today’s networks performance, as well as lead to a more resilient and survivable networks in the future. The primary concern of the communication networks is *reliability* and *availability*. These are the terms which are often used by industry when referring to the performance of communications networks. *Availability* refers to the percentage of time a communication network is

accessible for use and *Reliability* is the probability of successfully performing an intended function for a given time period. *Resilience* is closely related to *availability* and *reliability*, but it also includes the ability to limit and withstand disruptions/downtime. It also involves preparation for and adaptation to changing conditions, mitigation against the impact of future events, reducing the probability of occurring disruptions, and when they do occur, there is still a plan to recover quickly. Resilience encompasses the ability recovering from a disaster event such that the infrastructure can also be rebuilt to a higher standard with respect to the initial condition. Consequently, by enhancing the resilience of communications infrastructure, the *availability (amount of downtime)* and *reliability (frequency of downtime)* can be improved. The resilience of a communication network also dependent on its capacity, which is a key parameter especially during and immediately after disaster events when there is an increase in demand of the communication and information systems during and immediately after disaster events (Jrad et al. 2005).

It is infeasible and impractical to design and deploy hardened structures, equipment, and transmission facilities that never fail and can withstand any disaster. Therefore, an alternative approach is to design and provide mechanisms that can recover and react to disasters quickly. Thus, the desired outcome of disaster resilience is for a network to recover from a disaster with an acceptable level of performance by a set of mechanisms within a short amount of time. Such mechanisms can be either *proactive* or *reactive*, or a combination of them.

Usually, *proactive approaches* include redundancy in a cost-effective manner; hence, the network is sufficiently reliable for addressing a failure or an attack. In the case of *reactive approaches*, the network may react by rerouting through backup capacity, or, in some cases, by rapidly deploying ad hoc networking capability. Thus, reactive approaches may include emergency communication mechanisms during and after a disaster.

One of the key aspect of a communication network is the coordination of recovery plans between the first emergency responders and the community leaders right after a hazardous event. The direct involvement of residents in the emergency response and recovery plan is determinant, because if well coordinated, they can improve the recovery process. In fact, residents may help identifying an emergency and they can play a significant role in the recovery process. The ability of residents and professional emergency responders to exchange information during an emergency is necessary to provide a more accurate portrait of the loss assessment following major disasters. Interaction and collaboration between residents and experts lead to improve the resilience of a given community (Cimellaro and Reinhorn 2010; Cimellaro et al. 2010). “Mobile devices” and “Resilience” are two terms that nowadays regularly appear in the emergency management field. Mobile technologies and Internet provide means for use in a community when a response is needed, especially since individuals are getting comfortable with the use of technological devices. Mobile devices facilitate response in large scale emergencies by enabling individuals to report information. Using smart phones in emergency management will help build community disaster resilience. This section

explores the viability of using mobile communication technologies (smart phones) and the Web to develop response systems that would aid communities after a major disaster, providing channels for allowing residents and responders to upload and distribute information, related to structural damages coordinating the damage field reconnaissance. A mobile application that can be run by residents and specialists on smart phones has been developed (Cimellaro et al. 2014a), to give an initial damage evaluation of the area right after a disaster, which is going to be useful when resources (e.g. the number of experts) are limited.

8.6.1 Literature Review

In a society where information and telecommunications technologies have become so vital to everyday life, the nature of telecommunications policy must constantly be evolving to meet new social developments (Mileti 1999).

Mobile technologies can be harnessed to create a previously unavailable social benefit to communities and to individuals. It could be a revolution in the use of technology and infrastructure to help individuals and communities to respond and recover from disaster. Technologies such as smart phones and Internet can be better employed by coordinating community response to major disasters more effectively. Advanced disaster management technology could provide a critical support system for emergency authorities during crises. Such technology can also provide important inputs for any disaster management plan of action in modern times.

Natural disasters, such as the latest “Tsunami” in Asia and the earthquake in Niigata, Japan, are contributing to residents’ awareness of the need of pre-disaster procedures. There is also a growing recognition by governments and private institutions that a mobile disaster management system could help to minimize the fatalities of human lives when natural disasters occur. Because of this recognition, countries such as Australia, Czech Republic, France, England, Hong Kong, Japan and Singapore, and others, have increased their efforts to develop disaster management applications which use mobile technology to enhance their response capabilities during a disaster. A few examples of these applications are given by Fujii et al. (2012) and Arcidiacono and Cimellaro (2013) which developed a system for supporting building damage assessment. However, their proposed application is not multi-platform, because it is available only in the Android operating system, which is a drastic limitation for the residents when they are affected by the earthquake. A smart phone application of the ATC-20 (2005) standard methodology for building seismic safety assessment termed ROVER (Rapid Observation and Visual Estimation of Risk) is also available (FEMA 2011). The application can be installed on any Windows Mobile Phone, but it shares the same limitations of the other applications. In any emergency, problems often derive from “collaborative problem solving” and other problems of coordination (Mileti 1999). Studies have repeatedly demonstrated the difficulties of coordination between responders, residents, government agencies, businesses, volunteers, and

relief organizations in an emergency (Jones and Mitnick 2006; Kapucu 2006; McEntire 1997, 2012; Lord 1992). Coordination in terms of informational sharing, communication, and collaborative action present enormous social and behavioral problems for emergency response (Kapucu 2006). Major disasters are “occasions in which the boundaries between organizational and collective behavior are blurred” (Kapucu 2006). As a result, communication and coordination between residents and responders are the most pressing issues during an emergency (Haddow et al. 2008).

Conceptually, the preparation for responding to emergencies can be seen as a cycle with information sharing and communication being keys throughout the cycle (Lord 1992; Pelfrey 2005). “Sharing information, willingness to collaborate, and shared values” are vital bases of effective information sharing and communication in major disasters (Kapucu 2006). A considerable amount of data and information is necessary for effective decision-making at any stage of natural disasters – from prediction to reconstruction and rehabilitation. The most important procedures relating information from disasters are monitoring, recording, processing, sharing, and dissemination. Experience has proved that information technology simplifies the receiving, classifying, analyzing, and dissemination of information for appropriate decision-making. A critical component of any successful rescue operation is time. Prior knowledge of the precise location of landmarks, streets, buildings, emergency service resources, and disaster relief sites saves time – and saves lives. Such information is critical for disaster relief teams and public safety personnel to protect life and reduce property loss. The ability of residents and professional emergency responders to exchange information directly during an emergency is necessary to provide a more accurate portrait of the severity and breadth of major disasters. The direct involvement of residents is extremely important during the emergency, because it can improve the response and recovery process (Kweit and Kweit 2004). “Community engagement equips leaders to face the complex and ever-shifting realities of an extreme event” (Schoch-Spana et al. 2007).

A higher number of resident responders will allow decision-makers to better allocate government resources where they are needed and supplement the limited resources, helping them to go further (Schoch-Spana et al. 2007). In the context of a community response grid, emergency response will firmly remain the job of professional emergency responders, except in the most dire of circumstances. The community members will generally be serving as support for professional emergency responders, helping the affected individuals in community support roles that fall outside the traditional functions of emergency response.

Literature shows that mobile-based information systems can be a solution to benefit responders in different ways. Implementation of new information technologies in emergency response can potentially improve communication and coordination (K. 1999; Comfort and Kapucu 2006). A more robust information network with greater distribution will further improve communication and coordination in major disasters (Comfort and Kapucu 2006; Graber 2003). After a major disaster, community involvement through mobile devices is essential for increasing residents trust of the emergency information and for promoting coordination between residents and responders. The possibility of using mobile technologies and the Web to build and



Fig. 8.43 Standard damage assessment


foster response systems could aid communities before, during, and after emergency, uploading and distributing information, and coordinating the responses.

8.6.2 Standard Earthquake Damage Assessment in Italy

One common scenario during disasters is that the activity of rescue and relief is not well-coordinated. Emergency authorities must receive and record the data related to damage of physical infrastructures (e.g. house, buildings, etc.) and then they must be processed to coordinate emergency response as fast as possible. The acquisition of damage reports starts from the residences that require a first-level damage report – i.e. certificates of occupancy. Then the Operative Center organizes many technical teams to evaluate and perform the damage reports that are processed and organized according to their importance (Fig. 8.43).


Specialists and technicians from various regions perform the earthquake damage assessment of buildings right after the earthquake using AeDES forms (Fig. 8.44). AeDES (Agibilit  e Danno nell’Emergenza Sismica) inspection forms are used by Italian civil engineers during earthquake damage assessments following an earthquake.

In the past, post earthquake surveys in Italy were performed using vulnerability forms which were conceived to detect vulnerability and damage without any specific concern for building usability. AeDES forms were created with the idea of limiting the time required for each inspection and evaluation of the post earthquake usability of ordinary buildings. The AeDES form that was used in 2012 Emilia earthquake is composed by nine sections: (1) identification of the building, (2) characterization of the building, (3) structural typology, (4) structural damage and emergency measures, (5) non-structural damage and emergency measures, (6) external risk from other structures and emergency measures, (7) soil typology and damage, (8) judgment of



Presidenza del Consiglio dei Ministri
Dipartimento della Protezione Civile

CONFERENZA DELLE REGIONI E DELLE
PROVINCE AUTONOME



**SCHEDA DI 1° LIVELLO DI RILEVAMENTO DANNO, PRONTO INTERVENTO E AGIBILITÀ
PER EDIFICI ORDINARI NELL'EMERGENZA POST-SISMICA**
(AeDES 06/2008) Codice Richiesta _____

SEZIONE 1 Identificazione edificio		IDENTIFICATIVO SOPRALLUOGO _____ giorno mese anno Squadra _____ Scheda n. _____ Data _____	
Provincia: _____ Comune: _____ Frazione/Localtà: _____ (denominazione Istat) 1 <input type="radio"/> via _____ 2 <input type="radio"/> corso _____ Num. Civico _____ 3 <input type="radio"/> vicolo _____ 4 <input type="radio"/> piazza _____ 5 <input type="radio"/> altro _____ (Indicare: contrada, località, traversa, solita, etc.)		IDENTIFICATIVO EDIFICIO Istat Reg. _____ Istat Prov. _____ Istat Comune _____ N° aggregato _____ N° edificio _____	
Coordinate geografiche (E500 - UTM fuso 32-33) E _____ Fuso _____ N _____		Cod. di Località Istat _____ Tipo carta _____ Sez. di censimento Istat _____ N° carta _____	
Denominazione edificio o proprietario _____		Dati Catastali Foglio _____ Allegato _____ Particelle _____	
Posizione edificio 1 <input type="radio"/> Isolato 2 <input type="radio"/> Interno 3 <input type="radio"/> D'estremità 4 <input type="radio"/> D'angolo		Codice Uso _____	
Fotocopia dell'aggregato strutturale con identificazione dell'edificio			

SEZIONE 2 Descrizione edificio																																								
<i>Dati metrici</i>			<i>Età</i>		<i>Usa - esposizione</i>																																			
N° Piani totali con interrati 1 <input type="radio"/> 2 <input type="radio"/> 3 <input type="radio"/> 4 <input type="radio"/> 5 <input type="radio"/> >12 6 <input type="radio"/> 7 <input type="radio"/> 8 <input type="radio"/>	Altezza media di piano [m] 1 <input type="radio"/> ≤ 2.50 2 <input type="radio"/> 2.50+3.50 3 <input type="radio"/> 3.50+5.0 4 <input type="radio"/> > 5.0 Piani interrati A <input type="radio"/> 0 C <input type="radio"/> 2 B <input type="radio"/> 1 D <input type="radio"/> ≥3	Superficie media di piano [m ²] A <input type="radio"/> ≤ 50 I <input type="radio"/> 400 +500 B <input type="radio"/> 50 + 70 L <input type="radio"/> 500 +650 C <input type="radio"/> 70 + 100 M <input type="radio"/> 650 +900 D <input type="radio"/> 100 + 130 N <input type="radio"/> 900 +1200 E <input type="radio"/> 130 + 170 O <input type="radio"/> 1200 +1600 F <input type="radio"/> 170 + 230 P <input type="radio"/> 1600 +2200 G <input type="radio"/> 230 + 300 Q <input type="radio"/> 2200 +3000 H <input type="radio"/> 300+ 400 R <input type="radio"/> > 3000	Costruzione e ristrutturaz. [max 2] 1 <input type="checkbox"/> ≤ 1919 2 <input type="checkbox"/> 19 ÷ 45 3 <input type="checkbox"/> 46 ÷ 61 4 <input type="checkbox"/> 62 ÷ 71 5 <input type="checkbox"/> 72 ÷ 81 6 <input type="checkbox"/> 82 ÷ 91 7 <input type="checkbox"/> 92 ÷ 01 8 <input type="checkbox"/> ≥ 2002	Uso A <input type="checkbox"/> Abitativo B <input type="checkbox"/> Produttivo C <input type="checkbox"/> Commercio D <input type="checkbox"/> Uffici E <input type="checkbox"/> Serv. Pub. F <input type="checkbox"/> Deposito G <input type="checkbox"/> Strategico H <input type="checkbox"/> Turis-ricet.	N° unità d'uso _____ _____ _____ _____ _____ _____ _____ _____	Utilizzazione A <input type="radio"/> > 65% B <input type="radio"/> 30+65% C <input type="radio"/> < 30% D <input type="radio"/> Non utilizz. E <input type="radio"/> In costruz. F <input type="radio"/> Non finito G <input type="radio"/> Abbandon.	Occupanti <table style="width: 100%; text-align: center;"> <tr><td>100</td><td>10</td><td>1</td></tr> <tr><td>0</td><td>0</td><td>0</td></tr> <tr><td>1</td><td>1</td><td>1</td></tr> <tr><td>2</td><td>2</td><td>2</td></tr> <tr><td>3</td><td>3</td><td>3</td></tr> <tr><td>4</td><td>4</td><td>4</td></tr> <tr><td>5</td><td>5</td><td>5</td></tr> <tr><td>6</td><td>6</td><td>6</td></tr> <tr><td>7</td><td>7</td><td>7</td></tr> <tr><td>8</td><td>8</td><td>8</td></tr> <tr><td>9</td><td>9</td><td>9</td></tr> </table>	100	10	1	0	0	0	1	1	1	2	2	2	3	3	3	4	4	4	5	5	5	6	6	6	7	7	7	8	8	8	9	9	9
100	10	1																																						
0	0	0																																						
1	1	1																																						
2	2	2																																						
3	3	3																																						
4	4	4																																						
5	5	5																																						
6	6	6																																						
7	7	7																																						
8	8	8																																						
9	9	9																																						
Proprietà A <input type="radio"/> Pubblica B <input type="radio"/> Privata																																								

Fig. 8.44 AeDES printed forms

usability, and (9) other observations. Moreover, after filling the form, six levels of building usability can be indicated: (A) usable building, (B) temporarily unusable (all or part) building but usable with emergency interventions, (C) partially unusable building, (D) temporarily unusable building for review with deepening, (E) unusable building, and (F) unusable building for external risk.

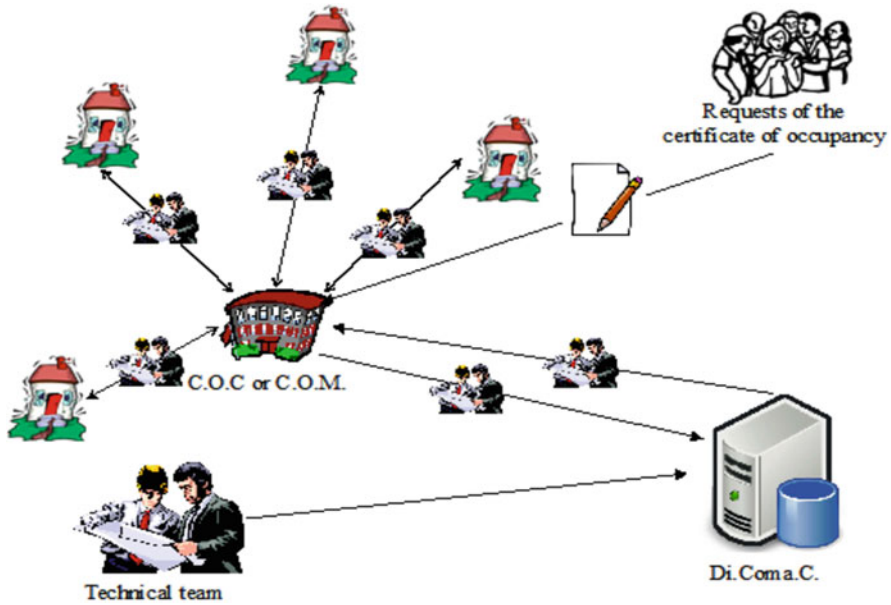


Fig. 8.45 Standard procedure of building damage assessment following an earthquake (Arcidiacono and Cimellaro 2013)

As a general information the final summary of the earthquake damage assessment for the inspected residential buildings after 2012 Emilia earthquakes in Italy using the data collected in the field with the *AeDES* forms are the following: 14,112 (36.4 %) of A, 6,827 (17.6 %) of B, 1,644 (4.2 %) of C, 208 (0.5 %) of D, 13,825 (35.7 %) of E, and 2,110 (5.4 %) of F.

The visual inspections in the field have been made by specialized teams of experts. The standard damage assessment procedure (Fig. 8.45) following the earthquake was the following:

- Requests of hardcopy certificates of occupancy made by residents at the Commissioner Operative Center (C.O.C.) or Mixed Operative Center (C.O.M.);
- Organization of technical teams;

Then for each technical team the following procedure is followed:

- Registration of the team at the Direction and Control Center (Di.Coma.C.) located in Bologna;
- Get the daily list of buildings to be investigated at the C.O.C. or C.O.M.;
- Fill the *AeDES* form (certificate of occupancy) for each building in the list;
- Compile the summary report to be submitted at the C.O.C. or C.O.M.;
- Reach the accommodation.
- Revision of the filled *AeDES* forms at the Di.Coma.C. in Bologna.

8.6.3 Proposed Earthquake Damage Assessment Using Mobile Phone Technology

A critical component of any successful rescue operation is time. Immediate knowledge of the precise location of landmarks, streets, buildings, emergency service resources, and disaster relief sites saves time – and saves lives. Such information is critical to disaster relief teams and public safety personnel to protect life and reduce property loss. Therefore, there is a need for a system that will improve the efficient resource allocation of rescue and relief in the disaster-affected areas.

Generally following an earthquake there is a limit on the number of specialists with adequate assessment skills who can access the damaged area for building damage assessment. Since the use of smart phones is proliferating among the population, this section is proposing a simplified application for building damage assessment using photos of damaged houses taken by residents or volunteer fire corps in damaged area without any specific skill.

The application has been tested for the first time after 2012 Emilia Earthquake to show the efficiency of the proposed method in improving the emergency response and compare it with previous data collection. The use of technology enables residents and responders to work together in community response to emergencies. Residents could report incidents and receive emergency information that would facilitate coordinated responses with emergency services. They could employ mobile devices like smart phones to provide information, GIS coordinates and photos. Multiple platforms (e.g. mobile devices, Internet etc.) and content types (e.g. text, photo, video etc.) ensure that community response grids will function with surviving infrastructure during and after an emergency, while supporting two-way communications among residents and responders. Professional emergency responders could be collecting information via smart phones, residents could be reporting and receiving information via website, and communities could be sharing information simultaneously to respond to a crisis of any magnitude. Professional staff could separate out suspicious or low priority reports, assigning appropriate resources to the major problems. The input from structural engineers would provide a more accurate portrait of the severity of disasters. A coordinated response from emergency services could be designed to use available resources with the option of requesting assistance from neighboring jurisdictions or secondary support services. The first responders need to communicate quickly, effectively, efficiently and frequently. Efficient, rapid and effective communication between mobile units and professional emergency responders is a key factor in responding successfully to the challenges of emergency management.

The proposed platform can support teams of professional emergency responders in the first hours after the disaster by using smart phone-based infrastructure and can also be scaled up to handle a much larger number of users. It is a set of pluggable, mobile-based disaster management solutions, that provides solutions to problems caused by the disaster and it is designed to help during the relief phase of a disaster.

The response phase includes search and rescue operations as well as the provision of emergency relief. In this phase, efficiency is important because during this kind of situation, timing is essential.

The idea is to consider residents that have a smart phone as a network of *mobile sensors* that can rapidly collect the first emergency response information immediately after a seismic event to improve community resilience through its recovery.

Since the use of smart phones is gaining interest in people, a simplified damage assessment system was implemented as a smart phone application. There are several mobile development environments in the market; therefore, initially it was decided to use Android, which is an open and comprehensive platform for mobile devices created by the Open Handset Alliance. Android was selected because it is designed to be more open than other mobile operating systems so that developers, wireless operators, and handset manufacturers will be able to make new products faster and at lower costs. However, because the application shouldn't be limited to only one operating system, it was decided to translate the code using a multiplatform language, Titanium, which can develop native applications for iOS, Android, BlackBerry, Windows, and mobile web through a single code base. So the current application named EDAM (Earthquake Damage Assessment Manager) (Cimellaro et al. 2014a) is able to run on Google's Android operating system, in the IOS operating system by Apple and in BlackBerry.

The only type of data collected with the proposed mobile application is I level accuracy data (damage data and building type data) because of the large amount of buildings to be surveyed in the phase post-earthquake. Damage data can be classified in different ways, according to the accuracy of the data and the time when the data are collected and then through statistical analysis it is possible to correlate damage and building type with seismic intensity. The simplified mobile application has been developed and kept accessible in order to be understandable by non experts (e.g. residents) who can collect different types of data and information right after a seismic event. The data can be grouped as: (i) residents personal data, (ii) structural damages, (iii) location and features of buildings and infrastructure damages. The part about the insertion of resident's personal data (name, last name, age, occupation, mobile number) also allows signing the document digitally, as it can also be downloaded in pdf after filling all the form. The position of the observer with respect to the building (inside or outside) is also required. This is an important aspect, because one problem in giving an initial damage evolution based only on pictures is that most of the time is not known from which position the picture is taken, therefore a tool to draw a sketch of the position of the observer is also added (Fig. 8.46). In other words, every time a picture or a video is taken, it is requested that the user add the position from which the picture is taken to the initial drawing of the building.

The reliability of the data comes from unambiguous terms in the computer form of the mobile application. Forms with multiple choices and multiple answers seem to perform better. As an example, the answer "none" has always been inserted in the form and not simply deduced from the fact that no answer is marked. However,

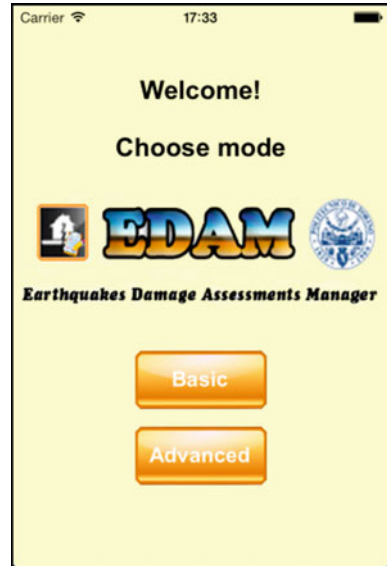
Fig. 8.46 Screen shot of the drawing graphical interface of the mobile application running on IOS



validation of data collected is always necessary; therefore, inspection of the same building by specialists is mandatory. In addition, the mobile application can also be used by experts, because it allows the user to log in with different accounts. For example if you log in as an expert (Advanced in Fig. 8.47), the complete form for the damage assessment evaluation appears (AeDES form). In this case, the type of data collected with the mobile application for specialist can be summarized as follows:

1. Identification: Name, address, cadastral unit, photographs;
2. Dimensional data: Mean surface, number of stories, height;
3. Function: Property, function, percentage of use, number of dwellings and inhabitants;
4. Building type: Material, structural schemes, age of construction, maintenance, position;
5. Soil condition, geomorphology, landslide;
6. Building damage: damage levels and their extension in different components, overall measure of damage;
7. Social data: homeless and family evacuated;
8. Countermeasures: urgent barricades, already done or to be done;
9. Quality of the inspection (complete, partial, from the exterior);
10. Usability assessment;
11. Notes.

Fig. 8.47 Initial screen shot of the mobile application



The application is user-friendly and it reduces the bureaucratic procedures, while it simplifies the evaluation and the acquisition of the certificates of occupancy (Fig. 8.48).

If the area affected by damage is extensive, there will be difficulties in managing a large amount of data, such as pictures, videos, sound records etc. In order to solve this problem, the application is working in combination with software which manages the data provided by the smart phones connected in the network. In summary, the system for uploading the photos of damaged houses has been developed as mobile communication service, while the remote system for specialists to assess the damage level has been developed as web service. The web service is developed in Java and run on a server which collects all the data sent by the mobile application. The data sent by the mobile are automatically collected and geo-referenced in damage maps using a system similar to the one proposed by Erdik (2013), but the maps of Google Earth are used as background for the software, so it will be easy to select the data related to a specific marked area. Search tools are also provided, which enhance the capacity to deal with large data.

8.6.4 Survey on Building Earthquake Damage Assessment

The possibility of collecting the earthquake damage assessment by residents was taken in account before the creation of the proposed platform. Therefore, a survey was carried out between non-specialists to understand if they were able to identify structural damages in a building subjected to an earthquake (Cimellaro et al. 2014a;



Fig. 8.48 Screen shot of the mobile application for residents running on Android

Scura et al. 2013). People were asked to match 36 pictures of damaged buildings (mainly from 2009 L’Aquila earthquake) with 22 type of failure mechanisms.

The survey was made first in Turin (Italy) and then in Buffalo (USA). In both cases, the ages of the sample were between 18 and 30 years (which is the age range in which the highest number of people uses smart phones). The comparison of the survey between the two sites revealed no significant differences in the comparison between Turin and Buffalo. By analyzing the results organized by pictures, (Fig. 8.49) it appeared that for some buildings there is a high error rate, which may be due to the low quality of the pictures, as in case 7. However, for other buildings, the percentage of people who have correctly identified the damages is high, as in case 1.

The different failure mechanisms have been ordered in Fig. 8.50 according to the level of difficulty in identifying them for the two locations, Turin and Buffalo. Overall, according to the survey the percentage of error in the damages’ identification by non-specialists is insignificant. However, it was decided not to rely on their judgments, because even a small error in percentage could falsify the damage assessment dramatically. Therefore, it was decided to focus on smart phones cameras power and consider residents not as experts who can give damage evaluation on buildings, but rather as “moving sensors”, which can collect data

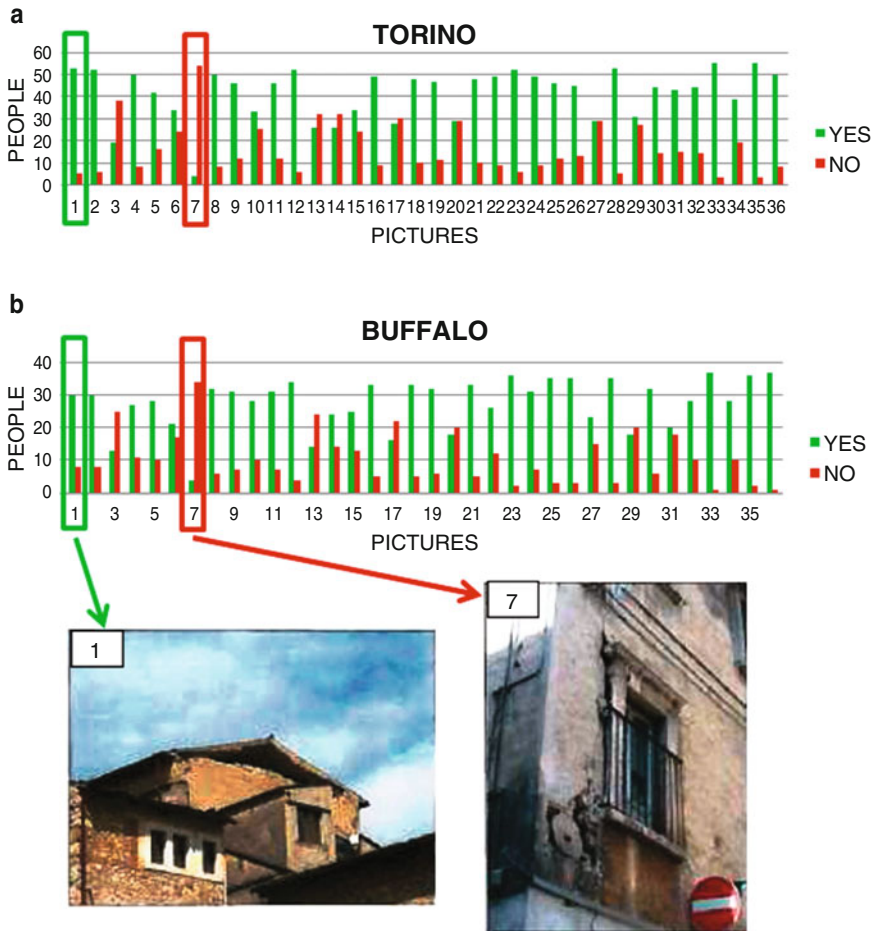


Fig. 8.49 Survey results for different pictures – (a) Torino; (b) Buffalo

and information following the directions given by the apps without adding any evaluation. The function of taking pictures of damaged buildings was included in the application and it was asked that residents take pictures of the most important part of the buildings.

Those parts are obviously the most critical from the structural point of view and are useful for specialists to give a post-event damage assessment. In detail, the parts pointed out by the application are: the entire facades; external and/or internal corners; boundaries between adjacent buildings; bottom of each facade; top of each facade; access; roofs; ground around the perimeter of the building; internal walls; ceilings; floors; stairs and/or elevators; everything that is different from usual (e.g. fractures, deformations, displacements etc.). Regarding the position, the application allows the automatic loading of the coordinates (WGS 84 system) as it

is geo-referenced through the GPS localization of the device. Additionally, people can fill different fields such as province, municipality, village or locality, address. The system in fact allows the localization of buildings directly on a map.

Regarding the building topology, the application provides for the collection of the following information: web, number of basements, number of levels and use of the building. In addition, it is possible to draw a digital sketch of the building (e.g. plan view, lateral view, etc.) directly on the screen. Regarding the infrastructure damages, the application allows for the collection of information on: (i) ground fractures along the building perimeter, (ii) water and gas leakage and (iii) power outage. All the collected information is filled into a form, which is prepared in pdf format directly from the app. Therefore, the application allows the user to save data and sending them directly to the centralized server of the operative center together with the attached pictures whenever an internet connection is available (Fig. 8.50). In this way, the collected data can be digitally stored in a database and/or printed once they have been received (Fig. 8.51).

Once received in real-time, all data from mobile sensors (of non-specialists), specialists and technicians at the operative center analyze these data and make a first

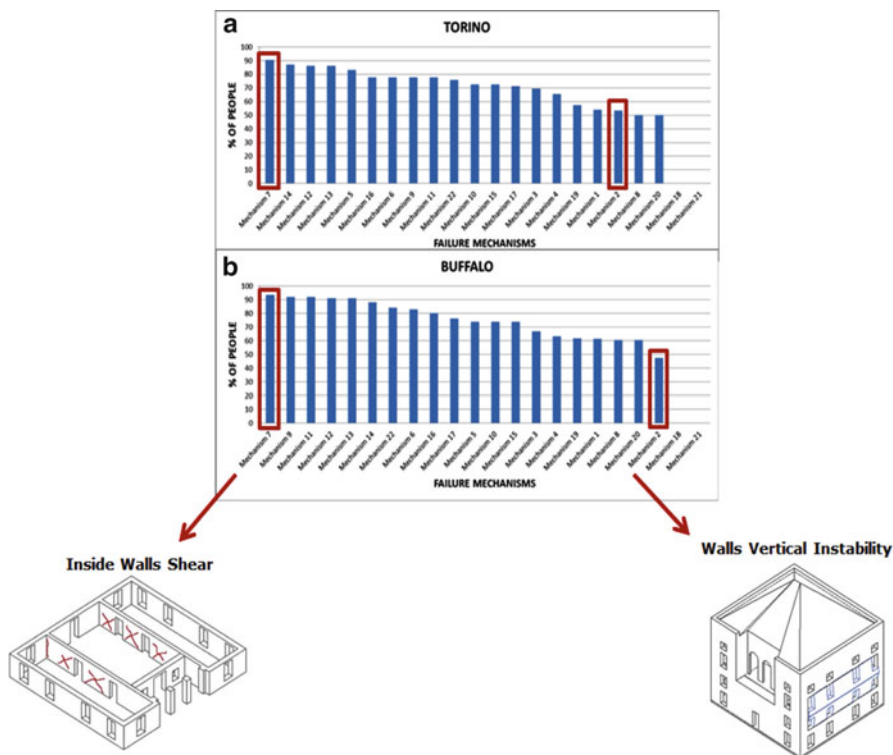


Fig. 8.50 Survey results for different failure mechanisms – (a) Torino; (b) Buffalo



Fig. 8.51 Example of Collected Data in the proposed mobile application

damage assessment. Therefore, they can quickly have an initial rough knowledge of the level of damage which can lead to a better organization of technicians carrying out recovery operations. Once a complete map is obtained with the localization of the buildings and a first damage evaluation, thanks to the interaction between ordinary residents and experts (e.g. specialists, technicians, engineers, etc.), emergency authorities have an overall view of the areas affected by the earthquake. In this way, the operations of technicians for a more detailed damage assessment (AeDES forms) can be planned accordingly, improving the post-event recovery phase as well as its recovery and efficiency. Therefore, a new procedure is proposed in this section (Fig. 8.52) to obtain a first damage assessment during emergencies more rapidly and efficiently by removing all bureaucratic procedures, reducing the damage evaluation time; organizing the recovery phase. The proposed method is defined in a step-by-step procedure as follows:

1. Download of the App;
2. Collection of data by residents using the mobile application and sending them to an Operative Center;
3. Requests of certificates of occupancy in digital format made by residents directly sending the data collected;
4. First damage assessment by technicians at the operative center by means of collected data analysis;
5. Organization of technical teams;
6. Second more efficient and more detailed damage assessment following the common procedure to establish a final judgment of building usability.

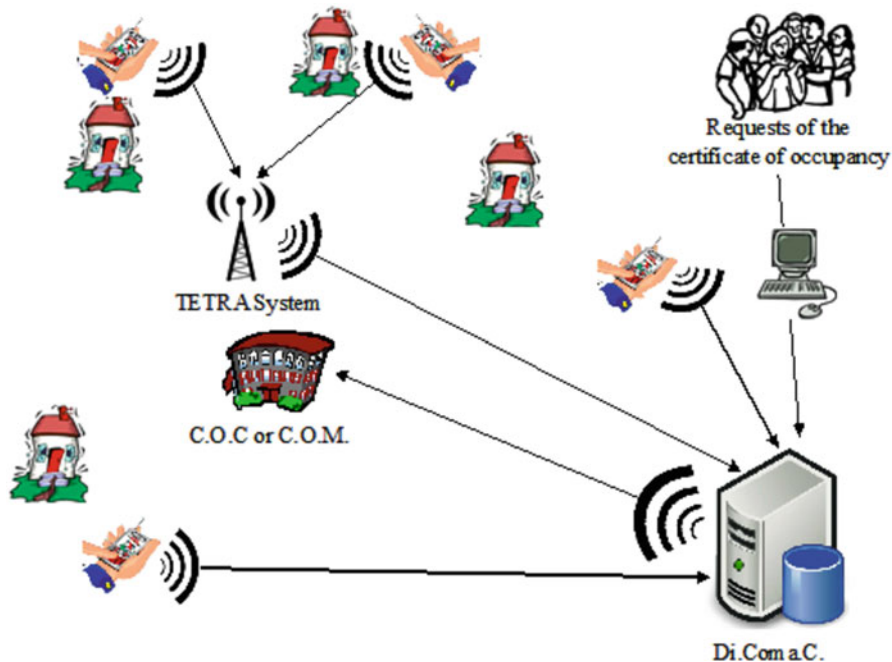


Fig. 8.52 Structure of the proposed methodology (Arcidiacono and Cimellaro 2013)

Based on the experience of the authors during 2012 Emilia earthquake, the experts spent a lot of time in the field, but most of the time they were not sent to places where the need was more urgent. They were organized by public governmental officers who never experienced an earthquake before and they did not have enough training. Most of the capabilities of the proposed software were performed directly by them, but manually on paper. It is strongly believed that the proposed package will assist them during the emergency when working in collaboration with experts.

8.6.5 Application of the Digitalized Earthquake Damage Assessment

The application was tested in the post-earthquake response of the 2012 Emilia Earthquake in order to enhance the data collection of the emergency authorities and compare it with the previous method. The application was tested by the residents of the town of Mirandola, who requested the damage assessment for their buildings just after the seismic event by following the existing standard procedure. In detail, they were provided with a smart phone on which the implemented application

Judgment			
A	Usuable building		
B	Usuable building with measures		
C	Partially usuable building		
D	Building to be reviewed		
E	Unusable building		
F	Unusable building for external risk		

Building	Address	Standar Procedure	Proposed Method
1	Via Curiel 4	E	E
2	Via Curiel 50	C	B
3	Via Curiel 44	A	A
4	Via Curiel 52	A	A
5	Via Curiel 25	A	A
6	Via Curiel 1	E	E
7	Via Voltorno 20	E	E
8	Via Voltorno 24	A	A
9	Via Voltorno 31	B	B
10	Via Castelfidardo 25	B	E
11	Via Castelfidardo 29	B	B
12	Via Castelfidardo 41	E	E
13	Via Luosi 4	A	A
14	Piazzale Garibaldi 25	E	E
15	Via Luosi 8	A	A
16	Via Luosi 10	A	A
17	Via Luosi 14	A	A
18	Via Fulvia 14	F	C
19	Via della Libertà 12	E	E
20	Via Martiri di Belfiore 10	A	A
21	Via Martiri di Belfiore 14	A	A
22	Via Martiri di Belfiore 27	A	A
23	Via Case Popolari 5	E	E
24	Via Case Popolari 9	A	A

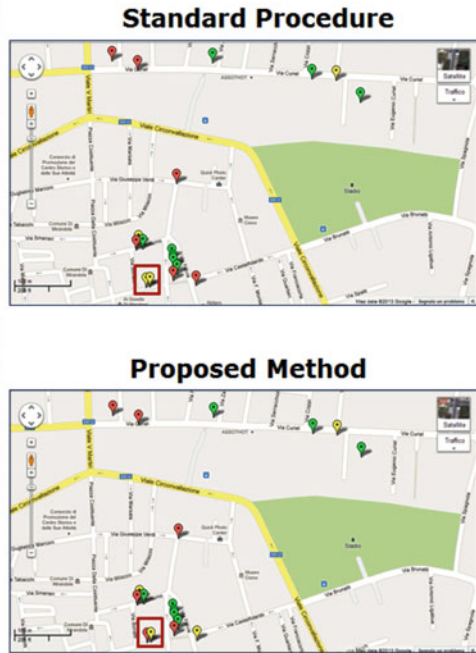


Fig. 8.53 Results of the damage evaluation using the proposed procedure using the 2012 Emilia earthquake

was installed and they were asked to use this application for scientific research purposes. In this way, it was possible to test the efficiency of the proposed method compared with the standard procedure. Twenty four households were selected and the digitalized form was sent to a centralized server located in the Operative Center. The data collected in digitalized form has been analyzed by five professional civil engineers for each building; a first damage evaluation was requested using only the data provided through the smart phone (Fig. 8.53). The most probable damage evaluation for each building was selected by comparing the five damage evaluations. Five different evaluations have allowed taking into account the biased judgment of every single operator. The final damage evaluation related to the building was then compared with the results of the field reconnaissance obtained by the AeDES forms that were filled in by technicians after the seismic event (Fig. 8.53).

It is evident that there are a few differences between the results of the AeDES forms and the damage evaluation obtained from the analysis of data collected by means of the mobile application, as was expected. The percentage of accuracy A of the proposed method shows the goodness of the proposed procedure to prove the

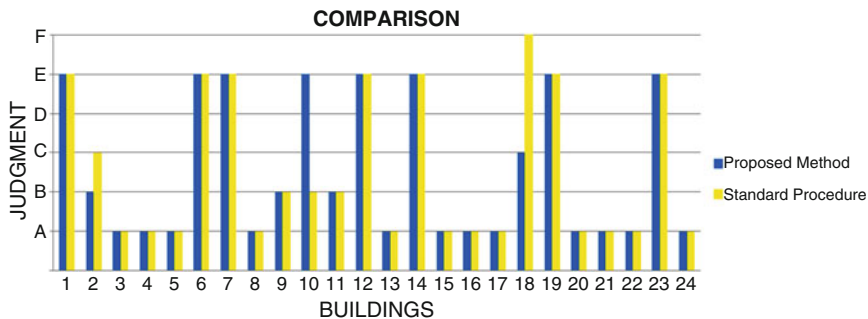


Fig. 8.54 Comparison between standard and proposed procedure results

usability of disaster evaluation made by residents via smart phones. It is given by the following equation:

$$A(\%) = \frac{N_p}{N_{TOT}} \times 100 \tag{8.50}$$

where N_p = number of buildings with the same damage evaluation using the two methods, while N_{TOT} = total number of evaluated buildings. From the analyzed data it was obtained that $N_p = 21$, while $N_{TOT} = 24$, therefore the final percentage of accuracy is 87.5 %. Even though the analyzed sample is very small due to the difficulty in convincing people to fill out the digitalized form, after having already filled the standard paper form, the percentage of accuracy of the proposed method is nonetheless very high (Fig. 8.54).

Once a complete map is obtained with the localization of buildings and a first damage evaluation, the specialists at the Operative Center can have a first overall view of damage in the entire area affected by the earthquake. In this way, the emergency management operations of structural engineers can be optimally planned using the limited recourses of personnel. It is important to mention that the field damage evaluation using the AeDES forms of specialists cannot be avoided with the proposed procedure, but the post-event damage evaluation can be managed in a more efficient way.

In Fig. 8.55 a sketch of functionality is shown, using the damage knowledge QDK of the buildings in Mirandola right after 2012 seismic event as indication. The damage knowledge is null when the seismic event happens (May 20th, 2012). Then by following the standard damage assessment, there is a complete recovery in terms of functionality after almost 7 months (December, 2012). Instead, following the proposed digitalized earthquake damage assessment, it is possible to reach a very high level of damage knowledge after just 1 week. Consequently the full damage knowledge will be reached by following a more efficient (exponential curve) procedure – thanks to well organized teams of specialists. In conclusion, by comparing the standard damage assessment with the proposed damage assessment

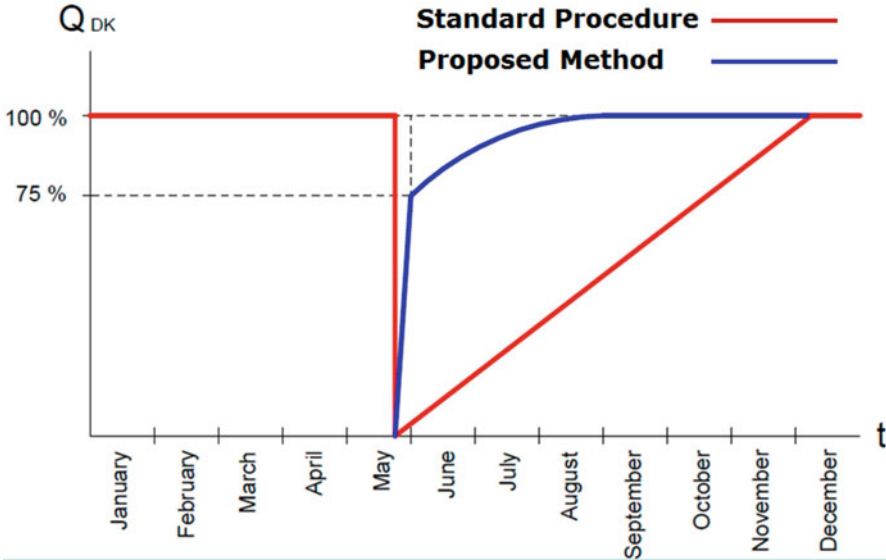


Fig. 8.55 Comparison in terms of recovery

method, it can be observed that the damage knowledge in the area of Mirandola will reach full knowledge (100 %) more rapidly than with the standard procedure. Indeed, the implemented mobile application can be used during the response phase of a disaster, especially when time is crucial.

8.7 Remarks and Conclusions

This chapter presents several applications of the PEOPLES framework focusing on the physical infrastructure dimension. Several examples are provided for the transportation, water, gas and communication network. In particular, the first case study will present a method to assess resilience of a transportation network, by evaluating the optimal recovery plan that maximizes the resilience index and minimizes the recovery time. In the second case study, the PEOPLES framework is applied to evaluate the resilience performance of a water distribution network. A new resilience index to measure the performance of a water distribution network is proposed, which combines both the technical, the environmental and social dimension of the PEOPLES framework.

In the third case study, a resilience index is proposed and applied to the gas distribution network of the municipalities of Introdacqua and Sulmona, two small towns in the center of Italy which were affected by 2009 earthquake.

In the fourth case study, a methodology to assess resilience of a power distribution network is presented. In the fifth case study, a methodology to improve the

field reconnaissance damage assessment of buildings following an extreme event is proposed. In all the examples presented in this chapter, the infrastructure interdependencies are neglected. Instead next chapter (Chap. 9) focuses on the applications on the physical infrastructure dimension taking into account interdependencies.

References

- Adachi T, Ellingwood BR (2008) Serviceability of earthquake-damaged water systems: effects of electrical power availability and power backup systems on system vulnerability. *Reliab Eng Syst Saf* 93(1):78–88. doi:[10.1016/j.res.2006.10.014](https://doi.org/10.1016/j.res.2006.10.014), <GotoISI>://WOS:000250637000005
- Advantica_Ltd(Germanische-Lloyd) (2009) Synergie gas software 4.3.2 – user’s manual
- ALA (2001) Seismic fragility formulations for water systems part I – guidelines. Report, American Lifeline Alliance (ALA), American Society of Civil Engineers (ASCE)
- Ambraseys NN, Douglas J, Sarma SK, Smit P (2005) Equations for the estimation of strong ground motions from shallow crustal earthquakes using data from Europe and the middle east: horizontal peak ground acceleration and spectral acceleration. *Bull Earthq Eng* 3(1):1–53
- Arcidiacono V, Cimellaro GP (2013) Damage report with smartphones during Emilia earthquake, 2012. In: 4th international conference on computational methods in structural dynamics and earthquake engineering (COMPDYN2013), Kos Island, 12–14 June, 2013
- ATC-20 (2005) Atc-20 procedures for post earthquake safety evaluation of buildings, 2nd edn. Report, Applied Technology Council
- Ballantyne DB, Berg E, Kennedy J, Reneau R, Wu D (1990) Earthquake loss estimation modeling of the Seattle water system. Technical report. Kennedy/Jenks/Chilton, Federal Way, 139p
- Bocchini P, Frangopol D (2011) A stochastic computational framework for the joint transportation network fragility analysis and traffic flow distribution under extreme events. *Probab Eng Mech* 26(2):182–193
- Chen WW, Shih B, Chen YC, Hung JH, Hwang HH (2002) Seismic response of natural gas and water pipelines in the ji-ji earthquake. *Soil Dyn Earthq Eng* 22(9–12):1209–1214. doi:[10.1016/S0267-7261\(02\)00149-5](https://doi.org/10.1016/S0267-7261(02)00149-5). <GotoISI>://WOS:000180004500056. ISI Document Delivery No.: 628PG Times Cited: 9 Cited Reference Count: 7; Chen WW, Shih B, Chen YC, Hung JH, Hwang HH (2001) 10th international conference on soil dynamics and earthquake engineering (SDEE 01) Oct 07–10, Philadelphia. Elsevier Science Ltd
- Choo YW, Abdoun TH, O’Rourke MJ, Ha D (2007) Remediation for buried pipeline systems under permanent ground deformation. *Soil Dyn Earthq Eng* 27(12):1043–1055. doi:[10.1016/j.soildyn.2007.04.002](https://doi.org/10.1016/j.soildyn.2007.04.002). <GotoISI>://WOS:000250641100001. Times Cited: 2
- Cimellaro G, Reinhorn AM, Bruneau M (2010) Framework for analytical quantification of disaster resilience. *Eng Struct* 32(11):3639–3649. doi:[10.1016/j.engstruct.2010.08.008](https://doi.org/10.1016/j.engstruct.2010.08.008)
- Cimellaro GP (2013) Computational framework for resilience-based design (RBD) CH11. Woodhead Publishing Limited, Sawston, book section 11, p 810
- Cimellaro GP, Reinhorn AM (2010) Multidimensional performance limit state for hazard fragility functions. *J Eng Mech* 1(1):156. [http://link.aip.org/link/?EMX/1/156/1http://dx.doi.org/10.1061/\(ASCE\)EM.1943-7889.0000201](http://link.aip.org/link/?EMX/1/156/1http://dx.doi.org/10.1061/(ASCE)EM.1943-7889.0000201)
- Cimellaro GP, Scura G, Renschler C, Reinhorn AM, Kim H (2014a) Rapid building damage assessment system using mobile phone technology. *Earthq Eng Vib* 13(3):519–533. doi:[10.1007/s11803-014-0259-4](https://doi.org/10.1007/s11803-014-0259-4)
- Cimellaro GP, Solari D, Bruneau M (2014b) Physical infrastructure interdependency and regional resilience index after the 2011 Tohoku earthquake in Japan. *Earthq Eng Struct Dyn* 43(12):1763–1784. doi:[10.1002/eqe.2422](https://doi.org/10.1002/eqe.2422)
- Comfort LK, Kapucu N (2006) Inter-organizational coordination in extreme events: the world trade center attack, Sept 11, 2001. *Nat Hazards* 39:309–327

- Davis CA (2014) Water system service categories, post-earthquake interaction, and restoration strategies. *Earthq Spectra* 30(4):1487–1509
- Eguchi R (1983) Seismic vulnerability models for underground pipes. In: *Proceedings of earthquake behavior and safety of oil and gas storage facilities, buried pipelines and equipment* (ASME 1983) New York, pp 368–373
- Erdik M (2013) Post earthquake rapid information generation. In: *Supersites coordination workshop*, Brussels, 10–11 June 2013
- FEMA (2005) Hazus-mh version 1.1, fema's software program for estimating potential losses from disasters, technical manual. Report, Federal Emergency Management Agency and U.S. Army Corps of Engineers
- FEMA (2011) Fema p-154 rover cd, rapid observation of vulnerability and estimation of risk. Report, Federal Emergency Management Agency
- Finch JC, Ko DW (1988) Tutorial – fluid flow formulas. PSIG annual meeting, pipeline simulation interest group, Toronto, 20–21 Oct 1988, PSIG-880
- Fragiadakis M, Christodoulou SE (2014) Seismic reliability assessment of urban water network. *Seism Reliab Assess Urban Water Netw* 43(3):357–374
- Fujiu M, Ohara M, Meguro K (2012) Development of remote building damage assessment system during large-scale earthquake disaster. In: *15th world conference on earthquake engineering (15WCEE)*, Lisbon, 24–28 Sept 2012
- Galli P (2000) New empirical relationships between magnitude and distance for liquefaction. *Tectonophysics* 324(3):169–187
- Graber DA (2003) *The power of communication: managing information in public organizations*. CQ Press, Washington, DC
- Haddow G, Bullock J, Coppola D (2008) *Introduction to emergency management*. Elsevier Limited, Oxford
- Han ZY, Weng WG (2011) Comparison study on qualitative and quantitative risk assessment methods for urban natural gas pipeline network. *J Hazard Mater* 189(1–2):509–518. doi:10.1016/j.jhazmat.2011.02.067. <GotoISI>://WOS:000289870100067. Times Cited: 0
- Hwang HHM, Lin H, Shinozuka M (1998) Seismic performance assessment of water distribution systems. *J Infrastruct Syst ASCE* 4(3):118–125
- Hyman SI, Stoner MA, Karnitz MA (1975) Gas flow formulas – an evaluation. *Pipeline Gas J* (Dec 1975 and Jan 1976)
- Jayaram N, Srinivasan K (2008) Performance-based optimal design and rehabilitation of water distribution networks using life cycle costing. *Water Resour Res* 44(1):W01,417. doi:10.1029/2006WR005316
- Jeon SS, O'Rourke TD (2005) Northridge earthquake effects on pipelines and residential buildings. *Bull Seismol Soc Am* 95(1):294–318. doi:10.1785/0120040020. <GotoISI>://WOS:000228042800019. Times Cited: 10
- Jo YD, Crowl DA (2008) Individual risk analysis of high-pressure natural gas pipelines. *J Loss Prev Process Ind* 21(6):589–595
- Jones C, Mitnick S (2006) Open source disaster recovery: case studies of networked collaboration. doi:http://dx.doi.org/10.5210/fm.v11i5.1325. URL:http://firstmonday.org/issues/issue11_5/jones/index.html
- Jrad A, Uzunalioglu H, Houck DJ, O'Reilly G, Conrad S, Beyeler W (2005) Wireless and wireline network interactions in disaster scenari-os. doi:10.1109/MILCOM.2005.1605710
- K CL (1999) *Shared risk: complex systems in seismic response*. Emerald Group Publishing Limited, New York
- Kapucu N (2006) Interagency communication networks during emergencies: boundary spanners in multiagency coordination. *Am Rev Publ* 36(2):207–225
- Kweit MG, Kweit R (2004) Citizen participation and citizen evaluation in disaster recovery. *Am Rev Publ Adm* 34(4):354–373
- Lord JoP (1992) Disaster relief or relief disaster? A challenge to the international community. *Disasters* 16(1):1–8

- Markov I, Grigoriu M, O'Rourke T (1994) An evaluation of seismic serviceability water supply networks with application to the San Francisco auxiliary water supply system. Technical report NCEER-94-0001, National Center for Earthquake Engineering Research (NCEER)
- Markowski AS, Mannan MS (2009) Fuzzy logic for piping risk assessment. *J Loss Prevent Process Ind* 22(6):921–927
- McEntire D (1997) Reflecting on the weaknesses of the international community during IDNDR: some implications for research and application. *Disaster Prevent Manag* 6(4):221–233
- McEntire D (2012) Coordinating multi-organisational responses to disaster: lessons from the March 28, 2000, Fort Worth Tornado. *Disaster Prevent Manag* 11(5):369–379
- Miles S, Chang S (2006) Modeling community recovery from earthquakes. *Earthq Spectra* 22(2):439–458. <http://link.aip.org/link/?EQS/22/439/1>
- Miles SB, Chang S (2011) Resilus: a community based disaster resilience model. *J Cartogr GIS (CAGIS)* 38(1):36–51
- Mileti D (1999) *Disasters by design: a reassessment of natural hazards in the United States*. Joseph Henry Press, Washington, DC
- Montiel H, Vilchez JA, Arnaldos J, Casal J (1996) Historical analysis of accidents in the transportation of natural gas. *J Hazard Mater* 51(1–3):77–92. doi:10.1016/s0304-3894(96)01819-5. <GotoISI>://WOS:A1996WB58400006. times Cited: 18
- O'Rourke TD, Erdogan FH, Savage WU, Lund LV, Tang A, Basoz N, Edwards C (2000) Water, gas, electric power, and telecommunications performance. *Earthq Spectra* 16(S1):377–402
- Panza G, Mura CL, Peresan A, Romanelli F, Vaccari F (2012) Seismic hazard scenarios as preventive tools for a disaster resilient society. *Adv Geophys* 53:93–165
- Panza G, Peresan A, Magrin A (2014) Neo-deterministic seismic hazard scenarios for Friuli Venezia Giulia and surrounding areas. Report, ISPRA- Istituto Superiore per la Protezione e la Ricerca Ambientale – Servizio Geologico d'Italia
- Park J, Seager T, Rao P, Convertino M, Linkov I (2013) Integrating risk and resilience approaches to catastrophe management in engineering systems. *Risk Anal* 33(3):356–567
- Pelfrey W (2005) The cycle of preparedness: establishing a framework to prepare for terrorist threats. *J Homel Secur Emer Manag* 2(1):1–5
- Poljansek K, Bono F, Gutierrez E (2012) Seismic risk assessment of interdependent critical infrastructure systems: the case of European gas and electricity networks. *Earthq Eng Struct Dyn* 41(1):61–79. doi:10.1002/eqe.1118. <GotoISI>://WOS:000298591500004. Times Cited: 1
- Porter K (1992) Performance of water supply pipelines in liquefied soil. In: Equchi RT (ed) *Proceedings of the fourth US-Japan workshop on earthquake disaster prevention for lifeline systems*, Washington, DC. U.S. Department of Commerce, 1992, NIST special publication, vol 840, pp 3–17
- Prasad TD, Park NS (2004) Multiobjective genetic algorithms for design of water distribution networks. *J Water Resour Plan Manag ASCE* 130(1):73–82
- Rossmann LA (2000) *Epanet users manual*. Report EPA/600/R-00/057, National Risk Management Research Laboratory
- Scawthorn C, Johnson GS (2000) Preliminary report – Kocaeli (izmir) earthquake of 17 August 1999. *Eng Struct* 22(7):727–745. doi:10.1016/s0141-0296(99)00106-6. <GotoISI>://WOS:000085896100001
- Schoch-Spana M, Crystal F, Nuzzo J, Usenza C (2007) Community engagement: leadership tool for catastrophic health events. *Biosecur Bioterrorism* 5(1):8–25
- Scura G, Arcidiacono V, Cimellaro GP, Renschler C, Reinhorn AM (2013) Integrated damage assessment communication system using smartphone network during 2012 Emilia earthquake
- Shinozuka M, H H, M M (1992) Impact on water supply of a seismically damaged water delivery system. *Lifeline Earthquake Engineering in the Central and Eastern US*, Technical Council on Lifeline Earthquake Engineering Monograph No5 Ballantyne, D B, ed, ASCE, Reston, VA pp 43–57
- Shinozuka M, Cheng TC, Feng M, Mau S (1999) Seismic performance analysis of electric power systems. Report, Research Progress and Accomplishments 1997–1999, The Multidisciplinary Center for Earthquake Engineering Research

- Shinozuka SECTFMOTDSMADXJXWY M; Chang, Shi P (2003/2004) Resilience of integrated power and water systems. Report, MCEER
- Spallarossa D, Barani S (2007) Disaggregazione della pericolosità sismica in termini di m-r. progetto dpc-ingv s1, deliverable d14. Report
- Taylor CE (1991) Seismic loss estimation for a hypothetical water system. Monograph (Technical Council on Lifeline Earthquake Engineering, ASCE, Reston), vol 2. The Society, New York
- TNO (1997) Tno – methods for the calculation of physical effects – yellow book. Report, TNO – The Netherlands Organization of Applied Scientific Research
- Todini E (2000) Looped water distribution design using a resilience index based heuristic approach. *Urban Water* 2(2):115–122
- Whitman R, Anagnos T, Kircher C, Lagorio H, Lawson RS, Schneider P (1997) Development of a national earthquake loss estimation methodology. *Earthq Spectra* 13(4):643–662
- Yamin LE., Arambula S, Reyes JC, Belage S, Vega Á, Gil W (2004) Earthquake loss estimation for a gas lifeline transportation system in Columbia. In: 13th world conference on earthquake engineering, Vancouver, Paper no. 2941
- Yuhua D, Datao Y (2005) Estimation of failure probability of oil and gas transmission pipelines by fuzzy fault tree analysis. *J Loss Prevent Process Ind* 18(2):83–88

Chapter 9

The Physical Infrastructure Dimension Taking into Account Interdependencies

Abstract Interdependencies between infrastructures can generate cascading failures or amplification effects, which can affect the restoration measures right after an extreme event and generate a reduction of the resilience index. In the chapter, is proposed a method to evaluate a resilience index of physical infrastructures taking into account their interdependencies. The weights assigned to each infrastructure, which are used to determine the resilience index, are evaluated using the degree of interdependency indicators, determined by the time series analysis. The advantage of the proposed method consists in the capacity to identify the critical lifelines, being unbiased from subjective judgment. However, when the time series is including coupled events, the coupling effect generates distortion in the evaluation of the cross correlation coefficient $S_{i,j}$. This is the case for example when there are strong after-shocks during the lifeline restoration phase right after the main shock. A method to overcome this problem is presented and applied to the physical infrastructure restoration curves recorded during March 11th 2011 Tohoku Earthquake in Japan.

9.1 Interdependencies Between Networks

In this chapter are described applications on lifelines which belong to the physical infrastructure dimension of the PEOPLES framework (Fig. 9.1), however with respect to Chap. 8 in this chapter is described how to deal with interdependencies.

9.1.1 Literature Review

A resilience index is used to quantify preventive measures, emergency measures, and restoration measures of complex systems, such as physical infrastructures, when they are subjected to natural disasters like earthquakes, hurricanes, floods etc. Interdependencies among these systems can generate cascading failures or amplification effects, which can also affect the restoration measures right after an extreme event and generate a reduction of the resilience index.

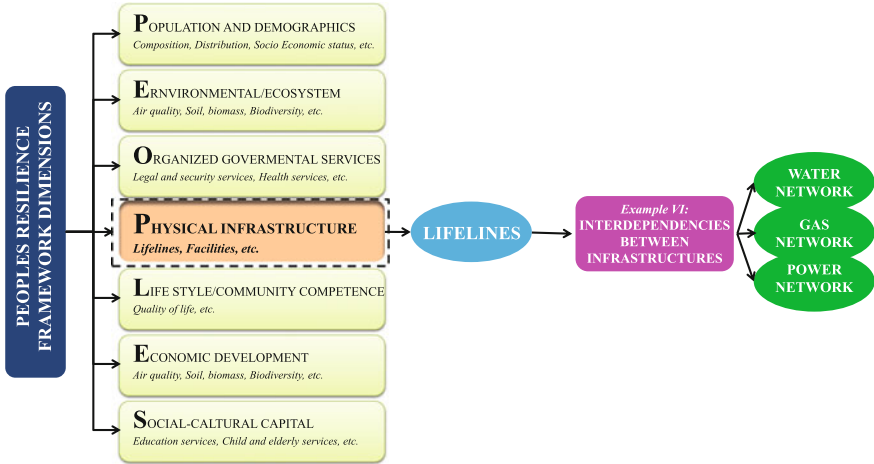


Fig. 9.1 Chapter 9 outline

In recent years, the scientific community has become increasingly interested in lifelines interdependencies and resilience assessment (Cimellaro and Reinhorn 2010; Cimellaro 2013), and several recent studies address the evaluation of interdependency indicators for infrastructures (Arcidiacono and Cimellaro 2012). These works published in the last decade all use the taxonomy of lifeline interdependencies, which is given in the fundamental work by Rinaldi et al. (2001). Paton et al. (2006) have provided numerical quantification of the dependencies among different infrastructures by using an empirical approach in which the degree of dependency among different infrastructures is a function of the strength of dependency (high, medium, low dependency). Bigger et al. (2009) have collected different interdependent lifeline information associated with the 2004 hurricane season in Florida. Delamare et al. (2009) have studied the potential effect of interdependencies that may occur between the telecommunication and the electrical network and they have proposed a model that describes the behavior of these interdependent systems.

Kakderi et al. (2011) have summarized the available methodologies and models for the vulnerability and risk assessment of systems of systems. In their work, they summarized and illustrated definitions of the interaction of complex dependencies available in literature. The classification schemes of dependencies were reviewed, and the available methods for the simulation of interdependencies were summarized and classified into five categories. Furthermore, the main characteristics, advantages and limitations of each category of interdependency were also reported. Alternatively, Kongar and Rossetto (2012) provided a review of the literature using a matrix approach, and used it to describe gaps in knowledge. Based on this review, Kongar and Rossetto (2012) proposed a methodological framework for the assessment of infrastructure vulnerability accounting for interdependencies.

Kjolle et al. (2012) have used contingency analysis (power flow), reliability analysis of power systems, and cascade diagrams for investigating interdependencies. Poljansek et al. (2012) have studied the seismic vulnerability of the European gas and electricity transmission networks from a topological point of view; network interdependency was evaluated using the strength of coupling of the interconnections, together with the seismic response.

Recently, Dueñas-Osorio and Kwasinski (2012) have proposed an approach based on post-analysis of restoration curves. The interdependency index between infrastructures was calculated by an empirical equation that depends on the maximum positive value of the cross correlation function (CCF) of the two data series.

In this section, a method is proposed for evaluating the resilience of a region affected by a disaster considering infrastructure interdependency. The resilience index of every infrastructure in the region is combined with others through the use of weight coefficients, which are calculated starting from a modified version of the interdependence index proposed by Dueñas-Osorio and Kwasinski using cross correlation functions (CCF). A new method to evaluate the interdependency index is proposed and compared with other methods available in literature. The regional resilience index is evaluated taking into account weights coefficients evaluated for every region and infrastructure considered in the analysis. Finally, a method for the treatment of restoration curves is proposed for the case when aftershocks are included in the restoration curves. The method is described using the restoration curves of the physical infrastructures of the twelve regions in Japan which were affected by March 11th 2011 Tohoku Earthquake.

9.1.2 Restoration Curves of Physical Infrastructures After the 2011 Tohoku Earthquake

The proposed method for the evaluation of the interdependency index and the weight coefficients necessary to evaluate the regional resilience index is based on the evaluation of the CCF for different restoration curves. In this part, the restoration curves used for the analysis are the time series recorded during the March 11th 2011 Tohoku Earthquake, in the twelve nearby Japanese prefectures of Miyagi, Ibaraki, Fukushima, Yamagata, Akita, Ibaraki, Tochigi, Aomori, Chiba, Gunma, Saitama and Kanagawa (listed here by increasing distance from the epicenter).

The functionality $Q(t)$ in the y axis of Fig. 9.2 is defined as the restoration ratio between the number of households without service and the total number of households. In particular, Fig. 9.2 shows the restoration curves for three different types of lifelines (*Power delivery*, *Water supply*, *City Gas delivery*) for Miyagi, Iwate, Fukushima, Ibaraki, Aomori and Saitama. For Yamagata, Akita, Tochigi and Gunma, only data on Power delivery and Water supply are available, whereas for the Chiba and Kanagawa prefecture, only restoration curves for the Power delivery and City Gas delivery are available. Figure 9.2 also shows the effects on the restoration

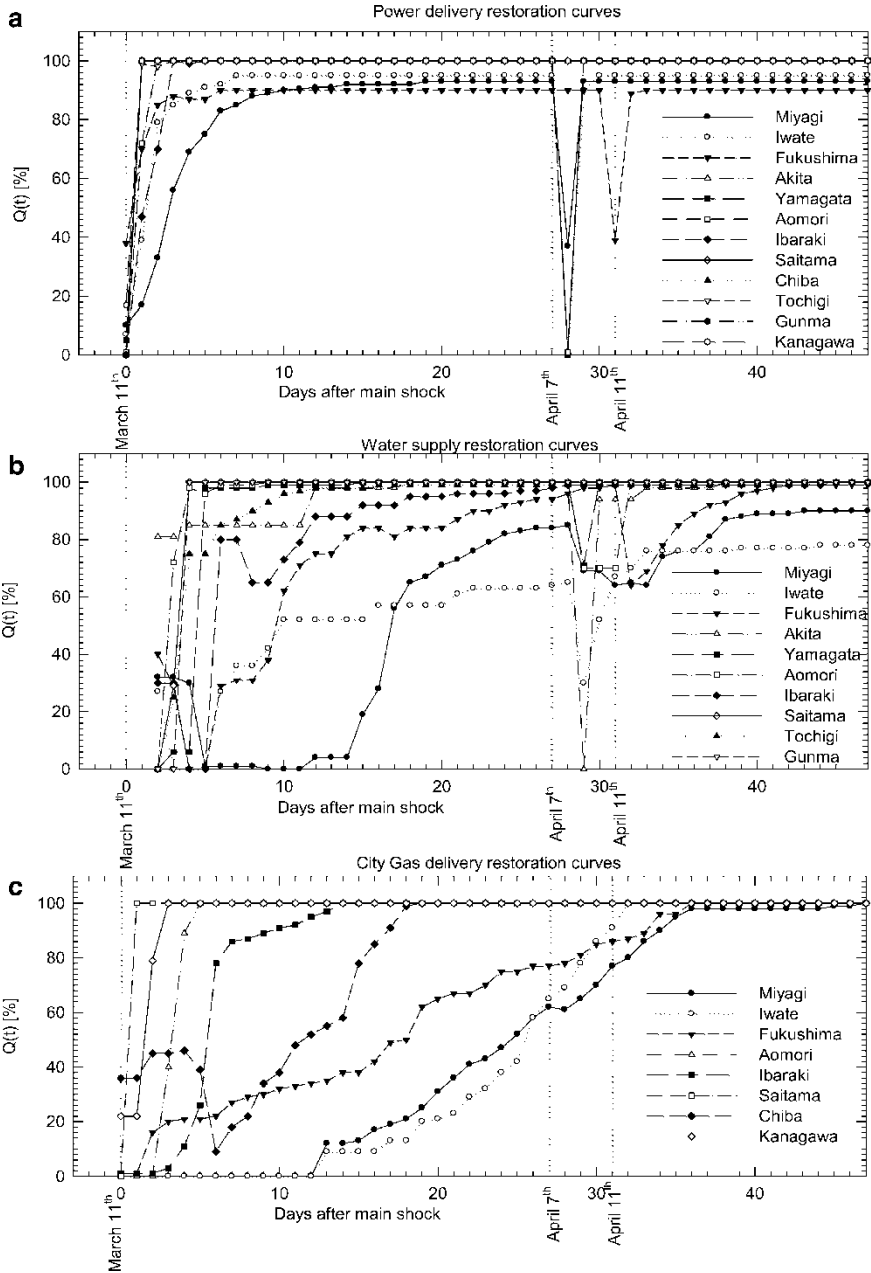


Fig. 9.2 Restoration curves for different Japan prefectures after the 2011-03-11 Mw=9.0 earthquake for three infrastructures: Power delivery (a), Water supply (b), City Gas delivery (c) (three infrastructures: power delivery)

curves of two main aftershocks, which occurred on April 7th ($M=7.2$) and on April 11th ($M=7.0$), on the different infrastructures and regions respectively. The first aftershock reduced the serviceability in the regions located near the epicenter of the main shock, whereas the second aftershock reduced the serviceability of lifelines in the Fukushima prefecture only. City Gas delivery was not influenced by the two aftershocks in any region.

9.1.3 Evaluation of Interdependency Index

To calculate the CCF functions of the different restoration curves, the time series must be at least weakly stationary (Shumway and Stoffer 2011). To minimize the effects of non-stationary data and to obtain meaningful statistical analyses, the time series data have been logarithmically transformed and second-differenced (Fig. 9.3a). This transformation stabilizes the variability, and the mean value which remains constant throughout time, while the auto-covariance values decay rapidly and only depend on the time-difference $h = t_1 - t_2$ between the data series, where t_1 and t_2 are arbitrary points in time (Shumway and Stoffer 2011). An example of the results of the transformation, about Power delivery and Water supply for the Miyagi region, is shown in Fig. 9.3a. After the logarithmic transformation and the second-differenced of the data series, it is possible to evaluate the CCF functions for different combinations of the restoration curves.

Figure 9.3b shows an example of the CCF function between Power delivery and Water supply for the Miyagi region. In the x-axis is the lag, analytically defined as a fixed time displacement which corresponds to the number of periods, $k > 0$, that a variable occurring at time $t + k$ is lagging behind to predict the variable occurring at time t . Four different approaches and equations for the evaluation

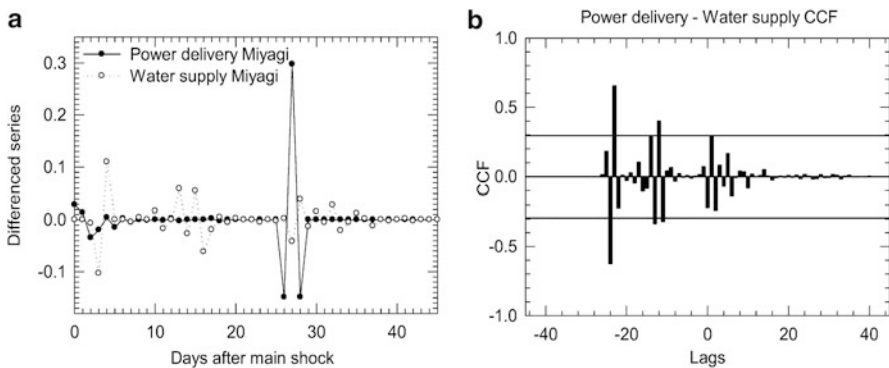


Fig. 9.3 Miyagi region data: (a) Power delivery and Water supply restoration curves logarithmically transformed and second differenced; (b) Cross correlation function of power delivery and water supply

of the interdependency index $S_{i,j}$ among different infrastructures are proposed (Eqs. 9.2, 9.3, 9.4, and 9.5), and compared with the results of Eq. 9.1 which has been proposed by Dueñas-Osorio and Kwasinski;

$$S_{i,j} = \begin{cases} \frac{\rho_{i,j}^+(h)}{1+\sqrt{|h|}} \times \text{sgn}(h) & \text{when } h \neq 0 \\ \rho_{i,j}^+(h) & \text{when } h = 0 \end{cases} \quad (9.1)$$

where $\rho_{i,j}^+(h)$ corresponds to the maximum positive CCF value, which occurs at the peak lag time value h with absolute value $|h|$, and the sign function (sgn) is used to keep track of the dominant system. The i th system leads [lags] the restoration of the j th system when $S_{i,j}$ is positive [negative] (Dueñas-Osorio and Kwasinski 2012). The four proposed alternative equations are:

$$S_{i,j} = \begin{cases} \frac{\rho_{i,j}^+(h)}{h} & \text{when } h \neq 0 \\ \rho_{i,j}^+(h) & \text{when } h = 0 \end{cases} \quad (9.2)$$

$$S_{i,j} = \frac{1}{N} \sum_{k=1}^N \begin{cases} \frac{\rho(h_k)}{1+\sqrt{|h_k|}} \times \text{sgn}(h_k) & \text{when } \rho(h_k) \geq \rho_{tr} \text{ when } h_k \neq 0 \\ \rho(h_k) & \text{when } \rho(h_k) \geq \rho_{tr} \text{ when } h_k = 0 \end{cases} \quad (9.3)$$

$$S_{i,j} = \frac{1}{N} \sum_{k=1}^N \begin{cases} \frac{\rho(h_k)}{h_k} & \text{when } \rho(h_k) \geq \rho_{tr} \text{ when } h_k \neq 0 \\ \rho(h_k) & \text{when } \rho(h_k) \geq \rho_{tr} \text{ when } h_k = 0 \end{cases} \quad (9.4)$$

$$S_{i,j} = |A_{i,j}|^{\frac{1}{N}} \cdot \text{sgn}(A_{i,j}) \quad (9.5)$$

$$A_{i,j} = \frac{1}{N} \sum_{k=1}^N \begin{cases} \frac{\rho(h_k)}{1+\sqrt{|h_k|}} \times \text{sgn}(h_k) & \text{when } \rho(h_k) \geq \rho_{tr} \text{ when } h_k \neq 0 \\ \rho(h_k) & \text{when } \rho(h_k) \geq \rho_{tr} \text{ when } h_k = 0 \end{cases} \quad (9.6)$$

where $\rho_{i,j}^+(h)$ corresponds to the maximum positive CCF value, which occurs at the peak lag time value h ; $\rho(h_k)$ corresponds to the CCF values which occur at lag time h_k ; ρ_{tr} is the value of the positive threshold of statistical significance (the threshold is shown in Fig. 9.3 with the two horizontal solid lines); and N corresponds to the number of CCF values that exceed the upper bound of statistical significance.

The n -infrastructure restoration curves are analyzed and the results are organized in an $n \times n$ matrix where every element ranges between -1 and 1 . Positive values of this index shows that the i th infrastructure (row) leads the restoration process of the j th infrastructure (column), while negative value of the index shows that the i th infrastructure (row) is lags behind the restoration process of the j th infrastructure (column). The magnitude of the dependence is given by the absolute value of the index; when it is close to 1 , the dependency is high, while when it is close to 0 the dependency is weak (zero value indicates absence of dependency).

The results for the March 11th 2011 Tohoku Earthquake are shown in Table 9.1, while in Fig. 9.4 the comparison of the different interdependency indicators $S_{i,j}$ is

Table 9.1 Comparison of different interdependency indices from different equations (TLC = 47 days)

Region		Sij Eq. (8.22) (Dueñas-Osorio and Kwasinski 2012)	Sij Eq. (8.23)	Sij Eq. (8.24)	Sij Eq. (8.25)	Sij Eq. (8.26)
Miyagi	Power – Water	-0.11	-0.10	-0.03	-0.03	-0.35
	Power – Gas	-0.15	-0.15	-0.05	-0.05	-0.19
	Water – Gas	0.10	0.03	0.04	0.00	0.31
Iwate	Power – Water	0.33	0.07	0.66	0.21	0.55
	Power – Gas	-0.10	-0.13	-0.03	-0.08	-0.56
	Water – Gas	-0.10	-0.04	-0.08	-0.03	-0.38
Fukushima	Power – Water	0.22	0.04	0.44	0.14	0.47
	Power – Gas	-0.11	-0.10	-0.02	-0.03	-0.35
	Water – Gas	-0.15	-0.15	-0.11	-0.11	-0.23
Yamagata	Power – Water	-0.13	0.02	-0.03	0.16	0.31
Akita	Power – Water	0.46	0.46	0.93	0.93	0.93
Ibaraki	Power – Water	0.14	0.14	0.09	0.09	0.20
	Power – Gas	0.19	0.16	0.12	0.12	0.49
	Water – Gas	0.87	0.87	0.87	0.87	0.87
Tochigi	Power – Water	0.29	0.29	0.26	0.26	0.45
Aomori	Power – Water	-0.13	-0.13	-0.03	-0.03	-0.15
	Power – Gas	-0.11	-0.11	-0.03	-0.03	-0.13
	Water – Gas	0.72	0.72	0.72	0.72	0.72
Chiba	Power – Gas	0.15	0.15	0.11	0.11	0.23
Gunma	Power – Water	0.26	0.26	0.23	0.23	0.40
Saitama	Power – Water	0.29	0.29	0.27	0.27	0.46
	Power – Gas	1.00	1.00	1.00	1.00	1.00
	Water – Gas	-0.29	-0.29	-0.27	-0.27	-0.46
Kanagawa	Power – Gas	0.28	0.28	0.55	0.55	0.55

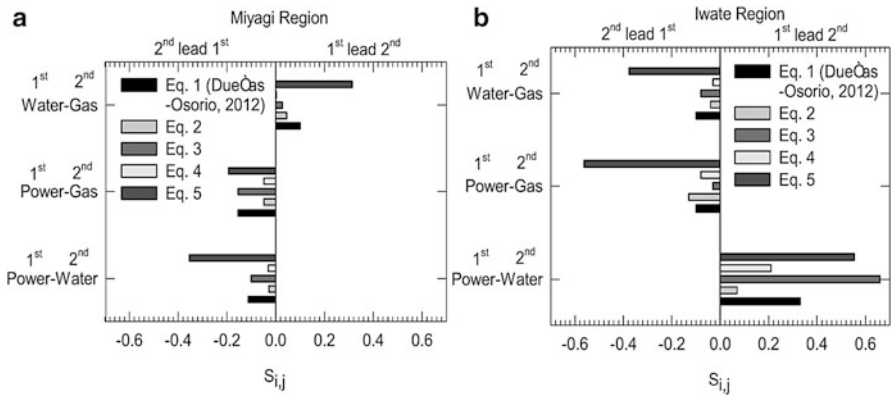


Fig. 9.4 Comparison of different interdependency index proposed for Miyagi (a) and Iwate regions (b)

shown, evaluated with the different equations for the regions of Miyagi and Iwate respectively. Equation 9.5 generally gives the highest values of the interdependency index, while the other equations have lower values of $S_{i,j}$. Equations 9.3 and 9.4 have the lowest values of the interdependency index, because the $S_{i,j}$ index are evaluated from the average of the values of the CCF function, which exceed the positive threshold of statistical significance. From Table 9.1, it is observed that the interdependency index relative to the Power-delivery evaluated with the different equations using the restoration curves of 47 days, often has negative value, which has no physical meaning. This behavior is also well highlighted in Fig. 9.4, where the interdependency indicators resulting from all the different equations taken into consideration are reported. All equations used for the evaluation of the $S_{i,j}$ index give results that are consistently of the same sign, but differences are observed in the absolute values.

9.1.4 Evaluation of the Weight Coefficients of the Infrastructures

The weights coefficients, w_i for the different infrastructures, which are necessary to assess the regional resilience, are calculated with Eq. 9.7. The matrix $S_{i,j}$ is a square matrix in which the terms on the diagonal are always equal to 1, whereas the terms outside the diagonal can range from -1 to $+1$. Positive values indicate that the lifeline in the row “leads” the lifeline in the column. The weight coefficients are calculated using the positive values of the interdependency matrices ($S_{i,j}$) corresponding to different lifelines. First all the positive terms are added, per row. Second, the weight coefficients are calculated as the ratio between the sum of the positive values in one row and the sum of all positive terms in the matrix $S_{i,j}$, namely:

$$w_i = \frac{\sigma_i}{\sum_i \sigma_i} \quad (9.7)$$

where σ_i is the sum of the positive values of the i th row of the interdependence matrix $S_{i,j}$, given by:

$$\sigma_i = \sum_j S_{i,j} \text{ when } S_{i,j} > 0 \quad (9.8)$$

The physical meaning of the weights coefficients can be explained with an example, by assuming that the infrastructures are independent. In this special case the S matrix is an identity matrix; therefore, the weight coefficients evaluated with Eq. 9.7 will all be identical. Equal weight coefficients in this particular condition have physical meaning because in this case no infrastructure is leading another one, so no one can be considered more important than the other ones. The different weight coefficients were evaluated using Eqs. 9.2, 9.3, 9.4 and 9.5 for the 12

Table 9.2 Weight coefficients for the computation of regional resilience

Si,j Eq. (8.22) (Dueñas-Osorio & Kwasinski)		Si,j Eq. (8.23)	Si,j Eq. (8.24)	Si,j Eq. (8.25)	Si,j Eq. (8.26)	Same weight	
Miyagi	Power	0.30	0.32	0.30	0.32	0.26	0.33
	Water	0.36	0.34	0.34	0.34	0.43	0.33
	City Gas	0.34	0.34	0.35	0.34	0.31	0.33
Iwate	Power	0.38	0.44	0.42	0.46	0.37	0.33
	Water	0.28	0.27	0.39	0.38	0.24	0.33
	City Gas	0.34	0.29	0.19	0.17	0.39	0.33
Fukushima	Power	0.35	0.40	0.40	0.44	0.39	0.33
	Water	0.29	0.28	0.38	0.38	0.27	0.33
	City Gas	0.36	0.32	0.22	0.18	0.34	0.33
Yamagata	Power	0.47	0.49	0.75	0.78	0.65	0.50
	Water	0.53	0.51	0.25	0.22	0.35	0.50
Akita	Power	0.59	0.66	0.59	0.66	0.66	0.50
	Water	0.41	0.34	0.41	0.34	0.34	0.50
Ibaraki	Power	0.26	0.24	0.15	0.13	0.27	0.33
	Water	0.37	0.38	0.43	0.44	0.36	0.33
	City Gas	0.37	0.38	0.43	0.44	0.36	0.33
Tochigi	Power	0.56	0.56	0.56	0.56	0.59	0.50
	Water	0.44	0.44	0.44	0.44	0.41	0.50
Aomori	Power	0.21	0.22	0.21	0.22	0.21	0.33
	Water	0.40	0.39	0.40	0.39	0.40	0.33
	City Gas	0.39	0.39	0.39	0.39	0.39	0.33
Chiba	Power	0.54	0.53	0.54	0.53	0.55	0.50
	City Gas	0.46	0.47	0.46	0.47	0.45	0.50
Gunma	Power	0.56	0.55	0.56	0.55	0.58	0.50
	Water	0.44	0.45	0.44	0.45	0.42	0.50
Saitama	Power	0.41	0.41	0.41	0.41	0.42	0.33
	Water	0.18	0.18	0.18	0.18	0.17	0.33
	City Gas	0.41	0.41	0.41	0.41	0.42	0.33
Kanagawa	Power	0.56	0.61	0.56	0.61	0.61	0.50
	City Gas	0.44	0.39	0.44	0.39	0.39	0.50

Japanese prefectures affected by the 2011 earthquake and for the three lifelines considered above. All the results are shown in Table 9.2, and part of these results are shown in Fig. 9.5 for Miyagi and Iwate prefectures.

9.1.5 Evaluation of the Regional Resilience Index

As described in Chap. 2, resilience is defined as “a normalized function indicating capability to sustain a level of functionality or performance for a given building,

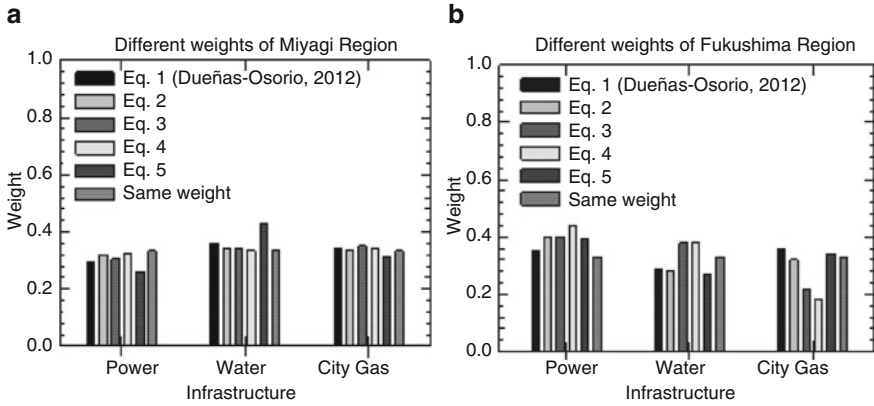


Fig. 9.5 Comparison of different weights coefficients for Miyagi region (a) and for Fukushima region (b) for the three different infrastructures

bridge, lifeline, networks or community over a period of time T_{LC} (life cycle, life span etc. etc)”. Analytically the resilience index of each infrastructure is given by the following equation:

$$R_i = \int_0^T \left(\frac{Q_i(t)}{T_c} \right) dt \quad (9.9)$$

where R_i is the resilience value of the i th infrastructure, $Q_i(t)$ is the functionality of the i th infrastructure at time t , T_c is the control period that is taken in this case to be 47 days (i.e., the length of available records for the March 11th 2011 Tohoku Earthquake). Once the weight coefficients are known, the regional resilience index is evaluated, multiplying the resilience of each lifeline by the corresponding weight coefficient (i.e., the one corresponding to the row on which the lifeline is situated in the matrix $S_{i,j}$) and adding the results obtained inside all regions. The regional resilience is evaluated with Eq. 9.10 using the weights of the different infrastructures calculated with Eq. (9.7).

$$R = \sum_i (R_i \times w_i) \quad (9.10)$$

Results are shown in Table 9.3 and in Fig. 9.6 for different weights of infrastructure’s resilience.

Results in Fig. 9.6 confirm that the major damage occurred in the regions near the epicenter of the main shock (as intuitively expected).

Discrepancies on this trend are observed only for the prefectures facing the Pacific coast (Miyagi, Iwate, Fukushima, Ibaraki, Aomori, Chiba, Kanagawa), in which the tsunami caused relevant damage (lower values of the resilience index) in areas far from the epicenter. For example, Chiba suffered more damage than Tochigi even if Chiba is more distant from the epicenter of the earthquake than Tochigi.

Table 9.3 Comparison of different interdependency indices from different equations

Region	Eq. (8.22) (Dueñas-Osorio and Kwasinski 2012)	Eq. (8.23)	Eq. (8.24)	Eq. (8.25)	Eq. (8.26)	Same weight
Miyagi	0.61	0.62	0.62	0.62	0.61	0.63
Iwate	0.67	0.69	0.69	0.70	0.66	0.65
Fukushima	0.75	0.78	0.77	0.79	0.76	0.76
Yamagata	0.92	0.94	0.92	0.94	0.94	0.92
Akita	0.95	0.95	0.95	0.95	0.95	0.94
Ibaraki	0.88	0.87	0.88	0.87	0.88	0.89
Tochigi	0.94	0.94	0.94	0.94	0.94	0.94
Aomori	0.97	0.97	0.97	0.97	0.92	0.96
Chiba	0.90	0.90	0.89	0.89	0.90	0.89
Gunma	0.95	0.95	0.95	0.95	0.95	0.95
Saitama	0.93	0.93	0.93	0.93	0.97	0.93
Kanagawa	0.97	0.97	0.98	0.98	0.98	0.97

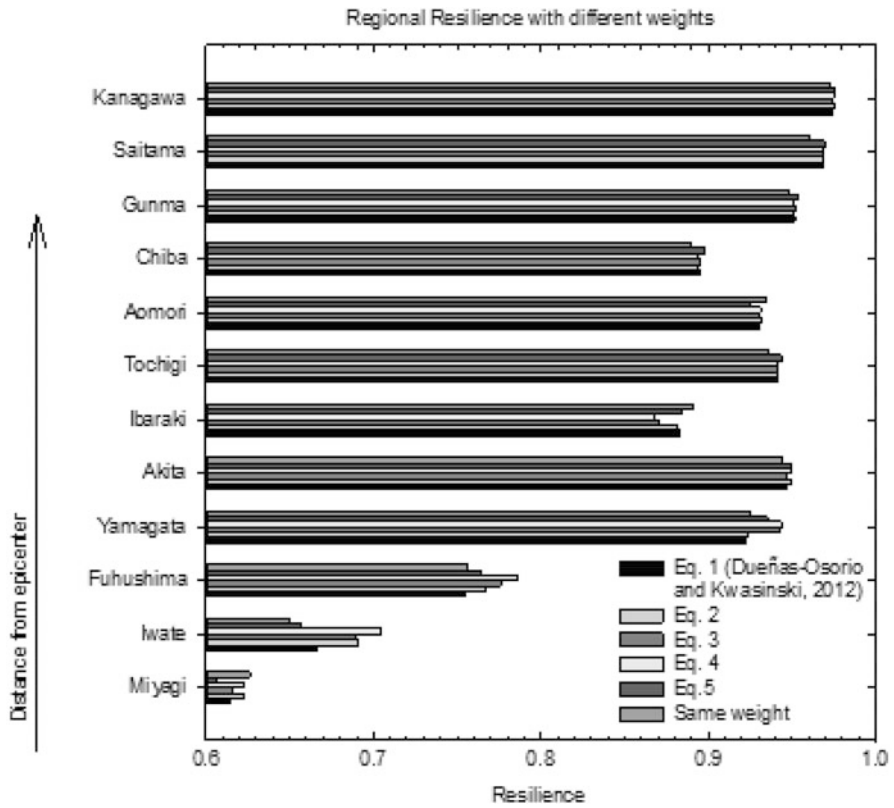


Fig. 9.6 Regional resilience calculated using different methods to calculate weight coefficients starting from the resilience index of every infrastructure

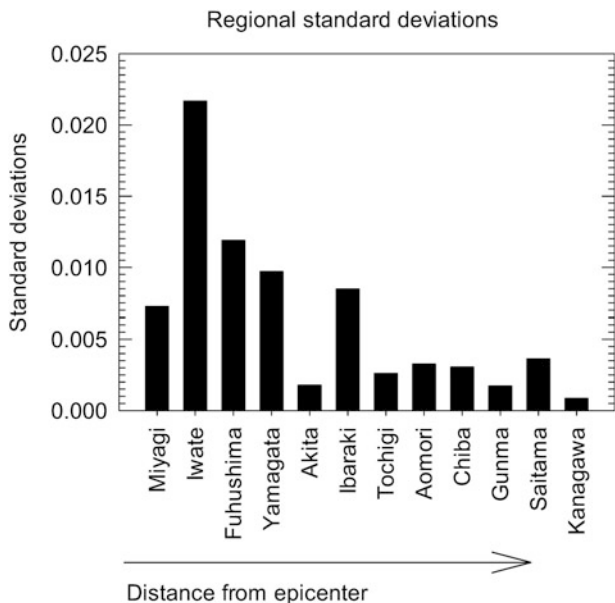


Fig. 9.7 Standard deviation of regional resilience

This is because Chiba is on the Pacific coast, while Tochigi is an interior region. Note that resilience in this context should be understood to be a response parameter and not an intrinsic property of the community; therefore higher values of resilience in region far from the epicenter such as Kanagawa does not necessarily mean that the community itself is resilient to earthquakes that could occur closer. To translate these results into community resilience, another parameter independent from the earthquake input (or normalizing results in terms of local level of ground shaking), which is beyond the scope of this section, should be taken into account.

Figure 9.7 shows the standard deviation of the regional resilience index ordered by region according to distance from the epicenter. Near the epicenter the higher values of standard deviation are observed; those then decrease farther from the epicenter. So results in Figs. 9.6 and 9.7 show that the type of approach taken to calculate the weight coefficients does not significantly influence the values of the resilience index for regions far from the epicenter.

9.1.6 Discussion on the Evaluation of the Interdependency Indices

The regional resilience index defined in Eq. (9.10) depends on the weight factors (Eq. (9.7)), which themselves depend on the interdependency indicators $S_{i,j}$. Therefore, a proper methodology for evaluating $S_{i,j}$ is necessary in order to evaluate

resilience. By comparing the interdependency indicators proposed above, it can be observed that Eqs. (9.1), (9.3) and (9.5) have the denominator term proportional to $\sqrt{|h|}$ that has the effect of amplifying the interdependency index, compared to Eqs. (9.2) and (9.4) that have the denominator term proportional to h (Fig. 9.4). In fact, Eqs. (9.1), (9.3) and (9.5) give more weight to the lags which are more distant from lag 0, with respect to Eqs. (9.2) and (9.4). Therefore if the CCF function has one peak only to lag (typical for Power delivery CCF functions), Eqs. (9.1) and (9.2) give a value of $S_{i,j}$ which is roughly half of the one obtained using Eqs. (9.1) and (9.3).

Equations (9.1) and (9.2) consider only the peak positive value of the CCF function in their formulation, neglecting the corresponding threshold of statistical significance. Instead, Eqs. (9.3) and (9.5) consider only the positive values of the CCF function above the respective threshold. According to the authors, the approach followed by Eqs. (9.3), (9.4) and (9.5) is statistically meaningful, because all peak positive values below the statistical threshold don't have any statistical significance. Therefore the follow observations focus on results obtained from the last three equations.

Equation (9.3) gives values of $S_{i,j}$ which are lower with respect to the ones obtained using Eqs. (9.4) and (9.5) (because of the form of the denominator described above), when the CCF functions have only one peak to lag, which is usually the case for the Power delivery CCF functions. In fact, after the main shock, the power delivery network suffers a rapid drop in functionality before the other infrastructures as shown in Fig. 9.2. However, the electric network is also the first lifeline that is repaired after a disaster, because other infrastructures depend on it. These considerations provide good reasons to disregard Eq. (9.3). Because of the structure of the denominator, Eq. (9.4) is less sensitive to the values of the CCF far from lag 0, and, in general, gives lower values of the interdependency index with respect to the other equations, as shown in Fig. 9.4. In fact, Eq. (9.4), by averaging the values of the CCF functions above the positive threshold, provides lower values of the interdependency index, especially when the CCF functions have one of these values that is small, which is usually the case when it is distant from lag 0. Because of the lesser sensitivity in those cases, Eq. (9.4) is less desirable. Equation (9.5) provides higher values of $S_{i,j}$, with respect to Eq. (9.1), when there is more than one value of the CCF function above the positive threshold of statistical significance. Furthermore, Eq. (9.5) is the only one that provides meaningful results, because as shown in Fig. 9.4b, Equation provides the highest $S_{i,j}$ value for Power delivery and the lowest values (maximum negative values of $S_{i,j}$) for other infrastructures dependent on this factor (which is consistent with engineering judgment). Therefore, based on the considerations above, Eq. (9.5) is retained as the recommended approach for the evaluation of the interdependency indicators $S_{i,j}$. Therefore, to investigate robustness of the formulation, sensitivity analysis has been conducted on Eq. (9.5) with different hypothetical CCF function shapes (Fig. 9.8) and the results are compared with the Eq. (9.1) proposed by Dueñas-Osorio and Kwasinski.

Figure 9.8a shows a CCF function with a constant value less than 1 (0.8) with the threshold value assumed equal to 0.5., meanwhile, in Fig. 9.8b the response of

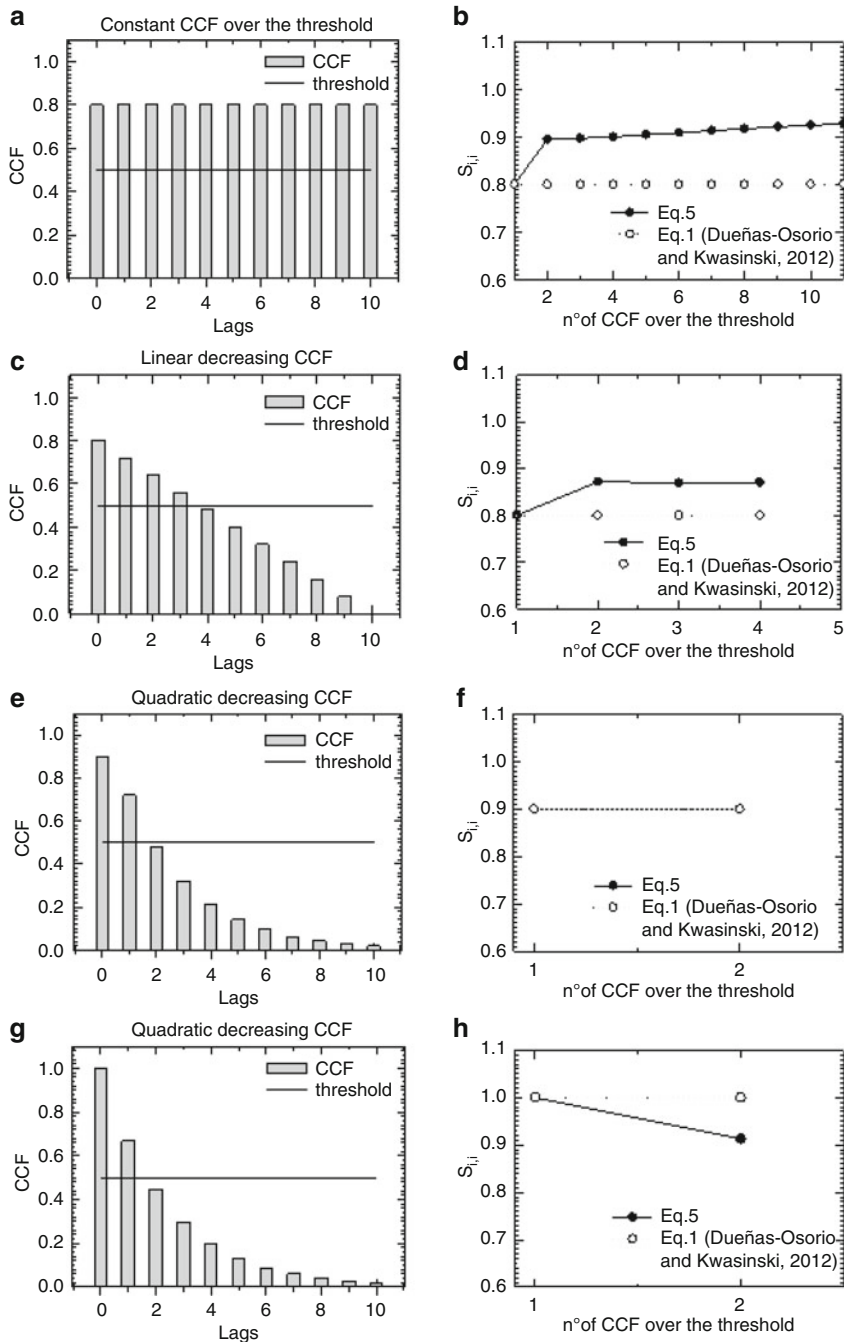


Fig. 9.8 Comparison of the Interdependency Index between Eqs. (9.1) and (9.5) with quadratic decreasing CCF values

Eqs. (9.1) and (9.5) is plotted as a function of the number of CCF values over the threshold taken into account for the calculation of $S_{i,j}$. It's observed how, if one considers only the first value at lag 0 over the threshold, the two equations give the same result. However, when increasing the number of CCF values taken into account, Eq. (9.5) gives a value of $S_{i,j}$ higher than that which would be achieved using Eq. (9.1). It is also observed that the difference between the two functions increases when increasing the values of the CCF function above the threshold taken into consideration in the calculation.

In fact, Eq. (9.5) produces an increment of the interdependency index when there is more than one value of the CCF function above the threshold of statistical significance. For example, Fig. 9.8c shows a CCF function which starts from lag 0 with a value of 0.8 and linearly decreases until the value of 0 for a lag of 10. The threshold is also equal to 0.5 in this case. For comparison, Fig. 9.8d shows the response obtained by Eqs. (9.1) and (9.5) as function of the number of CCF values over the threshold taken into account for the calculation of $S_{i,j}$. Again, if one considers only the first value at lag 0 over the threshold, the two equations give the same result. When increasing the number of CCF values taken into account, Equation gives $S_{i,j}$ values higher with respect to Eq. (9.1), but the difference between the two functions remains constant; in particular, the difference between the results of Eqs. (9.1) and (9.5) is less, compared to the case shown in Fig. 9.8b.

Figure 9.8f shows a boundary behavior of Eq. (9.5), which gives the same results as Eq. (9.1) regardless the number of CCF values (shown in Fig. 9.8e) considered in Equation for the computation of $S_{i,j}$. This behavior appears every time the ratio between the value of the CCF function at lag 1 and the value of the CCF function at lag 0 is equal to a certain value, which is a function of the value that assumes the CCF function at lag 0.

Figure 9.9 plots the ratio of the 2nd CCF value/1st CCF value vs. the 1st CCF value, and compares Eqs. (9.1) and (9.5) by identifying two regions of solutions, namely: Region 1 (where Eq. (9.5) gives a lower $S_{i,j}$ values with respect to Equation, as shown in Fig. 9.8g, h) and Region 2 (where Eq. (9.5) gives a higher $S_{i,j}$ values with respect to Eq. (9.1)). In particular, the curved line in this figure corresponds to the case in which Eq. 9.1 gives the same result as Eq. 9.5, which corresponds to the case shown in Fig. 9.8e, f. Furthermore, it is observed from this figure that when the first value of the CCF function at lag 0 ranges between 0 and 0.5, Eq. (9.5) gives higher values of $S_{i,j}$, regardless the CCF function value at lag 1.

The sensitivity analysis of the $S_{i,j}$ index evaluated with Eq. (9.5) has been performed to identify the interval of significance, as well as the advantages and limitations of the proposed equation. In fact, in Region 1 an increment of the $S_{i,j}$ index using Eq. (9.5) appears when more than one value of the CCF function exceeds the threshold of statistical significance (Fig. 9.8), while when the $S_{i,j}$ index appears in Region 2 (Fig. 9.9), Eq. (9.5) underestimates the $S_{i,j}$ index with respect to Eq. (9.1).

Finally, Fig. 9.10 shows the comparison of Eqs. (9.1) and (9.5) for a real CCF function resulting from the cross correlation of the restoration curves recorded after the March 11th 2011 Tohoku Earthquake, relating City Gas delivery and Water supply for the prefecture of Iwate in Japan. In this real case where more than

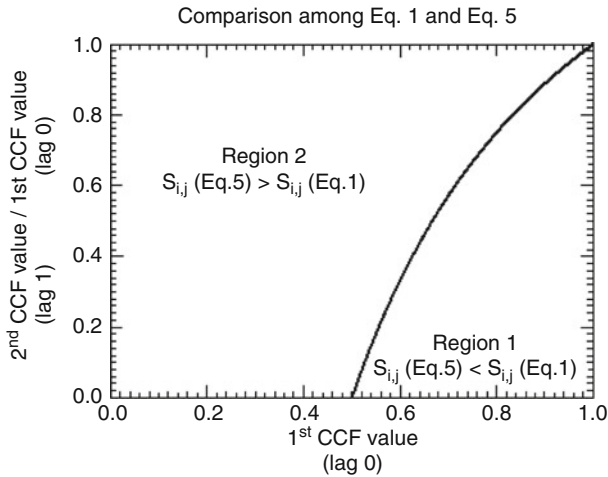


Fig. 9.9 Comparison of CCF values between Eq. (9.1) proposed by Dueñas-Osorio and Kwasinski and Eq. (9.1)

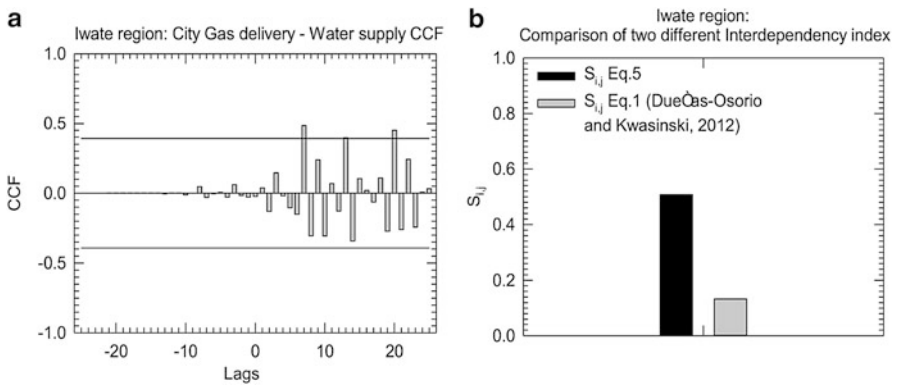


Fig. 9.10 Comparison of interdependency indicators for City Gas delivery and Water supply in Iwate region using Eqs. (9.1) and (9.5)

one value of the CCF function exceeds the threshold for statistical significance, Eq. (9.5) provides $S_{i,j}$ values higher than those obtained with the Equation proposed by Dueñas-Osorio and Kwasinski.

The two equations have also been compared for earthquakes other than Tohoku earthquake. In particular, the restoration curves of the infrastructures for the 2010 Chile earthquake have been used for comparison using the restoration curves of Region VIII, one of the fifteen first-order administrative divisions in Chile. The $S_{i,j}$ indicators have been plotted in Fig. 9.11, where it appears that the proposed Eq. (9.5) provides higher values of the indicators with respect to Eq. (9.1) for all the cases analyzed, in particular when there is more than one value of the CCF function

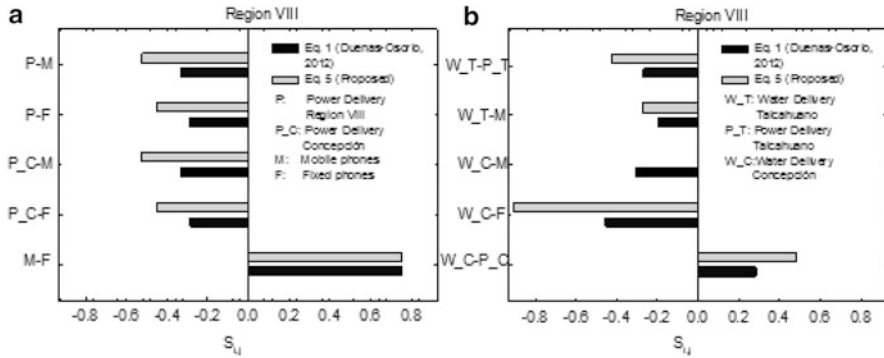


Fig. 9.11 Comparison of different interdependency index (Eqs. (9.1) and (9.5)) for region VIII of February 27, 2010 Chile earthquake

over the positive threshold of statistical significance. In conclusion the same trend of Tohoku earthquake shown in Fig. 9.4 has been observed in Chile Earthquake.

9.1.7 Decomposition of the Restoration Curves in Intervals Ranging Between Two Consecutive Shocks

Careful analysis of the results shown in Fig. 9.4a revealed an anomalous behavior of the interdependency index in the Miyagi prefecture, as results indicated a negative value for the combinations of Power-Water and Power-Gas. This negative value would have implied that Power delivery was controlled by Water supply and Gas delivery. This was not logical, because electricity normally leads in affecting the performance of the other networks (for example, electricity is needed for the operation of pumps and valves, which are themselves essential for the proper function of aqueducts and gas pipelines). This incoherent behavior of the interdependency index was also observed in Fig. 9.4b for the Iwate prefecture, in which the index of interdependency had a negative value for the combination Power-Gas.

This anomaly was found with all equations considered, including the one proposed by Dueñas-Osorio and Kwasinski and it was found to be a consequence of the nature of the restoration curves under consideration. The numerical error derives from the data collected after the main shock over a time period during which two strong aftershocks occurred. In fact, these aftershock events have affected the functionality of lifelines, perturbing the restoration curves. The solution to this problem can be found by dividing the data into homogeneous parts of the restoration curves corresponding to the elapsed time between two consecutive strong shocks. Figure 9.12 shows this operation for the Miyagi region. Figure 9.12a shows the entire data set recorded from the main shock on March 11th, 2011, for 47 consecutive days. The vertical dotted lines correspond to the main shocks and

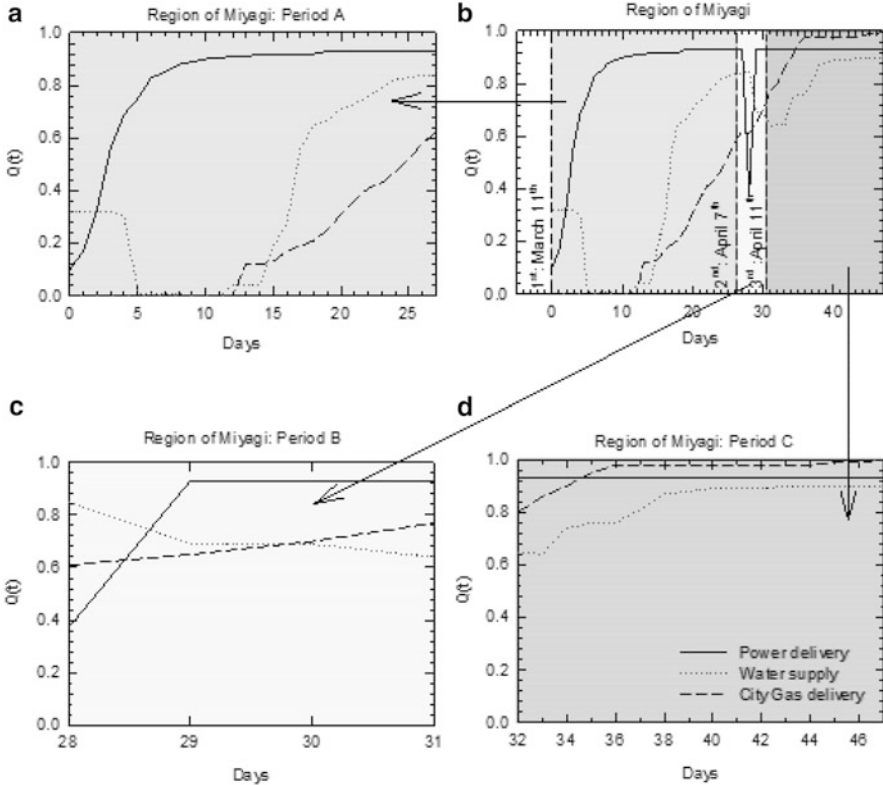


Fig. 9.12 Restoration curves from main shock to the end of the records of data (a). Restoration curves between main shock and first strong aftershock (b). Restoration curves between first strong aftershock and second strong aftershock (c). Restoration curves between second strong aftershock and the end of available records of data (d)

aftershocks. Three period ranges are identified: the first from the main shock of March 11th to April 7th when the first main aftershock occurred (Fig. 9.12b); the second from April 7th to April 11th, when the second main aftershock occurred (Fig. 9.12c); the third from April 11th to until the end of recorded data (Fig. 9.12d). Re-analysis is then performed for each region examined, using the same period range as reference. For each period, the cross-correlation analysis of the restoration curves are performed after the logarithmic transformation and the second differences as described above.

Figure 9.13 shows the cross-correlation function for the region of Miyagi calculated over the first period range (period A) of the time series. Looking at the cross-correlation function between Power delivery and City Gas delivery (Fig. 9.13b), it is noted that, now, Power delivery lead the City Gas delivery restoration process during period A, because there is a high positive value of CCF, over the statistical threshold, at positive lag. This leads to a positive value of

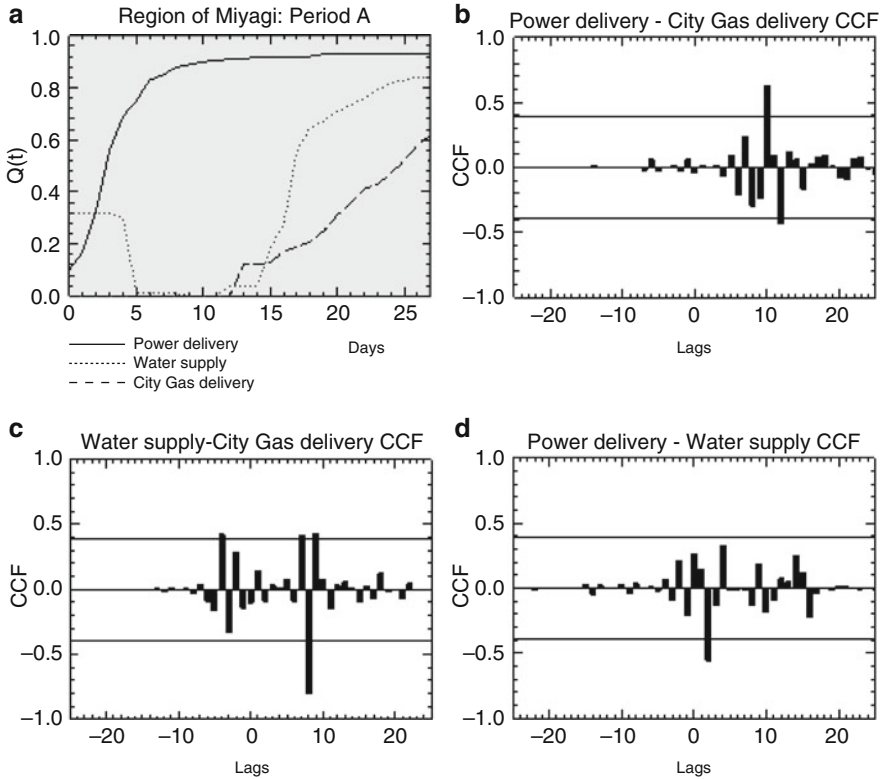


Fig. 9.13 Region of Miyagi: cross-correlation functions for the data of restoration curves from main shock to first strong aftershock

the interdependency index, regardless of the type of equation used to calculate it. Instead, when the entire time series (47 days) is considered, all the equations used to evaluate the interdependency index give a negative value of $S_{i,j}$ in correspondence to the cross-correlation between Power delivery and City Gas delivery. Results from the re-analysis indicate that dividing the time series in intervals between subsequent shocks leads to more logical results compatible with experience-based expectations, because Power delivery is now found to lead the restoration process of City Gas delivery. Looking at other results, such as the cross correlation function between Water supply and City Gas delivery (Fig. 9.13c), it is observed that Water supply weakly leads the City Gas delivery restoration process during period A. In fact, there are two small positive values of CCF above the statistical threshold at positive lags and only one small positive value of CCF above the statistical threshold, at negative lag. The results for Water supply and City Gas delivery obtained in Fig. 9.13c for the period A of the time series is similar to the results obtained for the entire time series of 47 days shown in Fig. 9.4a, because the value of the interdependency index is positive for both period ranges.

The CCF function between Power delivery and Water supply in Fig. 9.13d shows a weak dependence of Water supply on Power delivery, because the largest positive value of the CCF function which occurs at positive lag is below the positive threshold of statistical significance, following the definition of weak dependence provided by Dueñas-Osorio and Kwasinski.

Applying Eq. (9.1) to the cross-correlation function in Fig. 9.13d related to the first time interval (period A), the value of the interdependency index $S_{i,j}$ is different from zero, because it is using values of the CCF function below the threshold of statistical significance. Instead, according to Eq. (9.5), the value of the interdependency index $S_{i,j}$ is equal to zero, because there is no positive value of the CCF function above the positive threshold, therefore the restoration processes of Power delivery and Water supply are independent. On the other hand, when the second time interval (period B) is considered, the $S_{i,j}$ values do not seem logical, possibly because the time interval considered in that period is too short. To address this issue, it was decided to combine periods B and C. This aggregation is partially justified by the fact that the second aftershock that occurred on April 11th affected only the restoration curves of the prefecture of Fukushima. After this aggregation by repeating the same procedure, the $S_{i,j}$ values became logical again (results not shown in this book).

Table 9.4 shows the S matrices calculated using Eq. (9.5) for two different time intervals: (i) the maximum duration of the time series (47 days) and (ii) the time interval between the main shock and the first strong aftershock of April 7th (27 days). In gray, the values of the interdependency indicators related to the Power delivery are highlighted, switching from negative values to positive values when the time range of analysis is reduced from 47 to 27 days. The physical meaning of this variation is that it results in the Power network leading the other networks (as mentioned earlier). Furthermore, it is shown that the $S_{i,j}$ values become consistent with actual dependencies when considering the time range (27 days) between the main shock and the first strong aftershock, regardless the type of equation used. In fact, the same trend is also observed using Eq. (9.1). From the consideration above, it is suggested that the $S_{i,j}$ values should be evaluated using the time interval between the main shock (March 11th) and the first strong aftershock (April 7th). In this way, the perturbation effects of the aftershocks on the restoration curves will be reduced, by focusing only on the perturbation effects of the main shock.

9.1.8 Calculation of the Weight Coefficients on the First Period

In order to evaluate the resilience index given in Eq. (9.10), it is first necessary to evaluate the weight coefficients (Eq. (9.7)) which depend on the values of interdependency indicators. Table 9.5 presents a comparison of the weight coefficients obtained using Eq. (9.1) with the weight coefficients obtained using Equation,

Table 9.4 Comparison of interdependency index among different time: in gray are highlighted the values that increase

Region		Si,j 47 days Eq. (8.26)			Si,j 27 days Eq. (8.26)		
		Power	Water	City Gas	Power	Water	City Gas
Miyagi	Power	1.00	-0.35	-0.19	1.00	0.00	0.20
	Water	0.35	1.00	0.31	0.00	1.00	0.31
	City Gas	0.19	-0.31	1.00	-0.20	-0.31	1.00
Iwate	Power	1.00	0.55	-0.56	1.00	0.20	0.13
	Water	-0.55	1.00	-0.38	-0.20	1.00	0.51
	City Gas	0.56	0.38	1.00	-0.13	-0.51	1.00
Fukushima	Power	1.00	0.47	-0.35	1.00	0.00	0.49
	Water	-0.47	1.00	-0.23	0.00	1.00	-0.27
	City Gas	0.35	0.23	1.00	-0.49	0.27	1.00
Yamagata	Power	1.00	0.31	-	1.00	0.35	-
	Water	-0.31	1.00	-	-0.35	1.00	-
Akita	Power	1.00	0.93	-	1.00	0.20	-
	Water	-0.93	1.00	-	-0.20	1.00	-
Ibaraki	Power	1.00	0.20	0.49	1.00	0.20	0.27
	Water	-0.20	1.00	0.87	-0.20	1.00	0.87
	City Gas	-0.49	0.87	1.00	-0.27	0.87	1.00
Tochigi	Power	1.00	0.45	-	1.00	0.45	-
	Water	-0.45	1.00	-	-0.45	1.00	-
Aomori	Power	1.00	-0.15	-0.13	1.00	0.42	0.33
	Water	0.15	1.00	0.72	-0.42	1.00	0.80
	City Gas	0.13	0.72	1.00	-0.33	0.80	1.00
Chiba	Power	1.00	-	0.23	1.00	-	0.23
	City Gas	-0.23	-	1.00	-0.23	-	1.00
Gunma	Power	1.00	0.40	-	1.00	0.40	-
	Water	-0.40	1.00	-	-0.40	1.00	-
Saitama	Power	1.00	0.46	1.00	1.00	0.46	1.00
	Water	-0.46	1.00	-0.46	-0.46	1.00	-0.46
Kanagawa	City Gas	1.00	0.46	1.00	1.00	0.46	1.00
	Power	1.00	-	0.55	1.00	-	0.54
	City Gas	-0.55	-	1.00	-0.54	-	1.00

calculated from the interdependency indices evaluated using the procedure shown in the previous paragraph and the dataset of 27 days (from March 11th to April 7th).

The highest weight coefficients calculated using Eq. (9.1) correspond to the Power delivery network in all the regions with the exception of Ibaraki and Aomori. The exception is extended to the regions of Miyagi and Iwate when Eq. (9.5) is adopted. However, the weight coefficients tend to increase when passing from Eqs. (9.1) to (9.5) in general. It is expected that the lifeline that has the highest weight coefficient in a developed country like Japan should certainly be the Power

Table 9.5 Comparison of weights from Eqs. (9.1) and (9.5): are highlighted in gray the highest values in each region gray the highest values

Region		Wi from Eq. (8.22) (Dueñas-Osorio and Kwasinski 2012)	Wi from Eq. (8.26)
Miyagi	Power	0.37	0.34
	Water	0.33	0.37
	City Gas	0.30	0.28
Iwate	Power	0.37	0.35
	Water	0.34	0.39
	City Gas	0.30	0.26
Fukushima	Power	0.39	0.40
	Water	0.28	0.27
	City Gas	0.33	0.34
Yamagata	Power	0.55	0.57
	Water	0.45	0.43
Akita	Power	0.54	0.54
	Water	0.46	0.46
Ibaraki	Power	0.26	0.28
	Water	0.37	0.36
	City Gas	0.37	0.36
Tochigi	Power	0.56	0.59
	Water	0.44	0.41
Aomori	Power	0.29	0.33
	Water	0.36	0.34
	City Gas	0.36	0.34
Chiba	Power	0.54	0.55
	City Gas	0.46	0.45
Gunma	Power	0.56	0.58
	Water	0.44	0.42
Saitama	Power	0.41	0.42
	Water	0.18	0.17
	City Gas	0.41	0.42
Kanagawa	Power	0.56	0.61
	City Gas	0.44	0.39

delivery because many infrastructures operate through electric power. Applying Eq. (9.5) leads to an increment of the weight coefficients of the Power network in many regions with respect to Eq. (9.1). This could be considered a benefit of the proposed equation.

As explained above, the only exceptions to this trend were found in the regions of Miyagi and Iwate. The probable cause of this anomaly in the weight coefficients is related to the fact that these two regions have common characteristics with the restoration curves that are slower for the prefectures closer to the epicenter.

Some of these anomalies in terms of interdependency indicators can be physically justified. For example, after the earthquake, the water supply suspension occurred in 2,300,000 households, but since most of the residents in the area flooded by the tsunami have not lived since the event, most of the damaged pipelines have not yet been repaired. Therefore, the restoration curves of the water distribution network in these regions were slower (e.g. Miyagi, Iwate, Fukushima) as shown in Fig. 9.2. As a results of interdependency, the water distribution network appears to be dependent on power and gas distribution network as shown in Table 9.4.

Furthermore, in Miyagi Prefecture, the regional water supply system takes water from Dams and rivers outside the Prefecture. Large-diameter welded steel transmission pipelines of these trans-municipal water supply systems suffered major damage, significantly hindering recovery work during a few weeks. The configurations of these water transmission networks are tree-like structures. Because of poor redundancy of tree networks, the downstream areas of the most upstream location of pipe failures lost water supply. Recovery works of the failed pipes had to be conducted from the upper part in order to restore connection between water sources to users. Therefore, remote areas from the water source experienced longer disruption of water. Results show dependency of the water networks in the remote areas from the network in the upstream areas, because the restoration process started from the most upstream locations of pipe failures towards the downstream locations.

Regarding the gas network, the most damaged supplier was the Gas Bureau of City of Sendai. The Minato LNG plant was devastated by a tsunami, which was the main cause of the city gas outage at 359 thousand households (78.2 % of the total outage). Fortunately, the long-distance high-pressure pipeline network transmitting natural gas from Niigata Prefecture to Sendai performed well. Transmission of natural gas was shut off immediately after the earthquake at Shiroishi junction valve station. However, after completing safety inspection along the transmission line to Sendai, including 15 valve stations, the network system restarted its operation on March 23th, contributing to rapid recovery thereafter. The rapid recovery of the gas distribution network in the Miyagi Prefecture generated a dependency of all the other infrastructures (water and power) on the gas distribution network as shown in Table 9.4.

9.1.9 Numerical Results of the Regional Resilience Index

The previous section highlights the importance of properly selecting the data range on which the calculation of the interdependency index is based and, consequently, the calculation of the weight coefficients. It was shown that, when the total time interval includes more than one catastrophic event, the calculation of the index $S_{i,j}$ and, consequently of the weight coefficients, can be problematic, and that better results are obtained when the evaluation is performed only on the first period interval (between the main shock and the first aftershock) that causes a loss of functionality in at least one of the considered lifelines. Therefore, the weight coefficients of the

lifelines calculated for the time series of 27 days (from March 11th to April 7th) using Eq. (9.5) were used to calculate the resilience index values using Eq. (9.9) based on four different periods (T_c).

The first period has a length of 1 week (7 days). The second period has a length of 2 weeks (15 days). The third one has a length of 27 days (i.e., the time interval between the main shock and the first aftershock that generates a drop of functionality in at least one lifeline) while the fourth period T_c has a length of 47 days (that is the length of the complete set of data recorded after the main shock). These different values of T_c were assumed to evaluate the index of resilience at different intervals. A resilience index evaluated a week after the main shock gives information about the extent of the damage suffered by the physical infrastructure in a region and can give information about the vulnerability of a region and its ability to restore services to the previous condition in relation with a hazard to a comparable magnitude. The resilience index is mainly influenced by physical and geographical interdependencies. The lifeline interdependencies or the proximity to the epicenter of the earthquake, as well as the proximity of a region to the East coast are the predominant factors in the short time interval.

The resources available for the reconstruction have minor importance at this stage, while they become more important as time goes on. Resilience indices are shown in Table 9.6, where the maximum and minimum values within each time interval are highlighted in gray. Analyzing the results in Table 9.6, it is observed that for the time intervals equal to 15 days, 27 days and 47 days, the region closest to the epicenter (Miyagi) and the one farthest from the epicenter (Kanagawa) have the lowest and the highest value of resilience, respectively. The only exception is for the period of 7 days in the Akita region, which is the one shown to have the highest resilience index even though it is not the region farthest from the epicenter. This anomaly can be explained by the fact that the Akita region, although not far from the epicenter of the earthquake, is on the west coast, which is on the opposite coast of Japan and did not suffer damage from the tsunami that devastated the East Coast of Japan after the main shock.

Figure 9.14 shows a comparison of the resilience index for the Miyagi prefecture in the different chosen time ranges, calculated using the weights obtained by the interdependency index of Eqs. (9.1) and (9.5). For comparison, the value of the resilience index obtained using the same weights for each lifeline is shown in that figure. It can be observed that the three values that change in time are not so different (Fig. 9.14). This implies that the weight coefficients do not influence the results significantly. It would be less computationally demanding to assign the same weight to all the infrastructures to obtain a value of the regional resilience index.

However, the methodology presented here provides a mathematical approach to the problem, by creating a rational procedure for evaluating the weight coefficients. Furthermore, the methodology presented is also useful to identify the most

Table 9.6 Regional resilience with Eq. are highlighted in gray the maxima and minima values within each time interval

Region	Infrastructure	Tw	Wi	Rtot 7 days	Rtot 15 days	Rtot 27 days	Rtot 47 days
Miyagi	Power		0.34				
	Water	07 Apr.	0.37	0.26	0.30	0.46	0.63
	City Gas		0.28				
Iwate	Power		0.35				
	Water	07 Apr.	0.39	0.36	0.45	0.53	0.66
	City Gas		0.26				
Fukushima	Power		0.40				
	Water	07 Apr.	0.27	0.45	0.55	0.66	0.76
	City Gas		0.34				
Yamagata	Power	07 Apr.	0.57	0.67	0.83	0.90	0.93
	Water		0.43				
Akita	Power	07 Apr.	0.54	0.86	0.91	0.95	0.95
	Water		0.46				
Ibaraki	Power		0.28				
	Water	07 Apr.	0.36	0.44	0.67	0.80	0.88
	City Gas		0.36				
Tochigi	Power	07 Apr.	0.59	0.69	0.84	0.91	0.94
	Water		0.41				
Aomori	Power		0.33				
	Water	07 Apr.	0.34	0.65	0.83	0.90	0.93
	City Gas		0.34				
Chiba	Power	07 Apr.	0.55	0.64	0.70	0.83	0.90
	City Gas		0.45				
Gunma	Power	07 Apr.	0.58	0.72	0.86	0.92	0.95
	Water		0.42				
Saitama	Power		0.42				
	Water	07 Apr.	0.17	0.82	0.91	0.95	0.97
	City Gas		0.42				
Kanagawa	Power	07 Apr.	0.61	0.85	0.93	0.96	0.98
	City Gas		0.39				

important lifelines, which correspond to the ones with the highest value of the weight coefficients in the region. Finally, analyses results here may have been influenced by the fact the restoration curves were available for only three types of lifelines. Probably, by increasing the number of lifelines in the analysis, the resilience index could have been more sensitive to the weight coefficients. Finally, Fig. 9.15 geographically displays the regional resilience indicators for all the regions affected by the earthquake, as calculated using the procedure described above.

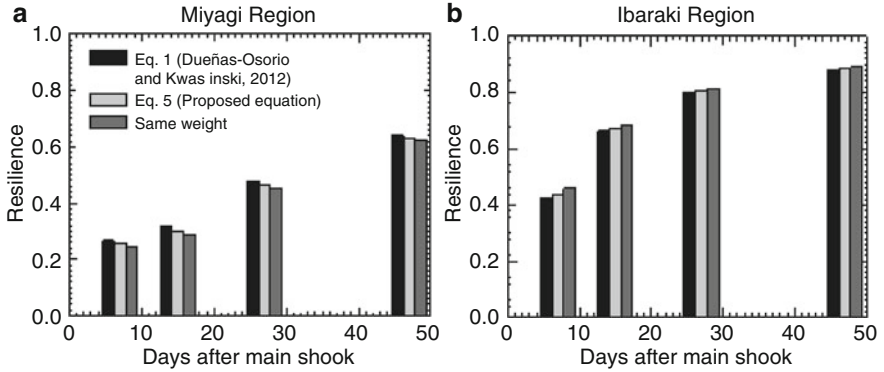


Fig. 9.14 Comparison between the new regional resilience indicators obtained using three types of weight coefficients for the regions of Miyagi (a) and Ibaraki (b)

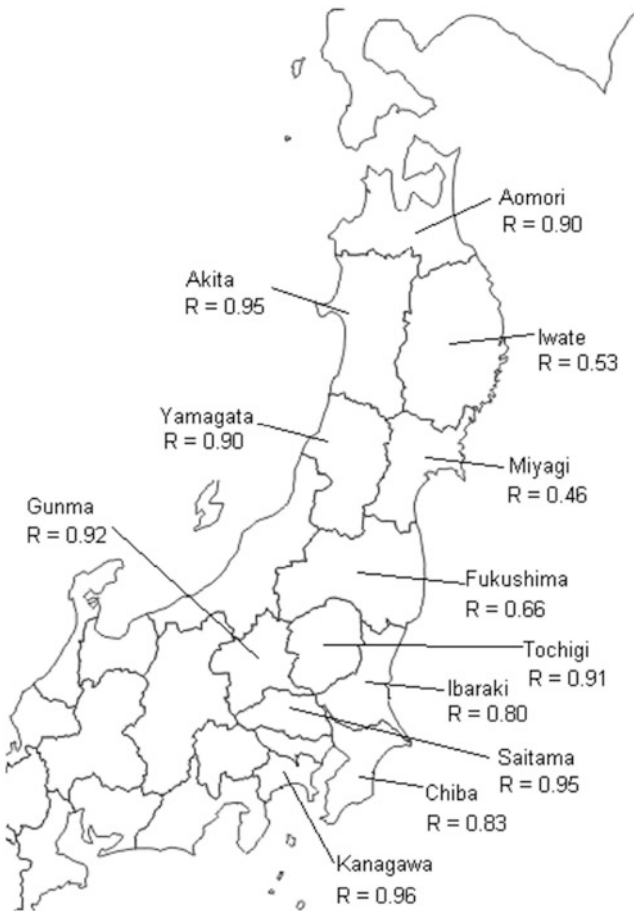


Fig. 9.15 Regional resilience 27 days after the main shock evaluated using Eq. (8.26) to evaluate the weight coefficients

9.1.10 *Remarks and Conclusions*

A methodology has been proposed for the calculation of a hybrid regional resilience index taking into account interdependency starting from the values of resilience indicators for individual infrastructures. The resilience index of each infrastructure is evaluated with Eq. (9.9) proposed by Cimellaro et al. (2014) using restoration curves data from the 2011 Tohoku earthquake in Japan. The resilience indicators of the individual lifelines are then combined using weight coefficients which are calculated on the basis of a matrix of interdependency $S_{i,j}$ calculated for each region. Once the weight coefficients are known, the regional resilience index is evaluated, by multiplying the resilience of each lifeline with the corresponding weight coefficient and adding the results obtained for all regions. A detailed analysis of the interdependency index has been performed, and a new equation that improves the one proposed by Dueñas-Osorio and Kwasinski has been presented. The proposed equation takes into account the level of statistical significance for each CCF function, considering only the values above the statistical threshold. More importance has been given to the peak values, and to the number of times in which the CCF function exceeds the threshold of statistical significance. Although it was observed for this particular example that the weight coefficients did not significantly influence the resulting value of the resilience index, the methodology presented in this section provides a mathematical approach to the problem by creating a rational methodology to select the weight coefficients. Furthermore, it is suggested that the optimal period range of the restoration curves that should be used for the evaluation of such weight coefficients is the period range between the main shock and the first aftershock.

Finally, it is recognized that the results presented here may have been influenced by the fact that only the restoration curves of three lifelines have been considered. Future research may focus on testing the proposed methodology for the calculation of the regional resilience index, using a higher number of restoration curves and earthquake data sets.

References

- Arcidiacono V, Cimellaro GP, Reinhorn AM, Bruneau M (2012) Community resilience evaluation including interdependencies. In: 15th world conference on earthquake engineering (15WCEE), Lisbon, 24–28 Sept 2012
- Bigger JE, Willingham MG, Krimgold F, Mili L (2009) Consequences of critical infrastructure interdependencies: lessons from the 2004 hurricane season in Florida. *Int J Crit Infrastruct* 5(3):199–219
- Cimellaro GP (2013) Computational framework for resilience-based design (RBD) CH11. Woodhead Publishing, Sawston, p 810 (Book section 11)
- Cimellaro GP, Reinhorn AM (2010) Multidimensional performance limit state for hazard fragility functions. *J Eng Mech* 1(1):156. [http://link.aip.org/link/?EMX/1/156/1http://dx.doi.org/10.1061/\(ASCE\)EM.1943-7889.0000201](http://link.aip.org/link/?EMX/1/156/1http://dx.doi.org/10.1061/(ASCE)EM.1943-7889.0000201)

- Cimellaro GP, Solari D, Bruneau M (2014) Physical infrastructure interdependency and regional resilience index after the 2011 tohoku earthquake in Japan. *Earthq Eng Struct Dyn* 43(12):1763–1784. doi:[10.1002/eqe.2422](https://doi.org/10.1002/eqe.2422)
- Delamare S, Diallo AA, Chaudet C (2009) High-level modelling of critical infrastructures' interdependencies. *Int J Crit Infrastruct* 5(1–2):100–119
- Dueñas-Osorio L, Kwasinski A (2012) Quantification of lifeline system interdependencies after the 27 February 2010 m-w 8.8 offshore manic, Chile, earthquake. *Earthq Spectra* 28:S581–S603. doi:[10.1193/1.4000054](https://doi.org/10.1193/1.4000054). <GotoISI>://WOS:000308573000029
- Kakderi K, Argyroudis S, Pitilakis K (2011) State-of-the-art literature review of methodologies to assess the vulnerability of a “system of systems”. Report, Aristotle University of Thessaloniki
- Kjolle GH, Utne IB, Gjerde O (2012) Risk analysis of critical infrastructures emphasizing electricity supply and interdependencies. *Reliab Eng Syst Saf* 105:80–89. doi:[10.1016/j.res.2012.02.006](https://doi.org/10.1016/j.res.2012.02.006). <GotoISI>://WOS:000307085400010
- Kongar I, Rossetto T (2012) A framework to assess the impact of seismic shocks on complex urban critical infrastructure networks. In: 15th world conference on earthquake engineering (15WCEE), Lisbon
- Paton D, McClure J, Burgelt P (2006) Disaster resilience: an integrated approach. Charles C. Thomas Publisher, Springfield
- Poljansek K, Bono F, Gutierrez E (2012) Seismic risk assessment of interdependent critical infrastructure systems: the case of European gas and electricity networks. *Earthq Eng Struct Dyn* 41(1):61–79. doi:[10.1002/eqe.1118](https://doi.org/10.1002/eqe.1118). <GotoISI>://WOS:000298591500004 (times cited: 1)
- Rinaldi SA, Peerenboom JP, Kelly TK (2001) Identifying, understanding, and analyzing critical infrastructure interdependencies. *IEEE Control Syst Mag* 21(6):11–25. doi:[10.1109/37.969131](https://doi.org/10.1109/37.969131). <GotoISI>://WOS:000172368500002. ISI Document Delivery No.: 495YT Times Cited: 144 Cited Reference Count: 26 Rinaldi, SA Peerenboom, JP Kelly, TK IEEE-Inst Electrical Electronics Engineers Inc
- Shumway RH, Stoffer DS (2011) Time series analysis and its applications with R examples, 3rd edn. Springer, New York

Chapter 10

Applications of Seismic Resilience for Health Care Facilities and School Buildings

Abstract In the recent earthquakes in Chile, New Zealand, and Japan, a great number of critical facilities, including hospitals, schools, bridges, factories, etc. experienced extensive damage resulting in loss of functionality, and consequently substantial economic losses. The recovery process is estimated to last from several years to few decades in these regions. As a result, increased attention is being placed on strategies to design facilities that are both safe and damage resistant. It is often presumed that such an approach increases costs to an unacceptable level. In this chapter Performance-based earthquake evaluation tools are used to estimate repair costs and times for five different hazard levels considering two occupancy types critical for recovery: health-care and school building. A typical three-story steel building is used considering two design levels: conventional fixed-base and damage resistant base-isolated moment resisting frame system. The buildings are located in a seismic region in western North America. It is shown that using seismic isolation to enhance damage resistance results in significantly smaller repair cost, repair time, and improved resilience for the base-isolated alternative compared to a conventional fixed-base design.

10.1 Introduction

Following recent hazard events, a great number of critical facilities have experienced extensive damage. These damages resulted in their loss of function and consequently substantial economic losses. Heavily affected communities were paralyzed for months following these large seismic events and the complete recovery process is estimated to last from several years to a few decades.

In particular this chapter focuses on the evaluation of Resilience metrics for Physical Infrastructures (Fig. 10.1). To this purpose, the PEOPLES framework is applied to two principle occupancy types of structures: healthcare and school. In the event of failure, healthcare facilities and schools present a substantial hazard to human life (occupancy category III, per ICC IBC, 2012) and on the other hand they are also critical during the recovery phase to comply the organized governmental services. Therefore, they are designed to follow more stringent design requirements than buildings with residential and commercial occupancy.

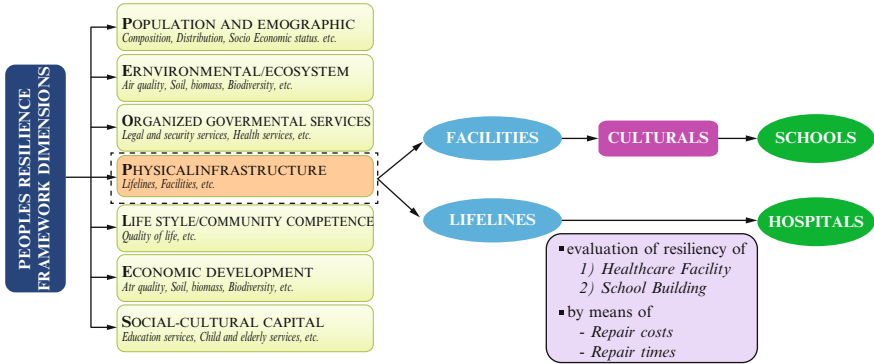


Fig. 10.1 Chapter 10 outline

In the recent large earthquakes in Chile, New Zealand, and Japan, healthcare facilities and schools were generally safe. However, there are cases of healthcare and school closures due to extensive structural and nonstructural damage that resulted in the loss of their function (Miranda and Taghavi 2003). As a result, increased attention is being placed on strategies to design facilities that are both safe and damage resistant. Key indicators for these physical infrastructure include the number of available response units and their capacity to re-establish its function following a hazard event. In order to assess this dimension, two loss metrics including; repair costs and repair times are defined in this chapter to estimate effectiveness of isolation system as a strategy to design both safe and damage resistant facilities.

To do this, each building component and content is associated with a fragility curve that correlates engineering demand parameters (i.e. median values of maximum and residual story drifts and floor accelerations) to the probability of that item reaching a particular damage state. The component’s damage is then related to a loss (e.g., repair cost or repair time) utilizing consequence functions. The total loss at a hazard level is then estimated by integrating losses over all components of a system. Then a business downtime as a function of time is characterized to estimate the resiliency of the systems and the revenue losses resulting from the business interruption. Finally the level of resiliency is measured by integrating the recovery function of the system within a certain period of time.

10.2 Buildings Description

The study considers a three-story steel building located in a seismic region in western North America, Oakland, California. The basic building plan dimensions are 120 ft (36.5 m) by 180 ft (54.9 m) with a bay spacing of 30 ft (9.1 m) in each direction. The building is located on relatively stiff soil (site class C/D with

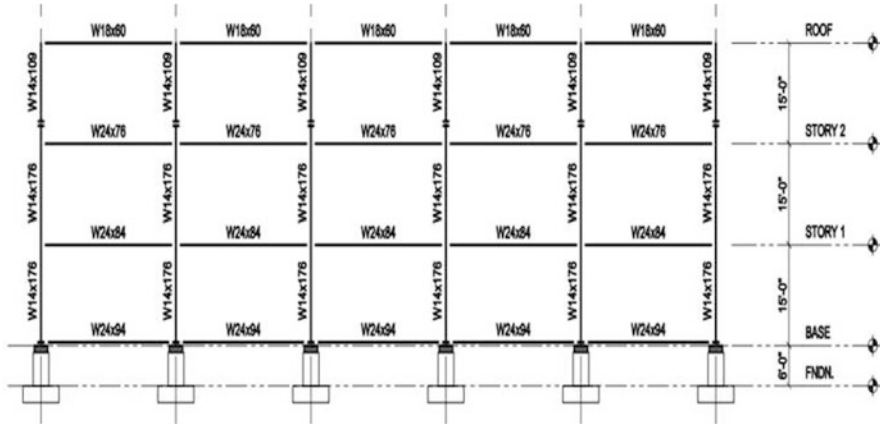


Fig. 10.2 Lateral force resisting system configuration-BI-IMRF

reference shear wave velocity = 180 to 360 m/s). Code spectral accelerations were selected to be $S_s = 2.2g$ for short periods and $S_1 = 0.74g$ at a period of 1 s. The designs of the two considered systems, fixed-base and base-isolated moment resisting frames, are consistent with what might be used by many engineers and are compliant with the code standards for design according to the Equivalent Lateral Force Method (ASCE 2010).

The HP-SMRF was designed with a force reduction factor (R/I_e) of 6.4 (8/1.25), an inter-story drift limit of 1.0 % (more stringent than 2 % required by code – ASCE (2010)), and utilized pre-qualified WUF-W beam-to-column connections (AISC 2005). Such design resulted in fundamental period of the fixed-base system of 0.67 s. Compared to the HP-SMRF, the BI-IMRF (Fig. 10.2) was designed utilizing lower R/I_e factor ($1.69 = (3/8) \times (4.5/1)$) and the same drift limit (1.0 %).

The IMRF uses simpler connection details and does not require a strong column-weak girder design approach. The isolation system is designed to have a maximum displacement of 30 in. under the maximum capable earthquake (MCE) event. It utilizes triple friction pendulum bearings (TFPB) with the friction coefficients of the four sliding surfaces of 0.01, 0.01, 0.03, and 0.06, and the effective pendulum lengths of 20, 122, and 122 in. Under the MCE event, this bearing has the effective period of 4.35 s and the effective damping of 15.1 %. More details on designs of these two systems can be found in Mayencourt (2013) and Terzic et al. (2014).

10.3 Ground Motion Selection

The set of ground motions used in the analysis were selected to match the uniform hazard spectrum (UHS) (USGS 2014) and associated causal events for the Oakland site. Forty three-component ground motion records were selected to represent

the ground motion hazard at each of three hazard levels, with probabilities of exceedance in 50 years of: 2 %, 10 %, and 50 %. More information on these motions can be found in Baker et al. (2011). To better characterize the seismic hazard at the site, two additional sets of records representative of hazard levels at 5 % and 20 % probabilities of exceedance are also included in the analysis. Each of the two additional sets of ground motions had 25 three-component ground motion records, derived following the selection criteria given in Baker et al. (2011). Figure 10.3 compares:

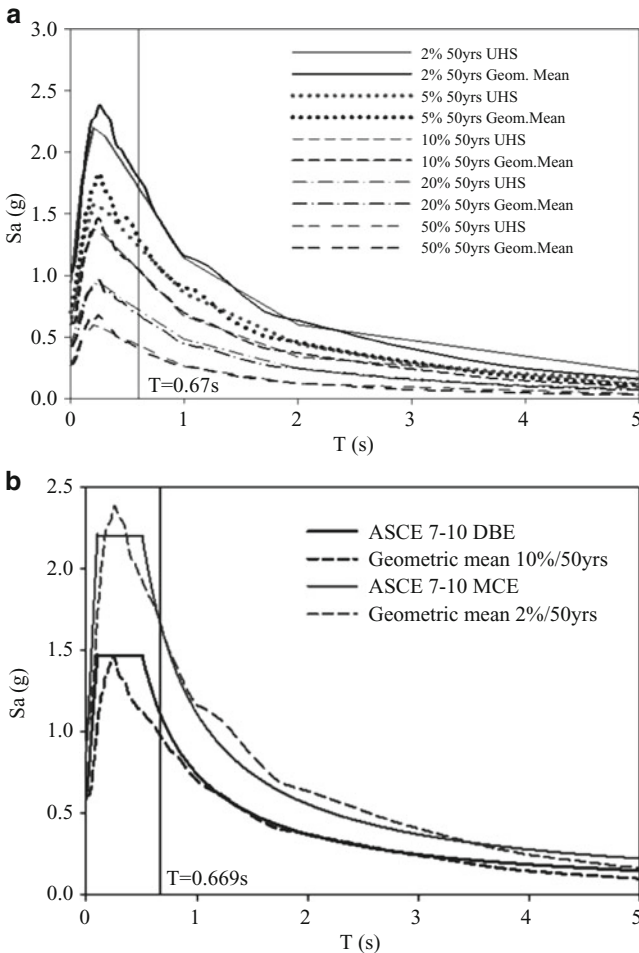


Fig. 10.3 Comparison of: (a) uniform hazard spectra with the median pseudo-acceleration response spectra at five considered hazard levels (2 %, 5 %, 10 %, 20 %, and 50 % probabilities of exceedance in 50 years) and (b) median pseudo-acceleration response spectra for the selected ground motions at 10 % and 2 % in 50-year hazard level with the spectra for the code design basis earthquake (DBE) and max. capable event (MCE)

- UHS with the median pseudo-acceleration response spectra for the selected ground motions at five considered hazard levels (Fig. 10.3a);
- Median pseudo-acceleration response spectra for the selected ground motions at 10 % in 50-year and 2 % in 50-year hazard level events with the spectra for the code design basis earthquake (DBE) and MCE (Fig. 10.3b).

10.4 Analysis-Models and Methods

To simplify the analysis for this study, time history analyses were performed on appropriately modeled two-dimensional (2D) frames utilizing OpenSees (McKenna and Fenves 2004). This simplification is valid because the lateral load resisting frames are located only on the perimeter of the building and do not have common elements. Gravity-load-only type connections were used elsewhere in the structure. Details of numerical models and modeling assumptions are described in Terzic et al. (2014).

In short, (i) floor slabs were assumed to be axially inextensible, (ii) all elements of the two moment resisting frames were modeled utilizing force-based beam-column elements of OpenSees, (iii) isolators were modeled with zero-length elements (horizontal springs), one beneath each column of the structural frame, and tri-linear uniaxial material representative of a hysteretic behavior of triple pendulum friction bearing, (iv) P - δ effects from the gravity columns were accounted for by using a single leaning column, (v) the effects of large deformations of beam and column elements were accounted for utilizing P - δ nonlinear geometric transformation, (vi) damping was assigned to the frames using Rayleigh damping model and the damping ratio of 3 %, (vii) the frames were subjected to horizontal and vertical components of ground motions.

10.5 Comparison of Structural Response

By comparing the average peak values of engineering demand parameters (EDP) based on story drifts, floor accelerations, and residual drifts for the five considered hazard levels, the relative performance characteristics of the systems can be assessed. The severity of damage to various structural and nonstructural components associated with these EDPs can be quantitatively assessed using fragility relations from FEMA P-58 (FEMA 2012). Losses associated with this damage will be evaluated in the next section.

Base-isolated moment frame substantially reduces accelerations and drifts compared to the fixed-base frame (Fig. 10.3). While the effectiveness of the isolation system in reducing the story drifts increases with the increasing intensity of ground shaking (from 20 % to 62 % with an average of 49 %), the reduction of acceleration is high at all hazard levels (from 84 % to 90 % with an average of 88 %).

The BI-IMRF, with the uniform acceleration profile over the height of the building and the peak median value reaching 0.22 g at the 2% in 50-year hazard level, most likely will not trigger any damage of the acceleration sensitive components (e.g., ceiling, MEP, contents). At the 50% in 50-year hazard level, the HP-SMRF develops maximum median drift of 0.46%, 20% larger than maximum median drift of the BI-IMRF of 0.37% (Fig. 10.3a). Because both moment frames are expected to yield at drift ratios slightly larger than 1%, elastic structural behavior is anticipated at this hazard level. The damage to interior partitions is expected for both the HP-SMRF and BI-IMRF system, since the median drift associated with initiation of damage to partition walls commonly used in healthcare facilities and schools is 0.21% (FEMA 2012). Median horizontal accelerations in the HP-SMRF range from 0.26 to 0.67g over the height of the building (not shown), triggering damage to piping, electronic and medical equipment in the upper levels (FEMA 2012). At the 20% in 50-year hazard level, greater differences in story drift demands were observed between the two systems (Fig. 10.3b).

Compared to the BI-IMRF, the fixed-base HP-SMRF had a drift ratio about 2 times larger at every level, with the peak median value reaching 0.84%. This would likely result in a greater damage to partition walls and initiation of damage to stairs (that initiates at drift of 0.5%, per FEMA 2012). At this hazard level, damage to structural elements is not anticipated. Median horizontal accelerations in the HP-SMRF range from 0.37 to 1.13g over the height of the building (not shown).

These accelerations extend the regions of the building that undergoes acceleration-related damage, and trigger additional damage to ceilings, chillers, fire sprinkler drops, bookcases, and filing cabinets (FEMA 2012). At the 10% in 50-year hazard level, Fig. 10.4c shows even greater differences in story drift demands between the two systems (Fig. 10.4b). The fixed-base HP-SMRF had the peak median drift ratio of 1.24%, which suggests initiation of yielding of the system and probable extensive damage to wall partitions and moderate damage to stairs.

The BI-IMRF, with the peak median drift ratio of 0.57% is anticipated to remain elastic with slight damage to wall partitions and stairs. Median horizontal accelerations in the HP-SMRF ranged from 0.59 to 1.54g over the height of the building (not shown). These accelerations extend the regions of the building that undergoes acceleration-related damage observed at lower hazard levels, trigger additional damage to cooling tower, HVAC ducts, and air handling units. At the 5% and 2% in 50-year hazard levels, the fixed-base HP-SMRF had median peak story drifts of 1.57% (5% in 50 years) and 2.24% (2% in 50 years) (Fig. 10.4d, e), suggesting damage to both structural and nonstructural components, requiring substantial repair.

The BI-IMRF, with the peak median drift ratios of 0.62% (5% in 50 years) and 0.83% (2% in 50 years) is anticipated to remain elastic with slight non-structural damage. Median horizontal accelerations in the HP-SMRF range from 0.78 to 1.61g for the 5% in 50-year hazard level and from 0.97 to 1.81g for the 2% in 50-year hazard level (not shown), causing damage to all acceleration sensitive non-structural components and content except for the electrical systems and components.

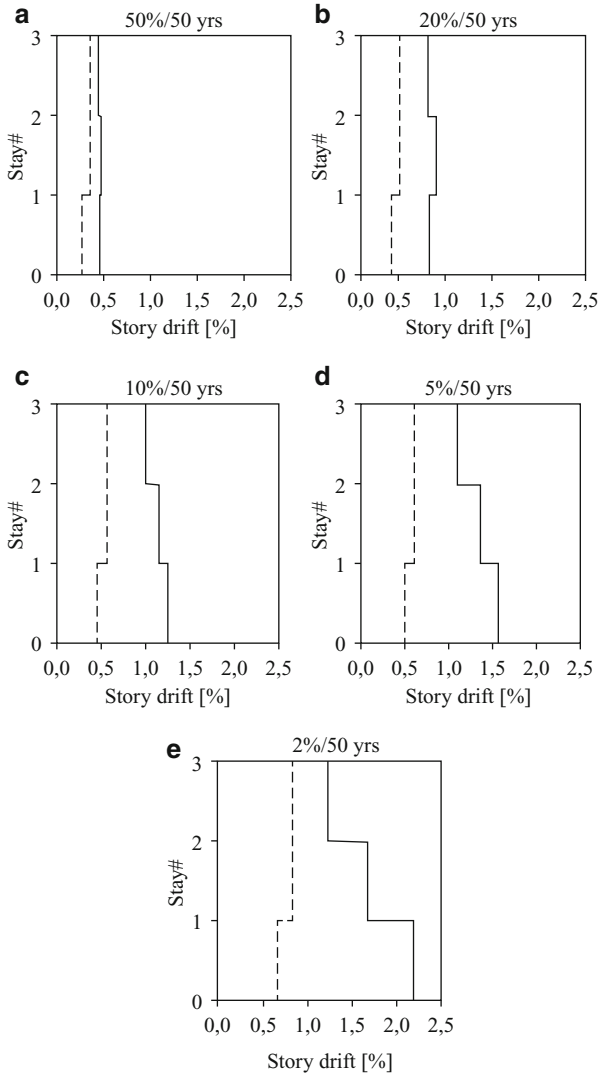


Fig. 10.4 Median story drifts of the HP-SMRF and the BI-IMRF on TFPBs for five hazard levels

10.6 Loss Analysis

Two loss metrics used to estimate effectiveness of isolation system in reducing the total financial losses are: (1) financial losses associated with the cost required to implement repairs and (2) repair time. The computer software Performance Assessment Calculation Tool (PACT) (ATC 2012) is used to calculate the repair

costs and the repair times for the two systems (fixed-base and base-isolated moment frames) and two occupancy types (healthcare and school), at each of the five considered hazard levels.

In PACT, each building component and content is associated with a fragility curve that correlates EDPs to the probability of that item reaching a particular damage state. The component's damage is then related to a loss (e.g., repair cost or repair time) utilizing consequence functions. The total loss at a hazard level is then estimated by integrating losses over all components of a system. To account for the many uncertainties affecting calculation of seismic performance, the FEMA P-58 methodology uses a Monte Carlo procedure to perform loss calculations (FEMA 2012). The type and quantities of most non-structural components and contents used in the loss analysis were determined using the normative quantities recommended by FEMA P-58 (FEMA 2012).

The components considered in this study included: (i) *structural*: moment connections, shear tab gravity connections, base plates, and column splices, (ii) *non-structural*: partition walls, curtain walls, cladding, ceiling, lighting, stairs, elevators, and MEP components, and (iii) *content*: bookcases, filing cabinets, computers, servers, and medical equipment. Isolator devices and utilities at the isolation level are not included in the loss model due to unavailability of their fragility functions in PACT. For the healthcare occupancy, the fragility functions for the medical equipment (not available in PACT) are adopted from Yao and Tu (2012).

These fragility functions are derived by investigating 41 healthcare buildings in the aftermath of the 1999 Chi-Chi earthquake. The consequence functions, relating damage of medical equipment to the repair cost, are developed based on an estimate that the medical equipment cost is 44 % of the total building cost (Miranda and Taghavi 2003). The consequence functions, relating damage of medical equipment to the repair time, were not developed due to unavailability of data. Replacement costs for the buildings, which are input for the loss analysis with PACT, are equal to the initial construction cost increased by 20 % to include cost allowances for demolition and site clearance (FEMA 2012).

The initial construction costs of the school are estimated to be \$17,823,000 for the HP-SMRF and \$17,408,000 for the BI-IMRF, the same as if it was a commercial building (Terzic et al. 2014; Ryan et al. 2010). The initial construction cost of the healthcare facility was calculated using the metric of \$597.7/sq ft (estimate by Mayencourt 2013). Considering the footprint of the three-story building, the initial construction cost of the healthcare is estimated to be \$38,730,960, the same for the two considered structural systems.

10.6.1 Repair Cost and Repair Time

Repair cost estimates can provide the design engineers with valuable insights regarding the desirability and cost-effectiveness of enhancements to the structural system. Figure 10.5 shows the median repair costs for the fixed-base and

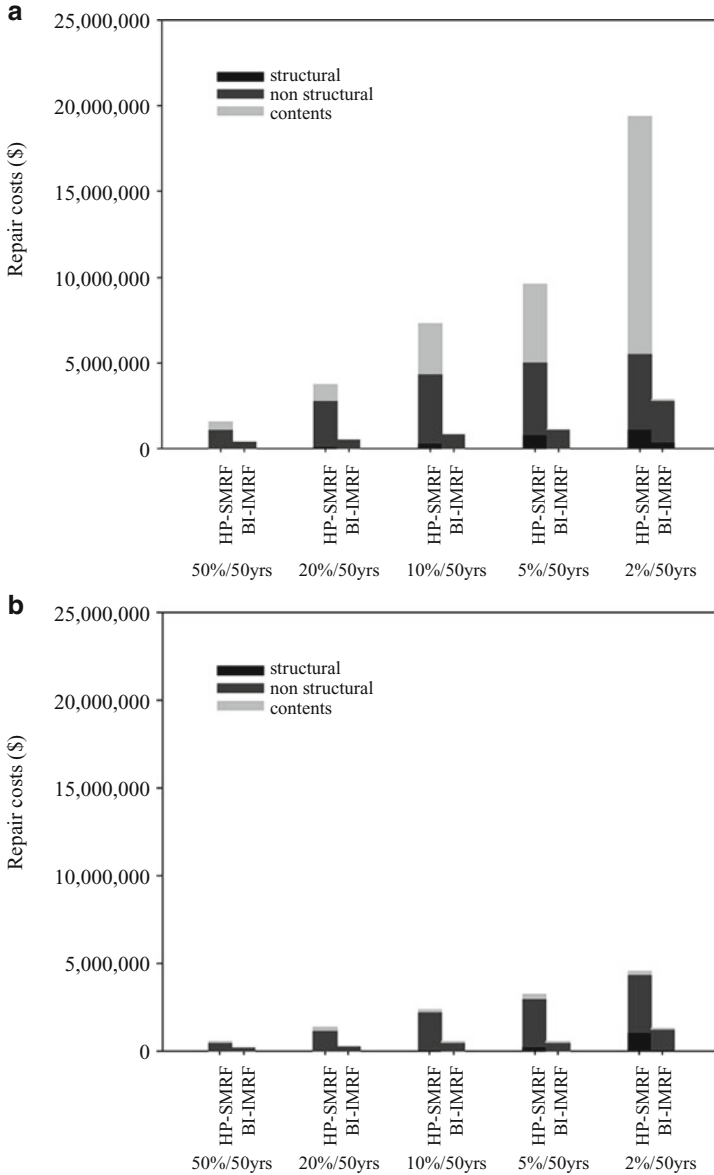


Fig. 10.5 Median repair costs for the HP-SMRF and the BI-IMRF for five hazard levels

base-isolated moment frames for the five considered hazard levels and the two occupancy types: healthcare and school. It clearly shows effectiveness of base-isolated system in mitigating damage. Reduction in cost of damage repair is consistently high at all hazard levels for the both occupancy types. For the healthcare

occupancy, the reduction in repair cost ranges from 76 % to 88 % with an average of 85 %, and for the school it ranges from 66 % to 82 % with an average of 76 %.

Cost of damage repair is several magnitudes higher for the healthcare (more expensive facility) than for the school (Fig. 10.5b). Healthcare facility, whose initial cost is double that of the school cost, has 3–4 times greater losses than the school if the fixed-base HP-SMRF is utilized, and about 2 times greater losses if the BI-IMRF is utilized. While the fixed-base system generates dis-proportionally greater losses for the more expensive facility, the base-isolated system generates proportionally greater losses. To identify the major contributors to the losses, the total repair cost is disaggregated into structural components, non-structural components, and contents (Fig. 10.5).

Non-structural components and content of the healthcare facility dominate the losses. In the case of the fixed-base healthcare facility, non-structural components dominate the losses (72 % contribution) at the lower hazard levels (50 % and 20 % in 50 years). At the 10 % and 5 % in 50-year hazard levels, non-structural components and content have almost equal contributions to the total repair cost. At the 2 % in 50-year hazard level, damage to the medical equipment, which is the primary source of the content damage, dominates the losses (71 % contribution). For the fixed-base school, the base-isolated school, and the base-isolated healthcare facility, nonstructural components dominate the losses (contribution greater than 73 %), but to a smaller extent for the base-isolated buildings. The restoration cost of structural components, although minor for the fixed-base system at higher hazard levels (up to 23 % for the school occupancy), reduces with the base-isolation system.

To facilitate the decision to repair or replace a building damaged after an earthquake, the repair costs can be expressed in terms of loss ratio, which FEMA P-58 defines as the minimum repair costs divided by the building's replacement costs. According to FEMA P-58 (FEMA 2012), building owners typically elect to replace a building rather than repair it when the loss ratio exceeds 40 %; however, other replacement triggers may also be used. Figure 10.6 plots loss ratios for each system at the five considered hazard levels. Although the fixed-base healthcare and school buildings have significantly higher loss ratios than the base-isolated buildings at all hazard levels, the highest loss ratio of the fixed-base system of 0.26 is significantly smaller than the FEMA P-58 replacement threshold of 0.4.

To estimate the resilience of the system and the revenue losses resulting from the business interruption following an earthquake event, business downtime needs to be characterized as a function of time. Business downtime should include the time required to: (1) identify damage, design repairs or upgrades, obtain permits and financing, and to mobilize supplies and manpower; and (2) make the repairs necessary to restart operations. Although business models exist for the commercial occupancy type (e.g., Terzic et al. 2014) such a model could not be found for a school or a healthcare facility. Therefore, the study presented herein will use repair time as a metric for comparing the two systems and the two occupancy types.

Estimating the time required to repair a structure is difficult without specific information about the availability of workers and material. To calculate repair time, a number of assumptions are made. It is assumed that supplies and workers are

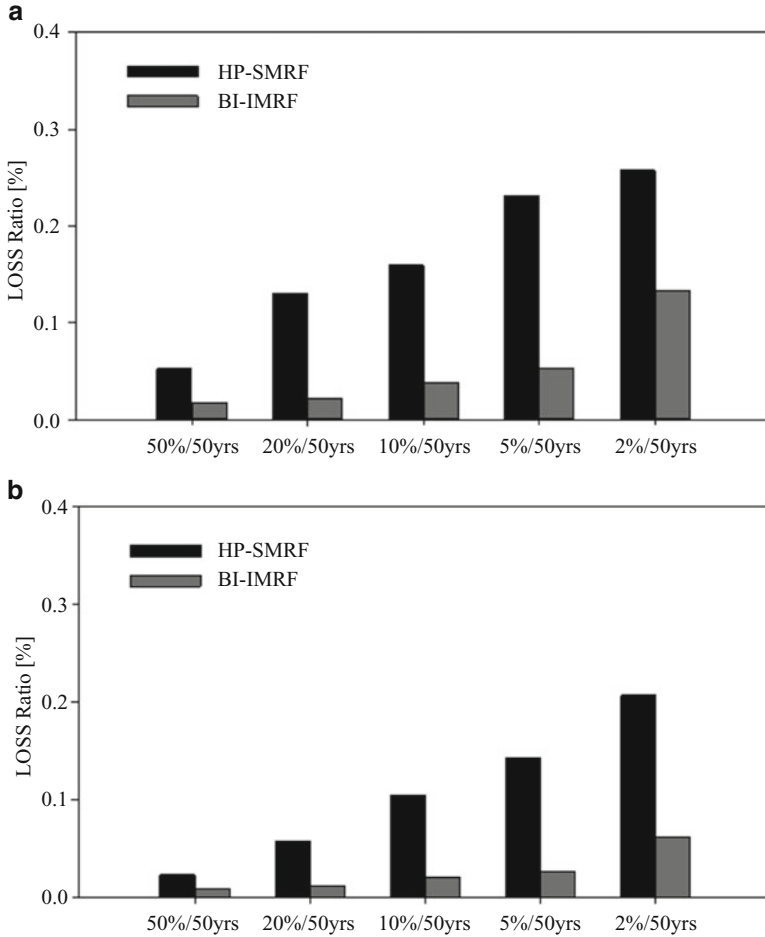


Fig. 10.6 Median loss ratio for the HP-SMRF and the BI-IMRF for five hazard levels and two occupancy types: (a) healthcare and (b) school

available to permit necessary work. A high density of workers (one worker per 500 ft^2) is used, assuming that the building will not be occupied during the repair of the damaged building components. The repair time is calculated considering two repair schemes: (1) *parallel scheme* that assumes simultaneous repair at all three floors, and (2) *serial scheme* that assumes sequential repair at three floor levels (FEMA 2012). Both repair schemes assume sequential repair of all damaged components within one floor level. These repair schemes are not optimal but provide a good estimate of the lower and upper bound of the repair time for the chosen density of workers. While the assumptions made may be feasible for the systems with the smaller extent of damage (i.e., isolated system), they may be hard to achieve for the systems with more extensive damage (i.e., the fixed-base system). Therefore, these

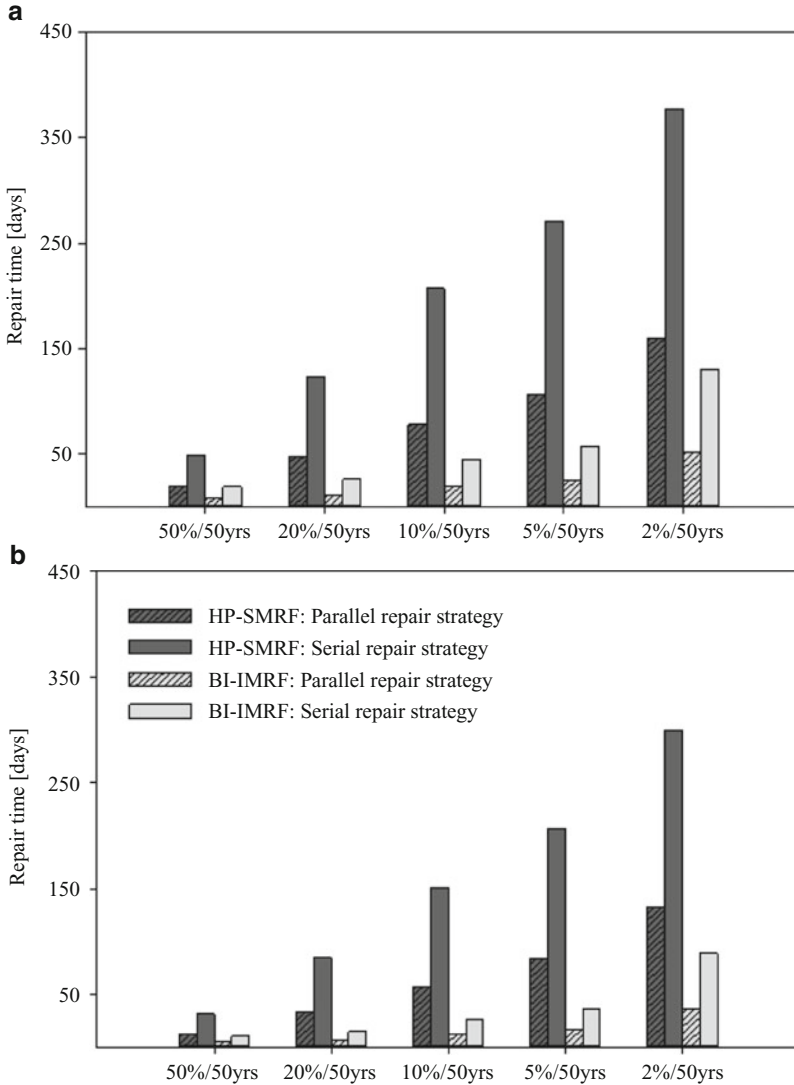


Fig. 10.7 Median repair times for the HP-SMRF and the BI-IMRF for five hazard levels and two occupancy types: (a) healthcare and (b) school, considering two repair strategies, parallel and serial

assumptions are advantageous for the HP-SMRF relative to the base isolated system as they reduce relative benefits of the isolated system. This is in line with the goal of this comparative study: estimation of minimum benefits of the isolated system in reducing the potential losses.

Figure 10.7 shows the median repair times for the HP-SMRF and the BI-IMRF for five hazard levels, for the school and the healthcare facility, considering two

repair strategies, parallel and serial. Base-isolation is again effective in reducing the repair time, which also implies significantly smaller downtime of the isolated buildings.

Upper (serial) and lower (parallel) bounds of the repair times are both several magnitudes smaller for the isolated buildings than for the fixed-base buildings. For the 50 % in 50-year hazard level, the repair times of the base-isolated buildings are 2–3 times smaller than for the fixed-base buildings. For the higher hazard levels, 20 %, 10, and 5 % in 50 years, the base-isolation has 4–6 times smaller repair times. For the 2 % in 50-year hazard level, the reduction in repair time is 3–4 times which is still significant.

While repair costs were significantly larger for the fixed-base healthcare facility than for the school, their repair times are of the same order of magnitude (Fig. 10.7). If the repair time of the medical equipment was included in the loss analysis, a greater difference between repair times of the school and the healthcare facility, and also between the fixed-base and the base-isolated healthcare facility would be anticipated.

10.7 Resiliency

As described in Chap. 3, resiliency is the ability of a system to re-establish its function following a hazardous event. The level of resiliency is measured by integrating the recovery function of the system within a certain period of time (Cimellaro et al. 2010a,b). To quantify the resiliency of the considered building, a recovery function needs to be known. For the considered systems, it can be easily observed that the base-isolated buildings are more resilient than the fixed-base buildings as they have significantly smaller repair times and will therefore recover faster.

However, to better quantify resilience an attempt is made towards developing resilience functions considering school occupancy and an earthquake with a 2 % probability of exceedance in 50 years. For this hazard level, it is assumed that both the fixed-base and the base-isolated system incur enough damage to trigger the closure of buildings. The probable lower and upper bounds for the recovery and therefore resiliency are established based on the lower (parallel scheme) and upper (serial scheme) bounds of repair times. Figure 10.8 clearly shows higher values of resilience for the base-isolated structure with respect to the fixed-base system. In fact the fixed-base system starts to re-establish its function between 133 and 145 days after the earthquake, while the base-isolated system starts to recover its function earlier – between 22 and 36 days. Resiliency functions (Fig. 10.8b) are much steeper for the base-isolated school building, indicating faster recovery. Considering the recovery time of 365 days, the resiliency factor for the fixed-base school is between 0.41 and 0.63, while it is higher for the base-isolated building between 0.85 and 0.9.

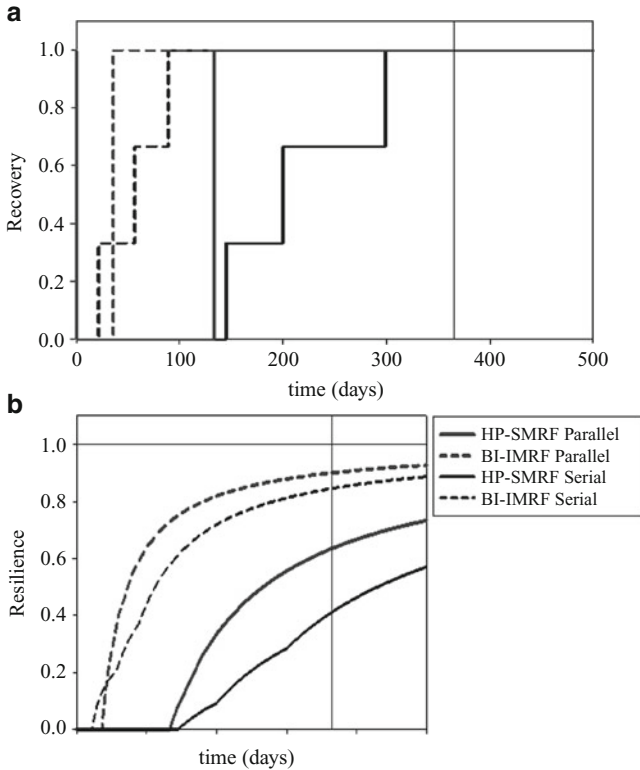


Fig. 10.8 Recovery and resilience functions of the HP-SMRF and the BI-IMRF considering school occupancy and the 2% in 50-year hazard level

10.8 Remarks and Conclusions

Over the past two decades, performance-based earthquake evaluation has developed to a point where it can be effectively used in the design of structures. For a healthcare facility and a school building located in Oakland (California), the base-isolated system provides significant median damage savings and repair time reduction compared to the fixed-base system. This stems from the substantial reduction in accelerations, drifts, and residual drifts when isolated system is utilized at the base of the building. For the healthcare occupancy the reduction in repair cost ranges from 76% to 88% with an average of 85%, and for the school it ranges from 66% to 82% with an average of 76%. Such big reduction in cost of damage repairs of base-isolated systems comes primarily from preventing damage of the expensive equipment and structural components, and from minimizing the damage of non-structural components. Repair times are 3–6 times smaller for the isolated buildings relative to the fixed-base buildings. For the design basis earthquake (10% probability of exceedence in 50 years) and healthcare occupancy, the repair time of the

fixed-base building is expected to be in the range of 78 and 207 days, while it is in the range of 19 and 45 days for the base-isolated building. Such dramatic reduction in repair time implies significantly smaller downtime and higher resilience of the base-isolated buildings. This chapter is indicative of the effectiveness of the base isolation in mitigating damage and associated losses as well as increasing resiliency.

References

- AISC (2005) Prequalified connections for special and intermediate steel moment frames for seismic applications. Technical report, American Institute of Steel Construction
- ASCE (2010) Minimum design loads for buildings and other structures. Technical report, American Society of Civil Engineers
- ATC (2012) Performance assessment computation tool (pact). Technical report, Applied Technology Council
- Baker JW, Lin T, Shahi SK, Jayaram N (2011) New ground motion selection procedures and selected motions for the peer transportation research program. Technical report, Pacific Earth. Eng. Research Center, University of California, Berkeley
- Cimellaro G, Reinhorn AM, Bruneau M (2010a) Framework for analytical quantification of disaster resilience. *Eng Struct* 32(11):3639–3649
- Cimellaro GP, Reinhorn AM, Bruneau M (2010b) Seismic resilience of a hospital system. *Struct Infrastruct Eng* 6(1–2):127–144
- FEMA (2012) Next-generation methodology for seismic performance assessment of buildings. Technical report, Applied Technology Council for the Federal Emergency Management Agency
- Mayencourt P (2013) Seismic life cycle cost comparison of a frame structure. Ph.D. thesis, Swiss Federal Institute of Technology Zurich (ETHZ)
- McKenna F, Fenves GL (2004) Open system for earthquake engineering simulation (OpenSees). Pacific Earthquake Engineering Research Center (PEER), PEER, University of California, Berkeley
- Miranda E, Taghavi S (2003) Response assessment of nonstructural building elements. Technical report, Pacific Earthquake Engineering Research Center, University of California, Berkeley
- Ryan KL, Sayani PJ, Dao ND, Abraik E, Baez YM (2010) Comparative life-cycle analysis of conventional and base-isolated theme buildings. In: 9th US national & 10th Canadian conference on earthquake engineering, Toronto
- Terzic V, Mahin S, Comerio M (2014) Comparative life-cycle cost and performance analysis of structural systems. Technical report, Earthquake Engineering Research Institute, Anchorage
- U.S.G.S. (2014) The 2014 U.S. geological survey (USGS) national seismic hazard maps. <http://earthquake.usgs.gov/research/hazmaps/>
- Yao C, Tu Y (2012) The generation of earthquake damage probability curves for building facilities in taiwan. Technical report, Proceedings of the international symposium on engineering lessons learned from the 2011 Great East Japan earthquake

Chapter 11

A Model to Evaluate Disaster Resilience of an Emergency Department

Abstract Hospitals are critical infrastructures which are vulnerable to natural disasters, such as earthquakes, manmade disasters and mass casualties events. During an emergency, the hospital might also incur in structural and non-structural damage, have limited communication and resources, so they might not be able to treat the large number of incoming patients. For this reason, the majority of medium and large size hospitals have an emergency plan that expands their services quickly beyond normal operating conditions to meet an increased demand for medical care, but it is impossible for them to test it before an emergency occurs. In this chapter is presented a simplified model that can describe the ability of the Hospital Emergency Department to provide service to all patients after a natural disaster or any other emergency. The waiting time is the main response parameter used to measure hospital resilience to disasters. The analytical model has been built using the following steps. First, a discrete event simulation model of the Emergency Department in a hospital located in Italy is developed taking into account the hospital resources, the emergency rooms, the circulation patterns and the patient codes. The results of the Monte Carlo simulations show that the waiting time for yellow codes, when the emergency plan is applied, are reduced by 96 %, while for green codes by 75 %. Then, using the results obtained from the simulations, a general metamodel has been developed, which provides the waiting times of patients as function of the seismic input and the number of the available emergency rooms. The proposed metamodel is general and it can be applied to any type of hospital.

11.1 Introduction

The capacity of a community to react to and resist an emergency, regardless the spatial scale of the area of interest is strictly related to the proper functioning of its own critical infrastructure systems. To this purpose, hospitals have been recognized critical networks as part of the organized governmental services which must continue to function when an emergency occurs.

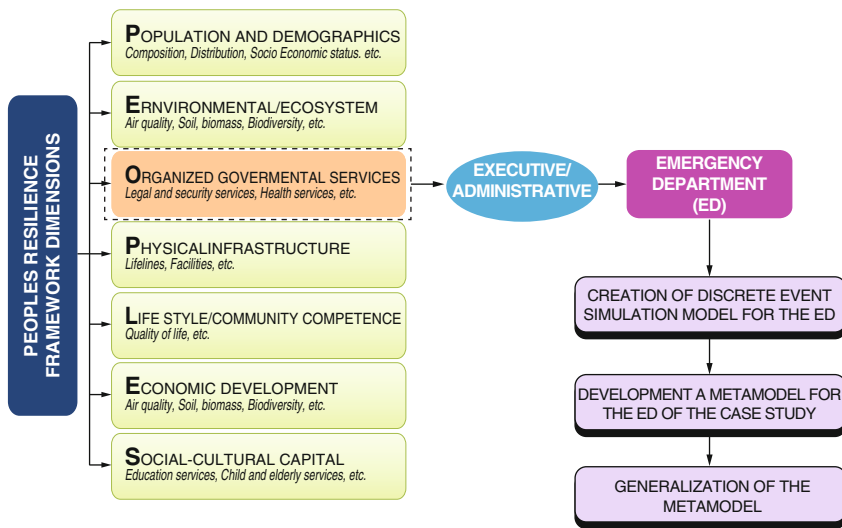


Fig. 11.1 Chapter 11 outline

Within a short period, the majority of medium and large size hospitals have an emergency plan that expands their services quickly beyond normal operating conditions to meet an increased demand for medical care, but it is impossible for them to test it before an emergency occurs.

Between all the hospital departments, the Emergency Department (ED) is the key area in the hospital during a disaster. In fact, the ED plays a pivotal role in the delivery of acute ambulatory and inpatient care, providing immediate assistance request during a 24 h period (Morganti et al. 2013).

In particular this chapter focuses on the evaluation of Resilience metrics for organized governmental services in term of emergency response (Fig. 11.1). This chapter develops a simplified model that can describe the ability of the Hospital Emergency Department to provide service to all patients after a natural disaster or any other emergency (Cimellaro et al. 2010). The waiting time is the main response parameter used to measure hospital resilience to disasters. To this purpose, first, a discrete event simulation model of the Emergency Department in a hospital located in Italy is developed taking into account the hospital resources, the emergency rooms, the circulation patterns and the patient codes. Then, using the results obtained from the simulations, a general metamodel that can be applied to any type of hospital is developed, which provides the waiting times of patients as function of the seismic input and the number of the available emergency rooms.

11.2 Literature Review

The majority of studies which focus on evaluating the service quality and efficiency of the healthcare facilities are based on the *patients' waiting time*, which is the time the patient has to wait before receiving assistance by a doctor (Dansky and Miles 1997). Many studies have been developed over the years to analyze how to decrease the patient waiting times. One of the earliest studies was conducted by Fetter and Thompson (1965), which analyzed the doctors utilization rates with respect to patient waiting time using different input variables (e.g. patient load, patient early or late arrival patterns, walk-in rates, physician service etc.). Later, in the 1990s, Kirtland et al. (1995) developed some of the first studies in the optimization of human resources analyzing how to improve patient flow in an ED. They identified three alternatives that can save an average of 38 min of waiting time per patient. Later, Martin et al. (2003) analyzed the parameters and the strategies which can be used to decrease the patient waiting time and therefore to improve the hospital performance.

Takakuwa and Shiozaki (2004) proposed a procedure for planning emergency room operations that minimize patient waiting times. They found that patient waiting time was substantially reduced by adding a more appropriate number of doctors and medical equipment. A similar study to assess the effect of some possible changes in the ED processes was also presented by Mahapatra et al. (2003) which showed that the addition of a care unit improved the average waiting times by at least 10 %.

Later, Lau (2008) studied new patient scheduling rules for three Orthopedic Clinics across Ontario in order to find solutions to long patient waiting times by proposing a new scheduling algorithm.

Santibáñez et al. (2009) provided a framework on how to reduce the waiting time and improve the resource allocation using a computer simulation model of the Ambulatory Care Unit (ACU).

Later, Yerravelli (2010) studied the patients' waiting times at KCH Emergency Department. The objective of the research was to evaluate the hospital performance, as well as to identify the opportunity by reducing waiting times using the KCH ED model. Furthermore, resource utilization was taken into account in order to determine the required staffing levels and to minimize the operating costs. Duda (2011) examined whether hospital strategies were aligned with its processes. In particular, he analyzed the patients' flow, the time spent in the hospital before receiving assistance. His goal is to identify which processes need to be changed and which alternatives need to be considered to increase the effectiveness of the patient flow processes and to reduce the waiting time. More recently, Hu (2013) studied an optimal human resource allocation to reduce the patient waiting time using Discrete Event Simulation models (DES) on an existing Clinic. DES models are widely used to simulate hospitals, because healthcare facilities are complex systems with multiple interactions between patients, doctors, nurses, technicians, different departments and circulation patterns. The interaction between all these components

is described realistically through DES models. Many studies have been performed over the years and nowadays it is possible to find several references related to this field (Günel and Pidd 2010). DES models are also used as a communication tool between the hospital administration and the model developers helping the administrators to understand the performance of the different healthcare processes (Van der Meer et al. 2005; Morales 2011). Moreover, DES model allows the investigation and planning for the use of the hospital resources (Šteins 2010). Below are some additional examples of ED which have been modeled using DES models.

Samaha et al. (2003) developed a DES model of the ED and tested different scenarios by concluding that the waiting time is *process related* and not *resource related*, so according to the authors the *triage* with – fast track – area can reduce the patient waiting time.

Later, Komashie and Mousavi (2005) conducted sensitivity analysis by varying the number of beds, doctors, nurses in the simulation model to reduce the waiting time.

Davies (2007) developed a new approach called “See” and “Treat” method, where the triage process is eliminated and the patients are directed by a qualified receptionist to the doctor or to a emergency nurse practitioner (ENP) based on the patient’s condition. This approach is supposed to eliminate the patient waiting time by simplifying the service.

Medeiros et al. (2008) developed a DES model for the ED by implementing a new approach known as PDQ (Provider-Directed-Queuing) which can reduce non-critical patients waiting time and increase the room availability for the critical patients. Recently, DES models have also been used by Morgareidge et al. (2014) to optimize the design of the ED space and the care process for a specific case study.

11.3 Methodology

Outlined in this paragraph is the methodology used here to develop the metamodel of an ED, using the step-by-step procedure described below:

1. Creation of a discrete event simulation model for the ED with and without an emergency plan, using as input data the estimated patient arrival rate in normal as well as in emergency operating conditions;
2. Development of a *metamodel* (Cimellaro et al. 2010) to evaluate the hospital waiting time using a reduced number of input parameters: the magnitude of the seismic input and the number of non functional emergency rooms;
3. Development of a *general metamodel* that can be applied to any hospital;

In the next paragraphs the different steps of the procedure are described.

11.4 Discrete Event Simulation Model for the ED

Simulation modeling is the process of creating a discretization of an existing physical system to predict its performance in the real world. The steps for developing the model are described in the following paragraphs.

11.4.1 Description of the Case Study

The hospital considered for the analysis is the Umberto I Mauriziano Hospital located in Turin, Italy (Fig. 11.2). The hospital is located in the southeast part of the city, approximately 3 km far from the center. It was built in 1881, but it was bombed several times during World War II, so several parts have been rebuilt or extended. Currently it includes 17 units, which correspond to different departments, and it covers an overall surface of 52,827 m². While developing the simulation model, only the Emergency Department, which is located in the building 17, has been considered (Fig. 11.3).

The ED consists of an entrance area in which “triage” is carried out, and four macro areas corresponding to the four different color codes, that represent the severity of injury. In particular, these four color codes are *red*, *yellow*, *green* and *white*. *Red codes* (emergency) identify patients with compromised vital functions, already altered or unstable whose lives are at risk. *Yellow codes* (urgency) are patients who are not in immediate danger of life, but present a partial impairment of vital functions. *Green codes* (minor urgency) have a no critical situation, so their lives are not at risk and their lesions do not affect vital functions. White codes (no



Fig. 11.2 Umberto I Mauriziano hospital, Turin

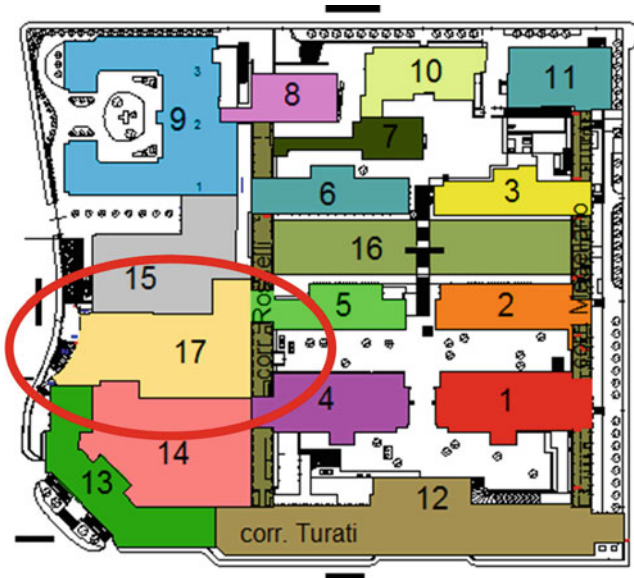


Fig. 11.3 Hospital's units – emergency department building



Fig. 11.4 Emergency department color-codes areas

urgency) include all patients who have neither serious nor urgent injuries and who do not really need to be in the ED, so their treatment can be provided by a general doctor.

The ED is normally divided into four main areas but, when the Emergency Plan is applied, the number of areas is reduced to three (Fig. 11.4), because in emergency conditions the white codes are sent to another facility outside the ED. In emergency

conditions, the red code area is located immediately in front of the ambulance entrance and contains two rooms in which patients receive the first treatments. Parallel to this area, there is the yellow codes' area composed of three emergency rooms, while the green codes' area is situated perpendicular to yellow and red codes' areas and includes two emergency rooms. Each area is provided with waiting rooms in which patients can wait before being treated. Moreover, inside the ED there are recovery rooms in which patients can stay before being discharged or recovered in another part of the hospital.

11.4.2 Description of the Model and Assumptions

In this research, the ED (Fig. 11.5) has been simulated using a discrete event simulation (DES) model built in ProModel[®] 7.00, (downloaded on February 15, 2014) (ProModel 2014). ProModel is a discrete-event simulation software that is used to plan, design and improve complex systems such as tactical and operational systems. Discrete Event Simulation (DES) model has been selected to study the hospital, because the ED is a complex and dynamic system in which the state variables change continuously over time. In addition, DES models allow users to test different asset allocations which are characterized by complex relationships between system processes.

In detail, in the model, it is assumed that the hospital structural and non-structural elements remained undamaged after the earthquake. Four codes have been considered to divide the patients arriving in the ED: red, yellow, green and white. Actually, the Emergency Plan of the hospital also considers blue and black codes that represent respectively “*compromised vital functions*” and “*death*”. While

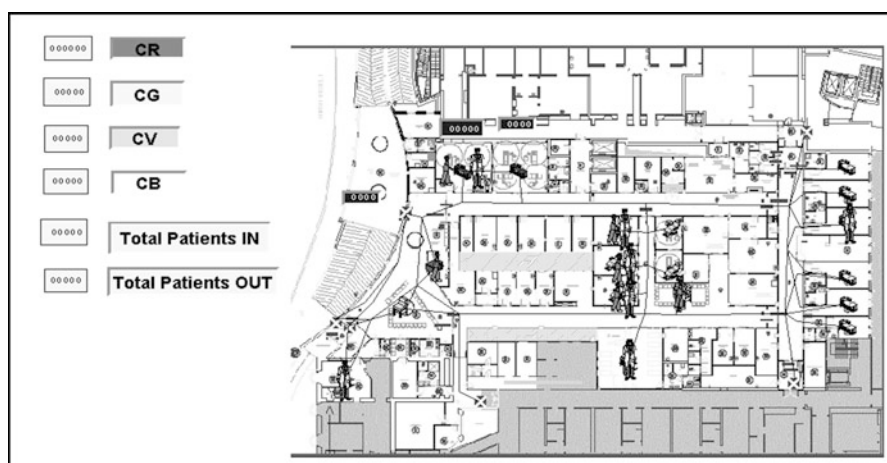


Fig. 11.5 DES model of the Maurizioano ED

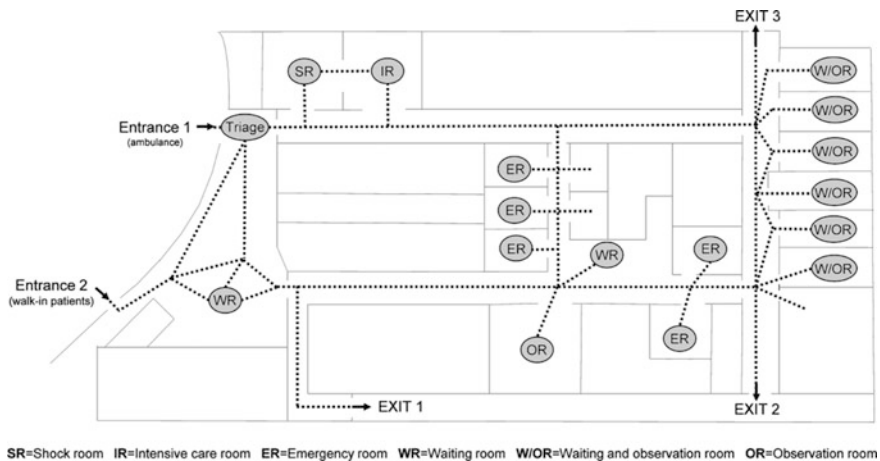


Fig. 11.6 Patient path in the emergency department

developing the model, these two additional codes have not been considered because they have no influence on patients' waiting times. It is also assumed, that once the code is assigned according to the triage, the patients cannot change their status while their staying in the ED.

All the assumptions in the model have been approved by the Emergency Department Staff and the Emergency Plan Director of the Hospital. The ED of the case study consists of emergency rooms (ER) which are different for each color code area, two waiting rooms (WR), a triage room (Triage), an exams area, a critical area, one shock room (SR) and one intensive reanimation room (IR), several observation rooms (OR) and some separate stations (Fig. 11.6).

There are two entrances to the ED, one is for ambulance only, while the second is for patients and visitors. The first one is located in the northwest part of the ED, near the red code area, while the second one is in the southwest side. Therefore, the patients that arrive by ambulance or car (e.g. red codes) enter through the north entrance, which is closest to the shock and intensive care rooms. On the other hand, all the other walk-in patients use the south entrance that is nearest to the yellow and green codes areas. There are three exits from the ED, which are used according to the patient destination (healthcare facilities, hospital wards, dismissed). They are situated in the south, northeast and southeast sides of the ED. Each place is called "*location*" according to Promodel terminology and have a given assigned capacity. Some locations, such as the entrances, the exits, and the waiting rooms, have an infinite capacity while others, like the emergency rooms, the shock room, the intensive care room, have a defined number of patients who can be treated at the same time.

Inside the locations, the "*entities*" carried out their duties. In this model, the entities are the patients visiting the ED, who are categorized according to the severity of their injury. In particular, they have been divided into four categories

Table 11.1 Resources definition

Color codes area	Work schedule	Resources
Red area	Hours 8/20	2 doctors, 4 nurses
	Hours 20/8	2 doctors, 3 nurses
Yellow area	Hours 8/20	5 doctors, 3 nurses
	Hours 8/20	5 doctors, 3 nurses
Green area	Hours 8/20	3 doctors, 5 nurses
	Hours 8/20	2 doctors, 3 nurses

corresponding to the four color codes: red, yellow, green and white codes. An entry, a path and a travel speed has been assigned to each patient type. For example, yellow, green and white codes travel at the speed of 50 mpm, while red codes travel at the speed of 60 mpm.

Patients, nurses and doctors follow a predefined “*network path*” (Fig. 11.6) composed of nodes and edges (dotted lines) which can be unidirectional or bidirectional. Not all the paths are accessible to all the entities. For example, the passage from the red to the yellow area is accessible only to the medical staff. Furthermore, if multiple path options are available at a single node, then the shortest distance path is selected.

The “*resources*” correspond to the medical doctors, nurses, health care operators, etc. They are divided into two categories: those that provide service from a fixed station and those that travel through the ED. Each resource has its own schedule which is summarized in Table 11.1, according to the color code.

The “*processes*” are all the actions that the entities carry out within the ED, such as the patients’ movements from one location to another, how much time they spend in each location and how and for how long they use a particular resource. Below is given a description of all the actions which have been modeled according to the color codes.

Red Codes; Red codes generally arrive by ambulance at entrance 1. As soon as they arrive, due to the severity of their condition, they are sent directly to the shock room and the intensive care room in the red zone, where critical patients are treated immediately. After receiving the first treatment in these two rooms, some patients are displaced to the yellow area in the ED, others are transferred to the hospital ward and the remaining part leave the hospital (they could move to another healthcare facility or be dismissed).

Yellow Codes; Yellow code patients generally can arrive from both Entrance 1 and 2. After the triage, they wait in the waiting room reserved for the yellow codes until one of the emergency rooms is available. While waiting, some of them are kept in the observation room where they receive the first treatments. After being visited in the emergency rooms, some patients leave the hospital while others are sent to the examination room. Once the check is done, the patients are sent back to the emergency rooms or to the green codes area. From the emergency rooms, a part of them leaves the ED (toward the hospital wards or others healthcare facilities) while the remaining patients are sent back to the examination room until their condition is identified and they can leave the ED.

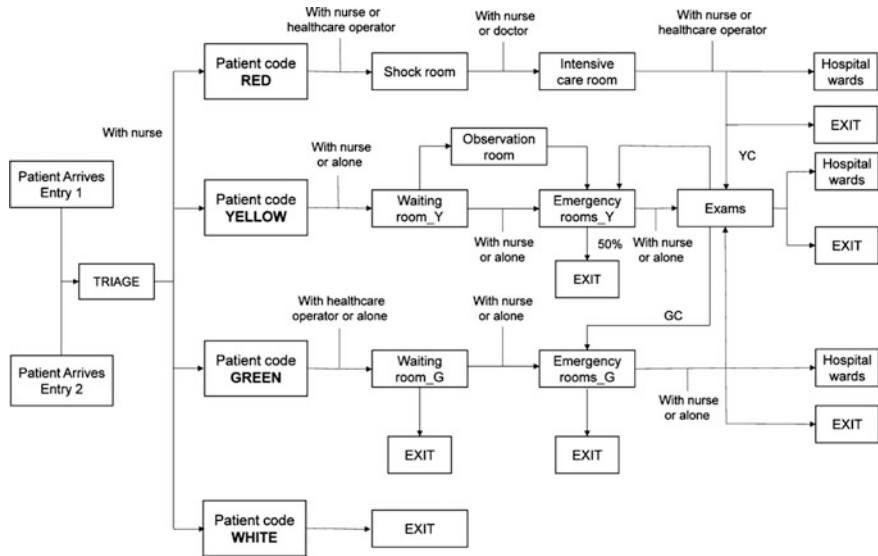


Fig. 11.7 Process map for the emergency department

Green Codes; In general, green codes go in from the entrance 2. After the triage, they are sent to the observation rooms in the green area. Over there, any available nurses treat the green codes with less injury, so that they can leave the ED earlier. The others wait for an available emergency room. After receiving treatment, they leave the hospital or move to an examination room and then they go to the hospital wards or are dismissed.

White codes; White codes also go in from the entrance 2. After the triage, if the emergency plan is active, the white codes leave the ED, because they have minor injuries.

All the *processes* and *patient paths* that take place in the ED during an emergency have been identified through interviews with the staff and the personnel of the ED. The results of these interviews are shown in the flow map (Fig. 11.7), which has been approved by the hospital’s personnel. It is important to mention that the input data for the emergency plan have been determined from public interviews with hospital’s medical staff, since the current emergency plan has never been applied in the hospital.

11.4.3 Calibration of the Model in Normal and Emergency Operating Condition

The *patients’ arrival rates* under normal operating conditions have been calculated using the hospital’s register statistics. However, other information has also been extracted by the hospital’s register statistics, such as the patient’s inflow, the

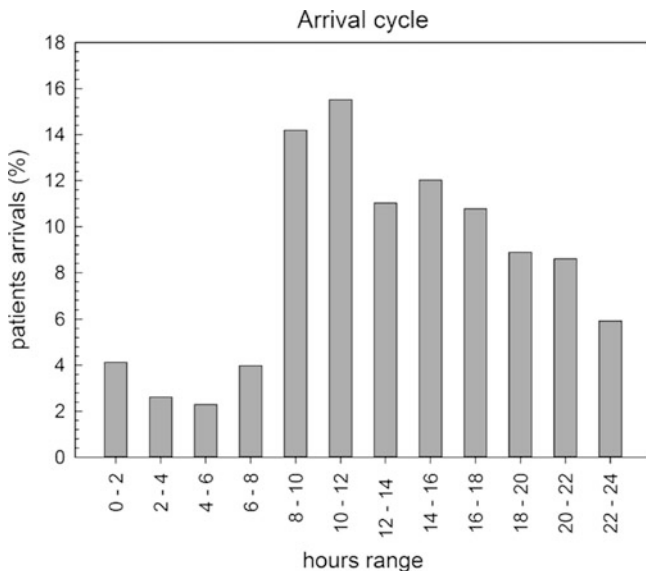


Fig. 11.8 Percentage of patients entering the ED hourly in normal operating conditions

check-in and checkout time, the time spent in each room as well as patients’ movements from one location to another. Moreover, the patient arrivals in the ED vary from hour to hour and, in order to determine the patient arrival distributions, an arrival cycle has been defined using the data provided by the hospital database that have been used to calibrate the model. The distribution is shown in Fig. 11.8. The patient arrival rate during a seismic event has also been considered in the analysis, using the data collected by a Californian hospital during 1994 Northridge Earthquake (Stratton et al. 1996; Peek-Asa et al. 1998; McArthur et al. 2000). The shape of the patient seismic wave related to Northridge earthquake is available in Cimellaro et al. (2011), however in the current research the patient’s arrival rate has been scaled to adapt to the seismic hazard in the region (Turin, Italy). In particular, an earthquake with a return period of 2500 years has been considered in the analysis, assuming a nominal life for a strategic building like a hospital of 100 years according to the Italian seismic standards (NTC-08 2008). Initially a scaling procedure based on the PGA has been used, but because of its limitations, another procedure based on the Modified Mercalli Intensity (MMI) scale has been selected. In Fig. 11.9 three days of patient arrival rates following Northridge earthquake are shown, which have been scaled with respect to the corresponding PGA and MMI values. Then the number of patients has been grouped in different color codes, following a similar distribution proposed by Yi (2005).

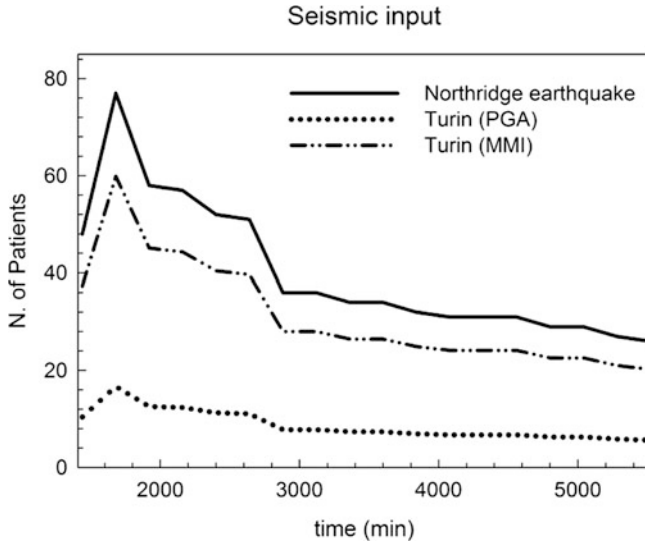


Fig. 11.9 Arrival rates for Northridge earthquake and arrival rate scaled with respect to PGA and MMI

11.4.4 Emergency Plan

After a disaster occurs, the number of incoming patients rises significantly. A change in patients' arrival rates entails an increase of crowding, prolongs injured waiting times to be treated by an emergency provider and enhances the risk of aggravating patients conditions. Considering all these factors, the hospitals' Emergency Departments should have an emergency plan to be implemented during catastrophic events. The Emergency Plan (EP) consists of a number of procedures designed to guarantee the essential health services during an emergency when the number of incoming patients increases. It is also developed to assure adequate medical resources for the continuation of patient care, equipment and treatment materials availability and an appropriate interaction with others critical infrastructures during an emergency. Generally, the EP is activated when the number of ill or injured exceeds the normal capacity of the ED to provide the quality of care required. According to the Mauriziano hospital's provisions, the EP is activated when there is the simultaneous access (or within a short period) of 10 or more patients with critical health condition (red and yellow codes). However, according to the personnel in the hospital, this condition has never happened so far. Therefore, the only possibility to test the effectiveness of the EP is using a *discrete-event simulation model*, which represents a useful tool for testing the response of the EP with an increasing number of incoming patients. According to the EP, the patients with critical health conditions are red and yellow codes, so in order to check if the EP can be activated, the total number of red and yellow code incoming patients has been plotted in Fig. 11.10. The

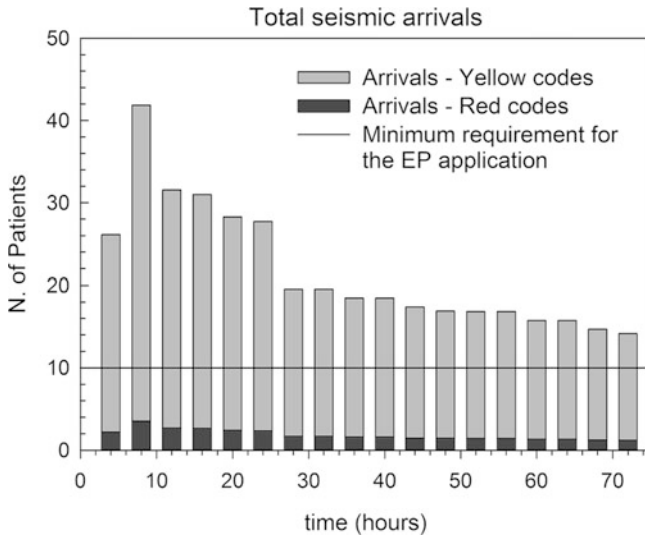


Fig. 11.10 Total arrival rate during an emergency (*red and yellow codes*)

figure shows the amount of patients arriving in the ED during the three days period following an earthquake with 2500 years return period. In this case, the threshold of the EP is exceeded and the plan is activated.

11.4.5 Numerical Results

The model has been validated and verified by comparing the numerical results in normal operating conditions with the real data provided by the hospital. Monte Carlo simulation has been performed using 100 runs for each scenario considered. The total time of each run in the simulation is 13 days, which has been divided into three parts. First, the simulation runs for two days using the patient arrival rate under normal operating conditions, in order to make the system stable and remove any influence by the initial conditions. Then for three days, the patient arrival rate generated by the seismic event is used. Finally, the last eight days of simulation again use the patient arrival rate in normal operating conditions, in order to bring back the system to the steady state it had before the earthquake occurs. The numerical output of the simulation is the patient waiting time vs. time, divided according to the color code for different scenarios (e.g. with and without the Emergency plan, etc.). In Fig. 11.11 the average waiting time vs. time in normal and emergency operating conditions is shown, assuming the same distribution of incoming patients.

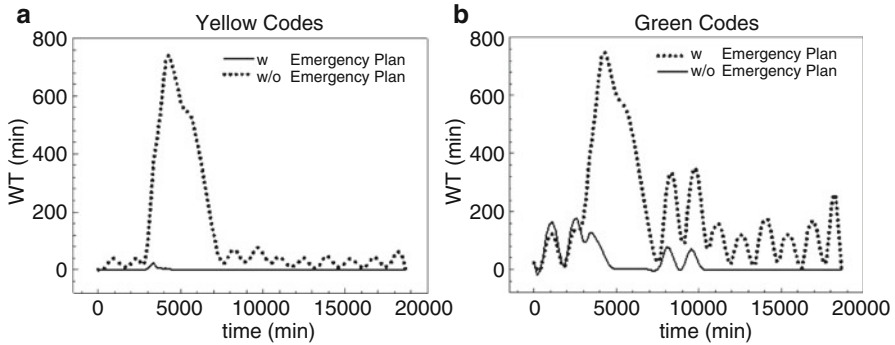


Fig. 11.11 Comparison with and w/o emergency plan with $MMI = VI$ for (a) yellow codes; (b) green codes

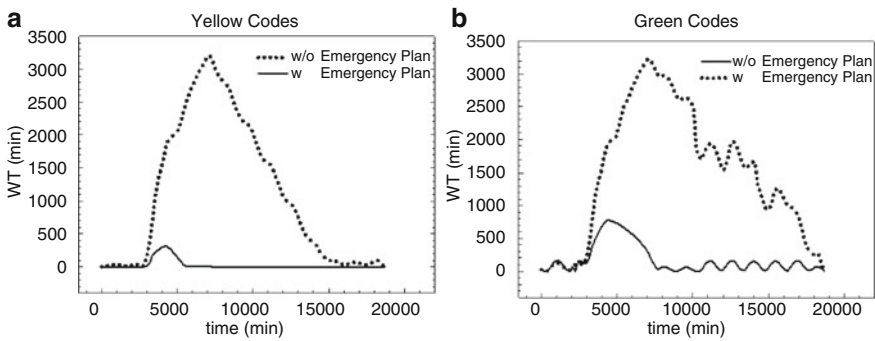


Fig. 11.12 Comparison with and w/o EP with an amplified seismic input ($MMI = XI$) for (a) yellow codes; (b) green codes

The numerical results show that the waiting time is drastically reduced when the emergency plan is active. The results reveal that both yellow and green code patients experience longer waiting time under normal operating conditions during an extreme situation. In particular, the average patient waiting time for yellow codes reaches a peak value of about 720 min, while for green codes it reaches about 750 min without an emergency plan. On the contrary, when the emergency plan is active, the average patients waiting time reaches a peak value of about 30 min for yellow codes and about 190 min for the green codes. In percentage, there is a reduction in waiting time of 96 % for the yellow codes and of 75 % for the green codes respectively, when the emergency plan is applied.

Sensitivity analysis has been performed using six different increasing levels of earthquake intensities from $MMI = VI$ to $MMI = XI$. Monte Carlo simulations have been run and, in Fig. 11.12 the average waiting time vs. time with and without emergency plan is shown, assuming the same distribution of incoming patients corresponding to an earthquake with $MMI = XI$. The numerical results show that the effect of the emergency plan is more evident for high intensity earthquake.

In fact, the average patients waiting time for yellow codes reaches a peak value of about 3200 min, while for green codes of about 3250 min without an emergency plan. On the contrary, when the emergency plan is active, the average patients waiting time reaches a peak value of about 300 min for yellow codes and about 785 min for the green codes. In percentage, there is a reduction of waiting time of 91 % for the yellow codes and of 76 % for the green codes respectively, when the emergency plan is applied.

Although the emergency plan plays a positive role in reducing the waiting time, the green code in emergency conditions have to wait about 800 min (13 h) when an earthquake with $MMI = XI$ strikes. The long waiting can delay the diagnosis and the consequent treatment, leading to complications and putting patients' lives and well-being in jeopardy. Therefore, the possibility of improving the existing emergency plan in the hospital has been analyzed, by adding additional resources such as doctors and emergency rooms. The possibility of adding one doctor without simultaneously adding the respective emergency room has also been considered, because the green codes can also receive treatment outside their emergency room.

The results of the sensitivity analysis by adding different resources are given in Fig. 11.13, where it is shown that, when one additional doctor is considered, the average peak of waiting times decrease of around 39 %. On the other hand, if an emergency room is added, a reduction of 74 % with respect to the initial emergency plan is observed. Finally, adding both a doctor and an emergency room, the waiting time reduces to a peak of about 90 min, generating a total reduction of 88 % with respect to the initial emergency plan (13 h). Between the different options, the addition of an emergency room only is more feasible and recommended, because an emergency room is already available in the ED. So it can be used by the existing personnel, at no extra cost, while in the other cases a doctor has to be hired by the

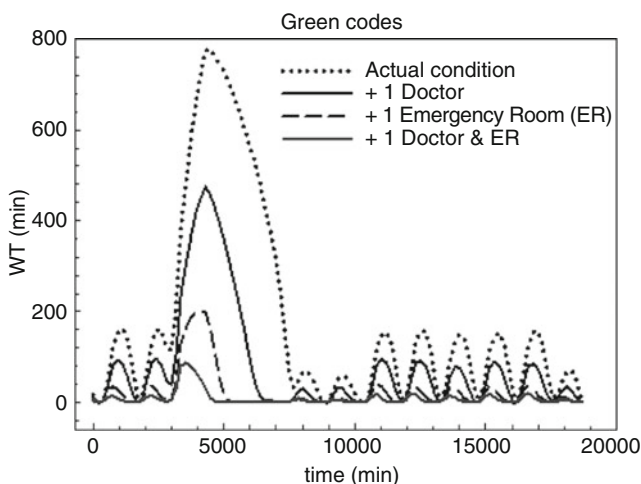


Fig. 11.13 Sensitivity of additional resources on the performance of the ED with emergency plan

hospital. In fact, the solution with extra costs is not justified by a reduction of the waiting time of only 14 % with respect to the recommended solution.

11.5 Metamodel for the ED of the Mauriziano Hospital

However, the proposed DES model has some limitations. First, it is computationally demanding, therefore it is difficult to run multiple simulations in real time to determine the patient waiting time during the emergency. Secondly, DES models generate a significant amount of numerical data that is difficult to interpret, because generally, the person who analyzes the data is not the same one who built the model and, in most cases, this person has no experience with the simulation software. For the reasons above, a simplified model, called “metamodel” has been developed. The metamodel is an analytical function describing the system behavior using a reduced number of parameters with respect to the DES model.

In this paragraph, to explain the methodology, the metamodel of a complex system like the Mauriziano Emergency Department has been built. There are two input parameters of the proposed metamodel: the seismic arrival rate (α) and the number of non-functional emergency rooms (n) due to the earthquake, while the output parameter is the patients’ waiting time (WT).

Sensitivity analysis has been performed by changing both input parameters. First, the number of non-functional ER has been increased and the seismic inputs have been amplified. Monte Carlo simulations has been run for all the different combinations and then non-linear curve regression methods have been used to identify the coefficients of the analytical quadratic equation, which is issued to determine the average patient waiting time.

The main assumption of the metamodel is that it has been built based on numerical simulation data obtained by the results of the DES model described in previous paragraph, so it shares the same assumptions with which the DES model has been built. It is also assumed that the configuration of the ED does not change during the emergency, so the doctors, the nurses, their paths and the emergency rooms remain the same. Below the procedure to evaluate the coefficients for the average patient waiting time of the yellow codes is shown. A similar procedure can be followed for all the other patient codes.

11.5.1 Architecture of the Metamodel

The general formulation of the metamodel is given by

$$WT = f(t, n, \alpha) \quad (11.1)$$

where WT represents the patients’ waiting time, n is the number of not functional waiting rooms, α is a parameter proportional to the intensity of the seismic input

and t is the time in minutes. In detail, a lognormal function has been selected to describe the average patients' waiting time which is given by

$$WT(t, n, \alpha) = \frac{a_n}{t} * \exp \left(-0.5 * \left(\frac{\ln t/b_n}{c_n} \right)^2 \right) \tag{11.2}$$

where a_n , b_n , and c_n are coefficients which are function of the t , n and α . All the coefficients have been calibrated using the numerical data from the DES models for both the normal and emergency operating condition.

11.5.2 Calibration of the Model in Normal Operating Condition

In this paragraph is described in detail the procedure to determine the coefficients, a_n , b_n , and c_n in Eq. (11.2) for the case of patients with yellow code. First, Montecarlo simulations have been performed assuming a constant value of n and increasing values of MMI. The resulting average WT is shown in Fig. 11.14. The trend is that by increasing the seismic input, the corresponding waiting time increases.

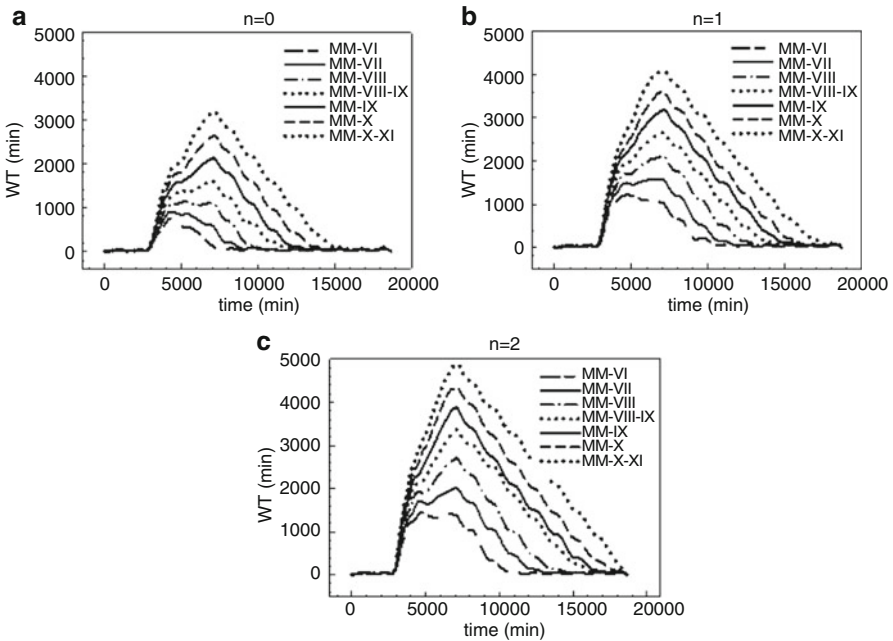


Fig. 11.14 Simulations results w/o emergency plan for different values of MMI and damage states (a) $n = 0$; (b) $n = 1$; (c) $n = 2$

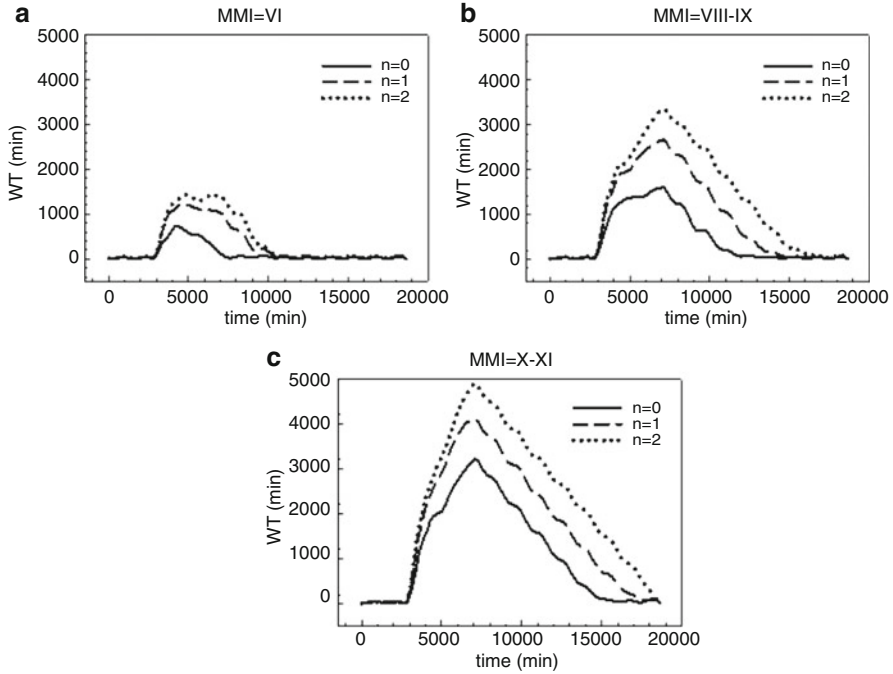


Fig. 11.15 Simulations results w/o emergency plan with different damage states for (a) $MMI = VI$; (b) $MMI = VIII-IX$; (c) $MMI = X-XI$

Then, Montecarlo simulations have been run considering a constant value of seismic intensity (MMI) and a variable value of emergency rooms n . In other words, it is simulated the closure of the emergency rooms (n), assuming they are not functional following a seismic event. The results of the simulations are shown in Fig. 11.15 for three different values of MMI. It is observed that by closing the ERs, the WT increases significantly. In particular, when $MMI = XI$ and two emergency rooms are not functional, the average WT reaches a peak of about 5000 min, which corresponds to approximately 84 h (three and a half days). This means that the system is congested due to a high volume of patients that exceeds the hospital capacity.

In order to describe the trend shown in Figs. 11.14 and 11.15, the bell shape curve given in Eq. (11.2) has been adopted where the coefficients a_n , b_n , and c_n have been determined using regression analysis assuming they are quadratic functions of α given by

$$a_n(\alpha) = a_0 + a_1\alpha + a_2\alpha^2 \quad (11.3)$$

$$b_n(\alpha) = b_0 + b_1\alpha + b_2\alpha^2 \quad (11.4)$$

$$c_n(\alpha) = c_0 + c_1\alpha + c_2\alpha^2 \quad (11.5)$$

where the coefficients $a_0, a_1, a_2, b_0, b_1, b_2, c_0, c_1, c_2$ are function of n and are also determined by regression analysis. The resulting quadratic functions for the case of normal operating conditions is the following

$$\begin{cases} a_0(n) = 21,178,533.7 - 50,687,867.5 \cdot n - 10,938,560.2 \cdot n^2 \\ a_1(n) = -49,405,307.7 + 86,079,082.9 \cdot n - 19,905,188.7 \cdot n^2 \\ a_2(n) = 31,467,171.4 - 30,777,131.8 \cdot n + 8,057,254.1 \cdot n^2 \end{cases} \quad (11.6)$$

$$\begin{cases} b_0(n) = -0.5166 + 1.1094 \cdot n - 0.3743 \cdot n^2 \\ b_1(n) = 1.121 - 1.529 \cdot n + 0.5132 \cdot n^2 \\ b_2(n) = -0.3514 + 0.5445 \cdot n - 0.1776 \cdot n^2 \end{cases} \quad (11.7)$$

$$\begin{cases} c_0(n) = -3955.3 + 3131.5 \cdot n - 1393.7 \cdot n^2 \\ c_1(n) = 11,100.9 - 1821.2 \cdot n + 1262.6 \cdot n^2 \\ c_2(n) = -2328.4 + 45.4 \cdot n - 200.1 \cdot n^2 \end{cases} \quad (11.8)$$

11.5.3 Calibration of the Model with the Emergence Plan

The same procedure described above can be used to evaluate the coefficients of the model in Eq. (11.2) when the Emergency plan is active in the model. Similarly, Montecarlo simulations have been performed assuming a constant value of n and increasing values of MMI. The resulting average WT is shown in Fig. 11.16. Similar trends to the ones shown in Fig. 11.14 have been observed, however an additional consideration can be added. The effectiveness of the Emergency plan is more evident when all the ERs are functional, while when most of them are not functional ($n = 2$), the emergency plan does not have any effect in reducing the average patient waiting time.

Instead by keeping constant the seismic intensity and increasing the number of non functional ERs, it can be observed that for high seismic intensities $MMI = XI$ when two ERs are not functional, the WT can reach peaks of about 6000 min (around 4 days) (Fig. 11.17c). This peak is even higher with respect to the same condition when the Emergency Plan is not applied (Fig. 11.14c).

The reason for this unexpected behavior can be explained because when the Emergency Plan is not active, there are five ERs for both the green and the yellow codes. When the EP is active 3 ERs are reserved for the yellow codes only, while the green codes are treated in different parts of the hospital. When two ERs are not functional ($n = 2$) and the EP is not active, the yellow codes have three ERs available and they have priority with respect to the green codes, so it can be assumed that yellow codes use two of the three rooms available.

On the other hand, when the EP is active, but two ERs are not functional, the yellow codes can be treated in only one ER. For the reasons above, the WT for the yellow codes following a high seismic intensity event ($MMI = XI$) is smaller when the EP is not active. Equations (11.3), (11.4) and (11.5) are also valid when the

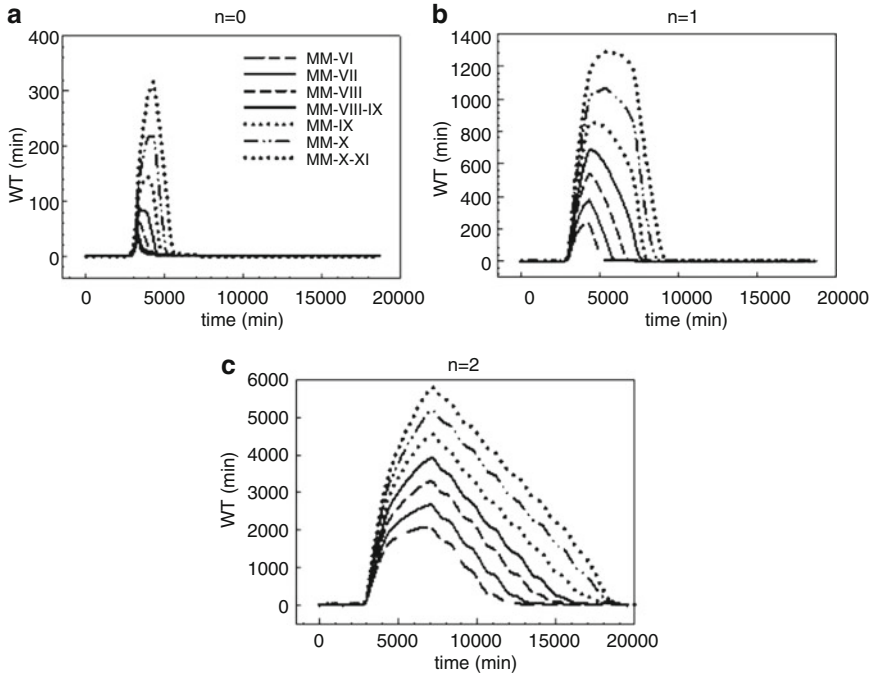


Fig. 11.16 Simulations results with emergency plan for different values of MMI and damage states for (a) $n = 0$; (b) $n = 1$; (c) $n = 2$

emergency plan is applied, but the new coefficients $a_0, a_1, a_2, b_0, b_1, b_2, c_0, c_1, c_2$ which are function of n are given by the following equations

$$\begin{cases} a_0(n) = 4,313,145 + 13,231,212.6 \cdot n - 9,439,291.9 \cdot n^2 \\ a_1(n) = -8,170,064.6 - 25,095,914.1 \cdot n - 14,299,370.7 \cdot n^2 \\ a_2(n) = 3,947,395.5 + 6,797,542.2 \cdot n + 1,122,876.7 \cdot n^2 \end{cases} \quad (11.9)$$

$$\begin{cases} b_0(n) = -0.1195 - 1.099 \cdot n + 0.6206 \cdot n^2 \\ b_1(n) = 0.1625 + 1.728 \cdot n - 0,8719 \cdot n^2 \\ b_2(n) = 0.0033 - 0.61 \cdot n + 0.3148 \cdot n^2 \end{cases} \quad (11.10)$$

$$\begin{cases} c_0(n) = 3304.5 - 6345.4 \cdot n + 3260.9 \cdot n^2 \\ c_1(n) = -939.3 + 8878.9 \cdot n - 3687 \cdot n^2 \\ c_2(n) = 945.1 - 2823.8 \cdot n + 1415.2 \cdot n^2 \end{cases} \quad (11.11)$$

After the model has been built, the numerical results have been compared with the DES model.

In Table 11.2 the error in the estimation of the maximum waiting time between the DES model and the metamodel with and without emergency plan are listed. The

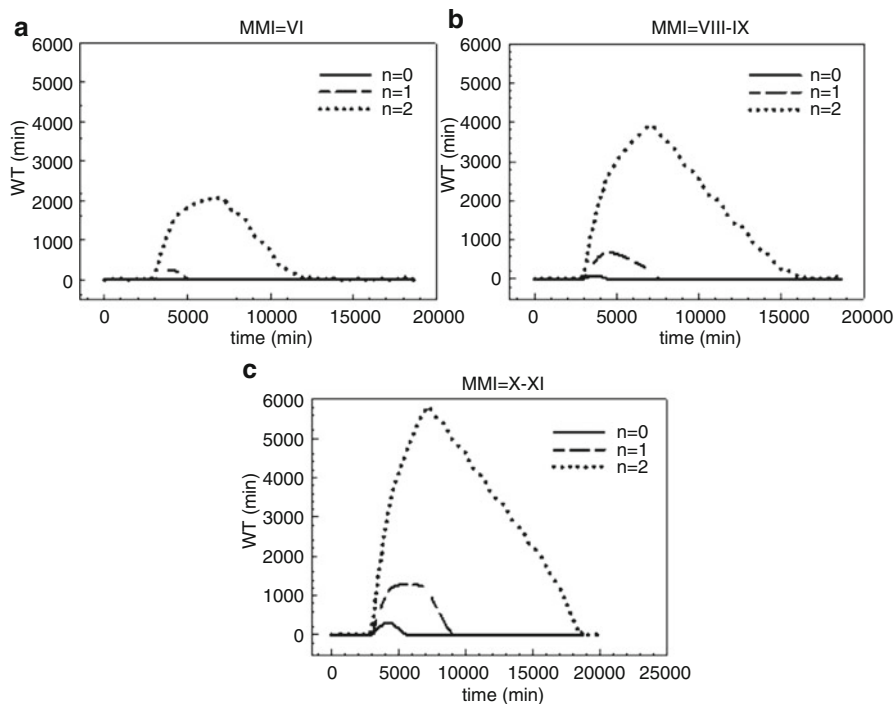


Fig. 11.17 Simulations results with emergency plan with different damage states for (a) MMI = VI; (b) MMI = VIII-IX; (c) MMI = X-XI

Table 11.2 Error in the estimation of the maximum WT between the proposed metamodel and the DES model with and w/o EP

MMI	Without emergency plan			With emergency plan		
	Error (%), n = 0	Error (%), n = 1	Error (%), n = 2	Error (%), n = 0	Error (%), n = 1	Error (%), n = 2
VI	5.43	2.94	7.53	8.00	9.17	5.31
VII	3.84	8.96	5.44	15.20	1.05	3.71
VIII	10.81	4.35	1.03	7.93	1.11	0.93
VIII-IX	2.23	0.37	1.11	8.13	5.24	0.38
IX	2.60	2.72	4.40	6.89	8.96	1.63
X	3.22	1.35	3.26	7.33	11.21	1.92
X-XI	0.32	1.00	3.92	1.89	9.82	2.41

comparison shows that the metamodel is able to provide an accurate description of the ED with an error in the range between 0.32 % and 15.2 % and with an average value which is below 5 %.

11.6 Generalization of the Metamodel

The main limitation of the model proposed in Eq. (11.2) is that can only adequately represent, in real time, the dynamic response of the Maurizioano hospital's Emergency Department. Therefore, it is necessary to develop a general metamodel that can be applied to any ED. However, the problem is rather complex because each ED is substantially different from the other, so it will be impossible to create a general model with the same level of accuracy of a model which has been built "ad hoc" for a specific ED. So in order to have more flexibility with respect to the metamodel proposed in previous paragraph an additional parameter has been added for the calibration. In particular, the number of parameters selected for characterizing a generic ED is three. They are the *number of emergency rooms*, the *number of doctors* and the *seismic intensity*.

One of the assumptions made in the general metamodel is that the total number of emergency rooms (m) is equal to the number of doctors (q). This assumption is generally reasonable because one emergency room is equipped to provide care to only one patient, so the presence of an additional doctor would be useless. The form of the lognormal equation of the generalized metamodel used for estimating the WT is the following:

$$WT(t, \alpha, m) = \frac{a(\alpha, m)}{t} * \exp\left(-0.5 * \left(\frac{\ln\left(\frac{t}{b(\alpha, m)}\right)}{c(\alpha, m)}\right)^2\right) \quad (11.12)$$

where m is the total number of emergency rooms per color area equivalent to the total number of doctors, t is the time in minutes and a, b, c are nonlinear regression coefficients obtained using Eqs. (11.3), (11.4) and (11.5).

Instead, the coefficients $a_0, a_1, a_2, b_0, b_1, b_2, c_0, c_1, c_2$ have been expressed as a function of the total number of emergency rooms m in the ED. The calibration has been performed using different DES models of the ED with increasing number of emergency rooms and increasing level of incoming patients. For all the possible combinations, several functions of the coefficients have been fitted and finally the same type of equation has been selected for all the coefficients. The coefficients of the generalized metamodel appearing in Eqs. (11.3), (11.4) and (11.5) are the following:

$$a_1(m) = 132,611,723 + m^4 \left(2,072,754 - \frac{26,999,059}{m} + \frac{124,474,864}{m^2} - \frac{233,300,000}{m^3} \right) \quad (11.13)$$

$$a_2(m) = 16,657,792 + m^4 \left(-543,784 + \frac{6,227,391}{m} - \frac{22,646,870}{m^2} + \frac{22,339,458}{m^3} \right) \quad (11.14)$$

$$b_0(m) = 5.57 + m^4 \left(0.08 - \frac{1.04}{m} + \frac{4.89}{m^2} - \frac{9.34}{m^3} \right) \quad (11.15)$$

$$b_1(m) = -7.65 + m^4 \left(-0.12 + \frac{1.58}{m} - \frac{7.34}{m^2} + \frac{13.67}{m^3} \right) \quad (11.16)$$

$$b_2(m) = 2.79 + m^4 \left(0.04 - \frac{0.54}{m} + \frac{2.54}{m^2} - \frac{4.78}{m^3} \right) \quad (11.17)$$

$$c_0(m) = 28,475.3 + m^4 \left(338.6 - \frac{4684.3}{m} + \frac{22,726}{m^2} - \frac{43,551.1}{m^3} \right) \quad (11.18)$$

$$c_1(m) = -43,772 + m^4 \left(-578.5 + \frac{8013.6}{m} - \frac{38,812}{m^2} + \frac{74,209.6}{m^3} \right) \quad (11.19)$$

$$c_2(m) = 11,604.2 + m^4 \left(123.1 - \frac{1811}{m} + \frac{9196.2}{m^2} - \frac{18,167.4}{m^3} \right) \quad (11.20)$$

11.6.1 Validation of the Metamodel

In order to validate the proposed generalized metamodel, its numerical results have been compared with the respective DES model of the Mauriziano hospital in Turin and another hospital located in San Sepolcro, Tuscany.

In Fig. 11.18a, b the comparison in term of waiting time between the generalized metamodel of the Mauriziano ED ($m = 3$) with the respective DES model is shown for two different levels of seismic intensity, MMI = VI and MMI = XI. As observed, the two models match each other well. To generalize the results, the model has also been validated using another hospital located in San Sepolcro, Tuscany that has 4 ERs ($m = 4$). Similarly, the results for the same two levels of seismic intensity are shown in Fig. 11.19a, b, highlighting also in this case a good match with the DES model. The error in the term of maximum WT between the DES models and the generalized metamodel is given in Table 11.3.

In this case, the maximum error in the estimation of the maximum waiting time is around 25 % for the San Sepolcro hospital. From the results shown in Figs. 11.18, 11.19 and Table 11.3, it can be concluded that for both hospitals, the generalized metamodel is able to describe the ED behavior.

11.7 Summary and Remarks

Healthcare facilities play a key role in our society, especially during and immediately following a disaster. Generally several potential hazards might occur in a geographic area, so it is essential that hospitals ensure their functionality during emergencies. Thus, during a disaster a healthcare facility must remain accessible

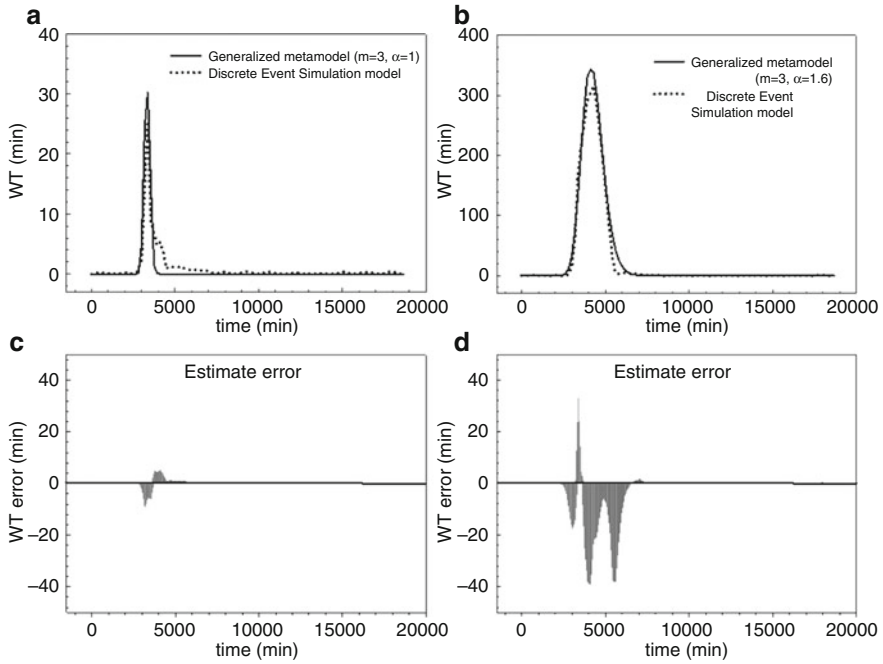


Fig. 11.18 Comparison between metamodel and DES model of the Mauriziano's hospital for (a) MMI = VI, (b) MMI = XI; (c), (d) error bars

and able to function at maximum capacity, providing its services when they are most needed. Discrete event simulation is a powerful tool for representing complex systems such as hospitals. It has been used widely in the medical industry since the mid 1980's. In this chapter, the patients' waiting time (WT) has been identified as the main parameter for evaluating the resilience indicator of an Emergency Department. A discrete event simulation model has been built for the hospital's emergency department, with and without the emergency plan. Results have been collected, and the waiting times calculated when the emergency plan is applied, have been compared with the results under normal operating conditions, showing the efficiency of the existing emergency plan. However, building a DES model is time consuming; therefore, a simplified model called "*metamodel*" has been developed. In order to build the metamodel, different scenarios have been considered, taking in account the intensity of the seismic input and the number of functional emergency rooms. The proposed model can be used by any hospital to measure the performance of its Emergency Department without running complex simulations and for estimating its resilience to disasters. It can also be used by decision-makers to measure the performance of a hospital network in real time during an emergency or to develop some pre-event mitigation actions by optimizing the resources allocated and comparing different emergency plans.

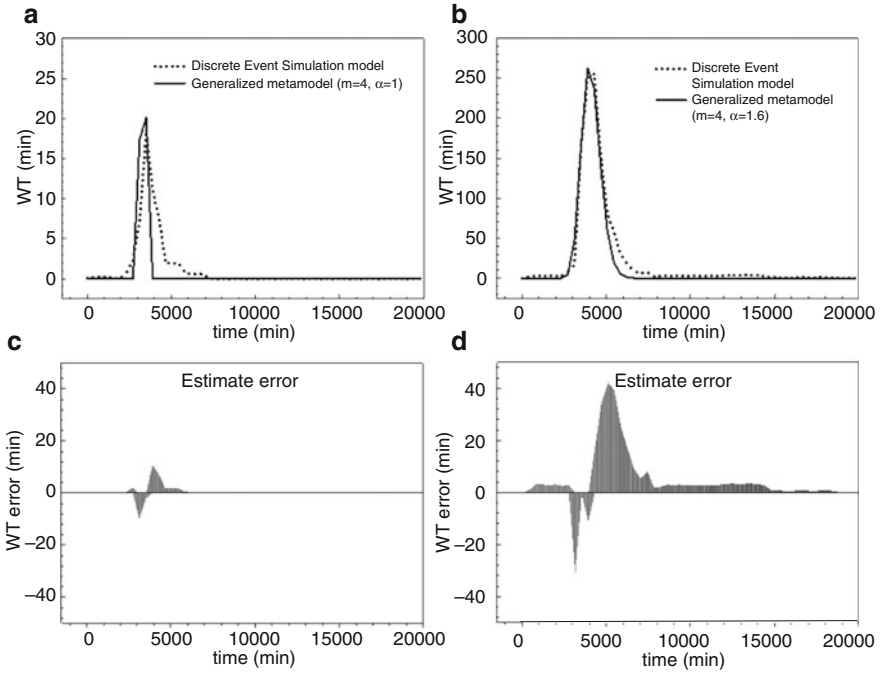


Fig. 11.19 Comparison between analytical metamodel and San Sepolcro’s experimental data for (a) $\alpha = 1$, (b) $\alpha = 1.6$; (c), (d) error bars

Table 11.3 Error between the DES model and the generalized metamodel evaluated at the peak value for Mauriziano and San Sepolcro hospitals

Seismic intensity	Error (%) Mauriziano ED	Error (%) San Sepolcro ED
MMI	19.60	10.70
VI	16.90	25.40
VII	13.80	24.30
VIII	9.30	21.20
VIII–IX	17.20	15.30
IX	13.10	5.10
X	5.90	1.70

References

Cimellaro GP, Reinhorn AM, Bruneau M (2010) Seismic resilience of a hospital system. *Struct Infrastruct Eng* 6(1–2):127–144

Cimellaro G, Reinhorn AM, Bruneau M (2011) Performance-based metamodel for health care facilities. *Earthq Eng Struct Dyn* 40(11):1197–1217

Dansky KH, Miles J (1997) Patient satisfaction with ambulatory healthcare services: waiting time and filling time. *Hosp Health Serv Adm* 42(2):165–177

- Davies R (2007) “see and treat” or “see” and “treat” in an emergency department. In: Henderson SG, Biller B, Hsieh MH, Shortle J, Tew JD, Barton RR (eds) *Proceedings of the 2007 Winter Simulation Conference*, Washington DC IEEE, pp 1498–1501
- Duda CI (2011) *Applying process analysis and discrete event simulation to improve access and customer service times at the Ronald Reagan UCLA Medical Center*. Ph.D. thesis, University of California, Los Angeles (UCLA), Los Angeles
- Fetter RB, Thompson JD (1965) The simulation of hospital systems. *Oper Res* 13(5):689–711
- Günal M, Pidd M (2010) Discrete event simulation for performance modelling in health care: a review of the literature. *J Simul* 4:42–51
- Hu X (2013) *Optimization analysis of patient waiting time and resource utilization in an ob/gyn clinic – a simulation approach*. Ph.D. thesis, University of Central Arkansas
- Kirtland A, Lockwood J, Poisker K, Stamp L, Wolfe P (1995) Simulating an emergency department “is as much fun as...”. In: *Proceedings of the 1995 winter simulation conference*, Arlington, pp 1039–1042
- Komashie A, Mousavi A (2005) Modeling emergency departments using discrete event simulation techniques. In: *Proceedings of the winter simulation conference*, Orlando. IEEE
- Lau R (2008) *Applying discrete-event simulation to orthopaedic clinics: case studies and perspectives*. M.A.Sc., University of Toronto, Toronto
- Mahapatra S, Koelling C, Patvivatsiri L, Fraticelli B, Eitel D, Grove L (2003) Pairing emergency severity index5-level triage data with computer aided system design to improve emergency department access and throughput. In: *Proceedings of the 2003 winter simulation conference*, New Orleans, pp 1917–1925
- Martin E, Gronhaug R, Haugene K (2003) Proposals to reduce over-crowding, lengthy stays and improve patient care: study of the geriatric department in Norway’s largest hospital. In: *Proceedings of the 2003 winter simulation conference*, New Orleans, vol 2, pp 1876–1881
- McArthur DL, Peek-Asa C, Kraus JF (2000) Injury hospitalizations before and after the 1994 Northridge, California earthquake. *Am J Emerg Med* 18(4):361
- Medeiros DJ, Swenson E, DeFlicht C (2008) Improving patient flow in a hospital emergency department. In: Mason SJ, Hill RR, Mönch L, Rose O, Jefferson T, Fowler JW (eds) *Proceedings of the 2008 Winter Simulation Conference*, Miami. IEEE, pp 1526–1531
- Morales G (2011) *Using discrete event computer simulation to analyze the effects of proposed changes to personnel in a hospital medical laboratory*. M.S., The University of Texas – Pan American, Ann Arbor
- Morganti KG, Bauhoff S, Blanchard JC, Abir M, Iyer N, Smith AC, Vesely JV, Okeke EN, Kellermann AL (2013) *The Evolving Role of Emergency Departments in the United States*. RAND Corporation, Santa Monica
- Morgareidge D, Hui CAI, Jun JIA (2014) Performance-driven design with the support of digital tools: applying discrete event simulation and space syntax on the design of the emergency department. *Front Archit Res* 3(3):250–264
- NTC-08 (2008) *Nuove norme tecniche per le costruzioni (ntc08)* (in Italian)
- Peek-Asa C, Kraus JF, Bourque LB, Vimalachandra D, Yu J, Abrams J (1998) Fatal and hospitalized injuries resulting from the 1994 northridge earthquake. *Int J Epidemiol* 27(3):459–465
- ProModel C (2014) *Promodel 2014 user guide*
- Samaha S, Armel WS, Starks DW (2003) The use of simulation to reduce the length of stay in an emergency department. In: *Proceedings of the 2003 winter simulation conference*, New Orleans, pp 1876–1881
- Santibáñez P, Chow V, French J, Puterman M, Tyldesley S (2009) Reducing patient wait times and improving resource utilization at British Columbia cancer agency’s ambulatory care unit through simulation. *Health Care Manag Sci* 12(4):392–407
- Šteins K (2010) *Discrete-event simulation for hospital resource planning – possibilities and requirements*. Ph.D. thesis, Linköping University, Norrköping
- Stratton SJ, Hastings VP, Isbell D, Celentano J, Ascarrunz M, Gunter CS, Betance J (1996) The 1994 northridge earthquake disaster response: the local emergency medical services agency experience. *Prehosp Disaster Med* 11(3):172–179

- Takakuwa S, Shiozaki H (2004) Functional analysis for operating emergency department of a general hospital. In: Proceedings of the 2004 winter simulation conference, Washington DC, pp 2003–2010
- Van der Meer RB, Rymaszewski L, Findlay H, Curran J (2005) Using or to support the development of an integrated musculo-skeletal service. *J Oper Res Soc* 56(2):162–172
- Yerravelli S (2010) Computer simulation modeling and nurse scheduling for the emergency department at Kishwaukee community hospital. Ph.D. thesis, Northern Illinois University, Schaumburg, 60173, United States
- Yi P (2005) Real-time generic hospital capacity estimation under emergency situations. Ph.D. thesis, State University of New York at Buffalo, Buffalo

Chapter 12

Application of Economic Resiliency of Communities Affected by Natural Disasters

Abstract The chapter is proposing a model that describes the economic effects and characteristics that should be taken into account to predict the monetary impact of natural disasters, focusing in particular on the economic interdependencies of industries and lifelines. Different losses are considered using real economic data provided by surveys on natural disasters such as Northridge earthquake, Des Moines flood, etc. The Economic Resilience Index provided in the PEOPLES framework is adopted and applied to the specific case study of the San Francisco Bay Area using the data provided by HAZUS for the physical damage. Sensitivity analysis is performed for each economic sector considered in the analysis.

12.1 Introduction

In the decades, many catastrophe models have been developed for measuring economic losses. However, the data paucity and the complexity of the problem, have caused significant levels of uncertainties. In fact, the factors that drive the economic recovery process before, during, and after natural disasters needs to be determined to select the optimal resources allocation and preparedness measures right after an extreme event. In most of catastrophe models interdependencies between physical and non-physical infrastructures are neglected. Instead the chapter describes the evaluation of Resilience metrics for Economic development (Fig. 12.1) and focuses on the impact of natural disasters on different economic sectors in a given community considering their interdependencies. A model is proposed that describes the economic effects and characteristics that should be taken into account to predict the monetary impact of natural disasters, focusing in particular on the economic interdependencies of industries and lifelines. For this purpose, losses are divided into two main categories: direct and indirect. The direct losses include economic losses caused by physical damage to buildings and utilities, while the indirect losses stem from the interdependence between different economic sectors. Finally, according to PEOPLES framework, a global economic resilience index as a measure of the economic ability of a community to withstand catastrophic events is developed and applied to the specific case study of the San Francisco Bay Area.

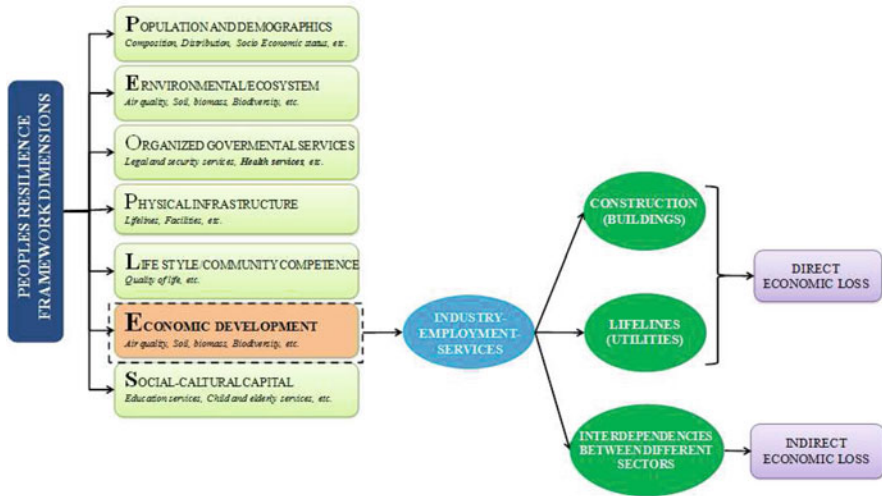


Fig. 12.1 Chapter 12 outline

12.2 Description of Methodology

Natural disasters may cause intent economic losses at both, the local (regional) and global level. In general, the regional losses are significantly higher than the global losses, so the chapter will focus on regional losses. To estimate the total economic losses of a region struck by a natural disaster, the losses are disaggregated into direct and indirect. The direct economic losses are associated with the business-interruption cost due to physical damage of structures (buildings and lifelines) while the indirect losses are associated with the inter-industry transactions.

12.2.1 Economic Loss Framework

The proposed framework for assessing economic losses due to hazardous events, is schematically presented in Fig. 12.2, as an extension of HAZUS framework. HAZUS is a software developed by FEMA to estimate different types of losses generated by a natural hazard. The framework divides the losses into direct and indirect. The direct losses stem from building, from utility damage and are associated to the cost of reconstruction and business interruption, however HAZUS is neglecting interdependencies. The indirect losses in the methodology are estimated as general equilibrium effects of a disrupted inter-industry economy instead of being computed through the traditional Input-Output model of HAZUS.

Three main modifications to the framework are applied to capture all the types of possible losses, as shown in Fig. 12.2. The first is represented by the analysis of the

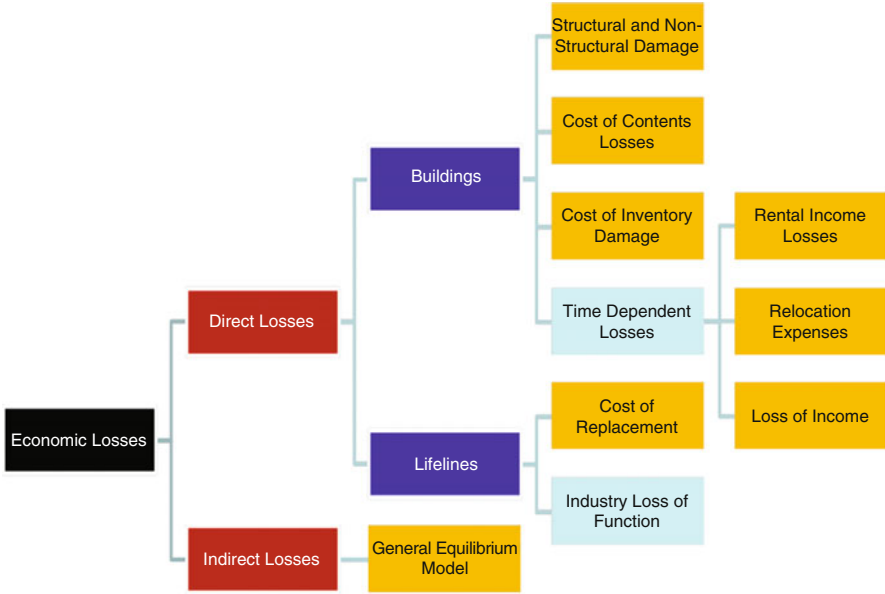


Fig. 12.2 Economic loss framework

industry loss of function due to the disruption of utilities. The second is given by a new method which is able to find the probabilistic distribution of the time-dependent direct losses that affect a specific region of interest. Finally, the *structural growth model (SGM)* is applied instead of the usual *Input-Output model*, to quantify the indirect effects that arise as a cascade effect due to the business interdependencies.

12.2.2 Direct Time-Dependent Losses

The proposed methodology refines the analysis of the *time-dependent direct losses* related to the building physical damage. The basic model, inspired by HAZUS, assumes that *relocation* occurs if the damage state of the building is greater than or equal to moderate and in that case the losses are given by *relocation expenses (RE)*, *rental income losses (RIL)*, and *loss of income (LI)*. Otherwise, the *time-dependent direct losses* are given only by the LI due to the loss of functionality that could arise even with slight damage to the building. Besides, since the goal of the chapter is to quantify the global economic effects of a disaster on a specific region of interest, it should be taken in account that relocation can occur in different ways that influence the losses.

To accomplish this goal, Eqs. (12.1), (12.2) and (12.3) have been implemented. The difference with respect to the HAZUS approach stems from two observations. Since the goal is to model the losses of a specific region, it is important to distinguish

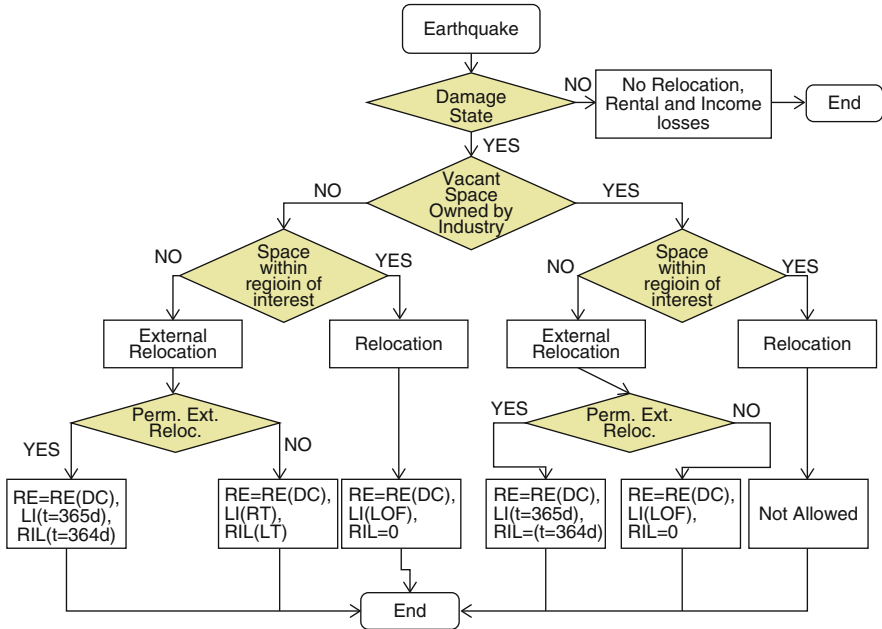


Fig. 12.3 Time dependent losses algorithm for owner-occupied businesses

between inside and outside relocation. Moreover, HAZUS does not take into account the possibility that the industries which are forced to relocate own extra space in which they could move the activity, and that this space may be again inside or outside the region of interest. The implemented algorithm takes into account these different possibilities by choosing different time windows used to compute LI and RIL (while in HAZUS they are always computed using the loss of function and the recovery time respectively, which take into account mobilization time) and considering or not new rental costs or rental losses, depending on if the property is business-owned. The flowchart of the method that refers to businesses that are owner occupied is represented in Fig. 12.3.

$$RE_i = \left[(1 - \%OO_i) \cdot \sum_{DS=3}^5 (POSTR_{DS,i} \cdot DC_i) + \%OO_i \cdot \sum_{DS=3}^5 (POSTR_{DS,i} \cdot (DC_i (+RENT_i \cdot RT_{DS}))) \right] \tag{12.1}$$

$$LI_i = (1 - RF_i) \cdot FA_i \cdot INC_i \cdot \left(\sum_{DS=1}^5 POSTR_{DS,i} \cdot t_{DS} \right) \tag{12.2}$$

$$RIL_i = (1 - \%OO_i) \cdot FA_i \cdot RENT_i \cdot \left(\sum_{DS=3}^5 POSTR_{DS,i} \cdot t_{DS} \right) \tag{12.3}$$

where:

- $\%OO_i$ = percent owner occupied for occupancy i ;
- $POSTR_{DS,i}$ = probability of occupancy i being in structural damage state DS ;
- DC_i = disruption costs for occupancy i ;
- $RENT_i$ = rental cost for occupancy i ;
- RT_{DS} = recovery time for the damage state DS ;
- RF_i = recapture factor for occupancy i ;
- INC_i = income per day per square foot for occupancy i ;
- t_{DS} = period of time which depend on DS , business property and place of relocation (see Fig. 12.3).

The yellow blocks in the flowcharts (Fig. 12.3) are the decision blocks. Due to the scarcity of data, it is difficult to obtain exact data for these blocks. For this reason, a probabilistic approach has been adopted to take into account for the uncertainty of the decisional variables. However, if more data regarding the decision blocks are available, they could easily be substituted in the method to obtain outcomes that are more reliable.

The methodology implemented in this chapter is based on three assumptions. The first is that the greater is the business size, the higher is the possibility that the businesses own vacant space to relocate the activity. The second is that the probability that the vacant space is located within the region of interest is equal to the percentage of vacant buildings in the region (this value is approximated using HAZUS database). Finally, it is assumed that the longer the recovery time, the higher is the probability that the external relocation will be permanent. It should also be noted that the *income losses* considered refer to the *output losses* suffered by the industries, which eventually represent the loss of functionality of each sector. A more detailed description of the methodology is provided in Martinelli et al. (2014b). The *cost of business interruption* due to the physical damage of buildings is represented by a graph which shows the normalized output losses as a step function, where the different steps shown in Fig. 12.4 for the Educational sector represents the number of damage states that contribute to the loss of business functionality.

After computing the building damage losses, the business losses due to lifelines disruptions are also taken into account in the proposed methodology. However, due to the scarcity of data, a hybrid approach has been adopted where both simulated and real data have been used. The lifeline functionality after the event is obtained by using the simulated data given by HAZUS. The real data are represented by the *probability of business closure due to lifeline disruption*. They have been derived using a procedure similar to the one explained by Chang et al. (2002) using data collected with surveys conducted on two natural disasters (Northridge earthquake and Des Moines flood) described in the works of Tierney and the simulated results given by Rose. In particular, a new function called an *autonomy curve* which corresponds to the *probability of business closure* for a given lifeline is derived using Eqs. (12.4) and (12.5). These *autonomy curves* represent the ability of each

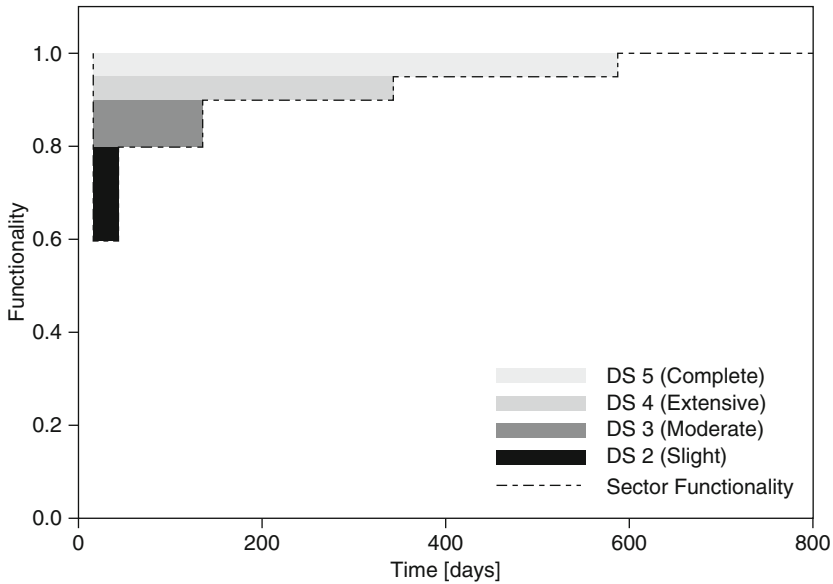


Fig. 12.4 Loss of functionality for the educational sector

economic sector to withstand a utility outage of a different entity without losing functionality.

$$AF_i = 1 - P_{BI,i} \quad (12.4)$$

$$P_{BI,i} = P_{BC,j} \bullet P_{UO,i,j} \bullet \alpha_i \quad (12.5)$$

where:

- P_{BI} = probability of business interruption due to utility i outage;
- $P_{BC,j}$ = probability of business closure for occupancy j ;
- $P_{UO,i,j}$ = percentage of business with utility i outage for occupancy j ;
- α_i = average percentage of businesses that closed due to utility i outage.

The *autonomy curves* have been calibrated using the temporal lifeline outage data of the case study, while different types of curves have been selected depending on the type of utility considered. For example, when analyzing the *Retail and Wholesale sector*, for the electricity, water, and phone network a four parameters logistic function has been chosen, while for the waste and gas system, a multi-linear curve has been selected as shown in Fig. 12.5. All the figures shown in this chapter refer to the San Francisco Bay Area case study.

The influence of each utility disruption on the economic sector functionalities is modeled by applying the *autonomy curves* (AF), determining the new sector functionalities using the following equation:

$$f_{sector}(t) = f_{utility}(t) [1 - f_{utility}(t)] \bullet AF_{utility}(t) \quad (12.6)$$

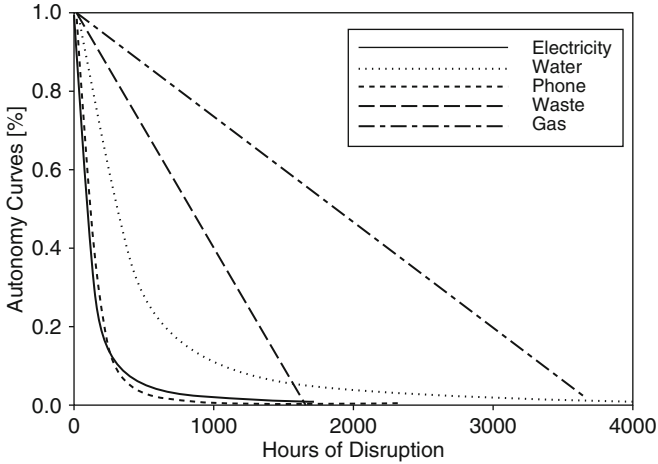


Fig. 12.5 Autonomy factor curves of different lifelines for the retail and wholesale sector

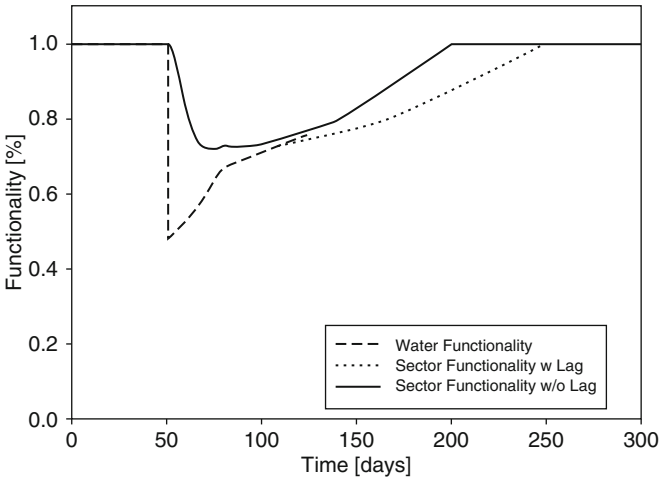


Fig. 12.6 Sector functionality influenced by the water service restoration

where f_{sector} =functionality of the economic sector; $f_{utility}$ =functionality of the utility and AF =autonomy curves. The limitation of Eq. (12.6) is that the normal operating condition after lifeline disruption is reached at the same time for both the lifeline and the economic sector, as shown in Fig. 12.6 which considers the example of the water service.

In reality, a lag exists between economic sector and lifeline recovery. So Eq. (12.6) can be used until the economic sector begins to recover. Then a lag factor θ is introduced to take into account the delay of functionality with respect to the other. The mathematical formulation for the lag factor is given by:

$$\begin{cases} \theta = 0 & t < t_r \\ \theta = \frac{t-t_r}{X_{gg}} & t_r < t < t_{fr} \end{cases} \quad (12.7)$$

$$f_{sector}(t + \theta \bullet t_r) = f_{utility}(t) + [1 - f_{utility}(t)] \bullet AF_{utility}(t) \quad (12.8)$$

where:

- t_r = time instant when the recovery of the economic sector starts when using Eq. 12.6;
- t_{fr} = time instant when the recovery of the economic sector ends using Eq. 12.6;
- X_{gg} = lag time of the economic sector with respect to the utility;
- $AF_{utility}$ = autonomy curves of the economic sector with respect to the utility.

The lag time needs to be calibrated, however as a first approximation, the lag time θ for the economic sector is assumed to be a fraction of the utility restoration time. Once all the *autonomy curves* which describe the interdependencies between the economic sector and the different lifelines are determined, they are combined with the economic sector functionality for determining the effect of all the different utilities. The new updated functionality curves are then combined to determine a single functionality curve for each economic sector, which captures the interdependencies between each lifeline.

It is important to mention that the methodology overestimates the losses due to utility disruption since it has been assumed that the businesses were affected separately by the utilities which affect mostly the sector functionality. Moreover, interdependencies are considered separately one by one, and it is not taken into account the possibility that businesses that are forced to close due to utility disruption can reduce their losses by interacting with other utilities, or by making up production at different times. To reduce this overestimation, the recapture factors provided by HAZUS have been used to decrease the losses.

Finally, the losses due to utilities disruption for each economic sector have been summed with the output losses due to building damage and a loss range is determined. The lower bound of this loss range is represented by the envelope of the two functionality curves affected separately by physical damage and the utilities disruption. The upper bound is represented by the sum of the two functionality losses. Then, depending on the conditional probability that a business will be affected simultaneously by building physical damage and utility disruption, a probable value has been found within this range. Equation (12.9) is adopted to compute the global functionality which is given by

$$F_{tot,sec} = \min(F_{sec,utilities}; F_{sec,building}) - P(BD \cap UO) \bullet (1 - \max(F_{sec,utilities}; F_{sec,building})) \quad (12.9)$$

where:

- $F_{sec.utilities}$ = functionality of the sector influenced by the utilities;
- $F_{sec.building}$ = functionality of the sector influenced by the building damage;
- $P(BD \cap UO)$ = probability that business is simultaneously affected by building damage (BD) and utility outage (UO).

12.2.3 Indirect Losses

After estimating the direct effect of the disaster event on each economic sector, the methodology applies the structural growth model to the scenario of interest, as described in Martinelli et al. (2014a), to estimate the indirect effects that stem from the interdependence between the sectors. In other words, the model applies to the business functionalities an initial perturbation that corresponds to the direct damages experienced by the sectors and then evaluates the recovery process which is controlled by the *price adjustment velocity* and by the *depreciation factors* of the goods. At the end of the analysis, it is possible to obtain a graph, shown in Fig. 12.7 which depicts the general equilibrium effects and from which the monetary losses due to the business interdependences can be derived.

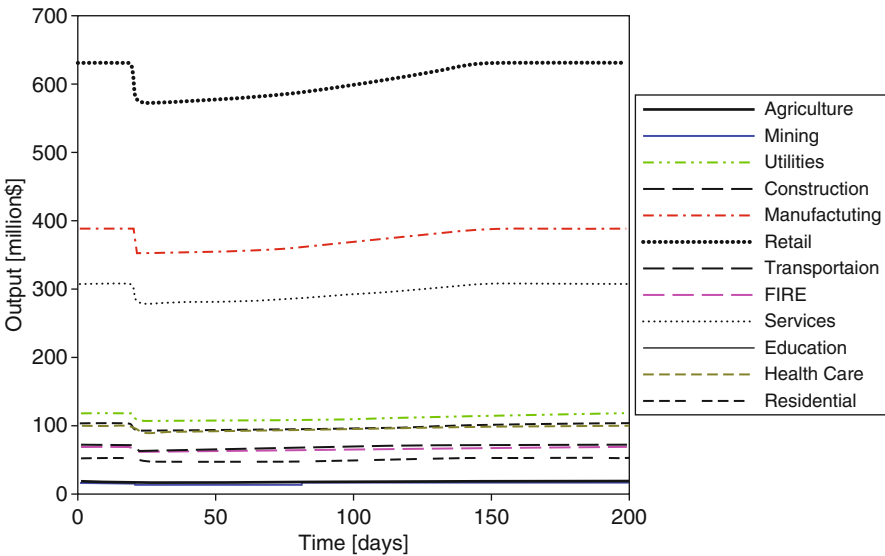


Fig. 12.7 Indirect general equilibrium effects for the different sectors

12.2.4 Economic Resilience Index (R_{EC})

Finally, the methodology evaluates the economic behavior of the analyzed region using a comprehensive resilience index R_{EC} determined according to the PEOPLES framework. In detail, R_{EC} is the area under the function which is the sum of the direct losses and of the indirect losses normalized with respect to the value of the business functionality over the same control period.

12.3 The San Francisco Bay Area Case Study

The SF Bay Area shown in Fig. 12.8 is considered as a case study to show the implementation issues of the methodology. Since the predictions of the USGS estimated the maximum probability of 30% for a $M > 6.7$ in the Hayward Fault, the baseline scenario chosen is a $M 6.9$ earthquake close to Oakland in the Hayward fault. The structural and non-structural losses and the utilities functionalities have been derived from HAZUS after having loaded the soil map and the liquefaction susceptibility map of the region.

Then the methodology described above is implemented to estimate the direct time-dependent losses. To do that, the values of INC_i in Eq. 12.2 have been updated coherently with the output data of each sector published by the Economic Census. The *loss distributions* for the economy in the region obtained by the methodology are shown in Fig. 12.9. The estimated *relocation expenses* are \$1.5 and \$2.1 billion



Fig. 12.8 Region considered in the SF Bay Area case study

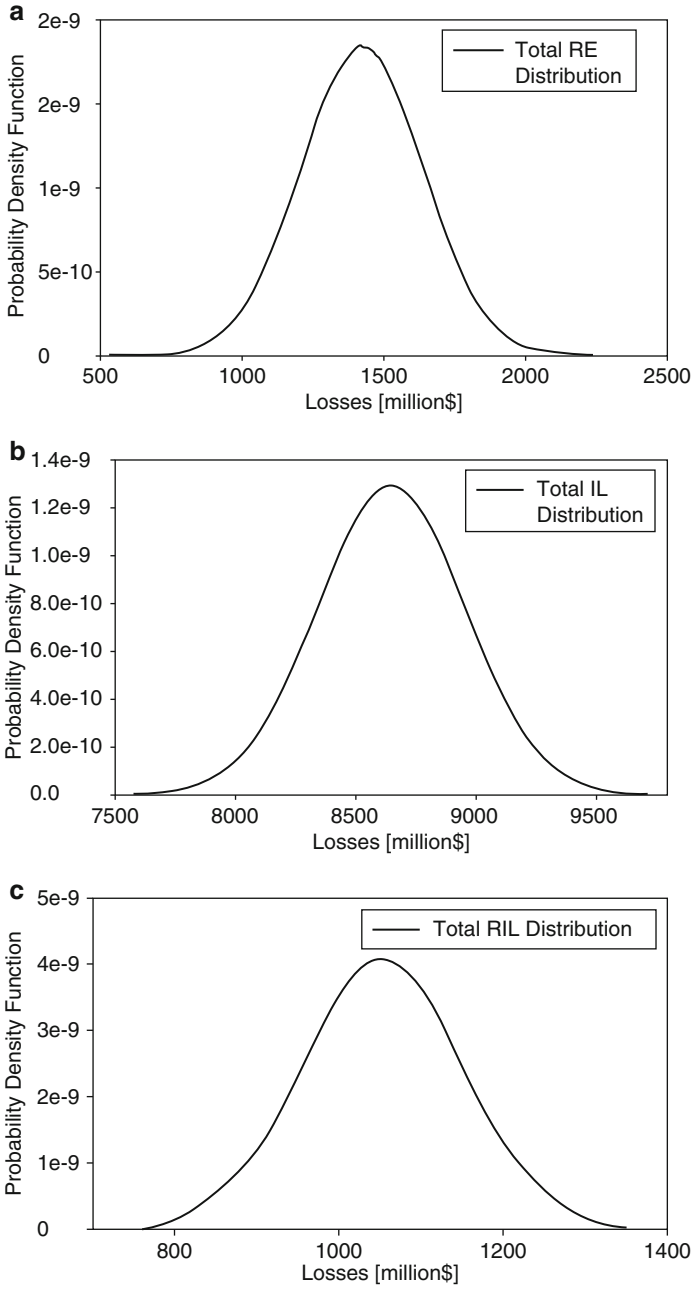


Fig. 12.9 Relocation expenses RE (a), loss of output IL (b), rental income losses RIL (c)

with the proposed methodology and with HAZUS respectively, while the estimated *rental income losses* are \$1.06 and \$1.21 billion respectively. In Fig. 12.10a the mean and the dispersion of the direct output losses are represented for each sector due to building damage while in Fig. 12.10b the losses are also shown taking into account the utility disruption. The contribution of utility disruption to business loss of function has been computed assuming that the mean number of utilities which lost their businesses is 2.5 and that a business has about 50 % probability of being affected by both building damage and utility disruption. The results show that for the Bay Area, the sectors which have greatest losses are the Retail & Wholesale, the Residential and the Services & Government while the Mining and Agriculture experienced smaller losses. While for the Retail & Wholesale and the Services & Government sectors, the great part of the loss stem from the interdependencies which affect the business interruption, for the Residential sector, a significant contribute is given by the relocation expenses. The small losses of the Mining and Agriculture sectors are mainly due to the relatively small volume of business.

The *structural growth model* has been applied to estimate the indirect losses. The proposed method starts computing the Input-Output matrix of the region of interest using the procedure explained by Chamberlain (2011) from the *Make and Use* matrices provided by the BLS (Bureau of Labor Statistics). Since public data are available only at the national level, the San Francisco Bay Area Input-Output matrix has been derived assuming a scaling factor based on the GDP value which has been applied to the US Input-Output matrix.

The final indirect losses are represented in Fig. 12.10c. Similar to what has been done to estimate the output losses due to building damage and utility disruption, the indirect losses have been reduced using the recapture factors provided by HAZUS to take into account for the ability of business to make up production at different times. It should be noted that the direct output losses has not been represented for the Utilities and the Transportation sector due to the unavailability of the data necessary to apply the described methodology but have been taken into account in the total loss analysis considering the data provided in HAZUS. Finally, in the specific case study, the indirect losses represent approximately 15 % of the direct losses.

12.3.1 Sensitivity Analysis

Performing sensitivity analysis is useful for showing how the total losses are influenced by the different parameters. In Table 12.1 the different analysis performed for the total direct-time dependent losses are reported, each one distinguished by a specific assumption listed sideways. The different outcomes are summarized in Fig. 12.11. As made clear in Fig. 12.11b, the most important thing to avoid is the permanent external relocation of businesses that quadruples the loss of productivity of the sectors in the region; moreover, it does not allow the economy of the region to bounce back to the pre-event levels of productivity since part of the functionality is lost forever.

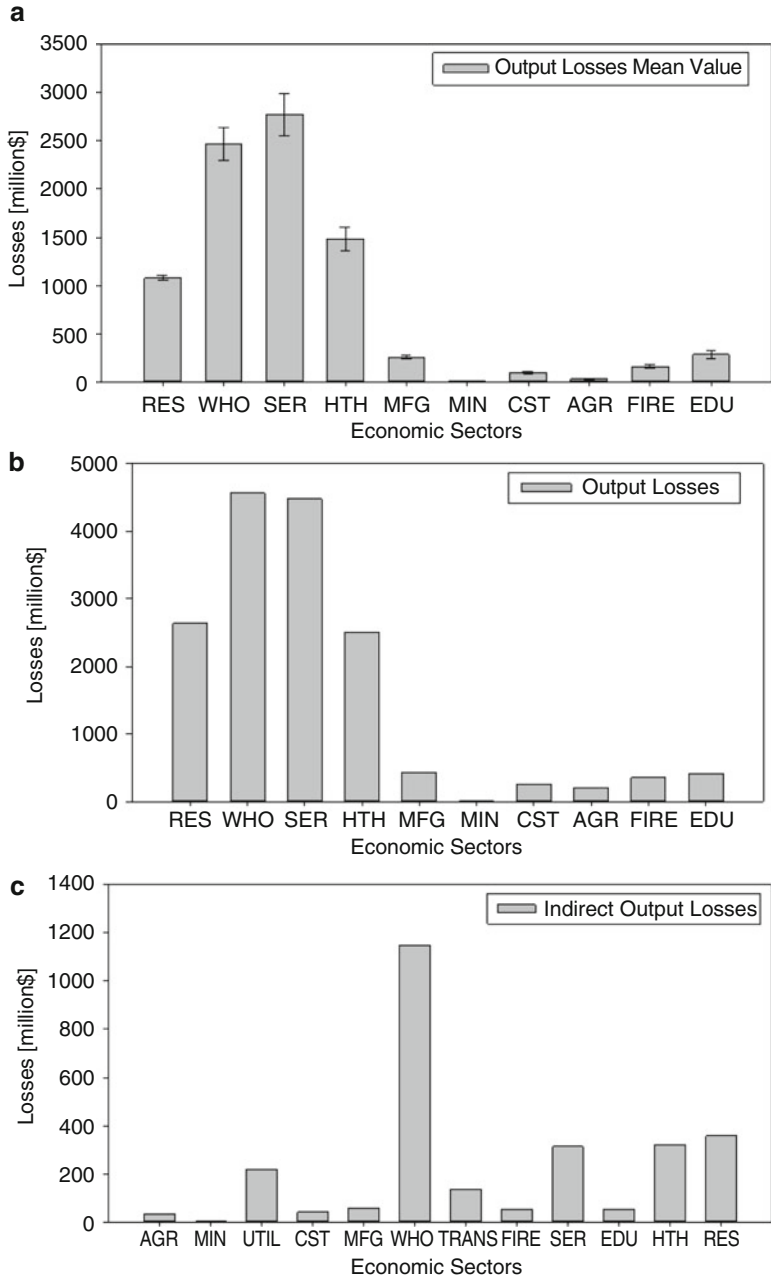


Fig. 12.10 Mean value and dispersion of the output direct losses due to (a) building and (b) building + utility damage; (c) indirect losses

Table 12.1 Assumptions implemented in the sensitivity analysis

1	No excess capacity or vacant space owned by the business which relocate
2	Probability of vacant space within the region equal to 50 %
3	Probability of vacant space within the region equal to 97 %
4	High probability of permanent external relocation
5	Probability of excess capacity or vacant space owned by the industry close to 100 %
6	Medium probability of permanent external relocation

Indeed, the smaller losses are found by assuming a high probability of vacant space within the region. Though it seems difficult to reach this condition in reality, this observation can be used as a guideline for the preventive measures implemented in the individual industries. To show the uncertainty stemming from the unknown magnitude of the earthquake, Fig. 12.12 represents the differences in the cases of three different earthquakes. Finally, Table 12.2 summarizes the outcomes of the baseline case study from the R_{EC} index point of view.

12.4 Summary and Conclusions

This chapter proposes a new methodology for evaluating the economic losses following a natural disaster. A new probabilistic framework to estimate economic losses has been presented, where the indirect losses have been estimated using the structural growth model (SGM), while interdependencies between the different economic sectors and lifelines during disruption are modeled using the *autonomy curves*. Uncertainties in different parameters have been analyzed and a final global economic resilience index R_{EC} has been obtained, which can be used in a general community resilience framework (e.g. PEOPLES), to estimate the effects of the economic dimension. The *autonomy curves* have been derived using the probabilities of business closure collected from business surveys and simulation conducted mainly in California, so that they are only representative of the case study analyzed. However, these *autonomy curves* represent the main findings of the study. In fact, as shown by the sensitivity analysis which simulates different earthquake magnitudes, the M7.5 earthquake causes less direct and indirect output losses compared with M7.3 earthquake in Oakland, even if it has a higher magnitude. The justification can be found in the fact that the M7.5 earthquake in San Francisco considering the HAZUS approximation will cause less utility losses and therefore the costs due to business interruption will be smaller.

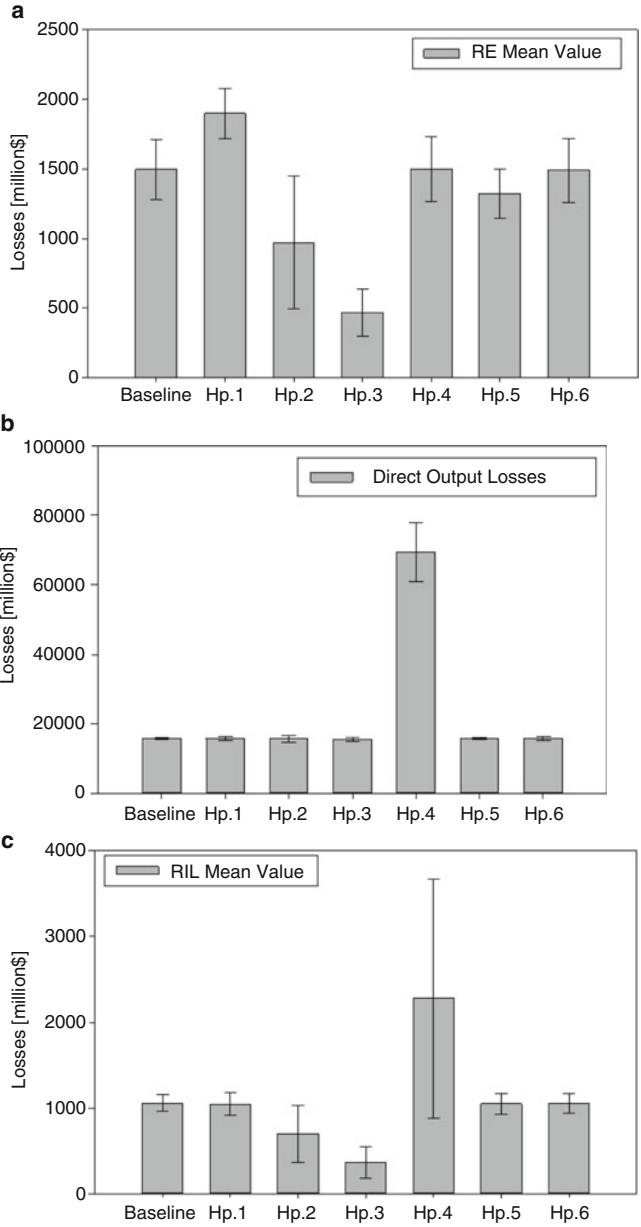


Fig. 12.11 Time-dependent relocation expenses (a), direct output losses (b), and rental income losses (c) for the different scenarios

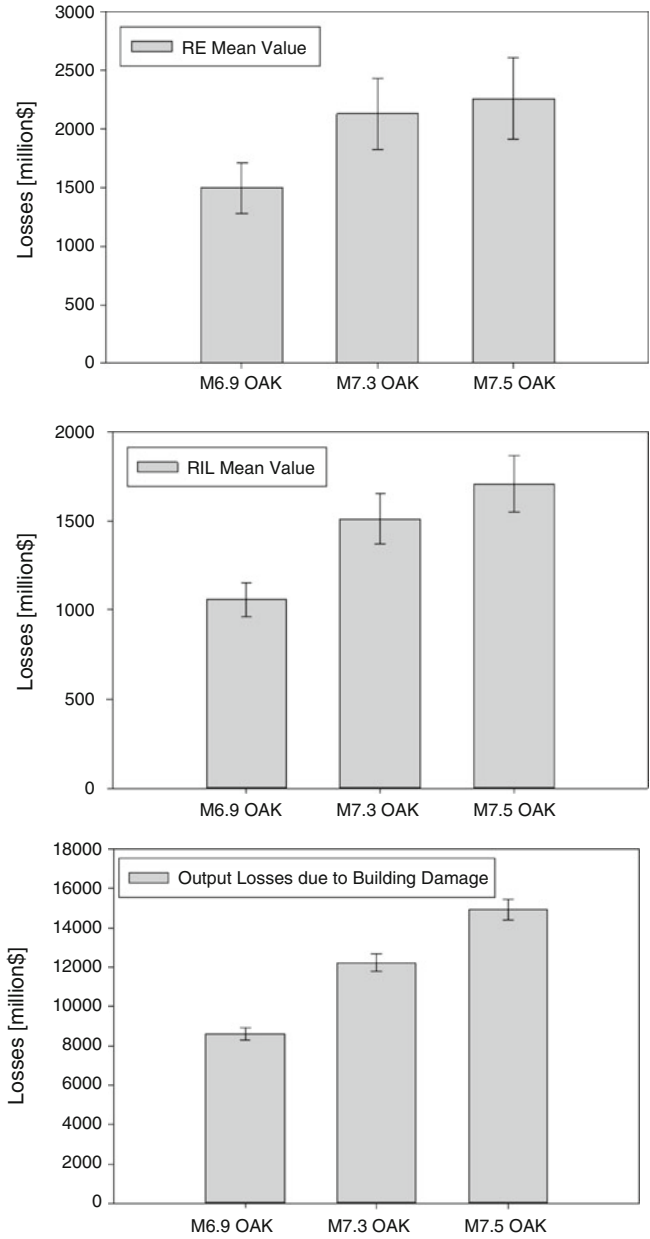


Fig. 12.12 Variation of the total direct time-dependent economic losses for the different assumed earthquake magnitudes

Table 12.2 Summary of total economic losses and resilience indexes for the case study

	M6.9	M7.3	M7.5
Total relocation expenses (million\$)	1498	2129	2258
Total rental income losses (million\$)	1057	1511	1709
Total direct output losses (million\$)	18,407	29,094	25,267
Total indirect output losses (million\$)	2555	4198	2359
Total structural/non-structural losses (million\$)	29,388	42,804	49,108
<i>R_{EC}</i>	0.96	0.938	0.955

References

- Chamberlain A (2011) Methodology paper: developing square U.S. input-output tables from B.E.A. Make and Use tables. Chamberlain Economics L.L.C., La Jolla
- Chang SE, Svekla WD, Shinozuka M (2002) Linking infrastructure and urban economy: simulation of water-disruption impacts in earthquakes. *Environ Plan B* 29(2):281–302
- Martinelli D, Cimellaro GP, Renschler C (2014a) Quantification of the economic resilience from the community level to the individual business level: the bay area case study. In: *Proceedings of the 2014 structures congress (SEI 2014)*, ASCE – American Society of Civil Engineering, Reston, paper 1087
- Martinelli D, Cimellaro GP, Terzic V, Mahin S (2014b) Analysis of economic resiliency of communities affected by natural disasters: the bay area case study. *Procedia Econ Financ* 18(2014):959–968. doi:10.1016/S2212-5671(14)01023-5

Part III
Resilience Mitigation Actions and Tools

Chapter 13

Building More Resilient Communities

Abstract After the description of the methods to assess resilience (part 1) and show some applications (part 2) the goal of this chapter is to show what actions should be taken to make communities more resilient. After categorizing the different interventions according to the structural type, and presenting the three international frameworks for disaster risk management (Yokohama, Hyogo and Sendai framework), the chapter focuses on the different initiatives developed in New York City after Hurricane Sandy to make the region more resilient.

13.1 Introduction

Disasters brought on by supernatural events are now the most threatening sources of danger to long term advancement around the globe. In the course of the most recent two decades, they have killed 1.3 million individuals, damaged 4.4 billion, and created over 2 trillion USD in financial losses. Nowadays, it is worldwide accepted that the activities and choices of people, communities, and countries have a remarkable difference whether a hazard transforms into a disaster. Decisions made with the point of diminishing the human effect of common perils can be portrayed as disaster risk reduction (DRR) in the broadest sense (UNDP 2014a).

13.1.1 *Disaster Risk Management*

Disaster risk management (DRM) refers to the systematic process of using administrative decisions, organization, operational skills, and capacities to implement policies, strategies, and coping capacities of the society and communities to reduce the impacts of natural hazards and related environmental and technological disasters. This includes all forms of actions, such as structural and nonstructural measures to avoid (prevention) or to limit (mitigation, preparedness, and response)

the adverse effects of hazards (adapted from UNISDR 2004). DRM is usually divided into three main areas of activity:

1. Disaster risk reduction (prevention, mitigation, and preparedness),
2. Disaster response (rescue and relief), and
3. Disaster recovery (rehabilitation and reconstruction).

Even if these areas are kept separate in reality they overlap and affect each other, however in the following paragraphs is kept this separation to have an organized description of the following actions.

13.1.2 State-of-Art on Existing Plans for Developing Resilient Communities

Several plans exist to develop resilient communities. Among them it is worth to mention the Plan that the National Institute of Standards and Technology (NIST) recently released, called new Community Resilience Planning Guide for the Built Environment and Infrastructure Systems (Version 1.0) (NIST 2015), prepared with experts and stakeholders from around the nation. The planning guide details a six-step, integrated approach that communities can follow to achieve a more resilient, less disaster-prone future. The six steps are the following:

1. Form a collaborative planning team
2. Understand the situation
3. Determine goals and objectives
4. Plan Development
5. Plan preparation, review, and Approval
6. Plan implementation and Maintenance

It is surprising that the US, however, are not among the leading countries when it comes to disaster risk reduction. According to UNDP (2014a), US falls within the “Medium priority” in the disaster risk reduction classification. It is noteworthy here to mention New Zealand as one of the countries that have given high priority to Disaster Risk Reduction (DRR). New Zealand’s Civil Defence Emergency Management Act of 2002 (DRM law) does not indicate from its title that it gives a high priority to DRR, but the law has been described as being based on five key principles (UNDP 2014b):

1. Risk management
2. Integration
3. Comprehensiveness
4. Subsidiarity
5. An all hazards and all risks approach to emergency management.28

The DRM law of New Zealand describes an entire DRR process, from risk assessment to monitoring and review. Another interesting feature of the New Zealand DRM laws objectives is the use of the terms “sustainable management of hazards”, “acceptable levels of risk”, and “cost-effective risk reduction”. These place government efforts on DRR within the broader context of national development, recognizing that there may be limitations on the resources and/or capacity available to manage hazards sustainably (UNDP 2014a).

13.2 Resilience as a Preventive Action

13.2.1 Improving Disaster Preparedness

Ideally, buildings and (NIST 2015) infrastructures and their ability to support individuals and social institutions of government, business, education, etc., should not be affected or disrupted in the occurrence of a hazard event. Realistically, hazardous events can disrupt the community functions so extensively that they result in permanent damages. Despite the fact that most people are unprepared to cope with the loss of functionality, the built environment is not always able to retain full service after significant hazardous events occur. This harsh reality is faced every time a significant hazardous event occurs. Two events which have caused extensive damages across communities in the U.S. are the Hurricane Katrina, in 2005, and the Super-storm Sandy, in 2012- events which have left the communities still in need of years to recover. During the period from January 2000 to January 2011 there were between 45 and 81 Presidential disaster declarations in the US yearly for floods, hurricanes, tornadoes, earthquakes, fire events, and severe storms (FEMA 2011). Many of the disaster declarations were for hazard events with loads lower than current design levels. Whether the hazard is due to severe weather, fire, floods, earthquakes, infrastructure failures, cyber attacks, technological accidents, sea level rise, man-made hazards or other disruptive events, each community will eventually need a period of recovery from the event. The ultimate outcome of the recovery depends on *planning, preparedness, mitigation, response, and facilitation of the recovery*. A community that has not been prepared to face a disaster often requires decades to recover and may never achieve full restoration. The best way to improve *disaster preparedness* is to persuade organization and coordination to understand the hazard that has to be faced and to reduce its risk. This task should be developed jointly by civil society, by citizen groups and by building authorities that prepare the society and ensure that all departments understand their role in disaster risk reduction and preparedness. It is a necessity that all cities have an institutional basis for implementing risk reduction, and it should be multi-sectorial and involve all relevant stakeholders in the area. At the *local level*, cities or regional governments have to create councils, committees, agencies and other local disaster risk management institutions for emergency preparedness, response,



Fig. 13.1 Destruction in the wake of superstorm Sandy on Wednesday, Oct. 31, 2012, in Seaside Heights, NJ (Source: <http://blogs.pjstar.com/eye/2012/11/02/aerial-photos-of-destruction-left-by-superstorm-sandy/>)

disaster risk, climate change and resilience. To strengthen the *city-level* institutional and coordination capacity, a lead entity has to be established, to lead a coordination mechanism among departments. The roles and responsibilities of those departments have also to be defined in detail. Not only council institutions have to work together, but also volunteers, business, NGOs and emergency services have to be involved as well. Those emergency services have to work together, so that a collaborative strategy can be generated to integrate all units responsible for emergency response (Fig. 13.1).

However, it is better to work under a *national-level framework*. National disaster risk reduction legislation has to enable the development of city-level, and to provide a supportive funding structure. To facilitate the coordination across sectors, the responsibilities should be designated at national level and thus be delegated through to the local level. Furthermore, to ensure that these authorities are working at their best, it would be great to institutionalize them. Alliances and networks beyond cities have to be created by developing partnerships with local, national or international universities that can provide data, expertise and research. Exchange programs with cities should be considered, between communities in other countries that face similar risk patterns or challenges. In the Philippines, different cities work together in the field of disaster preparedness to develop an authority community-scale structure for disaster risk management. Today's communities are riddled with issues, policies, and regulations that require attention and demand both time and investment. Without a government mandate or recent event to draw community interest, *low probability-high consequence* hazardous events become a lower priority. These incidents illustrate the role of resilience planning in making a major difference in the

way a community and that the idea of resilience should be an integral part of normal planning and operations. Chile, as a country, is no stranger to seismic activity. In 1960, following a catastrophic occurrence, Chile began to make efforts to develop and update stringent building codes and emergency response procedures. Another earthquake of similar magnitude occurred in 2010, disrupting areas from Santiago in the North to Concepcion 500 miles to the south and generating a large tsunami. The newly implemented emergency response procedures that were encouraged by past experience, in combination with greatly improved building standards that had been in place for 50 years, resulted in decreased damages, especially to high-rise residential buildings. Power restoration to critical infrastructure began within days and over 50,000 provisional homes were constructed within a few months. It took only 3 years to complete infrastructure repairs and nearly all subsidized home rebuilding projects were complete within 4 years. Despite the widespread damage to older buildings and infrastructure systems, the proliferation of modern construction and response and recovery plans assisted the communities ability to manage the event and swiftly rebuild in a way that better prepared them to face another seismic event (Fig. 13.2).

In the past 15 years, a variety of efforts related to community resilience have been initiated in the United States, and there are constantly individual communities that are working to recover from hazard events. Cedar Rapids, Iowa, has multiple sources of natural hazards, including: floods, severe weather, tornadoes, severe windstorms, and heat waves. This city is precariously situated just downstream from a commercial nuclear power facility. The community is well equipped with an evacuation plan for dealing with a nuclear disaster. During the flooding of 2008 when the river crested at well above its predicted 500-year flood event, these plans played a key role, protecting the lives of the residents who were all safely evacuated



Fig. 13.2 Chile as a resilient city in a resilient nation (Source: en.wikipedia.org)



Fig. 13.3 Downtown Cedar Rapids, Iowa is engulfed by the Cedar River (2008) (Source: en.wikipedia.org)

(NRC 2012). The response by the community and government was so successful because the City Council and City Manager instituted a community engagement process, developing a shared vision and planning system months before the 2008 flood. Currently, the Recovery and Reinvestment Plan is being rapidly implemented, improving the community resilience in the case of flooding events (CARRI 2013) (Fig. 13.3).

The circumstances surrounding the 2005 Hurricane Katrina had been frequently predicted and even focused on by multiple State and Federal response exercises. One scenario considered went so far as envisioning the levee breach. However, following the disaster, numerous communities and industrial facilities that support national fuel supplies were damaged severely. Communities were not cognizant of the threat posed by storm surge or the predictions and therefore were unprepared for response and recovery at the local level (APA 2014). The recovery was stalled by the lack of suitable design codes, response plans, processes to coordinate various local, state, and Federal agencies, and local leadership. A new department in the local government, the New Orleans Redevelopment Authority, was added after the hurricane in order to facilitate land stewardship, commercial revitalization, and affordable housing. Although their efforts are sometimes criticized, service organizations such as Habitat for Humanity, Make-it-Right Foundation, and Rebuilding Together New Orleans have made significant strides in aiding homeowners to return to their communities and rebuild their lives, though collaboration with local government and community leaders. The population of New Orleans is at approximately 75 % of its pre-Katrina levels, 10 years after the disaster (APA 2014) and it may be decades before the city can make a full recovery from hurricane Katrina. On the cutting edge of disaster preparedness is the city of San Francisco, in California (USA). San Francisco is exposed to several seismic hazards. The city is recognized as a leader in sustainability and preparedness against disasters and its buildings have a demonstrated great resilience. The San Francisco Planning and Research

Association (SPUR) began to establish this style of resilience planning in 2007. Their work focuses on the community level, creating policies and programs which aim to make San Francisco a Disaster Resilient City. Multiple policy papers and recommendations regarding the broad issues of disaster resilience have been produced as a result of SPURs work. Their policy recommendations focused on community needs before, during and after responding to a disastrous event. There are key questions related to disaster planning on which previous disaster work has focused. The following is a list of the problems that are addressed regarding preparedness: ensuring a quick recovery of our built environment after a major earthquake, deciding which buildings should be retrofitted and to what level, encouraging better performance in new buildings and strengthening infrastructure so that the buildings are serviceable after an earthquake. Disaster Response focuses on activities during the days and weeks following a catastrophic event will include activities referred to as disaster response, this concerns: damage assessment, responder safety, communications and control, evacuation, public health and safety, and the restoration of vital systems. The goals addressed by the disaster task force after the event include: preparation for rebuilding the city to an improved state, employing plans and systems of governance in order to put the city in a position to rebuild and extracting lessons from recovery experiences in lower Manhattan, New Orleans, Haiti, Chile, China, and beyond. This task force is working to evaluate and understand long-term recovery, in the areas of transportation, governance, planning, and housing cite (NI) (NIST 2015). This resilience is the product of its comprehensive institutionalization of disaster risk reduction. The City and County of San Francisco (CCSF) assigns a budget for disaster risk reduction (staffs and projects) every year. The Mayor and City Administrator are responsible for coordinating the work of these agencies, as well as the correct distribution of the budget to ensure that the goal of contributing to enhance the overall resilience of the City is accomplished. The programs of the CCSF include Disaster Preparedness Coordinators for each department. The CCSF Disaster Council, chaired by the Mayor, ensures stakeholders participation in emergency planning. The CCSF Lifelines Council, chaired by the City Administrator, increases lifelines resilience. A Ten Year Capital Plan connects all the city stakeholders and advises the Mayor regarding future capital project bond issuance. The CCSF has created the Neighborhood Empowerment Network (NEN), which is an alliance of residents, communities, NGOs, universities, private and public agencies. The NEN generates programs, resources and tools for residents in order to increase communities resilience.

13.2.2 Mitigating Natural Hazard

Floods, hurricanes, earthquakes, wild fires and other natural hazards can't be prevented, but through planning, prioritization and sustained follow-through efforts, communities can decrease the impacts of these shocks and shorten the road to full recovery. In the last decade there have been a shift on hazard reduction from one

solely protecting people to protect the built environment to the extent necessary to allow rapid recovery.

In this paragraph are shown the approaches adopted in US for mitigating natural hazards, because many of these plans can be also applied elsewhere. The Federal Emergency Management Agency (FEMA) is a department of the United States Central Government. Its main goal is to coordinate the response after a disaster in US. Nearly 24,000 communities in the U.S. have used FEMA to guide the development of mitigation plans, these communities encompass 80 % of American residents. According to its plan, the State has to submit a plan including a mitigation strategy to reduce the losses by identifying the risk assessment. This plan aims at different goals, which should be related to other State and local jurisdictions plans and policies. By having the goals well defined, it is easier to achieve a long-term hazard protection, however it is also important to identify the funding, that could be from local or private sources. The first step should be to review the previously approved plans and to update them to demonstrate that progress has been made to implement new mitigation strategies. The mitigation strategy updating provides the chance to discuss the goals and objectives of the State and local plans. Since *mitigation* is a component of resilience, these plans evolve a community towards resilience. A comprehensive understanding of community resilience is provided through a planning process which includes a detailed analysis of the built environment as outlined in the Disaster Resilience Framework and incorporates ongoing mitigation planning. The next step after the establishment of community mitigation planning structure is to expand the scope to resilience. There are similar roles and responsibilities to the ones involved in mitigation activities that are necessary for resilience. An important part of the mitigation planning process is the public participation for coordinating strategies with targets, actions and priorities. Existing mitigation plans and techniques related to the built environment can be used as the framework for community resilience plans. The Presidential Policy Directive 8 (PPD-8) on National Preparedness delegated to FEMA the task of producing a series of frameworks to address the spectrum of prevention, protection, mitigation, response, and recovery. Each Mission Area includes a framework document, which describes the roles and responsibilities of the whole community.

13.2.2.1 Hazard Mitigation Objectives

The goals defined in the State plan aim at long-term hazard mitigation and loss reduction. Integration of long-term planning and implementation of measures of improving resilience can be positive for a community, providing an attractive, vibrant place for residents to live and a reliable environment for the location of businesses. There are also daily benefits of having a resilient community, such as reduced daily disruptions with the adoption of improved design and construction practices. The community resilience plan will therefore begin to improve the performance of buildings and infrastructures against cascading effects due to interdependencies.

It is necessary to describe how these goals were developed and why they have been chosen. With these goals in mind, it is possible to implement a guide of mitigation actions, by describing the objectives and explaining the connection between goals, objectives and actions. The goals should focus on local and State risk assessment and represent a long-term vision for hazard reduction or enhance mitigation capabilities. The resources allocation and priorities are evaluated by considering the desired performance goals in comparison to the anticipated performance of the built environment to hazard events, as well as their expected recovery sequences, time and costs provides. Ideally, community resilience planning can achieve improved social and economic well-being in the long-term by integrating it with long-term plans for economic development. This approach to resilience planning has been developed and implemented in San Francisco (SPUR 2009).

13.2.2.2 Estimation of State Capability

A State shall define its financial and legal situation and its capability to program and carry out mitigation actions both before and after a disaster. The mitigation strategy has to focus on the existing capabilities of mitigation and as well as address areas in which strengthened capabilities are needed. Without this evaluation, the implementation of the plan could fall through because of inadequate supplies. The State shall also conduct an evaluation of the laws, policies, regulations and programs that are related to hazard mitigation as well as to develop new ones if it is necessary. The emergency programs have to be discussed, assessing its implementation opportunities and problems, chances to improve them and possible problems related with private development projects in hazard-prone areas. The State should prioritize and highlight tools and policies that have achieved mitigation objectives. Finally, the discussion should include positive aspects and problems that came up.

13.2.2.3 Estimation of Local Capability

The local mitigation policies, programs and capabilities should be accurately defined. These pre- and post-disaster polices have to be described and evaluated to determine their effectiveness. The description of these capabilities can be general and does not need to be detailed for all localities. Basically, the proceeding is the same used for the State capability assessment, but now at a different level.

13.2.2.4 Estimation of Mitigation Actions

The mitigation actions should be identified through both local and state planning process. The State should define the agencies and organizations that have been involved in identifying the *priorities* and the *mitigation actions*. This necessitates

the involvement of all stakeholders that are essential for setting the recovery goals of community resilience. A governance structure is required to set direction and provide services, while the built environment is required to support the social institutions of the community. The recovery process is directed by the governance, paced by financing and supported and propelled by the members of the community. The foundation of the recovery is established by the built environment.

A *resilience plan* is developed through collaboration between the office of a Chief Executive, such as the Mayor, City Council or Board of Supervisors, community departments and key stakeholders, including representatives of the social institutions, representatives of the physical infrastructure systems, and concerned community members. The holistic nature of the plan and the role that support plays in a successful implementation, lends itself to a public-private partnership for its development. The FEMA Local Mitigation Planning Handbook provides guidance for building a planning team. FEMA suggests using existing community organizations or committees as a starting point and involving all agencies and organizations which have a role in hazard response and mitigation planning. These actions were evaluated along with the correspondence between these actions with the plans mitigation goals, which should be directly associated in order to ensure the achievement of the objectives. The actions can be different in nature: statewide or property specific, targeted at government agencies or private organizations, regulatory or programmatic, construction activities or public outreach.

13.2.2.5 Identifying and Describing a Natural Hazard

The hazards likely to affect the area shall be identified and described by the local risk assessment. This is a critical step, due to the fact that the foundation of the plan and the factual basis for the mitigation strategy is the identification of the hazards that can affect the jurisdiction. All the hazards that are commonly recognized as threats to the jurisdiction have to be identified, if not, this plan cannot receive a satisfactory score. In this way, it is necessary to describe how these hazards have been identified and explain why a hazard has been disregarded. The process for identifying hazards could involve the reviewing of the policy and mitigation plans of the State, talking to experts, searching information in different sources and interviewing long-term residents. A list of potential hazard is given in Sect. 1.1.1.

Communities should then consider three levels of *intensity* or *magnitude* for each hazard selected, in order to apply it in the framework. The terms used to define these levels should be consistent with the design (NIST 2015).

- *Routine*: This hazard level is below the expected (design) level, but is of a higher frequency of occurrence. Full functionality of buildings remains and the infrastructure systems should not experience any significant damage or disrupt daily life.
- *Expected*: This is the design hazard level, according to the codes, possibly greater than the minimum required by codes, or could be based on other criteria

surrounding the building or infrastructure system. Buildings and systems should remain functional and capable of supporting the recovery and response period of the community. This level is based on the typical design level used for buildings.

- *Extreme*: This hazard level exceeds the expected (design) level. The hazard level doesn't necessarily have to be the largest possible hazard level that can be envisioned, but is one that the community intends to be able to recover from, however long it may take. At this level, critical facilities and infrastructures should remain functional. It is expected that infrastructures and other buildings should perform at a level to protect the occupants and allow them to safely and easily evacuate. Emergency response should be prepared for scenarios at this hazard level.

There are standards and code specifications for the national minimum hazard levels of design, for example, *Standard 7–10 Minimum Design Loads for Buildings and Other Structures* (ASCE 2013) defines minimum hazard levels for design nationwide and then communities may define the size of a hazard they wish to consider for each level.

The *impact* of a hazard depends on the size of the area affected, the conditions and development in the affected area, and the community ability to respond. However, the size of the area affected in a disaster as well as the geographic distribution of the intensity depends on the particular hazard.

After identifying a hazard it should be described using the following criteria:

- Probability that the hazard occurs in the area;
- Information of damages due to past events occurred in the community;
- Level of severity of past events;
- Date and duration of previous hazards;
- Sources of information for assembling these past events;
- Maps identifying the affected areas by previous episodes and composite maps combining information;
- Characterize the area describing the topography, meteorology and other conditions that could mitigate or exacerbate the potential of the hazard;

13.3 Resilience as Restorative Care

13.3.1 *Post-disaster Recovery*

Disaster recovery (rehabilitation and reconstruction) refers to the resolutions and actions taken after a disaster with the goal of restoring or improving the pre-disaster living conditions of the stricken community, while encouraging and facilitating necessary changes to reduce disaster risk. Recovery affords an opportunity to develop and apply disaster risk reduction measures (UNISDR 2004). When a disaster strikes in a poor community, it cause serious loss of life and property and it

often threatens the livelihoods and futures of those who survived. This is especially the case where productive household members have been lost or permanently disabled. For many households, not only will their short-term economic and social vulnerability be increased, but their ability to cope with future shocks may also be eroded. These pressures can increase poverty in a society. They can exacerbate tensions or conflicts that may have already existed within or between communities prior to the disaster. In the case of regularly recurring hazard events or shocks, many poor communities live in a constant state of recovery, where temporary relief has become a permanent coping strategy. For example, in Malawi drought occurs with such frequency that people have little time to recover before another drought hits. This has resulted in expanding poverty, chronic food insecurity, and aid dependency. Thus, in order to be effective and sustainable, recovery initiatives must be linked to the national and local development context and processes, as well as an understanding of the economic, social, and political conditions that were prior to the disaster. Some of these are likely to have been contributing factors to the risk and vulnerability that turned the hazard event into a disaster; others for instance, underlying structural issues may have an impact on the strategies adopted for recovery. Lack of understanding of these processes can lead to poorly targeted and inappropriate assistance. This is the case for infrastructure rehabilitation and reconstruction. There are many examples of schools and health centers rebuilt after natural disasters that could not afford ongoing maintenance costs or the staff to run them.

13.3.2 The Role of Legislators

Laws and regulations are considered the foundation for building community resilience. They are essential for reducing existing danger posed by natural hazards, preventing new risks from growing and making the world safer. Following this international guidance, many countries have sought to strengthen their laws and regulations. The *Post-disaster recovery* is an essential part of the disaster risk reduction. Most of the countries nowadays have already started doing intensive work in this field. The Federal Emergency Management Agency (FEMA), for example, released the National Disaster Recovery Framework (NDRF) in September 2011. This guide wants to promote effective recovery, particularly for those incidents that are large-scale or catastrophic. The NDRF provides the overarching inter-agency coordination structure for the recovery phase of “Stafford Act incidents”, and elements of the framework may also be used for significant “non-Stafford Act incidents”.¹ It also defines core recovery principles, roles and responsibilities of recovery coordinators and other stakeholders, a coordinating structure that facili-

¹The Stafford Act is a United States federal law designed to encourage state and local governments to develop comprehensive disaster preparedness plans, prepare for better intergovernmental

tates communication and collaboration among all stakeholders, guidance for pre- and post-disaster recovery planning, and the overall process by which communities can capitalize on opportunities to rebuild stronger, smarter, and safer (FEMA 2011).

13.4 Land Use Intervention Planning

Applying and enforcing risk *compliant building regulations* and *land use planning* are effective tools to mitigate the damage after an earthquake or other kind of natural hazards. This land use planning can be applied in several ways as (i) *an upgrade of informal settlements* or (ii) the *identification of safe lands* for incoming citizens. However, these two approaches for reducing disaster risk are not easy to implement. Upgrading informal settlements is politically controversial and has become the norm in some cities. Instead the identification of safe lands of incoming citizens is not an easy task, because no one can ensure that people will buy there and even worse, the government can't guarantee that low-income households can afford safe sites. It is important for the city government to integrate hazard risk information into their urban planning processes. A wider understanding of disaster risk is needed to develop urban plans and land-use management. Likewise, good inter-sectorial coordination as well as detailed local data on hazards and its reduction are required. Safer infrastructures are definitely achieved when standards are in place through building codes and regulations. They are a valuable way to mitigate disaster vulnerability and risk from extreme natural hazards. The responsibility of its application belongs to the local authorities. Different aspects have to be taken into account to develop efficient land-use intervention planning:

- The municipal regulations and laws shall include codes for design, location and construction that minimizes the disaster risk. These codes shall also enforce the investigation of building capacity to make them more resilient and increase public awareness. The regulations should be different for each type of construction.
- The disaster risk reduction should be incorporated into the urban land-use plan and regulations, underpinned on the city risk assessment, also including the peripheral land around the city.
- These plans have to prevent and control the development of the risk and mitigate it. The plans include restrictions on building type, use, density and occupancy in high risk areas. In vulnerable buildings already built, the plan should implement other ways to reduce risk.
- Identify escape routes and routes for the delivery of relief supplies. Provide the city with evacuation shelters, critical infrastructure, emergency services and lifelines.

coordination in the face of a disaster, encourage the use of insurance coverage, and provide federal assistance programs for losses due to a disaster.

Fig. 13.4 Mudslide after Santa Teclas earthquakes in 2001



- Take into account the populations needs and difficulties of swiftly changing existing building practices. Relocate informal settlements to safer locations when possible.
- Promote the design of more resilient, safer ways of constructions and strengthening of non-engineered buildings.
- Share and show the safer construction techniques to the public with campaigns to aware the population.

An example of how useful these building regulations are can be shown in the construction details. To provide a building of more resilient elements would increase its cost from 1 % to 5 %. But in non-structural elements, the cost saving is huge. For instance the cost of replacing a damaged electric generator could be up to 50,000 dollars, but if a seismic isolator device is installed (that its cost is about 250 dollars) the damaged situation can be avoided. Another example is the measures that were taken in Santa Tecla (Fig. 13.4), in the city of San Salvador (capital of El Salvador), after the two earthquakes stroke in 2001. Two tremors in 5 s caused more than 700 deaths, displaced 20 % of the city and damaged 38 % of the infrastructure. The mayor of the city announced a 10-year plan in order to make the city more resilient when disaster strikes. This plan involved the citizens. The government created citizen groups to encourage their participation, to have periodic discussions and to help make decisions.

13.5 Public Policy

Policies can be categorized according to the structural type as follow:

1. *built environment*
2. *infrastructures*
3. *communities*

By strengthening the resilience of its built environment, a community is better able to maintain vital functions during an emergency and to recover efficiently so that “normal life” can resume within a reasonable time after the hazard has passed. According to FEMA, the main local policies related to the mitigation of disasters are

- *Building codes*, adopted by the States, which local governments are required to adopt and also to build up. These codes are applicable to the design and construction of buildings in order to withstand natural hazards such as winds, floods and earthquakes. They are effective in all structures that have been erected after 1999 with the new building code.
- *Zoning laws and ordinances*. Regulate development by dividing the communities into zones and by setting development standards for each zone. Restrictive zoning can keep inappropriate development out of areas prone to natural hazards. It has been proved in 8 out of the 12 counties of the United States which have applied space ordinances that these regulations are totally favorable to the disaster mitigation process.

FEMA has also planned future local policies:

- *Land-use planning*, prevents the development in hazardous areas or if it is necessary to build anyway, it allows the development in a manner that minimizes hazard risks. With this planning, local governments can identify areas subject to hazards and work on it.
- *Subdivision regulations*, sets construction and location criteria for subdivision layout and infrastructure.
- *Capital improvements planning*, identifies where the biggest public outgoes will be made over the next 5–10 years. It is really useful for planning because it can identify utilities that have to be strengthened, replaced or realigned.

13.6 Role of Policy Makers

There is an ascending acknowledgment among policymakers at all levels that disaster risk reduction, climate alteration, and sustainable development are connected. These issues show commonly subordinate difficulties, which require joint effort, incorporated systems, solid, comprehensive administration structures, sound urban arranging practices, and creative technological and financial arrangements. Since

economic development and risk aggregation take after the same way, as urban cities populations and economies expand, regional governments will assume an undeniably critical part in standing up to the difficulties emerging from more incessant, contained compelling occasions, which can negatively affect the social, ecological, and economic infrastructure and organizations on which lives and jobs depend. Generally, local pioneers must have the political will to enhance disaster resilience. Especially where considerable changes to the norm are vital, political will has demonstrated essential as far as presenting new and dynamic risk reduction policies. In the meantime, on the grounds that a high turnover in leadership is frequently the chief obstruction to supporting urban risk reduction programs, local policymakers must advance a society of strength from the base up. This begins with an eagerness to draw in communities, grassroots associations, organizations, and different accomplices, as well as taking an interest in information imparting stages and exchanges to other local policymakers. Local leaders should likewise enable a city's specialized and expert staff to build civic capacity and guarantee the congruity and attainment of risk reduction activities. Local policy makers have the ability to significantly impact nationals' choices and responsibility. This can prompt a more productive, fair, and composed way to deal with risk management, which can at the same time support other urban plans, including social and economic advancement, safety and security, resource management, and natural assurance. For example, enhancing citywide storm and surface drainage systems to adapt to extreme precipitation can give chances for reusing the water, parks, or community services. Similarly, building stock and other infrastructure that are intended to withstand high winds or seismic movement can improve vitality proficiency and tap into green development opportunities (UNISDR 2013).

13.7 Policy Actors

In this section the primary policy actors are identified and the parts they play in building effective legislative framework. In some cases these groupings frame a plainly defined lobby, in different cases they are a loose coalition of interest. The TEARFUND (Christian action with the world's poor) in their report about the legislation mainstreaming disaster risk reduction (Pelling and Holloway 2006) distinguished six possible actors for risk reduction legislation. They are classified in the following paragraphs.

13.7.1 *Policy Insiders and Outsiders*

Policy coalitions work best when they assemble (a) *policy insiders* who have the ear of policy-makers, and might incorporate abnormal state legislators, yet who may not have specialized knowledge; and (b) *policy outsiders* who have technical mastery but are not routinely counseled in the policy making process. Insiders can

be considered as policy-navigators, and thus who might be liable to be excited or hesitant to backing change. Such mindfulness is extremely helpful when lobbying for change.

It is critical that DRR has a comprehensible policy character that separates itself from prior disaster management work directed towards response and relief. Policy discussions are also significantly helped by an evidence base to show the benefits to be gained in social and economic improvement and in environmental protection by adding a DRR approach to deal with existing disaster management. DRR acknowledges the need for disaster response, however it will at least improve the increasing size of vulnerability and loss in society. The responsibility of external facilitators can be essential in both elucidating the connections between DRR and other segments, and obligations in other national settings, and by representing the social, economic and environmental gains of a DRR approach when home data is small.

13.7.2 Civil Society Policy

Coalitions can be significant and incorporate grassroots actors that are capable of activating local resources and prevalent opinion to advocate for change as well as line ministries. Civil society actors are important because they can provide a vehicle for bringing bits of knowledge from the grassroots, a component for the representation of popular views, and the potential for legitimacy and oversight.

13.7.3 Policy Champions Processes of Reform

Policy supports processes of reform can be simplified when the leadership is provided by policy champions with high-level administrative office. For instance, the Madagascar program for DRR has a top-level political support (the President is involved in the design of hurricane-resistant buildings). Its programme has also developed training programs for district-level officials. The champions must be respected by several policy actors, to be effective in the multi-sectoral environment of risk reduction legislation and policy-making. Reliability in leadership is a great asset in building trust and technical competency. For instance, the India DRR legislation was supported by Shri Shivraj Patil, Minister for Home Affairs, who took the initiative of piloting the legislation and succeeded in guiding the drafting of the law, introducing the bill and controlling it through both houses of Parliament.

13.7.4 Sub-national Government

In some cases, the national framework need to be enacted through regional, local or metropolitan governments. For instance, the Ghana disaster management plan

is managed through a National Disaster Management Organization situated in the Ministry of the Interior and upheld by 10 local, 140 regional and 900 zonal (town and metropolitan) workplaces and contact points. In some cases, the laws on risk reduction may cause a variation in the relationship between national and sub-national governments. For instance India has encountered such vulnerability with the state government assuming a central role in disaster mitigation and reconstruction, however, the national government has managed the discussion on risk reduction inserting it in the plan and financial programs.

13.7.5 Scientific and Technical Bodies

Practical skills are required as soon as a decision has been made to explore the chances that need to be done in the legislation. For example, in Iran, experimental and technical interests has lead and push for the development of the national disaster risk reduction plan that has been endorsed by the Council of Ministers in 2003.

13.7.6 International Actors

There are many examples of countries learning from each other. International actors such as the ISDR and UNDP-BCPR have been active in organizing meetings between people interested in developing national legislation programs and experts from other countries where the legislation has been drawn up.

13.8 International Schemes for Disaster Risk Management

This paragraph reviews the literature regarding the United Nations International Strategy for Disaster Reduction (UNISDR), such as the Hyogo Framework for Action (HFA), and how community institutions (are recommended to) engage in disaster risk reduction (DRR) practices. The United Nations International Strategy for Disaster Reduction (UNISDR) is a global strategy to engage a wide range of actors in a coordinated effort to reduce the risks of disasters and to build “a culture of prevention” in society as part of sustainable development” (UNISDR 2011a). The UNISDR designs and uses cooperative mechanisms (most recently, the biennial Global Platform for Disaster Risk Reduction), through which governments, intergovernmental organizations, international financial institutions, technical institutions and networks, nongovernmental organizations, and civil society organizations interact, share information, and collaborate on risk reduction initiatives. Primarily, UNISDR coordinates the partnerships and leads a global DRR movement focused on meeting the objectives of the Hyogo Framework of Action (UNISDR 2011b).

The United Nations International Strategy for Disaster Reduction (UNISDR) has done a significant work in the field of disaster risk reduction. It is worth to mention the world Conference on Disaster Risk Reduction which is a series of United Nations conferences focusing on disaster and climate risk management in the context of sustainable development. The World Conference has been convened three times, with each edition to date having been hosted by Japan: in Yokohama in 1994, in Kobe in 2005 and in Sendai in 2015. As requested by the UN General Assembly, the United Nations Office for Disaster Risk Reduction (UNISDR) served as the coordinating body for the Second and Third UN World Conference on Disaster Reduction in 2005 and 2015.

13.8.1 Yokohama Strategy for a Safer World (1994)

The United Nations General Assembly, based on the growing concern and recognition of the devastating outcomes of natural disasters, announced 1990–1999 as the International Decade for Natural Disaster Reduction. The First World Conference on Natural Disasters in Yokohama was a significant event that took place during this period. The main result of the mid-term review of the decade was the Yokohama Strategy for a Safer World and its Plan of Action. The strategy lists ten principles on preparedness, prevention and mitigation of natural disasters (UNISDR 1994):

1. Risk assessment is a required step for the adoption of adequate and successful disaster reduction policies and measures;
2. Disaster prevention and preparedness are of primary importance in reducing the need for disaster relief;
3. Disaster prevention and preparedness should be considered integral aspects of development policy and planning at national, regional, bilateral, multilateral and international levels;
4. The development and strengthening of capacities to prevent, reduce and mitigate disasters is a top priority area to be addressed during the Decade so as to provide a strong basis for follow-up activities to the Decade;
5. Early warnings of impending disasters and their effective dissemination using telecommunications, including broadcast services, are key factors to successful disaster prevention and preparedness;
6. Preventive measures are most effective when they involve participation at all levels, from the local community through the national government to the regional and international level;
7. Vulnerability can be reduced by the application of proper design and patterns of development focused on target groups, by appropriate education and training of the whole community;
8. The international community accepts the need to share the necessary technology to prevent, reduce and mitigate disaster; this should be made freely available and in a timely manner as an integral part of technical cooperation;

9. Environmental protection as a component of sustainable development consistent with poverty alleviation is imperative in the prevention and mitigation of natural disasters;
10. Each country bears the primary responsibility for protecting its people, infrastructure, and other national assets from the impact of natural disasters. The international community should demonstrate strong political determination required to mobilize adequate and make efficient use of existing resources, including financial, scientific and technological means, in the field of natural disaster reduction, bearing in mind the needs of the developing countries, particularly the least developed countries.

This strategy served as international model in disaster reduction. Communities were aware that natural disasters posed a big threat to human life and economic losses and concluded that the solution to this problem was mainly disaster prevention. The objective of the next World Conference would have been the complete review of the Yokohama Strategy with the intention of providing an updated guide and framework on disaster reduction. Following the idea of working on disaster prevention, the conference aimed at increasing the global awareness and importance of building disaster reduction policies, with a focus on developing countries where disasters have a greater impact.

13.8.2 Hyogo Framework for Action (HFA) (2005)

The Second World Conference on Natural Disasters concluded introducing the *Hyogo Framework for Action (HFA)* to the participating members as a common strategy to work on disaster risk reduction.

Adopted in 2005, the HFA was developed to substantially reduce the losses to social, economic, and environmental assets of communities and countries from disasters (UNISDR 2009). The HFA is the international blueprint for DRR and has been adopted by 162 UN member states. Its overarching goal is to build the resilience of nations and communities to disasters, [and] achieving substantive reduction of disaster losses by 2015 (Nkala and Helena Graziosi 2010).

The HFA outlines five priorities to be addressed and acted upon in order for vulnerable communities to build and maintain resilience.

1. Ensure that DRR is a national and a local priority with a strong institutional basis for implementation;
2. Identify, assess, and monitor disaster risks and enhance early warning;
3. Use knowledge, innovation, and education to build a culture of safety and resilience at all levels;
4. Reduce the underlying risk factors;
5. Strengthen disaster preparedness for effective response at all levels.

Hyogo framework is the framework used to determine adequate Disaster Risk Reduction (DRR). It is the structure of resilience and preparedness created by the United Nations International Strategy for Disaster Reduction (UNISDR). Twigg (2007) simplified the HFA into five thematic areas, they are: *governance, knowledge and education, risk management and vulnerability reduction, risk assessment, disaster preparedness and response*. According to the study, the sub-themes of the themes are more or less the characteristics of resilient communities.

Governments applying HFA had to submit their reports during four different periods of 2 years each. In these reports, each priority is met with a different set of core indicators that are evaluated with a score from 1 to 5, 1 being the least progress achieved and 5 being the highest. In order to fill these reports and give a score, countries need to answer specific questions for each indicator in an effort to give as much information as possible for every step they took towards disaster reduction.

After the application of the HFA, some DRR specialists and activists have communicated doubts and dissatisfaction with the administrative course, contending that the numerous new laws and policies that have been produced to deliver DRR appear not to have had the effect they guaranteed, referring to, specifically, crevices and gaps in execution at the community level (UNDP 2014a). The International Federation of Red Cross and Red Crescent Societies (IFRC) and the United Nations Development Program (UNDP) in their report (UNDP_&_IFRC 2015) claim that since the endorsement of the framework, and succeeding the staggering impacts of recent immense scale catastrophes, many nations have looked to amend and enhance their legal systems for disaster risk reduction (DRR), particularly by embracing new laws for disaster risk management. Throughout this process, several governments have been asking: “What works? In what capacity would we be able to gain from different nations experiencing the same process?” in the meantime, various reports relating to HFA execution have demonstrated moderate advancement in decreasing disaster risk at the community level, and an absence of clear data and examination on the role of legislation. To label this gap, in 2012, the International Federation of Red Cross and Red Crescent Societies (IFRC) and the United Nations Development Program (UNDP) left in a joint activity went for supporting the fortifying of domestic legislation for disaster risk reduction (DRR). The program conceived the development of two items:

- A multi-nation report on the DRR-related legislation of 31 nations, and
- A ten-point Checklist on Law and Disaster Risk Reduction.

A blend report of the largest comparative study of enactment for disaster risk reduction embraced to date, titled A report titled “Effective law and regulation for disaster risk reduction: a multi-country report” (UNDP_&_IFRC 2014), was released on June 2014, which include the largest comparative study of enactment for disaster risk reduction. The findings of the synthesis report and case studies, together with the opinions and practical knowledge of stakeholders accumulated through ten consultations held around the globe, were then used to be added to the Checklist on Law and Disaster Risk Reduction (UNDP 2015).

13.8.3 Sendai Framework (2015)

The Hyogo Framework for Action has given the basic directions to minimize the disaster risk and has made some steps towards the accomplishment of the Millennium Development Goals. Its execution has, nonetheless, highlighted various gaps in addressing the basic disaster risk variables, in the creation of objectives and priorities for action, in the need to encourage disaster resilience at all levels and in guaranteeing a satisfactory method for implementation. The gaps demonstrate a need to grow an action-oriented system that Governments and important partners and stakeholders can implement in a strong and correlative way, and which recognizes disaster risks to be overseen and directs investments to enhance resilience (UNISDR 2015).

This has prompted the Third United Nations World Conference on Disaster Risk Reduction that took place in Sendai, Miyagi, Japan in March 14–18th, 2015, attracting more than 6,000 representatives to the conference itself and 50,000 individuals to the related Public Forum. The Sendai Framework for Disaster Risk Reduction 2015–2030 (SFDRR) is a 15-year non-binding agreements which perceives that the State has the essential part to decrease disaster risk, yet this obligation ought to be imparted to different partners and stakeholders including local government and the private sector. It is the first global policy framework and represents a step in the direction of global policy coherence with explicit reference to health, development, and climate change. To develop SFDRR, the United Nations Office for Disaster Risk Reduction (UNISDR) organized and facilitated several global, regional, national, and intergovernmental negotiations and technical meetings in the period preceding the World Conference on Disaster Risk Reduction (WCDRR) 2015 where SFDRR was adopted. UNISDR also worked with representatives of governments, UN agencies, and scientists to develop targets and indicators for SFDRR and proposed them to member states for negotiation and adoption as measures of progress and achievement in protecting lives and livelihoods.

The Sendai Framework for Disaster Risk Reduction 2015–2030 aims to protect lives, health, livelihoods, ecosystems, cultural heritage, and critical infrastructure from natural and human-caused hazards over the next 15 years. It seeks to bring about “the substantial reduction of disaster risk and losses in lives, livelihoods and health and in the economic, physical, social, cultural and environmental assets of persons, businesses, communities and countries” (UNISDR 2015). The Sendai Framework outlines seven global targets:

- a substantial reduction in global disaster mortality;
- a substantial reduction in numbers of affected people;
- a reduction in economic losses in relation to global GDP;
- a substantial reduction in disaster damage to critical infrastructure and disruption of basic services, including health and education facilities;
- an increase in the number of countries with national and local disaster risk reduction strategies by 2020;

- enhanced international cooperation for developing countries; and
- increased access to multi-hazard early warning systems and disaster risk information and assessments.

Implementation of the Sendai Framework for Disaster Risk Reduction requires strong commitment and political leadership both at national and local levels. This is essential to ensure stronger risk governance and capable institutions that can take the lead and mobilize and motivate stakeholders. A key outcome of the 15-year strategy must be the development of communities that are not only risk informed but are also knowledgeable about risk, and therefore understand how to eliminate or mitigate underlying drivers of risk and how to build back better after a disaster.

13.8.4 Decision Making

The hierarchy of the causal factors of disasters is unique to each community. Hazards that occur in different geological locations with different cultural traditions, standards of living, and social expectations makes “best practices” or universal rules obsolete and makes DRR fundamentally contingent. It is in the communities best interest to design their own DRR structure based on their particular causal factors, their culture, and their way of life. It is important that different livelihood strategies are taken into account because understanding or at least recognizing ways that different types of communities live will help us understand how other types of communities and cultures cope with hazards (Wisner et al. 2006). Similarly, the way different communities view and analyze risks as well as what causes a disaster and their impacts can affect the modes and types of decision-making drastically.

Petal (2007) explains that origins of disasters can be assessed at three overlapping levels of social organization: (1) the *micro level*, or individuals and households, (2) the *meso-level*, which comprises schools, businesses, local governments, faith-organizations, etc., and (3) the *macro-level*, consisting of regional, national, and international policy making entities. Petal (2007) also explains that there are three primary actions considered when conducting DRR. These are risk assessment and planning, physical protection, and response capacity development. It is crucial to think of the different levels of social organization and the different actions taken in order to effectively create and enforce DRR. Understanding these fundamental characteristics of community institutions will help shape an understanding of their level of engagement and capacity in DRR. The following are examples of how the fundamental characteristics of *meso community* institutions can shape their types of engagement in DRR (across risk assessment and planning, physical protection, and response capacity and development).

1. Government can implement legislation and policies dictating how far to build off of the shore of a hurricane swept beach;
2. Schools can educate students about how they can protect themselves at school and at home;

3. The private sector can advocate for DRR and therefore strengthen the resilience of their businesses; Healthcare facilities can be prepared for a high magnitude event, both in the availability of their services as well as in the accommodations they provide;
4. Grassroots organizations can reach out to those who are unable to increase their coping capacity and provide them a safer location to live, a safer building in which to live, and mandate certain maintenance take place in order for the tenant to remain safe.

There are many options that community institutions can take, at various levels, in order to implement the idea of reducing risk. By understanding the causal factors of disasters, a general level of risk can be assessed, which can inform community institution's decision-making and actions.

13.9 Case Study of Hurricane Sandy

Several initiatives can be implemented to increase the community resilience of a region affected by an extremely disruptive event in order to make it able to withstand and recover from similar events in the future. A precise set of initiatives cannot be put in place prior to an event, nor can they be selected to encompass every region and type of event. For each specific scenario, it is necessary to evaluate what the best strategy is to adopt. This means that decision-makers need to be guided in choosing one or more of the initiatives to implement, and this selection can be made based on certain criteria: the type of event and the risks that an area may face, the goals to reach in order to obtain resiliency, the funding made available to reach those goals or to recover from that specific event. These are just some of the parameters to consider when making a decision. The extent of damage and economic loss in communities and specific infrastructures can also support this choice and lead to the prioritization of initiatives to adopt. By categorizing initiatives based on this and other criteria, it is possible to provide a tool to better plan an intervention strategy in order to increase preparedness before, during, and after an event. The application of these initiatives has a broad impact on entire communities and individual infrastructures in terms of increasing of their ability to withstand the threats posed by climate change. In the end, the goal is always to mitigate the effects of natural and man-made disasters on communities, giving them the instruments to bounce back to their state prior to the event, or to an even better situation, and improving their ability to withstand future similar events. This paragraph describes the initiatives proposed by the New York City government to increase the resilience of the infrastructure sectors hit by Hurricane Sandy, organized according to the type of infrastructure and the intervention strategy they have in common. Among the more than 200 initiatives reported, this analysis focuses only on those proposed for utilities, liquid fuel, and transportation infrastructures. Finally, to better understand the features of these several possible initiatives, and thus the best one for each specific situation, they are further organized according to the selection criteria described above.

13.9.1 Initiatives Proposed in New York City

After Hurricane Sandy, the New York City government understood the need for a long-term plan to increase resiliency in the city's several infrastructures. In the aftermath of the first recovery phase, when all attention was focused on repairing the damage caused by the storm, it was clear that there was a need to intervene in order to solve several problems presented before, during, and after the event, which caused delays in restoring the area to its previous situation and made the impact worse than expected. The efforts put in place to prevent the worst were not enough and something needed to be done to prevent this situation from happening again. The extent of damage suffered was unexpected and the recovery phase took longer than predicted, despite some resiliency efforts that had made the region more prepared and protected. In December 2012, the New York City government launched the Special Initiative for Rebuilding and Resiliency (SIRR), a program specifically for resilience that addressed the consequences of the hurricane itself and the risks posed by similar future events. The SIRR produced a plan of strategies to adopt in order to strengthen the protection of New York's infrastructures, buildings, and communities from the impacts of future climate risks, published in the report *PlaNYC: A Stronger, More Resilient New York*. The plan outlines more than 200 initiatives for several infrastructure sectors that should be implemented to increase the preparedness, strength, and resilience of New York City against future events. These initiatives make New York a reference model of a resilient city able to address climate change and are an example of what decision-makers can do to have a more reliable and resilient infrastructure. The focus now is on the initiatives proposed to increase resiliency in utilities, liquid fuel, and transportation systems, since several analyses of Hurricane Sandy itself and other natural and man-made events showed that intervention in these sectors must be focused on better planning and recovering from these events. The reason for this is due to the fact that these sectors are key in the overall infrastructure network, therefore intervening in them would have a wide effect on the other sectors that rely on them. Initiatives in other sectors are also equally important, but their effect are mostly limited to the sector in which they are organized, as they are not crucial to the network. After explaining the initiatives focused on in this chapter and describing some examples of their effects on their sector and others, the reason for their emphasis will be more evident. A brief analysis of these initiatives is provided to answer the following questions:

- Why is the initiative needed?
- What will be/has been done to solve this problem?
- What is goal needs to be achieved?
- What are the consequences/effects/benefits of the application of the strategy on increasing the resiliency of a sector and other sectors that rely on it?

A complete analysis of the each initiatives features, in terms of reason, description, goal, and benefits, is summarized in a table at the end of the chapter. This table summarizes and explains more in depth the features of each initiative, following the same structure used to briefly describe them within the chapter.

13.9.2 Initiatives for Utilities

The utilities sector includes power, natural gas and steam systems, which are the critical energy infrastructures that provide electricity, heat, hot water, and other services to several facilities. These systems are highly interconnected, making each one of them more vulnerable to disruptive events that occur to one or more of them. The initiatives for increasing resiliency in utilities are organized into the following strategies:

- Redesign the regulatory framework to support resiliency
- Harden existing infrastructure to withstand climate events
- Reconfigure utility networks to be redundant and resilient
- Reduce energy demand
- Diversify customer options in case of utility outage

Each strategy focuses on different aspects of the utilities sector, from the regulatory framework to the physical single infrastructures and overall network, and aims to achieve one or more goals. Overall, these strategies are designed to increase the resiliency of the utilities systems by upgrading their features and assets, reducing their possibility of being disrupted and the time it takes to restore them when these disruptions occur.

13.9.2.1 Strategy: Redesign the Regulatory Framework to Support Resiliency

The initiatives to accomplish this first strategy are thought to reduce the lack of laws and rules that characterize the energy systems. This will make utilities systems more resilient by assisting utilities and regulators in carrying out several projects. For this reason, the initiatives that utility companies and regulators should work together for are:

- Develop a cost-effective upgrade plan of utilities systems
- Consider climate risks in system design and equipment standards
- Define a set of performance metrics for climate risk response
- Develop a cost-effective upgrade plan of utilities systems

Utilities generally are not required by regulators to account for the possibility of losing entire facilities due to severe weather events, yet they can guarantee energy supply during minor weather events or when a single part of the facility fails. This means that utility systems are not designed to address events like Sandy with low-probability and high-impact consequences. In order to solve this issue, some actions have already been taken by the Office of Long-Term Planning and Sustainability (OLTPS), such as the development of a probability risk assessment model to efficiently plan the use of budgets or the quantification of possible customer outages and economic losses. Other actions planned are the development of costs, benefits,

and risks analysis tools by utilities and the upgrade of their systems to withstand risks related to future high-impact events by giving them a reasonable motivation to recover those investments with an improvement of the ratemaking process. This initiative aims to better prepare utilities to address high-impact climate risks, by forcing them to take into account storm probabilities and future surge heights and by providing them with a tool on which they can base storm hardening investment decisions. This upgrade makes them more resilient in the future, in addition to it being affordable and sustainable.

- Consider climate risks in system design and equipment standards

The second initiative addresses the fact that utility systems are not able to remain operational during extreme weather events and recover quickly when parts of the system fail. If on one hand the systems are considered reliable through adequate system planning approaches and design standards, on the other hand these approaches and standards do not guarantee resiliency needed to withstand climate risks. For this reason, the impact of climate change has to be considered when evaluating system planning decisions, e.g. taking into account temperature and humidity forecasts, the possibility of extended exposure to flooding and saltwater, and stronger and more sustained winds when planning for the strengthening and update of power systems and equipment design standards. Voltage reduction is another solution that can be put in place to address the impact of heat waves and other events that cause a high-peak system demand. In this way, the goal of optimizing reliable systems resiliency and obtaining adequate power supply for climate change can be achieved.

- Define a set of performance metrics for climate risk response

The third initiative highlights the need for establishing performance metrics, since they are often not considered when evaluating utility performance in the different stages of the events impact. To accomplish this, updated resiliency metrics and realistic performance standards need to be developed, and utilities need to publish annual progress reports to show their preparedness and investments for climate risks. This strategy aims to increase resiliency and reduce vulnerability through increasing preparedness and the ability to plan and manage emergencies and through upgrading system asset characteristics to improve their reliability. It provides several benefits for the utilities sector and for all the others that are directly dependent on it. If an upgrade plan is determined, utility systems will be strengthened and their possibility of failure will be reduced, decreasing, at the same time, the possibility of cascading effects on dependent systems. Based on performance metrics, utility companies will be more capable of identifying the priorities in terms of what damaged areas need to be repaired first. They will also be able to deal with critical situations that limit the availability of resources better. Moreover, buildings, health care and other facilities would have a lower chance of power outages from line overloads because of upgraded systems, while

transportation, fuel, and telecommunication sectors would be more resilient and able to withstand future events if systems and equipment design standards are updated. These are just some examples of the benefits.

13.9.2.2 Strategy: Harden Existing Infrastructures to Withstand Climate Events

Sandy and other past disruptive events showed that existing power infrastructures are vulnerable to severe damage and that the interruption of power supply is caused mainly by the failure of key nodes in the energy supply systems, like power generators, transmission and distribution infrastructures. There is therefore the need to identify and harden vulnerable high-priority nodes of the power infrastructure against climate risks. The hardening strategy regards different utilities, from electric to gas to steam in the case of New York, and involves several agencies to work to:

- Harden key power generators against flooding
- Harden key electric transmission and distribution infrastructure against flooding
- Harden vulnerable overhead lines against winds
- Harden natural gas system against flooding
- Harden steam plants against flooding
- Harden key power generators against flooding

The first initiative focuses on the most important assets of the electric infrastructure, which are the power generators. More than half of NYC generators are currently at high risk of flooding and almost all of them will be in 2050. Moreover, the owners of these power plants are not obliged to protect them with flood-protection measures, since no regulations exist. Plant owners, utilities, and regulators have to work together to prioritize, plan, and budget for the hardening of key in-city assets. Through a cost-benefit analysis, some existing plants will be upgraded to withstand at least a 100-year flood, while new ones will be built with a 500-year flood protection, through different measures and timeframes for completion that need to be determined. The aim of this initiative is to put in place all the measures needed to allow plants to remain operational during, or recover quickly from, a 500-year flood event.

- Harden key electric transmission and distribution infrastructure against flooding

The second initiative focuses on the hardening of other key infrastructures of the power system, such as transmission and distribution substations, utility tunnels, and underground equipment, which are all at risk of flooding as they are located in the flood maps: 37% of transmission substations are currently in the 100-year floodplain and 63% will probably be by 2050. Starting with those considered priority due to their role in network reliability, the customers they serve, and the impact their failure would have on the economy, several site-specific measures can be adopted to harden these systems against flooding. The elevation above flood level of certain assets and the replacement of tunnels underground equipment with

waterproof ones are just a few of them. Together with other ideas, the protection of transmission and distribution infrastructures from future flood events can be guaranteed.

- Harden vulnerable overhead lines against winds

The third initiative deals with the hazard of high-speed winds that, like in the case of Sandy, can down trees over overhead line equipment, like electric poles, transformers, and cables. To address this problem, utilities are requested to perform ordinary and extra tree maintenance when hazardous events are forecasted, strengthen their overhead lines, and eventually consider the possibility of rerouting some of them underground. Since this option is expensive and not practical, a cost-benefit analysis is needed to evaluate its applicability. The goal of increasing the protection of overhead lines from these threats can be achieved including wind risks in the overall regulatory framework that governs system reliability.

- Harden natural gas system against flooding

The fourth initiative instead focuses on the actions needed to ensure higher protection of the natural gas systems and so that utilities can better control and monitor them. Sandy showed that the gas system was affected by the failure of remote operation of parts of it and by localized outages to the distribution system caused by the infiltration of water. The idea is to harden all city-gates, interface regulator stations, and control equipment against flooding through, for example, replacing inefficient equipment that is at risk of corrosion, fixing leaks and cracks, and installing devices to prevent water from infiltrating into the gas.

- Harden steam plants against flooding

Finally, the fifth initiative stresses the need to increase resiliency in the steam system. After electricity and gas, steam is the third power source in the city in terms of the number of customers served. Most steam plants are located in the current floodplain, and are thus vulnerable to future flooding. Several flood-protection measures can be adopted to achieve the resiliency goal. Among these, some are the same of those proposed for other systems, like the elevation of equipment; others are specifically designed for the steam system, like the installation of floodwalls and of flood-protected, natural gas-fired back-up generators. Overall, the hardening strategy puts together initiatives to increase the protection of existing infrastructure assets. These hardening initiatives mainly address flooding, which is one of the main features of coastline hurricanes due to their ability to move high volumes of water inland via high speed winds, and can be worse than expected due to their superposition with high tide during the full moon. Flooding, together with wind, is the main cause of most damage to utility systems reported after similar events. These systems are vulnerable to such kind of hazard because they are often located in the most recent floodplain maps. Several physical measures can be adopted to physically harden these systems. Among these, the most common and feasible one is elevating key nodes of the power system chain, such as power stations and substations, above flood level. Due to the extent of the number of

systems in need of hardening, attention is focused on high-priority infrastructures that are fundamental to keep the most critical infrastructures operating, like health care and other emergencies facilities. Hardening initiatives are, essentially, mostly physical measures to implement on the existing utility network of systems, which is vulnerable to several consequences of an extreme event, like a hurricane, which are mostly flooding and wind. Due to their nature, these initiatives can be implemented in a short time with short-term planning, but with term effects. A choice cannot be made among the initiatives for power utility, since they regard different assets of the same utility that are in need of the same protection. The impact of these hardening initiatives is broad and leads to improvements in the resiliency of other infrastructures that are not utilities. Despite the fact that they are proposed specifically based on the number of damage caused to utilities by Sandy, they can be considered in various geographical contexts and can reduce the consequences of several other events, like heavy rainfall. The hardening of these systems allows utilities to have better control of them during the recovery phase following an event and to better manage repair crews that can be then deployed to repair the most critical damage, like the one of local systems in buildings, rather than the one in power plants. Some economical and feasibility evaluations are needed to harden overhead lines, which are the most damaged by strong winds that tear down trees. Burying power lines is expensive and makes them prone to flooding, therefore frequent tree maintenance and overhead line strengthening is preferred rather than the rerouting of overhead lines underground. Gas and steam systems showed to withstand the impact of the hurricane; however, this does not mean that they do not need hardening against flooding. Since their key assets are located in the current floodplain, their lines need to be protected from water infiltration, which causes localized outages to the distribution system. There are several benefits of applying this strategy both on the utilities sector and others. Despite reducing the possibility of power outages from downed trees or flooding of critical assets, utility infrastructures would have less damage because of their ability to better withstand these extreme events and their consequences, like flooding. Moreover, utility repair crews would be able to focus only on those critical situations where damage occurred despite the protection put in place. By reducing the number of criticalities to repair, it would also be possible to reduce recovery time and repair costs and guarantee the availability of utility infrastructures during the recovery phase. In addition to these benefits to the utility sector, several others regard other sectors. Through protection measures against flooding and wind, transportation equipment, like traffic lights, switches, and other facilities, would also work if the area was flooded and physical transportation infrastructures, such as roads and railways, would not be interrupted by downed overhead lines. Buildings and healthcare facilities would not be affected by power outages and would not need backup generators to keep functioning, and therefore these structures would not need to be evacuated like the case during Sandy.

13.9.2.3 Strategy: Reconfigure Utility Networks to Be Redundant and Resilient

After hardening, reconfiguration of utilities with the aim of redundancy and resiliency through these measures is essential to reduce the probability of failure of the utility systems and to ensure faster service restoration in the event of failures. To increase redundancy and resiliency of utility infrastructures, the initiatives that several regulated utilities and private companies working together have put in place include:

- Strengthen New York City's power supply
- Require more in-city plants to be able to restart quickly in the event of blackout
- Develop a long-term resiliency plan for the electric distribution system
- Minimize electric outages in areas not directly affected by climate impacts
- Implement smart grid technologies
- Speed up service restoration for critical customers via system configuration
- Speed up service restoration via pre-connections for mobile substations
- Expand and diversify natural gas supply
- Strengthen the in-city gas transmission and distribution system
- Launch an energy infrastructure resiliency competition
- Strengthen New York City's power supply

The first initiative considers the fact that the majority of power generation plants are old, at risk of flooding because they are located in the 100-year floodplain, and rely on natural gas and liquid fuel supplies to function. Their supplies themselves are susceptible to interruption caused by extreme events, consequently making power supply increasingly vulnerable to these events. The goal to achieve with this initiative is to diversify and improve the sources of the city's power supply by increasing the number of power lines linked to other external markets and the number of supply sources, considering, for example, low-carbon electricity generation and re-powered, upgraded older and inefficient power plants.

- Require more in-city plants to be able to restart quickly in the event of a blackout

In addition, as highlighted by the second initiative, many New York City power generation plants, both oldest and newest, need external power sources to be restarted after extensive outages. In order to increase the ability to recover these assets more quickly, the so-called black-start capacity has to be implemented in existing plants, since this requirement was not established by regulations at the time they were built, and considered when building new plants, since this requirement has now been implemented by State regulators.

- Develop a long-term resiliency plan for the electric distribution system

On the other hand, with the third initiative, the focus is directly on increasing the resilience of the electric distribution system, rather than focusing on hardening, since utilities actually develop their long-term expansion plans without accounting for resiliency. Several actions can be put in place to make the electric distribution

system more able to withstand heavy blows from extreme weather, such as storm and heat waves. For example, new systems can be built inland to reduce the load on coastal ones and to avoid the geographical concentration of systems in vulnerable areas. New links and transmission corridors can be created to strengthen the connection to out-of-city electric supplies, as well.

- Minimize electric outages in areas not directly affected by climate impacts

Often customers are subjected to power disruptions not because they are directly damaged by flooding, but because of so-called sympathetic outages, which are preemptive shutdowns determined by utilities to prevent larger damage to parts of the network that have the probability of being flooded. Therefore, with the aim of solving this, the fourth initiative focuses on building new network boundaries and installing new equipment for controlling power line sections to address this effect, thus reducing the number of customers affected by an outage, especially in critical infrastructures like hospitals.

- Implement smart grid technologies

The implementation of new technologies would allow utilities to evaluate system conditions in real-time and dispatch crews and equipment to the highest priority problem locations better and quicker. This initiative is needed because utilities actually base the identification of location and extent of damage solely on information obtained through customer reports of power outages and on-site inspections by crews. Together with inaccessible roadways and other similar problems, this only way to identify damages can increase the time needed to collect information and thus delay the dispatch of repair crews. Low-cost sensor technologies, system integration, automated control, decision-aided tools, and smart meters are just some of the new technologies that utilities could implement to achieve that goal.

- Speed up service restoration for critical customers via system configuration

Damaged customer equipment has to be repaired or replaced before utilities can restore power service to individual customers. Critical customers, such as hospitals, are also subjected to this dependence on efficient equipment and can be just as impacted by it as less critical customers are. To avoid service interruption to critical customers and to restore their service quicker than other customers, the first initiative regarding service restoration defines several solutions for system configuration that can be adopted to isolate the critical customers from the rest of the network, e.g. installing switches and other equipment along feeders that supply them.

- Speed up service restoration via pre-connections for mobile substations

Another way to accomplish the same goals of avoiding service interruption is to provide customers with the necessary equipment to connect to mobile substation units. Often times, these units cannot be immediately used because of missing pre-connections in the system, even if they are critically important because they allow electrical distribution circuits to have partial functionality restored while utilities are

proceeding with the repair of damaged substations. To use mobile substations during this recovery time, the initiative suggests that necessary connections in the system have to be pre-installed, and ways to source them must be found. After a primary technical evaluation for the effectiveness of utilizing of these units as a strategy for high priority substations, the idea is to permanently implement them for individual customers or for neighboring regions, by sharing mobile units to reduce their cost.

- Expansion and diversification of natural gas supply

The two initiatives regarding natural gas supply focus on different things that have occurred in the past. The first initiative regards the five city-gate connections that are all needed during high-demand days to prevent disruptions. Despite the fact that the existing natural gas connections to New York City generally are able to provide the city's customers with gas, an increase of their capacity is needed. This can be obtained through the installation of additional city-gate capacities, linking the city to new natural gas pipelines, and the construction and completion of new pipelines, such as the Spectra pipeline. This is an effective way to increase gas supply redundancy and avoid forced shutdowns.

- Strengthen of the in-city gas transmission and distribution system

On the other hand, the capacity of New York's natural gas system to move gas supply through transmission and distribution systems has to be strong enough to move the current and the extra gas supply provided by new sources. The second initiative addresses this limitation, due to which significant outages could be recorded during high demand days because the system is not able to supply an area through a different source if that area's city gate is down, meaning the system lacks redundancy. In order to avoid this, natural gas outage risks have to be evaluated and the transmission systems have to be strengthened according to specific plans.

- Launch of an energy infrastructure resiliency competition

The last initiative focuses on the need to find new cost-effective approaches to protect these utility systems in the future, despite floodwalls and equipment elevation, which are among the many resiliency solutions for the city's already available energy systems. To accomplish this need, the Resilience Technologies Competition, an energy infrastructure resiliency competition, was launched in the summer of 2013 to explore and compare new projects that use innovative technologies to increase building and infrastructure resiliencies. Some initiatives aim to diversify and improve the sources of the city's power supply in order to reduce the chance of power outages, since several sources can feed the same systems and it is highly improbable that multiple sources are unavailable at the same time. Other initiatives want to reduce restoration time in different ways otherwise utilities may not be able to restore electric service to individual customers until damaged customer equipment is repaired or replaced. For this purpose, new technologies can be used to reduce the number of interventions needed and to understand more quickly priority interventions where repair crews and equipment can be reasonably dispatched. Redundancy will also mean letting repair crews work at their own pace,

since the service is being provided anyway through other sources, and reducing the dependency of power plants on natural gas and liquid fuel supplies. The initiatives for gas supply will surely increase system redundancy and consequently increase the availability of gas, especially during high-demand peak days, by reducing forced shutdowns on these days caused by limited gas supply. Finally, the energy infrastructure resiliency competition can provide decision-makers with several new ideas to implement in order to increase building and infrastructure resiliencies.

13.9.2.4 Strategy: Reduce Energy Demand

One further strategy to consider when planning for increasing resilience, in order to address rising temperatures that will lead to higher peak energy demand, is to manage this high demand by reducing it, a more effective and economic approach than increasing the energy supply. The initiatives put forward for this strategy, which imply utilities, regulators, the government and private sector partners working together, are:

- Expand citywide demand response (DR) programs
- Increase the energy efficiency of buildings
- Expand citywide demand response (DR) programs

Demand response can be defined as “a wide range of actions which can be taken at the customer side of the electricity meter in response to particular conditions within the electricity system, such as peak period network congestion or high prices. DR programs include activities such offering time-based rates and other forms of financial incentives to reduce or shift customers electric usage. The first initiative is thus proposed because, despite a new demand response capacity of 500 MW being built in recent years to manage brief periods of peak electrical demand, this new capacity demonstrated not being enough for demand, and thus its increase is needed and can be obtained in different ways. A reduction of the price of DR generation to the price of traditional generation is a first incentive for DR participation to increase capacity. A further increase of the existing number of large customers that participate in DR can be obtained by improving the participation standards and increasing the importance and participation of private companies that manage DR capacity among many small users. This would also avoid costly system expansions that could be needed to manage peak demand periods.

- Expand the energy efficiency of buildings

On the other hand, the expansion of energy efficiency programs for buildings is another way to reduce both their energy demand and overall energy demand. If these programs are implemented, buildings themselves can withstand a power outage for a longer period of time, as they rely on a lower energy demand in order to function. Buildings owners would also save money and the chance of peak season outages, together with carbon emissions, would be reduced. These programs include several actions, such as the adoption of energy use benchmarking, audit

and retro-commissioning requirements, the upgrade of lighting, and the creation of centers to improve the knowledge of best practices for lighting and building system integration. These two initiatives thus highlight the need to focus on energy efficiency efforts to increase utilities' ability to recover from extreme events that lead to higher peak energy demand. For this purpose, they both focus on the development of expansion programs of the existing actions already taken for energy efficiency. If these initiatives are implemented, several effects and benefits can be obtained. More buildings could be supplied with energy and could all together maintain their functions at the same time during a reduction of power supply and their recovery can be faster since less power would be required to run them. The chance of outages during high peak demand due to overload would be reduced and, consequently, system reliability and stability would be increased. Critical facilities such as hospitals would also be able to work with a reduced energy supply and telecommunication systems would always be able to function. Overall, the impact of high peak demand on people's lives, such as pollution, for example, would be reduced.

13.9.2.5 Strategy: Diversify Costumer Options in Case of Utility Outage

The last strategy for the utility sector takes into account the importance of alternative energy sources in addition to the main networks, as this could fail even if it is reliable. The initiatives are therefore focused on increasing the redundancy of the utility sector, both at level of individual customers and districts, since its insufficiency makes the sector vulnerable. In order to diversify customers options in case of a utility outage, the initiatives proposed are:

- Scale up distributed generation (DG) and micro-grids
- Incorporate resiliency into the design of City electric vehicle initiatives and pilot storage technologies
- Improve backup generation for critical customers
- *Scale up distributed generation (DG) and micro-grids*

Distributed generation (DG) refers to the production of power in the proximity of the final users through the employment of small-scale technologies, like solar photovoltaic systems (PV) and other systems to produce renewable energy. Micro-grids are defined as local energy grids with control capability, which means they can be disconnected from the traditional grid and operate autonomously, (CITE) and can thus be seen as the expansion of the DG concept at the neighborhood level. A significant expansion of the DG systems in New York is constrained by regulatory structures, financing challenges, and lack of information. Therefore, the first initiative aims to promote the diffusion of these systems by addressing regulatory, financing, and information barriers, e.g. by changing the existing tariff structures and interconnection standards related to DG and by providing incentives for its expansion, especially in critical facilities such as hospitals. The initiative

also supports further studies of the applications of PV systems during outages and the technical and regulatory solutions for enabling cost effective and safe implementations of them. On the other hand, utilities do not take micro-grid expansion into account in their planning. To encourage micro-grid adoption as an effective alternative power source to use during outages, several actions can be underlined. Among others, this includes the clarification of the rules governing the export of energy and feasibility studies of the effects of micro-grid technology on buildings and on the entire energy network.

- *Incorporate resiliency into the design of City electric vehicle initiatives and pilot storage technologies*

Electric vehicle (EV) fleets could potentially be used as alternative energy sources, e.g. to power a small home for a day, thus redundancy can be obtained with the second initiative by improving the adoption of this fleet, looking at the resiliency benefits it can provide during outages. Despite the lack of power flow standards between vehicles and chargers, the idea is to make the EV infrastructure sturdy and resilient for when these standards will be available. The adoption of new storage technologies, such as batteries to add to buildings, is also considered another good action to adopt to improve grid reliability, provide emergency power to critical systems, and manage peak loads.

- *Improve backup generation for critical customers*

Critical customers, such as hospitals, nursing homes, police and fire stations, and wastewater treatment plants, should have backup generators working in-place. Less critical users, such as gas stations, pharmacies, and food supply stores, should be able to connect to backup generators, too. For this purpose, the last initiative is focused on preventing the failures demonstrated by backup generators during extreme events and reducing the impossibility of several users to connect to backup generators that utilities put in place at the time. To achieve this goal, the City proposes, among several actions, to increase the capacity to supplement the backup generator needs of different kinds of customers and to develop a generator plan to pre-wire a subset of less critical facilities to accept backup generators when needed. This strategy puts together different kind of initiatives to accomplish the goal of redundancy. It highlights the need to expand existing power generator systems and the need for new power sources to supply disrupted areas when disruptions occur, focusing on the need to guarantee the operability of systems and facilities that are considered to be critical both during normal times, but especially during emergencies. The interventions listed show that both individual customers and utilities can do something to increase the redundancy of the utility system at different scales. Several benefits of the utilities sector and of other dependent sectors can be obtained with this strategy. For example, the diffusion of alternative power sources would imply a reduction in the probability of extensive outages during hazardous events, since a certain area would be supplied by many sources and there is a low likelihood that would be disrupted all together at once. This initiative would also increase the availability of clean energy and reduce

costs, complexity, interdependencies, and inefficiencies associated with classic transmission and distribution systems, since it would guarantee more ability of isolating single customers and clusters of buildings in case of widespread power outages. EVs would reduce air pollution and increase independency from fuel, while also increasing the possibility of powering the most remote facilities. Together with storage technologies that are to be developed, they would reduce the risk of insufficient supply for high demand facilities. Finally, improving backup generators for critical customers would make different facilities more capable of restarting more quickly after a disruption to their main power systems and would make it easier for them to connect to temporary backup generators implemented for the occasion. Generally, these solutions would make several critical facilities able to perfectly perform their operations during emergencies. Hospitals and other critical infrastructures, for example, wouldn't risk being evacuated due to the failure of backup generators.

13.9.3 Initiative for Liquid Fuel

The liquid fuel sector is one of the most important sectors in the network of critical infrastructures, as well as one of the most damaged by Hurricane Sandy. Its importance is clearly demonstrated through the fact that it powers vehicles, heats buildings, fuels airplanes, works as an alternative energy source for power and steam generators, and overall provides the flexibility needed during disruptions to other energy sources. Disruptions were reported at nearly every level of the fuel supply chain, causing a wide impact on the whole network due to the high reliability of other sectors on liquid fuel. The lack of fuel supply and the consequent lines at gas stations were the most visible effects of the damage experienced by the sector. Three strategies are proposed by the government to accomplish the goal of making the sector resilient and preventing the supply disruptions that occurred because of Sandy. These strategies are:

- Seek to harden the liquid fuel supply infrastructure
- Enhance the ability of the supply chain to respond to disruptions
- Improve the City's ability to fuel first responders and private critical fleets

Each strategy focuses on one or more specific interventions that can be carried out in order to increase the overall resiliency of the liquid fuel sector. Hardening, increasing preparedness, and improving response are just some the objectives that can minimize the frequency and severity of disruptions and minimize their impacts. Overall, the initiatives proposed for the liquid fuel sectors have a broad impact on the entire network of critical infrastructure systems.

13.9.3.1 Strategy: Seek to Harden the Liquid Fuel Supply Infrastructure

The initiatives to accomplish the first strategy address the vulnerability of the fuel supply infrastructure by hardening its key assets in order to decrease disruptions and

allow for faster restoration. In order to obtain this, the municipal government wants to work with federal government and New York State to:

- Develop a fuel infrastructure hardening strategy
- Develop a reporting framework for fuel infrastructure operators
- Build pipeline booster stations in New York City
- Provide incentives for the hardening of gas stations
- Ensure that a subset of gas stations and terminals have access to backup generators in case of widespread power outages
- *Develop a fuel infrastructure hardening strategy*

New York City relies mainly on liquid fuel infrastructures located along New Jersey's coastline, which are vulnerable to the effects of coastal hazardous events, like wind and flooding. In the case of Sandy, they were the most damaged and the main cause of the widespread fuel supply shortage in the area. One of the reasons for which this happened is that the current regulatory framework does not require owners to harden their liquid fuel infrastructures against climate change. The other reason is that often they are not able to adopt the resiliency measures needed to harden their waterfront assets because they lack the necessary resources and long-term outlook. The first initiative focuses therefore on bringing together the necessary stakeholders to develop a common hardening strategy for all the infrastructures that are critical to maintain the fuel supplies in the region. This is needed because the City and State of New York have no regulatory or legislative authority on the infrastructure in New Jersey, which means they cannot control actions taken by their owners.

- *Develop a reporting framework for fuel infrastructure operators*

On the other hand, the government considers worthwhile the development of a reporting framework in order to allow infrastructure operators to better understand the actions and the challenges that must be dealt with in the aftermath of a disruptive event like Sandy. Delays in recovery and restoration efforts are also caused by the lack of updated information reported about the operational status of all the sectors infrastructures, such as terminals, pipelines, refineries, and gas stations. By developing a global IT system and information-reporting framework, it would be possible to better support post-emergency restoration and monitor the operational status of fuel facilities. This framework includes the employment of several IT systems, like automated sensors, and streamlined reporting protocols for operators, so as to increase the ability to access the most updated information needed during the emergency.

- *Build pipeline booster stations in New York City*

The third initiative is proposed because many existing pumping stations located along pipelines are not hardened against extreme weather. Pipeline booster stations ensure the pressurization of liquid fuel inside the pipelines and would allow additional fuel supply to be brought especially during emergencies, making the

management of fuel shortages easier. For this reason, one or more booster stations need to be installed and verified to be able to withstand the worst climate change impacts.

- *Provide incentives for the hardening of gas stations*

Gas stations can be considered as one of the weakest nodes of the liquid fuel sector since they are vulnerable to several threats, such as power outages, fuel shortages, and flooding. The last two initiatives mainly address their vulnerability to widespread power outages that would make fuel supply unavailable, even if the lack of fuel was shown to cause the most gas station inoperability in the aftermath of Sandy. Therefore, gas stations need to be hardened to withstand extreme weather events. Those located in critical points, such as in the proximity of controlled access roads and designed evacuation routes, are already required to be able to function during emergencies. For example, they need to enter into supply contracts for emergency generators and implement the necessary equipment to connect these generators quickly when a power loss occurs. Further hardening can be obtained with the development of effective hardening incentive programs for key retail fueling stations in vulnerable areas, which include hardening measures against flooding or other climate-related risks. These measures are not considered in the generator connection program, another effort that needs to be designed and implemented for the same hardening purpose.

- *Ensure that a subset of gas stations and terminals have access to backup generators in case of widespread power outages*

The New York State Energy Research and Development Authority (NYSERDA) is in charge of developing a generator pool program for vulnerable gas stations and creating a pre-event positioning plan. These plans can ensure the access to backup generators to a subset of gas stations and terminals and the faster deployment of generators to impacted areas immediately after a disaster. As seen, the goal of hardening can be achieved both with physical interventions, like the installation of booster stations to increase supply, and with several upgrade programs and plans, like the generator connection program, that have to be planned and put in place. This means that not only the actual liquid fuel infrastructures have to be strengthened but a review of the actual regulatory framework is also needed. This would prevent the liquid fuel sector from failing during future disruptive events and would help operators to better control and manage their infrastructures. Moreover, the strategy shows the dependency of New York City on liquid fuel infrastructures located in New Jersey, highlighting that both States and their governments have to collaborate in the development of a common hardening intervention approach. Due to the high number of assets that would need to be strengthened, the focus is on those considered to be critical during emergencies because of their geographical position. Hardening the fuel supply infrastructures would reduce the need to import fuel from abroad and thus the extra costs that this entails. The strategy would reduce the recovery time in several ways: by improving the ability to control fuel infrastructures, and consequently speeding up the intervention to damaged ones;

by improving communication among several operators; and by reducing the extent of damage that can occur to fuel assets. Moreover, if updated information were more accessible, owners would be more able to understand the emergency actions to take in the immediate aftermath and thus optimize the deployment of repair crews. This means that repair crews would waste less time waiting to know where to go or waiting for other interventions that have priority, thus they would be able to restore more places at the same time. Booster stations would increase the ability to import fuel during emergencies, which means more fuel available in these situations and consequently shorter lines at gas stations. Finally, incentives programs would increase the willingness of petrol companies to harden their assets and the availability of backup generators to run in order to maintain gas stations operations. It is clear that the other dependent sectors would benefit from this strategy too, in particular the transportation sector. Regular and temporary transportation services put in place would work with the usual number of customers and wouldn't be overcrowded because most of the people would be able to fuel and use their own cars. Traffic would be normal, less congestion would be reported in the proximity of gas stations, and less fuel trucks would circulate to cover the disruption of the usual fuel supply chain. Airport activities wouldn't be delayed because of the unavailability of fuel to pump into airplanes. Limited fuel shortages also mean that more power plants would be able to function, as well as more backup generators to run buildings and other facilities and heating oil could keep homes warm and water hot.

13.9.3.2 Strategy: Enhance the Ability of the Supply Chain to Respond to Disruptions

This strategy focuses on the need to improve the response of the fuel supply chain during and after extreme events that can cause its disruption despite the hardening focused on in the previous strategy. The lack of redundancy and market flexibility needed to respond to such disruptions slowed down the restoration of fuel supply. They can be addressed through market and regulatory changes, which are focused on by the following initiatives:

- Creation of a transportation fuel reserve
- Modification of price-gouging laws and increase of flexibility of gas station supply contracts
- Development of a package of City, State, and Federal regulatory actions to address liquid fuel shortages during emergencies
- *Creation of a transportation fuel reserve*

The goal to reach with the first initiative is to temporally supply the private market during disruptions. For this purpose, several entities are involved in the evaluation of feasibility and cost of the creation of a transportation fuel reserve. This program also allows the support of restoration and relief efforts in the event of widespread disruption to the fuel supply chain.

- *Modification of price-gouging laws and increase of flexibility of gas station supply contracts*

The second initiative addresses two issues that came up in the circumstances of widespread disruption of fuel supplies. The first one is the lack of clarity in New York State price-gouging laws, which results in the unwillingness of retail fuel station owners to raise prices after a disruption to pay for out-of-the-region supplies. The solution to this problem is to allow and control the increase in prices during fuel supply emergencies, while still ensuring fair pricing. The second one refers to the contractual obligations that prevent station owners from temporarily sourcing fuel from different suppliers. This other problem can be solved by including a “force majeure” clause in fuel supply contracts to let franchised stations to temporarily supply fuel from any wholesaler if the retailer’s usual suppliers are unable to deliver. Overall, the initiative aims to increase fuel availability during disruptions, and specifically to also cover the additional transportation costs to bring fuel into the city during a liquid fuels shortage.

- *Development of a package of City, State, and Federal regulatory actions to address liquid fuel shortages during emergencies*

The last initiative of this strategy highlights the need to change various regulations relating to the transportation and consumption of fuels in New York City that limit the flexibility of the market when responding to disruptions. There are multiple objectives: to quickly mitigate the supply-demand imbalances in the fuel supply, to allow foreign-flagged ships to deliver fuel into the region, to bring and sell within the city fuel that is normally consumed upstate and elsewhere, and to use heating fuel to power vehicles. In order to achieve these goals, a fuel-rationing plan has to be developed and regularly maintained, as well as a package of regulatory waivers and modifications to implement immediately after the declaration of a liquid fuel shortage. This strategy is proposed because the fuel supply chain showed to be unprepared to withstand and respond to the impact of Sandy. Each initiative proposes a specific solution to fuel shortage, aiming to increase preparedness to future disruptions, as evidenced by the creation of a fuel reserve, or market flexibility and redundancy, as reported by the other two initiatives. Moreover, the first initiative would surely reduce the dependence on imported fuel and increase the ability to withstand long-term widespread supply disruption through more fuel available to use during this time. It would also allow for a faster deployment of fuel to critical users, thus reducing their disturbance and increasing their ability to intervene during emergencies. Overall, through the several actions listed, the strategy would increase the availability of fuel in the aftermath of disruptive events and would affect the other sectors in several ways. For example, the transportation of goods and the entire food supply chain, as well as the deployment of utility repair crews, would not be delayed. Furthermore, transportation services that require fuel to work (buses, planes, etc.) would not be limited due to fuel rationing and water and wastewater services would not be interrupted.

13.9.3.3 Strategy: Improve the City’s Ability to Fuel First Responders and Private Critical Fleets

Fuel supply must always be guaranteed for first responders and private critical fleets that are fundamental for emergency response, infrastructure rebuilding, and disaster relief, so as to avoid a lack of emergency management that can cause the amplification of the impact on the community. The only initiative proposed for this strategy is to:

- *Harden municipal fueling stations and enhancing of mobile fueling capability*

This initiative is needed to guarantee continued service to City, government, and critical fleets and to by-pass the regular supply chain. These goals can be obtained by using the municipal network of gas stations and mobile fueling trucks during a widespread disruption to the retail liquid fuels market. The use of additional equipment that can also be quickly deployed everywhere (mobile fueling trucks, generators, light towers, forklifts, water pumps) can provide the mobile fueling capability needed to run emergency fueling operations immediately following a disruption in the supply chain. Furthermore, other options can be evaluated for sourcing fuel to first responders and critical fleets during emergencies, so as to ensure that the municipal fuel supply is not used for them. By providing fuel to these fleets through the several ways listed, the strategy would improve the ability of local and national institutions of intervention and the management of emergency situations, preventing them from being slowed down by the disruption of the usual fuel supply chain, as normal users would be. For example, emergency vehicles would be able to regularly respond to emergencies, doctors and nurses who treat patients would not be delayed, and the overall restoration of other critical infrastructures would not be delayed.

13.9.4 Initiative for Transportation

The New York region’s transportation network is considered to be the largest public transportation system in the U.S. and is demonstrated to be one of the most impacted along Sandys path, as well as the one that influenced and delayed the peoples and communities return to normality in general. A highly dense network of infrastructures, made up of busy highways, railways, ports, bridges, tunnels, etc., provides mobility to millions of people that visit, live, and work in the region, giving them the option to use their own vehicles or several public transportation systems, such as buses, trains, subways, ferryboats, etc. These systems are also heavily used by commuters to travel to/from and move inside New York City for all of their activities. The sectors area infrastructures are old, unreliable, in need of improvements and, because of their geographical position, vulnerable to disruptions that could be caused by many extreme events, such as flooding and wind. Sandy itself caused several damages to vehicular tunnels, subway stations,

roads, and airports, and lead to an extensive transportation outage that affected 8.5 million public transit riders, 4.2 million drivers, and 1 million flyers, as reported by the New York City government report. Generally speaking, extreme events like Sandy demonstrated the importance of the transportation system to the city's economy and overall ability to function. Given the size and complexity of it, the goal of resiliency represents a major challenge. Several initiatives are proposed to make the transportation system more resilient, focusing on upgrading the existing infrastructures and improving the reliability of its systems. These initiatives are organized according to the following strategies:

- Protect assets to maintain system operations
- Prepare the transportation system to restore service after extreme climate events
- Implement new and expanded services to increase system flexibility and redundancy

13.9.4.1 Strategy: Protect Assets to Maintain System Operations

The first strategy aims to increase the protection of existing infrastructures by implementing interventions to restore and harden them against damages and loss of service. The initiatives to account for this objective are:

- Reconstruction and resurfacing of key streets damaged by Sandy
- Integration of climate resiliency features into future capital projects
- Elevation of traffic signals and provision of backup electrical power
- Protection of NYCDOT tunnels from flooding
- Installation of watertight barriers for mechanical equipment of bridges
- Protection of Staten Island Ferry and private ferry terminals from climate change-related threats
- Integration of resiliency into planning and project development
- Implementation of protection strategies to address climate change threats
- *Reconstruction and resurfacing of key streets damaged by Sandy*

Several roadways were damaged in varying degrees by wave action and flooding generated by Sandy, leading to building inaccessibility and the interruption of transportation services. These damages were the most visible impact of the storm on the transportation systems, because they were also reported from several locations. In order to address these damages and prevent future ones in road infrastructures, the streets that reported serious damages have to be reconstructed or repaired following upgraded resiliency measures. On the other hand, some may only need to be resurfaced because of underlying structures still in good condition. The New York City Department of Transportation (NYCDOT) was in charge of reconstructing 60 lane-miles and resurfacing 500 lane-miles of streets damaged by Sandy.

- *Integration of climate resiliency features into future capital projects*

The current roadway network is vulnerable to several threats, such as surface flooding from heavy downpours, wave action from storm surge, and asphalt damage from heat waves. The overall impact of these threats can be mitigated with the adoption of several storm water management best practices and tools. These include, for example, the raising of street grades and bulkheads and the installation of pre-cast permeable concrete gutters and bioswales (planted areas in the sidewalk designed to capture stormwater from the adjacent roadway). The adoption of these measures allows water captured on the streets to soak into the ground rather than flow into the sewer system. Many others climate resiliency features can be considered for the development of future capital projects.

- *Elevation of traffic signals and provision of backup electrical power*

The most critical assets for the management of the transportation network are the traffic signals. The third initiative focuses on their protection against damages from flooding and power losses caused by several extreme events. The goal is to maintain the roadway network operational efficiency and avoid the placement of New York City Police Department (NYPD) traffic agents to control traffic. In order to achieve these objectives, controllers and electrical hardware vulnerable to flooding need to be raised and possibly placed above the 100-year flood elevation (flooding has 1 % of probability of occurrence per year). For a more immediate intervention when power outages occur, NYPD vehicles could be provided with power inverters to be used as alternative power sources for critical traffic signals.

- *Protection of NYCDOT tunnels from flooding*

Road and rail tunnels were among the most damaged transportation infrastructures by the storm. NYCDOT, Amtrak, and MTA tunnels under the Hudson and the East River were flooded and reported remarkable structural and equipment damage. Therefore, there is the need to reduce their vulnerability to flooding from storm surges and heavy downpours. To achieve this goal, several flood protection strategies can be put in place, e.g. tunnel entrances and ventilation structures can be raised above flood elevations and floodgates can be installed at tunnels entrances and closed at the occurrence. These actions would therefore provide protection from water infiltration and from damage to sensitive mechanical and electric equipment and overall prevent the disruption of these critical assets of the transportation network.

- *Installation of watertight barriers for mechanical equipment of bridges*

On the other hand, the bridges withstood the impact of Sandy well. Despite this evidence, their mechanical equipment is still vulnerable to flooding. This equipment controls the opening/closure of bridges needed to provide a clear path for marine traffic, thus damages occurring to it could block the bridges in either one of the two positions, impacting marine or roadway traffic. The solution proposed is

the installation of watertight barriers to protect movable bridge machinery and to prevent the occurrence of this situation, so as to ensure the proper functioning of these critical crossings.

- *Protection of Staten Island Ferry and private ferry terminals from climate change-related threats*

The last initiative that directly addresses the risk of flooding focuses on the protection of ferry services that, due to their nature/geographical position, are vulnerable to disruptions and damages caused by flooding and wind. Several actions can be put in place to avoid the consequent service suspension and reduction of mobility and to allow quicker service restoration. On one hand, physical improvements can be carried out on several terminal infrastructures. On the other hand, critical equipment of these facilities can be protected, e.g. waterproofing or relocating them.

- *Integration of resiliency into planning and project development*

Climate adaptation and resiliency are not considered critical factors in planning, funding, and developing capital projects that address the vulnerability of the city's transportation network to climate change. These factors need to be included and prioritized in the federal legislation funding surface transportation. Moreover, there is the need for a joint planning for resilience and climate adaptation among the various transportation agencies in the region, in order to avoid duplicate investments.

- *Implementation of protection strategies to address climate change threats*

Another way to address climate change threats is to increase transportation system flexibility, whose critical assets otherwise could remain vulnerable to damage and disruption from future events. Therefore, a comprehensive implementation of appropriate investments in resiliency and protection strategies across all transportation systems is needed to ensure their protection against the aforementioned threats, as well as their preparedness for quick restoration. Transportation agencies are called to implement hardening and preparation measures to protect several infrastructures (vehicular, rail and subway tunnels; bus depots, terminals, and other facilities that are critical to providing bus service; rail, subway yards, and other facilities that are critical to providing rail service; runways, lighting systems, navigation systems, terminal buildings, and other airport facilities; port and marine facilities) and to also support projects to expand the flexibility and redundancy of the transportation network. (These projects include the Amtrak Gateway Project; the extension of the MTA New York City Transits seven subway line to New Jersey, or alternatives that would significantly expand cross-Hudson commuting capacity; transit improvements along the North Shore of Staten Island; and extension of Metro-North Railroad service to Penn Station.) As seen, the strategy focuses mostly on physical measures needed to protect and harden existing infrastructures. The initiatives included mainly address the risk of flooding of several vulnerable assets that were not originally designed taking this risk into account. Some of these

initiatives refer only to the protection of specific transportation infrastructures and equipment, while others are thought to have a broad application to the entire sector, like the last two. Each initiative focuses on addressing something specific to reduce the sectors vulnerability, like the need to upgrade existing assets or increase the flexibility of the whole sector.

Overall, the strategy leads to several benefits. For example, by upgrading the existing infrastructures through the interventions considered by the first and second initiatives, the impact of future events causing mobility disruption would be surely reduced, as more roads would satisfy the resiliency requirements, would not be flooded, and thus would be able to withstand such events. At the same time, the accessibility to damaged areas in need of repair would be increased. The elevation of critical assets would surely reduce traffic congestion, allow for the deployment of police officers where actually needed (i.e. not controlling traffic), and speed up the restoration of traffic management services. Actions conceived for tunnels and bridges would guarantee mobility especially during recovery phases, reducing congestion in other access points, and also reducing the amount of equipment that has to be replaced, allowing for a faster reopening of crucial infrastructures. Many other sectors would benefit from this strategy too. Utility repair crews would not be delayed by closed roads and consequent detours, as well as emergency services (ambulance, police, firefighters, etc.). Damaged buildings would be reached and repaired faster. Waste service would continue its operation, and thus prevent the accumulation of waste, causing further problems. Food delivery to major and minor customers would not be delayed by a lack of access to warehouse and delivery locations. Fuel would be delivered to gas stations and other critical users faster.

13.9.4.2 Strategy: Prepare the Transportation System to Restore Service After Extreme Climate Events

The second strategy focuses on increasing redundancy, preparedness, and the ability for a quick response following a disruption, listing a series of initiatives that mostly regards temporary services to restore mobility and specific assets of the transportation system. In fact, its extent, complexity, and age make challenging to act with an overall intervention. For these purposes, the government proposes to:

- Plan for temporary transit services in the event of subway system suspensions
- Identify critical transportation network elements and improve transportation responses to major events through regular resiliency planning exercises
- Implement High-Occupancy Vehicle (HOV) requirements
- Plan for and install new pedestrian and bicycle facilities
- Construct new ferry landings
- Deploy the Staten Island Ferrys Austen Class vessels on the East River Ferry and during transportation disruptions
- Improve communication about the restoration of transportation services

- *Plan for temporary transit services in the event of subway system suspensions*

The forecasted impact of Sandy on the transportation system led, among others, to the total shutdown of the subway system for the entire length of the storm and the provision of limited service for the few days following. The subway system usually runs non-stop, 24 h a day, 365 days a year, and provides most of the transportation network capacity. As a consequence, its partial or total suspension brings this capacity to a reduction, and the rest of the regular network cannot handle the resulting increased volume of commuters and other travelers. Temporary transit services can be adopted to address this reduction of transit capacity. The initiative proposes the development and regular updating of temporary transportation plans, such as those regarding several services like high-capacity bus bridges, already successfully implemented during Sandy, point-to-point ferries, dedicated bus lanes, and necessary enforcements to adopt for the time needed. To understand the best type of temporary services needed in every situation, it is recommended that companies identify and study potential threats and their impacts on their infrastructures and evaluate the level and type of support they could provide. Another solution is to allow temporary access to other transit service through cross-honoring. This solution is often adopted during several transit service disruptions and has been proven to relieve system stress. Overall, the initiative aims to provide alternative mobility options during the partial or total suspension of the transportation system.

- *Identify critical transportation network elements and improve transportation responses to major events through regular resiliency planning exercises*

The second initiative aims to improve the response of transportation agencies to several possible transportation outages and restoration scenarios and to allow them to understand where to focus their resources in the different stages of emergency management. This need is highlighted by the vulnerability to disruption and the damage of critical transportation facilities that are needed during disaster response. Their interruption can potentially delay the delivery of emergency services, the supply of goods, and the restoration of critical non-transportation infrastructures and economic activity. To avoid this, transportation agencies and other stakeholders have to work to identify the critical elements of the network that have to be quickly available following different types of events. This can be done, for example, through a series of detailed and multi-disciplinary resiliency planning exercises, including live drills. Focusing on these elements, resiliency investments can be prioritized and response can be improved.

- *Implement High-Occupancy Vehicle (HOV) requirements*

The use of HOV lanes is an effective way to reduce the volume of circulating private vehicles. Especially when extended transportation disruptions occur, this volume can overwhelm road capacity (which may already be reduced by damages) and create gridlocks. The requirement adopted by New York City immediately after Sandy was that vehicles entering the city needed to have three or more occupants, while, at the time, HOV lanes permitted only vehicles with a minimum of two

passengers. Given the positive results exhibited during the storm, the idea is to develop standard protocols for the implementation of HOV requirements in the occasion of similar disruptions to the transportation network. This also implies the establishment of minimum conditions that must be satisfied in order to adopt these protocols and other details, such as their exemptions.

- *Plan for and install new pedestrian and bicycle facilities*

Another initiative created to provide additional capacity during subway interruptions focuses on the expansion of pedestrian and bicycle paths, which were overwhelmed by the extra number of people walking and biking due to this disruption. To overcome this problem, several actions can be undertaken, such as the deployment of temporary facilities to increase pedestrian and bicycle capacity in the event of an emergency situation and the expansion of the bike-sharing network to cover the areas vulnerable to transportation interruptions. Overall, the initiative proposes to improve connectivity to key transportation hubs through transportation options that do not rely on electricity to function.

- *Construct new ferry landings*

Waterways can be used as alternative methods of providing mobility when emergencies and other events occur and disrupt regular land transportation services. The initiative focuses on the expansion of the network of ferry landings available for both regular and emergency use in order to provide a more dense transportation service via water. This goal can be achieved in several ways: on one hand, through the design and deployment of ferry landing barges as temporary landings, in order to provide basic ferry service to potential locations vulnerable to climate-related transportation interruptions; on the other hand, by designing new mobile permanent ferry landings that can be temporarily relocated to provide alternative transit services where needed. In this way, private and emergency ferry services are enhanced and made available during extreme events.

- *Deploy the Staten Island Ferrys Austen Class vessels on the East River Ferry and during transportation disruptions*

The Staten Island Ferrys Austen Class vessel is a type of boat that can carry 10 times the number of passengers of a typical East River Ferry. As it can be seen, this initiative specifically refers to the context of New York City, but it can surely be considered in other circumstances where there is a similar level of service. This vessel can be deployed during transit service disruptions that cause large numbers of commuters to use ferry services in order to supplement the increased demand that otherwise would exceed the capacity of typical private ferry vessels.

- *Improve communication about the restoration of transportation services*

The last initiative focuses on the need to improve the reliability of communication between the several agencies involved in the restoration process and the general public. The lack of reliable information during and immediately following an emergency situation can lead to additional unreliable communication

and considerable confusion. The goal is to provide accurate and trustworthy information, for example, to truck companies and drivers about detours to follow during emergencies, in order to minimize their impact on sensitive infrastructures and to facilitate the safe, fast, and efficient delivery of relief supplies. For these purposes, standardized communication protocols need to be developed for use during transportation disruptions in order for agency stakeholders and the public to receive proper information regarding system status and interim measures. As seen, the strategy's goals can be achieved through different measures. Several transportation systems are in need of interventions to increase their ability to withstand extreme events. The strategy highlights how the entire transportation network can suffer from the suspension of one or more of these systems, but also how there are several actions that can be taken to make up for it. The last initiative, in particular, shows how distribution of information has a key role in the development, adoption, and effectiveness of the temporary solutions suggested. The importance of waterways as alternative transportation, which, because of this, need to be reinforced, is something that can be considered in other contexts rather than NYC, despite one initiative being written specifically for ferry transportation in the New York Harbor. Overall, the strategy would increase the preparedness of all the agencies involved in the management of these events. Through the several temporary transportation services listed, it would be possible to maintain service capacity in certain directions, especially for users who do not own a car, and prevent the overcrowding of regular transportation services that are still functioning. As a result, less people would be forced to use their own cars, and thus less accidents would take place due to, for example, unfamiliar drivers who are not used to the traffic. Resiliency planning exercises would increase agencies preparedness for several extreme events, as well as their ability to adopt emergencies actions and thus reduce the time needed to restore critical infrastructures. The installation of new pedestrian and bicycle facilities would provide an incentive for the use of these alternative transportation systems during a disruption of the regular ones and would reduce the overcrowding of existing bike and pedestrian paths. Finally, buildings and health care facilities would be accessible as usual, since temporary service would still guarantee people access to them, and emergency services and supplies of food, fuel, and medicine would not be impaired by transportation disruptions. Overall, the restoration of several other critical infrastructures and economy activities would not be delayed.

13.9.4.3 Strategy: Implement New and Expanded Services to Increase System Flexibility and Redundancy

The last strategy focuses on the expansion of several temporary transportation services that demonstrated to be effective for the entire transportation network in the aftermath of Sandy, preventing other means of transportation from being overwhelmed. As seen in its title, the strategy seeks to increase flexibility and redundancy to increase the networks overall resiliency to a variety of weather events

and other emergency situations, in addition hardening existing assets and creating additional capacity and responsiveness. To achieve these goals, this strategy includes three initiatives:

- Expand the city's Select Bus Service network
- Expand the network of bus priority strategies on arterial highways
- Expand ferry services in locations citywide
- *Expand the city's Select Bus Service network*

The Select Bus Service (SBS) is a bus service designed by MTA to specifically address general mobility challenges by reducing travel time and increasing customers level of comfort. The SBS network is made up of several corridors that cover portions of the city that are not directly served by subway service. These routes represent the backbone of the alternative high-capacity bus service network, which accounts for the reduction of capacity following subway disruption, and include what are also known as high-capacity bus bridges. Therefore, a significant expansion of the current SBS network, with the addition of several new routes, would allow for an increase in the efficiency of this service.

- *Expand the network of bus priority strategies on arterial highways*

Congestion on the region's highways reduces regular mobility and, above all, can slow recovery efforts put in place during emergency situations. Bus priority strategies for express, local, and intercity buses represent a solution to account for this problem. These strategies include solutions such as median bus lanes and the use of shoulders for bus traffic. The idea is to expand the current network with the creation of 15 new miles of these bus priority corridors on major arterial highways as they are improved or reconstructed. The goal of the NYC government is to implement these strategies as soon as possible.

- *Expand ferry services in locations citywide*

Ferry services provide an additional transportation option especially during other transit services disruption. However, they are vulnerable to damages suffered by key crossings, which can therefore limit waterway movement. To address this problem, the last initiative focuses on the expansion of current ferry service beyond existing routes, to guarantee service in critical locations in the city. The strategy proposes to expand already existing transportation services that proved to be useful during the reduction of transportation capacity. Despite the reliability of the entire transportation network, during its disruption, alternative mobility options must be taken into account, otherwise the impact of the disruptive event is further amplified. Overall, the strategy brings several benefits to the transportation sector. For example, the first of the two initiatives designed for bus service would increase its capacity during unusual service interruptions, similar to the subway interruption, and would increase and guarantee mobility to areas that can only be reached by certain transportation services. On the other hand, the second initiative would increase bus service reliability, due to its independence from local traffic. It would also allow

for faster movement of buses along critical roadways and a reduction of transit service congestions along them. Finally, the last initiative would increase the ability to use waterways as an alternative to regular transportation service. The strategy would also reduce the impact of transportation disruption on other sectors. Several businesses, e.g. food services, would suffer less economic loss, as people would be able to reach certain places despite the emergency situation. Critical buildings and health care facilities located close to waterways could also be reached by water more easily and quickly.

13.10 Summary and Remarks

Each community has to develop a resilience plan from its unique perspective. This involves accounting for the risk toleration, anticipation of provided services, and the planning process which are all specific to the community. The success and endurance of a community plan depends on its unique adaptations. In order for a plan to be developed and implemented in a community, it requires extensive support. The resilience target isn't necessarily expensive, but for each community the process is different and will take time to implement and to see results. A resilient community is achieved through maintenance and on-going efforts. The process involves intensive planning, aiming at a combination of mitigation before the hazardous event, along with phases of emergency response, restoration and long-term reconstruction after the occurrence of the event. The process of achieving disaster resilience requires concentration, persistence and efforts to understand the current social institutions, governance, economics, the buildings, and infrastructure systems and their effectiveness, as well as the consequences that the occurrence of a hazardous event would cause. The basis of resilience planning is formed by the intersection of community daily needs and the anticipated damage from hazardous events. Communities are currently making efforts to reduce threats and vulnerabilities through adoption and enforcement of codes, standards, and regulations, as well as exercising preparedness, mitigation, emergency management and codes and standards-based design. These activities are necessary and prudent, but they are not enough to make a community resilient. Proper community resilience also requires that the built environment can sustain acceptable levels of functionality during and after events. Therefore, there should be a specified time frame for which communities have developed the plans to recover the built environment to its full functionality. The recovery times are determined by the function and importance of each facility or system within the community and the extent of disruption that the facility can tolerate and still remain functional. During an emergency, short term plans and interim solutions can be developed for implementation, if the event occurs tomorrow. In the long term, plans will provide the roadmap for eventually achieving disaster resilience. This process begins with the vision of a better outcome, a better understanding of your community, the development of a resilience plan, and the initiation of the implementation.

References

- APA (2014) Planning for post-disaster recovery: next generation. American Planning Association, Washington, DC
- ASCE_7-10 (2013) Minimum design loads for buildings and other structures (ASCE/SEI 7–10). American Society of Civil Engineers, Reston, p 636
- CARRI (2013) Community and regional resilience institute, community resilience system. <http://www.resilientus.org/recent-work/community-resilience-system>
- FEMA (2011) Fema p-154 rover cd, rapid observation of vulnerability and estimation of risk. Report, Federal Emergency Management Agency
- NIST (2015) Community resilience planning guide for buildings and infrastructure systems. Report, National Institute of Standards and Technology
- Nkala DMV, Helena Graziosi A (2010) Local governments and disaster risk reduction: good practices and lessons learned. Report, United Nations International Strategy for Disaster Reduction (UN/ISDR)
- NRC (2012) Disaster resilience: a national imperative. National Research Council, The National Academies Press, Washington, DC
- Pelling M, Holloway A (2006) Legislation for mainstreaming disaster risk reduction. Report, TEARFUND. www.tearfund.org
- Petal M (2007) Disaster risk reduction education: material development, organization, and evaluation. Reg Dev Dialogue J 28:1–25
- SPUR (2009) The dilemma of existing buildings: private property, public risk. Report, San Francisco Planning, Urban Research Association, 1 Feb 2009. www.spur.org
- Twigg J (2007) Characteristics of a disaster-resilient community – a guidance note. Report, DFID Disaster Risk Reduction Interagency Coordination Group
- UNDP (2014a) Effective law and regulation for disaster risk reduction: a multi-country report. Report, United Nation Development Program & International Federation of Red Cross and Red Crescent Societies
- UNDP (2014b) New Zealand: country case study report – how law and regulation support disaster risk reduction. Report, United Nation Development Program & International Federation of Red Cross and Red Crescent Societies
- UNDP (2015) The checklist on law and disaster risk reduction (pilot version, march 2015). Report, United Nation Development Program & International Federation of Red Cross and Red Crescent Societies
- UNDP_&_IFRC (2014) New Zealand: country case study report – how law and regulation support disaster risk reduction. United Nation Development Program & International Federation of Red Cross and Red Crescent Societies, Geneva
- UNDP_&_IFRC (2015) The checklist on law and disaster risk reduction (Pilot version, Mar 2015). United Nation Development Program & International Federation of Red Cross and Red Crescent Societies, New York
- UNISDR (1994) Yokohama strategy and plan of action for a safer world, guidelines for natural disaster prevention, preparedness and mitigation. In: World conference on natural disaster reduction, Yokohama, 23–27 May, 1994
- UNISDR (2004) Living with risk: a global review of disaster reduction initiatives. Report, United Nations International Strategy for Disaster Reduction (UN/ISDR)
- UNISDR (2009) 2009 UNISDR terminology on disaster risk reduction. Report, United Nations International Strategy for Disaster Reduction (UN/ISDR)
- UNISDR (2011a) Third session. In: Global platform for disaster risk reduction and world reconstruction 2011, Geneva. United Nations International Strategy for Disaster Reduction (UN/ISDR)
- UNISDR (2011b) Towards a post-2015 framework for disaster risk reduction. Report, United Nations International Strategy for Disaster Reduction (UN/ISDR)

- UNISDR (2013) Making cities resilient: summary for policymakers, a global snapshot of how local governments reduce disaster risk. Report, United Nations Office for Disaster Risk Reduction (UNISDR)
- UNISDR (2015) Sendai framework for disaster risk reduction 2015–2030. *Aust J Emerg Manag* 30:9–10
- Wisner B, Blaikie P, Cannon T, Davis I (2006) *At risk: natural hazards, people's vulnerability, and disasters*. Taylor & Francis Group/Routledge, London

Chapter 14

Computational Tools and Software for Resilience Assessment

Abstract The first part of the chapter describes the current commercial software and research tools available in literature to assess resilience of critical infrastructures against extreme event. The second part of the chapter focuses on the comparison of different virtual city simulators considering their capability to model different types of infrastructures, hazards and their visualization capabilities.

14.1 Introduction

A complete overview of commercial software is presented in this chapter. The software are used in the field of seismic engineering to analyze the system behavior when subjected to extreme events. Each of them is capable of operating in a specific direction, and is focused on a particular objective:

- **RISe for SELENA.** This software is able to analyze and evaluate the seismic risk and the losses using the capacity spectrum method. In particular, RISe (Lang and Corea 2010) allows plotting on a Google Earth map, the results obtained using SELENA.
- **REDARS** (Werner et al. 2006). This software is used for analyzing a highway network and takes into consideration both bridges and traffic flow data. It provides information about changes in the network conditions due to a simulated disruption.
- **HAZUS** (Whitman et al. 1997; FEMA 2001). It is the most articulate software which is able to work on a multilevel layer configuration. Furthermore, It takes into account possible interconnections between different lifelines and buildings.
- **GIRAFFE** (GIRAFFE 2008). It offers assistance in understanding problems related to lifelines. It is able to model and manage disruptions on the hydraulic network.
- **OpenQuake.** The idea behind the software is making the Global Earthquake Model Foundation (GEM) a uniform, independent standard for calculating earthquake risk worldwide.
- **EQVIS.** This is an advanced seismic loss assessment and risk management software developed in the SYNER-G project. The SYNER-G project is a

European collaborative research project focusing on systemic seismic vulnerability, buildings risk analysis, transportation, utility networks and critical facilities.

- **ResilUS** (Miles and Chang 2011). It is limited to buildings and lifelines (transportation network, electrical network, water supply, and critical facilities) and uses a macro-sub division of the area contained within a broader community such as the neighborhood subdivision. Then it subdivides the community into three elements which are: the physical built environment, economics, and humans (i.e., health).

In the following paragraphs a detailed description of each software is provided.

14.2 RISE and SELENA Software

Predicting the consequences of an earthquake is important for several reasons. Nowadays, a vast number of software tools are available for estimating physical building damage and associated losses. SELENA is an open-source software tool Molina et al. (2009) for computing seismic risk, economic and human losses. It has been developed by the International Center of Geohazards (ICG), through NORSAR. Its name is the acronym of **SE**ismic **L**oss **E**stimation using a logic tree **A**pproach and makes use of the capacity spectrum method (CSM). SELENA is based on C programming language and to make the input process as transparent and comfortable as possible, both the input and the output are plotted to the main part of the GIS (Geographic Information Systems) systems, so the user can apply his preferred program. Experience has proven that it can be difficult to implement maps with GIS, and to solve this difficulty, RISE (**R**isk **I**llustrator for **S**elena) has been developed. RISE is a open-source software tool free of charge which can convert SELENAs input and output into KML files, the ones used by Google™ Earth, so it is possible to illustrate the results with Google™ Earth.

14.2.1 Step-by-Step Procedure Using RISE and SELENA

Figure 14.1 shows that SELENA is used as a pure computational tool, while RISE illustrates the geo-referenced information in input and output files. Different steps must be followed:

1. Boundary of Geographical Districts for Aggregation with Google™ Earth. SELENA considers the minimum geographical unit as the smallest area unit, which can be *building blocks* or *city districts*. The size of each unit (geo-unit) depends on several factors, such as the soil conditions and the topography. It is necessary to define the center points (centroids) and borders of each geo-unit by using the place mark and polygon tools available in Google™ Earth.

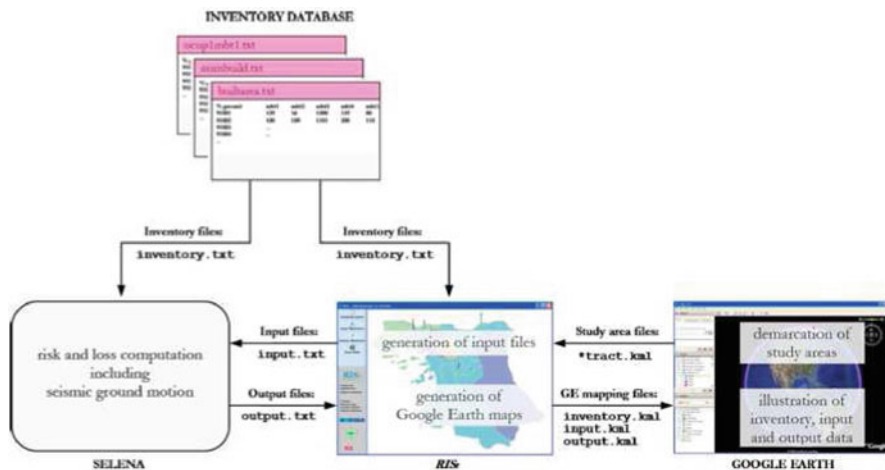


Fig. 14.1 SELeNa and RISEs flow chart (Illustrates the integration of RISE into a seismic risk and loss analysis. RISE is basically an intermediary tool between SELeNa and Google™ Earth to support in the preparation of input file, KML files generation, inventory and output files)

Table 14.1 Soil classification according to the NEHRP provisions (FEMA 1997) used by the international building IBC-2006 (ICC IBC 2015)

Index	NEHRP site class	Site class description	Shear-wave velocity $v_{s,30}$ [m/s]
1	A	Hard rock	>1500
2	B	Rock	760–1500
3	C	Very dense soil and soft rock	360–760
4	D	Stiff soil	180–360
5	E	Soft soil	<180

2. Generation of Input Files with RISE. The files referring to the centroid and boundaries generated with Google™ Earth can be used with SELeNa as input data. Therefore, it is possible to categorize near-surface soil conditions. Soil amplification factors are associated with each geo-unit depending on its soil class (Table 14.1).
3. Computation of Risk and Losses with SELeNa, as ground-motion values, damage probabilities, absolute building damage, casualties and economic losses.
4. Generation of Google™ Earth Mapping Files. RISE automatically recognizes files containing geo-reference data and it illustrates them. Different mapping types are required to illustrate input and output, since the number of input and output files which are suitable for conversion differs from case to case.

The three different types of mapping are

- Color-Shaded plot. A single data type can be plotted for each geographical unit, for example soil class information or ground motion values (Fig. 14.2).

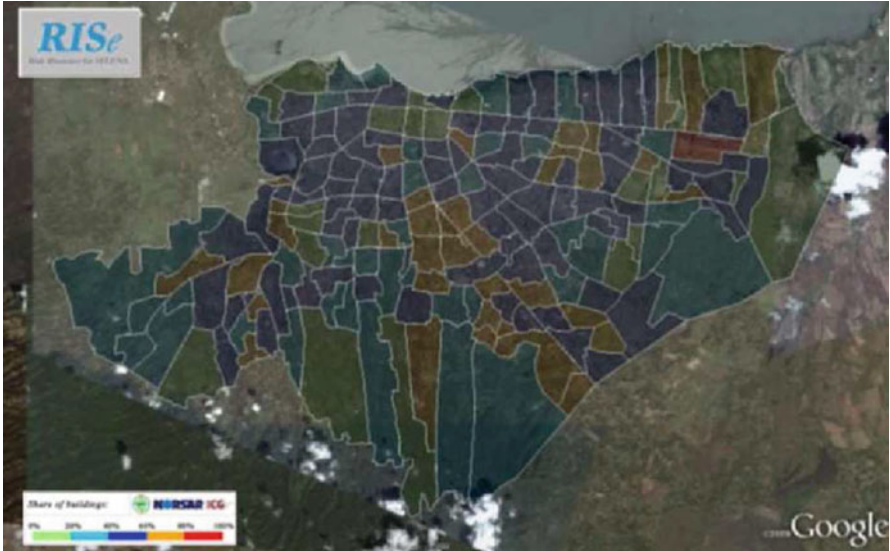


Fig. 14.2 Color-shaded plot

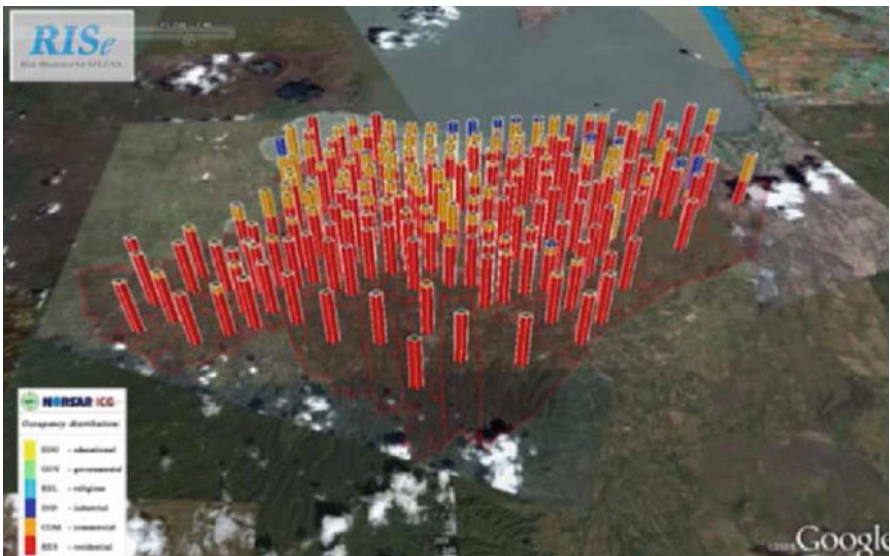


Fig. 14.3 Normalized bar-chart plot

- Normalized bar-chart plot. Mapping type to illustrate the shares of the main occupancy types or damage probabilities in the five different damage states. The heights of the column are identical and represent 100 % of cumulative damage probability (Fig. 14.3).

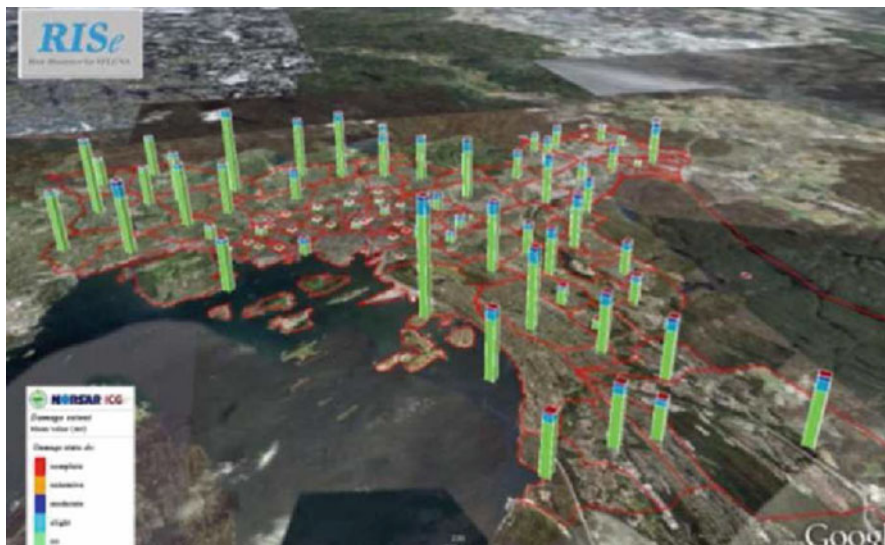


Fig. 14.4 Absolute bar-chart plot

- Absolute bar-chart plot. Mapping type for illustrating absolute values of risk and loss results in the five different damage states. The heights of the columns are different and represent the amount of damage, economic loss or casualties in the respective geographical unit (Fig. 14.4).

14.2.2 Seismic Risk and Loss Assessment Using RISE

The graphical representation of seismic risk and losses allows us to detect possible errors in input data or computation process. For large inventory databases, this option is important due to its vast number of geographical units, building types and occupancy classes.

The two-dimensional color-shaded maps (which can have different projection angles) are especially used for mapping of inventory and input files, and for the output files containing ground-motion parameters.

On the other side, the bar-chart maps are especially customized to illustrate the SELeNa output files, in particular the damage and loss results. Seismic risk and loss assessment software SELeNa commutes physical building damage estimates for different states of damage, classified into the five damage states: *none*, *slight*, *moderate*, *extensive* and *complete*, as defined by HAZUS.

These generalized damage limit states are used by SELeNa to describe structural damage as a measure of building deformation under lateral earthquake loading. The representation of the output can be provided using a three-dimensional bar-chart

map. The total height of the columns depicts cumulative damage probabilities for the five different damage states mentioned above, allowing the user to quickly recognize regions where one particular building typology may undergo higher damage.

The main advantages of RISE in competition with other GIS programs are summarized below:

- Output files are plotted on top of satellite images, which are available in sufficient resolution for nearly every built environment worldwide.
- RISE is stand-alone software that does not need procedure of installation of other commercial software.
- RISE is used with Google™ Earth, a program well known worldwide and already installed by most users.
- Erroneous results can be quickly identified by visual checks and corrected during all stages of the rise computation.
- RISE allows five different types of illustration of the output results depending on the needs of the input data.

14.3 REDARS

Earthquake damage in a highway system can provoke a major traffic disruption, which can impact the economic recovery and the emergency response in the region (Basoz and Mander 2008; Basz and Kiremidjian 1996). The impact will depend on the seismic performance of the components and on the properties of the system itself, such as its network configuration and roadway characteristics. Those are not usually taken into account in seismic risk reduction activities. REDARS 2, developed by FHWA, is a new methodology for *Seismic Risk Analysis* (SRA), which can estimate the seismic hazard through the highway system, the damage state of each component in the system, and how each component can be repaired, along with its cost (Cho et al. 2006). REDARS 2 is usually considered a post-earthquake tool, but it can also be considered as a pre-earthquake tool, because it can estimate the effectiveness of the hypothetical seismic-upgrade options.

14.3.1 *Seismic Risk Analysis Using REDARS*

REDARS 2 enables users to achieve deterministic (multiple simulations with a complete set of system SRA results) or probabilistic (one of the results is developed for one set of randomly-selected parameters) SRA from any highway system within the U.S.A.

REDARS2 methodology is modular because it includes a series of *seismic analysis modules* containing input data; It is a synthesis of models; it has a wide

range of results, for example before, during or after an earthquake and import wizard, to carry out SRA of the infrastructure systems of study.

14.3.1.1 Seismic Analysis Modules

The system module contains input data and models characterizing the highway system and its seismic performance before, during and after an earthquake. Input data contained in the System Module includes all the features of the highways, the OD zones considered in the SRA and the traffic-management measures for modifying the system.

The *Transportation Network Analysis Procedure* estimates the post-earthquake traffic flows throughout the highway system. First of all, it represents the latest well-developed technology for flow evaluation. Then it describes the reduction in travel time demand after an earthquake and it accommodates various types of travel options along the highway system. Finally, with a minimum-path algorithm it reduces the computer time for estimating post-earthquake traffic flows.

The *Hazards Module* contains input data and models for characterizing system-wide seismic hazards for each scenario earthquake and simulations considered in the SRA of the Highway system.

Deterministic SRA in REDARs 2 can be based on a single earthquake from the walk through table and Shake-map input data, with real-time maps of ground motion and shaking intensity.

The *Component Module* contains input data and models for evaluating: seismic response for each component, the component “damage state” and how the damage could be restored, the costs and the repair time, and the “traffic state” that will vary with time after the earthquake.

14.3.1.2 Analysis Procedure

The various steps of the analysis can be summarized as follows:

1. *Initialization.* This step involves the development of input data that defines the highway system to be examined, the attributes and the locations of the several components that contend this system and conditions of the soil, OD zones and pre-earthquake trip demands; all these data are obtained from Import Wizard and in addition the frequency of occurrence of damage is calculated.
2. *System analysis.* Step 2 consists of a full system of analysis for one particular earthquake scenario and one set of site, consisting of a hazard study, a direct loss and system state evaluation, transportation network analysis and economic impact evaluation.
3. *Check need for additional system analysis.* If the analysis is deterministic, another study is needed only if the user wants to consider different scenarios.

On the other hand, if SRA has probabilistic data, once they are considered good, the SRA proceeds to the final aggregation of all the probabilistic results.

4. *Aggregate results.* This is carried out only if the analysis is probabilistic and an aggregation of data has to be made. When the process of aggregation is completed, the SRA has ended.

14.3.1.3 Use of SRA for Decision Making and Seismic Risk Reduction

The process of decision making through REDARS 2 is based on the recognition that it is not possible to achieve a zero seismic risk. An “acceptable” level of risk is the one in which the costs of further reduction in the residual risks are no longer acceptable. If the costs to further reduce residual risks are no longer acceptable, you can define the “acceptable” level of risk. Below is given a “guideline” to be followed:

1. Identify seismic decision alternatives (Fig. 14.5).
2. Establish seismic performance requirements.
3. Apply SRA for baseline condition and each seismic decision alternative.
4. Evaluate the seismic design alternatives and select the preferred alternative.

Strategy	Description
Prioritization of Bridges for Seismic Retrofit	Evaluation of what retrofit sequence should be adopted for various bridges in the region, in order to optimize the benefits of the retrofit to the seismic performance of the highway system. SRA would be applied for different retrofit sequences, and would assess which sequence leads to the optimum seismic performance of the system.
Establishment of Design Acceleration Level for Bridge Design or Retrofit	Selection of alternative design acceleration levels should be considered for design of a new bridge or retrofit of an existing bridge. This should consider the initial construction costs associated with each design acceleration level, the potential for bridge damage, and its impact on the seismic performance of the highway system.
Emergency Response Planning	Evaluation of effects of various seismic decision options on access/egress times to or from key locations (e.g., hospitals, fire stations, airports, emergency command centers, centers of commerce). This could guide establishment of seismic retrofit priorities and design acceleration levels for components along emergency response routes. SRA can also be used in real-time assessment of seismic performance of a highway system after an actual earthquake, to guide real-time emergency response decision making.
Assessment of Available Repair Resources	Roadway downtimes due to earthquake damage will depend on available equipment, material, and labor for repair. SRA can assess how losses due to travel time delays are affected by these downtimes, and optimal repair resources for reducing these losses, by considering relative costs and benefits of various repair resource options.
System Enhancement	Assessment of how construction of new roadways that are being planned could improve the seismic performance of the highway system, as well as the effectiveness of possible short term traffic management strategies (e.g., conversion of selected roadways from one-way to two-way traffic) in improving system performance.

Fig. 14.5 Strategies and its description

14.3.2 Earthquake Modeling and Hazards Module

The seismic hazards imposed on a highway system will depend on the magnitudes, locations and frequencies of earthquakes in the sector, so it is important to know how earthquake scenarios are modeled in REDARS 2.

14.3.2.1 Earthquake Scenarios

Individual scenarios are necessary for evaluating the correlation effects of earthquakes. REDARS 2 enables users to specify earthquake scenarios in three ways: as a walk through table of earthquake base on established regional models, as an earthquake with a customized user-specified moment magnitude and as an earthquake with ShakeMap estimates.

The walk through analysis procedure for probabilistic SRA applications is developed as follows:

1. Total duration of walkthrough table can be decided. Typically thousands of years.
2. Scenario earthquake during each year of walkthrough. The number of potentially dangerous earthquakes and the locations and its magnitudes can be established.

14.3.2.2 Ground Motion Hazards

Highway components can be susceptible to damage from strong ground shaking; this ground shaking distribution is not random. It tends to reduce with increasing distance from the seismic source and with increasing earthquake magnitude. REDARS 2 keeps in mind this attenuation to estimate ground motion at each component.

14.3.3 Component Module

For characterizing the seismic performance of a given earthquake scenario, it is necessary to describe the traffic state at various times after the earthquake and evaluate the costs for repairing the damaged components. With these two parameters the total economic loss due to earthquake damage of the highway system is estimated. The step-by-step procedure for calculating the two values is the following:

1. Evaluation of the damage state,
2. An estimation of the repairs,
3. Analysis of the traffic state and repair costs.

The use of default models will greatly increase the efficiency of the highway system SRA, which use simplified methods to develop first-order estimates of the previous parameters. Models for determination of component performance can be deterministic or probabilistic (taking into account various uncertainties). REDARS 2 provides default models for three types of components: bridges, approach fills and pavements. The default models for bridges are probabilistic, while the default model for approach fills and pavements are deterministic.

14.3.3.1 Default Models for Bridges

Input data for analysis of the seismic response of a bridge should include information that can be accomplished from as-built drawings for individual bridges, and can be a laborious task when many bridges are involved. This information is about bridge geometry, the materials of construction, reinforcement, bearings, joints, seat widths, foundations, soil conditions and abutments.

14.3.3.2 Pushover Capacity Spectrum

The pushover capacity spectrum is a plot of equivalent 5% damped spectral acceleration against spectral displacement. Each capacity spectrum was obtained as the sum of the capacity of the piers and the three-dimensional arching action of the deck.

14.3.4 System Module

The first applications were based on a simpler theory than actual REDARS 2, using a *network-analysis process* that was based on:

1. User-equilibrium model
2. Fixed trip demands
3. One trip type
4. Minimum path algorithm

The improvements introduced in REDARS 2 are listed below:

1. Variable-trip demands: that accounts for the effects of traffic congestion
2. Dual-simplex minimum path algorithm, which is less computationally intensive
3. Multiple trip types

14.3.5 Economic Module

Damage to the highway system affects the system itself, the surrounding buildings and the industrial capacity. The objectives of the Economic Module are to provide data for estimating the economic losses due to earthquake damage. REDARS 2 considers the repair cost, as well as the losses due to earthquake-induced travel-time delays and the losses from trips foregone due to traffic congestion.

14.3.5.1 General Approach for Developing Default Loss Estimates

Repair parameters are based on the construction experience of the California Department of Transportation, used as an outlet for developing repair models for highway systems in other parts of the country. Construction procedures, repair resources and experience will differ from region to region, so REDARS 2 users should override the current default repair-model.

14.3.5.2 Loss Sources

Default repair costs are represented as percentages of the estimated total replacement cost for the component. REDARS 2 variable-demand network-analysis method takes into account possible increases in travel times and reductions in trip demands. Various types of trips throughout the system will have different economic values, and consequently separate travel-time delays for each trip type have to be estimated. It is supposed that post-earthquake trip demands are equal to pre-earthquake demands. The economic losses due to travel-time increases and trip reductions are estimated as the product of a unit loss and the area of the trapezoid in the following figure defined by P_1 and P_2 and D_1 and D_2 , while the corresponding losses due to trips foregone are represented by the area of the triangle defined by P_1 and P_2 and D_1 and D_2 multiplied by the unit loss (Fig. 14.6).

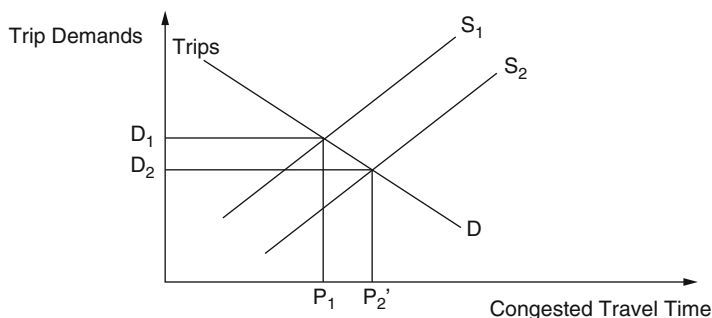


Fig. 14.6 Variable-demand model for earthquake-damaged highway system

14.3.5.3 Unit Losses

A *unit loss* represents the cost of the travel-time delays and trip foregone. User-specified estimates are applied as vehicle occupancy rates, truck-trip dollar value, cost of excess fuel, and others to develop these unit costs. It is measured in dollars per hour per passenger-car-unit.

14.3.6 Advantages of REDARS 2

The advantages of using REDARS are listed below:

1. Improved models and procedures can be introduced due to its modular structure.
2. It is a multidisciplinary method based on a synthesis of models.
3. As it is able to provide several results to deterministic and probabilistic SRA, it can meet the various needs of potential users nationwide.
4. The probabilistic framework has been extended through the development of a variance-reduction procedure, so fewer simulations are needed to achieve acceptable confident intervals.
5. A module has been included to estimate system-wide site-specific ground shaking and ground-displacement. It uses walkthrough tables and a wide range of different sources.
6. New models for estimating earthquake damage and the restoration process have been used.
7. The network module has been improved too.
8. The economic losses now include component repair costs and increased travel times and reduced trip demands.
9. The input data facilitates the location of openly available databases with the Wizard. Study of region boundaries and the establishment of various networks, soil and bridge input database within REDARS 2.
10. Possibility to be programmed into a REDARS 2 software packages with an internal GIS capability.

14.4 HAZUS

The program HAZUS was developed by the National Institute of Building Sciences (NIBS) and the Federal Emergency Management Agency (FEMA 1999, 2001, 2005a) for multi hazard risk assessment. Its name is in reference to the words **HAZ**ard and **US**, since it is nationally applicable software and has not the possibility to be applied to an out-of-USA scenario, because of the lack of a specific database. It uses GIS software to map and represent hazard data and results in a probable

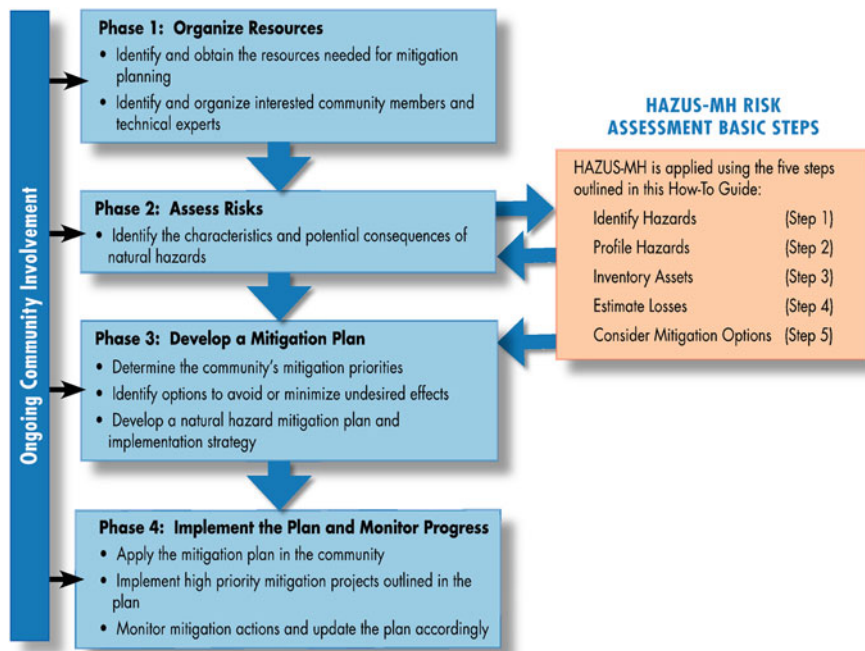


Fig. 14.7 Hazard mitigation planning process (FEMA 2005b)

risk estimate for infrastructures and buildings. The inputs and outputs can be overlaid on GIS-based maps. Thanks to an inventory of several elements it is able to classify components like building, population, transport system, lifeline utilities and hazardous materials (Fig. 14.7).

14.4.1 Risk Assessment Using HAZUS

Although it has been developed with as much capability as possible, there are certain situations for which there are no methods for rigorous calculation of damage, like for flooding and fire.

Collection of inventory is without question the most costly part of performing the study. This methodology produces crude estimates of losses based on a minimum of local input, while quality and uncertainty of the results is related to the detail of the inventory and the economic and demographic data provided. The software is able to estimate the consequences of hazard events like earthquakes, floods and hurricanes.

The software allows different levels of customization, based on the users resources and analysis needs, identified with an analysis Level 1 through Level 3:

- Level 1 (*Default Data Analysis*). It is the simplest type of analysis, since the user is not expected to have any knowledge about the software.
- Level 2 (*User-Supplied Data Analysis*). It requires more extensive inventory data than Level 1. It is the most commonly used since it integrates HAZUS provided data with more accurate and recent ones (especially for regions).
- Level 3 (*Advanced Data and Models Analysis*). It consists of an improvement of the loss estimation models used for loss analysis.

In conclusion, the primary limit on the type of analysis will be the user's ability to provide the required data. Even with perfect data, the methodology would not be able to precisely estimate earthquake loss.

14.4.2 Risk Assessment Process Using HAZUS-MH

Several steps of risk assessment process have been followed as it is shown in Fig. 14.8. Below is given a description of the five steps in details.

Step 1: Identify the Hazards

First of all, the area of study has to be defined and its boundaries marked (Fig. 14.9). The “detail level” must also be defined to make a good analysis, usually dependent on the smallest detail needed. This area of study is usually represented on a map (Fig. 14.10), using GIS, that allows interacting graphically with the representation. In the HAZUS-MH interface, it is possible to decide the level of aggregation through a menu. A more detailed zone can provide supplementary details during the analysis. After the definition of the study region, HAZUS-MH will be used to draw a base map, which gives a graphical representation of the defined area. In order to allow easy identification of hazards, the map layers may include the study region boundary, geographic frames of reference including roads, water bodies and main buildings. At this moment, is also possible to add local data to supplement provided, furnishing specifications about peculiar characteristics of some elements.

Step 2: Profile Hazards

The second step in the risk assessment process is to outline the hazard of interest in your study. It has to take into account, depending on the priorities, the likelihood of occurrence of the hazard, its possible magnitude and the historical events on the community of study. HAZUS provides historic data regarding the location and magnitude of earthquakes events which have occurred in the USA (Fig. 14.12). This is useful for providing communication of risks to the decision makers and for explaining to people the possible hazards. In the same way, by profiling hazard it is possible to create a scenario to carry out the Loss Estimation. At the end of this step, HAZUS provides maps showing the areas impacted by each hazard of interest and its characteristics (Fig. 14.11).

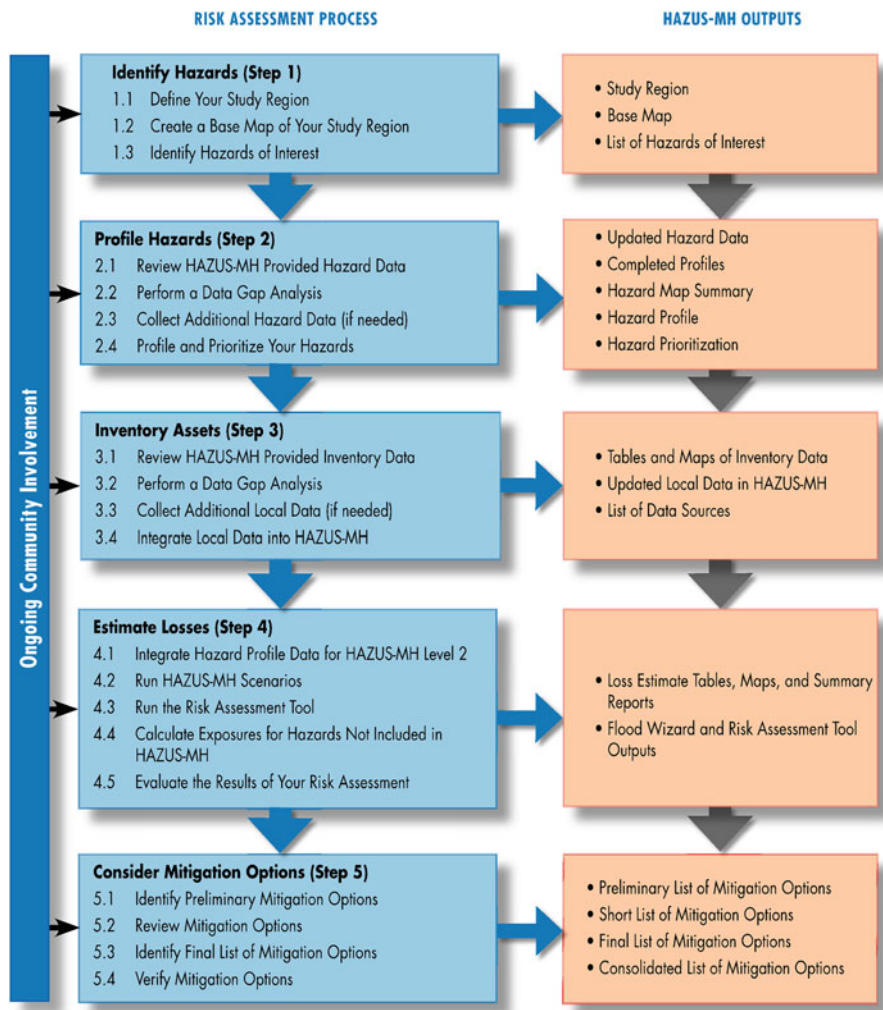


Fig. 14.8 HAZUS risk assessment process and outputs (FEMA 2005b)

Step 3: Inventory Assets

In this step (Fig. 14.13), risk quantification is provided as a combination of hazard exposure and vulnerability. HAZUS includes several inventories for each geographic study region in order to support the user in the loss estimation and risk studies (Fig. 14.14). This inventory has seven different categories:

1. *General Building Stock*; HAZUS-MH categorizes general building stock into 36 model building types (i.e. light wood frames, steel-braced concrete, masonry etc.), 28 occupancy classes (i.e. single-family, retail trade, heavy industry,

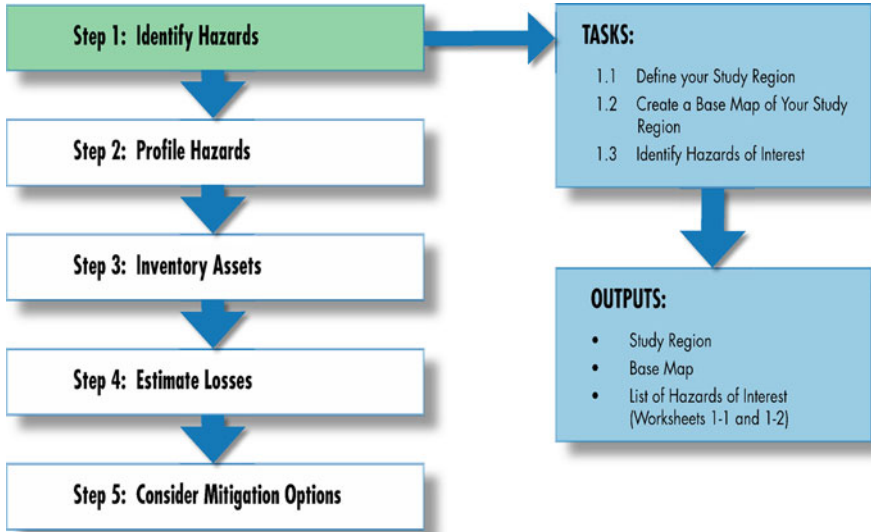


Fig. 14.9 Step 1 tasks and outputs (FEMA 2005a)

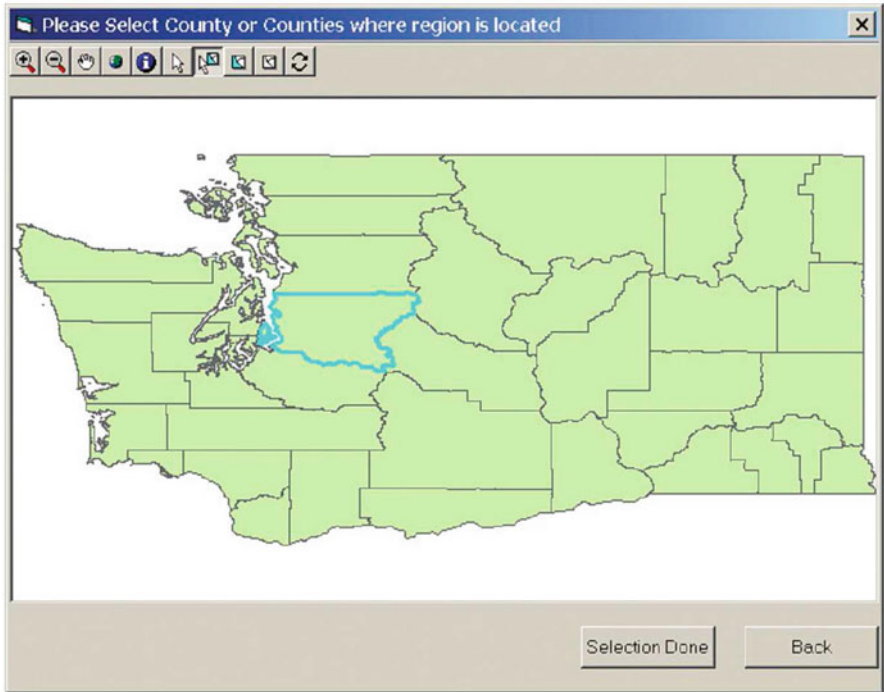


Fig. 14.10 County selection map (FEMA 2005b)

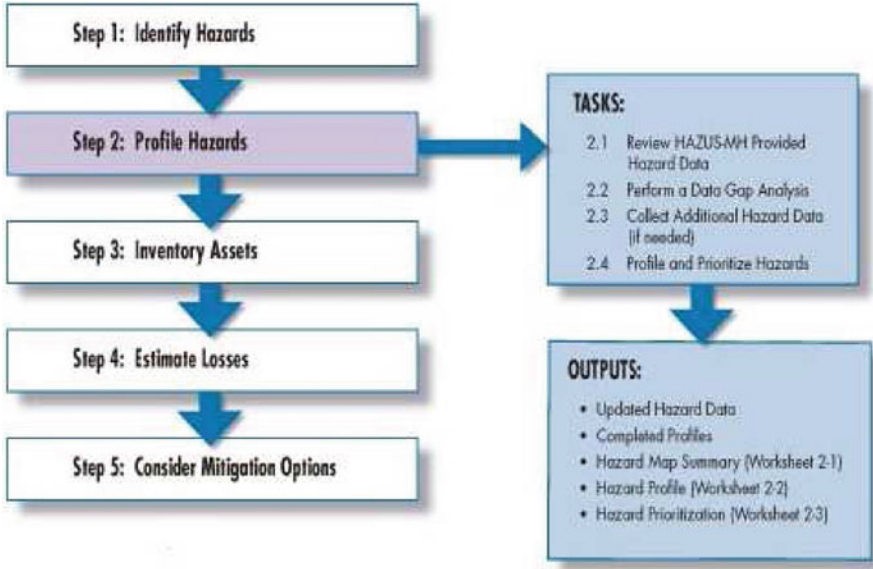


Fig. 14.11 Step 2 tasks and outputs (FEMA 2005a)

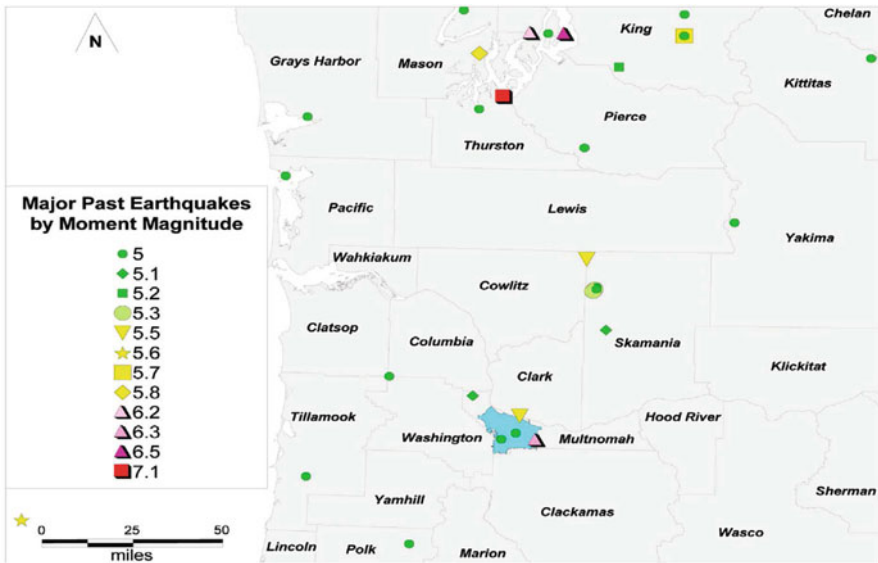


Fig. 14.12 Example: major past earthquakes for the Pacific Northwest, 1600–2002 (FEMA 2005a)

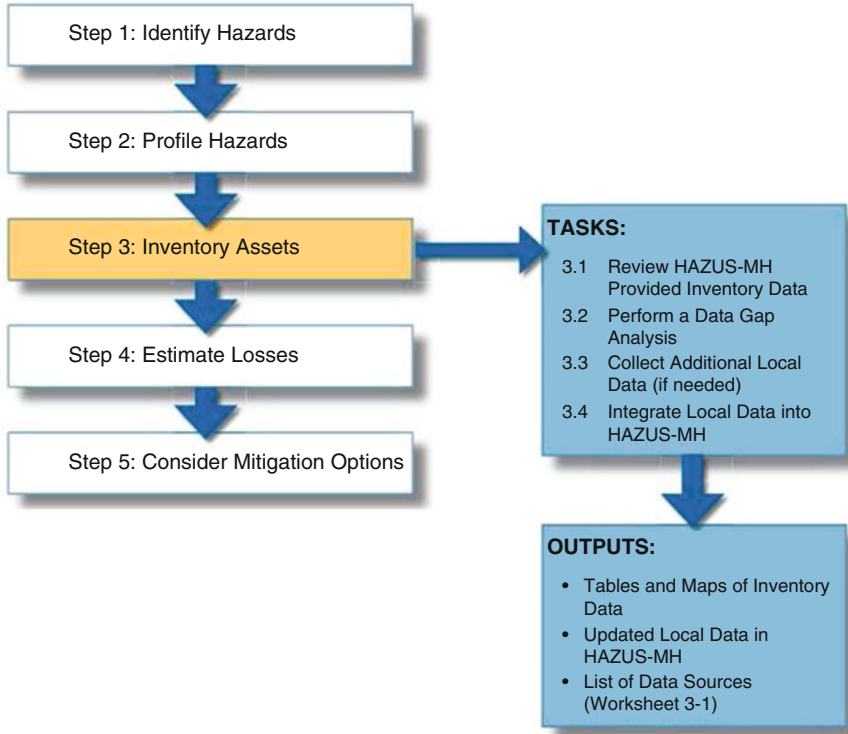


Fig. 14.13 Step 3 tasks and outputs (FEMA 2005a)

churches etc.) and 7 classes of occupancy (residential, commercial etc.). The parameters affecting building damage and loss can be structural or non-structural, referring to its occupancy or the variability of its characteristics within the classification.

2. *Essential Facilities*; groups the facilities essential to the health and welfare of the community. Its fundamental role in organization and supporting rescue make them important after earthquakes.
3. *Hazardous Material Facilities*; it includes all the stock in which potential dangerous materials are located (i.e. explosive, corrosive, flammable, radioactive materials).
4. *High Potential Loss Facilities*; these are the facilities that, if affected by disaster, would have a high loss or impact on the community (i.e. nuclear power plants, dams, levee etc.)
5. *Transportation Lifeline Systems*; this includes each typology of transportation possibilities.
6. *Utility Lifeline Systems*; this includes potable water and wastewater, electric power, gas and communication systems.

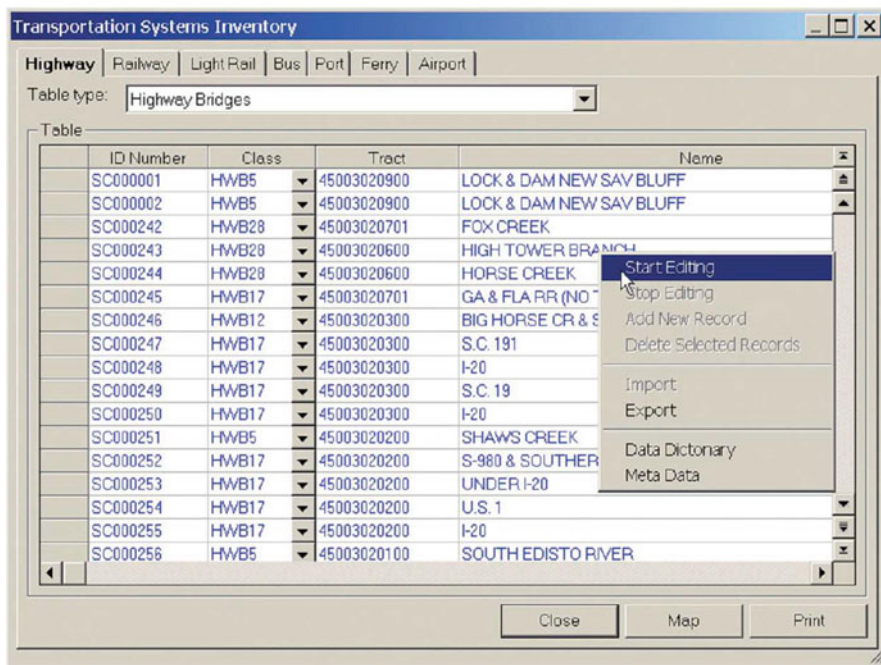


Fig. 14.14 Example of an inventory table (FEMA 2005b)

7. *Demographics*; referring to population statistics (i.e. age, gender, income distribution, number of householders and renters etc.).

On the maps these categories can be represented with

- Points, for site-specific facility locations that may have high potential;
- Lines, for locations connected by pipelines for utility lifeline systems;
- Roads for transportation lifeline;
- Polygons features, those represent a group of facilities.

At the end of this step, inventory data will be collected and integrated into HAZUS, including all the categories presented before.

Step 4: Estimate Losses

HAZUS has loss estimation models that have to be implemented in this step for the evaluation of the hazard events, the simulation of damage scenarios and the estimation of the hazard. With HAZUS-MH, a tool called “Risk Assessment Tool” (RAT) is provided. It makes the preparation of the risk assessment outputs for earthquakes easier, so that it is quicker to assess inventory exposure and loss for a studied region.

HAZUS provides running both deterministic and probabilistic scenarios. Anyway, it is advisable to use the probabilistic one because the estimated losses are the average expected value of loss in any 1-year and this can help decision-makers

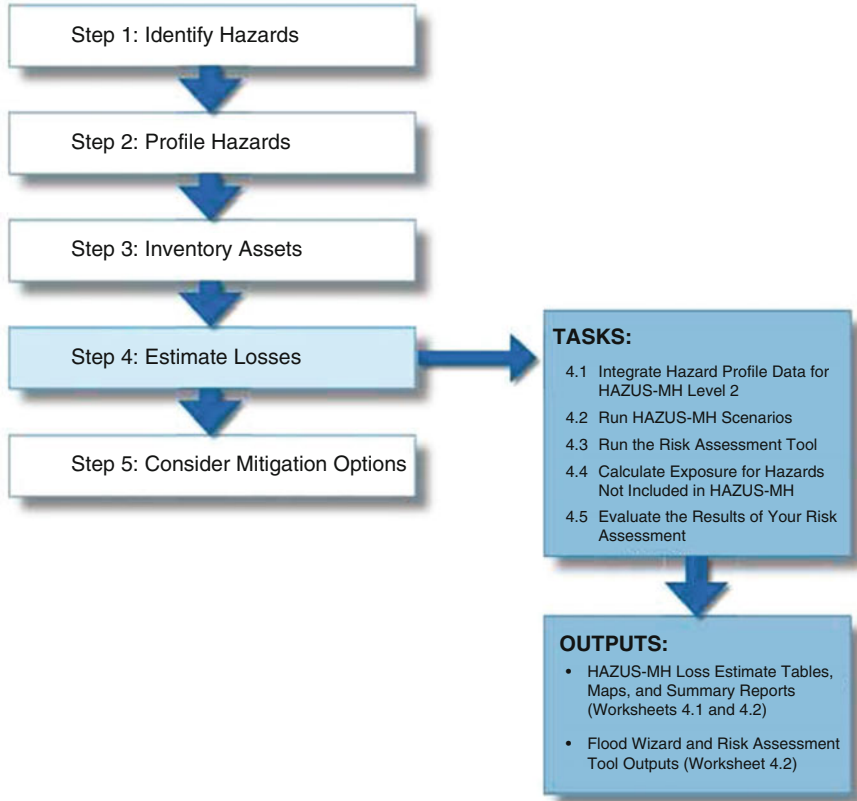


Fig. 14.15 Step 4 tasks and outputs (FEMA 2005a)

plan cost-effective budgets and mitigation measures. Deterministic analysis relies on the laws of physics or on correlations developed through experience or testing to predict the outcome of a particular hazard scenario. Therefore, HAZUS focuses on probabilistic analysis. The deterministic approach should be used for a more reality-correspondent result, since it is based on real measured data (Fig. 14.15).

Examining in a particular way the procedure requested to run a probabilistic earthquake scenario, the instructions below should be followed:

1. Select the Earthquake Hazard Scenario, define a new one if necessary, and load hazard maps for that scenario.
2. Run a Probabilistic Hazard assessment, select the return period and the moment magnitude of interest (Fig. 14.16).
3. Save the scenario and store it in the memory.
4. Now it is possible to run the Analysis, selecting the desired option for general buildings, essential facilities, other types of buildings, transportation systems, direct social losses, indirect economic impact and contour maps.

Fig. 14.16 Probabilistic hazard selection menu (FEMA 2005b)

At the end of this step, the user should have a clear idea of which assets are subject to the greatest potential damages and which hazards are likely to produce the greatest potential losses or present the greatest hazard exposure.

Step 5: Consider Mitigation Options

Step 5 will help the user to identify and evaluate several available mitigation options that are directly associated with the losses identified in the previous step. HAZUS losses are estimated based on the cost to repair or replace damage or loss of the building inventory. The attenuation measures consist of reduction in destructive effects of earthquakes and other causes of damage.

Mitigation measures can be viewed from many perspectives, favoring strategies that address the goal of mitigation with respect to building and infrastructure, minimizing the destructive and disruptive effect of hazard events on the built environment. For this objective, mitigation options are described in three categories:

- *Regulatory measures*; which include legal and other instruments used by the governments to prevent, reduce, or prepare for the losses associated with hazard events. In this case, building codes are the most widely used earthquake mitigation dispositions.
- *Rehabilitation of existing structures*; that concerns structural and non-structural modifications of elements in existing structures and infrastructures. Improving the safety and structural integrity of existing building and infrastructures is probably the best way to reduce the impact of hazardous events.
- *Protective and control measures*; these focus on protecting structures by deflecting the destructive forces from vulnerable structures, building and building protective barriers.

Now the mitigation options evaluated before are grouped and FEMA provide useful criteria for creating a short list of mitigation options for the specific

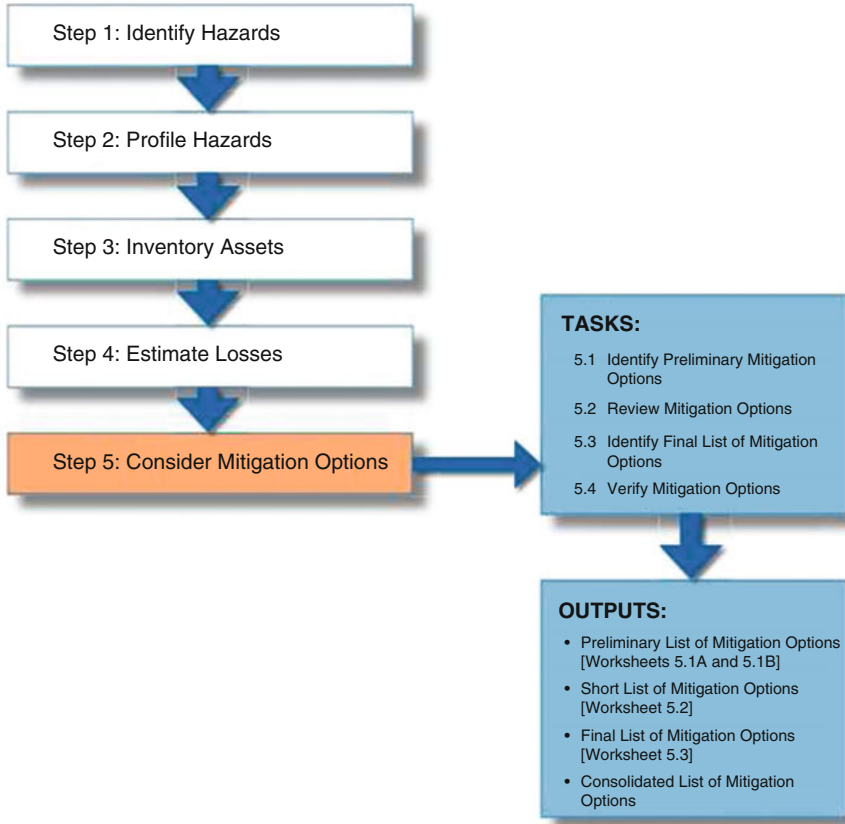


Fig. 14.17 Step 5 tasks and outputs (FEMA 2005a)

case. It consists of a common set of evaluation criteria, known as STAPLEE: Social, Technical, Administrative, Political, Legal, Economic and Environmental opportunities and constraints of formulating a tailored mitigation measure using a consistent framework (Fig. 14.17).

14.5 GIRAFFE

GIRAFFE is the acronym for **G**raphical **I**terative **R**esponse **A**nalysis for **F**low **F**ollowing **E**arthquake (GIRAFFE 2008). It was developed at Cornell University, New York, USA, and was written using C++ code, working iteratively with the EPANET hydraulic network analysis engine (Markov et al. 1994; Wang and O'Rourke 2008). It works using an iterative procedure for negative pressure elimination and, as in the software seen previously. It performs probabilistic (Monte

Carlo) and deterministic simulations and provides results linked to GIS creating spatial analysis and map representations.

GIRAFFE takes care of the water supplies. They have the key role of supporting fire protection and providing water for potable household, both for civil and industrial or commercial use.

As usual, water is conveyed mostly in underground pipelines. The lifelines are vulnerable to earthquakes due to the direct effect of the ground shaking. The lifelines performance, during and after an earthquake event, depends on the available flow and pressure in the damage system. To simulate this performance, an algorithm has been developed to model pipe breaks and leaks, and to integrate this algorithm into an analysis program for simulation purposes.

14.5.1 Overview of the GIRAFFE Simulation

GIRAFFE is a stand-alone software and its installation is accompanied by the installation of EPANET, a software to help users to visualize the hydraulic network and simulations. It can perform two different types of simulations: the *deterministic* one, in which damages to the network are added and then the analysis is performed, and *Monte Carlo simulation*, where the user can decide the number of simulations. Either way, a complete GIRAFFE simulation includes these modules: system definition, seismic damage, earthquake demand simulation, hydraulic network analysis and compilation of results.

14.5.1.1 Earthquake Demand Simulation

The earthquake demand simulation module implicitly considers the effects of damage to small diameter distribution pipelines by increasing nodal demands. The fragility curves are developed on the basis of Monte Carlo simulations of the LADWP (Los Angeles Department of Water and Power) distribution networks. Because the earthquake demand is simulated probabilistically by fragility curves, this module only works for probabilistic simulations.

14.5.1.2 Hydraulic Network Analysis

In this module, the use of EPANET is required to work in an iterative way to solve the damaged hydraulic network and to eliminate negative pressures. GIRAFFE checks the nodal pressures, and identifies the lowest nodal pressure in the system. If the lowest pressure is higher than the preset pressure limit (zero), the hydraulic analysis stops. On the other hand, if it is lower than the pressure limit, the program eliminates the node linked to the elements. After each step of elimination, GIRAFFE performs a hydraulic network analysis again, and this process continues until there is no pressure lower than the pressure limit in the system (zero) (Fig. 14.18).

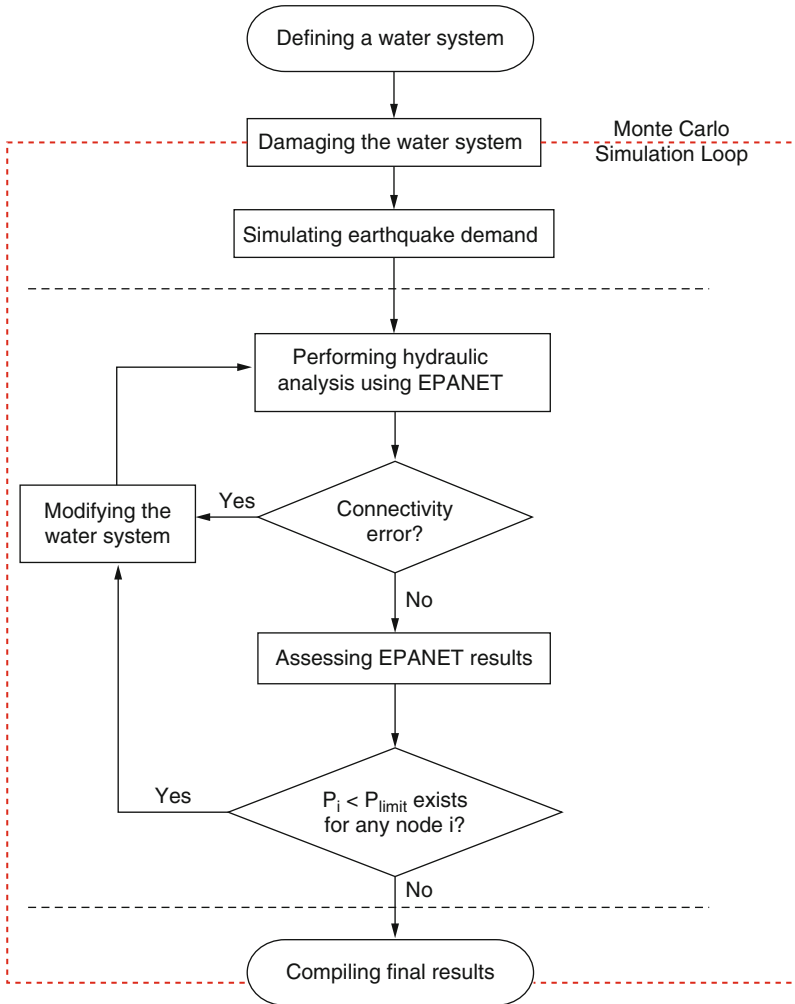


Fig. 14.18 Step 5 tasks and outputs (FEMA 2005a)

14.5.1.3 Compilation of the Results

The results of the analysis are compiled into a format compatible with GIS. It also provides a performance index to measure the system serviceability. Generally, a hydraulic network model consists of two basic classes of elements: nodes, which represent facilities at specific locations, and links, which define relationships between nodes. Typical nodal elements include junctions and storage nodes, while typical link elements are pipes. Other components, such as valves and pumps, can be modeled as either links or nodes, depending on different modeling techniques.

Table 14.2 Summary table for physical components in an EPANET hydraulic network model

Components		Descriptions	Inputs	Outputs	
Junction		Points where links join together and where water enters or leaves the network	Coordinates; elevation; demand	Hydraulic head; pressure	
Storage Node	Reservoir	Constant Level	Unlimited capacity water sources with constant water level during simulation time	Coordinates; hydraulic head (a constant value)	
		Variable Level	Unlimited capacity water sources with water level varying with simulation time	Coordinates; hydraulic head curve (hydraulic head vs. time)	
	Tank	Cylindrical	Limited capacity water sources with cylindrical shape	Coordinates; bottom elevation; diameter; initial, minimum, and maximum water level	Hydraulic head
		Variable Area	Limited capacity water sources with variable cross-sectional area	Coordinates; volume vs. hydraulic grade curve	Hydraulic head
Pipe		Links conveying water from one node in the network to another	Start and end node; diameter; length; roughness and minor loss coefficients; status (open, closed, or containing check valve)	Flow rate; head loss	
Pump	Constant Power		Pumps which a supply constant amount of energy to water	Start and end node; diameter; energy; status (open or closed)	
	One-Point		Pumps with characteristic curves defined by one point	Start and end node; diameter; operation flow and head gain; status (open or closed)	
	Three-Point		Pumps with characteristic curves defined by three points	Start and end node; diameter; pump curve; status (open or closed)	
	Multiple-Point		Pumps with characteristic curves defined by multiple points	Start and end node; diameter; pump curve; status (open or closed)	

Component	Description	Input	Output
Valve	Check (CVs)	Allow water through one direction (built in pipe)	None (presence is indicated by a "CV" at the end of a pipe definition line)
	Pressure Reducing Valves (PRVs)	PRVs limit the pressure on their downstream end to not exceed a pre-set value when the upstream pressure is above the setting. If the upstream pressure is below the setting, then flow through the valve is unrestricted. If the downstream pressure exceeds the upstream pressure, the valve closes to prevent reverse flow.	Start and end node; diameter; minor loss coefficient; downstream pressure setting; status (open or closed)
	Pressure Sustaining Valves (PSVs)	PSVs attempt to maintain a minimum pressure on their upstream end when the downstream pressure is below the setting. If the downstream pressure is above the setting, then flow through the valve is unrestricted. If the downstream pressure exceeds the upstream pressure, the valve closes to prevent reverse flow.	Start and end node; diameter; minor loss coefficient; downstream pressure setting; status (open or closed)
	Pressure Breaker Valves (PBVs)	PBVs force a specified pressure loss to occur across the valve. Flow through the valve can be in either direction.	Start and end node; diameter; minor loss coefficient; pressure setting; status (open or closed)
	Flow Control Valves (FCVs)	FCVs limit the flow to a specified amount.	Start and end node; diameter; minor loss coefficient; flow setting; status (open or closed)
	Throttle Control Valves (TCVs)	TCVs simulate a partially closed valve by adjusting the minor head loss coefficient of the valve.	Start and end node; diameter; minor loss coefficient; status (open or closed)
	General Purpose Valves (GPVs)	GPVs are used to represent a link where the user supplies a special flow-head loss relationship instead of following one of the standard hydraulic formulas.	Start and end node; diameter; head loss vs. flow rate curve; status (open or closed)

In the Table 14.2, all the physical components are summarized. For a deterministic simulation, the outputs for the five types of components are reported. For a probabilistic simulation, the outputs for the five types of components are reported for each run of the Monte Carlo simulation.

14.5.2 Hydraulic Network Analysis

Hydraulic network analysis is a mathematical model of a water supply system where the components of the system are represented as nodes and links. This model can be used to predict pressure and flow conditions in a water supply system under different operational scenarios. The hypothesis is that a pipeline network is always full and pressurized with incompressible water, governed by two principle laws: the laws of mass and energy conservation. The major unknowns that need to be determined are flows in links and hydraulic head at nodes.

14.5.2.1 EPANET Software

This is commercial software for hydraulic network analysis, designed to be a research tool for improving the understanding of the movement of drinking water constituents in water distribution systems. EPANET models a water supply system as a collection of links connected to nodes, representing junctions and storage nodes, including tanks and reservoirs. Figure 14.19 illustrates how these objects can be connected to one another to form a network. Each reservoir, tank, pump, and valve, because of its different physical properties and/or functions, can have different modeling options.

14.5.2.2 EPANET Input

EPANET stores all input data in a text file with the file extension, *.inp*. The *.inp* file is organized into sections with each section beginning with a key word enclosed in brackets. The various sections are listed in Table 14.3.

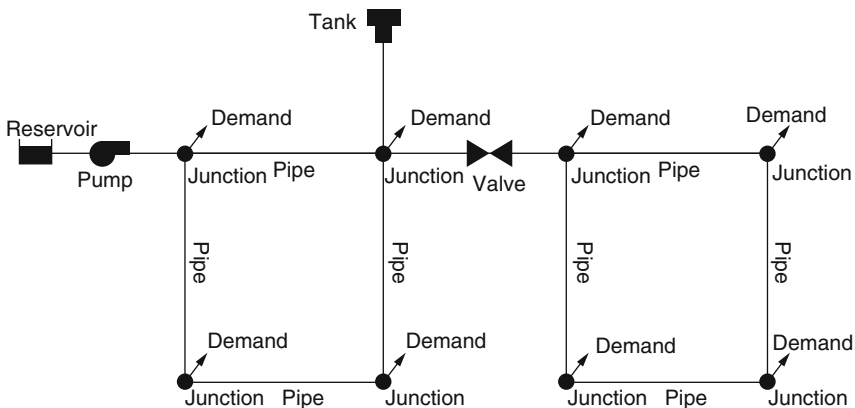


Fig. 14.19 Physical components in an EPANET hydraulic network (GIRAFFE 2008)

Table 14.3 Sections in an EPANET input file

Network Components	System Operation	Water Quality	Options and Reporting	Network Map/Tags
[TITLE]	[DEMANDS]	[SOURCES]	[ENERGY]	[COORDINATES]
[JUNCTIONS]	[CURVES]	[QUALITY]	[OPTIONS]	[VERTICES]
[RESERVOIRS]	[PATTERNS]	[REACTIONS]	[TIMES]	[END]
[TANKS]	[ENERGY]		[REPORT]	
[PIPES]	[STATUS]			
[PUMPS]	[CONTROLS]			
[VALVES]				

14.5.2.3 EPANET Output

The outputs from the EPANET engine are generated in a text file with the extension of file name, *.rpt*. An output file can contain four sections: status, energy, nodes and links.

14.5.3 Pipe Damage Modeling

To predict the conditions of pressure and flow in a damaged water supply system, a hydraulic network analysis and a pipe damage model (leaks and breaks) are required. GIRAFFE methodology for pipe damage simulation begins with the definition of pipe leaks and breaks, then is proposed a classification for leak types to determine the opening area of each leak type. A break is defined as the complete separation of a pipeline, no flow will pass between the two adjacent sections of the broken pipe. A leak is defined as a small disclosure in a pipeline, such that water will continue to flow through the pipeline, albeit with some loss of pressure and flow rate being delivered.

14.5.3.1 Pipe Leak Simulation

Leaks are classified into five different types, as shown in Table 14.4, and the leak area is simulated as a function of the pipe diameter. A pipe leak is essentially an orifice in the pipe wall or at a pipe joint, which allows water to be discharged into the surrounding soil (ALA 2001). In GIRAFFE, a pipe leak is simulated as a fictitious pipe with one end connected to the leaking pipe and the other end open to the atmosphere, simulated as an empty reservoir.

Table 14.4 Representation of possible leak types

Type of leak	Schematic Drawing
Annular Disengagement	
Round Crack	
Longitudinal Crack	
Local Loss of Pipe Wall	
Local Tear of Pipe Wall	

14.5.3.2 Pipe Break Simulation

It is assumed that a break occurs in a pipe, which is connected to the upstream node and downstream node. GIRAFFE simulates the break by eliminating the pipe from the network, and by adding two new empty reservoirs. Their elevation is determined by linear interpolation of the elevations of upstream and downstream nodes. Two more pipes are added, which have the same diameter and roughness as the deleted pipe (Fig. 14.20).

14.5.4 Earthquake Demand Simulation

One technique for simulating a complex system is to decouple various parts of it, applying models with appropriate levels of complexity to each part, and integrating

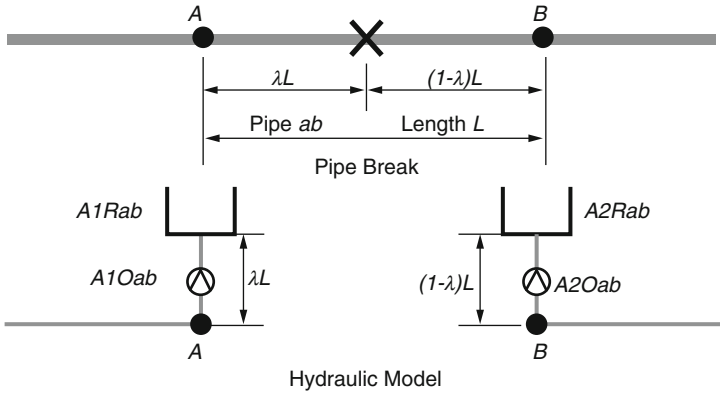


Fig. 14.20 GIRAFFE model for pipe break

the decoupled analyses to show system performance. A possible technique for simulating a complex water supply system is therefore to decouple the trunk and distribution systems. The local response of the system can be simulated using distribution network models, which cover a small local area but include small diameter distribution lines. Using multi-scale modeling, a complex water supply system can be decoupled into several systems, which have manageable complexity.

GIRAFFE provides a method for simulating the earthquake demand associated with the distribution networks. The earthquake demands are simulated by means of fragility curves relating demand to repair rate in local distribution networks. The repair rate is correlated with seismic hazard parameters, including peak ground velocity and permanent ground deformation.

14.5.5 GIRAFFE Inputs and Outputs

The input for GIRAFFE simulations includes control parameters and data files. The input data includes files for system definition, pipe damage generation, and earthquake demand simulation. The major outputs from GIRAFFE simulations are hydraulic analysis results of network physical components, including junctions, tanks, pipes, pumps, and valves, and the serviceability of the damaged system.

14.5.5.1 Input Data

GIRAFFE can perform both deterministic and probabilistic simulations. For probabilistic simulations, users can either specify the number of Monte Carlo simulation runs, or let the program determine this number using the self-termination algorithm

built into the code. For both deterministic and probabilistic simulations, users need to input some common control parameters to specify the system definition file.

14.5.5.2 Output Data

The major outputs for GIRAFFE simulations are the hydraulic analysis results for each type of network physical component, including reports about the serviceability of the damaged system.

The main outputs of deterministic simulations are hydraulic analysis results for the components of the system, written in a text file, as well as reports about the serviceability of each demand node and the entire system, written into a text file.

The main outputs of the Monte Carlo simulation are system serviceability, reported in a matrix format. For every Monte Carlo simulation run, the serviceability is reported for each demand node and for the entire system. The mean of the nodal and system serviceability for all Monte Carlo simulation runs is also calculated and reported.

14.6 OpenQuake of GEM

The **Global Earthquake Model (GEM)** is a public/private union initiated by the Global Science Forum of the Organization for Economic Cooperation and Development (OECD-GSF). It is used to support decisions and actions to reduce earthquakes losses, helping homeowners, governments and decision-makers to know all the information before take any mitigation action. GEM started in 2009 and it is the first global, open source model for seismic risk assessment at a national and regional scale, and aims at achieving broad scientific participation and independence.

OpenQuake is a suite of open-source software that allows the GEM community to use data, best practise and applications collaboratively being developed. The suite comprises the Platform, the Engine, and a great variety of (desktop) Tools for modeling, and for accessing and exploring GEM products, as well as uploading and sharing data & findings.

14.7 EQVIS

EQVIS is an advanced seismic loss assessment, and risk management software developed during the SYNER-G project. SYNER-G developed the Consequence-based Risk Management (CRM) methodology for the assessment of physical as well as socio-economic seismic vulnerability at the urban/regional level. The built environment is modeled according to a detailed taxonomy into its component

systems, grouped according to the following categories: buildings, transportation and utility networks, and critical facilities. CRM provides the philosophical and practical bonds between the cause and effect of the disastrous events and mitigation options.

EQVIS follows the CRM methodology using a visually-based, menu-driven system (Fig. 14.21) to generate damage estimates from scientific and engineering principles and data. It tests multiple mitigation strategies, and supports modeling efforts to estimate higher level impacts of earthquake hazards, such as impacts on transportation networks, social, or economic systems.

EQVIS is based on the open-source-platform MAE Viz developed by the Mid-America Earthquake (MAE) Center and the National Center for Supercomputing Applications (NCSA) which employs the advanced workflow tools to provide a flexible and modular path. It requires the following inputs: hazard, inventory and fragility models. This information is useful to estimate the damage and the losses.

With respect to *buildings*, it estimates structural and non-structural damage, economic losses and liquefaction damage. With respect to *bridges*, it computes damage, loss of functionality and repair cost analysis. Concerning *lifelines*, it

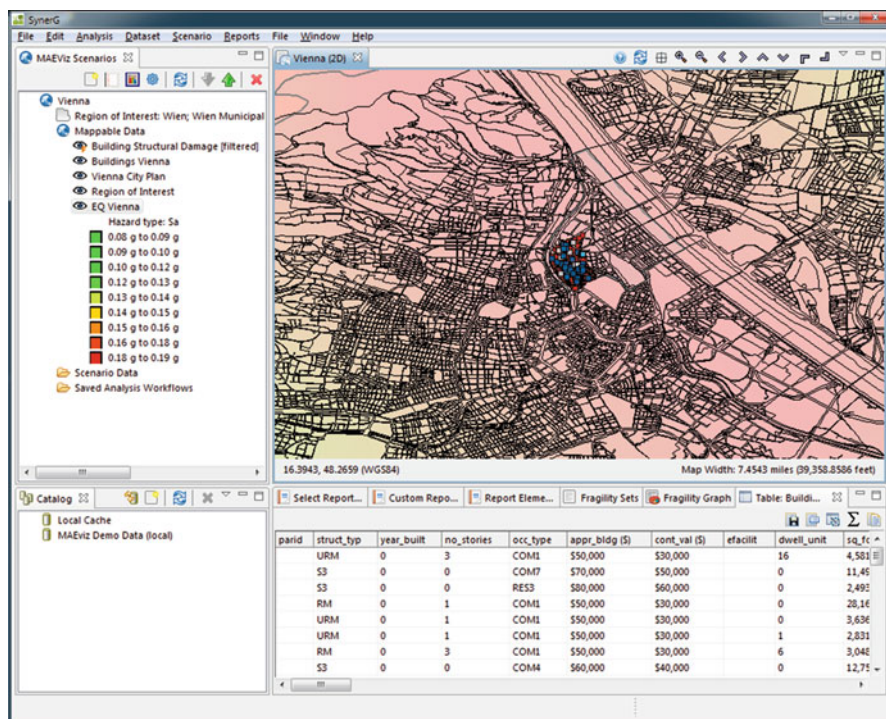


Fig. 14.21 GUI EQVIS

calculates the damage network and the repair rate analysis. Finally, it computes socio-economic losses such as shelter needs, fiscal and business interruption.

14.8 ResilUS

Recently, the ResilUS framework (Miles and Chang 2006, 2007, 2011) has been developed. It is limited to buildings and lifelines (transportation network, electrical network, water supply, and critical facilities) and uses a macro-sub division of area contained within a broader community such as the neighborhood subdivision. The community is divided into three elements:

1. *the physical built environment,*
2. *economics,*
3. *humans (i.e., health).*

The method relies on two generic indicators of resilience:

1. *the ability to perform*
2. *the opportunity to perform*

These recovery indicators are specifically represented by multiple variables. For example, the indicator of ability to perform for households is represented by household health, while the reconstruction time is influenced by the size (single-family vs. multi-family) of the respective building in addition to the construction capacity in the community (opportunity to perform). The model has four recovery curves, but currently the software ResilUS uses only one curve, that returns to pre-disaster conditions. The framework, therefore, facilitates the creation of a database for infrastructures and defines multiple resilience indicators making the optimal solution difficult to find, but different functionality models already available in the literature can be adopted.

14.9 Virtual City Simulators

A comparison between virtual city simulators is performed in this section. A virtual city software is a fundamental tool for Resilience assessment when paired with an agent-based model. The term “virtual city” is used to describe a two- or three-dimensional computer generated environment which can be explored and interacted with by a person. That person becomes part of this virtual world or is immersed within this environment and, whilst there, is able to manipulate objects or perform a series of actions.

The assessment focuses on both open access software packages and commercial models. A list of the simulators considered is provided in Table 14.5. These software

Table 14.5 List of software packages analysed

Proprietary software	Open source models
Aimsun 8.1 (TransportSimulationSystems 2001)	NetLogo (NorthwesternUniversity 2001)
Cities in motion (ParadoxInteractive 2000)	OpenCity (Nguyen 2004)
Cities:Skylines (ParadoxInteractive 2014)	OpenTTD (OpenTTD 2004)
Cities XL platinum (FocusHomeInteractive 2008)	Repast simphony (Sourceforge 1999)
SimCity (Markov et al. 1994)	RoboCup rescue simulator (Kleiner 2004)
	Simutrans (PanamaCityPC 2003)

are easily obtainable and currently supported, with active discussion forums in which users share their designs and models.

14.9.1 Comparison Between Virtual City Software Packages

The parameters of comparison taken into account are:

- Infrastructures (Lifelines)
- Hazards
- Visual graphic display

14.9.1.1 Parameter of Comparison: Lifelines

Following the work of Kongar and Rossetto (2012), 16 infrastructures have been identified: *Electricity (Power delivery)*, *Oil delivery*, *Transportation*, *Telecommunication*, *Natural Gas delivery*, *Water supply*, *Wastewater treatment*, *Financial system*, *Building services*, *Business*, *Emergency services*, *Food supply*, *Government*, *Health care*, *Education and Commodities*.

These infrastructures have been divided in two main groups: the *core lifelines* (Electricity, Oil delivery, Transportation, Telecommunication, Natural Gas delivery, Water supply, Wastewater treatment) and the *socio-technical networks* (Financial system, Building services, Business, Emergency services, Food supply, Government, Health care, Education, Commodities).

Cities:Skylines, followed by SimCity, is the software package that models more lifelines with respect to the others. Both of them are proprietary software.

NetLogo (Dawson et al. 2011), *Repast Symphony* (Felsenstein and Grinberger 2014) and *RoboCup Rescue Simulator (RCRS)* (Skinner and Ramchurn 2010), marked with an asterisk, are simulators that reproduce conditions similar to an urban post-hazard event with the purpose of testing mitigation strategies for disasters. In order to reach this objective, the platforms try to simulate the real world scenarios as accurately as possible, introducing all the useful lifelines. The number of infrastructures assigned to these three simulation programs (Fig. 14.22) is taken

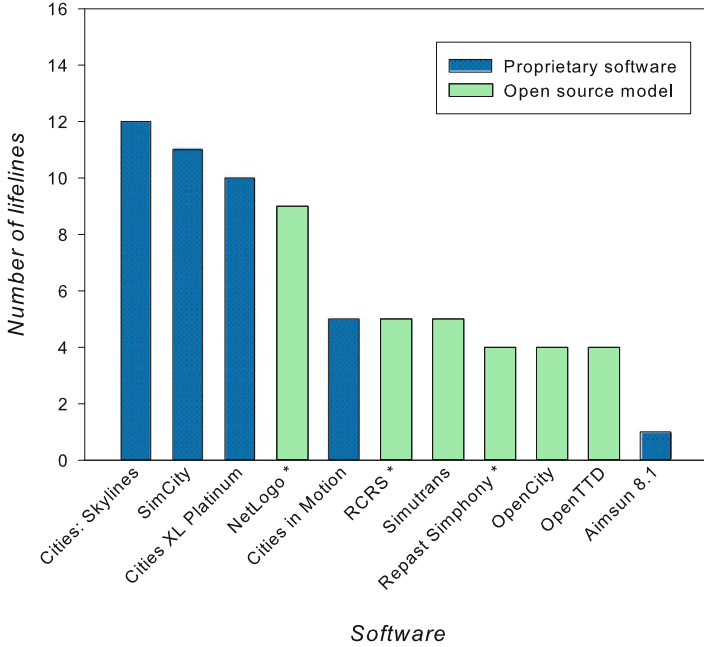


Fig. 14.22 Comparison between simulators based on the number of lifelines modeled

from documents and projects already realized and shared on the official websites and on the community forums.

According to the information obtained, among the open source simulators NetLogo is on top, with nine infrastructures modeled: power supply, transportation, telecommunication, water supply, financial system, emergency services, food supply, government and health care.

Of the seven lifelines missing in NetLogo, two are included in other open source software packages. These are the Commodities and Business lifelines, both covered by OpenTTD and Simutrans. Of the remaining five infrastructures, three are modeled only in proprietary solutions, while Building Services is not included in any software at all. This is reasonable when considering that all these programs focus mainly on the urban environment as a whole, and not on the single building conditions. Natural gas delivery is not modeled by any program as well.

14.9.1.2 Parameter of Comparison: Hazards

A Hazard is a threat, a future source of danger. It has the potential to cause harm to people (death, injury, disease and stress), human activity (economic, educational etc.), property (property damage, economic loss of amenities), environment (loss fauna and flora, pollution) and infrastructures.

The main hazards that could damage infrastructures and people are:

- Earthquake – faulting, ground shaking, landslides
- Fire – wild land fire, urban/building
- Flood – tsunami, urban, coastal, ponding
- Snow or rain – winter storm, hailstorm, avalanche
- Wind – tornado, storm, hurricane/typhoon
- Man-made – blasts, bomb incident, civil disorder, contamination

From Table 14.6 it can be observed that RCRS, NetLogo and Repast can simulate all the hazards, since these programs provide the creation of a “ad hoc” disaster-scenario for a specific agent-based simulation.

There are four simulators which don’t include any hazard in their code: Simutrans, Cities XL Platinum, Cities in Motion, OpenCity and Aimsun 8.1, which have been developed for different purposes. Aimsun 8.1 (TransportSimulationSystems 2001) is a traffic simulation software. Simutrans (PanamaCityPC 2003) and Cities in Motion (ParadoxInteractive 2000) are transportation simulation platforms. Cities XL Platinum (FocusHomeInteractive 2008) and OpenCity (OpenTTD 2004) are urban planning models.

The definition of the possible levels of hazard and of the fragility curves is needed in order to immediately define different levels of recovery strategy. Having a clear distinction allows for a quicker and more precise response.

None of the software analyzed takes into account the structural characteristics of the buildings, therefore it is not possible to implement all the damage levels and fragility curves for each one of them. RCRS has taken the first step towards this type of analysis, introducing brokenness (meaning how much structurally damaged the building is) and fieriness, that describes the fire related damage in the building (da Silva et al. 2013).

Table 14.6 Comparison between simulators based on the number of hazards modeled

		Hazards					
		Fire	Wind	Earthquake	Flood	Snow or rain	Man-made
Software	Repast simphony	✓	✓	✓	✓	✓	✓
	RCRS	✓	✓	✓	✓	✓	✓
	NetLogo	✓	✓	✓	✓	✓	✓
	SimCity	✓	✓	✓	✗	✗	✗
	Cities:Skylines	✓	✗	✗	✗	✗	✗
	OpenTTD	✓	✗	✗	✗	✗	✗
	Simutrans	✗	✗	✗	✗	✗	✗
	Cities XL platinum	✗	✗	✗	✗	✗	✗
	Cities in motion	✗	✗	✗	✗	✗	✗
	OpenCity	✗	✗	✗	✗	✗	✗
	Aimsun 8.1	✗	✗	✗	✗	✗	✗

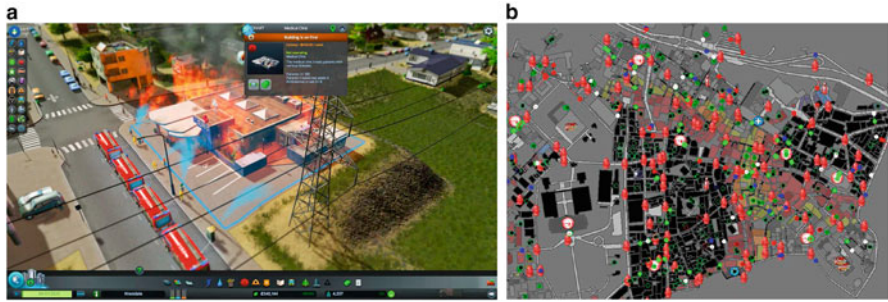


Fig. 14.23 different types of software visualization. (a) cities:skylines. (b) robocup rescue

Table 14.7 Comparison between simulators based on visual graphic display

		Visual output quality		
		High	Medium	Low
Software	Cities:Skylines	✓		
	SimCity	✓		
	Cities XL platinum	✓		
	Cities in motion	✓		
	Repast symphony		✓	
	RCSR		✓	
	OpenTTD		✓	
	Simutrans		✓	
	NetLogo			✓
	OpenCity			✓
	Aimsun 8.1			✓

14.9.1.3 Parameter of Comparison: Visual Graphic Display

Visualization is the primary tool used to speed up the understanding of hazard in a region. Visual representations of information, data or knowledge is intended to present information quickly and clearly.

It is useful to discern between the realistic approach (Fig. 14.23a), focused on representing real-time damage of buildings/vehicles in realistic fashion, and a more detailed one (Fig. 14.23b), focused on giving a bigger spectrum of information, sacrificing the realism. The two can coexist to a certain degree and an optimal balance should be obtained.

An evaluation of the software visual output, divided in three main sections: high, medium an low, is shown in Table 14.7.

The higher visualization level is given to the proprietary simulators: (a) *Cities: Skylines*, (b) *SimCity*, (c) *Cities XL Platinum* and (d) *Cities in Motion* (Fig. 14.24). All these software packages have a 3D visualization tool, with the possibility of orbiting around the buildings. Being sold as video games, they have been developed with a definite focus on visual performances.



Fig. 14.24 Software packages with high visual graphic display. (a) Cities:Skylines. (b) SimCity. (c) Cities XL platinum. (d) Cities in motion

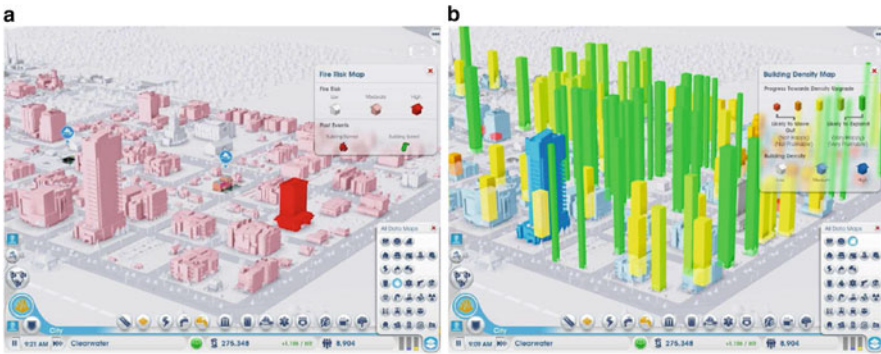


Fig. 14.25 SimCity info views. (a) Fire info view. (b) Density distribution info view

In the case of *SimCity*, the developers implemented tilt-shift photography in order to achieve a better visual impact on users (Fig. 14.23b).

In *SimCity* (Fig. 14.25) a player can also dig in to see how systems work, and look under the surface for deeper clues on how the city is functioning. The user can discover for example the fire risk (color-coded in white, pink and red) or the density distribution (with the height of the columns and different colors).

Cities:Skylines (Fig. 14.26) features 20 info views to highlight various information about the city. Some of them include multiple tabs for different, but related,

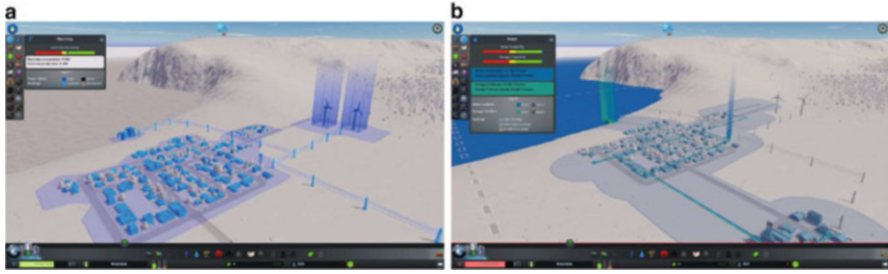


Fig. 14.26 Cities:Skylines info views. (a) Power delivery info view. (b) Water supply info view



Fig. 14.27 Cities XL PLatinum graphic visualization



Fig. 14.28 Software packages with medium visual graphic display. (a) OpenTTD. (b) Simutrans

data (such as water availability and sewage treatment (Fig. 14.26b)). The water info view displays the currents, the direction of the water flows and highlights all the water network buildings. It also shows the pipes that run underground.

Cities XL Platinum, instead, is the only software that includes a ground-level perspective, allowing the player to walk among the buildings (Fig. 14.27).

Other simulators such as *Simutrans* and *OpenTTD* (Fig. 14.28) focus mainly on the transportation network, so the purpose of the two softwares is to connect the pre-built cities with road and rail connections. The buildings have a medium level

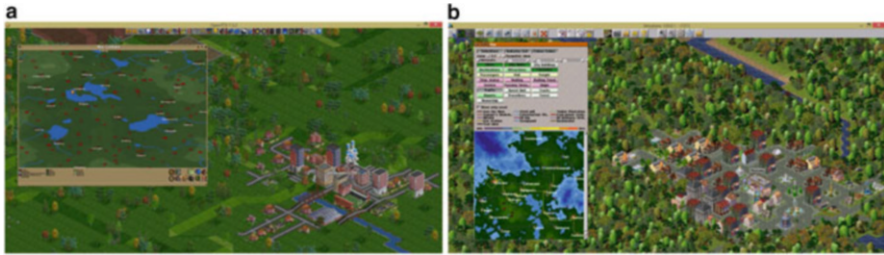


Fig. 14.29 Software 2D maps. (a) OpenTTD. (b) Simutrans

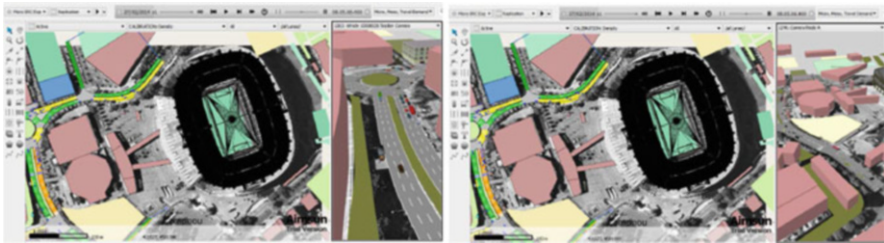


Fig. 14.30 Aimsun 8.1 visual graphic display

of graphic detail and there is no personalization of their location. The visualization is isometric with the possibility to zoom in and zoom out, to pan the view, but not to orbit around the buildings. Furthermore *Simutrans* also gives the possibility to rotate the view, but only from the 4 fixed cardinal points (Fig. 14.29).

In *OpenTTD* the user can open a 2D map which shows cargo flows, transport routes, vegetation, landowners, industries, vehicles and land contours. In *Simutrans*, the 2 dimensional map of the region shows all the cities names, their limits and the color dots refer to different network buildings such as iron ore mines, oil fields, incinerators and others.

Aimsun 8.1 allows to create buildings and draw the transportation system on a map. The traffic simulation can be seen both in 2D and in 3D visualization, positioning on the map different cameras to get different point of view (Fig. 14.30).

NetLogo, *Repast Symphony* and *RCRS* are a clear examples of different approaches for the visualization of the information, which is based on the 2-dimensional display of the city environment (Figs. 14.31, 14.32, and 14.33). The information on the lifelines and the hazards is presented with the use of colors and symbols: it allows to immediately see all the significant data.

Furthermore, for *Repast* and *RoboCup simulations* 3D plots are also available. Within the *Repast* framework it is possible to generate 3D display-platform using the Google Earth APIs. The kind of visualization shown in Fig. 14.34 also permits to orbit around the buildings (Lichter et al. 2015).

Fig. 14.31 NetLogo 2D visualization



Fig. 14.32 Repast simphony 2D visualization

With regards to RCRS, the documentation of the winning project of the “Infrastructure Competition” at RoboCup Rescue Simulation 2005 in Portugal (Kleiner 2004) describes the capability to render the animation of agents in three dimensions (Fig. 14.35) or in two dimensions by projecting the 3D scene into the plane (Fig. 14.36) (Kleiner and Göbelbecker 2004).

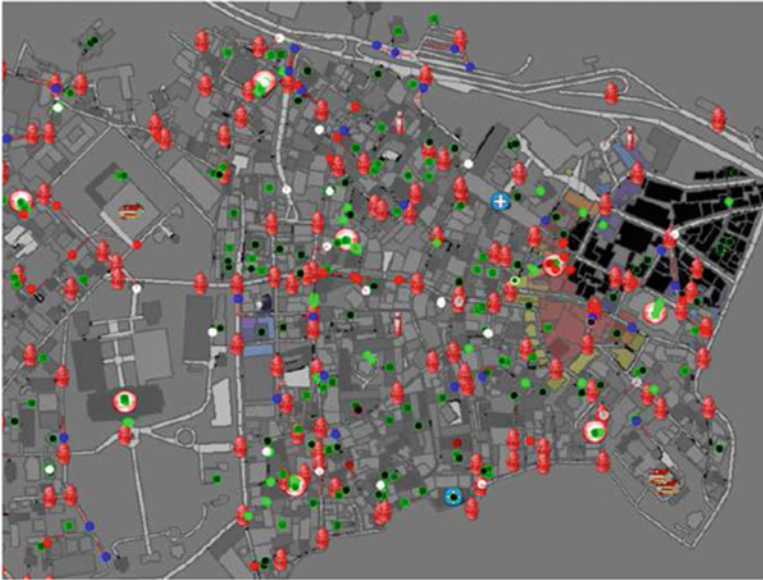


Fig. 14.33 RCRS 2D plot



Fig. 14.34 3D visualization with Google Earth APIs as platform (The height of the columns represents the value of the variable selected on the left-hand menu. The color refers to the different type of structures)

Fig. 14.35 3D visualization of the Kobe City, Japan with RCRS (*Green* buildings indicate refugees, *red* buildings fire stations, *white* buildings ambulance stations and *yellow* buildings police offices)

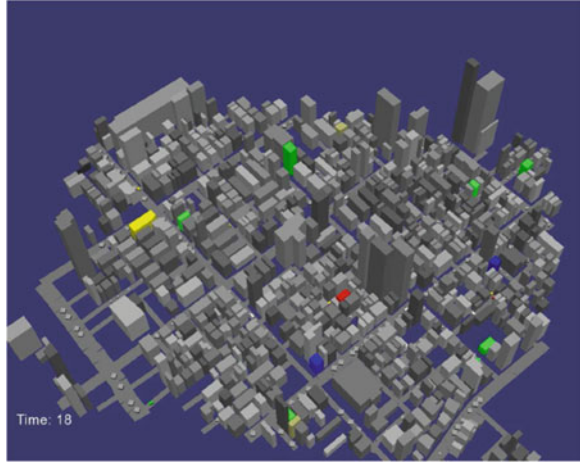
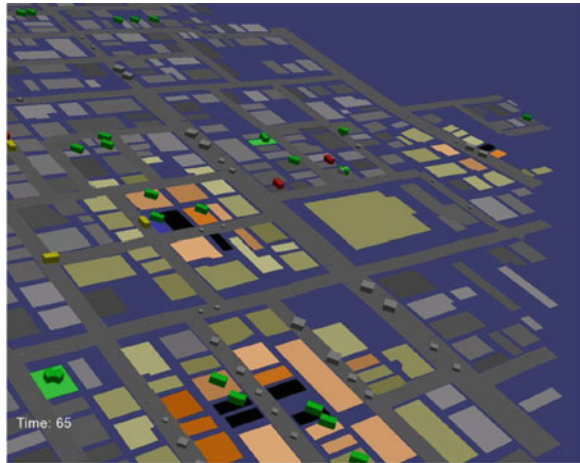


Fig. 14.36 A two dimensional visualization of Kobe City, Japan with RCRS



14.10 Summary and Remarks

This chapter focuses on the analysis of both commercial and research software available in literature for the analysis of communities following an extreme event such as an earthquake. Each software focuses on specific objectives. For example, *RISe* analyzes and evaluates the seismic risk and the losses, using the capacity spectrum method along with Google™ Earth, processing this information without requiring the installation of other commercial software. The *RISe* program then plots the output files on top of satellite images, with enough resolution for any built environment.

REDARS is another tool used for Seismic Risk Analysis. In particular, it estimates the seismic hazard of highway system, the damage state of each component and

how it can be repaired, and it also evaluates the cost. Therefore REDARS can be considered a tool that can be used for preparedness and mitigation actions, since both deterministic and probabilistic analysis can be performed.

The most known tool for the estimation of damage and loss due to earthquakes is *HAZUS*. This tool utilizes GIS technology and works in a multi-layered configuration. *HAZUS* can be used both as a pre-event and post-event tool, by using ShakeMap for the post-event study.

GIRAFFE models and manages disruptions on the hydraulic network and assists in the assessment of problems related to lifelines.

OpenQuake is an open source software developed within GEM that is applied at the national and regional level of seismic risk assessment. It can be used to support decisions and actions which aim to reduce losses resulting from an earthquake.

EQVIS, a program developed during the SYNER-G project sponsored by the European Commission, is based on the open-source-platform MAEviz. This program estimates the systemic seismic vulnerability, buildings risk analysis, loss of functionality and repair cost for the bridges, utility network and the repair rate analysis. It also computes socio-economic losses incurred by shelter needs, fiscal and business interruption. Lastly, the recently developed tool *ResilUS* was designed based on the two generic indicators of resilience concept, which are: the ability to perform and opportunity to perform.

In the second part of the chapter, a comparison between virtual cities software packages is proposed.

The comparison includes both commercial programs (*Aimsun 8.1*, *Cities in Motion*, *Cities:Skylines*, *Cities XL Platinum* and *SimCity*) and open source models (*NetLogo*, *OpenCity*, *OpenTTD*, *Repast Symphony*, *RoboCup Rescue Simulator* and *Simutrans*) The parameters of comparison adopted are: (i) infrastructures, (ii) hazards and (iii) visual graphic display.

Cities:Skylines is the software package that models the higher number of lifelines (12 out of 16) with respect to the others. The number of infrastructures which can be modeled with *NetLogo*, *Repast Symphony* and *RCSR* have been selected by analyzing existing projects where different mitigation strategies have been tested. For example, from the analysis it was concluded that *NetLogo* can model up to nine different types of infrastructures, and between the lifelines it can not model (7), two of them can not be model by any software at all. In term of hazard simulation, *RCSR*, *NetLogo* and *Repast* can simulate any type of hazard, while there are four simulators which can not model any hazard (*Simutrans*, *Cities XL Platinum*, *Cities in Motion*, *OpenCity* and *Aimsun 8.1*).

The higher visualization scores are given to the proprietary simulators, which have a 3D visualization capability. *SimCity* and *Cities Skylines* are able to highlight various data about the cities. However, other softwares such as *Cities XL Platinum* includes a ground-level perspective, while the buildings in *Simutrans* and *OpenTTD* have a medium level of graphic detail. In *Aimsun 8.1* the traffic simulation can be seen both in 2D and in 3D visualization, positioning on the map different cameras to get different points of view. Finally *NetLogo*, *Repast Symphony* and *RCSR* can represent the output of their analysis in a 2D visualization of the city, while for *Repast* and *RoboCup 3D* plot simulations are also available.

References

- ALA (2001) Seismic fragility formulations for water systems Part 1 – guidelines. Report, American Lifeline Alliance (ALA), American Society of Civil Engineers (ASCE)
- Basoz N, Mander JB (2008) Enhancement of the highway transportation module in HAZUS. Report, National Institute of Building Sciences
- Basz N, Kiremidjian A (1996) Risk assessment for highway systems. Report No 118, John A Blume Earthquake Engineering Center
- Cho S, Ghosh S, Huyck C, Werner SD (2006) User manual and technical documentation for the REDARSTM import wizard. Report MCEER-06-0015, Multidisciplinary Center of Earthquake Engineering Research
- da Silva ABM, Nardin LG, Sichman JS Robocup rescue simulator tutorial. http://roborescue.sourceforge.net/2013/robocup_rescue_simulator-tutorial.pdf
- Dawson RJ, Peppe R, Wang M (2011) An agent-based model for risk-based flood incident management. *Nat Hazards* 59(1):167–189
- Felsenstein D, Y, G (2014) Desurbs deliverables 4.2 urban simulation modeling, 4.3 probability estimation, 4.4 optimization. European Union's Seventh Framework Programme (FP7), Designing Safer Urban Spaces (DESURBS), Brussels
- FEMA (1997) Fema 273 NEHRP guidelines for seismic rehabilitation of buildings. Report, Federal Emergency Management Agency
- FEMA (1999) HAZUS99, technical manual, earthquake loss estimation methodology. Report, Federal Emergency Management Agency
- FEMA (2001) HAZUS99 for mapinfo, service release 2. Report, Federal Emergency Management Agency
- FEMA (2005a) HAZUS-MH version 1.1, FEMA's software program for estimating potential losses from disasters, technical manual. Report, Federal Emergency Management Agency and U.S. Army Corps of Engineers
- FEMA (2005b) Improvement of nonlinear static seismic analysis procedures. Report, Federal Emergency Management Agency
- FocusHomeInteractive (2008) Cities xl. <http://www2.citiesxl.com/en/community>
- GIRAFFE (2008) Giraffe users manual version 4.2 january 2008
- ICC IBC (2015) International building code. International Code Council, New York
- Kleiner A (2004) Rescue3d. <http://kaspar.informatik.uni-freiburg.de/~rescue3D/index.html>
- Kleiner A, Göbelbecker M (2004) Rescue3D: making rescue simulation attractive to the public. <http://kaspar.informatik.uni-freiburg.de/~simrescue3D>
- Kleiner A, Göbelbecker M (2004) Rescue3d: making rescue simulation attractive to the public
- Kongar I, Rossetto T (2012) A framework to assess the impact of seismic shocks on complex urban critical infrastructure networks. In: 15th world conference on earthquake engineering (15WCEE), Lisbon, pp 24–28
- Lang DH, Corea FVG (2010) RISE: illustrating georeferenced data of seismic risk and loss assessment studies using Google Earth. *Earthq Spectra* 26(1):295–307
- Lichter M, Grinberger AY, Felsenstein D (2015) Simulating and communicating outcomes in disaster management situations. *ISPRS Int J Geo-Inf* 4(4):1827–1847
- Markov I, Grigoriu M, O'Rourke T (1994) Evaluation of seismic serviceability of water supply networks with application to the San Francisco auxiliary water supply system, NCEER
- Miles SB, Chang SE (2006) Modeling community recovery from earthquakes. *Earthq Spectra* 22(2):439–458
- Miles SB, Chang SE (2007) A simulation model of urban disaster recovery and resilience: implementation for the 1994 Northridge earthquake. Report, MCEER technical report MCEER-07-0014, State University of New York at Buffalo (SUNY)
- Miles SB, Chang S (2011) ResilUS: a community based disaster resilience model. *J Cartogr GIS* 38(1):36–51

- Molina S, Lang DH, Lindholm CD (2009) SELENA – an open-source tool for seismic risk and loss assessment using a logic tree computation procedure. *Comput Geosci* 36(3):257–269
- Nguyen DK (2004) Opencity, another free 3D city simulator. www.opencity.info/
- NorthwesternUniversity (2001) Netlogo home page. <https://ccl.northwestern.edu/netlogo/>
- OpenTTD (2004) Openttd. <https://www.openttd.org/en/>
- PanamaCityPC (2003) Simutrans. <http://www.simutrans.com/en/>
- ParadoxInteractive (2000) Cities in motion. <http://www.citiesinmotion.com/>
- ParadoxInteractive (2014) Skylines wiki. <http://www.skylineswiki.com/Cities:SkylinesWiki>
- Skinner C, Ramchurn S (2010) The robocup rescue simulation platform. In: Proceedings of the 9th international conference on autonomous agents and multiagent systems: volume 1–Volume 1, International Foundation for Autonomous Agents and Multiagent Systems, Toronto, pp 1647–1648
- Sourceforge (1999) Repast simphony. http://repast.sourceforge.net/repast_simphony.php
- TransportSimulationSystems T (2001) Aimsun. https://www.aimsun.com/wp/?page_id=21
- Wang Y, O'Rourke T (2008) Seismic performance evaluation of water supply systems. Report, Multidisciplinary Center of Earthquake Engineering Research
- Werner SD, Taylor CE, Cho S, Lavoie JP, Huyck CK, Eitzel C, Chung H, Eguchi RT (2006) Redars 2 methodology and software for seismic risk analysis of highway systems. Report, Multidisciplinary Center of Earthquake Engineering Research
- Whitman RV, Anagnos T, Kircher CA, Lagorio HJ, Lawson RS, Schneider P (1997) Development of a national earthquake loss estimation methodology. *Earthq Spectra* 13(4):643–662

Appendix A

Probabilistic Formulation

A.1 Important Definitions

In the terminology of set theory, the set of all possibilities in a probabilistic problem is collectively a sample space, and each of the individual possibilities is a sample point. An event is then defined as a subset of the sample space.

- *Impossible event*: denoted \emptyset , is the event with no sample point;
- *Certain event*: denoted S , is the event containing all the sample points in a sample space, it is the sample space itself;
- *Complementary event \bar{E}* : of an event E contains all the sample points in S that are not in E (Fig. A.1).

A.2 The Venn Diagram

A sample space and its subsets (or events) can be represented pictorially with a Venn diagram. In many practical problems, the event of interest may be a combination of

Fig. A.1 A Venn diagram of sample space S

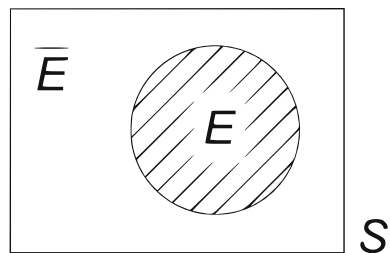


Fig. A.2 Venn diagram for $E_1 \cup E_2$

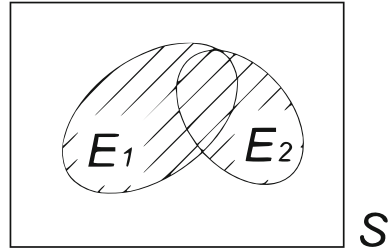
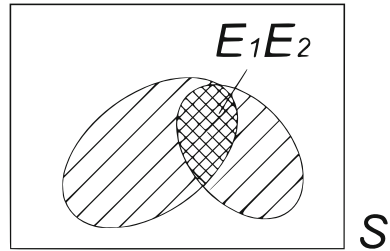


Fig. A.3 Venn diagram for $E_1 \cap E_2$



several other events; there are only two ways that events may be combined: *the union* or *intersection* (Figs. A.2 and A.3).

A.3 Mathematics of Probability

The theory of probability is based on certain fundamental assumptions, or axioms, that are not subject to proofs; these are as follows:

- **Axiom 1:** For every event E in a sample space S , there is a probability

$$P(E) \geq 0 \tag{A.1}$$

- **Axiom 2:** The probability of the certain event S is

$$P(E) = 1.0 \tag{A.2}$$

- **Axiom 3:** Finally, for two events E_1 and E_2 that are mutually exclusive (if the occurrence of one precludes the occurrence of the other event)

$$P(E_1 \cup E_2) = P(E_1) + P(E_2) \quad \textit{Addition Rule} \tag{A.3}$$

These equations constitute the basic axioms of probability theory, are essential assumptions and, therefore, cannot be violated.

A.4 Conditional Probability

There are occasions in which the probability of an event may depend on the occurrence (or nonoccurrence) of another event. If this dependence exists, the relevant probability is a *conditional probability*. For this purpose, we shall use the notation:

$P(E_1 | E_2)$ = the probability of E_1 assuming the occurrence of E_2 , or simply the probability of E_1 given E_2 .

The conditional probability $P(E_1 | E_2)$ may be interpreted as the likelihood of realizing a sample point of E_1 that is in E_2 ; hence the appropriate normalization, we obtain the conditional probability

$$P(E_1 | E_2) = \frac{P(E_1 \cap E_2)}{P(E_2)} \quad \text{Multiplication Rule} \quad (A.4)$$

A.5 The Theorem of Total Probability

On occasion, the probability of an event, say A , cannot be determined directly; its occurrence will depend on the occurrence or nonoccurrence of other events such as $E_i = 1, 2, \dots, n$ and the probability of A will depend on which of the E_i 's has occurred. On such an occasion, the probability of A would be composed of the conditional probabilities (conditioned on each of the E_i 's) and weighted by the respective probabilities of the E_i 's. Such problems require the theorem of total probability.

Formally, consider n events that are mutually exclusive and collectively exhaustive, namely E_1, E_2, \dots, E_n . That is, $E_1 \cup E_2 \cup \dots \cup E_n = S$. Then if A is an event in the same sample space S as shown in Fig. A.4, we derive the theorem of total probability as follows:

$$\begin{aligned} A &= AS \\ A &= A(E_1 \cup E_2 \cup \dots \cup E_n) \\ A &= AE_1 \cup AE_2 \cup \dots \cup AE_n \end{aligned} \quad (A.5)$$

Then

$$P(A) = P(AE_1) + P(AE_2) + \dots + P(AE_n)$$

And by virtue of the multiplication rule, we obtain the theorem of total probability as

$$P(A) = P(A | E_1)P(E_1) + P(A | E_2)P(E_2) + \dots + P(A | E_n)P(E_n) \quad (A.6)$$

Fig. A.4 Intersection of A and E_1, E_2, \dots, E_n in sample space S

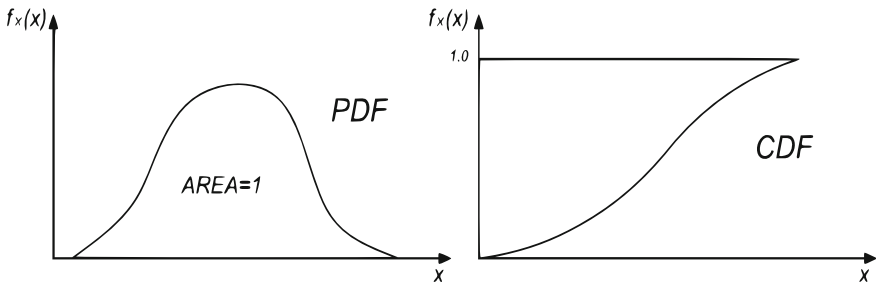
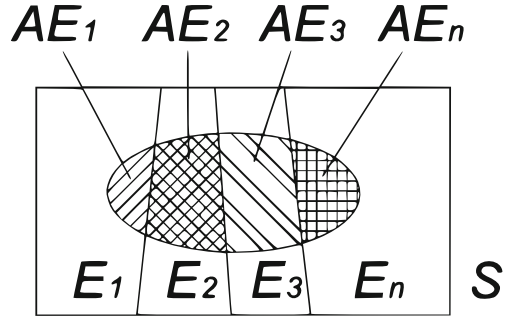


Fig. A.5 Probability distribution function and Cumulative distribution function

A.6 Probability Distribution of a Random Variable

A random variable is a mathematical vehicle for representing an event in analytical form. In contrast to a deterministic variable that can assume a definite value, the value of a random variable may be defined within a range of possible values. If X is defined as a random variable, then $X = x$, or $X < x$, or $X > x$, represents an event, where $(a < x < b)$ is the range of possible values of X .

As the values of a random variable represent events, the numerical values of the random variable are associated with specific probability. These probability measures may be assigned according to prescribed a probability law that is called *probability distribution function* (PDF). If X is a random variable, its probability distribution can always be described by its *cumulative distribution function* (CDF) (Fig. A.5).

A random variable may be discrete, continuous or mixed. X is a discrete random variable if only discrete values of x have positive probabilities; X is a continuous random variable if probability measures are defined for all values of x ; X is a mixed random variable if probability distribution is a combination of probabilities at discrete values of x as well as over a range of continuous values of x .

In the case of a continuous distribution, cumulative distribution function gives the area under the probability density function from minus infinity to x ,

$$F(x) = P(X \leq x) = \int_{-\infty}^x f(t)dt \quad \text{Cumulative distribution function} \quad (A.7)$$

A.7 Useful Probability Distributions

The best known and most used probability distribution is undoubtedly the Gaussian distribution also known as the normal distribution (Fig. A.6). Its PDF for a continuous random variable X, is given by

$$f_x(x) = \frac{1}{\sigma\sqrt{2\pi}} \exp\left[-\frac{1}{2}\left(\frac{x-\mu}{\sigma}\right)^2\right] \quad -\infty < x < +\infty \quad (\text{A.8})$$

where (in case of continuous random variable)

$$\mu = E(x) = \int_{-\infty}^{\infty} xf_x(x)dx \quad \text{Mean Value} \quad (\text{A.9})$$

$$\text{Var}(X) = \int_{-\infty}^{\infty} (x-\mu x)^2 f_x(x)dx \quad \text{Variance of X} \quad (\text{A.10})$$

$$\sigma = \sqrt{\text{Var}(X)} \quad \text{Standard deviation} \quad (\text{A.11})$$

$$P(a < x \leq b) = \frac{1}{\sigma\sqrt{2\pi}} \int_b^a \exp\left[-\frac{1}{2}\left(\frac{x-\mu}{\sigma}\right)^2\right] dx \quad (\text{A.12})$$

The logarithmic normal or simply lognormal distribution is also a popular probability distribution (Fig. A.7). Its PDF is

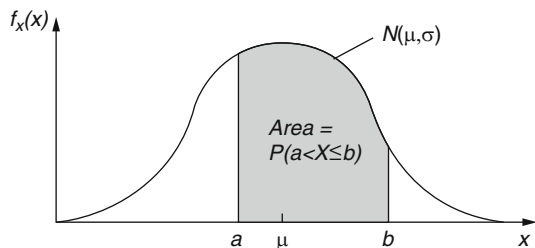
$$f_x(x) = \frac{1}{\sqrt{2\pi}(\zeta x)} \exp\left[-\frac{1}{2}\left(\frac{\ln x - \lambda}{\zeta}\right)^2\right] \quad x \geq 0 \quad (\text{A.13})$$

where

$$\lambda = E(\ln X) \quad \text{Mean value} \quad (\text{A.14})$$

$$\zeta = \sqrt{\text{Var}(\ln X)} \quad \text{Standard deviation} \quad (\text{A.15})$$

Fig. A.6 The Gaussian distribution



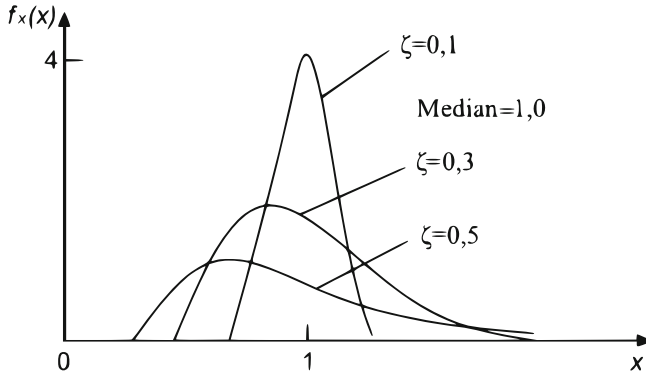


Fig. A.7 The lognormal PDFs for various values of ζ

$$P(a < X \leq b) = \frac{1}{\sqrt{2\pi}(\zeta x)} \int_b^a \exp \left[-\frac{1}{2} \left(\frac{\ln x - \lambda}{\zeta} \right)^2 \right] dx \tag{A.16}$$

A.8 Multiple Random Variables

The essential concepts of a random variable and its probability distribution can be extended to two or more random variables and their joint probability distribution. In order to identify events that are the results of two or more physical processes in numerical terms, the events in a sample space may be mapped into two (or more) dimensions of the real space; implicitly, we can recognize that this requires two or more random variables.

As any pair of values of the random variables X and Y represent events, there are probabilities associated with given values of x and y; if the random variables X and Y are continuous, the joint probability distribution may also be described with the joint PDF, $f_{X,Y}(x,y)$ that graphically is a surface

$$f_{X,Y}(x,y)dxdy = P(x < X \leq x + dx, y < Y \leq y + dy) \text{ Joint PDF} \tag{A.17}$$

Then

$$F_{x,y}(x,y) = \int_{-\infty}^x \int_{-\infty}^y f_{X,Y}(u,v)dvdu \text{ Joint CDF} \tag{A.18}$$

We observe the following probability

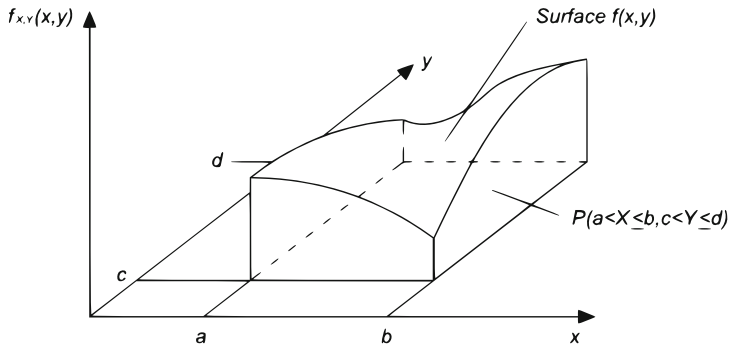


Fig. A.8 Volume under the PDF $f_{X,Y}(x,y)$

$$P(a < X \leq b, c < Y \leq d) = \int_a^b \int_c^d f_{X,Y}(u, v) dv du \tag{A.19}$$

Which is the volume under the PDF $f_{X,Y}(x,y)$ (Fig. A.8)

A.9 The Conditional and Marginal Distributions

For continuous X and Y, the conditional PDF of given Y is

$$f_{X|Y}(x|y) = \frac{f_{X,Y}(x, y)}{f_Y(y)} \tag{A.20}$$

From which we have

$$f_{X,Y}(x, y) = f_{X|Y}(x|y) f_Y(y) \text{ or } f_{X,Y}(x, y) = f_{Y|X}(x|y) f_X(y) \tag{A.21}$$

Finally, through the theorem of total probability, we obtain the marginal PDFs

$$f_X(x) = \int_{-\infty}^{\infty} f_{X|Y}(x|y) f_Y(y) dy = \int_{-\infty}^{\infty} f_{X,Y}(x, y) dy \tag{A.22}$$

This is called marginal density function and can be deduced from the probability density associated with, in a general case, the random variables X_1, \dots, X_n by integrating on all values of the $n - 1$ other variables.

In the probabilistic approach, we use this way to calculate the expected value of the resilience index considered a random variable dependent by other random variables.

Glossary

Accident an unforeseen and unplanned event or circumstances; or an unfortunate event resulting especially from carelessness or ignorance.

Classification The system of establishing classes for rating purposes.

Consequential loss A loss that arises as a result of direct damage to property for example, loss of rent. Some types of consequential loss are insurable under standard direct damage or time element coverage forms; others are not.

Crisis In risk management, any unplanned event or series of events that can cause death or injury to employees or the public or that can disrupt operations, cause physical or environmental damage, shut down the organization, or threaten the organization's financial standing or public image.

Database A database is a collection of organized information.

Direct loss Loss incurred due to direct damage to property, as opposed to time element or other indirect losses. It is also used sometimes by captives to identify losses under policies directly insured by the captive, as opposed to losses assumed from a front company.

Functionality the state or quality of being functional.

Hazard Conditions that increase the probability of loss.

Indicator An instrument used to monitor the operation or condition of an engine, furnace, electrical network, reservoir, or other physical system; a meter or gauge.

Indirect losses Income loss caused by a direct loss, such as when a firm cannot sell its merchandise due to a fire at its premises.

Resilience is "the ability [of a system] to cope with change.

Index

A

adaptive resilience, 40
AeDES forms, 297
AENS, 291
Agent based models, 155
Aimsun 8.1, 497
Aleatory uncertainties, 45
American Lifeline Alliance, 249
Analytical Recovery Models, 94
Android, 301
autonomy curves, 393

B

Bataclan theatre, 11
BI-IMRF, 347
Boston marathon terrorist attack, 13
Budgetary interdependency, 144
Business downtime, 354

C

CAIDI, 291
CAIFI, 291
capital improvements planning, 423
Cascading failure, 148
Charlie Hebdo, 12
Cities XL Platinum, 497
Cities:Skylines, 495
Civil society policy, 425
classical reliability indicators, 290
Classification of indicators, 56
Communicating Risk in RBD, 46
Communication Network, 292

Coupled failure, 148
cross correlation functions (CCF), 319
CTAIDI, 291
Cyber interdependency, 143

D

degree of interdependency, 149
Demand Driven Analysis (DDA), 247
depreciation rate, 75
Direct causalities losses, 75
Direct economic losses, 75
Disaster Preparedness, 411
Disaster risk management, 409
Discrete Event Simulation (DES) model, 367
downtime, 100
Durability, 42
Dutch TNO model, 271

E

Economic Development, 125
economic losses, 390
economic resilience, 389
Economic Resilience index, 398
Economic theory based models, 155
Electric Power Network, 287
Emergency Department, 361
Empirical approaches for interdependencies, 154
Empirical recovery models, 100
engineering demand parameters (EDP), 349
ENS, 291
Environmental/Ecosystem, 118

EPANET 2.0, 247
 EPANET software, 485
 Epistemic uncertainties, 45
 EQVIS software, 492
 Event tree, 178
 Event Tree Analysis, 175
 Excess Flow Automatic Gas Shutoff Valves, 283

F

Fault tree, 177
 Fault Tree Analysis, 175
 Florian, 15
 fragility functions, 78
 friction factor, 248
 Fukushima Daiichi nuclear power plant, 181
 Functionality of transportation networks, 234
 Fuzzy logic method (FL), 262

G

Gas Network, 261
 geographic scales, 34
 Geographical interdependency, 144
 GIRAFFE software, 484
 global reliability indicators, 291
 graph theory, 162
 Great East Japan earthquake, 7

H

HAZUS, 24
 HAZUS software, 474
 health care facilities, 345
 HP-SMRF, 347
 Hurricane Andrew, 5
 Hurricane Katrina, 5, 414
 Hurricane Sandy, 432
 Hyogo Framework for Action (HFA) , 428
 hysical interdependency, 142

I

Indian Ocean earthquake, 6
 indirect economic losses, 76
 Inherent resilience, 40
 input-output inoperability matrix, 129
 Input-output Inoperability Method, 156
 Input-Output model, 391
 Interdependency, 140
 Interdependency Index, 321

intradependencies, 142
 IOS, 301
 ITALGAS, 265
 Italian gas distribution network, 268
 Italian gas supply system, 267
 Italian National Institute of Geophysics and Vulcanology (INGV), 276

K

Kirchhoff law, 269

L

Land Use Intervention Planning, 421
 Leadership index, 150
 Lifelines, 227
 Lifestyle and Community Competence, 124
 Limit states, 82
 liquefaction effects, 274
 LOLP, 291
 Long term recovery models, 94
 Loss Assessment for Infrastructure, 73
 Loss Assessment models, 71
 Loss Function, 74
 loss of income (LI), 391
 low-pressure (LP) lines, 266

M

Manmade disasters, 7
 Market & Economy interdependency, 144
 matrix of interdependency, 151
 MCEER definition of Resilience, 32
 medium-pressure (MP) lines, 266
 metamodel, 376
 mitigation actions, 417
 Modified IIM, 160
 Mont Blanc and Tauern Tunnel fires, 9
 Multidimensional Performance Limit State Function, 82
 Multilayer approach for spatial interdependency, 165

N

natural gas, 261
 natural hazard, 4
 NetLogo, 495
 Network-based models, 154
 NIST, 22
 Non-Structural losses, 74

O

OpenCity, 497
 OpenQuake software, 492
 OpenSees, 349
 OpenTTD, 496
 Oregon Resilience Plan, 23
 Organized Governmental services, 120

P

patient arrival rate, 371
 PEER, 25
 PEER integral, 26
 PEOPLES framework, 111
 Performance Assessment Calculation Tool (PACT), 351
 Physical infrastructures, 122
 Policy actors, 424
 Policy insiders and outsiders, 424
 Policy/Procedural interdependency, 144
 Population and demographics, 116
 Pressure Driven Analysis (PDA), 247
 pressure reduction gas stations, 273
 Probability Risk Assessment, 173
 ProModel, 367
 Public Policy, 423

Q

qualitative indicators, 61
 quantitative indicators, 61

R

Rapid Observation and Visual Estimation of Risk, 295
 Rapidity, 36
 RE.MI. “Regolazione di misura”, 268
 REDARs software, 468
 Redundancies, 157
 Redundancy, 38
 Regional Resilience Index, 339
 Regional Seismic Losses Assessment Models (RSLA), 72
 relocation expenses(RE), 391
 rental income losses (RIL), 391
 Repair cost, 352
 Repair Rate, 249
 Repast Symphony, 495
 replacement building costs, 75
 Resilience, 16
 resilience indicators, 49
 Resilience performance levels, 132

resilience software, 463
 Resilience-Based Design, 31
 ResilUS software, 494
 Resourcefulness, 38
 Restoration curves of physical infrastructures, 319
 Reynolds Number, 248
 RISE and SELENA software, 464
 risk, 43
 Risk Curves, 289
 Risk of pipe failure, 251
 RoboCup Rescue Simulator (RCRS), 495
 Robustness, 37
 roughness, 248

S

SAIDI, 291
 SAIFI, 291
 San Andreas Fault earthquake scenario, 146
 school buildings, 345
 Scorecards, 50
 Sendai Framework (2015), 430
 Short term recovery models, 97
 SimCity, 495
 Simutrans, 496
 Societal interdependency, 144
 Socio-Cultural Capital, 127
 SPUR, 22, 415
 Standard earthquake damage assessment in Italy, 297
 Step recovery function, 100
 structural growth model (SGM), 391
 Structural losses, 74
 Subordination index, 150
 Survey, 303
 sustainability, 41
 System dynamics based models, 153

T

temporal networks, 153
 temporal scale, 34
 The four Rs for Resilience, 35
 total performance index, 132
 Transportation network, 228
 triage, 365
 triple friction pendulum bearings (TFPB), 347

U

Uncertainties of Limit States, 85
 Uncoupled failure, 148

uniform hazard spectrum (UHS), [347](#)
UNISDR, [23](#)

V

Virtual City Simulators, [494](#)
visual graphic display, [498](#)
vulnerability, [40](#)

W

Water Distribution Network, [238](#)
water network restoration plans, [257](#)
weight coefficients, [336](#)

Y

Yokohama strategy for a safer world, [427](#)